

**Advances in Isotope Hydrology
and its Role in Sustainable Water
Resources Management
(IHS – 2007)**

**Proceedings of a Symposium
Vienna, 21–25 May 2007**

Vol. 1



IAEA

International Atomic Energy Agency

ADVANCES IN ISOTOPE HYDROLOGY
AND ITS ROLE IN SUSTAINABLE
WATER RESOURCES MANAGEMENT
(IHS-2007)

The following States are Members of the International Atomic Energy Agency:

AFGHANISTAN	GREECE	NORWAY
ALBANIA	GUATEMALA	PAKISTAN
ALGERIA	HAITI	PALAU
ANGOLA	HOLY SEE	PANAMA
ARGENTINA	HONDURAS	PARAGUAY
ARMENIA	HUNGARY	PERU
AUSTRALIA	ICELAND	PHILIPPINES
AUSTRIA	INDIA	POLAND
AZERBAIJAN	INDONESIA	PORTUGAL
BANGLADESH	IRAN, ISLAMIC REPUBLIC OF	QATAR
BELARUS	IRAQ	REPUBLIC OF MOLDOVA
BELGIUM	IRELAND	ROMANIA
BELIZE	ISRAEL	RUSSIAN FEDERATION
BENIN	ITALY	SAUDI ARABIA
BOLIVIA	JAMAICA	SENEGAL
BOSNIA AND HERZEGOVINA	JAPAN	SERBIA
BOTSWANA	JORDAN	SEYCHELLES
BRAZIL	KAZAKHSTAN	SIERRA LEONE
BULGARIA	KENYA	SINGAPORE
BURKINA FASO	KOREA, REPUBLIC OF	SLOVAKIA
CAMEROON	KUWAIT	SLOVENIA
CANADA	KYRGYZSTAN	SOUTH AFRICA
CENTRAL AFRICAN REPUBLIC	LATVIA	SPAIN
CHAD	LEBANON	SRI LANKA
CHILE	LIBERIA	SUDAN
CHINA	LIBYAN ARAB JAMAHIRIYA	SWEDEN
COLOMBIA	LIECHTENSTEIN	SWITZERLAND
COSTA RICA	LITHUANIA	SYRIAN ARAB REPUBLIC
CÔTE D'IVOIRE	LUXEMBOURG	TAJIKISTAN
CROATIA	MADAGASCAR	THAILAND
CUBA	MALAWI	THE FORMER YUGOSLAV REPUBLIC OF MACEDONIA
CYPRUS	MALAYSIA	TUNISIA
CZECH REPUBLIC	MALI	TURKEY
DEMOCRATIC REPUBLIC OF THE CONGO	MALTA	UGANDA
DENMARK	MARSHALL ISLANDS	UKRAINE
DOMINICAN REPUBLIC	MAURITANIA	UNITED ARAB EMIRATES
ECUADOR	MAURITIUS	UNITED KINGDOM OF GREAT BRITAIN AND NORTHERN IRELAND
EGYPT	MEXICO	UNITED REPUBLIC OF TANZANIA
EL SALVADOR	MONACO	UNITED STATES OF AMERICA
ERITREA	MONGOLIA	URUGUAY
ESTONIA	MONTENEGRO	UZBEKISTAN
ETHIOPIA	MOROCCO	VENEZUELA
FINLAND	MOZAMBIQUE	VIETNAM
FRANCE	MYANMAR	YEMEN
GABON	NAMIBIA	ZAMBIA
GEORGIA	NETHERLANDS	ZIMBABWE
GERMANY	NEW ZEALAND	
GHANA	NICARAGUA	
	NIGER	
	NIGERIA	

The Agency's Statute was approved on 23 October 1956 by the Conference on the Statute of the IAEA held at United Nations Headquarters, New York; it entered into force on 29 July 1957. The Headquarters of the Agency are situated in Vienna. Its principal objective is "to accelerate and enlarge the contribution of atomic energy to peace, health and prosperity throughout the world".

PROCEEDINGS SERIES

ADVANCES IN ISOTOPE
HYDROLOGY AND ITS ROLE
IN SUSTAINABLE WATER
RESOURCES MANAGEMENT
(IHS–2007)

PROCEEDINGS OF AN INTERNATIONAL SYMPOSIUM
ON ADVANCES IN ISOTOPE HYDROLOGY
AND ITS ROLE IN SUSTAINABLE
WATER RESOURCES MANAGEMENT (IHS–2007)
ORGANIZED BY THE
INTERNATIONAL ATOMIC ENERGY AGENCY
AND HELD IN VIENNA, 21–25 MAY 2007

In two volumes

VOLUME 1

INTERNATIONAL ATOMIC ENERGY AGENCY
VIENNA 2007

COPYRIGHT NOTICE

All IAEA scientific and technical publications are protected by the terms of the Universal Copyright Convention as adopted in 1952 (Berne) and as revised in 1972 (Paris). The copyright has since been extended by the World Intellectual Property Organization (Geneva) to include electronic and virtual intellectual property. Permission to use whole or parts of texts contained in IAEA publications in printed or electronic form must be obtained and is usually subject to royalty agreements. Proposals for non-commercial reproductions and translations are welcomed and considered on a case-by-case basis. Enquiries should be addressed to the IAEA Publishing Section at:

Sales and Promotion, Publishing Section
International Atomic Energy Agency
Wagramer Strasse 5
P.O. Box 100
1400 Vienna, Austria
fax: +43 1 2600 29302
tel.: +43 1 2600 22417
email: sales.publications@iaea.org
<http://www.iaea.org/books>

© IAEA, 2007

Printed by the IAEA in Austria

December 2007

STI/PUB/1310

IAEA Library Cataloguing in Publication Data

International Symposium on Advances in Isotope Hydrology and Its Role in Sustainable Water Resources Management (2007 : Vienna, Austria)

Advances in isotope hydrology and its role in sustainable water resources management (IHS-2007) : proceedings of an International Symposium on Advances in Isotope Hydrology Hydrology and its Role in Sustainable Water Resources Management (IHS-2007) / organized by the International Atomic Energy Agency and held in Vienna, 21–25 May 2007. — Vienna, IAEA, 2007.

p. ; 24 cm. — (Proceedings series, ISSN 0074-1884)

STI/PUB/1310

ISBN 978-92-0-110207-2

Includes bibliographical references.

1. Radioisotopes in hydrology — Congresses.
 2. Hydrology — Congresses.
 3. Water-supply — Congresses.
- I. International Atomic Energy Agency.
II. Series: Proceedings series: (International Atomic Energy Agency).

FOREWORD

Access to safe freshwater is considered a basic human right. However, in many parts of the world, surface water and ground water resources are at risk because of indiscriminate use, rapidly growing populations, increasing agricultural demands, and the threat of pollution. These risks are often compounded by a lack of understanding about local conditions governing the occurrence, distribution and movement of surface and groundwater resources.

Historically, the IAEA has played a key role in advancing isotope techniques and in promoting the use of isotopes to address water resource sustainability issues worldwide. The quadrennial IAEA symposia continue to be an important component of the IAEA's mission in water resources management. The 12th symposium in the series was convened from 21 to 25 May 2007 in Vienna with the objectives of: reviewing the state of the art in isotope hydrology; outlining recent developments in the application of isotope techniques to water resources management; and identifying future trends and developments for research and applications.

Over 200 participants from 59 Member States participated in a series of invited lectures, poster sessions, round table discussions, and a scientific visit to the Danube River. The breadth of topics addressed was extensive and included analytical developments, the use of isotopes to understand land-atmosphere-biosphere interactions, rivers and surface water, development of deep groundwater resources, ecohydrology, urbanization and water resources management, carbon sequestration, waste management, artificial recharge, contamination problems, coastal zone hydrology, geothermal systems, agriculture and water resources management, and research frontiers.

Out of 152 oral and poster presentations, 136 contributions submitted by the authors are included in two volumes of the proceedings with editorial corrections. These proceedings are intended for those using isotopes for applied problems in hydrology as well as the research community. It is also hoped that these proceedings will promote increased use of isotopes for water resource sustainability problems and greater utilization of these techniques by hydrologists in general.

EDITORIAL NOTE

The papers in these Proceedings (including the figures, tables and references) have undergone only the minimum copy editing considered necessary for the reader's assistance. The views expressed remain, however, the responsibility of the named authors or participants. In addition, the views are not necessarily those of the governments of the nominating Member States or of the nominating organizations.

The report does not address questions of responsibility, legal or otherwise, for acts or omissions on the part of any person.

Although great care has been taken to maintain the accuracy of information contained in this publication, neither the IAEA nor its Member States assume any responsibility for consequences which may arise from its use.

The use of particular designations of countries or territories does not imply any judgement by the publisher, the IAEA, as to the legal status of such countries or territories, of their authorities and institutions or of the delimitation of their boundaries.

The mention of names of specific companies or products (whether or not indicated as registered) does not imply any intention to infringe proprietary rights, nor should it be construed as an endorsement or recommendation on the part of the IAEA.

The authors are responsible for having obtained the necessary permission for the IAEA to reproduce, translate or use material from sources already protected by copyrights.

Material prepared by authors who are in contractual relation with governments is copyrighted by the IAEA, as publisher, only to the extent permitted by the appropriate national regulations.

CONTENTS OF VOLUME 1

SUMMARY	1
----------------------	---

ORAL PRESENTATIONS

INVITED SPEAKERS

Compound specific stable isotope analysis: Research frontiers in isotope hydrology and water resources management (IAEA-CN-151/156)	9
<i>B. Sherwood Lollar, M.C.G. Chartrand, S.M. Hirschorn, M. Howlett, T.F. Bidleman, L.M. Jantunen, S. Mancini, J. McKelvie, G. Lacrampe-Couloume, E.A. Edwards</i>	
Application of stable isotopes and fluid chemistry to understanding anthropogenic CO ₂ -brine-rock interactions in sedimentary basins: Results from the Frio brine pilot tests, Texas, USA (IAEA-CN-151/163)	17
<i>Y.K. Kharaka, D.R. Cole, J.J. Thordsen, E. Kakouros</i>	
An integrated approach in evaluating isotope data of the Nubian Sandstone Aquifer System (NSAS) in Egypt (IAEA-CN-151/167)	31
<i>K. Froehlich, P.K. Aggarwal, W.A. Garner</i>	
Radionuclide tracers of submarine groundwater discharge (IAEA-CN-151/18)	47
<i>W.S. Moore</i>	
Stable isotopes as tools for watershed hydrology model development, testing and rejection (IAEA-CN-151/111)	59
<i>J.J. McDonnell, K.B. Vache, K.J. McGuire, A.B. Mazurkiewicz</i>	
Tritium/Helium-3 dating of baseflow — Southern Vienna Basin (IAEA-CN-151/17)	73
<i>D.K. Solomon, D. Rank, P.K. Aggarwal, A. Suckow, T. Vitvar, B. Stolp</i>	

A decade of environmental isotope research in a low permeability
aquitard system (IAEA–CN–151/146) 83
M.J. Hendry, L.I. Wassenaar

Variations in the isotopic composition of near surface water vapour
in the Eastern-Mediterranean (IAEA–CN–151/152) 101
D. Yakir, A. Angert, J.R. Gat

Advances in optical water isotope ratio measurements
(IAEA–CN–151/80) 115
E.R.Th. Kerstel

CASE STUDIES

Spatial variations of environmental tracer distributions in water
from a mangrove ecosystem: The case of Babitonga Bay (Santa
Catarina, Brazil) (IAEA–CN–151/23). 131
*V. Barros Grace, L.A. Martinelli, J. Mas Pla, T. Oliveira Novais,
J.P. Ometto, E. Sacchi, G.M. Zuppi*

Origin and effects of nitrogen pollution in groundwater traced
by $\delta^{15}\text{N}_{-\text{NO}_3}$ and $\delta^{18}\text{O}_{-\text{NO}_3}$: the case of Abidjan (Ivory Coast)
(IAEA–CN–151/31) 139
M.S. Oga Yei, E. Sacchi, G.M. Zuppi

Groundwater and its functioning at the Doñana Ramsar site
wetlands (SW Spain): Role of environmental isotopes to define
the flow system (IAEA–CN–151/158). 149
M. Manzano, E. Custodio, H. Higuera

Relationship between stable isotopes of precipitation and
atmospheric circulation – Case study: Application in a pilot basin
in Central Anatolia (IAEA–CN–151/78) 161
Y. Inci Tekeli, A. Unal Sorman

Assessment of groundwater dynamics in Uganda using a
combination of isotope tracers and aquifer hydraulics data
(IAEA–CN–151/108) 169
*C. Tindimugaya, R.G. Taylor, K.M. Kulkarni, T.C. Atkinson,
J. Barker*

Environmental isotopic study for groundwater of the North Plain of
Huai He River, China (IAEA–CN–151/154) 177
*Nian-Jun Ye, Jian-Shi Gong, Wei-Ya Ge, Jia-Ju Lu, Cheng-You Ha,
Wei-Zu Gu*

Environmental isotope and hydrochemical investigation on
groundwater recharge and dynamics of the coastal sedimentary
aquifers of Tiruvadanai, Tamilnadu State, India
(IAEA–CN–151/81) 187
*U. Saravanakumar, S. Sharma, A.S. Deodhar, H.V. Mohokar,
S.V. Navada, S. Ganesan*

Groundwater flow functioning in arid zones with thick volcanic
aquifer units: North–Central Mexico (IAEA–CN–151/118) 199
J.J. Carrillo-Rivera, A. Cardona, W.M. Edmunds

POSTER PRESENTATIONS

PRECIPITATION AND ATMOSPHERIC PROCESSES

Isotopic study of the water exchange between atmosphere and
biosphere at selected sites in Pakistan (IAEA–CN–151/15) 211
M. Ali, Z. Latif, M. Fazil, M. Ahmad

Geostatistical methods for producing stable isotope maps over
Central and Eastern Mediterranean (IAEA–CN–151/29) 221
A.A. Argiriou, S.P. Lykoudis

Isotopic composition of meteoric water in Sicily (IAEA–CN–151/67) 231
*M. Liotta, R. Favara, M. Fontana, E. Gagliano, A. Pisciotta,
C. Scaletta*

Factors controlling the stable isotopic composition of recent
precipitation in Spain (IAEA–CN–151/82) 239
M.F. Díaz, J. Rodríguez, E. Pérez, S. Castaño, L. Araguás-Araguás.

Application of environmental isotope techniques to selected
hydrological systems in Pampean, Argentina (IAEA–CN–151/90). 251
C. Dapeña, H.O. Panarello

Rainwater tracing using the stable isotope in the Western Mediterranean (case of Rif Chain in the North of Morocco) (IAEA–CN–151/93) 261
M. Qurtobi, H. Marah, A. El Mahboul, C. Emblanch

Modeling the altitude isotope effect in precipitations and comparison with the altitude effect in groundwater (IAEA–CN–151/103) 269
F. Gherardi, P. Bono, C. Fiori, M.F. Diaz Tejeiro, R. Gonfiantini

Isotopes in precipitations of Kinshasa area: Moisture sources and groundwater tracing (IAEA–CN–151/136) 279
L. Ndembo, Y. Travi, L.M. Moyengo, J.N. Wabakaghanzi

Non-mass dependent oxygen isotope effect observed in water vapour from Alert, Canada (IAEA–CN–151/153)..... 289
Y. Lin, L. Huang, R.N. Clayton

SURFACE WATER DYNAMICS

Dynamics of water transport through the Velika Morava catchment (IAEA–CN–151/2) 299
N. Miljevic, D. Golobocanin, A. Milenkovic, M. Nadezdic

Detection of water leaks in Foum El-Gherza dam (Algeria) (IAEA–CN–151/5) 309
N. Hocini, A.S. Moulla

Isotopic and chemical study of Lake Massaciuccoli, Tuscany. Hydrodynamic patterns, water quality and anthropogenic impact (IAEA–CN–151/30) 317
I. Baneschi, R. Gonfiantini, M. Guidi, J.L. Michelot, D. Andreani, G.M. Zuppi

Mean residence time of water from springs of the Plitvice Lakes and Una River area (IAEA–CN–151/45)..... 327
S. Babinka, B. Obelić, I. Krajcar Bronić, N. Horvatinčić, J. Barešić, S. Kapelj, A. Suckow

The use of tritium in river base flow to understand long-term changes in water quality (IAEA–CN–151/51)	337
<i>R.L. Michel, P.K. Aggarwal, T. Kurttas, L. Araguas Araguas, K.M. Kulkarni</i>	
Deuterium and oxygen-18 ratios in rainfall and streamflow in a major drinking water catchment near Sydney, Australia during drought (IAEA–CN–151/54)	345
<i>C.E. Hughes, M.J. Fischer, D.M. Stone, S.E. Hollins</i>	
New approaches for the detailed assessment of Meromictic Lakes by using stable isotopes (IAEA–CN–151/58)	349
<i>A. Seebach, K. Knöller</i>	
Do water isotopes reflect differences in timber harvest practices? Isotope ecohydrology in the Mica Creek watershed, Idaho USA (IAEA–CN–151/68)	357
<i>P. Koeniger, T.E. Link, J.D. Marshall</i>	
Evaluation of the impact of groundwater resources on surface water in Chihuahua, Northern Mexico (IAEA–CN–151/71)	365
<i>L.G. Hernández-Limón, J. Mahlkecht, A. Chávez-Rodríguez, A. Pinales-Munguía, R. Aravena</i>	
Internet GIS and water resource information (IAEA–CN–151/72)	375
<i>P. Deeprasertkul, R. Chitradon</i>	
Environmental isotopes in the water cycle in the catchment of the Quequen Grande River, Argentina (IAEA–CN–151/84)	381
<i>D.E. Martínez, C. Dapeña, T. Bentacur Vargas, H.O. Panarello, M. Quiroz Londoño, H.E. Massone</i>	
C-14 and Tritium concentrations along Romanian Danube Sector – Preliminary results (IAEA–CN–151/92)	389
<i>C. Varlam, I. Stefanescu, S. Cuna, I. Faurescu, I. Popescu, M. Varlam</i>	
The role of rivers in the Swiss network for the observation of isotopes in the water cycle (ISOT) (IAEA–CN–151/102)	399
<i>U. Schotterer, M. Leuenberger, P. Nyfeler, H.U. Bürki, R. Kozel, M. Schürch, W. Stichler</i>	

Ground water input to a rare flood event in an arid zone ephemeral river identified with isotopes and chemistry (IAEA-CN-151/110). 409
B.Th. Verhagen, M.J. Butler

Water flowpaths in the mountainous watershed traced by ¹⁸O isotope: experimental approach (IAEA-CN-151/139). 419
M. Sanda, M. Sobotkova, M. Cislerova

Preliminary isotope studies in Poyang Lake (IAEA-CN-151/160) 427
Wenbin Zhou, Maolan Wang, Chunhua Hu, Huayun Xiao Xiao

Linking water pathways and nutrient dynamics in a small head water catchment: results of a controlled sprinkler experiment using a deuterium tracer in western Oregon (IAEA-CN-151/165) 437
H.R. Barnard, W.J. van Verseveld, C.B. Graham, B.J. Bond, K. Lajtha, J.R. Brooks, J.J. McDonnell

Geochemistry of carbon stable isotope in Shatt AL-Arab River and Khor AL- Zubair Estuary, South Iraq (IAEA-CN-151/166). 447
A.H. Afaj, S.A. Thejeel

SURFACE WATER QUALITY

Long-term behavior of Chernobyl radionuclides in the Dnieper River Basin (IAEA-CN-151/43). 457
O. Zhukova, Zh. Bakarykava, M. Germenchuk

Examination of the source of salinity in water resources using isotope techniques. Case study: water resources of Shapoor River Basin (IAEA-CN-151/59) 467
F. Hatami, Y. Khalaj Amirhosseini, M. Kuhpour

Deuterium as indicator of the natural and anthropic stress on the waters of the Danube Delta, Romania (IAEA-CN-151/62) 475
V. Feurdean, L. Feurdean, C. David

Tritium concentrations in the Yukon River Basin and their implications (IAEA-CN-151/70) 487
R.L. Michel, P. Schuster, M. Walvoord

Combining hydrological, chemical and isotopic approaches to identify sources and fate of sulfate and nitrate in the South Saskatchewan River system, Canada (IAEA–CN–151/105) 493
B. Mayer, L.I. Wassenaar, L. Rock, J.E. McCallum

Isotope hydrology and hydrochemistry of some nutrient enrichment sources to the Densu River Basin, in Ghana (IAEA–CN–151/123) 501
J.R. Fianko, S. Osae, D. Adomako, D.G. Achel

UNSATURATED ZONE AND ARTIFICIAL RECHARGE

Application of isotope hydrology for the assessment of artificial ground water recharge in some areas of UAE (IAEA–CN–151/8). 509
A.S. Ekaabi

Quantification of the heterogeneity in water transport through the unsaturated zone of sandy soils using environmental isotopes (IAEA–CN–151/13) 519
C. Stumpp, P. Maloszewski, W. Stichler

Isotopic and geochemical impact of water releases from the Sidi Saâd Dam on groundwater in Kairouan plain (Central Tunisia) (IAEA–CN–151/22). 527
S. Belhadj Salem, N. Chkir, K. Zouari, R. Beji

Hydrochemical and isotopic study of Al-Mouh Sabkha evaporatic system (Syria) (IAEA–CN–151/32). 537
B. Abou Zakhem, R. Hafez

Stable isotopes as indicators of ecohydrological coupling at the watershed scale (IAEA–CN–151/36) 549
J.R. Brooks, H. Barnard, J.J. McDonnell, R. Coulombe, C. Burdick

Use of natural tracers (major ions, total organic carbon, stable isotopes) to understand volcanic aquifer functioning: An example from the Argnat Basin (Auvergne, France) (IAEA–CN–151/49) 559
G. Bertrand, H.Celle-Jeanton, G. Chazot, F. Huneau

Infiltration processes and impact on shallow groundwater in agricultural dry land areas (IAEA–CN–151/79)	567
<i>E. Garel, V. Marc, S. Ruy, C. Doussan, R. Simler, M. Daniel, F. Tison</i>	
Use of deuterated water as a conservative artificial tracer in the study of water movement in a coarse gravel unsaturated zone (IAEA–CN–151/87)	577
<i>N. Mali, J. Urbanc, A. Leis</i>	
Assessing agriculture pollution in the Beja aquifer using nitrogen isotopes (south Portugal) (IAEA–CN–151/101)	587
<i>E. Paralta, P.M. Carreira, L. Ribeiro</i>	
Deuterium tracer experiment in the unsaturated zone of fractured karst aquifers (IAEA–CN–151/113)	597
<i>B. Cencur Curk, W. Stichler</i>	
Carbon-13 and carbon-14 contents of groundwater located in sandy aquifer outcrops: Driving influence of the unsaturated zone (IAEA–CN–151/126)	605
<i>M. Gillon, F. Barbecot, E. Gibert, C. Marlin, M. Massault</i>	

ANALYTICAL DEVELOPMENTS

Compound-specific chlorine stable isotope of vinyl chloride by continuous flow-isotope ratio mass spectrometry (CF-IRMS) (IAEA–CN–151/14)	615
<i>O. Shouakar-Stash, S.K. Frappe, A. Gargini, M. Pasini, R.J. Drimmie, R. Aravena</i>	
Stable isotopes in Gacka River catchment: Installation of a laboratory for stable isotope analysis in Croatia (IAEA–CN–151/46)	625
<i>Z. Roller-Lutz, M. Mandić, D. Bojić, H.O. Lutz, S. Kapelj</i>	
Recent advances in modern ion chromatography for the analysis of environmental water samples: Reagent free ion chromatography systems using recycled eluent and their applications (IAEA–CN–151/132)	633
<i>S. Ghirlanda, D. Jensen</i>	

COASTAL ZONE HYDROLOGY

Submarine groundwater discharge to the Mediterranean Sea: A case study off Monaco (IAEA–CN–151/40)	641
<i>J.C. Scholten, M. Schubert, A. Schmidt, M.M. Rutgers van der Loeff, M. Schlüter, M.K. Pham, K. Knöller, J.-F. Comanducci, J.A. Sanchez-Cabeza</i>	
Application of stable isotopes to evaluate groundwater recharge of a coastal aquifer in North-Central Chile and its role in vegetation dynamics (IAEA–CN–151/52)	649
<i>E. Aguirre, F.A. Squeo, R. Aravena</i>	
Characterization of marine intrusion and origin of the mineralization in the oriental coastal aquifer of Cap Bon (Tunisia) (IAEA–CN–151/53)	659
<i>M.F. Ben Hamouda, K. Zouari, J. Tarhouni, C. Leduc</i>	
Isotopic characterisation of groundwater-seawater interactions (IAEA–CN–151/131)	667
<i>P.P. Povinec, P.K. Aggarwal, K.M. Kulkarni, M. Groening, L.F. Han</i>	
Use of environmental isotopes to evaluate the sources of submarine freshwater in the southern shoreline in Lebanon (IAEA–CN–151/137)	675
<i>Z. Saad, V. Kazpard</i>	
Chairpersons of Sessions	685
Programme Committee and Secretariat of the Symposium	687

SUMMARY

The 12th international symposium on Advances in Isotope Hydrology and its Role in Sustainable Water Resources Management (IHS-2007) was held in Vienna, from 21 to 25 May 2007. The symposium was divided into an opening session, a series of nine invited lectures, a series of eight case study lectures, three poster sessions (at which 135 posters were presented), a scientific side visit, two roundtable discussions, technology demonstrations, and a closing session. The poster sessions were very well attended and generated substantial interactions among participants. Technical presentations were organized through a series of themes which are described below. There were 213 registered participants, 14 observers, and 6 exhibitors. Participants came from 59 Member States, and 32 grants were provided to participants from developing countries. Four new aspects of this symposium were the focus on poster sessions over oral presentations, the scientific side visit, the roundtable discussions, and the technology demonstrations.

SURFACE WATER DYNAMICS AND QUALITY, INCLUDING THE UNSATURATED ZONE AND ARTIFICIAL RECHARGE

One highlight of this theme was a case study on a large wetlands area in Spain. Another was the large number of posters that described a wide range of water flow and water quality studies involving rivers, streams, lakes, artificial impoundments, and the role of the unsaturated zone. The number of posters on nitrate contamination was substantial, and this is an area where compound specific isotope analyses can be very important. Other studies demonstrated usefulness of isotope methods for quantifying artificial recharge through dams and enhanced bank infiltration.

SURFACE WATER-GROUNDWATER INTERACTIONS

A scientific side event on the River Danube was held mid-conference. The visit involved a boat trip from Melk to Vienna, and participants learned about the importance of surface water-groundwater interactions while on the river. Two keynote presentations were made on the boat and demonstrated the critical value of isotope methods in rivers and catchment studies, and the role of such data for development of conceptual and predictive models that integrate

both surface water and groundwater aspects. In addition, various rivers and aquifers interactions were discussed during the poster sessions.

GROUNDWATER DYNAMICS AND QUALITY

Two invited presentations showed how diverse isotope applications can be for addressing important issues involving groundwater dynamics. One presentation described the application of isotopes and geochemistry to carbon sequestration in brine aquifers. This work was also described in an article on the IAEA web page the week before the symposium. The second presentation showed how isotopes can be used to understand groundwater flow in systems with clay aquitards. These systems can isolate aquifers for long periods of time, making them potentially attractive for hazardous or radioactive waste disposal. Case studies described isotopes and aquifer hydraulic data that can be integrated to understand groundwater flow in Uganda, use of nitrogen isotopes to understand the origin of nitrate pollution in groundwaters of Côte d'Ivoire, and how isotopes and hydrogeochemical methods can be used to quantify groundwater dynamics in coastal sedimentary aquifers in India. Posters described many examples of application of isotopes used to understand groundwater flow and pollution problems.

GROUNDWATER SUSTAINABILITY, INCLUDING GEOTHERMAL SYSTEMS

Many of the posters presented focused on sustainability issues, showing the significance of this problem across the world. The highlights of this theme included an invited presentation on the Nubian aquifer in Africa, which described how isotopes are being used to characterize this large, complex, and important transboundary aquifer system. In addition, case studies described isotope studies of groundwater sustainability issues in semiarid/arid areas in China and Mexico. There were many posters on the application of isotopes in geothermal systems.

ANALYTICAL DEVELOPMENTS AND SAMPLING METHODS

New analysis and sampling methods help increase the breadth of isotope applications for water cycle problems, and in some cases make it easier to apply and use isotopes for applied problems and research. Highlights of this

theme include invited presentations on compound specific isotope analyses for understanding contaminant degradation and advanced laser methods for water cycle studies. Demonstrations of new laser analysis instrumentation for water samples and an automated precipitation/water sampling device for isotope studies were also highlights of this theme and drew a great deal of interest from participants. Several posters also presented innovative analysis or sampling methods for both stable isotopes and radioisotopes.

LAND-ATMOSPHERE AND GROUNDWATER-MARINE CONNECTIONS

The highlights of this session included an invited presentation of how radioisotopes can be used to quantify submarine groundwater discharge and how important this process is in many coastal areas. A second invited presentation described how isotopes are critical for understanding land-atmosphere interactions in the water, carbon, and oxygen cycles and that there is still much work to do in this area. Two case study lectures reinforced the importance of these connectivity issues. One case study presentation described the links between groundwater and coastal wetlands in Brazil and the factors that are impacting this important ecosystem. The other case study described how isotopes can be used to understand the relation between precipitation and atmospheric circulation patterns in Turkey.

ROUNDTABLE SESSIONS

The roundtable sessions were held to provide open forums for conference participants to discuss key issues related to the application of isotope methods. They were used as a way of identifying research needs and priority application areas, and to hear about isotopes application issues in developing countries. The roundtable outcomes will help the IAEA understand how best to align programmatic efforts and resources for future needs. One roundtable focused on the use of isotopes in developing countries, while the other focused on general issues involving the application of isotope techniques. Three of the main conclusions of the developing country roundtable were:

- The IAEA continues to play a critical role in promoting and facilitating the use of isotope methods in developing countries, and is helping to address important water issues. It can play an even stronger role, for

example, by increasing integrated isotope–geochemistry–basic hydrology training options with other UN organizations.

- The development of new isotope tools and approaches which can be more easily applied under the challenging circumstances in developing countries should be continued. The increasing need for developing countries to address contaminant and climate change issues requires new and/or easier to implement isotope methods.
- Isotope laboratories are difficult to operate, and maintaining analytical quality can be a problem in small laboratories in some developing countries. Isotope laboratories should not be established indiscriminately in developing countries. A focus on a few regional laboratories would enable those laboratories to have enough economy of scale for routine operation and to provide quality analyses. New ‘simpler’ technologies, such as laser machines, can also make it easier for countries to maintain isotope capabilities and adequate analytical quality.

The main conclusions of the roundtable on general isotope issues were as follows:

- There is a clear need for the increased use of isotopes in numerical modelling studies which is being driven by new regulations such as the European Union water framework. International organizations and research agencies should increase their focus on the integration of isotopes and modelling.
- The IAEA/WMO global network of isotopes in precipitation (GNIP) is more important than ever, not only because of groundwater/surface water applications, but also for understanding the role of the water cycle in climate and atmospheric processes, ecology and other disciplines. Moisture isotopes in the biosphere and atmosphere (MIBA) and global network of isotopes in rivers are also important, but because they are in the development stage, their impact is not currently as large.
- As a community, we need to identify problems where isotopes can have large impacts, and focus efforts on those problems. This focus includes doing more work to understand linkages and coupled processes. To this end, we need to encourage more collaborative research and interactions at meetings between isotope hydrologists and those working in fields such as ecohydrology, carbon and oxygen cycling, and the climate

ORAL PRESENTATIONS

INVITED SPEAKERS

COMPOUND SPECIFIC STABLE ISOTOPE ANALYSIS: RESEARCH FRONTIERS IN ISOTOPE HYDROLOGY AND WATER RESOURCES MANAGEMENT

B. SHERWOOD LOLLAR*, M.C.G. CHARTRAND*,
S.M. HIRSCHORN*, M. HOWLETT*, T.F. BIDLEMAN**,
L.M. JANTUNEN**, S. MANCINI*, J. MCKELVIE*,
G. LACRAMPE-COULOUME*, E.A. EDWARDS*

*Department of Geology,
University of Toronto,
Toronto, Ontario

**Centre for Atmosphere Research Experiments,
Environment Canada

Canada

Abstract

Compound Specific Isotope Analysis (CSIA) — the characterization of stable isotope compositions of individual contaminant compounds dissolved in groundwater, sparked a revolution in the interface between isotope geochemistry and contaminant hydrogeology. Stable isotope fingerprints can provide diagnostic tools to identify and differentiate sources of contamination. Furthermore CSIA rapidly proved a novel method for investigation of both abiotic and biotic remediation potential at contaminated sites. Several novel developments in CSIA are directly relevant to moving applications of this field from point source contamination to larger regional watershed and ground water resource management applications. The limits of sensitivity and detection limit are being pushed back to facilitate the application of CSIA to low concentrations of contaminants in more diffuse sources. Multi-isotope approaches such as incorporation of both carbon and hydrogen isotope signatures, which to date have been used primarily for non-chlorinated hydrocarbons, are now being extended to investigation of chlorinated hydrocarbon compounds. Improved detection limits and chromatography are facilitating applications of CSIA to new classes of compounds including pesticides, and chlorinated aromatics, where the presence of many isomers presents both an analytical challenge and a challenge for identifying promising lines of evidence for biodegradation.

1. INTRODUCTION

The past decade has witnessed a revolution in the application of stable isotope analysis to environmental contamination in soils and groundwaters. Compound specific isotope analysis provides a wide range of analytical advantages — one of the major being the ability to measure stable isotope signatures on individual compounds in a complex mixture at environmentally realistic concentrations ($\mu\text{g/L}$ to mg/L). To date, environmental applications in the laboratory and field have focused primarily on alkanes, petroleum hydrocarbons, fuel additives and chlorinated solvents. Recent technical advances and refinement of analytical procedures are opening new directions in terms of both applications of CSIA to new groups of contaminants, and multi-isotope applications of CSIA (i.e. incorporation of hydrogen and chlorine isotope analysis as well as carbon).

2. RECENT TECHNICAL ADVANCES AND ANALYTICAL DEVELOPMENTS

Applications of stable carbon isotope analysis by continuous flow CSIA to environmental geochemistry and contaminant hydrogeology have more recently been followed by compound specific isotope analysis of additional isotopic signatures — in particular hydrogen isotope analysis [1–8], and to a lesser extent, chlorine isotope analysis [9–11]; nitrogen isotope analysis [12–13]; and oxygen isotope analysis [14]. Complementary efforts to improve method detection limits [2, 15–17] and to establish standard procedures for analytical practices such as assessment of total uncertainty [17–19] have been an important step in standardizing QA/QC (quality assurance/quality control). These analytical developments, as well as the expanding interest not simply in point source contamination but in diffuse sources at the catchment and watershed scale are driving further developments in this research area to explore applications of CSIA to a wider range of contaminants of interest including POPs, PAHs, chlorinated aromatics, pesticides, agrochemicals and pharmaceuticals.

Of the multi-use isotope approaches, the most widespread to date has been integration of $\delta^{13}\text{C}$ and $\delta^2\text{H}$ values [1–8, 20]. Applications of continuous flow compound specific $\delta^2\text{H}$ analysis to chlorinated compounds however were delayed due to degradation of analytical performance and instrument deterioration related to the formation of HCL as a by-product of pyrolysis of chlorinated compounds. Recently Chartrand et al. (2007) Ref. [21] developed an HCL trapping system to resolve this problem and demonstrated that accurate

COMPOUND SPECIFIC STABLE ISOTOPE ANALYSIS

and reproducible compound specific $\delta^2\text{H}$ analysis of chlorinated hydrocarbons is feasible as a complement to the existing routine CF-CSIA techniques for carbon isotope analysis.

3. MULTI-ISOTOPE (C AND H) APPROACHES APPLIED TO CHLORINATED HYDROCARBONS

3.1. Source differentiation

The use of CSIA as a tool to differentiate between contaminant sources in the field is dependant on the contaminants having distinct isotope values when they enter the environment, and on other mass-dispersal processes such as dissolution, volatilization and sorption not significantly changing the isotope values of the contaminant. For chlorinated hydrocarbons ($\delta^{13}\text{C}$) and BTEX ($\delta^{13}\text{C}$ and $\delta^2\text{H}$) compounds, dissolution, volatilization and sorption processes are typically small to negligible within the analytical uncertainty associated $\delta^{13}\text{C}$

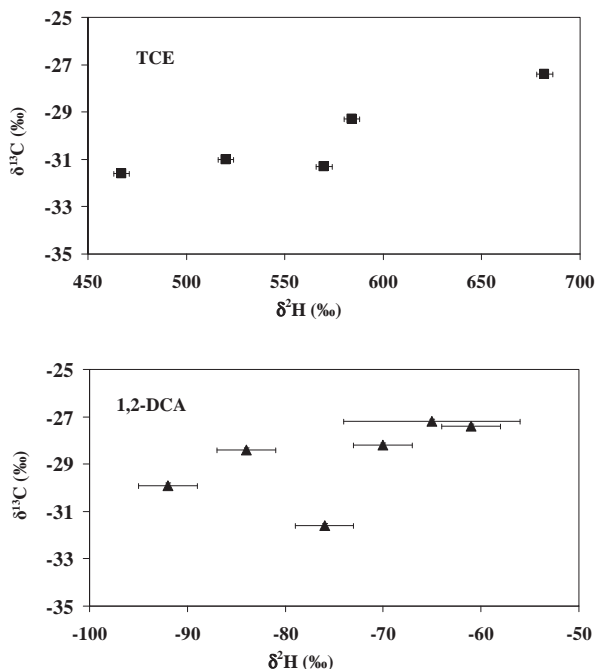


FIG. 1. Carbon and hydrogen isotope signatures for pure phase product from different manufacturers. A) TCE data after Shouakar-Stash et al. (2003) Ref. [26] (B) 1,2-DCA data after Chartrand et al. (2007) Ref. [21].

with CSIA [22–25]. In the absence of significant degradation of contaminants by abiotic or biotic processes, stable isotope signatures may remain relatively conservative and provide a means to identify and delineate different sources of contamination. Given that the range in $\delta^{13}\text{C}$ values for chlorinated solvents typically reflects the range in the petroleum feedstocks used to produce these materials (-35‰ to -25‰), $\delta^{13}\text{C}$ signatures alone can be insufficient to resolve different sources. Shouakar-Stash et al. (2003) Ref. [26] showed that incorporating $\delta^2\text{H}$ isotope values in addition $\delta^{13}\text{C}$ values can provide more ability to source differentiate based on $\delta^2\text{H}$ values for pure phase TCE between $+466.9$ and $+681.9 \text{‰}$, and $\delta^2\text{H}$ values for TCA between $+22.2$ and -23.1‰ for TCE and TCA obtained from different manufacturers (Figure 1A). Figure 1B demonstrates that not all chlorinated hydrocarbons show such a large range of $\delta^2\text{H}$ values, and in particular, not all chlorinated solvents have $\delta^2\text{H}$ values in the enriched range, but that nonetheless incorporation of both $\delta^2\text{H}$ and $\delta^{13}\text{C}$ isotope values can be critical to identifying product from different sources.

3.2. Delineation of mechanisms of microbial transformation and implications for quantification of biodegradation

Several studies have demonstrated that incorporation of $\delta^2\text{H}$ isotopic measurements are an important parameter for delineation of mechanisms of contaminant transformation as well [3, 7, 8, 20, 27]. Hirschorn et al. (2004) Ref. [27] suggested that for a compound such as 1,2-DCA, known to biodegrade via two different pathways under aerobic conditions, CSIA analysis of $\delta^2\text{H}$ values may be critical to both identification of the biotransformation pathway and to any attempt to quantify the extent of biodegradation. Biodegradation of 1,2-DCA under aerobic conditions can occur by two initial enzymatic reaction pathways: hydrolytic dehalogenation to form 2-chloroethanol, which results in large carbon isotopic fractionation (enrichment factor (ϵ) = -29‰), and oxidation to form 1,2-dichloroethanol, which results in small carbon isotopic fractionation (ϵ = -4‰) [27]. In both cases, as shown for the experimental data in Figure 2, the carbon isotope fractionation follows a Rayleigh degradation model as has been demonstrated for biodegradation of many organic contaminants. Using the Rayleigh model, governed by the equation:

$$((\delta^{13}\text{C}_w/1000)+1) = ((\delta^{13}\text{C}_0/1000)+1)f^{(a-1)} \quad (1)$$

by measuring the carbon isotope value of 1,2-DCA in a downgradient well for instance ($\delta^{13}\text{C}_w$), and comparing it to the carbon isotope value of 1,2-DCA in a well in the source zone ($\delta^{13}\text{C}_0$), the extent of biodegradation between the source

COMPOUND SPECIFIC STABLE ISOTOPE ANALYSIS

zone and downgradient plume (1-f) can be estimated if the fractionation factor (α) is known, where:

$$\epsilon = 1000(\alpha - 1) \quad (2)$$

As illustrated in Figure 2, if, for example, an enrichment trend in $\delta^{13}\text{C}$ values of 7‰ were observed (e.g. a shift from -27‰ to -20‰) in 1,2-DCA at a field site, this could be attributed to 18% 1,2-DCA biodegradation via a hydrolytic dehalogenation pathway ($\epsilon = -29\text{‰}$), or alternatively, 90 % 1,2-DCA biodegradation via an oxidation pathway ($\epsilon = -4\text{‰}$). Chartrand et al. (2007) Ref. [21] describes a trapping technique that facilitates routine $\delta^2\text{H}$ analysis of chlorinated hydrocarbons and provides a means to determine which degradation mechanism is occurring by differentiation between the hydrolytic dehalogenase pathway (characterized by a small secondary $\delta^2\text{H}$ fractionation and large $\delta^{13}\text{C}$ fractionation) and the oxidation pathway (characterized by a large primary $\delta^2\text{H}$ fractionation and small $\delta^{13}\text{C}$ fractionation).

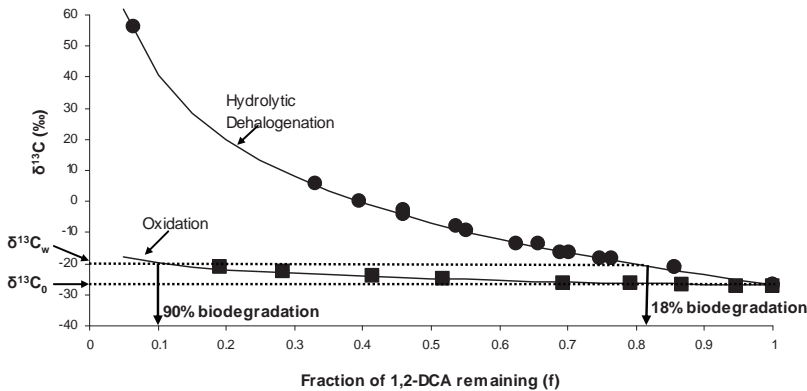


FIG. 2. Measured carbon isotope fractionation for 1,2-DCA during biodegradation via oxidation (squares) or via hydrolytic dehalogenation (circles) modified after Hirschorn et al. (2004) Ref. [27]. The solid curves represent the Rayleigh model through the measured data based on $\epsilon = -4$ ‰ (oxidation) and $\epsilon = -29$ ‰ (hydrolytic dehalogenation). For a hypothetical field site at which the source well contained 1,2-DCA with a $\delta^{13}\text{C}_0$ value of -27‰ and 1,2-DCA in a downgradient well had a $\delta^{13}\text{C}_w$ value of -20‰ , two estimates of the extent of biodegradation responsible for this isotopic enrichment can be calculated (see text) if the appropriate pathway is not known.

ACKNOWLEDGEMENTS

Financial support was provided by National Sciences and Engineering Research Council (NSERC) Strategic Grants program, Water Earth and Sciences Ltd., and an NSERC scholarship to MMGC. Helpful discussions with A. Hilker and G. Slater are gratefully acknowledged.

REFERENCES

- [1] WARD, J.A.M., et al., Hydrogen isotope fractionation during methanogenic degradation of toluene: Potential for direct verification of bioremediation, *ES&T* **34** (2000) 4577–4581.
- [2] HUNKELER, D., et al., Hydrogen and carbon isotope fractionation during aerobic biodegradation of benzene, *ES&T* **35** (2001) 3462–3467.
- [3] MORASCH, B., et al., Stable hydrogen and carbon isotope fractionation during microbial toluene degradation: Mechanistic and environmental aspects, *AEM* **67** (2001) 4842–4849.
- [4] GRAY, J.R., et al., Carbon and hydrogen isotopic fractionation during biodegradation of methyl tert-butyl ether, *ES&T* **36** (2002) 1931–1938.
- [5] MANCINI, S.A., et al., Hydrogen isotopic enrichment: An indicator of biodegradation at a petroleum hydrocarbon contaminated field site, *ES&T* **36** (2002) 2464–2470.
- [6] STEINBACH, A.R., et al., Hydrogen and carbon isotope fractionation during anaerobic biodegradation of aromatic hydrocarbons — A field study, *ES&T* **38** (2004) 609–616.
- [7] KUDER, T. et al., Enrichment of stable carbon and hydrogen isotopes during anaerobic biodegradation of MTBE: Microcosm and field evidence, *ES&T* **39** (2005) 213–220.
- [8] ZWANK, L. et al., New evaluation scheme for two-dimensional isotope analysis to decipher biodegradation processes: Application to groundwater contamination by MTBE, *ES&T* **39** (2005) 1018–1029.
- [9] HOLMSTRAND, H., et al., Chlorine isotope fractionation of a semi-volatile organochlorine compound during preparative megabore-column capillary gas chromatography, *J. Chromatog.* **1103** (2006) 133–138.
- [10] SHOUAKAR-STASH, O., et al., Compound specific chlorine isotope ratios of TCE, PCE and DCE isomers by direct injection using CF-IRMS, *Applied Geochem.* **21** (2006) 766–781.
- [11] VAN ACKER, M.R.D., et al., GC/Multiple collector-ICPMS method for chlorine stable isotope analysis of chlorinated aliphatic hydrocarbons, *Anal. Chem.* **78** (2006) 4663–4667.

COMPOUND SPECIFIC STABLE ISOTOPE ANALYSIS

- [12] HARTENBACH, A., et al., Using nitrogen isotope fractionation to assess abiotic reduction of nitroaromatic compounds, *ES&T* **40** (2006) 7710–7716.
- [13] BERG, M. et al., Compound specific nitrogen and carbon isotope analysis of nitroaromatic compounds in aqueous samples using solid-phase microextraction coupled to GC/IRMS, *Anal. Chem.* **79** (2007) 2386–2393.
- [14] STURCHIO, N.C., et al., Oxygen and chlorine isotope fractionation during perchlorate biodegradation: Laboratory results and implications for forensics and natural attenuation studies, *ES&T* (2007) in press.
- [15] ZWANK, L., et al., Compound specific carbon isotope analysis of volatile organic compounds in the low-microgram per liter range, *Anal. Chem.* **75** (2003) 5575–5583.
- [16] MORRILL, P.L., et al., Dynamic headspace: a single-step extraction for isotopic analysis of µg/L concentrations of dissolved chlorinated ethenes, *Rapid Comm. Mass. Spec.* **18** (2004) 595–600.
- [17] JOCHMANN, M.A., et al., A new approach to determine method detection limits for compound specific isotope analysis of volatile organic compounds, *Rapid Comm. Mass. Spec.* **20** (2006) 3639–3648.
- [18] ZWANK, L. Assessment of the fate of organic groundwater contaminants using their isotope signatures, PhD thesis, Swiss federal Institute of Technology (ETH), Zurich, CH (2004).
- [19] SHERWOOD LOLLAR, B., et al., An approach for assessing total instrumental uncertainty in compound specific carbon isotope analysis: Implications for environmental remediation studies, *Anal. Chem.* (2007) in press. Web release date 29-Mar-2007; article DOI:10.1021/ac062299v.
- [20] MANCINI, S.A., et al., Carbon and hydrogen isotope fractionation of benzene during anaerobic biodegradation of benzene, *AEM* **69** (2003) 191–198.
- [21] CHARTRAND, M.M.G., et al., Compound specific hydrogen isotope analysis of 1,2-dichloroethane: Potential for delineating source and fate of chlorinated hydrocarbon contaminants in groundwater, *Rapid Comm. Mass. Spec.* (2007) in press.
- [22] HUANG, L., et al., Carbon and chlorine isotope fractionation of chlorinated aliphatic hydrocarbons by evaporation, *Organic Geochem.* **30** (1999) 777–785.
- [23] POULSON, S.R., DREVER, J.I., Stable isotope (C, Cl and H) fractionation during vapourization of trichloroethylene, *ES&T* **33** (1999) 3689–3694.
- [24] SLATER, G.F., et al., Carbon isotope effects resulting from equilibrium sorption of dissolved VOCs, *Anal. Chem.* **72** (2000) 5669–5672.

**APPLICATION OF STABLE ISOTOPES AND
FLUID CHEMISTRY TO UNDERSTANDING
ANTHROPOGENIC CO₂-BRINE-ROCK
INTERACTIONS IN SEDIMENTARY BASINS:
RESULTS FROM THE FRIO BRINE PILOT TESTS,
TEXAS, USA**

Y.K. KHARAKA*, D.R. COLE**, J.J. THORSEN*,
E. KAKOUIROS*

*U. S. Geological Survey,
Menlo Park, CA

**Oak Ridge National Laboratory,
Oak Ridge, TN

USA

Abstract

To investigate the potential for the long-term storage of CO₂ in deep saline aquifers in sedimentary basins, 1600 t of CO₂ were injected at 1500 m depth into a 24-m-thick “C” sandstone section of the Frio Formation, a regional aquifer in the U.S. Gulf Coast. Stable isotopes of water, gases and solutes proved powerful tools in mapping the distribution, transport and interactions of the injected CO₂, and in tracking its leakage into the local shallow groundwater, and into the overlying Frio “B” sandstone, separated from the “C” by ~15 m of shale and siltstone. Fluid samples obtained from the “C” before CO₂ injection showed a Na-Ca-Cl type brine with ~93,000 mg/L TDS at saturation with CH₄, but only 0.3% CO₂. Following CO₂ breakthrough, samples showed sharp drops in pH, pronounced increases in alkalinity, Ca, Fe and Mn, and significant shifts in the isotopic compositions of H₂O, CH₄, DIC, and Sr. Gas and isotopic signatures coupled with perfluorocarbon tracers demonstrated significant CO₂ migration into the “B” sandstone. Results obtained to date from four shallow monitoring groundwater wells show no brine or CO₂ leakage through the Anahuac Formation, the regional cap rock. The δ¹⁸O values for brine and DIC, used to calculate brine/CO₂ ratios in the reservoir, gave results comparable to those obtained by geophysical methods.

1. INTRODUCTION

Global warming and the resulting climate change are arguably the most important environmental challenges facing the world in this century [1]. In 2006, global average temperature was about 0.7°C higher than during pre-industrial times, and model calculations show the temperature difference increasing to 2–6°C by year 2100 [2]. There is now a broad scientific consensus that global warming results primarily from increased concentrations of atmospheric greenhouse gases (GHG), especially CO₂ emitted largely from the burning of fossil fuels, petroleum and coal [3]. The amount of CO₂ annually added to the atmosphere in 2003 was 25 Gt of CO₂, and estimates by Energy Information Administration [4] show this increasing to 44 Gt in 2030. Increased anthropogenic emissions of CO₂ have raised its atmospheric concentrations from about 280 ppmv during pre-industrial times to about 380 ppm today. Based on several defined scenarios, atmospheric CO₂ concentrations were projected by Intergovernmental Panel on Climate Change (IPCC) to increase to up to 1,100 ppmv at year 2100 [5]. Carbon sequestration, in addition to energy conservation and increased use of lower carbon intensity fuels, is now considered necessary to stabilize atmospheric levels of GHG and global temperatures at values that would not severely impact global economic growth [1]. Sedimentary basins in general and deep saline aquifers in particular, are being investigated as possible repositories for large amounts of anthropogenic CO₂ that must be sequestered to stabilize atmospheric CO₂ concentrations [6–8]. These basins are attractive for CO₂ storage, because they have huge potential capacity, estimated at 350–11,000 Gt of CO₂ worldwide, and are located close to major CO₂ sources [9, 10].

In geologic sequestration, CO₂ captured from fossil fuel-fired power plants and other sources may be stored in:

- (1) structural traps such as depleted petroleum reservoirs, primarily as supercritical immiscible fluid (hydrodynamic trapping);
- (2) saline formation water as H₂CO₃^o, HCO₃⁻ and other dissolved C-species (solution trapping); and/or
- (3) carbonate minerals, including calcite, magnesite, siderite, and/or ankerite (mineral trapping) [11,12].

Initially, the bulk of injected CO₂ will be stored as supercritical fluid because the target reservoirs are likely to have temperatures and pressures higher than 31°C and 74 bar, the critical values for CO₂. The injected CO₂ will rapidly dissolve in formation water that contacts the fluid, in contrast to mineral trapping, which would be a slower, yet more permanent storage mechanism, dependent on the availability of reactive Ca, Mg and Fe [12,13]. In addition to storage capacity, key environmental questions include CO₂ leakage related to

the storage integrity and the physical and chemical processes that are initiated by injecting CO₂ underground [14–16].

The injected supercritical CO₂ likely will have a density of 0.6–0.8 g/mL, which makes it a buoyant fluid with a potential for upward migration and leakage that would negate some of the benefits of sequestration [17] and introduce elements of risk. The main risks from this CO₂ leakage, as well as from the large volumes of brine that would be displaced by the injected CO₂, are related to atmospheric release, groundwater contamination and induced seismicity [1]. Based on analogous experience in CO₂ injection technologies such as acid gas disposal and enhanced oil recovery, these risks appear to be minor and less than those of current oil and gas operations [10].

In this summary, we discuss geochemical results from Frio-I, a US DOE funded multi-laboratory field experiment to investigate the potential for geologic storage of CO₂ in saline aquifers. We emphasize the applications of water, solute and gas isotopes [18] and chemistry to understanding temporal changes in fluid compositions in the injection member, the Frio “C”, and deep monitoring of fluid leakage from “C” into the overlying “B” sandstone. Data obtained for deep monitoring above the injection zone proved more conclusive than shallow monitoring results obtained from four groundwater wells and soil gases sampled in four 1.5 m deep boreholes in the vadose zone and by capillary absorption tubes placed in 40, 0.3–1 m-deep, tubular aluminum installations [8].

2. REGIONAL SETTING AND METHODOLOGY

The Frio site is located within the South Liberty oil field, near Dayton, Texas, a region of the Gulf Coast where industrial sources of CO₂ are abundant. Wells in this field were drilled in the 1950s, with production from the Eocene Yegua Formation at depths of ~2900 m. An inactive oil well was recompleted and perforated in the Frio “C” sandstone at 1,528–1,534 m for use as an observation borehole. About 30 m down-dip, a new CO₂ injection well was drilled and perforated also in Frio “C” at 1,541–1,546 m. The Frio Formation has a dip of 16° to the south, and comprises several reworked fluvial sandstone and siltstone beds that are separated by transgressive marine shale. The Frio “C” injection zone is a subarkosic, fine-grained, moderately sorted quartz and feldspar sandstone, with minor amounts of illite/smectite and calcite. The zone has high mean porosity of 32% and permeability of 2–3 Darcies. Situated above the “C”, the “B” sandstone has a ~4 m thick reworked fluvial sandstone bed at the top, but is separated from “C” by ~15 m of shale, muddy sandstone and siltstone beds (Fig. 1). However, the main barrier to CO₂ leakage to surface is

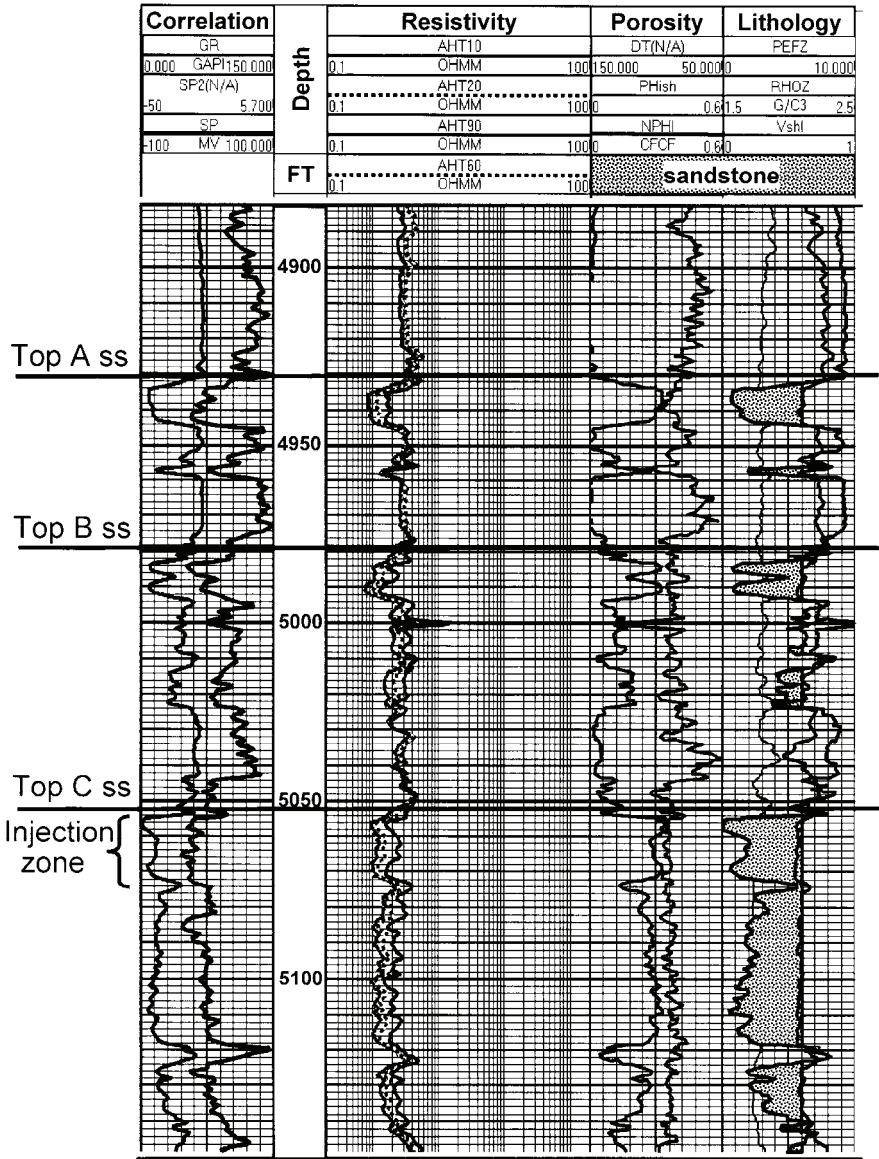


FIG. 1. Open-hole logs of the injection well. Note the relatively thick beds of shale and siltstone between Frio “C”, the injection zone and Frio “B”, used for subsurface monitoring of the injected CO₂.

expected to be the overlying regional thick marine shale beds of the Miocene-Oligocene Anahuac Formation [8].

Approximately 1,600 t of CO₂ were injected during October 4–14, 2004. More than 60 samples of water and gas were obtained from the “C” sandstone of both wells before, during and following CO₂ injection, using a variety of tools and methodologies [19], including the novel downhole U-tube system developed for this field experiment [20]. Surface and downhole fluid samples were also obtained (April 4–6, 2005) from the Frio “B” of the observation well, which was perforated (1506.0–1508.5 m) after cementing the earlier “C” perforations. Samples were collected after >300 bbl of brine were produced, and values of EC, pH, and alkalinity became constant, and concentrations of Rhodamine WT, the tracer used to tag the drilling fluids, were below background value of ~1 µg/L. To completely prevent any CO₂ leakage from “C” to “B” through the well casing, a plug was inserted between them before the final and more intensive fluid sampling carried out on January 23–27, 2006. Again sampling was not initiated until values of EC, pH, and alkalinity became constant, and concentrations of Rhodamine WT reached background values, which occurred after ~200 bbl of brine were produced.

3. RESULTS AND DISCUSSION

Chemical analysis of formation water and gas samples obtained from both wells prior to CO₂ injection show that the Frio brine is a Na-Ca-Cl type water, with a salinity of 93,000 ± 3,000 mg/L TDS. The brine also has relatively high concentrations of Mg and Ba, but low values for SO₄, HCO₃, DOC and organic acid anions [19]. The high salinity and the low Br/Cl ratio (0.0013) relative to sea water indicate dissolution of halite from the nearby salt dome (e.g., [21]). Careful measurements of the volumes of water and evolved gas obtained with downhole samplers show the Frio brine to have 40–45 mM/L dissolved CH₄, which is close to saturation at reservoir conditions (65°C and 150 bar). Gas analysis show that CH₄ comprises 95 ± 3% of total gas, but the dissolved CO₂ content of the gas is low at ~0.3% (Table 1).

During the CO₂ injection, October 4–14, 2004, more than 40 water samples were collected from the observation well using the U-tube system, and results from on-site measurements of electrical conductance (EC), pH and alkalinity are discussed in [19]. The EC exhibited only subtle increase from a pre-injection value of ~120 mS/cm (at ~22°C), whereas there were major changes in some chemical parameters as the CO₂ reached the observation well, including a sharp drop in pH (from 6.5 to 5.7) and high increases in alkalinity (from 100 to 3,000 mg/L as bicarbonate). Additionally, laboratory determinations showed

TABLE 1. COMPOSITION OF GASES (MOLE %) FROM FRIO “C” AND “B” SANDSTONES. NOTE THE RELATIVELY HIGH CO₂ IN “B”

Gas	“C” ¹	“C” ²	“B” ³	“B” ⁴
He	0.008	0	0.01	0.011
H ₂	0.040	0.19	0.92	0.012
Ar	0.041	0	0.13	0.010
CO ₂	0.31	96.8	2.86	0.28
N ₂	3.87	0.037	1.51	1.12
CH ₄	93.7	2.94	94.3	98.3
C ₂ H ₆ +	1.95	0.005	0.12	0.11

¹ background from injection well, before CO₂ injection.

² from observation well after CO₂ breakthrough.

³ from observation well ~ 6 mo after injection.

⁴ from the observation well ~ 15 mo after injection.

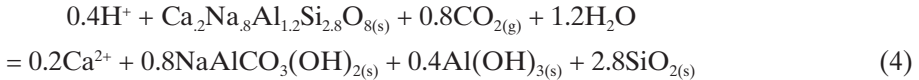
major increases in dissolved Fe (from 30 to 1,100 mg/L) and Mn, and significant increases in the concentration of Ca. The most dramatic changes in chemistry occurred at CO₂ breakthrough 51 hours after injection (Fig. 2), as evidenced also by on-site analysis of gas samples from the U-tube system that showed CO₂ concentrations increasing from 0.3 to 3.6% of total gas [20]. The CO₂ content of gas measured on site and in laboratory then quickly increased, reaching values of up to ~97% of total gas, with CH₄ comprising the bulk of the remaining 3% (Table 1). Significant shifts were also observed in the isotopic compositions of H₂O, DIC and CH₄ following CO₂ injection.

Results of geochemical modeling, using updated SOLMINEQ [22] indicate that the Frio formation water in contact with the supercritical CO₂ would have a pH of ~3 at subsurface conditions. This low pH causes the brine to become highly undersaturated with respect to carbonate, aluminosilicate and other minerals in the Frio (Fig. 3 in [19]). Because mineral dissolution rates are generally higher by one or more orders of magnitude at such low pH values [23], the observed increases in concentrations of Ca and equivalent concentration of HCO₃ likely result from the rapid dissolution of calcite, as depicted in reaction (1).



Maintaining reservoir integrity that prevents the ultimate escape of CO₂ back to the atmosphere by limiting its leakage to extremely low levels is essential to the success of injection operations [15]. Preventing brine and CO₂ leakage into overlying drinking water supplies is also important, because toxic organic and inorganic components are mobilized by the injected gas, in addition to the chemicals present in the pristine brine [19].

Results of chemical analysis of samples collected ~20 days, 6 and 15 months after CO₂ injection demonstrate decreases in the concentrations of Fe, Mn (Fig. 3), HCO₃ and Ca, and increases in pH. Geochemical modeling indicates that the brine pH increases from dissolution of carbonate and iron oxyhydroxide minerals discussed above, as well as from dissolution of oligoclase and other aluminosilicate minerals present in the Frio. Aluminosilicate mineral dissolution generally is not congruent, but likely follows an incongruent reaction (4), where dawsonite, gibbsite and amorphous silica are precipitated, and/or where kaolinite and amorphous silica are precipitated [1,16].



As the pH increases from mineral interactions and the mixing of CO₂-saturated and pristine brines, modeling indicates that mineral saturations reverse the trend discussed above, resulting in precipitation of carbonate and other minerals. The overall result is the brine gradually evolves toward its pre-injection composition, but additional modeling is planned to further investigate gas-water-rock interactions in such a system based on results from Frio II test.

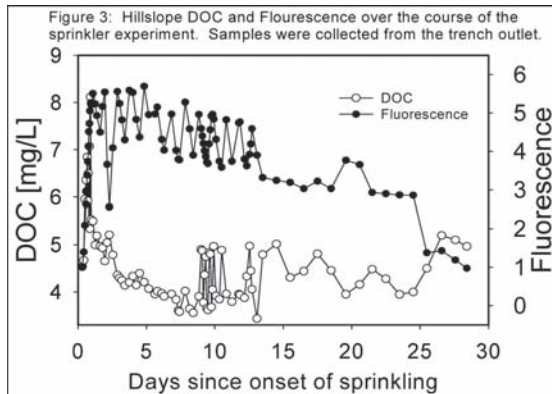


FIG. 3. Concentrations of Fe and Mn in Frio-I brine from June, 2004 to January, 2006. Note the sharp increases in metal content during October 6, 2004, at the time of CO₂ breakthrough, and slightly higher Fe and Mn in "B" samples from April, 2005.

3.1. Isotopic composition of water and gases

We observed significant shifts in the isotopic compositions of H₂O and DIC following CO₂ injection, but only subtle changes in the δD and δ¹³C values of CH₄. The δ¹³C values of DIC became profoundly lighter, shifting from -3 to -33 ‰, reflecting the fact that the injected CO₂ is the dominant C source and is depleted, with v¹³C = -34 to -44‰, depending on the mixing proportions of the two gas sources. The δ¹⁸O values of brine became isotopically lighter with time, shifting from 0.80 to -11.1‰, and there was a corresponding increase in the δ¹⁸O values of CO₂, from 9 to 43‰. Because water and CO₂ rapidly exchange oxygen isotopes even at low temperature, it is possible to use their δ¹⁸O values in mass balance equations to estimate the brine to CO₂ mass and volume ratios in the reservoir. The equation for a closed system and no isotopic exchange with minerals is given [26] by:

$$X_{\text{brine}}/X_{\text{CO}_2} = \frac{\delta^{18}\text{O}_{\text{CO}_2}^f - \delta^{18}\text{O}_{\text{CO}_2}^i}{\delta^{18}\text{O}_{\text{H}_2\text{O}}^i - \delta^{18}\text{O}_{\text{H}_2\text{O}}^f} \quad (5)$$

TABLE 2. CALCULATED BRINE/CO₂ VOLUME RATIOS IN THE FRIO FORMATION FOLLOWING CO₂ INJECTION BASED ON THE δ¹⁸O VALUES FOR BRINE AND CO₂.

Date	¹⁸ O shift	¹⁸ O shift	Brine/CO ₂ vol. ratio*
	Brine	CO ₂	
10-5-2004	0	0	∞
10-6-2004	0.37	32	43
10-6-2004	0.69	32	23
10-6-2004	0.77	32	21
10-6-2004	1.22	32	13
10-7-2004	2.24	32	7.1
11-3-2004	1.43	32	11
11-3-2004	1.74	32	9.1
4-4-2005	11.2	22	0.97
5-4-2005	11.7	22	0.93
6-4-2005	11.9	22	0.92

*To convert from mole oxygen basis (eq. 5) to brine/CO₂ volume ratio at reservoir conditions, we multiply by 0.495, using a density (gm/cc) of CO₂ = 0.60 and brine = 1.06.

where the superscripts “i” and “f” are the initial and final δ values for brine and CO_2 , respectively, and X is the atomic oxygen fraction in the subscripted component.

Results from the observation well (Table 2) show that initially the system is brine dominated, with CO_2 comprising ~10% of the fluid at reservoir conditions from one day after the CO_2 breakthrough on October 7, 2004 through November 3, 2004. However, samples collected from the injection well on April 4–6, 2005 yield a value of ~50% for the volume of CO_2 at reservoir conditions. The initial brine dominated system could indicate that the injected CO_2 acts like a piston pushing the pore water out with minimal mixing and isotopic exchange. Contact and isotopic equilibration with a larger volume of injected CO_2 is indicated from data of April, 2005. These results are comparable to ‘residual’ CO_2 -saturation values obtained with the reservoir saturation (RST) and other geophysical tools [8], indicating the usefulness of this isotopic approach.

3.2. Subsurface monitoring

Monitoring at and in close proximity to the surface for CO_2 leakage signal in soil gas was not effective primarily because of the induced perturbation as a result of injection operations. Significant amounts of CO_2 were released to the atmosphere during injection operations, and venting of CO_2 with PFT and other tracer gases during the purge cycle of the U-tube sampling system, released tracer to the atmosphere and the soils around the wells. Monitoring results obtained from the four shallow groundwater wells showed rapid chemical changes during the monitoring period, with a preinjection region of high salinity water migrating down-gradient across the monitoring array. Groundwater monitoring is continuing, but the observed chemical changes are tentatively attributed to the extraction of large amounts of groundwater for drilling and other field operations and to the construction of a large fresh-water mud disposal pit [8].

Because of the anticipated difficulty of near surface monitoring, we planned a rigorous program for monitoring immediately above the injection zone. Results of brine and gas analyses from the “B” sandstone, first perforated and sampled six months after CO_2 injection, showed slightly elevated concentrations of bicarbonate, Fe, and Mn and significantly depleted $\delta^{13}\text{C}$ values (–5.9 to –17.5 vs. ~ –4‰) of DIC relative to preinjection “C” composition. A more definitive proof of the migration of injected CO_2 into the “B” sandstone is obtained from the presence of two of the four (PMCH and PTCH) PFT tracers added to the injected CO_2 [27]. Additional proof of the migration of injected CO_2 into the “B” sandstone is obtained from the high concentration

(2.9 vs. ~0.3%) of CO₂ in dissolved gas obtained from one of the two downhole Kuster samples.

Results obtained from samples collected in January 23–27, 2006 indicate brine and gas compositions that are approximately similar to those obtained from the “C” sandstone before CO₂ injection. These results indicate the absence of significant amounts of injected CO₂ in the “B” fluids sampled. However, a contrary conclusion is indicated based on the fact that PMCH and PTCH were measured in the six samples also analyzed for PFT tracers [27]. It is possible that the measured PMCH and PTCH concentrations represent desorbed PFT tracers that were introduced into “B” earlier and do not represent migration of additional injected CO₂ into the “B” sandstone.

Results from the “B” sandstone show significant CO₂ migration from the “C” sandstone. We can not rule out migration through the intervening beds of shale, muddy sandstone and siltstone, but a short-term leakage through the failed squeeze on perforations in the “C” or remedial cement around the casing of a 50-year old well is a more likely explanation. These results highlight the importance of investigating the integrity of cement seals, especially in nearby abandoned wells, prior to the injection of large quantities of reactive and buoyant CO₂.

4. SUMMARY AND CONCLUSIONS

Deep saline aquifers in sedimentary basins provide advantageous locations close to major CO₂ sources and huge potential capacity for the storage of large amounts of this GHG [9,10]. The Frio brine field test demonstrated the relatively straight forward method of CO₂ injection and its rapid transport to the observation well. Our field geochemical methodologies, especially measurements of pH, alkalinity and gas compositions [20] proved highly effective for tracking the injected CO₂. The tracking of CO₂ was later confirmed by laboratory determinations of dissolved Fe, Mn, and Ca, and isotopes, especially δ¹⁸O values of brine and CO₂, and δ¹³C values of DIC (dissolved inorganic carbon) and CO₂ [19].

The chemical data coupled with geochemical modeling indicate rapid dissolution of minerals, especially calcite and iron oxyhydroxides caused by low pH brine. This dissolution could have important environmental implications with regard to creating pathways in the rock seals and well cements that could facilitate leakage of CO₂ and brine. Maintaining reservoir integrity that limits CO₂ leakage to very low levels is essential to the success of injection operations [15]. Preventing brine migration into overlying drinking water supplies is equally important, because dissolution of minerals would mobilize

Fe, Mn and other toxic metals, in addition to the chemicals in the pristine brine. Mobilization of organics, including BTEX, phenols and other toxic compounds, from this non oil-bearing aquifer would further compound the environmental severity of CO₂ and brine leakage.

ACKNOWLEDGEMENTS

We thank S. Hovorka (PI) and others at BEG, U. of Texas, Austin, TX, for leading this project. We also thank G. Ambats, and B. Topping for helping with sampling and analyses, and D. Collins and others at Sandia Technologies for logistical support. Funding was provided by US. DOE (NETL). (William O'Dowd and Karen Cohen, Program Managers).

REFERENCES

- [1] WHITE, C.M., et al., Separation and capture of CO₂ from large stationary sources and sequestration in geological formations--coalbeds and deep saline aquifer, *J. Air & Waste Management Assoc.*, **53** (2003) 645–715.
- [2] HOUGHTON, J.T., *Global Warming: The Complete Briefing*, Cambridge Univ. Press (2004).
- [3] BROECKER, W.S., The Holocene CO₂ rise: Anthropogenic or natural?, *EOS* **87** (2006) 27.
- [4] ENERGY INFORMATION ADMINISTRATION, *Annual Energy Outlook 2003, With Projections to 2030*, DOE/EIA-0484, Washington DC (2006).
- [5] PRENTICE, I.C., et al., The carbon cycle and atmospheric CO₂. Working Group I., *Third Assessment Report IPCC* (2001) 183–237.
- [6] KORBOEL, R., et al., CO₂ disposal— injection of removed CO₂ into the Utsira Formation; *Energy Convers. Mgmt.* **36** (1995) 509–512.
- [7] DUROCHER, K., et al., “Geochemical monitoring of the Weyburn CO₂-injection EOR site, Saskatchewan, Canada.” (Proc. 11th Int. Symp. Water-Rock Interaction, 2004), WANTY, R.B., SEAL II, R.R., Eds.), Balkema, Rotterdam (2004) 549–554.
- [8] HOVORKA, S.D., et al., Measuring permanence of CO₂ storage in saline formations — the Frio Experiment, *Environ. Geosciences* **13** (2006) 105–121.
- [9] HOLLOWAY, S., Storage of fossil fuel derived carbon dioxide beneath the surface of the earth, *An. Rev. Energy Environ.* **26** (2001)145–166.
- [10] BENSON, S.M., COOK, P., Chapter 5: Underground Geological Storage, *IPCC Special Report on Carbon Dioxide Capture and Storage*, Intergovernmental Panel on Climate Change, Interlachen, Switzerland (2005) 5–1 to 5–134, <http://www.ipcc.ch>.

APPLICATION OF STABLE ISOTOPES AND FLUID CHEMISTRY

- [11] GUNTER, W.D. et al., Aquifer disposal of CO₂-rich gases: reaction design for added capacity. *Energy Convers. Mgmt.* **34** (1993) 941–948.
- [12] PALANDRI, J.L., KHARAKA, Y.K., Ferric iron-bearing sediments as a mineral trap for CO₂ sequestration: iron reduction using sulfur-bearing waste gas, *Chem. Geol.* **217** (2005) 351–364.
- [13] HITCHON, B. (Ed.), *Aquifer Disposal of Carbon Dioxide*. Geoscience Publishing Ltd., Sherwood Park, Alberta, Canada (1996).
- [14] ALLIS, R., et al., Implications of results from CO₂ flux surveys over known CO₂ systems for long-term monitoring (Proc. DOE/NETL Fourth An. Conf. Carbon Capture & Sequestration, Alexandria, VA 2005), 1367–1388 (CD-ROM).
- [15] HEPPLER, R.P., BENSON, S.M., Geologic storage of carbon dioxide as a climate change mitigation strategy; performance requirements and the implications of surface seepage, *Environ. Geol.* **47** (2005) 576–585.
- [16] KNAUSS, K.G., et al., Preliminary reactive transport modeling and laboratory experiments conducted in support of the Frio Pilot Test (Proc. DOE/NETL 4th An. Conf. Carbon Capture & Sequestration, Alexandria, VA, 2005), ExchangeMonitor Publications (2005).
- [17] HERZOG, H. et al., An Issue of Permanence: Assessing the Effectiveness of Temporary Carbon Storage, *Climatic Change*, **59** (2003) 293–310.
- [18] AGGARWAL, P.K., GAT, J.R., FROEHLICH, K.F.O. (Eds.), *Isotopes in the Water Cycle: Past, Present, and Future of a Developing Science*, Dordrecht, Springer (2005).
- [19] KHARAKA, Y.K., et al., Gas-water-rock interactions in Frio Formation following CO₂ injection: Implications to the storage of greenhouse gases in sedimentary basins, *Geology* **34** (2006) 577–580.
- [20] FREIFELD, B.M., et al., The U-tube: A novel system for acquiring borehole fluid samples from a deep geologic CO₂ sequestration experiment, *J. Geophys. Res.* **110** (2005) B10203, doi: 10.1029/2005JB003735.
- [21] KHARAKA, Y.K., HANOR, J.S., “Deep Fluid in the Continents: I. Sedimentary Basins”, *Treatise on Geochemistry*, v.5 Surface and Ground Water, Weathering, and Soils (DREVER, J.I., Ed.) Elsevier Pergamon, Oxford (2007) 499–540.
- [22] KHARAKA, Y.K., et al., SOLMINEQ.88: A computer program for geochemical modeling of water-rock interactions, U.S. Geol. Surv. Water-Res. Invest. Rep. (1988) 88–4227
- [23] PALANDRI, J.L. KHARAKA, Y.K., A compilation of rate parameters of water-mineral interaction kinetics for application to geochemical modeling: U.S. Geol. Surv. Water-Res. Invest. Rep. 04-1068 (2004) 70.
- [24] KHARAKA Y.K., et al., Predicted corrosion and scale-formation properties of geopressured geothermal waters from the northern Gulf of Mexico basin, *J. Petrol. Tech.* **32** (1980) 319–324.

- [25] AHMAD, Z., Principles of Corrosion Engineering and Corrosion Control, Elsevier, Oxford (2006).
- [26] CLARK, I., FRITZ, P. Environmental Isotopes in Hydrogeology, CRC Press, Boca Raton, FL (1997).
- [27] PHELPS, T.J., et al., Monitoring geological CO₂ sequestration using perfluorocarbon gas tracers and isotopes (Proc. DOE/NETL Fifth An. Carbon Capture & Sequestration Conference, Alexandria, VA., Exchange Monitor Publications (2006).

AN INTEGRATED APPROACH IN EVALUATING ISOTOPE DATA OF THE NUBIAN SANDSTONE AQUIFER SYSTEM (NSAS) IN EGYPT

K. FROEHLICH, P. K. AGGARWAL, W.A. GARNER
International Atomic Energy Agency,
Vienna, Austria

Abstract

This paper presents an evaluation of isotope data on the NSAS in Egypt that have been collected by various project carried out over the last 40 years and are now available in the isotope hydrology database (ISOHIS) of the IAEA. The correlation of the $\delta^{18}\text{O}$ and $\delta^2\text{H}$ values reveals that the stable isotope composition of precipitation remained nearly constant during the pluvial phases over the last hundreds of thousands of years. The observed variation of the $\delta^{18}\text{O}$ and $\delta^2\text{H}$ values in the groundwater of the NSAS appears to be caused either by evaporation during formation of the groundwater or, especially in the case of sampling from dug wells, by evaporation due to exposure of groundwater to the atmosphere at present-day climatic conditions. The majority of the analysed groundwater samples represents a mixture of groundwater of various depths, which explains why ^{14}C can be found in groundwater taken from more than 1000 m depths by pumping wells. In these cases, the measured ^{14}C value represents the small contribution of the uppermost groundwater layers in the sample rather than a specific age of the groundwater in terms of time elapsed since its infiltration. Recently published ^{81}Kr and ^{36}Cl data of the NSAS in Egypt revealed apparent groundwater ages up to 1 million years. The data have been interpreted by a model that assumed recharge be inflow through the southern boundary rather than rain-fed recharge over the unconfined area of the aquifer system in Egypt. This paper presents a re-evaluation of the ^{36}Cl and ^{81}Kr data by an alternative conceptual model, which takes such distributed recharge into account. The model allows estimating the long-term average of recharge to the unconfined part of the aquifer system and discharge through leakages in the confined part. The values of recharge and discharge are 0.4 mm/year and 0.65 mm/year, respectively. The average flow velocity of the groundwater derived from the recharge value is about 0.8 m/year in the unconfined part which corresponds well with the commonly accepted value of about 1 m/year. The calculated mean transit time of groundwater through the system reaches up to 1 million years.

1. INTRODUCTION

Recently considerable effort is being taken towards more rational use of the groundwater resources in the Nubian Sandstone Aquifer System (NSAS) that covers an area of about 2.2 million square kilometres and is shared by the countries Chad, Egypt, Libya and Sudan. Over the last 40 years this system has been subject of numerous investigations, including geology, hydrogeology and geochemistry together with environmental isotopes. A synthesis of the studies carried out up to the middle of the 1990s has been published by [1]. In these previous studies, major emphasis was placed to assess groundwater resources on the basis isotope measurements and numerical flow modelling. Examining the distribution of the stable isotopes of hydrogen and oxygen in groundwater it was found that the groundwater of the NSAS was replenished during past pluvial phases by local rainfall that originated from air moisture transported by west-wind drift from the Atlantic source regions to the eastern Sahara [2]. Radiocarbon dating of groundwater indicated that recharge took place in the Late Pleistocene older than 20 kyr and in the Holocene between about 14 kyr and 4 kyr before present (BP). Nearly in all groundwater samples taken from various sites and various depths of the unconfined and confined parts of the aquifer system, the radiocarbon concentration was found to be above the detection limit of about 1 pMC. This finding has been interpreted as indication that the recharge during the various pluvial phases was distributed over the aquifer system rather than localized in certain areas, and that recharge could also enter confined parts of the system through leakages in the confining beds [1]. An alternative explanation for the occurrence of radiocarbon in very deep groundwater of the NSAS has been given by Himida [3], who compared the ages derived from first ^4He dating of artesian groundwater from the Kharga oasis with the results of the first radiocarbon measurements of groundwater collected from this area [4]. The apparent ^4He ages were in the order of 1 million years, while radiocarbon indicated apparent ages of about 30 kyr. Himida [3] concluded that the age derived from radiocarbon “most probably represents the age of some groundwater mixtures which were formed on account of contamination of the original artesian water with the locally infiltrated surface water” during the Holocene recharge period.

Since publication of these two pioneering papers in 1967, no further studies using dating methods for very old groundwater have been carried out in NSAS projects, and references to Himida’s paper hardly can be found in later publications on this subject. Only recently attempts have been made to investigate deep groundwater from the NSAS measuring long-living radioisotopes such as ^{234}U [5], ^{81}Kr [6] and ^{36}Cl [7]. Apparent ^{81}Kr and ^{36}Cl ages

AN INTEGRATED APPROACH IN EVALUATING ISOTOPE DATA

have been reported to range between less than 100 kyr and about 1000 kyr in deep groundwater with apparent ^{14}C ages in the order of 30 kyr.

This paper presents an attempt to clear the apparent contradiction between apparent ^{14}C and ^{36}Cl (^{81}Kr) groundwater and to contribute to a better understanding of origin and replenishment of groundwater resources in the NSAS. The paper refers to the Egyptian part of the NSAS, since only in this part both ^{14}C and the other long-living radioisotopes have been measured so far. At first, $\delta^2\text{H}$ and $\delta^{18}\text{O}$ data taken from the database of the IAEA (ISOHIS) are evaluated in terms of origin and formation of the groundwater. Then, all ^{14}C data available from ISOHIS are reviewed and evaluated together with the ^{36}Cl , ^{81}Kr and $^{234}\text{U}/^{238}\text{U}$ data on the basis of a conceptual model of the recharge-discharge regime in the study area.

2. ORIGIN AND FORMATION OF THE GROUNDWATER

The sites, for which isotope data are compiled in ISOHIS, are mainly located along the various depressions (oases) and the river Nile (Fig. 1). ISOHIS includes both data gathered by IAEA sponsored projects and data contributed by other institutions, in this particular case mainly by the University of Heidelberg, Germany.

Plotting the deuterium excess ($d\text{-excess} = \delta^2\text{H} - 8 \times \delta^{18}\text{O}$) versus $\delta^{18}\text{O}$ values, two group of groundwater in the study area can be distinguished. The

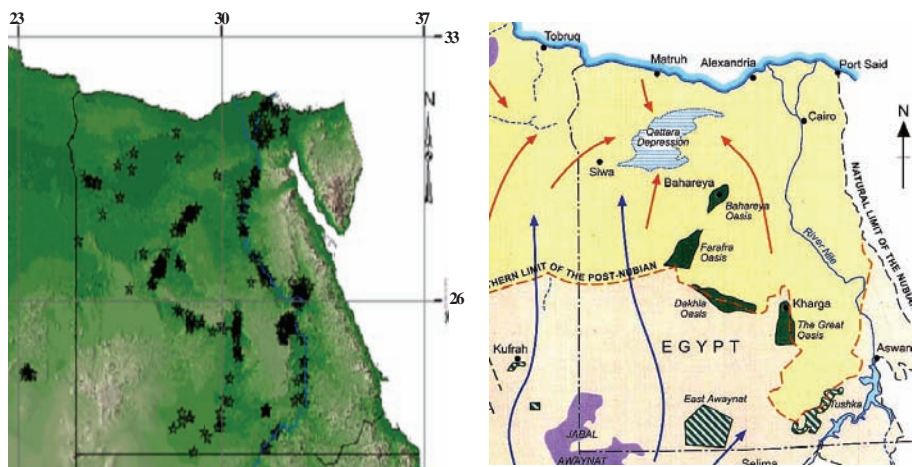


FIG. 1. Distribution of the sampling sites for which isotope data are available from ISOHIS (left). Right: NSAS in Egypt [8].

first group (left part of Fig. 2) comprises groundwater taken from springs and dug wells where the water is exposed to evaporation from the water surface

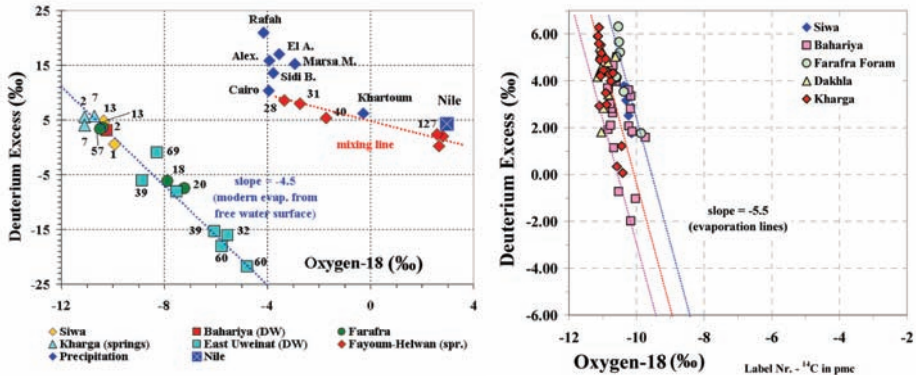


FIG. 2. Plot of d -excess versus $\delta^{18}\text{O}$ of groundwater exposed to atmosphere (springs, dug wells) and of modern precipitation (left) and groundwater of deep wells (right). The numbers at the measuring points represent the ^{14}C concentration (in pMC) of the given sample. The slopes of the dotted lines (-4.5 and -5.5 in the left and the right part, respectively) have been estimated by the Craig-Gordon model. The slope -4.5 has been obtained assuming evaporation of water exposed to the free atmosphere, while -5.5 has been calculated for evaporation from soil (sand).

to the free atmosphere, and the second group (right part of Fig. 2) represents groundwater collected from deep wells. The first group is characterized by a large fluctuation of the d -excess compared to the second one.

The data of the Fayoum and Helwan area fit a mixing line of two ‘end members’ that are represented by present-day Nile water ($^{14}\text{C} = 127$ pMC) and water of the old Nile that infiltrated during Holocene pluvial phases ($^{14}\text{C} = 27$ pMC). The generally lower $\delta^{18}\text{O}$ values for springs and dug wells in the oases of the NSAS indicate groundwater of the NSAS. The measuring points of this group of samples are spread along a line with slope -4.5 in the d -excess – $\delta^{18}\text{O}$ diagram. This value has been estimated by the Craig-Gordon equation, assuming evaporation of surface water that has been exposed to the atmosphere under present-day climatic conditions. The rather low d -excess and high $\delta^{18}\text{O}$ values of samples taken from dug wells in the East Uweinat region suggest an accordingly high evaporation loss (more than 20%).

AN INTEGRATED APPROACH IN EVALUATING ISOTOPE DATA

The slope -5.5 of the evaporation lines in the right part of Fig. 2 has been estimated by the Craig-Gordon equation assuming evaporation of water from soil/sand (higher kinetic fractionation factor than in case of evaporation from water surfaces). This slope suggests that (1) in pluvial phases the groundwater was subjected to evaporation during infiltration into soil/sand and (2) after pluvial phases it was exposed to evaporation from the shallow water table. — In this connection it is interesting to note, that already in the paper by Shata et al. [4] it was concluded that the rain water “underwent some evaporation before it disappeared in the subsurface”. — Since in pluvial phases the saturation deficit was lower than under (present-day) hyper-arid conditions, the evaporation effect was accordingly lower, as indicated by the lower spread of the d-excess values (cf. Fig. 2). In addition, the slight shift of the d-excess values (and the theoretical evaporation lines) along the $\delta^{18}\text{O}$ axis seems to be caused by variations in the air circulation pattern and rainout regime prevailing in the various pluvial phases that occurred during the last hundreds of thousands years.

The large variation of the d-excess values and the slope of -5.5 of the d-excess – $\delta^{18}\text{O}$ plot of samples collected in the south of the study area (Toshka, East Uweinat) indicate the effect of evaporation under arid (present-day) climate conditions (left part of Fig. 3). The d-excess decreases with the depth of the water table (right part of Fig. 3) and reaches a constant value below a depth of about 40 m, where evaporation through the sand layer appears to be negligible [9]. Most of the groundwater samples from these unconfined aquifers are of post-pluvial origin (see labels of Fig. 3, left part).

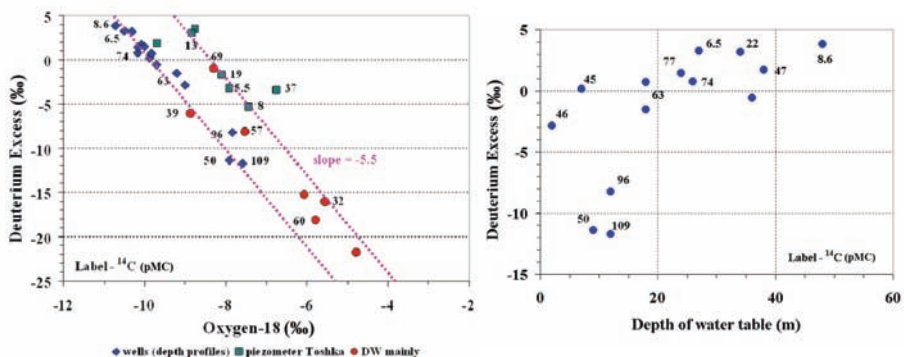


Fig. 3. D-excess vs. $\delta^{18}\text{O}$ of groundwater from wells/piezometers in East Uweinat and Toshka (left) and d-excess vs. depth of the water table in the East Uweinat region (right).

3. RECHARGE, FLOW AND DISCHARGE OF THE GROUNDWATER

3.1. ¹⁴C applications

East Uweinat is the only region for which filter depths of the wells sampled for ¹⁴C determinations, are known [10]. The sampling sites cover an area from 28.2°E to 29.9°E and 22°N to 23°N, and the filter depths range from some tens of metres to about 500 m. Plotting the ¹⁴C values as a function of the depth of the well filters, a general decrease of ¹⁴C with depths can be seen (Fig. 4), which points to vertical groundwater infiltration during the Holocene period including post-pluvial phases. Using the groundwater dating model by Vogel [11], a simple relationship can be derived for the infiltration (recharge) rate (R_{12}) during the periods defined by the ¹⁴C values at the beginning (C_1) and the end (C_2) of a given period:

$$R_{12} = \frac{\lambda p (z_2 - z_1)}{\ln(C_1 / C_2)} \quad (1)$$

where λ is the ¹⁴C decay rate, p the aquifer porosity (a value of 10% has been adopted from previous studies) and z is the depth. Geochemical effects on the change of ¹⁴C are considered to be negligible. Since the wells cover a rather wide area, neighbouring wells (except P3 – P5) have been combined for the calculation of the recharge rate. The results of well L6 and L1 have

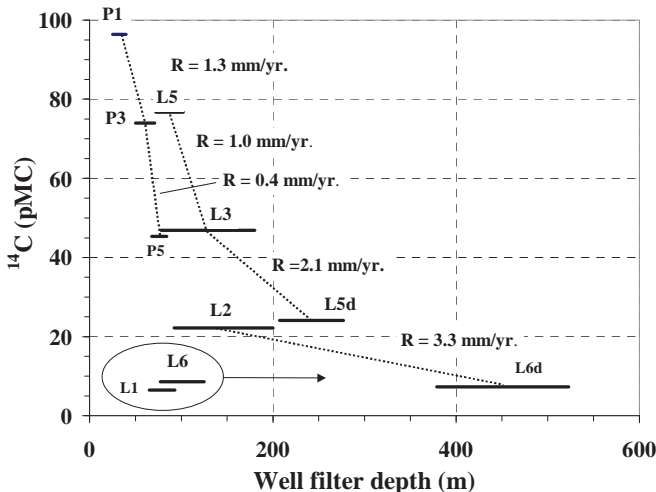


Fig. 4. ¹⁴C in groundwater in East Uweinat versus filter depth of the pump wells (P, L) from which samples have been taken. The horizontal bars represent the range covered by the filter.

been disregarded assuming that the water of these samples represent deeper groundwater as indicated by their filter depths. The results of Fig. 4 show that during the Holocene pluvial phases the recharge rate was between one and a few millimetres per year, and also during the post-pluvial phase some rain infiltrated below the groundwater table.

In contrast to the East Uweinat region, in all other regions of the NSAS in Egypt a systematic change of the ^{14}C values with depth of the wells is missing. The data plotted in Fig. 5 represent results from various studies and projects carried out during the last 40 years. Even in samples taken from pumping wells more than 1000 m deep, the ^{14}C values are well above the detection limit (about 1 pMC), which corresponds with an apparent ^{14}C age of less than about 35 kyr. Moreover, Fig. 6 demonstrates that, beyond East Uweinat, there is no systematic change of the ^{14}C values along the main flow direction of the groundwater. Also in samples from deep wells in the confined part of the system north of Dakhla oasis [12], ^{14}C values well above the detection limit have been measured.

However, due to recent ^{81}Kr and ^{36}Cl investigations [6, 7] this groundwater is hundreds of thousand years old and thus should be free of ^{14}C . Adopting the apparent ^{81}Kr and ^{36}Cl ages, four effects can be considered that may contribute to the occurrence of ^{14}C in very old groundwater samples:

- (1) Contamination during sampling by air- CO_2 due to a leaky extraction system or ^{14}C -contaminated chemicals. Vogel et al., [13] concluded from experimental studies, that such contamination could give rise to maximum 2 pMC in originally ^{14}C -free groundwater samples.
- (2) In-situ production of ^{14}C . Andrews and Fontes [14] reported that the underground production of ^{14}C by nuclear reactions (between aquifer rocks and products of the radioactive decay of radionuclides of the uranium and thorium decay series) can contribute about 1 to 2 pMC to the ^{14}C content.
- (3) Contamination of deep groundwater by locally infiltrated surface water [3], e.g. by leakages in the confined beds [1]. In fact, local recharge from last pluvial phases has been identified measuring the $^{234}\text{U}/^{238}\text{U}$ ratio in deep groundwater of the study area [5]. The estimated proportion of locally infiltrated groundwater ranges from about 5% (Baris oasis) to about 20% (Farafra and Bahariya oasis).
- (4) Contamination caused by mixing of groundwater from different layers (ages) during sampling. The groundwater samples have been collected by pumping wells that penetrate various layers with different groundwater ages in the stratified aquifer system. Under these conditions "pumping invariably results in mixtures of groundwater from the different layers" [15]. A simple mixing equation can be used to demonstrate this effect. Considering a sample with a measured ^{14}C content of 4 pMC taken

from a deep well (e.g. Bahariya wells of about 1000 m depth, cf. Fig. 5a), assuming that the uppermost layer contents pluvial groundwater with a present-day ^{14}C content of 40 pMC, and neglecting the ^{14}C content of the old groundwater below this layer, the proportion of the shallow pluvial groundwater in the mixed sample would be 10%, which would correspond with a depth of this layer of 100 m of a total depth of 1000 m. This result appears to be in qualitatively good agreement with the data of the diagram in Fig. 4.

In summary, these findings suggest the following conclusions:

- (1) The ^{14}C values of most of the samples collected so far from the study area, indicate mixing of groundwater from different layers in the stratified aquifer rather than the age of the groundwater. Therefore, ^{14}C appears to be useful as tracer to study the infiltration of contaminants in the aquifer system, e.g. due to agricultural activities.
- (2) Palaeoclimatic investigations using ^{14}C as age indicator should be reconsidered in the light of these findings.
- (3) The application ^{14}C dating in the NSAS is limited to the uppermost layers (cf. Fig. 4) and requires an appropriate sampling from well-defined depths in the aquifer.

3.2. Evaluation of the ^{36}Cl and ^{81}Kr data

In comparison to ^{14}C , the average ^{81}Kr and ^{36}Cl values in deep groundwater are in general insignificantly affected by small contributions of shallow (young) groundwater. Assuming for example that the proportion of young groundwater (initial ratio of $^{81}\text{Kr}/\text{Kr}$ and $^{36}\text{Cl}/\text{Cl}$ of 100%) is 4% in the bulk of deep groundwater with an average age of 200 kyr ($^{81}\text{Kr}/\text{Kr}$ of 54.6% and $^{36}\text{Cl}/\text{Cl}$ of 63.1%), groundwater mixing would result in $^{81}\text{Kr}/\text{Kr}$ of 56.8% and $^{36}\text{Cl}/\text{Cl}$ of 64.5%, which corresponds to a shift of the apparent ^{81}Kr and ^{36}Cl ages to 187 kyr and 191 kyr, respectively. Thus, the shift of the apparent age is insignificant in comparison to ^{14}C , which would result in a nearly ten times lower apparent age (25 kyr if a ^{14}C initial content of 85 pMC is assumed).

The ^{81}Kr and ^{36}Cl groundwater ages of the NSAS in Egypt [6, 7] range from a few ten thousand years to about 1 million years. A good agreement has been found between the ^{81}Kr and ^{36}Cl ages of selected samples. Patterson et al. [7] used a two-dimensional hydraulic model to discuss the dating results in terms of groundwater flow and replenishment in the aquifer system. The model assumes that the system is recharged by base flow through the southern boundary (at East Uweinat) and discharge occurs through the northern boundary north of Bahariya oasis. Thus, the model ignores recharge over the unconfined part of

AN INTEGRATED APPROACH IN EVALUATING ISOTOPE DATA

the system between Uweinat and Dakhla oasis, which implies negligible vertical age stratification. This assumption, however, is in contrast to measurements of ^{14}C in the East Uweinat region that show a well-developed vertical change of the ^{14}C values (Fig. 4) and, thus, unequivocally prove rain-fed local recharge in that unconfined aquifer region. Also for other parts of the aquifer system, local recharge during pluvial phases is recognized [1, 5].

In this paper a more realistic recharge regime is proposed, on the basis of which the available ^{81}Kr , ^{36}Cl and related data are re-evaluated. An evolutionary trend of the ^{36}Cl and ^{81}Kr data has been examined, which suggests an appropriate conceptual model of the recharge and flow regime. This approach avoids an „a priori” calculation of apparent ages of the individual groundwater samples which gives preference to the simple piston-flow regime and, moreover, requires

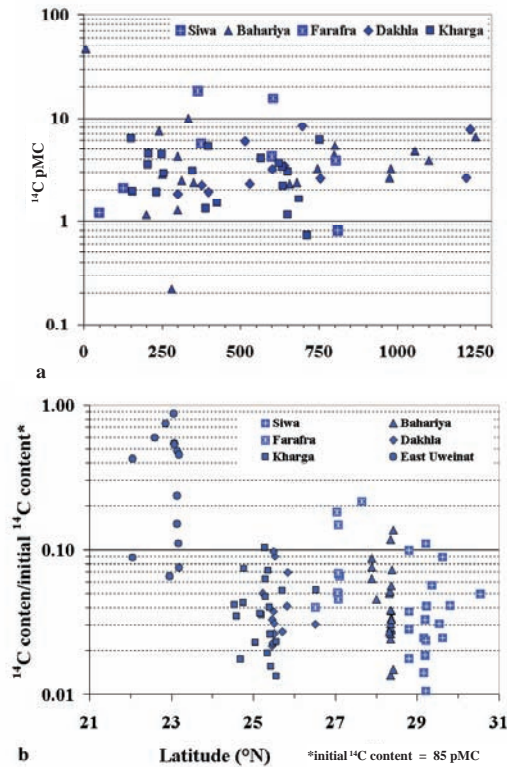


Fig. 5. ^{14}C content as function of depth of the sampling well (a) and of the latitude of the sampling sites (b). Given that the main flow direction of the groundwater is from south to north (Fig. 1, right part), the latitude differences in Fig. 5b are about proportional to the distance differences between the sampling sites in flow direction. It should also be noted that in Fig. 5b the ^{14}C values are normalized to an assumed ^{14}C initial content of 85 pMC.

laborious (sometimes difficult to verify) geochemical corrections. To examine a possible trend along the main flow direction, the coordinates of the sampling sites, not listed in the relevant papers, have been re-constructed. Plotting the ^{36}Cl and Cl^- values versus the latitude of the sites, rather high values and high fluctuations have been found in the unconfined part of the aquifer system. If atmospheric fallout (wet and dry) is anticipated as dominating source of the ^{36}Cl and Cl^- concentrations, this finding can be explained by build-up of chloride over several thousand years during arid phases followed by dissolution during pluvial phases. Since there is no remarkable difference in the enrichment of ^{36}Cl and Cl^- by evaporation and precipitation, the ratio of $^{36}\text{Cl}/\text{Cl}$ should be unaffected. This concept appears to be proved by the evolution of $^{36}\text{Cl}/\text{Cl}$ which shows no significant fluctuations in the unconfined part of the aquifer but a continuous decrease from the East Uweinat/Toshka area in northern direction (main flow direction). — Only one outlier with very high $^{36}\text{Cl}/\text{Cl}$ has been identified (site BA4 in the Kharga oasis). One of the possible explanations is additional ^{36}Cl production due to nuclear reaction of cosmic-ray neutrons with ^{35}Cl of salt deposits at the surface of this site. — By extrapolation in a semi-logarithmic plot of $^{36}\text{Cl}/\text{Cl}$ versus latitude of the sampling sites, the initial isotopic ratio $^{36}\text{Cl}/\text{Cl}$ has been estimated to be 130×10^{-15} . In this way, the relative ^{36}Cl and ^{81}Kr isotopic ratios could be plotted.

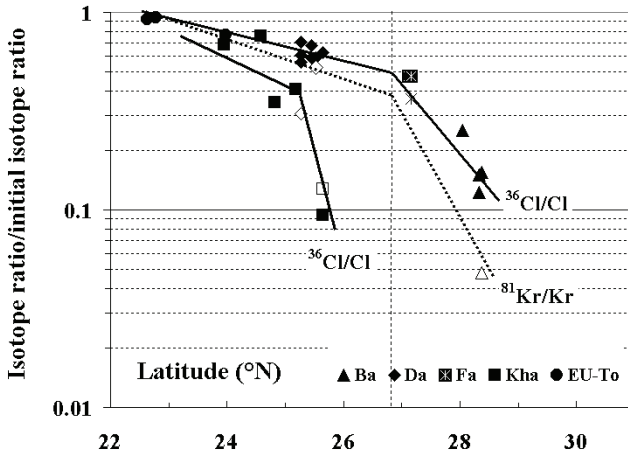


FIG. 6. Relative $^{36}\text{Cl}/\text{Cl}$ and $^{81}\text{Kr}/\text{Kr}$ ratios versus latitude of the sampling sites: Ba – Bahariya, Da – Dakhla, Fa – Farafra, EU-To – East Uweinat/Toshka. Full symbols represent ^{36}Cl values, the open symbols stand for ^{81}Kr values. The lines have been drawn to indicate possible evolutionary trends. The upper full and dashed lines suggest a trend in the main flow direction, while the lower line (only for ^{36}Cl because of insufficient data for ^{81}Kr) suggests a separate flow path to the eastern part of Kharga oasis.

AN INTEGRATED APPROACH IN EVALUATING ISOTOPE DATA

Fig. 6 suggests two different flow paths from south to north, one is connecting East Uweinat, Dakhla, Farafra, and Bahyriya oases and the other in the east includes sites of the Kharga oasis. This separation into two flow paths could be related to the Kharga Uplift, which stretches from East Uweinat (near Safsat) to the western part of the Kharga oasis (Thorweihe, [10], Fig.3). Furthermore, the rapid drop in the isotopic ratios from north to south of the Kharga oasis points to confined conditions in this region, increase of the aquifer thickness, and groundwater discharge through leakages in the confining beds. In the following, this flow path will not be discussed in more detail because of insufficient data.

The semi-logarithmic plot of the relative ^{36}Cl and ^{81}Kr ratios along the groundwater flow path from East Uweinat to Bahyriya oasis appears to be linear up to 26.7°N (north of the Dakhla oasis) followed by a rapid drop behind this latitude (Fig.6). Considering the geologic section of the aquifer system (Fig. 7), the strong bend of the lines could be explained by the change from unconfined to confined conditions. — Due to the geology of the system, this change in the geologic conditions is slightly more southern than the change in the isotope data. — Taking the geometry of the aquifer system into account and assuming constant recharge in the unconfined, and constant discharge in the leaky confined part, a conceptual model can be developed that describes the change of the isotopic composition along the groundwater flow path. For the sake of simplicity of this model, recharge, discharge and hydraulic permeability are assumed to be constant in the aquifer system. Recognizing, that the samples have been taken from pumping wells, it appears to be adequate assuming that the samples represent a mixture of groundwater from the whole aquifer depth.

On the basis of this conceptual model the following relationship has been derived for the isotope ratio (r) in the unconfined region

$$r = \frac{1 - \exp(-\lambda\tau_0(x/x_0))}{\lambda\tau_0(x/x_0)} \quad (2)$$

and for the leaky confined region

$$r = \frac{1 - \exp(-\lambda\tau_0)}{\lambda\tau_0} \exp\left[-\lambda\tau_0\left(\frac{x-x_0}{x_0 - (x-x_0)(\tau_0/\tau_L)}\right)\right] \quad (3)$$

where x (x_0) is the distance of a sampling site (transition zone from unconfined to confined conditions) from the southern boundary, and λ is the decay constant of ^{36}Cl and ^{81}Kr , respectively. The parameter τ_0 and τ_L are defined by the expressions

$$\tau_0 = \frac{pH_0}{R} \quad \text{and} \quad \tau_L = \frac{pH_0}{L} \quad (4a, b).$$

where H_0 is the maximum depth of the aquifer system (Fig. 7), p the porosity, R the recharge rate and L the discharge (leakage) rate. The geometric parameter x_0 and H_0 can be taken from Fig. 7, the average porosity of the aquifer system is known to be at about 10%. Therefore, the model allows to estimate parameter R by fitting the isotope data of the unconfined part to the theoretical curve given in equ.(2) and parameter L by fitting the data of the leaky confined part to equ.(3). In addition to the two parameters characterizing average recharge and discharge, also the flow velocity of the groundwater in the two parts of the system can be estimated. Under the given conditions, the groundwater flow velocity v follows the expression

$$v_{uc} = \frac{x_0 R}{H_0 p} \quad \text{and} \quad v_c = v_{uc} - \frac{(x - x_0)L}{H_0 p} \quad (5a, b)$$

where v_{uc} is the (distance) velocity in the unconfined and v_c in the leaky confined part.

In the following, only the evaluation of the ^{36}Cl ratios is presented. Although the relevant values derived from ^{81}Kr are close to the ones obtained by ^{36}Cl , the ^{81}Kr results will not be presented because of the insufficient ^{81}Kr data points. The fit of the measured ^{36}Cl ratios to the theoretical curves (Fig. 8) gives the following values of the relevant hydrodynamic parameters:

$$R = 0.4 \text{ mm/yr}, L = 0.65 \text{ mm/yr}, v_{uc} = 0.8 \text{ m/yr}$$

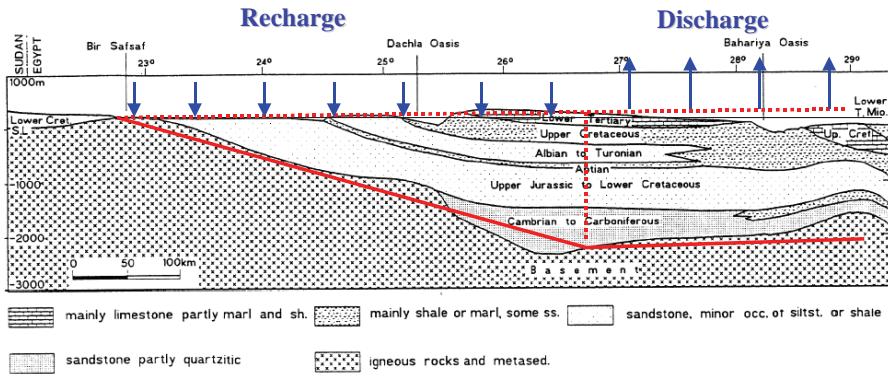


FIG. 7. Geologic section through the NSAS from the Sudanese border to Bahariya area in Egypt [12], and simplified geometry of the aquifer system used for modelling the groundwater flow and recharge regime. Arrows indicated recharge and discharge over the system.

AN INTEGRATED APPROACH IN EVALUATING ISOTOPE DATA

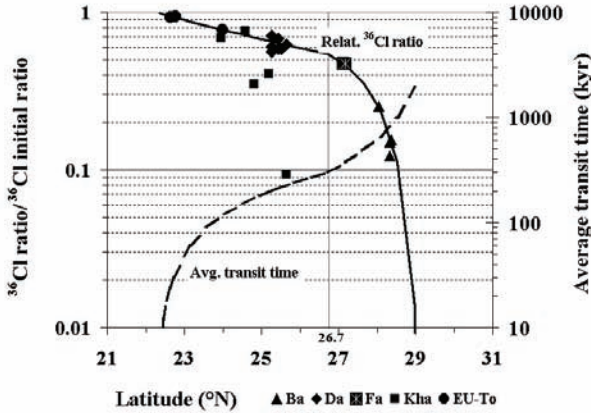


FIG. 8. Relative ³⁶Cl ratio and average transit time calculated on the basis of the conceptual model.

It should be noted that these parameters represent long-term averages over both pluvial phases (with higher recharge values) and arid phases (with no recharge at all) of the last hundreds of thousands years. Similarly, the discharge rate is higher in, or shortly after, pluvial phases and decreases in arid phases. Considering the relative extension of the recharge and discharge areas (Fig. 7), the estimated values of R and L result in a rather good balance of total recharge and discharge over the whole system. It should also be emphasized that according to this conceptual model, the groundwater flow velocity is constant in the unconfined part; the estimated value is close to the commonly accepted value of 1 m/yr. In the ‘confined’ part the velocity decreases due to leakages in the confining beds.

Finally, it should be emphasized that the apparent groundwater ages, estimated by Sturchio et al. [6] and Patterson et al. [7], appeared to be irrelevant for the data evaluation in terms of hydrogeologically (hydrodynamically) relevant parameters. Nevertheless, the groundwater age at a given location and depth of the groundwater can easily be derived from the geometry of the aquifer and the recharge and discharge values. For example, the vertically averaged groundwater age at a given distance x from the outcrop of the aquifer (‘average transit time’) is for the unconfined part of the aquifer given by the expression

$$t_{avg} = \frac{\tau_0}{2} \times \frac{x}{x_0} \tag{6}$$

The values calculated for both parts of the aquifer are shown in Fig. 8. In fact, this average transit time increases along the flow path up to about 1 million years.

REFERENCES

- [1] THORWEIHE, U., HEINL, M., Groundwater Resources of the Nubian Aquifer System NE Africa, Modified synthesis submitted to: Observatoire du Sahara et du Sahel (OSS, Paris) 1998: "Aquifers of Major Basins – non-renewable Water RESOURCE", OSS, PARIS (2002).
- [2] SONNTAG, C., KLITZSCH, E., LÖHNERT, E.P., EL-SHAZLY, E.M., MÜNNICH, K.O., JUNGHANS, C., THORWEIHE, U., WEISTROFFER, K., SWAILEM, F.M., Palaeoclimatic information from deuterium and oxygen-18 in carbon-14-dated north Saharan groundwaters: Groundwater formation in the past, In: Isotope Hydrology **1978** II (1979) 569–581, International Atomic Energy Agency, Vienna.
- [3] HIMIDA, I.H., Remarks on the absolute age determination of the artesian water of the oases of the Western Desert with a special reference to Kharga oasis, Bulletin de l'Institut du Désert d'Égypte **XII** 2 (1967) 61–124.
- [4] SHATA, A., KNETSCH, G., DEGENS, E.T., MÜNNICH, K.O., EL-SHAZLI, M., The geology, origin and age of the ground water supplies in some desert areas of U.A.R, Bulletin de l'Institut du Désert d'Égypte **XII** 2 (1967) 61–124.
- [5] DABOUS, A.A., OSMOND, J.K., Uranium isotopic study of artesian and pluvial contributions to the Nubian Aquifer, Western Desert, Egypt. Journal of Hydrology **243** (2001) 242–253.
- [6] STURCHIO, N.C., DU, X., PURTSCHERT, R., LEHMANN, B.E., SULTAN, M., PATTERSON, L.J., LU, Z.T., MÜLLER, P., BIGLER, T., BAILEY, K., O'CONNOR, T.P., YOUNG, L., LORENZO, R., BECKER, R., EL ALFY, Z., EL KALIOUBY, B., DAWOOD, Y., ABDALLAH, A.M.A., One million year old groundwater in the Sahara revealed by krypton-81 and chlorine-36. Geophys. Res.Lett. **31** (2004) L05503, doi:10.1029/2003GL019234.
- [7] PATTERSON, L.J., STURCHIO, N.C., KENNEDY, B.M., VAN SOEST, M.C., SULTAN, M., LU, Z.T., LEHMANN, B., PURTSCHERT, R., EL ALFY, Z., EL KALIOUBY, B., DAWOOD, Y., ABDALLAH, A., Cosmogenic, radiogenic, and stable isotopic constraints on groundwater residence time in the Nubian Aquifer, Western Desert of Egypt. Geochemistry Geophysics Geosystems, VOL. 6, Q01005, doi:10.1029/2004GC000779 (2005).
- [8] SALEM, O., PALLAS, P., The Nubian Sandstone Aquifer System (NSAS). In: Shammy, P. (ed.) International Shared (Transboundary) Aquifer Resources

AN INTEGRATED APPROACH IN EVALUATING ISOTOPE DATA

- Management – Their significance and sustainable management, A Framework Document, UNESCO, Paris (2001) 41–44.
- [9] CHRISTMANN, D., SONNTAG, C., Groundwater evaporation from East-Saharan depressions by means of deuterium and oxygen-18 in soil moisture. In: Proceedings of a Symposium on “Isotope Techniques in Water Resources Development”, IAEA (1987) 89–204.
- [10] THORWEIHE, U., Isotopic identification and mass balance of the Nubian Aquifer System in Egypt, In: Thorweihe, U. (ed.) Impact of Climatic Variations on East Saharian Groundwaters – Modelling of Large Scale Flow Regimes, Berliner geowissenschaftliche Mitteilungen (1986) 87–97.
- [11] VOGEL, J.C., Carbon-14 dating of groundwater, In: Isotope Hydrology 1970, IAEA Symposium, March 1970, Vienna (1970) 225–239.
- [12] KLITZSCH, E., Geological elements for preparing regional hydrogeological studies, based on the Nubian Aquifer example, In: Proc. Intern. Conf. Tripoli, Libya, on “Regional Aquifer Systems in Arid Zones – Managing non-renewable resources”. IHP, UNESCO (1999) 27–31
- [13] VOGEL, J.C., TALMA, A.S., HEATON, T.H.E., The age and isotopic composition of groundwater in the Stampriet Artesian Basin, SWA, Final Report of the Steering Committee for Water Research in SWA (1982).
- [14] ANDREWS, J.N., FONTES, J.C., Importance of in-situ production of ^{36}Cl , ^{36}Ar and ^{14}C in hydrology and hydrogeochemistry, In: Proc. Intern. Symp. on “Isotope Techniques in Water Resources Development”, IAEA, Vienna (1992) 245–269.
- [15] EDMUNDS, W.M., Integrated geochemical and isotopic evaluation of regional aquifer systems in arid regions, In: Proc. Intern. Conf. Tripoli, Libya, on “Regional Aquifer Systems in Arid Zones – Managing non-renewable resources”. IHP, UNESCO (1999) 107–119.

RADIONUCLIDE TRACERS OF SUBMARINE GROUNDWATER DISCHARGE

W.S. MOORE

Department of Geological Sciences,
University of South Carolina,
Columbia, South Carolina,
USA

Abstract

Radionuclide tracers have the ability to assess the flux of submarine groundwater discharge (SGD) over a range of temporal and spatial scales. Short-lived isotopes such as ^{222}Rn , ^{224}Ra , and ^{223}Ra can reveal sites where SGD impacts the coastal ocean and elucidate relationships between SGD and ocean forces such as tides and storms. Longer-lived isotopes such as ^{228}Ra and ^{226}Ra integrate the effects of SGD over longer scales. These isotopes can discriminate sources of SGD and evaluate total fluxes. This paper will investigate the application of radionuclide tracers to SGD in a variety of settings on different continents.

1. INTRODUCTION

The flow of groundwater from land to the sea is a major component of the hydrological cycle. This flow, called submarine groundwater discharge (SGD), consists of continental meteoric water mixed with sea water that has infiltrated the aquifer. The chemical composition of this mixture is usually different from that predicted by simple mixing because biogeochemical reactions in the aquifer modify the fluid chemistry. To emphasize the importance of mixing and chemical reaction in these coastal aquifers, they are often called subterranean estuaries [1].

Studies of SGD usually classify all saturated permeable materials in the coastal zone and on the continental shelf as aquifers. Thus, advective flow through such materials is considered SGD. This definition of SGD restricts the process to shallow depth (<150 m) [2]. SGD does not include such processes as deep-sea hydrothermal circulation, deep fluid expulsion at convergent margins, and density-driven cold seeps on continental slopes. Associated with SGD is submarine groundwater recharge (SGR), which occurs as the direction changes and surface ocean waters penetrate into the aquifer. Such recharge may occur

on short time scales due to tides and storms and long time scales due to sea level rise and inland groundwater pumping.

Two primary issues must be considered: (1) What is the flux of fresh water due to SGD? (2) What are the material fluxes due to chemical reactions of sea water and meteoric water with aquifer solids? Hydrologists are primarily concerned with the first question as it relates directly to the freshwater reserve in coastal aquifers and salinization of these aquifers through sea water intrusion. Oceanographers are also interested in this question because there may be buoyancy effects on the coastal ocean associated with direct input of fresh water from the bottom. Chemical, biological, and geological oceanographers are more concerned with the second question as it relates directly to alteration of coastal aquifers and nutrient, metal, and carbon inputs to the ocean (and in some cases removal from the ocean). Coastal managers should be concerned with both aspects.

We now recognize that SGD provides a major source of nutrients to salt marshes, estuaries, and other communities on the continental shelf. For example it is estimated that the fluxes of nitrogen and phosphorus to the South Carolin, USA, shelf from submarine groundwater discharge exceed fluxes from local rivers [3, 4]. Similar results have been obtained in South Korea [5] and Thailand [6]. Because nutrient concentrations in coastal groundwater may be several orders of magnitude greater than surface waters, groundwater input may be a significant factor in the eutrophication of coastal waters. Some have linked the nutrients supplied by SGD to harmful algae blooms [7].

2. COMPOSITION OF SGD

As freshwater flows through an aquifer driven by an inland hydraulic head, it can entrain seawater diffusing and dispersing upward from the salty aquifer that underlies it. Superimposed upon this terrestrially-driven circulation are a variety of marine-induced forces that result in flow into and out of the seabed even in the absence of a hydraulic head. Most SGD is a mixture of fresh groundwater and sea water. Although the salinity of SGD emerging from coastal aquifers may be used to determine the fraction of fresh groundwater that has diluted recycled seawater, the fluids that comprise SGD are often chemically distinct from these end-members. To emphasize the importance of mixing and chemical reaction in coastal aquifers, these systems have been called “subterranean estuaries” because they are characterized by biogeochemical reactions that influence the transfer of nutrients, metals, and carbon to the coastal zone in a manner similar to that of surface estuaries [1].

RADIONUCLIDE TRACERS OF SUBMARINE GROUNDWATER DISCHARGE

Because of organic matter oxidation, some subterranean estuaries are suboxic or anoxic. In these cases metals such as iron and manganese may be released from their oxides to solution. Other metals that were adsorbed to these oxide coatings would also be released. SGD from such subterranean estuaries will transfer these dissolved metals to the coastal ocean. Unlike dissolved metals that enter surface estuaries from rivers, metals that enter the coastal water from subterranean estuaries may bypass the estuary filter, that is the particle-rich and high productivity zones in many surface estuaries, where dissolved metals are sequestered. This process may be important for iron fluxes to the ocean. Significant additions of iron to the ocean are thought to occur along the southern coast of Brazil [8]. Sea water that recharges subterranean estuaries may transport dissolved metals that precipitate in reducing environments. Uranium may be removed from sea water by this mechanism [9].

The natural supply of nutrients and carbon by SGD may be necessary to sustain biological productivity in some environments. There is also an awareness that in some cases, SGD may be involved in harmful algal blooms and other negative effects. As coastal development continues, changes in the flux and composition of SGD are expected to occur. To evaluate the effects of SGD on coastal waters, it is necessary to know the current flux of SGD and its composition. Studies are underway along many coastlines to evaluate SGD and its effect on the environment.

3. MEASURING SGD

Attempts to quantify SGD have focused on three approaches: (1) using seepage meters to directly measure discharge; (2) using tracer techniques to integrate SGD signals on a regional scale; and (3) groundwater modeling. In this paper I will discuss various tracer techniques.

Regional estimation of SGD is complicated due to the fact that direct measurement over large temporal and spatial scales is not possible by conventional means. Measurements of a range of tracers at the aquifer-marine interface and in the coastal ocean provide a method to produce integrated flux estimates of discharge not possible by other means. Tracer techniques utilize chemicals (often naturally occurring radionuclides) that have high concentrations in groundwater relative to coastal waters and low reactivity in the coastal ocean. These techniques require an assessment of the tracer concentration in the groundwater, evaluation of other sources of the tracer, and a measure of the residence time of the coastal water. With this information, an inventory of the tracer in coastal waters is converted to an offshore flux of the tracer. This tracer flux must be replaced by new inputs of the tracer from SGD.

3.1. Radium isotopes

The discovery of high activities of ^{226}Ra in the coastal ocean (Fig. 1) that could not be explained by input from rivers or sediments coupled with measured high ^{226}Ra in salty coastal aquifers led to the hypothesis that SGD was responsible for the elevated activities [10]. These elevated ^{226}Ra activities, which have been measured along many coasts, provide the primary evidence for large SGD fluxes to the coastal ocean.

Because radium is highly enriched in salty coastal groundwater relative to the ocean, small inputs of SGD can be recognized as a strong radium signal. In many cases this signal can be separated into different SGD components using ^{228}Ra as well as ^{226}Ra , the two long-lived Ra isotopes. The short-lived Ra isotopes, ^{223}Ra and ^{224}Ra , are useful in evaluating the residence time or mixing

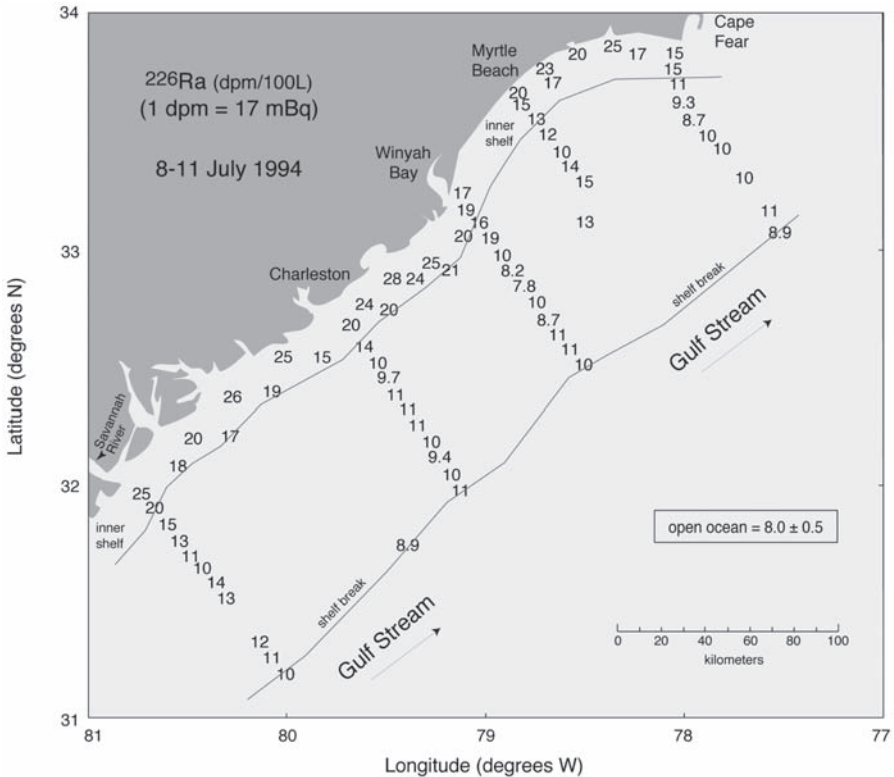


FIG. 1. The distribution of ^{226}Ra in surface water off the coast of South Carolina in July 1994. Note the strong concentration gradient between the inner shelf and the Gulf Stream. Adapted from [10].

RADIONUCLIDE TRACERS OF SUBMARINE GROUNDWATER DISCHARGE

rate of estuaries and coastal waters. Such estimates coupled with distributions of the long-lived Ra isotopes enable a direct estimate of radium fluxes. At steady state these fluxes must be balanced by fresh inputs of Ra to the system. If other sources of Ra can be quantified, the Ra flux that must be sustained by SGD can be evaluated. By measuring the Ra content of water in the coastal aquifers, the amount of SGD necessary to supply the Ra is determined. SGD fluxes of other components are determined by measuring their concentrations in the coastal aquifer or by determining relationships between the component and Ra and multiplying the component/Ra ratio by the Ra flux.

Moore [11] used the $^{228}\text{Ra}/^{226}\text{Ra}$ AR (activity ratio) to distinguish groundwater derived from the carbonate upper Floridan Aquifer (UFA) vs. the clastic surficial aquifer (SA) in samples collected from the Gulf coast of Florida. The results showed that most surface water samples fell along a mixing line having a $^{228}\text{Ra}/^{226}\text{Ra}$ AR = 2.5, indicating a surficial aquifer source. However, some offshore samples fell off this trend and toward a sample from an artesian well in the UFA. The low $^{228}\text{Ra}/^{226}\text{Ra}$ AR in the offshore plume indicated that the deeper aquifer was flushed slower than the near shore aquifer and/or that the $^{232}\text{Th}/^{230}\text{Th}$ AR of the solids was lower in the UFA. The $^{228}\text{Ra}/^{226}\text{Ra}$ AR in springs in the area showed that they were also influenced by the UFA source. Based on these data, Moore [11] developed a 3-endmember mixing model to assess the relative contributions of water from the open Gulf, the offshore UFA, and the near shore SA in the surface water samples. A result of the model was the presence of a significant and variable UFA component in the surface water.

A SGD intercomparison experiment in southern Sicily at Donnalucata compared estimates of SGD obtained from seepage meters, geochemical tracers, and hydrologic modeling. Springs from a limestone aquifer discharging on the beach and just offshore had a much lower $^{228}\text{Ra}/^{226}\text{Ra}$ AR than did shallow wells on the beach [12]. Samples collected in the near shore zone as well as samples collected in bags fixed to seepage meters fell between the isotopic compositions of these sources. Figure 2 illustrates the use of ^{228}Ra and ^{226}Ra in discerning these sources. Note that all of the beach wells and harbor seepage are elevated in ^{228}Ra with respect to the mixing line between the beach spring and the ocean. A mixing model based on these data revealed that approximately 80% of the flux was from diffuse sources rather than springs.

Charette and Buesseler [13] used a similar approach to distinguish between salt marsh derived groundwater and a shallow semi-confined aquifer in the Chesapeake Bay region. This study highlighted salt marshes as being particularly suited to the three-end member SGD approach, since the pore waters of the marsh sediments, which are repeatedly flushed on tidal time scales, are highly enriched in ^{228}Ra relative to ^{226}Ra compared with typical aquifer pore waters.

In some cases SGD in river-dominated areas can be significant but difficult to evaluate because of the high river-derived fluxes. Dulaiova et al. [6] used ^{222}Rn and radium isotopes (^{223}Ra , ^{224}Ra , ^{226}Ra , ^{228}Ra) to assess the magnitude of groundwater discharge in the Chao Phraya River and estuary (Gulf of Thailand). The isotopic results suggested that there are at least three different sources of these tracers in the estuary: river water, seawater, and groundwater. They estimated the extent of each input via a mixing model using ^{222}Rn , ^{223}Ra , and ^{224}Ra activities and $^{224}\text{Ra}/^{223}\text{Ra}$ A.R.. Their analysis showed that the largest groundwater outflow occurs near the mouth of the river. The estimated groundwater inputs represented about 20% of the river flow during low flow conditions (January) and 4% during high flow (July).

3.2. Radon

Other tracers also provide evidence of SGD and means to estimate the fluxes. The immediate daughter of ^{226}Ra , ^{222}Rn , is highly enriched in fresh and salty groundwater. High ^{222}Rn activities reveal regions of high SGD to coastal waters. Because ^{222}Rn can be measured continuously in situ, patterns of SGD

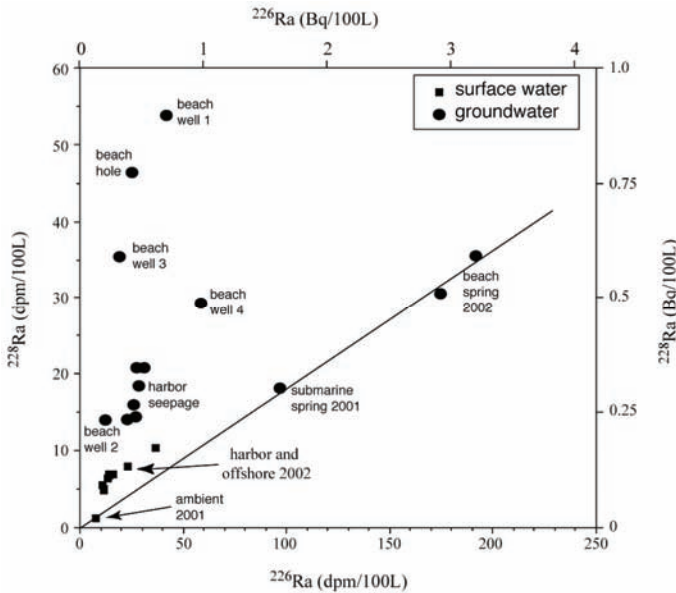


FIG. 2. Distribution of ^{226}Ra and ^{228}Ra in surface water and groundwater in Sicily. The data from the offshore springs follow a mixing line that is very different from the shallow beach groundwater. Surface water samples collected in 2002 reflect a contribution of each groundwater component. Adapted from [12].

RADIONUCLIDE TRACERS OF SUBMARINE GROUNDWATER DISCHARGE

through tidal cycles may be evaluated and compared to results from seepage meters. To estimate SGD fluxes via ^{222}Rn , losses to the atmosphere must also be considered.

The utility of ^{222}Rn as a tracer of SGD has been demonstrated in a wide range of environments from coastal embayments to the coastal ocean [14, 15, 16]. The very large enrichment of ^{222}Rn concentration in groundwater over surface waters (often 1000-fold or greater), its chemically unreactive nature, and short half-life ($t_{1/2} = 3.83$ d) make ^{222}Rn an excellent tracer to identify areas of significant groundwater discharge.

The approach for quantifying SGD using ^{222}Rn is similar to ^{226}Ra except: (1) ^{222}Rn loss to the atmosphere must be quantified, (2) there is no significant ^{222}Rn source from particles, and (3) decay must be accounted for owing to its relatively short half-life.

Atmospheric evasion is usually quantified using local wind speed measurements applied to theoretical gas exchange models. Experimental estimates of ^{222}Rn exchange with the atmosphere can also be made by evaluating the respective slopes of ^{222}Rn and ^{224}Ra in surface waters away from a common source of these radioisotopes. This works because ^{222}Rn and ^{224}Ra have very similar half-lives and are affected in the same manner by mixing processes, but only radon will emanate to the atmosphere. The common source could be SGD, river input, a hot spot of natural radioactive minerals or any localized enrichment of ^{222}Rn and ^{224}Ra . Dulaiova and Burnett [17] estimated the radon loss from surface waters in the Gulf of Thailand from the difference in the slopes of the ^{222}Rn and ^{224}Ra horizontal distributions across the inner shelf away from the mouth of the Chao Phraya River. The estimated gas exchange velocities based on their experimental results agreed well with theoretical models developed for lakes, estuaries and coastal systems.

3.3. Nutrient fluxes

A powerful use of the Ra-Rn SGD tracer has been its application to determine nutrient fluxes. The importance of coastal groundwater discharge in delivering dissolved nutrients, such as nitrate and phosphate, to coastal waters has often been overlooked, primarily because it is difficult to estimate [18, 19, 20]. The problem lies in the fact that SGD had been difficult to quantify using traditional methods such as seepage meters since the discharge is often patchy and may vary with time. Even if SGD is modest, dissolved nutrient concentrations in groundwater may be sufficiently high to have a significant impact on the nutrient budgets for receiving waters.

The approach via the radium tracer is relatively simple: the nutrient flux is the product of the Ra-derived SGD flux and the average nutrient concentration

in the groundwater endmember. An alternate approach is to multiply the nutrient/radium ratio in SGD by the radium flux. These studies must consider the potential nutrient transformations that may occur as water is discharged from the subterranean estuary. Studies should focus sampling on wells or temporary piezometers located as close to the point of discharge as possible.

In a study of the North Inlet, South Carolina, salt marsh system, Krest et al. [3] used the two long-lived Ra isotopes to determine nutrient mass balances for inorganic nitrogen and phosphorus. The calculated SGD-derived nutrient fluxes were such that the nutrient flux from the saline aquifer beneath the marsh was balanced by biological utilization and export to offshore waters. In addition, it was determined that this latter flux, when extrapolated to include other salt marshes along the coast, could be on par with riverine nutrient inputs to the coastal zone.

Moore et al. [21] examined SGD-derived nutrient fluxes on the southeastern US continental shelf using data from six monitoring wells located 15–20 km offshore. Some of the wells were set into a high permeability zone (HPZ) located ~2 m beneath the seabed; others were set into sand. A semi-diurnal cycle in temperature within the HPZ suggested that fluid was being exchanged with the overlying water column. The wells had a range of ^{226}Ra activity with a strong relationship between ^{226}Ra and both total dissolved nitrogen (TDN) and total dissolved phosphorous (TDP). Moore et al. [21] combined the $\text{TDN}/^{226}\text{Ra}$ and $\text{TDP}/^{226}\text{Ra}$ ratios in the wells with earlier estimates of ^{226}Ra flux to determine N and P fluxes from the seabed. When combined with the SGD fluxes to salt marshes estimated by Krest et al. [3], the resulting N and P fluxes from SGD clearly exceeded the sum of both riverine and atmospheric sources to waters on the continental shelf. Kim et al. [22] also used Ra isotopes to determine that SGD-derived silicate fluxes to the Yellow Sea were on the same order of magnitude as the Si flux from the Yangtze River, the fifth largest river in the world.

Hwang et al. [5] estimated SGD using a variety of tracers including ^{222}Rn and radium isotopes into Bangdu Bay, a semi-enclosed embayment on the Korean volcanic island, Jeju. Their estimated SGD inputs of $120\text{--}180 \text{ m}^3\cdot\text{m}^{-2}\cdot\text{yr}^{-1}$ are much higher than those reported from typical continental margins. The nutrient fluxes from SGD were about 90%, 20%, and 80% of the total input (excluding inputs from open ocean water) for dissolved inorganic nitrogen, phosphorus, and silica, respectively. The authors concluded that these excess nutrient inputs from SGD are the major sources of “new nutrients” to this bay and could contribute to eutrophication. Hwang et al. [23] took a unique approach to quantifying SGD and associated nutrient fluxes for Yeoja Bay, Korea. They solved simultaneous mass-balance equations for ^{226}Ra , ^{223}Ra , and dissolved silicate, which like Ra, also tends to have a strong groundwater

source. The resulting fluxes were an order of magnitude higher than previous studies in similar hydrogeologic environments suggesting that SGD was likely to play a significant role in the annual formation of harmful algae blooms in the offshore area of Yeolja Bay.

3.4. Metal fluxes

Several studies indicate that groundwater may contribute significant fluxes of trace metals to the oceans [24, 13, 8]. Charette and Buesseler [13] used radium isotopes to investigate the role of SGD in the delivery of copper to the Elizabeth River estuary, Virginia. They estimated that 730–1500 kg·yr⁻¹ of Cu may be derived from SGD. This flux was comparable with estimates of diffusive flux from benthic chambers, which highlighted the importance of considering advective inputs of trace metals through permeable sediments in addition to diffusive inputs from fine grained, less permeable sediments in coastal areas.

Windom et al. [8] reported a study of coastal waters of southern Brazil adjacent to a barrier spit that separates the Patos Lagoon from the South Atlantic Ocean. They used radium isotopes to quantify SGD advecting through coastal permeable sands and into the Atlantic. Measurements of dissolved iron in these beach pore waters were in the 1–180 µM range. This implied that there were large SGD Fe fluxes to coastal waters. Using mixing rates derived from the short lived Ra isotopes and dissolved Fe measurements in the coastal waters, they calculated a cross-shelf Fe flux from this 240 km coastline of 3.6×10^5 mol·day⁻¹, a flux equivalent to about 10% of the atmospheric flux to the entire South Atlantic Ocean.

Recently, the geochemical budget for uranium has been shown to be impacted by SGD. Unlike radium, uranium is enriched in seawater relative to groundwater. Uranium is typically conservative in oxic seawater where its oxidation state is +6 and it forms a strong complex with the carbonate ion [25]. As seawater circulates through the subterranean estuary, uranium may be removed if the conditions are reducing enough to convert U⁶⁺ to U⁴⁺. Such conditions frequently occur in organic-rich subterranean estuaries.

Several studies have documented uranium removal in subterranean estuaries. These include systems in Massachusetts [9], South Carolina [26], and southern Brazil [27]. The deficit of uranium in coastal waters may be an index of SGR into anoxic subterranean estuaries. It is likely that uranium removal in subterranean estuaries constitutes a significant sink in the global uranium cycle.

4. SUMMARY

We find evidence for the existence and importance of subterranean estuaries in the distribution of chemical tracers in the coastal ocean that must originate within coastal aquifers and enter the ocean as SGD. The tracer distribution in the coastal ocean provides a means of determining the exchange between the subterranean estuary and the coastal ocean. Studies of subterranean estuaries using tracers suggest that large volumes of water having chemical compositions very different from sea water or fresh groundwater enter the coastal ocean from these systems. Studies in systems worldwide demonstrate the importance of these unseen estuaries in supplying not only chemical tracers, but also nutrients and trace metals, to coastal waters. They may also constitute a significant sink for uranium.

REFERENCES

- [1] MOORE, W.S., The subterranean estuary: a reaction zone of ground water and sea water, *Mar. Chem.* **65** (1999) 111–125.
- [2] BURNETT, W.C., et al., Groundwater and pore water inputs to the coastal zone, *Biogeochem.* **66** (2003) 3–33.
- [3] KREST, J.M., et al., Marsh nutrient export supplied by groundwater discharge: Evidence from radium measurements, *Global Biogeochem. Cycles* **14** (2000) 167–176.
- [4] MOORE, W.S., Sources and fluxes of submarine groundwater discharge delineated by radium isotopes, *Biogeochem.* **66** (2003) 75–93.
- [5] HWANG, D. W., et al., Large submarine groundwater discharge and benthic eutrophication in Bangdu Bay on volcanic Jeju Island, Korea, *Limnol. Oceanog.* **50** (2005) 1393–1403.
- [6] DULAIIOVA, H., et al., Are groundwater inputs into river-dominated areas important? The Chao Phraya River — Gulf of Thailand, *Limnol. Oceanog* **51** (2006) 2232–2247.
- [7] SWARZENSKI, P.W., et al., Submarine groundwater discharge and its role in coastal processes and ecosystems, U.S.G.S. Open File Report (2004) 1004–1226.
- [8] WINDOM, H. L., et al., Submarine Groundwater Discharge: a Large, Previously Unrecognized Source of Dissolved Iron to the South Atlantic Ocean, *Marine Chem.* **102** (2006) 252–266.
- [9] CHARETTE, M.A., SHOLKOVITZ, E.R., Trace element cycling in a subterranean estuary: Part 2. Geochemistry of the pore water, *Geochim. Cosmochim. Acta* **70** (2006) 811–826.

RADIONUCLIDE TRACERS OF SUBMARINE GROUNDWATER DISCHARGE

- [10] MOORE, W.S., Large groundwater inputs to coastal waters revealed by Ra-226 enrichments, *Nature* **380** (1996) 612–614.
- [11] MOORE, W.S., Sources and fluxes of submarine groundwater discharge delineated by radium isotopes, *Biogeochem.* **66** (2003) 75–93.
- [12] MOORE, W.S., Radium isotopes as tracers of submarine groundwater discharge in Sicily, *Cont. Shelf Res.* **26** (2006) 852–861.
- [13] CHARETTE, M.A., BUESSELER, K.O., Submarine groundwater discharge of nutrients and copper to an urban subestuary of Chesapeake bay (Elizabeth River), *Limnol Oceanog.* **49** (2004) 376–385.
- [14] CABLE, J.E., et al., Estimating groundwater discharge into the northeastern Gulf of Mexico using radon-222, *Earth Planet. Sci. Lett.* **144** (1996) 591–604.
- [15] CABLE J.E., et al., Application of ²²²Rn and CH₄ for assessment of groundwater discharge to the coastal ocean, *Limnol Oceanog.* **41** (1996) 1347–1353.
- [16] CORBETT, D.R., et al., Radon tracing of groundwater input to Par Pond, Savannah River site. *J. Hydrol.* **203** (1997) 209–227.
- [17] DULAIOVA, H., BURNETT, W.C., Radon loss across the water-air interface (Gulf of Thailand) estimated experimentally from Rn-222-Ra-224, *Geophys. Res. Lett.* **33** (2006) doi:10.1029/2005GL025023.
- [18] JOHANNES, R.E., The ecological significance of submarine discharge of groundwater, *Mar. Ecol. Progr. Ser.* **3** (1980) 365–373.
- [19] NIXON, S.W., et al., Nutrients and the productivity of estuarine and coastal marine ecosystems, *J. Limnol. Soc. South Africa* **12** (1986) 43–71.
- [20] SIMMONS JR., G.M., Importance of submarine groundwater discharge (SGWD) and seawater cycling to the material flux across sediment/water interfaces in marine environments, *Mar. Ecol. Prog. Ser.* **84** (1992) 173–184.
- [21] MOORE, W.S., et al., Thermal evidence of water exchange through a coastal aquifer: Implications for nutrient fluxes, *Geophys. Res. Lett.* **29** (2002) doi: 10.1029/2002GL014923.
- [22] KIM, G., et al., Submarine groundwater discharge (SGD) into the Yellow Sea revealed by Ra-228 and Ra-226 isotopes: Implications for global silicate fluxes, *Earth Planet. Sci. Lett.* **237** (2005) 156–166.
- [23] HWANG, D.W., et al., Estimating submarine inputs of groundwater and nutrients to a coastal bay using radium isotopes, *Marine Chem.* **96** (2005) 61–71.
- [24] SHAW, T.J., et al., The flux of Barium to the coastal waters of the southeastern United States: The importance of submarine groundwater discharge, *Geochim. Cosmochim. Acta* **62** (1998) 3047–3052.
- [25] KOIDE, M., GOLDBERG, E.D., Uranium-234/uranium-238 ratios in sea water, *Prog. Oceanog.* **3** (1963) 173–177.
- [26] DUNCAN, T., SHAW, T.J., The mobility of rare earth elements and redox sensitive elements in the groundwater/seawater mixing zone of a shallow coastal aquifer, *Aquatic Geochem.* **9** (2003) 233–255.

MOORE

- [27] WINDOM, H., NIENCHESKI, F., Biogeochemical processes in a freshwater-seawater mixing zone in permeable sediments along the coast of Southern Brazil, *Marine Chem.* **83** (2003) 121–130.

STABLE ISOTOPES AS TOOLS FOR WATERSHED HYDROLOGY MODEL DEVELOPMENT, TESTING AND REJECTION

J.J. MCDONNELL¹
Water Resources Section,
TU Delft,
Netherlands

K.B. VACHE
Giessen University,
Germany

K.J. MCGUIRE
Plymouth University,
USA

A.B. MAZURKIEWICZ
Oregon State University,
USA

Abstract

Process representation in catchment model structure continues to be a vexing issue in hydrology. Complex hydrological descriptions at the hillslope scale have been difficult to incorporate within a catchment modeling framework due to the disparity between the scale of measurements and the scale of model sub-units. As a result, parameters represented in many conceptual models are often not physically-based or related to physical properties, and therefore cannot be established prior to a model calibration. While tolerable for predictions involving water quantity, when coupled with water quality simulations additional attention to transport processes, flowpath sources and ages is necessary. This paper examines how residence time may be used to explain process complexity and provide a simple, scalable evaluative data source for conceptual models at the catchment scale. We present a simple distributed hydrologic model along with a methodology to evaluate, through direct simulation, the residence time distribution of the model. A Monte Carlo framework is used to evaluate the identifiability of parameters and how values of mean residence time contribute to the evaluative process. Our results show that models that might otherwise be acceptable

¹ On leave from, Oregon State University, USA.

may be wholly rejected for an inability to capture residence time dynamics. This type of process-based rejectionist framework can be very helpful in the evaluation of conceptual models that include chemistry. Furthermore, the incorporation of soft, or highly uncertain and potentially qualitative data in model evaluation is a useful mechanism to bring experimental evidence into the process of model evaluation and selection, thereby providing a way to reconcile hillslope complexity with catchment scale simplicity.

1. INTRODUCTION

Conceptual models of catchment hydrology have proliferated over the past few decades [1]. These models have become valuable tools for water management problems (e.g., flood forecasting, water balance studies and computation of design floods) and in many ways, have become our de facto hydrological theory at the catchment scale. Increasingly, runoff models must meet new requirements to deal with problems of water quality (such as acidification, the development of Total Maximum Daily Loads (TMDLs), soil erosion, pollutant leaching, etc). When our conceptual models bridge water quantity with geochemical and ecological processes, they must incorporate more realism in the dominant flow pathways, storages and residence times of the conceptual model elements. This additional realism is necessary because contact time in the subsurface is a controlling feature of water quality [2]. Realistic water residence time within conceptual models is imperative. Despite these needs, hydrological modeling is faced by fundamental problems such as the need for calibration [3] and the equifinality of different model structures and parameter sets (i.e., the phenomenon that equally good model simulations might be obtained in many different ways) [4]. These problems are linked to the limited data availability, detailed process understanding, the natural heterogeneity of watersheds (e.g., [5–7]) and the procedures used for model testing [8, 9].

We assert that improvements in watershed-scale predictions will come when we devise new ways to capture process detail into more integrative measures (like a stream hydrograph). To date, experimentalists have not established measures that are both integrative and scalable. We argue in this paper that perhaps we have not made full use of the process understanding we have gained from our experimental work. Here, we build upon previous work from our group that has constrained parameterizations using additional experimental data sources such as tracers, groundwater levels, estimated saturation areas and other forms of soft data [10, 11]. More recently, we have described models that have focused on internal process dynamics and less on calibration-based schemes for reducing predictive uncertainty and in developing new model

descriptions that match the level of process understanding and available data [12]. In the present paper we explore further how to simplify observed hillslope process complexity at the small catchment scale to achieve parsimonious models that transcend spatial scales and represent dominant physical processes. We use residence time distribution (RTD) as a representation of the integrated hillslope and catchment scale response of diverse flow pathways, thus connecting process complexity with model simplification. Our overall approach is well outlined by Hooper [13] who indicated the need to incorporate the scientific method (ie. hypothesis generation, subsequent rejection, and from that the generation of new hypotheses) into catchment modeling. We apply a simple model that has the potential to explain observations – in this case discharge and distributed estimates of mean residence time (MRT).

This paper takes on the challenge of how we define model structures for catchment prediction. We use experimentally derived residence times to constrain parameterizations for storage in a conceptual rainfall-runoff model and provide a process basis for decisions regarding the complexity incorporated into the structure of the model. We argue that the incorporation of residence time estimates and their uncertainty into the model structure, may lead to better predictions of water and solute flux from hydrological models. We use the well-known Maimai watershed [14] as test-bed for these examinations. Our specific objectives in this paper are:

1. To propose, develop and apply a simple model designed to reflect the most basic first order controls on water flux at Maimai
2. To establish, within a Monte Carlo framework, the methodology and utility of direct simulation of water age within a relatively standard surface water catchment model
3. To evaluate the model as a hypothesis whose potential rejection is seen not as failure, but as significant progress

2. METHODS

2.1. Residence time theory

Water residence times are typically determined by black-box modeling of environmental tracers (e.g. ^{18}O and ^2H), in which input (rainfall) and output (discharge) tracer concentrations are used to estimate parameters of an assumed time-invariant distribution that represents the residence time [15]. The tracer composition of precipitation that falls on a catchment will be delayed by some timescale(s) according to its physical properties and current state. Explicitly,

the stream outflow composition at any time $\delta_{out}(t)$ consists of past inputs lagged $\delta_{in}(t-\tau)$ according to their travel time distribution $g(\tau)$ [15]:

$$\delta_{out}(t) = \int_0^{\infty} g(\tau) \delta_{in}(t-\tau) d\tau \quad (1)$$

where τ are the lag times between input and output tracer composition. This model is similar to the linear system approach used in unit hydrograph models; however, only tracer is considered here and thus, $g(\tau)$ represents the tracer transfer function. Equation 1 is only valid for systems at steady-state or when the mean flow pattern does not change significantly in time [15].

The convolution equation (1) must also include recharge weighting $w(t-\tau)$ so that the streamflow composition reflects the mass flux leaving the catchment [16]:

$$\delta_{out}(t) = \frac{\int_0^{\infty} g(\tau) w(t-\tau) \delta_{in}(t-\tau) d\tau}{\int_0^{\infty} g(\tau) w(t-\tau) d\tau} \quad (2)$$

The travel time or RTD or $g(\tau)$ describes fractional weighting of how mass (i.e. tracer) exists the system, which is equivalent to the probability density function (pdf) or transfer function of tracer in the stream. If the tracer is conservative, then the tracer RTD is equal to the water RTD. The definition of residence time herein is the time elapsed since the water molecule entered the catchment as recharge to when it exits at some discharge point (i.e. catchment outlet, monitoring well, soil water sampler, etc.). RTDs used in equation 1 are time-invariant, spatially-lumped characteristics of the catchment and thus describe average catchment behavior.

It is important to note that the timescale of the runoff response is different than the residence time because fluctuations in hydraulic head (the driving force in water flux) can propagate much faster than the transport of conservative tracer or individual water molecules. Thus, the timescales between the rainfall-runoff response and transport (i.e. residence time) are effectively decoupled. This partially explains why the majority of a stormflow hydrograph is composed of ‘old’ water even though runoff response to rainfall is often immediate.

2.2. Study site

The Maimai research catchments are a set of highly responsive, steep, wet watersheds on the west coast of the South Island of New Zealand. Maimai has a long history of hillslope hydrological research (see [14] for a complete review). Maimai M8 is the watershed examined in this study. M8 is a small 3.8 ha study catchment with short (<300 m) and steep (average 34°) slopes with local relief of 100–150 m. Stream channels are deeply incised and lower portions of the slope profiles are strongly convex. Areas that could contribute to storm response by saturation overland flow are small and limited to 4–7%. Mean annual precipitation is approximately 2600 mm, producing an estimated 1550 mm of runoff. The summer months are the driest; monthly rainfall from December to February averages 165 mm and for the rest of the year between 190 to 270 mm. On average, there are 156 rain days per year and only about 2 snow days per year. The M8 watershed is a textbook headwater research catchment: it is underlain by a firmly compacted poorly impermeable conglomerate and seepage losses to deep groundwater are negligible (estimated at 100 mm/yr based on 25 years of water balance data). In addition to being wet, the catchments are highly responsive to storm rainfall. Quickflow comprises 65% of the mean annual runoff and 39% of annual total rainfall. The period of record used for model simulation in this study was September–December, 1987. There were 11 major runoff events during this period with a maximum runoff of 6 mm/h.

A major difficulty in generalizing the Maimai perceptual model to other watersheds in the area or watersheds in other areas is the considerable heterogeneity of hillslope topography, soils, vegetation and most importantly, flowpath diversity. While the flow pathways to the stream are indeed complex at Maimai, as in other experimental watersheds, the residence times computed at the catchment outlet and internal to the hillslope show clear patterns of downslope aging. Stewart and McDonnell [16] showed that between-storm matrix water varied in age from approximately one week at the catchment divide to over 100 days at the main M8 channel margin. These are some of the shortest hillslope water residence times recorded in the literature and reflect the steep, wet, responsive nature of the catchment.

2.3. Hydrologic model structure

A simple, conceptual model structure was developed to correspond closely to the runoff generation processes that dominate in the Maimai catchments. The model represents a balance between a highly detailed conceptual model and the data available to support the numerical model. Our goal was to develop

a model with just enough complexity to provide estimates of the available measurements and residence times. Testing of this model structure against discharge and residence time measurements was then used to indicate whether additional complexity is warranted given the available data.

One of the first decisions in the development of model structure was the implementation of reservoir theory. The reservoir theory is based upon the understanding that there exists in the environment discreet units of space for which we can know volumes and fluxes, but that understanding the dynamics internal to those volumes would require more data than currently available. As a consequence of this lack of data, the reservoirs are often assumed to completely mix and can be combined, through fluxes to develop quasi-distributed simulations. The Maimai catchments are steep and are perennially wet, with the degree of saturation over 80 percent most of the year. In combination with the essentially impermeable bedrock, the climatology results in lateral water flow occurring in the transient saturated zone and moving under a gradient that is very well approximated by the topography. Measurements which have been used to develop this understanding have been distributed throughout the catchment, including upslope areas, through the use of wells and soil lysimeters. Given this level of detail, the reservoirs outlined within the model are distributed in space based upon a 10 m DEM. The volume of water within each reservoir is accounted for using the familiar continuity equation:

$$\frac{dV}{dt} = P + SS_{in} - ET - SS_{out} - SOF_{out} \quad (3)$$

where V is the specific volume of water in each reservoir (m), t is current time (days), P is the precipitation rate, ET is the evapotranspiration rate, K_d is the loss to groundwater (in this case set to the measured yearly average of 100mm), SS_{out} is the rate of subsurface outflow, SS_{in} the rate of subsurface inflow, and SOF_{out} is the output rate of saturation excess overland flow. An increase in water volume results in an increase in the depth of the saturated zone, and a corresponding decrease in storage of the unsaturated zones. These depths are characterized by model parameters representing soil depth (SD) and porosity (ϕ). Routing out of each reservoir and SS is based upon the multidimensional flow algorithm [17] (Equation 5). Transmissivity (T) is assumed to decline with depth as a power law, with the degree of decline modulated by the power law exponent (PLE). The decline is defined following from [18] as:

$$T(z) = \frac{K_s SD}{PLE} * \left(1 - \frac{z}{SD}\right)^{PLE} \quad (4)$$

where z is the depth to the water table measured from the soil surface. Subsurface flows (SS) follows from this equation as

STABLE ISOTOPES AS TOOLS FOR WATERSHED HYDROLOGY MODEL

$$SS_{i,j} = T_{i,j} * Slope_{i,j} \quad (5)$$

where subscripts indicate the multidimensional aspect of flow. We utilize calculated water surface elevations to determine slope in each direction. Infiltration is assumed to occur when the soil is not saturated, but when the saturation deficit reaches zero, infiltration cannot occur. In these instances, excess precipitation is ponded and subsequently delivered directly to the stream network as SOF. Existing data representing temperature based hourly ET estimates were read directly into the model during simulations. Instantaneous and complete mixing within each reservoir is assumed, and the unsaturated zone is not explicitly accounted for.

2.3.1. Conservative tracer: an additional state variable

Modeled tracer simulations were used to develop estimates of the MRT for simulations. The tracer model is similar to the hydrologic model, based upon reservoir theory and continuity. In this case, the model equation is defined as a mass balance of some arbitrary conserved tracer:

$$\frac{dM_t}{dt} = nC_e + tC_{in} - tC_t \quad (6)$$

where M_t is the tracer mass within the model unit, n is rainfall rate (m/d), C_e is the concentration of tracer in rainfall, t_{out} and t_{in} are the water flux rates out of and into the reservoir and C_{out} and C_{in} are the concentrations of tracer out of and into the reservoir (taken from the previous time). The incorporation of this model is designed to provide an ability to track the source of water within the model through time. Time source composition can be derived through clear assumptions about event and pre-event concentrations, and the standard 2 component mixing model. Geographic sources can be similarly tracked, but require that different tracers be 'applied' to different source areas.

2.3.2. Residence time

While unusual in the catchment modeling literature, the direct simulation of MRT within conceptual models, is well-established in the groundwater literature. The MRT can be derived by this concentration breakthrough and is defined as

$$MRT = \frac{\int_0^{\infty} tcdt}{\int_0^{\infty} cdt} \quad (7)$$

where c is breakthrough concentration and t is time. The numerator is the first moment (concentration weighted average) of the tracer distribution and the denominator is the zeroth moment, or total mass. At this point it is worth stating clearly that strictly speaking, the MRT defined by equation 6 is equivalent to that defined through convolution only when the direct simulation incorporates the same flowpath distribution as is incorporated by the isotope-based procedure (which is a top-down estimate of the true flowpath complexity within the catchment). The environmental tracers behind the convolution approach access the full catchment volume and more importantly is maintained within zones of essential immobility. Clearly, as a simplification, the catchment model would not be expected to incorporate that degree of heterogeneity. Our goal is evaluate the degree to which the simplification affects model residence time. If we can establish that the differences are highly significant, we can then successfully reject the model as a simulation of catchment chemistry due to over simplification, and use that as a sound basis to iteratively incorporate additional complexity.

3. RESULTS AND DISCUSSION

Input data at Maimai were available from September 3, 1987 – December, 30, 1987. While the period of record is suitable to establish reasonable discharge efficiencies, the 2 month isotope based residence times estimated by Stewart and McDonnell [16] for the watershed would likely not be reflected in a data record of this length. To adequately estimate the MRT, tracer breakthrough must be complete. To accommodate this longer timescale process, we doubled the record length by appending each dataset (20 minute rainfall and discharge and hourly ET estimates) to its end (Figure 1). The resulting 7 month simulation period provided enough time for complete tracer recovery, and estimates of MRT. The model was run under a Monte Carlo framework at a time step of 0.01 days, approximately 14.5 minutes, with data sampled for further analysis collected every 0.2 days (4.8 hours). 1750 total simulations were developed over a period of approximately 3 days. Initial soil saturation was assumed to be 50% and the first 30 days of simulation were allocated towards the stable redistribution of the initial conditions. Tracer application and the collection of error statistics occurred at the first time step on the 30th day of simulation. At that point in time, the concentration of tracer in soil water was set to 50 mg/L and no additional tracer was added to the system. Parameter data, efficiencies and MRTs were collected for simulations with Nash Sutcliffe efficiencies of untransformed efficiencies over 0.0. Time series data representing modeled discharge and tracer breakthrough for those simulations over 0.75 discharge efficiency were

STABLE ISOTOPES AS TOOLS FOR WATERSHED HYDROLOGY MODEL

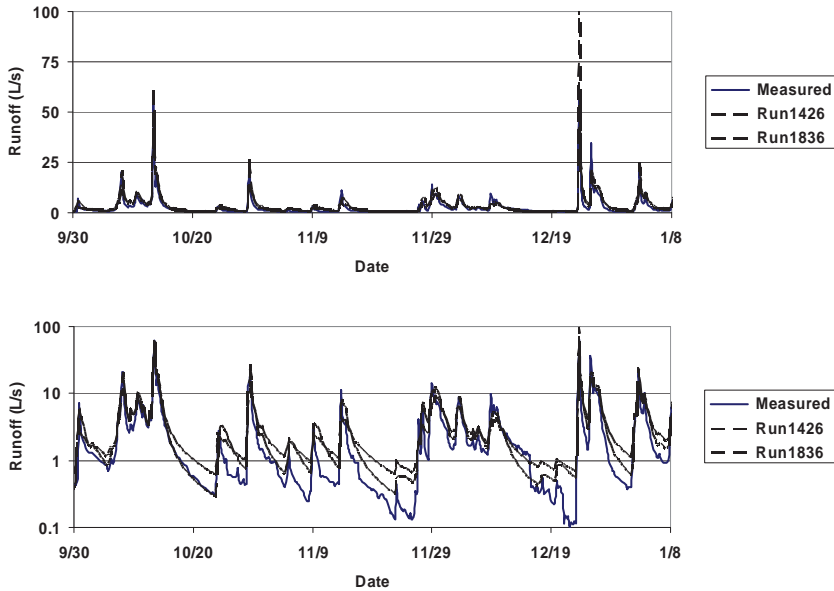


FIG. 1. Simulation results for stream discharge. The Y axis on the upper plate is log transformed to outline more clearly model failures at lower discharge. Calibration strategy focused on peak flows. The two simulations plotted as dashed lines represent the outside envelope of the 147 simulations found with Nash-Sutcliffe efficiencies over 0.75. Measured values are plotted as a solid line

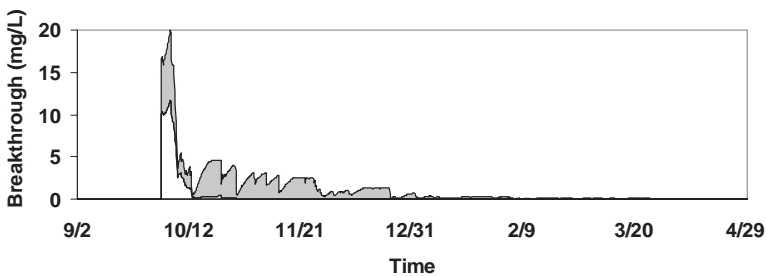


FIG. 2. Simulated tracer breakthroughs represented as an envelope incorporating data from all simulations with efficiencies over 0.75. All breakthrough curves occur within the plotted envelope. Maximum concentrations are not displayed as 50 mg/L due to the 0.2 day sampling period (with a 0.01 day simulation time step).

also collected and are represented in Figure 2. The initial concentration of tracer reported in the channel is less than the initial concentration of 50 mg/L because of rapid initial breakthroughs occurring prior to the first sampling step.

Nash Sutcliffe efficiencies of higher flows indicate that the model is capable of reproducing discharge in the catchment, even under the relatively restricted list of calibrated parameters. Maximum values of efficiency were 0.83. While low flow dynamics were clearly not as well represented (Figure 1 and the maximum efficiency), our use of untransformed discharge in the calculation of efficiency biased the results away from these values. Additional calibration using log transformed discharge may result in improved low flow estimates, but was not included in this analysis. As is common with conceptual models of this type, scatter plots of parameter value against efficiency indicates a significant degree of parameter uncertainty (Fig. 3). This lack of identifiability was most notable for the saturated hydraulic conductivity, for which the highest efficiencies could be established across the entire prior parameter range (Fig. 4). From the standpoint of storm discharges, we view these model simulations as acceptable. Given the number of parameters, and the tuning of three of them, this is not a surprising result. The next step is to evaluate the model against additional integrative criteria. In this case we utilize the unique MRT of each of the model simulations.

Directly simulated mean ages across the prior parameter range, varied from 30 to 95 days and results indicate a tradeoff between longer mean ages and discharge efficiency. Maximum efficiencies for the longer aged simulations dropped to a value of approximately 0.5. Parameter values versus efficiency are outlined in Figure 4, and indicate the importance of the storage term in this result. Lower porosities (in combination with the structure and other parameters) can successfully reproduce discharge characteristics, but result in short MRTs. An increase in total storage can result in longer residence times,

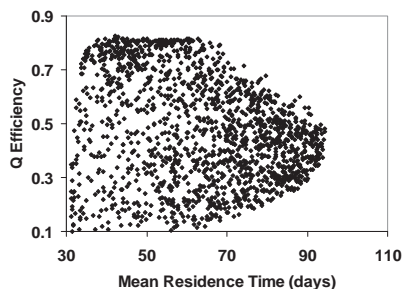


FIG. 3. Nash Sutcliffe discharge efficiency versus mean residence time. While modeled stream mean residence are always considerably less than measured values, a tradeoff exists between high discharge efficiency and longer, more realistic, residence times.

STABLE ISOTOPES AS TOOLS FOR WATERSHED HYDROLOGY MODEL

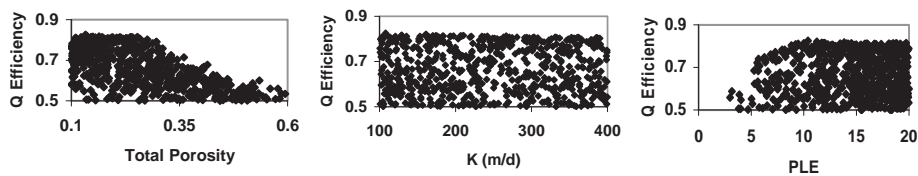


Figure 4. Monte Carlo results for the 3 tuned parameters.

but discharge simulations are negatively effected. This result, while not entirely unexpected, leads us to the conclusion that total available storage within the catchment is better approximated by models resulting in the longer MRT, but that this storage must be more variably allocated within the system.

While Figures 1 and 2 focused on stream water MRT, the distributed calculation of stocks and flows results in the estimation of MRT results at all discreet locations within the watershed. Stewart and McDonnell [16] developed a set of MRT values based on convolution of ^{18}O from an array of suction lysimeters in the northwest corner of the basin (Fig. 5). This work led to the hypothesis at Maimai that water ages in the downslope direction. Here we extended these data to the entire basin based on a 2 meter elevation grid from which we calculated the flowpath distance to the nearest stream channel, based on the single direction D8 algorithm. Flowpath lengths for each of the deeper suction lysimeters were collected and the simple linear relationship between flowpath length and water age was used to regionalize age estimates to the entire catchment. Results from the 2 m grid were averaged up to a 10 m grid to correspond in scale to model calculations (Fig. 5). We restricted the data to the deeper lysimeters that were representative of transient saturation because the hydrologic model does not explicitly simulate the vadose zone.

Distributed soil MRT were not collected for each of the high efficiency simulations, but were collected (subsequent to the Monte Carlo simulation) for a set of representative parameters. In this case we selected the set of parameters with the longest MRT for further examination. As suggested by Stewart and McDonnell [16], the direct simulations of MRT display increases in a characteristic fashion downslope, but MRT range is only approximately 4 days. This small directly simulated range is a direct reflection of the lack of spatial variability of the parameters. The distance from each reservoir (or grid cell) to the stream, along with local slopes, do vary in space. Given the explicit grid based routing scheme, this fact must result in some degree of downslope aging. However, porosities, soil depths, and other tunable model parameters were not varied in space. The choice to maintain spatial homogeneity of these parameters was justified if the results satisfactorily explained evaluative criteria. This was arguably the case if peak flows were the only criteria, but is

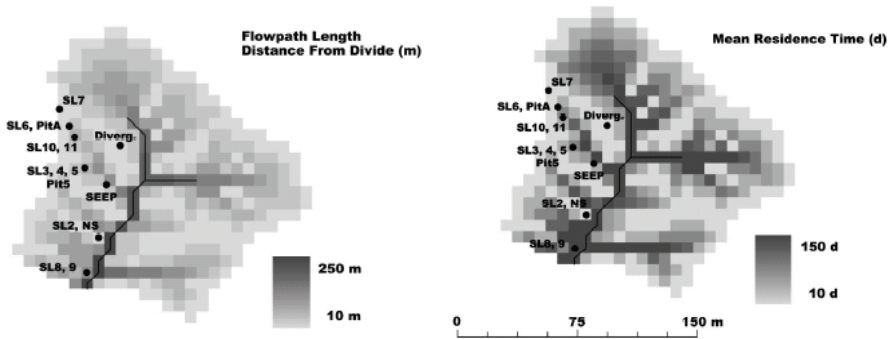


FIG. 5. Regionalized MRT based upon flowpath length: (left) calculated distance to the divide and (right) estimated MRT. While highly simplified, these regionalized data clearly indicate the relatively large range in residence times and the downslope aging. Approximate perennial channel network and suction lysimeter locations.

clearly not the case when looking at MRT. With this unambiguous rejection, along with the model's inability to capture both stream MRT and discharge dynamics with the same parameter set, the spatial variation of at least some of the model parameters is justifiable.

4. CONCLUSIONS AND OUTLOOK FOR THE FUTURE

Conceptual, physically based models are designed to reflect the main stocks and flows of water through catchments. A model that correctly captures discharge and water residence time is more realistic than one that captures only the former. More importantly, in some cases a model can perform reasonably well when evaluated for discharge alone, but additional compositional criteria can result in posterior rejection of the model structure itself. The incorporation of residence time into evaluation procedures is one mechanism to help understand the limitations of conceptual simulations of catchment hydrology, and to independently assess the need to incorporate additional process detail or heterogeneity.

Future work along these lines may include additional spatial variation in soil properties (parameters), the explicit inclusion of an immobile domain, an unsaturated zone model, and subsequent comparisons of the mobile versus immobile domains that will result. This list is not exhaustive, and other complexities, particularly for other basins and climate regimes, may also improve explanation of measured residence time parameters. Unavoidably, the

explicit incorporation of additional heterogeneity will lead to an increase in the number of parameters, but if we first reject the simpler versions as unable to explain observation, the additional complexity involved in the approach is fully justified.

ACKNOWLEDGEMENTS

This research was funded in part by USFS contract number PNW 02-CA-11261930-011 and by NSF grant EAR-0196381. We thank Jan Seibert, Markus Weiler and Brian McGlynn for useful discussions on Maimai and our conceptual model. This paper was originally written for a NATO Advanced Study Workshop on Hydrological Modeling.

REFERENCES

- [1] SINGH, V. P., Computer models of watershed hydrology. Highlands Ranch, CO, Water Resources Publications (1995).
- [2] BURNS, D.A., PLUMMER, L.N., MCDONNELL, J.J., BUSENBERG, E., CASILE, G.C., KENDALL, C., HOOPER, R.P., FREER, J.E., PETERS, N.E., BEVEN, K.J., SCHLOSSER, P., The geochemical evolution of riparian ground water in a forested piedmont catchment, *Ground Water* **41** (2003) 913–925.
- [3] DUAN, Q., SOROOSHIAN, S., GUPTA, V.K., Effective and efficient global optimization for conceptual rainfall-runoff models, *Water Resources Research* **28** (1992) 1015–1031.
- [4] BEVEN, K., How far can we go in distributed hydrological modelling? *Hydrology and Earth System Sciences* **5** (2001) 1–12.
- [5] BEVEN, K., WOOD, E.F., Flow routing and the hydrological response of channel networks, *Channel Network Hydrology*, K. Beven and M. J. Kirkby. Chichester, England, John Wiley & Sons, Ltd. (1993) 99–128.
- [6] O'CONNELL, P. E., TODINI, E., Modelling of rainfall, flow and mass transport in hydrological systems: an overview, *Journal of Hydrology* **175** (1996) 3–16
- [7] BRONSTERT, A., Capabilities and limitations of detailed hillslope hydrological modelling, *Hydrological Processes* **131** (1999) 21–48.
- [8] KIRCHNER, J.W., HOOPER, R.P., KENDALL, C., NEAL, C., LEAVESLEY, G., Testing and validating environmental models, *Science of the Total Environment* **183** (1996) 33–47.
- [9] MROCZKOWSKI, M., RAPER, G.P., KUCZERA, G., The quest for more powerful validation of conceptual catchment models, *Water Resources Research* **33** (1997) 2325–2335.

- [10] FREER, J.E., MCMILLAN, H., MCDONNELL, J.J., BEVEN, K.J., Constraining dynamic TOPMODEL responses for imprecise water table information using fuzzy rule based performance measures, *Journal of Hydrology* **291** (2004) 254–277.
- [11] SEIBERT, J., MCDONNELL, J.J., On the dialog between experimentalist and modeler in catchment hydrology: Use of soft data for multicriteria model calibration, *Water Resources Research* **3811** (2002) 1241, doi:10.1029/2001WR000978.
- [12] WEILER, M., MCDONNELL, J., Virtual experiments: a new approach for improving process conceptualization in hillslope hydrology, *Journal of Hydrology* **2851** 4 (2004) 3–18.
- [13] HOOPER, R.P., Applying the scientific method to small catchment studies: a review of the Panola Mountain experience, *Hydrological Processes* **15** (2001) 2039–2050.
- [14] MCGLYNN, B.L., MCDONNELL, J.J., BRAMMER, D.D., A review of the evolving perceptual model of hillslope flowpaths at the Maimai catchments, New Zealand, *Journal of Hydrology* 257 (2002) 1–26.
- [15] MALOSZEWSKI, P., ZUBER, A., Determining the turnover time of groundwater systems with the aid of environmental tracers. 1. models and their applicability, *Journal of Hydrology* **57** (1982) 207–231.
- [16] STEWART, M. K., MCDONNELL, J.J., Modeling base flow soil water residence times from deuterium concentrations, *Water Resources Research* **2710** (1991) 2681–2693.
- [17] WIGMOSTA, M.S., VAIL, L.W., LETTENMAIER, D.P., A distributed hydrology-vegetation model for complex terrain, *Water Resources Research* 30 (1994) 1665–1679.
- [18] IORGULESCU, I., MUSY, A., Generalization of Topmodel for a power law transmissivity profile, *Hydrological Processes* **119** (1997) 1353–1355.

TRITIUM/HELIUM-3 DATING OF BASEFLOW

Southern Vienna Basin

D.K. SOLOMON*, D. RANK**, P.K. AGGARWAL⁺, A. SUCKOW⁺,
T. VITVAR⁺, B. STOLP*

*Department of Geology and Geophysics,
University of Utah,
Salt Lake City, Utah,
USA

**Center for Earth Sciences,
University of Vienna,
Vienna, Austria

⁺Isotope Hydrology Section,
International Atomic Energy Agency,
Vienna

Abstract

Long-term time series of tritium in baseflow provide an indicator of the mean subsurface residence time (MRT) and hence a useful index of vulnerability/sustainability of surface water. Unfortunately, long-term time series are uncommon. We are investigating the use of tritium/helium-3 dating as a substitute for long-term time series in the Southern Vienna Basin, Austria. Preliminary results indicate that the apparent age of the water depends on sampling location. Apparent tritium/helium-3 ages range from about 2 to 12 years with the oldest water occurring at head-water springs. We have evaluated the exchange of helium-3 with the atmosphere by performing a gas tracer test and applying a gas exchange model. The model was then used to predict the observed change in the helium-3 (and hence apparent tritium/helium-3 age) with excellent agreement to observed values. This result suggests that while gas exchange is an active mechanism for noble gases in streams, it is possible to predict this exchange and hence “correct” tritium/helium-3 ages for this process.

1. INTRODUCTION

The mean residence time (MRT) of groundwater is a fundamental characteristic of a subsurface flow system. For example, the evolution of water

quality, the vulnerability of an aquifer to contamination, and the development of best management practices are all closely related to the mean residence time. Perhaps more importantly, the rate of recharge to an unconfined aquifer and the volume of water in storage are both directly proportional to the mean residence time [1]. Furthermore, as pointed out by [2], the MRT of groundwater is a remarkably robust attribute of a groundwater basin. In part, this is because the MRT is much more sensitive to fluid fluxes and the storage volume of the reservoir, than to the details of fluid movement within the system (i.e. fractured versus intergranular flow).

Potential approaches to estimating the MRT of baseflow include (1) tritium time series, (2) stable isotope time series, and (3) age dating. When the temporal variability of tritium (^3H) in precipitation (and recharge to groundwater) can be combined with temporal patterns of tritium in natural discharge areas (e.g. springs and streams at baseflow) the lag between peak input versus peak output values is a powerful method to evaluate the MRT of the system [3]. However, relatively few time series in baseflow are available making this method rather limited in scope. Stable isotopes of hydrogen and oxygen typically vary with season in precipitation and this time series can be measured in streams to provide an estimate of MRT. However, because longitudinal dispersion is typically large and the period of this input signal is typically 1 year, it can be difficult to derive a MRT greater than one year and typically it is impossible to quantify a MRT larger than about 4 years.

Precise groundwater dating using dissolved gases has become relatively common in recent years [4–6]. If groundwater ages were preserved in the baseflow of streams it might be possible to obtain flow-weighted mean residence time estimates even when long time series are not available. However, once groundwater discharges into streams, dissolved gases begin to equilibrate with the atmosphere. If gas exchange is rapid, one might expect stream water to fully equilibrate with the atmosphere and have a “modern” apparent age. Alternatively, if exchange is slow, a tracer signal might be present in streams. If the exchange could be estimated, it may be possible to interpret the tracer signal as an age or MRT.

The central hypothesis of this research is that gaining streams will not completely reach equilibrium with the atmosphere provided that the flux of non-modern groundwater can offset the rate of exchange with the atmosphere. We present results from a field study in the Southern Vienna Basin to test our hypothesis. Our results suggest that it may be possible to estimate the MRT and values for recharge and storage in an unconfined aquifer that provides water to streams. The integrated nature of such values makes them particularly useful for protecting groundwater resources and developing best management practices.

2. STUDY AREA AND METHODS

Samples for noble gases and have been collected from a gaining stream in the Southern Vienna Basin, approximately 35 km from the city of Vienna, Austria. Samples were collected from the Fischa-Dagnitz spring and in the 1st order stream that emerges at the spring. Fig. 1 shows the Fischa-Dagnitz study area. Stream discharge increases from about 50 L/s at the Fischa-Dagnitz spring to about 700 L/s 1.8 km downstream. Previous work [7] has shown that the likely source of water emerging at the spring is infiltration primarily from the Schwarza River with lesser amounts from the Pitten River both approximately 20 km to the south. Infiltration is into a gravel deposit that is of sufficient permeability that the Schwarza River does not flow beyond the infiltration section in mid to late summer. To the north of the infiltration section, perennial flow occurs in various gaining streams including the Leitha River. A diagram showing the infiltration section of the Schwarza River along with other hydrologic features is shown in Fig 2.

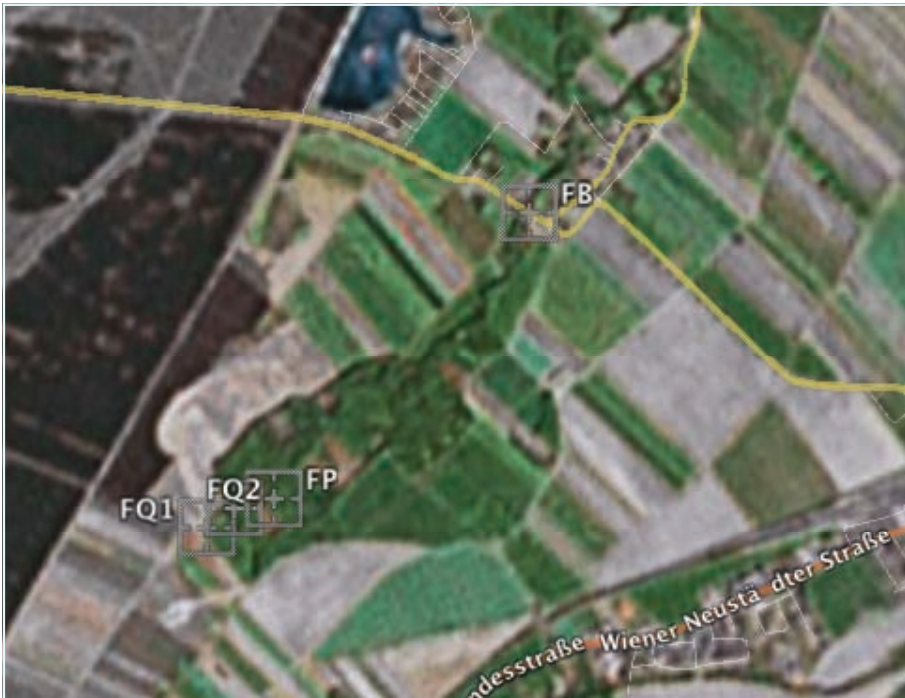


FIG. 1. Fischa-Dagnitz springs (FQ1 and FQ2), gauging station (FP), and highway bridge (FB) at the downstream end of the study area. The distance from FQ1 to FB is about 1.8 km.

Noble gas samples were collected using passive diffusion samplers. Gas from these samplers was inlet into a cryogenic cleanup system followed by analysis using a sector-field mass spectrometer for helium isotopes and a quadrupole mass spectrometer for neon, argon, krypton, and xenon isotopes. Recent tritium measurements were made at the Isotope Hydrology Laboratory of the IAEA. Apparent tritium/helium-3 ages were calculated using the method discussed by [8].

3. RESULTS

A long-term tritium record is available for the Fischa-Dagnitz as shown in Fig 3. Also shown in Fig. 3 is tritium in precipitation collected at Gloggnitz Austria. Peak values in precipitation occur in 1963 whereas the peak value at the spring is in the early to mid 1970s suggesting a lag time of approximately 10 to 12 years.

In 2007, noble gas and tritium samples were collected to obtain the apparent tritium/helium-3 age of the stream water. Samples were collected at various distances downstream from the Fischa-Dagnitz spring. As shown in Fig 4, apparent tritium/helium-3 ages range from 12 years near the spring to 2 years 1.8 km downstream.

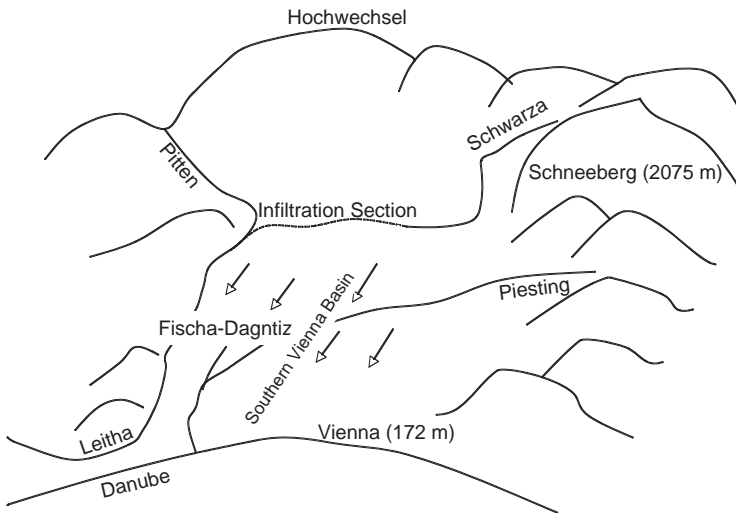


FIG. 2. Diagram showing the general hydrology of the Southern Vienna Basin. Note that diagram is looking to the south (i.e. north is as the bottom of the figure.)

TRITIUM/HELIUM-3 DATING OF BASEFLOW

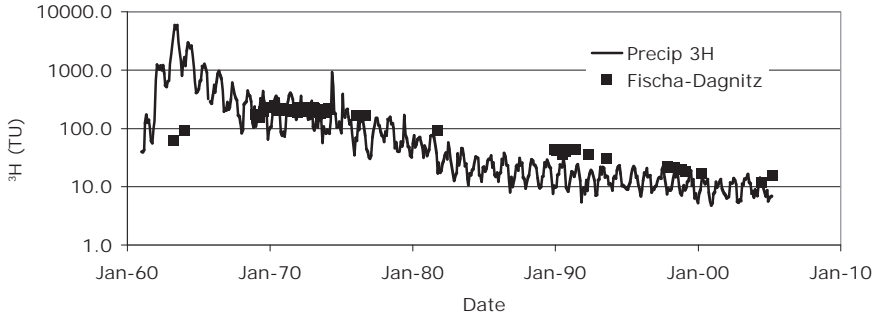


FIG. 3. Time series of tritium in precipitation at Gloggnitz Austria and at the Fischa-Dagnitz spring in the Southern Vienna Basin.

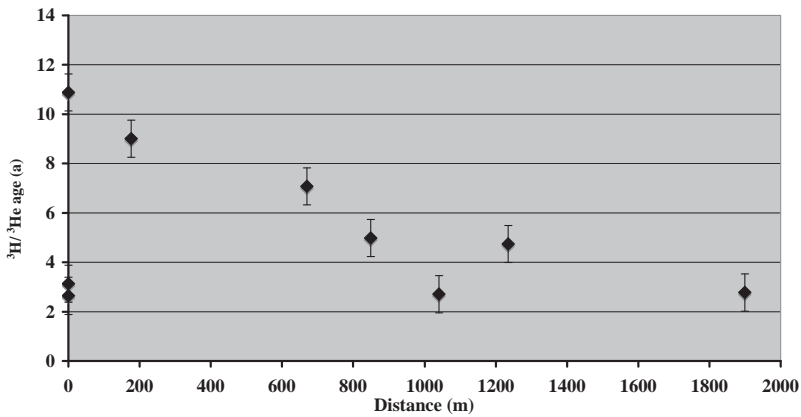


FIG. 4. Apparent tritium/helium-3 ages (year) at various distance downstream from the Fischa-Dagnitz spring.

There are several interesting aspects to the apparent tritium/helium-3 ages. First, it is clear that while helium-3 can (and is) lost to the atmosphere (thereby resetting the tritium/helium-3 clock), this loss is not complete even after nearly 2 km of travel in the stream. Second, the apparent age at the spring is variable depending on the exact location of the sample; however, the oldest apparent ages are similar to the travel time given by the long-term tritium record. In the remaining discussion we examine these issues in greater detail.

4. DISCUSSION

4.1. Gas Exchange

Fig. 4 shows the apparent tritium/helium-3 age as a function of distance downstream for the spring. The systematic decrease with distance downstream suggests that helium-3 is exchanging with the atmosphere causing the tritium/helium-3 clock to be reset. In order to evaluate gas exchange, we performed a gas tracer test by injecting helium and krypton into the stream. Fig. 5 shows the concentration of helium-4 both before and during this injection. Fig. 6 shows the concentration of krypton-84 before and during the injection. It is clear from both Fig. 5 and Fig. 6 that gas exchange reduces the stream concentrations, but even after nearly 2 km the water has not reached equilibrium with the atmosphere. This suggests that it may be possible to correct the stream concentrations of helium-3 in order to eliminate the effect of gas exchange on the apparent tritium/helium-3 age.

We have utilized a modified version of the OTIS (One-dimensional Transport with Inflow and Storage) simulator [9] to estimate the gas exchange parameters in the stream that give rise to the injected concentrations of the helium and krypton. The OTIS simulator accounts for advection and dispersion in the stream, the inflow of groundwater along the simulated section of the stream, mass exchange with pore waters in stream sediments, and exchange with the atmosphere. The gas transfer model assumes that the mass flux of dissolved gas is proportional to the concentration difference between the

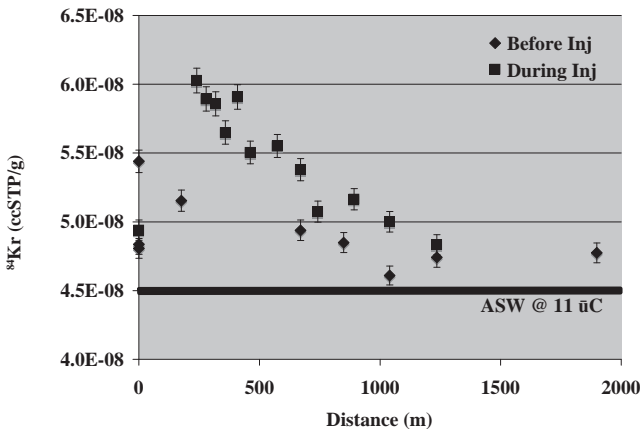


FIG. 5. Concentration of helium-4 versus distance downstream from the Fischa-Dagnitz spring before and during a gas tracer test. Also shown is the expected concentration for air saturated water (ASW) at the temperature and atmospheric pressure of the stream.

TRITIUM/HELIUM-3 DATING OF BASEFLOW

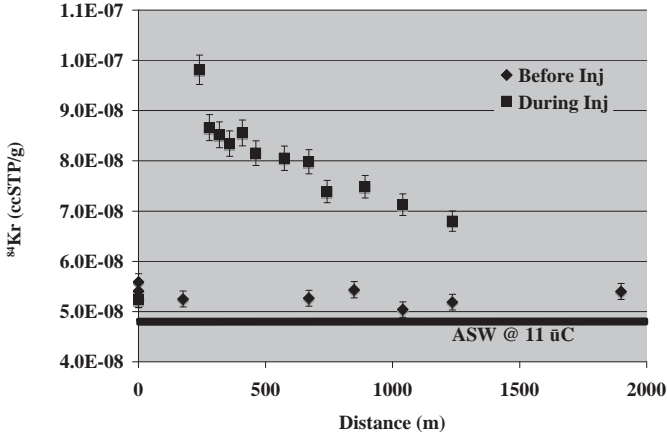


FIG. 6. Concentration of krypton-84 versus distance downstream from the Fische-Dagnitz spring before and during a gas tracer test. Also shown is the expected concentration for air saturated water (ASW) at the temperature and atmospheric pressure of the stream.

stream and the equilibrium value. The proportionality constant is the gas transfer velocity (units of length per time.) The gas exchange coefficient is given by the gas transfer velocity divided by the mean depth of the stream and has units of inverse time. The simulator requires a measure of groundwater inflow as a function of distance downstream in order to account for dilutions and/or additions of gas at locations downstream from the spring. We have utilized discharge measurement giving about 650 L/s of gain in the 1.8 km reach of the stream below the spring.

We adjusted the gas exchange coefficient for helium-4 and krypton-84 within the OTIS simulator to obtain a fit between observed and computed values as shown in Fig 7. A single value for gas exchange was used for the entire reach. The best-fit exchange coefficients are $6.5 \times 10^{-4} \text{ s}^{-1}$ and $2.0 \times 10^{-4} \text{ s}^{-1}$ for helium-4 and krypton-84. The corresponding gas transfer velocities are 61 cm/hr and 19 cm/hr.

According to gas exchange theory [10, 11], the relationship between the gas exchange coefficients (λ) for krypton and helium is

$$\frac{\lambda_{Kr}}{\lambda_{He}} = \left(\frac{D_{Kr}}{D_{He}} \right)^n \quad (1)$$

where D is the diffusion coefficient. The ratio of λ_{Kr} to λ_{He} that best fits both data sets is 3.25. By utilizing the krypton and helium diffusion coefficients ($1.2 \times 10^{-5} \text{ cm}^2 \text{ s}^{-1}$ and $5.8 \times 10^{-5} \text{ cm}^2 \text{ s}^{-1}$) from [11] along with Eq. 1, we calculate an exponent (n) of 0.77. According to gas exchange theory [11], an n value of

0.5 corresponds to turbulent flow conditions whereas a value of 1.0 corresponds to smooth flow at the air-water interface. Thus, the computed value of 0.77 seems reasonable for this system and implies that gas exchange is controlled mostly by molecular diffusion. Also, these results imply that while gas exchange in streams does occur, it is not instantaneous and thus it seems possible to correct tritium/helium-3 ages for this process if an independent estimate of the gas exchange coefficient is available.

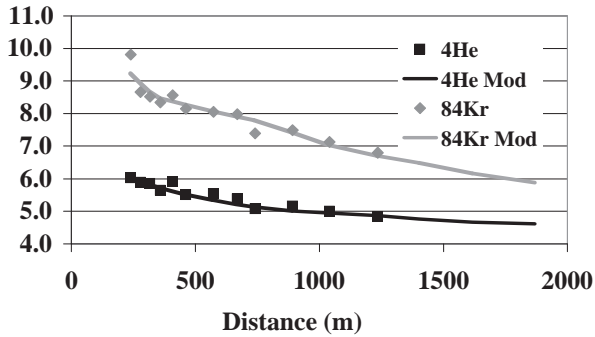


FIG. 7. Observed and simulated (using OTIS) concentration of helium-4 and krypton-84 injected downstream from the Fische-Dagnitz spring. The decrease downstream is due to gas exchange with an average gas transfer velocity of 61 cm/hr for helium-4 and 19 cm/hr for krypton-84.

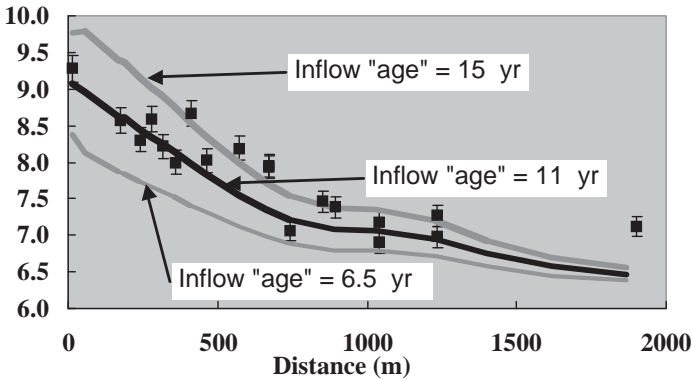


FIG. 8. Observed and simulated (using OTIS) concentration of helium-3 from the Fische-Dagnitz spring to 1.8 km downstream. The simulated values use different inflow concentrations that are equivalent to inflow ages of 15, 11, and 6.5 years; the best fit to the data is obtained with an inflow age of 11 years.

TRITIUM/HELIUM-3 DATING OF BASEFLOW

Having an independent estimate of the gas exchange coefficient from the gas tracer test, we have finally utilized the OTIS simulator to estimate the concentration (and hence apparent age) of helium-3 in groundwater that is discharging into the stream. Fig. 8 shows the fit between simulated and measured values of helium-3 for input concentrations that are equivalent to inflow ages 15, 11, and 6.5 years. The best fit of the data is obtained with an inflow age of about 11 years and has an uncertainty of about ± 2 to 3 years.

4.2. Tritium/helium-3 age versus long-term tritium time series

As discussed in the previous section, the concentration of helium-3 in baseflow of the Fischa-Dagnitz system is well explained by the exchange of helium-3 with the atmosphere using an exchange velocity that is consistent with the observed exchange of helium-4 and krypton-84 (after corrections for differences in diffusion coefficient.) The OTIS simulator utilized a helium-3 concentration for inflowing groundwater that is consistent with a tritium/helium-3 age of about 11 ± 3 years. By comparison, the long-term tritium record shown in Fig. 3 shows a lag that is about 12 ± 3 years. Thus, within the uncertainty of our measurements, the exchange corrected tritium/helium-3 age of baseflow is the same as the mean residence obtained from a long-term tritium record.

5. CONCLUSIONS

Tritium/helium-3 ages in the baseflow of a gaining stream decrease with distance downstream as a result of exchange with the atmosphere. However, this exchange is not instantaneous and appears to occur in a predictable manner such that a correction for this loss can be made. If samples are thoughtfully collected it is possible to capture most of the helium-3 signal. In the case of the Fischa-Dagnitz system the exchange is well estimated by performing a simple gas tracer test using helium-4 and krypton-84.

Apparent tritium/helium-3 ages collected directly from springs (before significant gas exchange is likely to occur), as well as the simulated concentration of helium-3 in dispersed groundwater that is discharging into the stream, are the same within uncertainty as the MRT determined using a long-term tritium time series. This study shows the potential for tritium/helium-3 dating to provide a powerful indicator of the MRT for groundwater that sustains the baseflow of rivers.

REFERENCES

- [1] COOK, P. G., BÖHLKE, J.K., Determining the timescales for groundwater flow and solute transport, in *Environmental Tracers in Subsurface Hydrology*, Eds. P.G. Cook and A. L. Herczeg,, Kluwer Academic Publishers, Boston (2000).
- [2] HAITJEMA, H.M., On the residence time distribution in idealized groundwatersheds, *J. Hydrology* **172** (1995) 127–146.
- [3] DINCERT., AL-MUGRIN, A., ZIMMERMANN, U., Study of the infiltration and recharge through the sand dunes in arid zones with special reference to the stable isotopes and thermonuclear tritium, *J. Hydrology* **23** (1974) 79–109.
- [4] BUSENBERG, W., PLUMMER, L.N., Use of chlorofluorocarbons (CCl₃F and CCl₂F₂) as hydrologic tracer and age-dating tools: the alluvium and terrace system of Central Oklahoma, *Water Resour. Res.* **28** (1992) 2257–2283, .
- [5] COOK, P. G., SOLOMON, D.K., Recent advances in dating young groundwater: chlorofluorocarbons, ³H/³He and ⁸⁵Kr, *J. of Hydrol.* **191** (1997) 245–265.
- [6] SOLOMON, D. K., COOK, P.G., ³H and ³He, in *Environmental Tracers in Subsurface Hydrology*, Cook and Herczeg, eds., Kluwer Academic Press (2000) 397–424.
- [7] RANK, D., PAPESCH, W., Determination of Groundwater Flow Velocity in the Southern Vienna Basin from Long-term Environmental Isotope Record, *Applied Environmental Geology* **228** (2003) 206-207.
- [8] SCHLOSSER, P., STUTE, M., SONNTAG, C., MÜNNICH, K.O., Tritiogenic ³He in shallow groundwater, *Earth Planet. Sci. Lett.* **94** 3/4 (1989) 245–254.
- [9] RUNKEL, R.L., One dimensional transport with inflow and storage (OTIS): A solute transport model for streams and rivers: U.S. Geological Survey Water-Resources Investigation Report 98-4018 (1998) 73.
- [10] WANNINKHOF, R., MULHOLLAND, P.J., ELWOOD, J.W., Gas exchange rates for a first-order stream determined with deliberate and natural tracers, *Water Resour. Res.* **26** 7 (1990) 1621–1630.
- [11] JAHNE, B., HEINZ, G., DEITRICH, W., Measurement of the diffusion coefficients of sparingly soluble gases in water, *J. of Geophys. Res.* **92** (1987) 10767–10776.

A DECADE OF ENVIRONMENTAL ISOTOPE RESEARCH IN A LOW PERMEABILITY AQUITARD SYSTEM

M.J. HENDRY

Department of Geological Sciences,
University of Saskatchewan

L.I. WASSENAAR

Environment Canada

Saskatoon, Saskatchewan,
Canada

Abstract

A decade of multi-isotope and hydrogeological research on a 160 m thick aquitard system has resulted in detailed, high-resolution profiles of stable and radiogenic isotopes (Tritium, δD and $\delta^{18}O$, ^{14}C -DOC and ^{14}C -DIC, ^{36}Cl , $\delta^{37}Cl$, 4He). The interpretations of these independent isotopic tracers reveal that late Pleistocene age porewater remains preserved in the aquitard between 35–55 m below ground. Transport modeling of isotopic profiles indicates this water was emplaced with the till upon deposition between 10 ka–20 ka BP, and that the late Holocene glacial-interglacial climatic transition occurred in this area between 7 ka–12 ka BP. Interpretation of the isotope profiles further shows transport of solutes in this aquitard is by molecular diffusion. These findings clearly demonstrate solute transport in homogeneous clay-rich aquitards is highly predictable over 20 ka and greater time scales. Long-term stability, plasticity, ease of access, and a high degree of confidence in transport predictability suggest thick aquitards could act as long-term repositories for the isolation and storage of hazardous and nuclear waste.

1. INTRODUCTION

Determining the residence times of porewater is critical for predicting the transport of contaminants in groundwater systems. In some cases, a rudimentary understanding of the hydrogeology (e.g., hydraulic conductivities, hydraulic gradients, porosities, and recharge rates) may be adequate for estimating residence times. However, a significantly greater level of confidence and accuracy in residence time determinations is required in situations where long-

term migration of contaminants is at issue. An increased confidence can only be attained by comparing and contrasting the results of physical hydrogeologic approaches with multiple, independent lines of evidence, especially isotopic tracer methods. Multiple, independent isotopic methods have been applied to relatively few regional aquifer systems, such as the well known Milk River aquifer in southern Alberta, Canada (c.f., [1]). In contrast, no comprehensive multi-tracer assessment approach to solute migration and residence times has been conducted in thick aquitards, despite their prevalence throughout the Northern Hemisphere and interest in their use as protective covers and for long-term waste repositories.

To date, the most commonly applied isotopic technique to examine solute migration and porewater residence time in aquitards has been the use of $\delta^{18}\text{O}$ and $\delta^2\text{H}$, whereby the distribution of these isotopes provides key information on groundwater flow, solute transport mechanisms, hydraulic conductivity (K), and the timing of climatic and geologic events [2–7]. These studies rely on the fact that water in glacially deposited aquitards originally had $\delta^2\text{H}$ and $\delta^{18}\text{O}$ values much lower than that of modern precipitation. However, detailed investigations using multiple, independent methods are few. In the past 10 years we applied a range of environmental isotopic methods to an archetypal surficial clay-rich till aquitard in Saskatchewan, Canada (King site; 51.09, -106.97). Multi-tracer studies included $\delta^2\text{H}$ and $\delta^{18}\text{O}$ [5, 8], $\delta^{37}\text{Cl}$ and ^{36}Cl [9], ^{14}C -DIC [10, 11], ^{14}C -DOC [12], ^4He [13], and $\delta^{81}\text{Br}$ [14]. In addition to these isotopes, detailed hydrogeologic [15–17] and geochemical [6, 18–27] studies have been conducted.

Here we provide a synopsis of independent and collaborative isotopic tracer research conducted at a single aquitard site over a 12-year period. The objectives of this paper are to describe the multi-isotopic and associated geochemical tracers with respect to: (1) defining the hydrodynamic age of the porewater, (2) estimating the timing of climatic or geologic events, (3) commenting upon the suitability of low permeability aquitards to contain contaminants over geologic time scales, and (4) identifying knowledge gaps for future aquitard research.

2. AQUITARD HYDROGEOLOGY

Four phases of drilling were carried out at the King site over the past 10 years, with collection of numerous core samples and installation of four sets of research grade piezometers (B-, BD-, BJ-, and BG-series). Cores were collected for geotechnical, geochemical, and isotopic analyses. Each piezometer series

was designed and constructed to meet specific experimental purposes and to avoid extrinsic contamination [23].

The near-surface geology at the King site consists of approximately 80 m of plastic, clay-rich, carbonaceous Battleford Till aquitard. The upper 3 to 4 m is oxidized and visibly fractured. The aquitard disconformably overlies 77 m of a late Cretaceous marine clay aquitard (Snakebite Member of the Bearpaw Fm; 72M–71Ma BP). The Snakebite is underlain by a regionally extensive sand aquifer (Ardkenneth Fm; 74.5M–72Ma BP). This aquifer forms the base of aquitard study (Figure 1).

Core samples collected between 11–15 m depth often contained a sand layer/streak within an overall fine-grained, clayey till matrix [17, 18]. Further, six piezometers installed after direct-push electrical conductivity (D-P EC) logging revealed these discontinuous sand streaks in 4 of 35 locations [18].

Hydraulic head was measured frequently in B-series piezometers between January 2001 and November 2004. Seasonal changes in water levels ranged from 2 m in the piezometer completed at 3.2 m to 0.4 m in the piezometer completed at 15.6 m deep. Water-level data in piezometers deeper than 22.7 m showed no seasonal fluctuations. The hydraulic gradient between 3.2 and 30.6 m depth was negligible at 0.0006 downward. The average hydraulic gradient, calculated from long-term static head distribution indicated downward vertical hydraulic gradients through the unoxidized till at 0.014 [17]. A peak in mean water-level elevation was observed at 15.6 m depth as a result of the discontinuous sand layers observed at about this depth. Based on water levels from three piezometers installed at the site prior to the start of our study (Christiansen, 1986; termed P-series piezometers) and regional data, the overall vertical hydraulic gradient thorough the Cretaceous clay was also downward but at a greater gradient than through the overlying till (0.6; [17]).

Hydraulic conductivities were determined from lab testing on core samples and water level responses in the piezometers. The matrix K of core samples were determined in the laboratory (K_1) using oedometer tests ($n = 17$), falling-head tests ($n = 4$), and constant-head triaxial tests ($n = 5$) [17]. No difference was found between test methods [17]. The geometric mean K_1 of the surficial aquitard was $2 \times 10^{-11} \text{ m s}^{-1}$. The geometric mean K_1 of the Cretaceous aquitard was $5 \times 10^{-12} \text{ m s}^{-1}$, almost an order of magnitude lower than that for the till. The K_1 reported for the clay was consistent with others [28] who report a geometric mean K_1 from constant head tests on till aquitard samples from 88 and 123 m depth ($5 \times 10^{-12} \text{ m s}^{-1}$, $n = 31$). Cores recovered from the sand layer yielded a K between 1×10^{-2} to $2 \times 10^{-2} \text{ m s}^{-1}$ [16].

Water-level recovery data from piezometers were used by [17] to estimate values of K for each piezometer (K_3) using the method of [29]. Routine measurements of water levels in these piezometers since 1995 were used to

recalculate K_s . The resulting K_s values were similar to those reported by [17]. The profile shows K_s is highest but more variable in the top 4–8 m depth. This was attributed to surficial fracturing. Between 10–15 m the value of K_s peaked at $\sim 5 \times 10^{-10} \text{ m s}^{-1}$ before decreasing to values $< 1 \times 10^{-10} \text{ m s}^{-1}$ throughout the remaining till. The peak in K_s at around 12–15 m depth corresponded to the sand streaks.

Groundwater flow in the upper oxidized till layer is dynamic and responds to spring snow melt and precipitation events, with the water table ranging from 0 to 3 m depth [17]. By contrast, the average downward porewater velocity through the unoxidized till and clay is between 0.5–0.8 m per 10 ka based on field determined K values and measured hydraulic gradients and porosity [17, 30].

3. ISOTOPE TRACERS OF WATER

3.1. Tritium

All piezometers completed in the unoxidized till were installed in “dry” boreholes. Over several years these piezometers slowly filled with water (reflecting their low K). Tritium (^3H) analyses were conducted on the first 500 mL of water entering piezometers in the unoxidized and unoxidized zones [30]. All values in the unoxidized till and clay were below detection level ($< 0.8 \text{ TU}$). However, water samples collected from the oxidized zone (2.3 and 2.8 m depth) were tritiated (12.4 and 9.2 TU, respectively), indicating the presence of post-1952 recharge water at shallow depths and emphasizing the dynamic nature of groundwater movement in this oxidized fractured zone.

3.2. Stable Isotopes of Water

Several sets of porewater δD and $\delta^{18}\text{O}$ analyses were conducted at the King site (1–13 occasions) between 1995 and 2006, and from domestic wells completed in the Ardkenneth aquifer. Comparative porewater water isotope analyses were also conducted using core samples and employing alternate techniques including radial cell diffusion [31] and direct porewater-equilibration [32].

All δD and $\delta^{18}\text{O}$ of porewater samples from piezometers and cores plot along the modern local Meteoric Water Line (MWL) (LMWL from June 1990 to February 2006 from L.I. Wassenaar). This confirmed the trend in $\delta^{18}\text{O}$ and δD with depth was not the result of evaporation or isotopic exchange with minerals, but due to diffusive mixing between modern and fossil porewaters [5, 7, 33]. The δD measurements versus depth are shown in Figure 1. A decrease

A DECADE OF ENVIRONMENTAL ISOTOPE RESEARCH

in δD values with depth was observed in the till reaching a minimum of -178‰ at 30 m. Between 30 and 46 m δD remained uniform at about -178‰ . The δD values increased across the till-clay interface to -144‰ at 105m. Below 105 m, the δD values in the clay and the underlying aquifer were constant at -144‰ .

The decrease in δD from near the water table to approximately 22 m is attributed to the rapid change in climatic conditions that occurred with the onset of the Holocene. The presence of low δD values ($< -175\text{‰}$) from 22 to about 60 m coupled with the low K of the till suggested this water was introduced into the till during its deposition during the late Pleistocene or shortly thereafter. The uniform δD values of -144‰ at depths greater than 105 m was attributed to post-depositional recharge. The δD profile between the clay (-144‰) and the till (-178‰) end members was attributed to long-term diffusive mixing from the clay into the till since deglaciation.

Initially, [5] used a simple 1D advection-diffusion model to with a laboratory determined value for the effective diffusion coefficient (D_e) for δD of $1.7 \times 10^{-10} \text{ m}^2 \text{ s}^{-1}$ to determine the time to simulate the isotopic profiles across the till-clay and from the water table to about 22 m depth for the King site. Best fits across the till-clay interface (Fig. 1) were obtained for a transport time (and hence an estimate of till deposition) of between 20 and 30 ka. Because

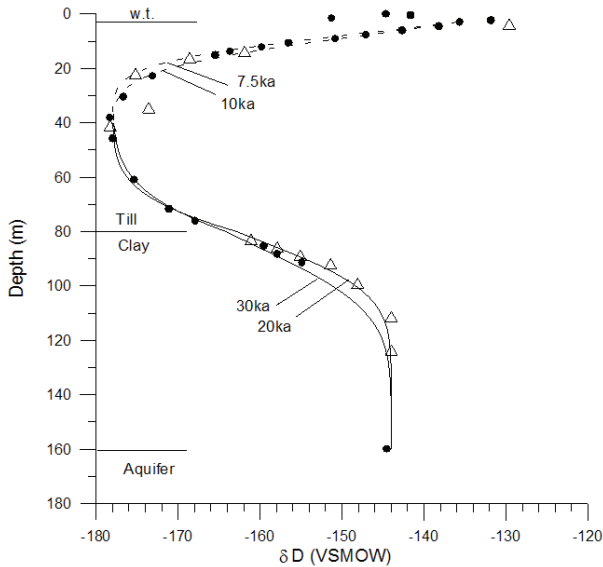


FIG. 1. Porewater δD values versus depth the B-series piezometers (solid circles; mean value) and core samples (direct equilibration and radial diffusion cells; open triangles). Best fit simulated diffusion transport profiles are presented as solid lines (after [5]).

of the presence of downward advection and upward diffusion of δD across the till-clay interface, best-fit simulated velocities of between 0.8 and 1.0 m per 10 ka were determined for the transport time period of 20 to 30 ka. In the case of the shallow δD profile, [5] obtained good fits (Figure 1) for a time of transport of between 7 and 10 ka, corresponding to the onset of the Holocene (modern precipitation). Bayesian inversion modeling of the $\delta^{18}O$ profile from the water table to 44 m [8] defines the onset of the Holocene at about 12 ka BP. This modeling also showed the onset of the Holocene occurred rapidly, but resolution of historic climatic variability (e.g., centennial scales) within the Holocene is not possible (i.e., Hypsithermal and Little Ice Age). Recently, [34] added a deuterium artificial tracer to several wells and determined the in situ D_e to be $3.5 \times 10^{-10} \text{ m}^2 \text{ s}^{-1}$. Using this value for D_e , the downward velocity through the till was determined to be 0.5–0.8 m/10 ka, the onset of glaciation to be between 15 and 20 ka BP, and onset of the Holocene to be between 5 and 8 ka BP.

3.3. Carbon-14 of DIC and DOC

Radiocarbon analyses were conducted on DIC and from high molecular weight (HMW) fulvic acids (DOC) from porewater [11, 12]. The HMW fraction of DOC was selected for ^{14}C analyses because it is considered geochemically inert, originates from the soil zone, and has been successfully used to estimate groundwater ages in aquifers [35, 36]. The ^{14}C -DIC and ^{14}C -DOC are presented in Figures 2 and 3. Both ^{14}C activities decreased with depth. The ^{14}C -DIC decreased with depth from post-bomb (109 pMC) values near the water table to background values of 3.2–4.9 pMC at 31 and 38 m depth. The ^{14}C -DOC decreased with depth, from 86.7 pMC at the water table (1.2 m depth) to background values of 14.6 and 13.2 pMC at 23 and 38 m depth.

Because the long-term migration of DIC could be simulated without invoking any geochemical carbonate reactions [6, 21] the ^{14}C -DIC activity is controlled solely by diffusion and radioactive decay [11]. Further, the apparent lack of biogeochemical redox and microbial activity in the unoxidized aquitard [6, 20] and lack of sorption and sieving of DOC [37] suggest ^{14}C activity in DOC is also solely controlled by diffusive transport and radioactive decay. As a result, the ^{14}C -DIC and –DOC activities from porewater samples collected from the glaciogenic zone in the till (where the activities attained their minimum background values) were applied to the simple form of the ^{14}C decay equation:

$$\text{age } (a) = -8267 \ln [A/A_o] \quad (1)$$

A DECADE OF ENVIRONMENTAL ISOTOPE RESEARCH

to estimate the age of DIC and DOC in the aquitard. In (1), A was the measured ^{14}C activity (3.2 and 4.9 pMC at 31 and 38 m depth for ^{14}C -DIC and 14.6 and 13.2 pMC at 23 and 38 m depth for ^{14}C -HMW) and A_0 was the initial ^{14}C content of the DIC and DOC at the time of till deposition. In both cases, A_0

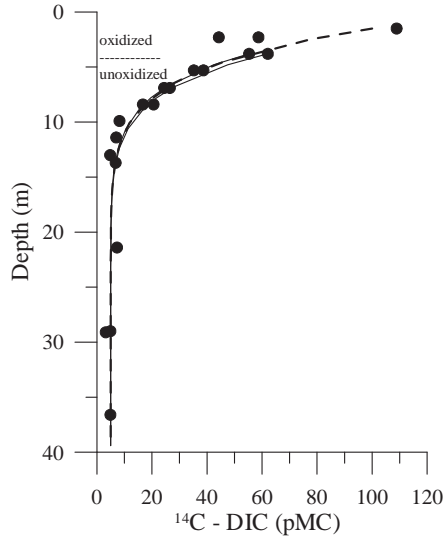


FIG. 2. ^{14}C -DIC measurements versus depth from B-series piezometers. Best fit simulated diffusive transport + radioactive decay are presented as solid lines (after [11]).

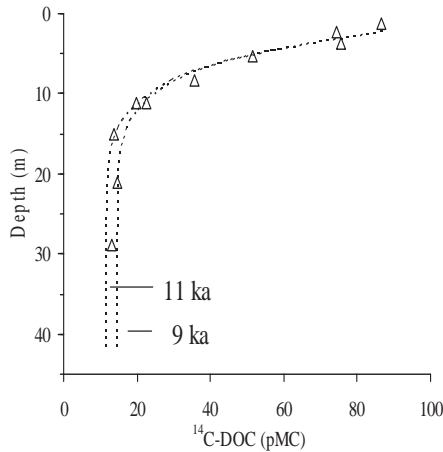


FIG. 3. ^{14}C -DOC measurements versus depth from B-series piezometers. Best fit simulated diffusive transport + radioactive decay are presented as solid lines (after [12]).

undoubtedly varied through glacial times. For ^{14}C -DIC, A_o could have ranged from 35 pMC [38] to >140 pMC [39]. For ^{14}C -DOC, the A_o was assumed to range between the ^{14}C specific activities observed in present-day recharge water at the site (87 pMC) and 100 pMC. Using these assumptions, the ^{14}C decay age associated with the glacial age water ranged between 15–31 ka BP and 15–17 ka BP for the ^{14}C - DIC and ^{14}C -DOC, respectively. Hendry and Wassenaar [12] suggest A_o values for ^{14}C -DIC of greater than 35 pMC were unlikely and the age of the glacial age water, based on ^{14}C -DIC, should be in the order of 15 ka. This age is in keeping with the ages estimated from the ^{14}C -DOC.

A diffusion transport model was used by [11] and [12] to evaluate whether observed ^{14}C -DIC and ^{14}C -DOC profiles could be modeled solely by diffusive transport from the oxidized till zone and radioactive decay. The best-fit results are in Figures 2 and 3. In both cases, the model fitted the data and showed ^{14}C profiles could be simulated with diffusion as the dominant transport mechanism and the depth trend could be attributed to the onset of soil development after deglaciation. The modeling of ^{14}C in DIC and DOC suggested the onset of soil organic carbon development following deglaciation occurred between 7 and 10 ka and 9 and 11ka BP, respectively (Figures 2 and 3), in good agreement with the water isotope model. Notably, conventional age-dating models based on piston-flow transport models are invalid under these diffusion-dominated conditions [11].

3.4. Helium-4

Concentrations of ^4He were measured in dissolved gases from B-series piezometers completed the till and clay, one domestic well in the Ardkenneth sand, and a surface runoff sample [13]. Overall, the helium data for all of the samples in the porewater profile revealed an exponential increase in concentration with depth (Fig. 4). Considering the higher ^4He concentrations measured in the Ardkenneth porewater sample, the observed profile of ^4He in the porewaters in the till and clay suggested upward diffusion of helium from the Ardkenneth and deeper formations. The dominant sources of ^4He in the clay and till included the upward diffusion of ^4He produced at depth greater than 160 m and the in situ release of ^4He from the clay and the till.

A diffusive transport model with an internal ^4He source term was used to model the observed changes in the dissolved ^4He profiles [13] assuming the measured ^4He concentrations were the result of diffusion dominated processes over time. Comparing the best fit modeled He profiles with the empirical ^4He data (Fig. 4) suggested residence times of 10 to 20 ka were required to produce the measured He profile in the till.

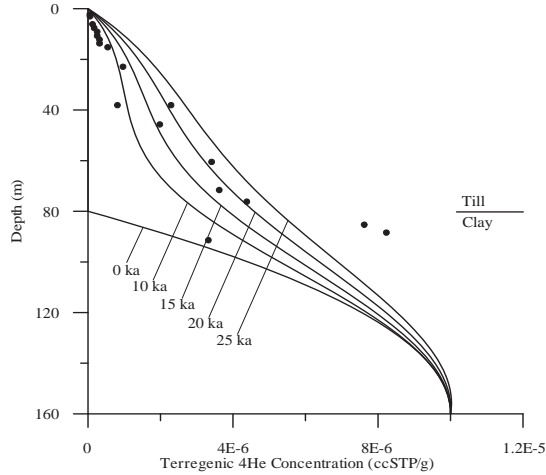


FIG. 4. ^4He measurements versus depth from B-series piezometers. Simulated diffusive transport + in situ production of radiogenic He are presented as solid lines (after [13]).

3.5. Chloride, $\delta^{37}\text{Cl}$ and ^{36}Cl

A synthesis of porewater Cl^- concentrations vs. depth from all four series of piezometers completed in the till are presented in Figures 5 and 6. The Cl^- profile exhibited an unusual but well defined spike in concentration between 10–20 m depth centered around the sand streaks. This trend was also observed in the $\delta^{37}\text{Cl}$ data (Fig. 5). The fact that no other isotopes or dissolved ions except Br (Fig. 5) exhibited peaks at this depth suggested the source water associated with the Cl^- peak underwent the same geochemical interactions as all other till porewater. Possible mechanisms for the Cl^- peak included: (1) salinity stratification in connate water at the time of till deposition, (2) evaporative concentration of rainfall at the ground surface during a period of higher aridity, and (3) off-site transport along the sand layers [9, 16]. This investigation suggested the Cl^- originated from an off site source area, likely to the north, and transported within the sand layer. The lack of a well-defined Cl^- trend with depth through the unoxidized till prevented its use to estimate the onset of weathering after deglaciation. However, based on 1-D solute transport modeling of the extent and shape of the peak between 4 and 13 m depth, [9] estimated the downward velocity to be about 1.5 m per 10ka. Further, near steady-state Cl^- concentrations at these depths existed for >2.5 ka (Figure 6).

^{36}Cl ($t_{1/2} = 3.01 \times 10^5$ yr) measurements were performed on dissolved Cl^- from nine B-series piezometers. The ^{36}Cl analyses are summarized in Figure

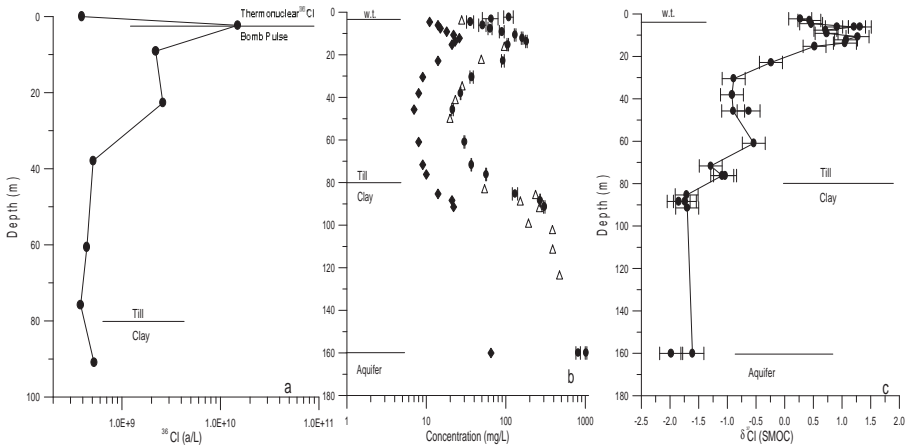


FIG. 5 Depth profiles of ^{36}Cl , Cl^- and $\text{Br}^- (\times 10)$, and $\delta^{37}\text{Cl}$ from the B-series (after [9]).

5 as concentrations of ^{36}Cl (a/L). In general, the $^{36}\text{Cl}/\text{Cl}^-$ ratios decreased with depth, whereas the ^{36}Cl concentrations remained relatively constant with depth. Tritiated porewaters within the oxidized till (see above) yielded $^{36}\text{Cl}/\text{Cl}^-$ ratios and ^{36}Cl concentrations of 3.7×10^{-12} to 7.2×10^{-12} and 3.9×10^8 to 1.5×10^{10} a/L, respectively, with the highest $^{36}\text{Cl}/\text{Cl}^-$ ratios and ^{36}Cl concentrations occurring at 2.2 m depth. The ^{36}Cl at this depth was of a similar magnitude to that expected for the levels of anthropogenic ^{36}Cl in groundwaters from thermonuclear bomb testing in the 1950's [40] and like tritium, defined the maximum depth of penetration of recent (post-1950) thermonuclear ^{36}Cl into the oxidized till.

The highest ^{36}Cl in the unoxidized till occurred at 9.3 and 22.7 m depth. The high ^{36}Cl value at 9.3 m was consistent with downward diffusive transport from the thermonuclear peak in the oxidized zone. The presence of high ^{36}Cl levels at 22.7 m, however, could not be attributed to downward diffusion from the oxidized zone but to a different source of ^{36}Cl in the porewater collected from this piezometer, in keeping with the presence of elevated Cl^- in this piezometer. The ^{36}Cl values throughout the remainder of the unoxidized till were largely invariant and similar to ^{36}Cl values measured in surface runoff. The ^{36}Cl levels of the porewaters from 30–76 m depth ($3.8\text{--}5.1 \times 10^8$ a/L) were similar to modern surface runoff (3.9×10^8 a/L) suggesting that little decay of ^{36}Cl occurred since the Cl^- was introduced into the till and that the Cl^- entered the till within the last 30 ka. ^{36}Cl was also measured on dissolved Cl^- collected from the Cretaceous clay at 91 m depth. $^{36}\text{Cl}/\text{Cl}^-$ ratios and ^{36}Cl concentrations for this porewater were 9.8×10^{-14} and 5.2×10^8 a/L. Using these data, [9] estimated the age of Cl^- in the porewater in the upper Cretaceous clay from 0.75 to 1.9 Ma.

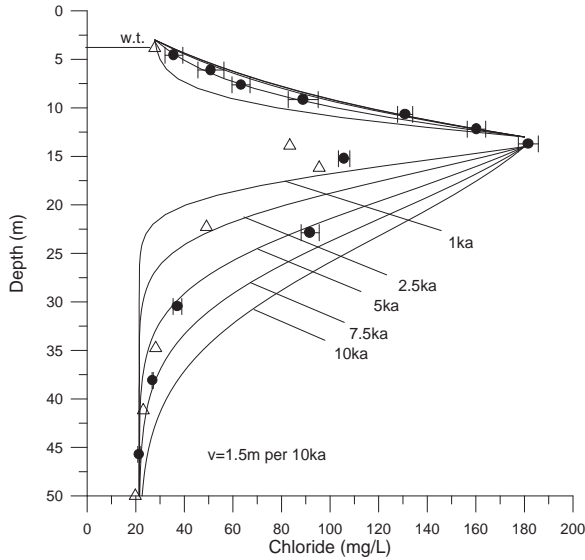


FIG. 6. Depth profiles of Cl from B-series piezometers in the upper 50 m of till. Best fit simulated diffusive transport for the Cl data are presented as a solid line (after [9]).

4. COMPARISON OF MULTI-TRACER AGES AND TIMING AND THEIR IMPLICATIONS

Following more than a decade of hydrogeologic and multi-isotope tracer research efforts, we show that solute transport in thick clay rich aquitards is almost universally controlled by molecular diffusion. This finding is supported by estimates of very low groundwater velocities through the till and clay from hydrogeologic data, and velocities determined from simulated best-fits to the δD profile across the till-clay boundary (Table 1). The discrepancies in velocities among these techniques are surprisingly minor, with velocities ranging from 0.5 to 1 m/10 ka. Most of the discrepancies among isotopic tracers can be attributed to unknown variability and assumptions in source, boundary and initial conditions. The similarity was unexpected given the velocity estimate for hydraulic data is based on recent hydraulic conditions in the aquitards, while in the case of the δD profile the estimated velocity represents aggregate conditions over tens of thousands of years.

Best-fit simulations for the δD and $\delta^{18}O$, ^{14}C -DIC and ^{14}C -DOC, and 4He profiles provide estimates of the time required for the individual isotopic profiles to develop. As the extent of various profiles are controlled by the timing of changes to boundary conditions and the D_e used in modelling,

these simulations yield our best estimates of the onset of: (1) till deposition (in the case of ^4He and δD), (2) the Holocene (δD), and (3) post glacial soils development ($^{14}\text{C-DIC}$ and $^{14}\text{C-DOC}$). Further, $^{14}\text{C-DIC}$, $^{14}\text{C-DOC}$ and ^{36}Cl measurements provide estimates of the age of the glaciogenic water in the till (between 23 and 38 m depth) and ^{36}Cl measurements were used to estimate of the age of the porewater near the top of the clay aquitard (91 m depth). These estimates are shown in Table 1. The $^{14}\text{C-DOC}$ age for the glaciogenic zone and the best-fit simulations for the development of the ^4He profile suggest the Battleford till was deposited on the clay between 10 and 20 ka BP (more likely 15 to 20 ka). This range in values is consistent with current estimates of the timing of the deposition of this till by [41] who determined the ^{14}C age on a sample of woody organic matter deposited below the Battleford till to be ~18ka BP. Although the range in $^{14}\text{C-DIC}$ ages for the glaciogenic water from [12] is great (15 to 31ka BP), it does bracket the known timing of till deposition. The broad range in $^{14}\text{C-DIC}$ ages can be attributed to a poorer understanding of its A_0 value than for $^{14}\text{C-HMW}$, as noted by [12] who suggest the $^{14}\text{C-DIC}$ age for

TABLE 1. SUMMARY OF INDEPENDENT ESTIMATES OF LONG-TERM GROUND WATER VELOCITIES (V), TIMING OF TILL DEPOSITION, AGES OF GLACIOGENIC WATER, AND THE ONSET OF THE POST-GLACIAL EVENTS¹

Profile	V	Till deposition	Post-glacial timing	Comment on post glacial-timing
hydrogeology	0.5–0.8			
δD^2	0.8–1.0	20–30	7–12	Onset of Holocene
δD^3	0.5–0.8	15–20	5–8	Onset of Holocene
$^{14}\text{C-DIC}$		15–31 (15 ⁶)	7–10	Development of soil zone
$^{14}\text{C-HMW}$		15–17	9–11	Development of soil zone
^4He		10–20		
Cl^-	1–2		>5 ⁴	
^{36}Cl		<30		
porewater chem ⁵			9	Development of soil zone

¹ All velocities are reported in m per 10 ka and timings are reported in ka BP

² using a laboratory determined D_e value for δD of $1.7 \times 10^{-10} \text{ m}^2 \text{ s}^{-1}$ [5]

³ using an *in situ* determined D_e value for δD of $3.5 \times 10^{-10} \text{ m}^2 \text{ s}^{-1}$ [34]

⁴ based on modeling of the Cl^- profile beneath the sand layer at 13 m depth.

⁵ from [6]

⁶ from [12]

the glaciogenic water is more likely about 15ka BP based on a reconsideration of A_0 . This value is in keeping with the results of ^{14}C -DOC and ^4He .

Best-fit simulations of the isotopic and chemical profiles that evolved from the top of the till aquitard and were associated with the onset of the Holocene and the development of a soil zone after deglaciation (δD , ^{14}C -HMW and -DIC) yielded internally consistent results with respect to the timing of the onset of the Holocene, suggesting it occurred between 7ka and 12ka BP. Simulations of depth profiles of major ions through the upper 45 m of till supported this determination, yielding estimates of the onset of geochemical changes attributed to the Holocene of about 9 ka BP [6] (Table 1). These values are in keeping with the development of Prairie soil zones prior to the Hypsithermal (ca. 7.5–5.0 ka BP) [42], knowledge of glacial retreat about 12,000 a BP [43], and the transition from cold climatic conditions of late Pleistocene to warm climatic conditions of the Holocene about 12,000 to 10,000 a BP [44].

Unlike the distribution of δD , ^{14}C -DIC and -DOC, the Cl^- and (other halides) and $\delta^{37}\text{Cl}$ exhibited atypical vertical profiles through the till, representative of the presence of the sand layer at about 13 m depth [9, 16]. This suggests the lack of deviation in one or more parameters from a well defined diffusive-depth trend cannot be used to rule out the presence of heterogeneity (e.g., a permeable sand layer), which could be an important consideration for solute transport.

The estimated timing of events using isotopic and hydraulic methods are in overall agreement. The small differences (about $\pm 25\%$) in ages between isotopic methods can be attributed at least in part to the D_e values used. This is exemplified by the differences in ages from the δD profile presented in [30] and [34] (Table 1). The sole difference between these models was the difference in the measured (laboratory vs. in situ) D_e values used. The difference between the two D_e values was small, differing by a factor of two. If more accurate estimates of ages are required, additional comparisons of D_e values determined for various solutes under both in situ and laboratory conditions are warranted.

Comparisons between the extensive data sets collected at the King site and data from other surficial clay aquitards in Canada suggest the diffusive transport conditions described for the King site are likely common in thick aquitards. Our findings clearly show that accurate prediction of the long-term migration of solutes through media is possible for time frames of up to 20 ka. As a result, clay-till aquitard systems may be promising candidates for long-term containment of contaminants, including hazardous and nuclear wastes.

ACKNOWLEDGEMENTS

Long-term financial support was provided by the Natural Sciences and Engineering Research Council of Canada and Cameco Co. Ltd. through the NSERC-Cameco Research Chair and by the Saskatchewan Potash Producers Association and Environment Canada. The assistance of numerous collaborators and students who contributed to the content of this paper is gratefully acknowledged.

REFERENCES

- [1] IVANOVICH, M., FROHLICH, K., HENDRY, M.J., Dating very old groundwater, Milk River Aquifer, Alberta, Canada, *Appl. Geochem.* (Special Issue) **6** 4 (1991) 367–472.
- [2] DESAULNIERS, D.E., CHERRY, J.A., Origin and movement of groundwater and major ions in a thick deposit of Champlain Sea clay near Montreal, *Can. Geotech. J.* **26** (1989) 80–89.
- [3] DESAULNIERS, D.E., CHERRY, J.A., FRITZ, P., Origin, age, and movement of pore water in argillaceous Quaternary deposits at four sites in southwestern Ontario, *J. Hydrol.* **50** (1981) 231–257.
- [4] FONTES, J.C.H., YOUSFI, M., ALLISON, G.B., Estimation of long-term, diffuse groundwater discharge in the northern Sahara using stable isotope profiles in soil water, *J. Hydrol.* **86** (1986) 315–327.
- [5] HENDRY, M.J., WASSENAAR, L.I., Implications of the distribution of deltaD in pore waters for groundwater flow and the timing of geologic events in a thick aquitard system, *Water Resour. Res.* **35** 6 (1999) 1751–1760.
- [6] HENDRY, M.J., WASSENAAR, L.I., Controls on the distribution of major ions in pore waters of a thick surficial aquitard, *Water Resour. Res.* **36** 2 (2000) 503–513.
- [7] REMENDA, V.H., VAN DER KAMP, G., CHERRY, J.A., Use of vertical profiles in delta18O to constrain estimates of hydraulic conductivity in a thick, unfractured till, *Water Resour. Res.* **32** (1996) 2979–2987.
- [8] HENDRY, M.J., WOODBURY, A.D., Clay aquitards ad archives of Holocene paleoclimate (in submission).
- [9] HENDRY, M.J., WASSENAAR, L.I., KOTZER, T., Chloride and chlorine isotopes (^{36}Cl and $\delta^{37}\text{Cl}$) as tracers of solute migration in a thick, clay-rich aquitard system, *Water Resour. Res.* **36** 1 (2000) 285–296.
- [10] WASSENAAR, L., ARAVENA, R., FRITZ, P., “Radiocarbon contents of dissolved organic and inorganic carbon in shallow groundwater systems”, *Isotope Techniques in Water Resources Development (Intl. Symp. Vienna, 1991)*.

A DECADE OF ENVIRONMENTAL ISOTOPE RESEARCH

- [11] WASSENAAR, L.I., HENDRY, M.J., Mechanisms controlling the distribution and transport of ^{14}C in a clay-rich till aquitard, *Ground Water* **38** 3 (2000) 343–349.
- [12] HENDRY, M.J., WASSENAAR, L.I., Origin and migration of dissolved organic carbon fractions in a clay-rich aquitard: ^{14}C and $\delta^{13}\text{C}$ evidence, *Water Resour. Res.* **41** (2005) W02021.
- [13] HENDRY, M.J., KOTZER, T., SOLOMON, D.K., Sources of radiogenic helium in a clay till aquitard and its use to evaluate the timing of geologic events, *Geochim. Cosmochim. Acta* **69** 2 (2005) 475–483.
- [14] VENGOSH, A., HENDRY, M.J., Chloride-bromide-delta 11B systematics of a thick clay-rich aquitard system, *Water Resour. Res.* **37** 5 (2001) 1437–1444.
- [15] BOLDT-LEPPIN, B.E.J., HENDRY, M.J., Application of harmonic analysis of water levels to determine vertical hydraulic conductivities in clay-rich aquitards, *Ground Water* **41** 4 (2003) 514–522.
- [16] HARRINGTON, G.A., HENDRY, M.J., ROBINSON, N.I., The impact of permeable conduits on solute transport in aquitards: mathematical models and their application, *Water Resour. Res.* (in press).
- [17] SHAW, J., HENDRY, M.J., Hydrogeology of a thick clay till and Cretaceous clay sequence, Saskatchewan, Canada, *Can. Geotech. J.* **35** 6 (1998) 1041–1052.
- [18] HARRINGTON, G.A., HENDRY, M.M., Chemical heterogeneity in diffusion-dominated aquitards, *Water Resour. Res.* **41** 12 (2005) doi:10.1029/2004WR003928.
- [19] JOHANNESSON, K.H., HENDRY, M.J., Rare earth element geochemistry of groundwaters from a thick till and clay-rich aquitard sequence, Saskatchewan, Canada, *Geochim. Cosmochim. Acta* **64** 9 (2000) 1493–1509.
- [20] LAWRENCE, J.R., et al., Distribution and Biogeochemical Importance of Bacterial Populations in a Thick Clay-Rich Aquitard System, *Microb. Ecol.* **40** (2000) 273–291.
- [21] TIMMS, W.A., HENDRY, M.J., Quantifying the impact of cation exchange on long-term solute transport in a clay-rich aquitard, *J. Hydrol.* **332** 1–2 (2007) 110–122.
- [22] TIMMS, W.A., HENDRY, M.J., Long-term reactive solute transport in an aquitard using a centrifuge model, *Ground Water* (in press).
- [23] WASSENAAR, L.I., HENDRY, M.J., Improved Piezometer Construction and Sampling Techniques to Determine Pore Water Chemistry in Aquitards, *Groundwater* **37** 4 (1999) 564–571.
- [24] YAN, X., HENDRY, M.J., KERRICH, R., Speciation of Dissolved Iron(III) and Iron(II) in Water by On-Line Coupling of Flow Injection Separation and Preconcentration with Inductively Coupled Plasma Mass Spectrometry, *Anal. Chem.* **72** (2000) 1879–1884.

- [25] YAN, X., et al., "Controls on the REE geochemistry of pore-waters in a till aquitard." The Geological Association of America (Ann. Meet. Salt Lake City, 1997).
- [26] YAN, X., KERRICH, R., HENDRY, M.J., Trace element geochemistry of a thick till and clay-rich aquitard sequence, Saskatchewan, Canada, *Chem. Geol.* **164** (2000) 93–120.
- [27] YAN, X., KERRICH, R., HENDRY, M.J., Distribution of arsenic(III), arsenic(V) and total inorganic arsenic in porewaters from a thick till and clay-rich aquitard sequence, Saskatchewan, Canada, *Geochim. Cosmochim. Acta* **62** 15 (2000) 2637–2648.
- [28] CEY, B.D., BARBOUR, S.L., HENDRY, M.J., Osmotic flow through a Cretaceous clay in southern Saskatchewan, Canada, *Can. Geotech. J.* **38** (2001) 1025–1033.
- [29] HVORSLEV, M.J., Time-lag and soil permeability in groundwater observations, (W.E.S. U.S. ARMY CORPS OF ENGINEERS, Ed.) Vicksburg, MS (1951).
- [30] HENDRY, M.J., LAWRENCE, J.R., MALOSZEWSKI, P., Effects of velocity on the transport of two bacteria through saturated sand, *Ground Water* **37** 1 (1999) 103–112.
- [31] VAN DER KAMP, G., VAN STEMPOORT, D.R., WASSENAAR, L.I., The radial diffusion method, 1. Using intact cores to determine isotopic composition, chemistry, and effective porosities for groundwater in aquitards, *Water Resour. Res.* **32** 6 (1996) 1815–1822.
- [32] KOEHLER, G., WASSENAAR, L.I., HENDRY, M.J., An automated technique for measuring $\delta^2\text{H}$ and $\delta^{18}\text{O}$ values of pore water by direct CO_2 and H_2 equilibration, *Anal. Chem.* **72** (2000) 5659–5664.
- [33] REMENDA, V.H., CHERRY, J.A., EDWARDS, T.W.D., Isotopic composition of old ground water from Lake Agassiz: Implications for late Pleistocene climate, *Science* **266** (1994) 1975–1978.
- [34] REIFFERSCHIED, L., In situ measurement of the coefficient of molecular diffusion in a fine grained till, MSc Thesis, University of Saskatchewan, Saskatoon (2007).
- [35] MURPHY, E.M., et al., ^{14}C fractions of dissolved organic carbon in ground water, *Nature* **37** (1989) 153–155.
- [36] WASSENAAR, L.I., et al., Organic Carbon Isotope Geochemistry of Clayey Deposits and Their Associated Porewaters, Southern Alberta, *J. Hydrol.* **120** (1990) 251–270.
- [37] HENDRY, M.J., et al., Geochemical and transport properties of dissolved organic carbon in a clay-rich aquitard, *Water Resour. Res.* **39** 7 (2003) 9–1 to 9–10.
- [38] WASSENAAR, L., et al., Radiocarbon in Dissolved Organic Carbon, a Possible Groundwater Dating Method: Case-Studies from Western Canada, *Water Resour. Res.* **27** 8 (1991) 1975–1986.

A DECADE OF ENVIRONMENTAL ISOTOPE RESEARCH

- [39] BARD, E., et al., ^{230}Th – ^{234}U and ^{14}C dates obtained by mass spectrometry on corals, *Radiocarbon* **35** (1993) 191–199.
- [40] BENTLEY, H.W., PHILLIPS, S.M., DAVIS, S.N., “ ^{36}Cl in the Terrestrial Environment”, *Handbook of Environmental Isotope Geochemistry* (FRITZ, P., FONTES, J.C., Eds.) Elsevier Science, New York (1986) 422–475.
- [41] CHRISTIANSEN, E.A., “Till in southern Saskatchewan, Canada”, *Till: A symposium* (GOLDTHWAIT, R.P., Ed.) The Ohio State University Press, Columbus, OH (1971).
- [42] SAUCHYN, D.J., A reconstruction of Holocene geomorphology and climate, western Cypress Hills, Alberta and Saskatchewan, *Can. J. Earth Sciences* **27** (1990) 1504–1510.
- [43] CHRISTIANSEN, E.A., Pleistocene stratigraphy of the Saskatoon area, Saskatchewan, Canada: an update, *Can. J. Earth Sci.* **29** (1992) 1767–1778.
- [44] GRIP_MEMBERS, Climate instability during the last interglacial period recorded in the GRIP ice core, *Nature* **364** (1993) 203–207.

VARIATIONS IN THE ISOTOPIC COMPOSITION OF NEAR SURFACE WATER VAPOUR IN THE EASTERN-MEDITERRANEAN

D. YAKIR, A. ANGERT, J.R. GAT
Department of Environmental Sciences
and Energy Research,
Weizmann Institute of Science,
Rehovot , Israel

Abstract

While the isotopic composition of precipitation is widely used in Global Climate Change studies, the use of water vapour isotopes is considerably more limited. Observations of the isotopic composition of atmospheric water vapour are important for four main reasons: (1) It is not limited only to rainy days. (2) Isotopic information contained in newly formed raindrops is scrubbed during rainout. (3) It is the principal tracer of water vapour sources, critical for eco-hydrology. (4) It is a key parameter in the estimating the isotopic enrichment in leaf water, and therefore in the application the oxygen isotopic composition of CO₂ and O₂ as a tracer of land vegetation activities. Here we present preliminary results from 9 years of atmospheric vapour measurements at a site in Israel. The measurements show firstly that our sampling station is representative of large spatial coverage. Secondly, that explaining the observed pronounced seasonal cycle requires three-dimensional consideration of local air turbulence and mixing patterns over the daily and seasonal cycles. Thirdly, a temporal trend in the vapour data over the sampling period is shown to reflect variations in sampling time, which is sensitive to daily planetary patterns in boundary layer mixing. The results demonstrate that even a single long-term monitoring station represent large spatial coverage and can provide much needed information on the controls over variations in the isotopic composition of water vapour across spatial and temporal scales.

1. INTRODUCTION

The stable isotope composition of atmospheric waters is potentially a useful tracer of the water cycle; in particular in identifying the source of the water and quantifying the atmospheric water balance as a result of the precipitation—re-evaporation processes. Further, based on the isotopic composition in climate proxies (such as ice cores, speleothems, cellulose or lake sediments) and aided

by atmospheric circulation models, a reconstruction of palaeo-climate conditions and calibration of the predictive models can be made.

With a few exceptions, our knowledge about the atmospheric water's isotope composition is based on measurements on precipitation provided by the GNIP programme and a few other local networks. While these data are of great value in specifying the input into the terrestrial water systems, they are quite deficient for the purpose of documenting the atmospheric waters because precipitation occurs only selectively in time and space, especially so in more arid zones, or where it has a marked seasonality such as in the Mediterranean Sea area. Furthermore only in the case of some precipitation conditions, namely fog deposition or moderate rainfall in the temperate zone, there is a clear (thermodynamic equilibrium) relationship between the isotope composition of the precipitation and that of the air mass. In many other cases, namely during snow fall, strongly convective systems or when there is a partial evaporation from droplets below the cloud base, the isotopic composition of the precipitation as measured at ground is an inadequate measure of the atmospheric waters' isotope composition.

The stable isotopologues of water (H_2^{16}O , HD^{16}O , H_2^{18}O , H_2^{17}O) have different saturation vapour pressures, and different diffusion rates, so the isotopic composition of precipitation integrates the effects of these processes over the life cycle of water in the atmosphere. The processes acting over this life cycle include evaporation at the surface, vertical and lateral transport and mixing in the atmosphere, recycling by ecosystems, in situ condensation and evaporation during cloud processes, and removal as rain or snow [1]. Insights into these processes can be gained by studying the isotopic composition of atmospheric water.

The stable isotopes ratios are usually presented in the normalized "delta notation" ($\delta^{18}\text{O}$, δD , where $\delta = \frac{R_{\text{sample}}}{R_{\text{standard}}} - 1$ in ‰, R is $^{18}\text{O}/^{16}\text{O}$ for $\delta^{18}\text{O}$ or $^2\text{H}/^1\text{H}$ for δD , and the standards is V-SMOW), and an additional important variable, termed deuterium excess (d) is calculated from the relationships between $\delta^{18}\text{O}$ and δD , and is defined as: $d = \delta\text{D} - 8 \times \delta^{18}\text{O}$ [2]. The deuterium excess is mainly determined by relative contribution of kinetic versus equilibrium isotopic exchange, which in turn depends on rates of evaporation, and in low temperature on the super saturation in ice formation. While interannual variations in climate and precipitation are compiled and well documented (for the time period 1870-present (e.g. [3]), there is a shorter (1961-present) and much sparser record of precipitation isotopes, and almost no record of the isotopic composition in atmospheric water vapour. The principal and comprehensive source of contemporary water isotope observations is the IAEA/WMO Global Network of Isotope in Precipitation (GNIP; IAEA 2001; <http://www.iaea.org/water>).

Studies of isotopes in precipitation in Israel started in 1960 [5, 6] and continue, with varying temporal and spatial resolutions, to date [7–11]. Vapour sampling at a single site was performed systematically from January 1969 to the end of October 1970 [12], and from December 1997 until present (Gat, Yam, and Yakir, unpublished results).

Precipitation in Israel occurs primarily during the winter months and is characterized by a d-excess value larger than that of the GMWL, close to $d = 20\text{‰}$ on the average. At the GNIP station Bet-Dagan for the period of 1961-1990, with a seasonal average precipitation of 543 ± 164 mm, the amount-weighted average of the isotopic composition of precipitation was $\delta^{18}\text{O} = -4.70 \pm 0.60\text{‰}$ ($\delta^{18}\text{O} = -5.15\text{‰}$ for the mid-winter months of December to March) [5]. Whereas there is a residual correlation of the data with the amount of precipitation, both in monthly and annual averages, it is often masked by the large scatter due to other causes. It was found, however, that an important factor for the isotope composition of the precipitation (both the δ -values as well as that of the d-excess) is the synoptic history of the air masses concerned [8, 10], including the rainout history along the flow path. Local rain intensity did not have a strong effect on its isotopic composition [9].

Most of the previous work discussed above, focused on isotopes in precipitation, and to a much smaller extent on water vapour isotopes near the surface. Observations of the isotopic composition of tropospheric water vapour are rare [4, 13, 14], but are important for three main reasons: (1) It is not limited only to rainy days. (2) Isotopic information contained in newly formed raindrops is lost during rainout. (3) It is the principal tracer of water vapour sources, critical for eco-hydrology. (4) It is a key parameter in the estimating the isotopic enrichment in leaf water, and therefore in the application the oxygen isotopic composition of CO_2 and O_2 as a tracer of land vegetation activities.

2. METHODS

Air was pumped by a vacuum pump from the building rooftop through an inverted funnel (i.e. facing the ground to prevent moisture intake), through a 6 mm OD plastic tubing (Bev-A-Line) and through a 10 mm OD Pyrex spiral cold trap (70 mL volume) immersed in ethanol–dry ice slush at about -80°C . Flow rate was 4 L/min, and moisture was collected in the trap for 5–9 hours starting at 8AM. At the end of the sampling period the trap was sealed at its two ends and warmed to room temperature. Water was mixed across the trap before decanting into a 5 mL vial and sealed. A similar system was also used on campaign basis to collect atmospheric water vapour at the top (19 m, 5 m above sparse canopy) of a flux measurement tower at the Yatir site [15].

An aliquot of 0.5 mL of each water sample was placed in a 7 mL tube, degassed under vacuum to 10^{-5} Torr, and 250 Torr of known CO_2 was added for equilibration. Equilibration was carried out over night at 29.5°C on a shaker and CO_2 was then cryogenically collected and sealed in a Pyrex tube for the isotopic analysis using automatic manifold on a Finnigan MAT 250 mass spectrometer. In the last couple of years, ^{18}O analysis was carried out by pyrolysis at 1500°C (Heckateck high temperature furnace) connected on-line to an Optima (GV, UK) IRMS for the isotopic analysis of the CO produced. Every other sample was also used for hydrogen isotopic composition. Aliquot of $2.8\ \mu\text{L}$ was added with 90 mg Zn (super dried) into a dry tube connected to a vacuum line. After degassing, the tube was sealed and heated to 497°C for 60 in and cooled to room temperature before isotopic analysis on the same mass spectrometer. Precision of the isotopic analysis was 0.1‰ and 1‰ for oxygen and hydrogen respectively.

3. RESULTS AND DISCUSSION

3.1. Site representativeness

To test the representativeness of our long-term roof-top data collection site, campaign-based short term comparison with data was obtained at an additional field site about 80 km east of the coast line (vs ~ 15 km for the permanent sampling site). Figure 1 shows that significant day to day variations in the vapour isotopes were similar in both sites and closely correlated with

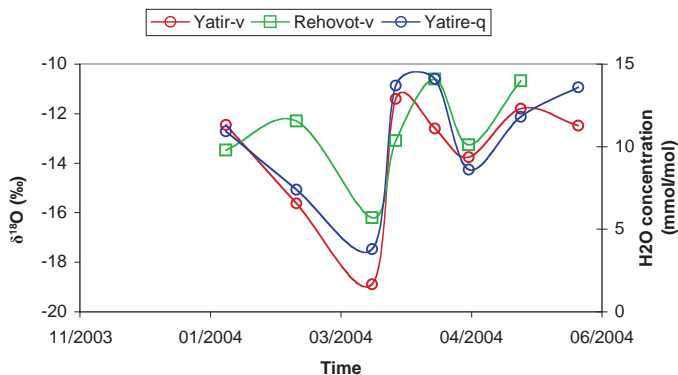


FIG. 1. Comparison of the $\delta^{18}\text{O}$ of atmospheric vapour obtained in the rooftop sampling site in Rehovot (~ 15 km east of the Mediterranean coastline) and at the Yatir field site ~ 80 km east of the coastline in southern Israel. Variations in the atmospheric moisture content during the campaign at Yatir are also reported.

variations in the local atmospheric moisture content. This clearly indicated that the our long-term sampling site at Rehovot provided information on the mixed planetary boundary layer and was not very sensitive to small-scale local effects. In addition, we used an isotope enabled GCM of Lee et al. [14] at $2.815^\circ \times 2.815^\circ$ resolution to show that capture well the hydrological cycle seasonality and patterns in the region. Comparing the grid cell centered on our sampling site with the regional grid cells, the model showed (data not shown) correlations of $r > 0.8$ in the seasonal timescale over the entire Mediterranean regions and correlation of $r > 0.7$ between interannual variability in the local grid-cell and the rest of the EM. These results further indicate that measurements of vapour isotopic composition in a single site have useful implication for understanding variations in isotopic composition of the vapour over a large area.

In the first stage of our study, five years of systematic vapour sampling, in part within the framework of the IAEA CRP on the “Isotopic composition of precipitation in the Mediterranean Basin in relation to air circulation patterns and climate”, established the patterns dictating the isotope composition, δ values and d-excess, in the atmospheric vapour. The isotopic composition of the vapour samples undergo the marked seasonal cycle noted before [12], with $\delta^{18}\text{O}$ values between -13‰ and -9‰ and the d-excess of $5\text{‰} \leq d \leq 22\text{‰}$ in summer. Winter values were more scattered ranging between $-10\text{‰} \leq \delta^{18}\text{O} \leq -18\text{‰}$ and with d-excess values up to $+40\text{‰}$. The data from spring and autumn follow a trend line between these two seasonal values. Samples from the rainy days show the most extreme values.

The results are summarized on a plot of d-excess vs. $\delta^{18}\text{O}$ in Figs. 2–5. The overall trend line for all samples is given by:

$$\delta D = (5 \times \delta^{18}\text{O} - 18.5)(\text{‰}) \quad (r^2 = 0.60)$$

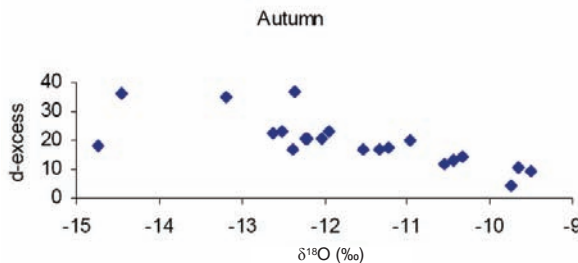


FIG. 2. Values of d-excess vs. $\delta^{18}\text{O}$ in water vapour collected at Rehovot during Autumn period.

which translates into the linear correlation: $d = -(3 \times \delta^{18}\text{O} + 18.5)(\text{‰})$. A weak temperature dependence of the data ($r^2 = 0.34$) is obviously a reflection of the seasonal pattern rather than pertaining to the individual samples.

In addition to the overriding control of the origin of the air-masses as well as its rainout-history (which applies primarily during the winter period), the measured values apparently reflect, as further discussed below, the degree of vertical mixing in the planetary boundary layer of air-masses with varying records (“memory”) of the evolution of their water content. It was shown that in this respect there is a noticeable change during the diurnal cycle which reflects the more stable configuration at night and increasing turbulence as the landscape heats up, including the effect of the onset of the sea-breeze in the afternoon (see discussion below). But similar arguments applies at the seasonal scale: Fig. 5 demonstrates the large scatter associated with the wide range of circulation patterns observed in the wet winter season, which sharply decays toward the summer with its rather constant conditions and fewer rain events.

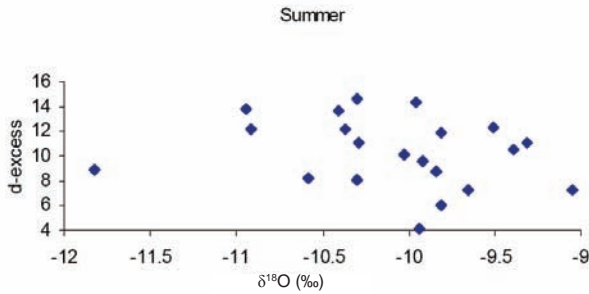


FIG. 3 Values of d -excess vs. $\delta^{18}\text{O}$ in water vapour collected at Rehovot during summer period.

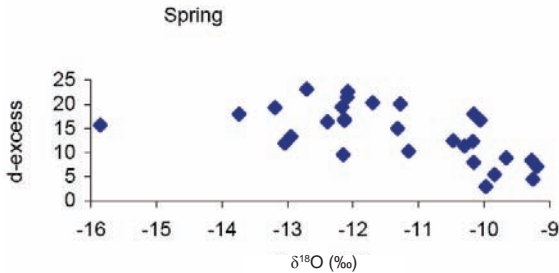


FIG. 4 Values of d -excess vs. $\delta^{18}\text{O}$ in water vapour collected at Rehovot during spring period.

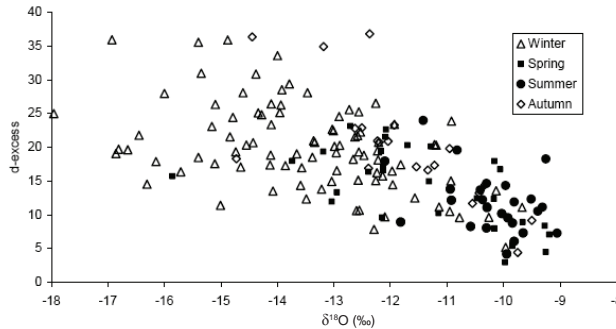


FIG. 5. Seasonal interactions on the relationship between *d*-excess and $\delta^{18}O$ values of vapour.

3.2. Seasonal variations in the vapour isotopic composition

The $\delta^{18}O$ data collected over the years 1998–2006, is presented in Fig. 6. The isotopic composition of the vapour samples showed a marked seasonal cycle, consistent with previous observations [12]. In summer, oxygen isotopic composition varied between -13‰ and -9‰ with a *d*-excess in the range $5\text{‰} \leq d \leq 22\text{‰}$. Winter values, more scattered as discussed above, ranged between $-10\text{‰} \leq \delta^{18}O \leq -18\text{‰}$ and with *d*-excess values up to $+40\text{‰}$. The data from spring and autumn follow a trend line between these two seasonal values. Samples from rain days often showed the most extreme values. The mean seasonality (monthly means averaged over all sampling years) of $\delta^{18}O$ and *d*-excess are presented in Fig. 7. Below we focus on the seasonal variations in $\delta^{18}O$ and *d*-excess as represented here.

Similar seasonal variability was observed in the isotopic composition of precipitation in Israel, but only for the rainy season (October through May; [5]). A recent study in Greece (Argiriou and Lykoudis, *J. Hydro. In press*) reported similar seasonal cycle in precipitation $\delta^{18}O$, over the entire year, and attributed it to the effect of temperature on the isotopic fractionation during the formation of precipitation. A similar control of temperature over the isotopic seasonal cycle was assumed by [16] for Egypt. As noted in an earlier study that explored the first data in our dataset [17], the vapour $\delta^{18}O$ was close to the equilibrium value for the prevailing surface temperature on rainy days. Examining selected sampling dates some relationships between the air mass trajectory and the observed isotopic composition was observed. It was also noted that days with marked changes in the height of the inversion layer, were accompanied by sharp changes in the vapour isotopic composition.

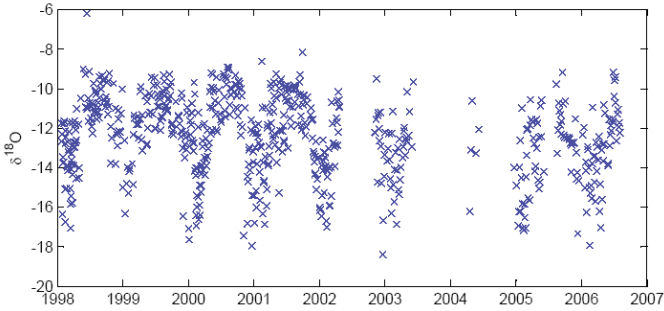


FIG. 6. A time series of $\delta^{18}\text{O}$ measured values showing a negative trend.

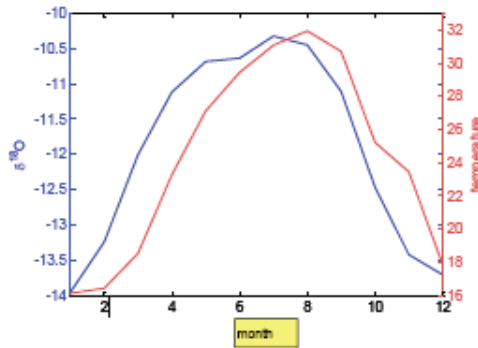


FIG. 7. The mean seasonal cycle values of $\delta^{18}\text{O}$ (blue) and temperature (red).

However, in contrast to the studies discussed above, in the present study the seasonal cycle is observed in the vapour isotopes, and includes changes during long rainless periods in the summer months, and the explanation invoked for rain is therefore inadequate.

Fig. 7 shows the mean seasonal cycle over the sampling period in comparison to that of the temperature at the site. The clear displacement of the isotopic and temperature record is key observations. It provides a strong indication that the seasonal cycle in vapour isotopes cannot be solely controlled by the regional evaporation process (Craig type) and rain out (Rayleigh type) processes. As discussed above (Fig. 5), vertical mixing patterns and advections are likely to play an important role. Indeed the importance of considering advection has clearly emerged from recent global modeling efforts (SWING; see <http://atoc.colorado.edu/~dcn/SWING>). We hypothesize that in the Eastern Mediterranean region vertical mixing is as important. This is related

to the summer synoptic conditions in our study area. In the summer months, the EM is subject to two primary factors: mid-upper level subsidence, which contributes to warming, and lower level cool advection from the northwest. The subsidence is associated with both the downward branch of the Asian monsoon and the downward branch of the Hadley cell across northern Africa [18]. The advection is associated with the Etesian winds, which are generated from a combination of the Persian Trough and the subtropical anticyclone of the Atlantic (Azores). The balance between the warming due to subsidence and cooling by advection controls surface temperature in summer in this region. Quantitative investigating (underway in our lab) requires vertical profile data, which are rarely available today, but are critically needed for future studies and for constraining models.

3.3. Is there a longtime trend in the vapour isotopes?

Plotting our entire data set versus time show a clear trend of decrease in $\delta^{18}\text{O}$ over the 9-year measurements period. A trend could be expected as over this time frame, strong warming was observed over the eastern-Mediterranean, considerably stronger than the mean global warming for this time frame [19].

Because vapour sampling for this study was carried only over several hours during the day, we checked for the possible effect of sampling duration. There was no correlation between individual samples collection times and $\delta^{18}\text{O}$ ($r = -0.06$). However annual mean $\delta^{18}\text{O}$ showed strong negative correlation with the annual mean collection duration ($r = -0.87$). Even if we exclude the extreme sampling times (>8 hours and $1 > 6.5$ hours; Fig. 8) a strong correlation with $\delta^{18}\text{O}$ ($r = -0.81$) is observed. This effect cannot be the result of decreasing efficiency in the collection system over time, since such effect would result with the opposite trend (heavy isotopes preferentially condensed with decreasing efficiency over time).

Why an effect of sampling time is manifested only in the annual mean values? It is likely that other effects, such as synoptic variability (on the days to weeks time-scale) and seasonal variation (on the longer scale) dominates over the effect introduced by change in sampling time. Only when we average over all other effects this smaller sampling effect becomes evident. But this leads to the question of how can sampling time influence the isotopic composition of the collected vapour?

The observed trend can probably be explained by the daily cycle in surface turbulence. The collection started at 8AM, and ended between 12 PM and 4 PM when the boundary layer is turbulent. The morning hours (specially in winter) are characterized by lingering nocturnal inversion with typical low wind speeds and, in turn, slow mixing of surface vapour with that from aloft

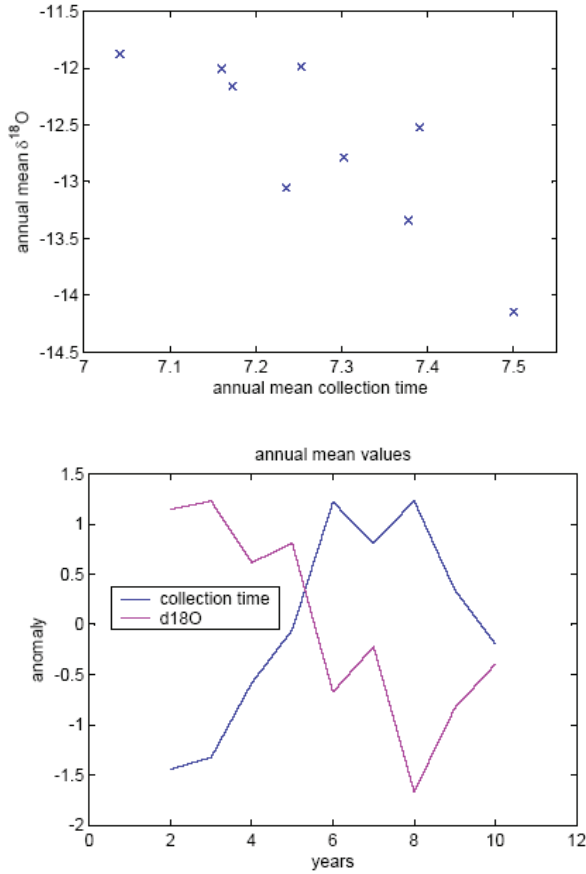


FIG. 8. Relationship between annual mean collection time (in hours) for all years of study and annual mean $\delta^{18}\text{O}$ (a and b).

(which have lighter isotopic composition, see discussion below). Warming of the ground by solar radiation during the day increases turbulence and mixing in the afternoon. In the summer, there is also a typical sea breeze front that reaches our sampling site in the late morning [20], and further increases turbulence. The increase turbulence along the daily cycle would be expected to mix down vapour with lighter isotopic composition (see discussion below) and could create the apparent link between longer sampling time (higher proportion of afternoon vapour) and lower delta values. Indeed, such afternoon decrease in $\delta^{18}\text{O}$ was observed in an earlier study in this region [21].

The significance of the small variations in sampling time (even $\frac{1}{2}$ hour) made it difficult to make conclusions regarding inter-annual variability or

longtime trends in our 9-years dataset. Future studies should consider such effect when determining a sampling strategy (e.g. use full 24 hours cycle, or the newly available diode-laser systems for real-time measurements). Note, however, that there was no relationship between sampling duration and month of year, and as a result, the mean monthly values are not correlated ($r = -0.12$) with the mean monthly collection time. Thus, there was no effect of sampling duration on the seasonal cycle, which is the focus of the discussion above.

The results of the detailed trend analysis indicated that the apparent temporal trend in the vapour isotopes cannot be attributed to climatic changes and likely reflect sampling uncertainties. However, it helps demonstrate first, the importance of considering the mixing patterns of the planetary boundary layer at the short time scales. And second, the potential of using short term effects studying the dynamics of boundary layer turbulence, and in studies of canopy evapotranspiration. In such studied the short term variations in vapour isotopes are used as tracers of surface water vapour fluxes, such as the contributions of soil evaporation and plant transpiration [22].

ACKNOWLEDGEMENT

The financial support from GLOW-JR, BSF and the MINERVA foundation is gratefully acknowledged.

REFERENCES

- [1] CRAIG, H., GORDON, L., Deuterium and oxygen-18 variations in the ocean and marine atmosphere, In: *Stable Isotopes in Oceanographic Studies and Paleotemperatures*, Ed. E Tongiorgi, Pisa, Lab. Geol. Nucleare (1965) 9–130.
- [2] DANSGAARD, W., Stable isotopes in precipitation, *Tellus* **16** (1964) 436–468.
- [3] DAI, A., FUNG, I.Y., DEL GENIO, A.D., Surface observed global precipitation variations during 1900–88, *J. Climate* **10** 2943–2962.
- [4] ROZANSKI, K., SONNTAG, C., Vertical-Distribution of Deuterium in Atmospheric Water-Vapour, *Tellus* **34** 2 (1982) 135–141.
- [5] GAT, J.R., CARMI, I., N., B., The isotopic composition of precipitation at Bet-Dagan, Israel: the climatic record (1961–1990), *Israel Meteorological Research Papers* **5** (1994) 10–19.
- [6] GAT, J.R., DANSGAARD, W., Stable isotope survey of freshwater occurrences in Israel and the Jordan Rift Valley, *Journal of Hydrology* **16** (1972) 177–211.

- [7] AYALON, A., BAR-MATTHEWS, M., SASS, E., Rainfall-recharge relationships within a karstic terrain in the eastern Mediterranean semi-arid region, Israel, *Journal of Hydrology* **207** (1998) 18–31.
- [8] GAT, J.R., Variability (in time) of the isotopic composition of precipitation: Consequences regarding the isotopic composition of hydrologic systems, *Use of Isotope Techniques in Water Resources Development*, IAEA (1987) 551–563.
- [9] GAT, J.R., ADAR, E., ALPERT, P., Inter- and intra storm variability of the isotope composition of precipitation in southern Israel: Are local or large scale factors responsible?, *International Conference on the study of environmental change using Isotope Techniques*. IAEA, Vienna (2001).
- [10] LEGUI, C., RINDSBERGER, M., ZANGWIL, M., ISSAR, A., GAT, J.R., The relation between the oxygen-18 and deuterium contents of rainwater in the Negev Highlands and air mass trajectories, *Isotope Geosciences* **1** (1983) 205–218.
- [11] LEVIN, M., GAT, J.R., ISSAR, A., Precipitation, flood and groundwaters of the Negev Highlands: an isotopic study of desert hydrology, *Arid Zone hydrology; Investigations with Isotope Techniques*, IAEA-AG (1980) 3–23.
- [12] TZUR, Y., Isotope effects in the evaporation of water into air, Ph.D. Thesis, The Weizmann Institute of Science, Rehovot (1971).
- [13] EHHALT, D.H., Vertical profiles of HTO, HDO and H₂O in the troposphere. NCAR-TN/STR-100, NCAR, Boulder, CO (1974).
- [14] LEE, X., SARGENT, S., SMITH, R., TANNER, B., In situ measurement of the water vapour O-18/O-16 isotope ratio for atmospheric and ecological applications. (vol 22, pg 555, 2005), *Journal of Atmospheric and Oceanic Technology* **22** 8 (2005) 1305–1305.
- [15] GRÜNZWEIG, J.M., LIN, T., ROTENBERG, E., YAKIR, D., Carbon sequestration potential in arid-land forest, *Global Change Biology* **9** (2002) 791–799.
- [16] EL-ASRAG, A.M., Effect of synoptic and climatic situations on fractionation of stable isotopes in rainwater over Egypt and East mediterranean, IAEA-Tecdoc-1453, IAEA, Viena (2005).
- [17] GAT, J.R., BEN-MAIR, R., YAMA, R., YAKIR, D., WERNLI, H., The Isotope Composition of Atmospheric Waters in Israel's Coastal Plain. IAEA-Tecdoc-1453, IAEA, Viena (2005).
- [18] ZIV, B., SAARONI, H., ALPERT, P., The factors governing the summer regime of the eastern Mediterranean, *International Journal of Climatology* **24** 14 (2004) 1859–1871.
- [19] ALPERT, P., KRICHAK, S.O., DAYAN, M., SHAFIR, H., Climatic trends over the Eastern Mediterranean: past and future projections. *CLIVAR Exchanges* **37** (2006) 12–13.

VARIATIONS IN THE ISOTOPIC COMPOSITION OF NEAR SURFACE WATER VAPOUR

- [20] ALPERT, P., RABINOVICH-HADAR, M., Pre- and Post-Sea-Breeze Frontal Lines — A Meso-gamma-Scale Analysis over South Israel, *Journal of the Atmospheric Sciences* **60** (2003) 2994–3008.
- [21] YAKIR, D., Oxygen-18 of leaf water: a crossroad for plant-associated isotopic signals, In: Ed. . Bios, Oxford. pp. 147-168, In: H. Griffiths (Editor), *Stable Isotopes and the Integration of Biological, Ecological and Geochemical Processes*. Bios, Oxford (1997) 147–168.
- [22] YAKIR, D., STERNBERG, L.S.L., The use of stable isotopes to study ecosystem gas exchange. *Oecologia* **123** (2000) 297–311.

ADVANCES IN OPTICAL WATER ISOTOPE RATIO MEASUREMENTS

E.R.Th. KERSTEL
Centre for Isotope Research,
University of Groningen,
Netherlands

Abstract

Isotope ratio mass spectrometers routinely achieve impressive measurement precisions and high throughput. In spite of this, a number of fundamental and practical problems are encountered. These are most notable in the case of water, arguably the most important molecule in the environment. Optical techniques to measure stable isotope ratios are able to address at least some of these issues; particularly, in relation to sample pretreatment and the difficulty of in-situ measurements. After discussing some general design criteria for infrared laser-based isotope ratio spectrometers, the case made above will be illustrated with a number of different instruments in applications from earthbound to the atmospheric: From laboratory based ice-core water isotope analyses to in-situ water isotope measurements in the upper troposphere and lower stratosphere.

1. INTRODUCTION

In this paper we present an overview of the state-of-the-art, and recent developments following a previous review by Kerstel and Meijer [1], in spectroscopic methods for measuring the stable isotope ratios of water as alternatives to isotope ratio mass spectrometry (IRMS). For a more detailed and wider discussion of stable isotope ratio infrared spectrometry of small molecules of environmental and biological importance, not limited to water, the reader is referred to [2].

IRMS is the conventional method for measuring isotope ratios and has benefited from over 40 years of research and development. Nowadays IRMS instrumentation is commercially available that reaches impressively high levels of precision, as well as throughput. Unfortunately, IRMS is incompatible with a condensable gas or a sticky molecule such as water. Therefore, in general, chemical preparation of the sample is required to transfer the water isotope ratio of interest to a molecule that is more easily analysed. For the ^{18}O isotope the method most used is that of oxygen-exchange between water and carbon

dioxide through the bicarbonate reaction [3]. Equilibration requires several hours and accurate temperature stabilization is needed in order to quantify the isotope fractionation associated with the reaction. The same technique also transfers the ^{17}O signature to CO_2 ; but due to mass-overlap, an accurate determination of the $^{17}\text{O}/^{16}\text{O}$ isotope ratio is difficult, if not impossible. For the $^2\text{H}/^1\text{H}$ ratio, several techniques, most still commonly used, exist, each with its specific problems [1]. Probably the most attractive of these is on-line pyrolysis of water in combination with a continuous-flow IRMS [4, 5]. This method is able to deal with very small sample sizes (of the order of $1\ \mu\text{l}$), provides a high throughput, and is able to achieve good precision.

It may be clear that for the larger part the required chemical conversion steps are time-consuming, and often compromise the overall accuracy and throughput [6, 7, 1]. Moreover, the two distinct sample preparations for $\delta^2\text{H}$ and $\delta^{18}\text{O}$ determinations potentially lead to uncorrelated (systematic) errors that do not (partially) cancel in the difference of the two measurements. This can be of importance in biomedical doubly labelled water studies and in the determination of the so-called deuterium excess parameter used in ice-core research. Apart from these drawbacks specific to water, IRMS instrumentation is expensive, voluminous and heavy, confined to a laboratory setting, and usually requires a skilled operator. All or most of these issues may be addressed by optical measurement techniques.

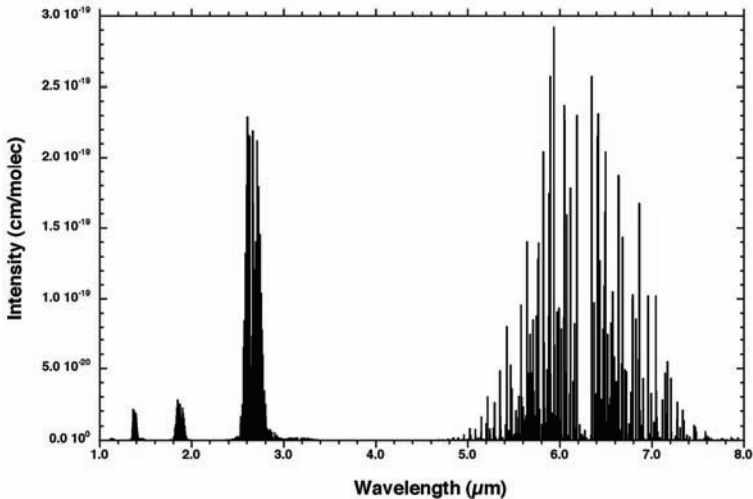


FIG. 1. Simulated (near) infrared spectrum of water based on the HITRAN database. The individual ro-vibrational transitions are assumed to be infinitesimally small.

2. INFRARED SPECTROMETRY

The near and mid-infrared absorption spectrum of gas phase water shows a large number of highly characteristic rotational-vibrational transitions that are very sensitive to isotopic substitution (in fact, such is the case for most small molecules). Figure 1 shows the spectrum of water over a wide range in the infrared. At sufficiently low vapour pressure and high instrumental resolution the individual ro-vibrational transitions are easily resolved, and can be uniquely assigned to a water molecule of particular isotopic composition (isotopologue). Even at higher pressure, or in the liquid phase, the unresolved vibrational bands of the deuterium isotopologue may be sufficiently displaced to be useful for a quantitative determination of the deuterium to hydrogen isotopologue ratio. Since the intensity of the experimentally recorded spectral features (whether individually resolved ro-vibrational transitions, or an unresolved vibrational band) may be directly related to the abundance of the absorbing species, recording the spectrum containing abundant and rare isotopologue features, in both an unknown sample and an isotopically well-known reference material, enables one to relate the isotopic composition of the sample to that of the reference material in a manner as described in, e.g., [2].

In Figure 2 we illustrate the basic principal of an isotope ratio measurement by means of infrared spectroscopy. It shows the spectra as a function of the light frequency ν in a small spectral region near $2.73 \mu\text{m}$ (3664 cm^{-1}) of two vapour-phase, water samples, one acting as the reference material (back-traceable to an international standard material such as Vienna Standard Mean Ocean Water, VSMOW), the other an ‘unknown’ sample. The absorption features correspond to ro-vibrational transitions in the most abundant isotopologue, H^{16}OH , and the rare isotopologues H^{17}OH , H^{18}OH , and H^{16}OD . The spectra were recorded as direct absorption spectra and converted to absorbance spectra by the application of the Beer law of linear absorption:

$$\frac{I_0 - \Delta I}{I_0} = e^{-\alpha \cdot l} \Leftrightarrow \alpha \cdot l = -Ln \left(\frac{I_0 - \Delta I}{I_0} \right) \quad (1)$$

In the above, ΔI represents the absorbed intensity of the incoming (laser) beam with intensity I_0 after traversing a length l of the absorbing medium, characterized by the absorption coefficient α .¹

The relative deviation ${}^x\delta_r(s)$ of the isotopic ratio of the sample (xR_s), with respect to that of the reference (xR_r) is given by:

¹Note that the definition of α here differs by a factor of l from the one in [2].

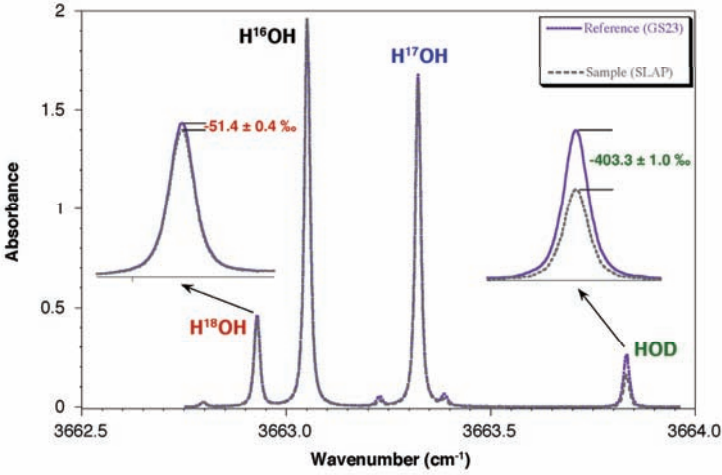


FIG. 2. Principle of the isotope ratio determination. In this figure, the absorbance spectra of sample and reference have been scaled to give equal H¹⁶OH absorbances. The isotope ratio may then be “read” directly from the ratio of the corresponding line intensities. In this case, the reference material was a local (Groningen) standard (²δ = -41.0‰, ¹⁷δ = -3.36‰, and ¹⁸δ = -6.29‰) and Standard Light Antarctic Precipitation was used as “unknown” sample (²δ = -428.0‰, ¹⁷δ ≈ -29.7‰, and ¹⁸δ = -55.5‰).

$${}^x\delta_r(s) \equiv \frac{{}^xR_s}{{}^xR_r} - 1 = \frac{\left(\frac{{}^xn}{{}^an}\right)_s}{\left(\frac{{}^xn}{{}^an}\right)_r} - 1 \quad (2)$$

The subscript s refers to the sample, r to the reference material. The superscripts a and x refer to the most abundant (H¹⁶OH) and the rare isotope species (H¹⁷OH, H¹⁸OH, or H¹⁶OD), respectively.

With a proper choice of experimental conditions, the δ-value follows directly from the intensities in the spectra:

$${}^x\delta_r(s) = \frac{\left(\frac{{}^x\alpha}{{}^a\alpha}\right)_s}{\left(\frac{{}^x\alpha}{{}^a\alpha}\right)_r} - 1 \quad (3)$$

Here, $\alpha = \alpha(v_0) = S \times f(v_0)n$ represents the experimentally determined (maximum) absorption coefficient at centre-line frequency, provided that the line shape, given by the normalized line shape function f, is the same for all transitions. If not, one has to use the integrated line intensity. In Eq. 3 the, normally justified, assumption has been made that the (effective) optical path

length l is the same for each isotopic species, or for the sample and reference spectra, or for both.

Since the line strength S depends on the number of molecules in the lower level of the transition, it is in general temperature-dependent: a change in temperature will redistribute the population over the rotational levels of the ground vibrational state (see, for example, [2]). Sample and reference spectra should therefore be measured at exactly the same temperature, and/or the isotopologue lines should be chosen such that their temperature coefficients are nearly equal. However, since to good approximation the measurement does not depend on the absolute temperature, but rather the difference between the sample and reference gas cells, passive stabilization with a good thermal contact between both gas cells is sufficient to make the temperature induced error negligible (i.e., $< 0.1\%$). Long-term absolute temperature stability is, however, important for measurement schemes that measure the sample and reference spectra not simultaneously but rather sequentially (in the same gas cell).

A careful selection of the spectral features is also important to assure that no interference from other species (whether other isotopologues of the water molecule, or entirely different molecules) is present, while a similar absorption of the different isotopologues is desired in order to assure a comparable signal-to-noise ratio on all spectral lines of interest, and eventually the best precision on the isotope ratio determination. This is generally achieved by searching for a set of lines with similar absorption coefficients (taking into account the natural abundances of the isotopologues). The alternative of compensating a lower absorption coefficient (usually for the rare isotopologue) with a correspondingly longer optical path length has been used first by Bergamaschi et al. [8], but so far not for water, as far as we are aware.

The search for the best spectral region is further complicated by the requirement that all isotopologue lines, including at least one belonging to the major isotopologue and one to (one of) the rare isotopologue(s), occur within a narrow wavelength range, limited by the tuning range of the laser. In fact, the simultaneous measurements of the three major isotopic ratios in water ($\delta^{18}\text{O}$, $\delta^{17}\text{O}$, and $\delta^2\text{H}$) was demonstrated to be possible, in both the fundamental band near $2.73\ \mu\text{m}$ [9] and the overtone band near $1.39\ \mu\text{m}$ [10], thanks to the fortuitous occurrence of suitable ro-vibrational lines of the H^{16}OH , H^{17}OH , H^{18}OH , and HO^2H isotopologues within a single laser frequency scan of about $1\ \text{cm}^{-1}$ wide. In both spectral regions, very few other possibilities, if any, exist. We have shown that this situation can be improved by the use of two lasers, each tuned to a different set of isotopologue lines [11]. In this scheme, the two lasers are wavelength modulated at different, incommensurate frequencies, and the two corresponding absorption spectra are retrieved from the detector signal using for each gas cell channel two phase-sensitive detectors, one for each

modulation frequency. An alternative to this dual-wavelength multiplexing technique would be to time-division multiplex the signals from each gas cell, resulting in a slightly less complex setup, but at the cost of an increased measurement time.

3. MULTIPLE-PASS SPECTROMETERS

A typical experimental layout is shown in Fig. 3, in this case of a wavelength modulated diode laser, dual gas cell, multiple-pass spectrometer. The laser is a distributed feedback, single mode laser, based on telecommunications technology. We have lasers operating near 1.4 μm in the OH-stretching overtone band and, since recently, devices that operate near 2.7 μm in the fundamental stretching vibrational band. The latter type of laser has essentially the same characteristics as its near-infrared counterpart, including room-temperature (thermo-electrically cooled), single mode operation and an output power of ~ 5 mW. Thanks to the one order of magnitude higher transition strength of the fundamental band (see Fig. 1), these lasers enable us to build more sensitive instruments, or to use a shorter effective absorption path length. This in turn allows for a more compact multiple-pass gas cell (and eventually a faster time-response if the sample gas is drawn through the cell). The gas cell alignment can also be made less susceptible to optical fringing (etaloning), which is often the limiting factor in the quest for the highest precision and accuracy. The output of the laser is split and the resulting two beams are directed to the two gas cells, where the laser beams make multiple passes through the cells between specially designed reflective optics for a total path length of ~ 20 m (1.39 μm) or ~ 4 m (2.73 μm). Before a measurement, the gas cells are flushed with dry nitrogen, evacuated, and then filled with between 1 and 10 μL (liquid) of water. The laser is repeatedly scanned over the spectral region of interest and frequency modulated, while a pair of phase-sensitive detectors (lock-in amplifier) recovers the absorption signal. In this manner we are able to measure the $\delta^2\text{H}$, $\delta^{17}\text{O}$, and $\delta^{18}\text{O}$ values of naturally occurring water samples with a precision of better than 0.5‰, 0.2‰, and 0.2‰, respectively, with an averaging time of 80 s [11]. The precision for $\delta^2\text{H}$ is comparable to that which can be obtained by IRMS, whereas $\delta^{17}\text{O}$ is difficult to determine by means of IRMS, making the laser determination quite unique. The $\delta^{18}\text{O}$ precision is almost one order of magnitude lower than possible with IRMS, but at higher, enriched ^{18}O concentrations, the accuracy of IRMS and our laser instrument become comparable again [12].

We have successfully used a (color center) laser based isotope spectrometer in applications in biomedicine (energy expenditure measurements by means

of the so-called doubly labelled water method) [12–14] and in ice-core studies to reconstruct the Earth's past climate [15]. The biomedical studies determine the CO_2 production as a direct measure of energy expenditure [16]. This is done by injecting a small amount of water, highly enriched in both ^2H and ^{18}O and following the decay of their concentrations. Since these studies use highly enriched samples, the accuracy of laser and IRMS instrumentation is comparable and the laser technique can compete effectively with IRMS, also in this respect [17].

The ice-core studies measured the $^2\delta$ -value (versus depth) as a proxy for the local (palaeo-) temperature, but also the so-called deuterium excess value, defined as $^2\Delta = ^2\delta - 8 \times ^{18}\delta$, which can be shown to depend on other important climate variables (such as the temperature and relative humidity in the source region of the precipitation). A precise determination of $^2\Delta$ thus requires a precise determination of $^2\delta$, and in particular $^{18}\delta$. Here, the laser setup cannot (yet) compete with the best IRMS instruments. Still, the laser measurements proved rather useful as a check on the absolute accuracy (a possible shift of the δ scale), as they are much less sensitive to sample contamination, in this case by residual drilling fluid [15].

In an ecological application of the $1.4 \mu\text{m}$ diode laser spectrometer, we observed, in real-time, the evolution of the isotopic signature of water evaporating from plant leaves that were held in a dry nitrogen atmosphere inside one of the spectrometer gas cells [18]. Similar experiments were carried out on the evaporation of small water droplets, with the aim of studying models of isotopic fractionation.

4. CAVITY ENHANCED TECHNIQUES

Understanding the process of dehydration of air entering the stratosphere through the tropical tropopause and the origin and microphysical properties of radiatively important thin cirrus clouds in the tropical tropopause layer, are among the key issues in Atmospheric Science.

In-situ measurement of the water isotopic composition is believed to be vital in addressing these. To this end we have developed a near-infrared spectrometer, based on the ultra-sensitive technique of optical feedback cavity enhanced absorption spectroscopy (OF-CEAS), a variation on the general technique of cavity ring down spectroscopy (CRDS) (for a review, see, e.g., [19, 20]). It should deliver a better sensitivity than a traditional multi-pass arrangement, as used in the airborne Alias water isotope spectrometer of Webster and co-workers [21], by creating an about two orders of magnitude longer effective optical absorption path length (7 km versus 80 m). At the same

time the gas cell volume is reduced by about the same factor (down to about 10 cc). This significantly reduces the flow rate needed to bring the gas exchange time, and therewith the memory-limited response time, down to an acceptable level, and, ultimately, the weight and size of the instrument. The instrument we built together with the group of Dr. Romanini (Grenoble) is lightweight (51 kg) and small (<50 L). Together with a low power consumption and the absence of cryogenics, this makes it uniquely suited for operation on Unmanned Aerial Vehicles and high altitude aircraft. In collaboration with Dr. Jost (then at NASA) it flew on both the NASA DC-8 research aircraft and the stratospheric WB-57F. In the summer of 2006 it participated in the African Monsoon Multidisciplinary Analysis (AMMA) campaign on board of the European M55 Geophysica stratospheric airplane, out of Ouagadougou, Burkina Faso. Its laboratory precision at a water mixing ratio of 40 ppm is between 5‰ (for $\delta^{18}\text{O}$) and 50‰ ($\delta^2\text{H}$) with a 50 s averaging time. Due to a temperature control problem, the effective averaging time during the Geophysica deployment was limited to about 1 s, with a corresponding penalty for the measurement precision.

Essentially the same device was used to analyze near-surface atmospheric moisture, sampled from just outside the Groningen laboratory. In this case, instrumental precision ranges from 0.1‰ ($\delta^{18}\text{O}$) to 2‰ ($\delta^2\text{H}$) for a 10 s averaging time for water mixing ratios of 2500 ppm and above.

We are aware of only one other water isotope ratio spectrometer that has been flown on a high altitude aircraft. This instrument, built by Moyer and colleagues [23], is, like ours, based on a CRDS technique, in this case called off-axis integrated cavity output spectroscopy (OA-ICOS), used in combination with a cryogenically cooled mid-infrared quantum cascade laser. The instrument is significantly larger and heavier than Iris, but has collected scientific quality data during the July 2005 and February 2006 AVE mission.

5. COMMERCIAL DEVELOPMENTS

Lee et al. [24] have reported on $^{18}\text{O}/^{16}\text{O}$ measurements in ecological water samples, using a modified version of the Campbell Scientific isotope ratio spectrometer. This commercial instrument uses a Pb-salt laser and MCT detector, which both require liquid nitrogen cooling. In principle, it could also measure $\delta^2\text{H}$, but so far, the low precision of the device in combination with calibration problems, have excluded practical application of this ability. With 20 s averaging time, the device is able to measure $\delta^{18}\text{O}$ with a precision of 1 to 2‰ and $\delta^2\text{H}$ with a precision of roughly 5‰.

ADVANCES IN OPTICAL WATER ISOTOPE RATIO MEASUREMENTS

Both Picarro (of Sunnyvale, CA) and Los Gatos Research (of Mountain View, CA) have developed sensitive near-infrared diode laser spectrometers, able to measure water isotope ratios. The Picarro spectrometer use CRDS with active locking of the cw laser to a triangular shaped cavity. It combines a high sensitivity with a small gas cell design, and thus fast gas exchange. We have not encountered applications of water isotopic analysis with the Picarro spectrometer in the literature. The Los Gatos spectrometer on the other hand has been subjected to a laboratory validation study by researchers of the IAEA Hydrology Section [25]. The device was found to yield standard deviations on repeated measurements of natural waters in the range of 0.1‰ to 0.4‰ for $\delta^{18}\text{O}$ and 1‰ to 3‰ for $\delta^2\text{H}$. In this case, the first one or two sample injections were possibly rejected for reasons related to previous sample memory, and a correction was applied for the injected amount of water. No sample measurement time was reported, but is estimated to be of the order of minutes.

All three spectrometers mentioned in this paragraph use only one gas cell. Consequently, the isotope ratios determined are sensitive to a drift in the gas temperature between the time of measurement of the sample and of the corresponding reference material, necessitating either a post-measurement correction (the strategy adapted by Los Gatos), or accurate temperature stabilization (Picarro).

6. FOURIER TRANSFORM SPECTROMETRY

An alternative detection technique is Fourier transform infrared (FTIR) spectrometry, in which a broadband light source illuminates the sample held in a gas cell inside the stationary arm of a Michelson interferometer. As the length of the second arm is changed in a periodic manner, an interferogram is recorded that is the Fourier transform of the sample gas absorption spectrum. The resolution of the instrument is proportional to the path length difference travelled by the mirror in the second arm. Fusch et al. [26] used a low-resolution (8 cm^{-1}) FTIR to determine $\delta^2\text{H}$ over a very wide range of enrichments (-500% to $16,000\%$) in $60\ \mu\text{L}$ liquid water samples with an accuracy ranging from 3‰ to about 45‰. Recently, Griffith and co-workers [27] used a medium-resolution (1 cm^{-1}) instrument in a 2-week field campaign to study the partitioning between evaporation and transpiration in a eucalypt forest in SE Australia by monitoring vertical profiles of atmospheric water vapour, and $\delta^2\text{H}$ with a precision of 1 to 2‰. The most recent version of this spectrometer uses thermo-electrically cooled detectors, doing away with the need for cryogens, facilitating long-term remote operation. Because of the highly congested spectrum (for such a small molecule),

the analysis of the oxygen isotopes in water requires a much higher resolution, and thus bigger and more expensive FTIR.

7. DISCUSSION

Optical isotope ratio measurements have clearly matured to the point where the deuterium analysis of water has become competitive with IRMS in terms of accuracy. Here, fractionation effects during sample handling constitute the dominant source of analytical errors. Although, it appears unlikely that an optical method will be able to reach the very high accuracy ($\sim 0.03\%$) possible with IRMS for $\delta^{18}\text{O}$ determinations on natural samples, current optical instruments are coming close, and are certainly able to satisfy the needs of many users. For highly enriched samples the precision and accuracy of laser spectrometry have already been shown to exceed those of IRMS. The possibility of using laser spectrometry to measure $\delta^{17}\text{O}$ easily may be used in relation with the mass-dependent fractionation relation [28] for independent verification of $\delta^{18}\text{O}$ measurements on the same sample [15], or to verify the applicability of this relation. Or in altogether more exotic applications, such as the determination of the ^{17}O concentration in the heavy water used in a solar neutrino experiment [29].

A growing number of spectrometers use CRDS, or one of its derivatives. This is a logical choice for an ultra-sensitive spectrometer for the isotope analysis of water at the extremely low water concentration encountered in the upper troposphere and lower stratosphere, but may not be so for an instrument designed to measure water at more elevated concentrations or liquid samples. One reason is that such an instrument is almost inevitably built with just one gas cell. Sample and reference are therefore measured sequentially, increasing the likelihood of a temperature difference between the two measurements producing an apparent isotope shift (typically several ‰ per degree K). For this reason we have implemented the possibility to measure a second H^{16}OH feature with a very different line strength temperature coefficient, thus providing a build-in gas thermometer by which to correct the measurements.

Of course, precision and accuracy are not the only factor to be considered when comparing laser spectrometry to IRMS. There are many applications for which other aspects, like robustness, portability, remote operation in a hostile environment, compactness, and the real-time measurement capability, are more important. Other advantages of optical methods that may be considered are the high selectivity, thus avoiding the need of chemical sample pretreatment, the non-destructive nature of the measurement, making it possible to recover the sample if needed, the absence of consumables (like an ionization source

filament), and, low cost. Last but not least, methods based on direct absorption are conceptually simple, which helps reduce the required scale correction and normalization with respect to IRMS.

The arrival of a number of commercial suppliers of optical spectrometers signals the acceptance of end users of the technique. The near future will surely see even more precise and accurate, as well as more sensitive, devices. Also, more attention will be paid to sample handling and calibration strategies.

ACKNOWLEDGEMENTS

We are indebted to past and present students and post-doctoral fellows who work(ed) in our laser spectrometry laboratory, and our colleagues Harro Meijer and Henk Visser. We also like to thank all our collaborators, and in particular Sigfus Johnsen, Gianluca Gagliardi, Livio Gianfrani, Daniele Romanini, Marc Chenevier, Samir Kassi, and, last but not least, Hans-Jürg Jost. Substantial financial support was obtained from the Dutch Foundation for Research on Matter (FOM), the Royal Academy of Arts and Sciences (KNAW), and the University of Groningen.

This paper is dedicated to the memory of Henk Visser, who passed away much too early on June 3, 2007, after a courageous and inspirational battle with cancer. His great enthusiasm and love for science will continue to guide us.

REFERENCES

- [1] KERSTEL, E.R.Th., MEIJER, H.A.J., Optical Isotope Ratio Measurements in Hydrology (Chapter 9), in: *Isotopes in the Water Cycle: past, present and future of a developing science*, P.K. Aggarwal, J. Gat, and K. Froehlich (Eds.), IAEA Hydrology Section, Kluwer (2005) 109–124.
- [2] KERSTEL, E.R.Th., Stable isotope ratio infrared spectrometry. *Handbook of Stable Isotope Analytical Techniques*, P.A. de Groot (Ed.) Elsevier (2004) 759–787.
- [3] EPSTEIN, S., MAYADA, T.K., Variations of O-18 content of waters from natural sources, *Geochim. Cosmochim. Acta* **4** (1953) 213–224.
- [4] BEGLEY, I.S., SCRIMGEOUR, C.M., High-precision $\delta^2\text{H}$ and $\delta^{18}\text{O}$ measurement for water and volatile organic compounds by continuous-flow pyrolysis isotope ratio mass spectrometry, *Anal. Chem.* **69** (1997) 1530–1535.
- [5] PHILLIPS, A., FOUREL, F., MORRISON, J., Oxygen-deuterium isotopic measurements using a variety of pyrolysis methods – IRMS continuous-flow techniques, *Isotopes in Environ. Health Stud.* **36** (2000) 347.

- [6] BRAND, W.A., AVAK, H., SEEDORF, R., HOFMANN, D., CONRADI, Th., New methods for fully automated isotope ratio determination from hydrogen at the natural abundance level, *Isotopes Environ. Health Stud.* **32** (1996) 263–273.
- [7] MEIJER, H.A.J., Isotope ratio analysis on water: a critical look at developments, *New Approaches for Stable Isotope Ratio Measurements (Proc. Advisory Group Meeting, 1999) IAEA-TECDOC-1247, IAEA, Vienna (2001)* 105–112.
- [8] BERGAMASCHI, P., SCHUPP, M., HARRIS, G.W., High-precision direct measurements of $^{13}\text{CH}_4/^{12}\text{CH}_4$ and $^{12}\text{CH}_3\text{D}/^{12}\text{CH}_4$ ratios in atmospheric methane sources by means of a long-path tunable diode laser absorption spectrometer, *Appl. Opt.* **33** (1994) 7704–7716.
- [9] KERSTEL, E.R.Th., TRIGT, R. van, DAM, N., REUSS, J., MEIJER, H.A.J., Simultaneous determination of the $^2\text{H}/^1\text{H}$, $^{17}\text{O}/^{16}\text{O}$, and $^{18}\text{O}/^{16}\text{O}$ isotope abundance ratios in water by means of laser spectrometry, *Anal. Chem.* **71** (1999) 5297–5303.
- [10] KERSTEL, E.R.Th., GAGLIARDI, G., GIANFRANI, L., MEIJER, H.A.J., TRIGT, R. van., RAMAKER, R., Determination of the $^2\text{H}/^1\text{H}$, $^{17}\text{O}/^{16}\text{O}$, and $^{18}\text{O}/^{16}\text{O}$ isotope ratios in water by means of tunable diode laser spectroscopy at 1.39 μm , *Spectrochim. Acta A* **58** (2002) 2389–2396.
- [11] GIANFRANI, L., GAGLIARDI, G., BURGEL, M. van, KERSTEL, E.R.Th., Isotope analysis of water by means of near-infrared dual-wavelength diode laser spectroscopy, *Optics Express* **11** (2003) 1566–1576.
- [12] TRIGT, R. van, KERSTEL, E.R.Th., VISSER, G.H., MEIJER, H.A.J., Stable isotope ratio measurements on highly enriched water samples by means of laser spectrometry, *Anal. Chem.* **73** (2001) 2445–2452.
- [13] TRIGT, R. van, KERSTEL, E.R.Th., MEIJER, H.A.J., MCLEAN, M., VISSER, G.H., Validation of the DLW method in Japanese quail at various water fluxes using laser and IRMS, *J. Appl. Physiol.* **93** (2002) 2147–2154.
- [14] KERSTEL, E., PIERSMA, T., GESSAMAN, J., DEKINGA, A., MEIJER, H., VISSER, H., Assessment of the amount of body water in the Red Knot (*Calidris canutus*): An evaluation of the principle of isotope dilution with ^2H , ^{17}O , and ^{18}O as measured with laser spectrometry and isotope ratio mass spectrometry, *Isotopes Environm. Health Studies* **42** (2006) 1–7.
- [15] TRIGT, R. van, Meijer, H.A.J., SVEINBJORNSDOTTIR, A.E., JOHNSEN, S.J., KERSTEL, E.R.Th., Measuring stable isotopes of hydrogen and oxygen in ice by means of laser spectrometry: the Bølling transition in the Dye-3 (South Greenland) ice core, *Ann. Glaciology* **35** (2002) 125–130.
- [16] SPEAKMAN, J.R., *Doubly Labelled Water, Theory and Practice*, Chapman & Hall: London (1997).
- [17] SPEAKMAN, J.R., The role of technology in the past and future development of the double labeled water method, *Isotopes Environm. Health Studies* **41** (2005) 335–343.

ADVANCES IN OPTICAL WATER ISOTOPE RATIO MEASUREMENTS

- [18] KERSTEL, E.R.T., Van der Wel, L.G., MEIJER, H.A.J., First real-time measurements of the evolving $^2\text{H}/^1\text{H}$ isotope ratio during water evaporation from plant leaves, *Isotopes Environm. Health Studies* **41** (2005) 207–216.
- [19] BERDEN, G., PEETERS, P., MEIJER, G., Cavity ring-down spectroscopy: Experimental schemes and applications, *Int. Rev. Chem. Phys.* **19** (2000) 565–607.
- [20] MAZURENKA, M., ORR-EWING, A.J., PEVERALL, R., RITCHIE, G.A.D., Cavity ring-down and cavity enhanced spectroscopy using diode lasers, *Annu. Rep. Prog. Chem., Sect. C*, **101** (2005) 100–142.
- [21] WEBSTER, C.R. HEYMSFIELD, A., Water Isotope Ratios D/H, $^{18}\text{O}/^{16}\text{O}$, $^{17}\text{O}/^{16}\text{O}$ in and out of Clouds Map Dehydration Pathways, *Science* **302** (2003) 1742–1745.
- [22] KERSTEL, E.R.T., IANNONE, R.Q., CHENEVIER, M., KASSI, S., JOST, H.-J., ROMANINI, D., A water isotope (^2H , ^{17}O , and ^{18}O) spectrometer based on optical-feedback cavity enhanced absorption for in-situ airborne applications, *Appl. Phys. B* **85** (2006) 397–406.
- [23] MOYER, E.J., HANISCO, T.F., KEUTSCH, F.N., SAYRES, D.M., ALLEN, N.T., St. CLAIR, J.M., WEINSTOCK, E.M., SPACKMAN, J.R., SMITH, J.B., PFISTER, L., BUI, T.P., ANDERSON, J.G., Measurements of the HDO/ H_2^{18}O relationship in stratospheric water vapour and implications for the cause of stratospheric isotopic enhancement, In preparation (2007).
- [24] LEE, X., SARGENT, S., SMITH, R., TANNER, B., In situ measurement of the water vapour $^{18}\text{O}/^{16}\text{O}$ isotope ratio for atmospheric and ecological applications, *J. Atm. Oc. Techn.* **22** (2005) 555–565.
- [25] AGGARWAL, P.K. GROENING, M., GUPTA, M., OWANO, T., BAER, D., Laser spectroscopic analysis of stable isotopes in natural waters. AGU poster, abstract H51D-504 (2006).
- [26] FUSCH, CH., SPRIRIG, N., MOELLER, H., Fourier Transform Infrared Spectroscopy Measures $^1\text{H}/^2\text{H}$ Ratios of Native Water With a Precision Comparable to that of Isotope Ratio Mass Spectrometry, *Eur. J. Clin. Chem. Clin. Biochem.* **31** (1993) 639–644.
- [27] GRIFFITH, D., personal communication (2007).
- [28] MEIJER, H.A.J., LI, W.J., The use of electrolysis for accurate $\delta^{17}\text{O}$ and $\delta^{18}\text{O}$ isotope measurements in water, *Isotopes in Environm. Health Studies* **3** (1998) 349–369.
- [29] KERSTEL, E.R.Th., O-17 Analysis of Ontario Hydro Heavy Water, Customer report No. 2001-32, Centre for Isotope Research, Groningen, The Netherlands (2001).

CASE STUDIES

**SPATIAL VARIATIONS OF ENVIRONMENTAL
TRACER DISTRIBUTIONS IN WATER FROM
A MANGROVE ECOSYSTEM: THE CASE OF
BABITONGA BAY (SANTA CATARINA, BRAZIL)**

V. BARROS GRACE**+, L.A. MARTINELLI**+, J. MAS PLA§,
T. OLIVEIRA NOVAIS+, J.P. OMETTO**+, E. SACCHI§§, G.M. ZUPPI*

*Dipartimento di Scienze Ambientali,
Università Ca' Foscari,
Dorsoduro, Venezia,
Italy

+University of UNIVILLE,
Depto Eng Ambiental,
Campus Universitário Bom Retiro s/nº,
Joinville, Santa Catarina,
Brazil

**Centro de Energia Nuclear na Agricultura,
Universidade de São Paulo,
Piracicaba, Brazil

§Dept. de Ciències Ambientals,
Facultat de Ciències,
Universitat de Girona,
Girona, España

§§Dipartimento di Scienze della Terra,
Università di Pavia,
Pavia, Italy

Abstract

The hydrologic complex of Babitonga Bay (Brazil) forms a vast environmental complex, where agriculture, shellfish farming, and industries coexist with a unique natural area of Atlantic rain forest. The origin of different continental hydrological components, the environmental transition between saline and fresh waters, and the influence of the seasonality on Babitonga Bay waters are evaluated using isotopes and

chemistry. The end of the dry season is marked by a fast response of continental water to the first rainfall, while in the Bay this change is delayed in time. At the end of the rainy season waters show a more homogeneous isotopic composition, suggesting the harmonisation of hydrological and hydrogeological systems. Moreover, $\delta^{13}\text{C}$ and $\delta^{15}\text{N}$ of DIC and POM allows for the definition of the biogeochemical processes originating and transporting chemical compounds in the coastal and transition areas and for the determination of three distinct end-members: terrestrial, marine and urban.

1. INTRODUCTION

Estuarine and transition areas constitute natural reaction zones in which heterogeneous processes may affect the ecological equilibrium due to local changes in the biogeochemical conditions. Besides the natural sources, other inputs provide significant contributions to the water chemistry. These include large volumes of poorly defined human waste inputs which may or may not be treated before entering rivers and bays. However, the interpretation of all geochemical data are complicated by the fact that bulk material represents mixtures of nutrients from several sources, and thus geochemical signatures reflect integration of different sources. Moreover, systems have variable inputs in space and time and, thus, it is difficult to separate mixing of multiple end members from the effects of matter alteration and transportation. The distinction between natural and human sources may be ambiguous. Babitonga Bay, one of the main estuarine formations and mangrove ecosystems in the south of Brazil, is an excellent location to monitor and understand such processes.

2. SITE DESCRIPTION

The hydrologic complex of Babitonga Bay (BB) is located 45 km northeast from the city of Joinville, which is the principle city (heavy industry and urbanization) of the Santa Catarina State (Southern Brazil). The drainage basin of this bay forms a vast environmental complex, where agriculture and shellfish farming as well as a spectrum of industries, coexist with a unique natural area of Atlantic rain forest. Babitonga Bay, the southern residual mangrove forests of Brazil, is connected to the Atlantic Ocean via an opening with a width of 1850 m and presents a salt-wedge circulation system. A significant tidal oscillation brings an appreciable water renewal to the whole ecosystem. Tides are mixed exhibiting semidiurnal dominance with diurnal inequalities [1].

The region is characterized by a humid subtropical climate with a rainfall average of 2000 mm/year. There are two distinguishable seasons: summer

(from November to April) and winter (from May to October). During summer, the weather is characterized by high temperatures and humidity, with intense precipitation caused by local convection processes strictly controlled by the regional orography. During winter, the influence of polar air-masses bring a decline of temperature and precipitation in the region.

3. HYDROGRAPHIC AND GEOLOGICAL SETTINGS

Geomorphological analysis reveals large variations in orography, lithology and structure, including the occurrence of well-developed Quaternary formations. The basin and range topography of the region generates pronounced altimetric contrasts of the Serra do Mar that raises up to 1500 m asl. The basin is divided into four hydrographic watersheds: Cachoeira, Palmital, Cubatão and Parati.

Among them the most important are: Cachoeira River entirely located within the urbanized area of Joinville, with a discharge varying between 3 to 5 m³/s and Cubatão River, with a mean discharge of 17.7 m³/s characterized by rapid fluctuations due to the intense precipitation events on the steep slopes of the Serra do Mar. The whole Babitonga basin is characterized by four geological domains including: granites with a complex Paleozoic tectonic basement; molasses; associated vulcanites; and sedimentary deposits from the Quaternary. The occurrence of groundwater is related to three main aquifer formations: weathered crystalline rocks, fractured granite complex, and quaternary sedimentary formations. The groundwater movement is generally towards Babitonga Bay. The hydraulic gradient around 10⁻⁴, is generally controlled by tidal oscillation. The underground discharge rate in the crystalline aquifer is up to 15 m³/h.

4. GEOCHEMICAL RESULTS AND INTERPRETATION

The sampling campaigns were made after the two extreme seasons in the region, i.e., after the austral summer (April 2004) and winter (October 2004). On the diagram (Figure 1) three groups of water appear:

1. Continental water samples related to the Cubatão River basin (CWCR) are characterised by the lightest isotopic content. Their shift from the Global Meteoric Water Line (GMWL) points out an isotopic enrichment that can be attributed to fractionation processes of local rainfall. Deuterium excess is around 25–30‰. The increase in d-excess inland is most easily explained by the contribution of recycled moisture

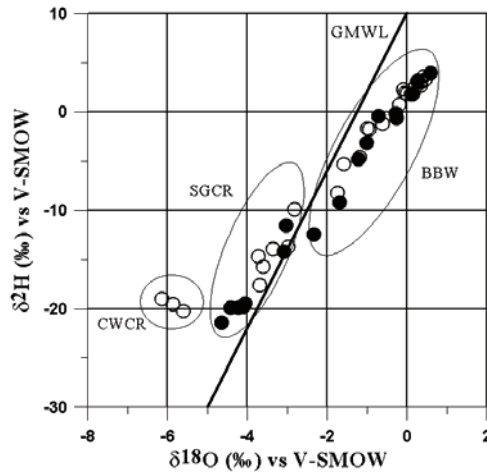


FIG. 1. Water stable isotope content in hydrologic complex of Babitonga Bay. Symbols represent: (●) April survey and (○) October survey.

via evaporation and re-precipitation. Moreover, the increase in d-excess suggests that evaporation/re-precipitation cycles occur repeatedly along the storm track. In fact, the high d-excess values of surface and ground waters indicates that an isotopically fractionated evapotranspiration flux contributes to the atmospheric water balance over the region, similar to the steady state evapotranspiration model developed for the Amazon Basin [2, 3]. Furthermore, d-excess values may also reflect a decrease in condensation temperature as indicated by the elevation of the Serra do Mar rising inland along this transect [4]. This interpretation also suggests that an altitude effect contributes to the control of the d-excess values of surface and ground waters.

2. Surface and ground water from the Cachoeira river (SGCR) (including the deep well TC from the April survey) as well as bay points 1S and 1F, and the island springs, within BB. Specifically, these first two groups show a very similar isotopic content in the April survey, almost indistinguishable in the plot. Such similarity is attributed to the effective recharge of rainfall and surface water to the aquifers during the wet season, suggesting the harmonisation of hydrological and hydrogeological systems.
3. Bay water (BBW). Isotopic results are arranged in a line extending from the second group towards the ocean isotopic composition in both surveys, and they reflect the variable influence of ocean water. Isotopic content of sampling point 5 is taken as the ocean reference. Mixing rates could be

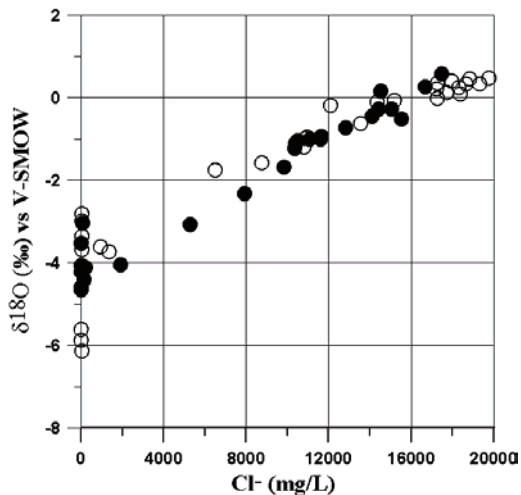


FIG. 2. Mixing processes between fresh and ocean water in BB. (●) April survey and (○) October survey.

inferred from such a distribution, although the influence of the first and second groups would not be clearly differentiated.

Mixing processes between fresh and ocean water are better represented in Figure 2, showing the relationship between chloride and $\delta^{18}\text{O}$ data and therefore combining chemical and isotopic information. Mixing lines have been drawn assuming an average linear composition of both components of the mixing system members. For the April survey, the homogeneity in the values of both components in the continental waters (previous groups 1 and 2) does not allow a further distinction of their origin.

In any case, data from the April survey convey a complete mixing process as actual data overlay the estimated mixing line. For the October dataset, two continental end-members are defined, based on the aforementioned first and second groups, and two distinct mixing lines are drawn accordingly.

^{13}C and ^{15}N in BB cannot be reasonably modelled by merely varying the proportion of a marine and a general terrestrial end-member. Those isotopes and the C/N ratio indicate that, although most of the organic matter have a riverine source in sample sites near the coast (1, 2 and 3), and a marine source in other sites (5, 6, 7, and 8), a component of sewage organic matter is present in several sampling sites of the Babitonga Bay. The mixing between continental system and the ocean is clearly described by the isotopic composition of POC and PON as a function of salinity (Fig. 3a and 3b). The more pristine continental

end-member, the River Cubatão had a $\delta^{13}\text{C}_{\text{POC}}$ value of -26.2‰ . On the other hand, the River Cachoeira had a higher $\delta^{13}\text{C}_{\text{POC}}$ value (-23.9‰) typical of sewage-impacted rivers. The sampling site closest to the Atlantic Ocean (7 and 8), had $\delta^{13}\text{C}$ values around -22 to -23‰ , which is typical of ocean samples. Most of the other samples plotted between these two extremes with a tendency of increase the $\delta^{13}\text{C}_{\text{POC}}$ as a function of salinity (Fig. 3a).

The $\delta^{15}\text{N}$ values describe a rather significant correlation with salinity than $\delta^{13}\text{C}$ (Fig. 3b). Overall, the $\delta^{15}\text{N}$ values of POM can be explained in terms of simple mixing between the terrestrial particulate matter (riverine or sewage derived) with generally lower $\delta^{15}\text{N}$ values, and marine phytoplankton, which has mainly inherited the $\delta^{15}\text{N}$ of nitrate from deeper oceanic waters. Larger $\delta^{15}\text{N}$ values were obtained at stations 7 and 8 near the BB mouth. These results therefore suggest that $\delta^{15}\text{N}$ of the oceanic water is around $+10\text{‰}$, slightly enriched in comparison to the latitudinal distribution pattern of $\delta^{15}\text{N}_{\text{POM}}$ reported in the literature [5, 6].

The above mentioned observations are in agreement with the information obtained using chloride and bromide. Halides support the idea that an effective bromine uptake by biological processes occurs in the Babitonga Bay, which is noticeable at those points located near the coast, which are characterized by shallow depths and are protected from the main tidal influences. Such facts illustrate the limit of bromine application as tracer of biogeochemical processes in complex hydrological systems such as the estuarine/mangrove systems.

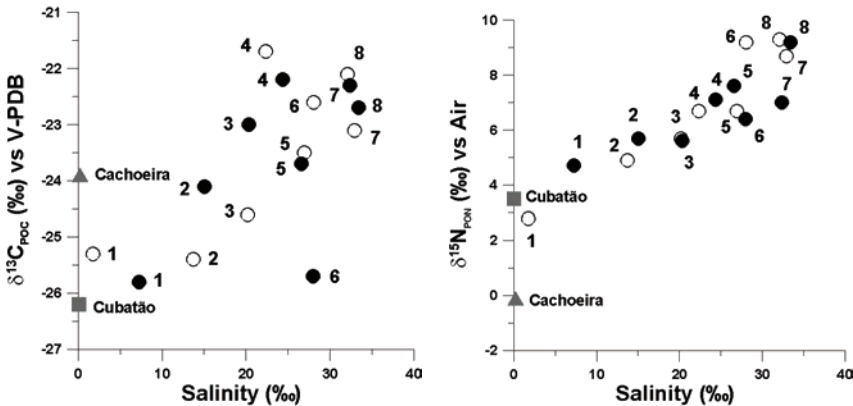


FIG. 3: (a) $\delta^{13}\text{C}$ values of the particulate organic carbon ($\delta^{13}\text{C}_{\text{POC}}$) versus salinity in the BB; (b) $\delta^{15}\text{N}$ values of the particulate organic nitrogen ($\delta^{15}\text{N}_{\text{PON}}$) versus salinity in the BB.

5. CONCLUSIONS

The Babitonga Bay could be considered as an exceptional natural model in predicting the future of natural environments stressed by recent anthropic activities, and provide a spectacular opportunity to develop a sound understanding of the changes induced to lagoon systems. In fact, the use of end-member mixing analyses with distinct components has helped to differentiate the origin of water flowing into the bay, the origin of particulate organic matter as well as to identify the non-conservative behaviour of bromine in such highly biologically active environments.

ACKNOWLEDGEMENTS

The authors thank Prof. R.L. Victoria for access to the analytical facilities at the Centro de Energia Nuclear na Agricultura (CENA), Universidade de São Paulo. This work was financially supported by the Region of Veneto and by UNIVILLE. The authors wish to thank Claudio Tureck and Mariele Simm (University of UNIVILLE - Joinville) for the collection of samples and Digital Cartography Laboratory (UNIVILLE) and Enrico Allais (ISO 4, Turin) for oxygen and deuterium analyses.

REFERENCES

- [1] SCHETTINI, C.A.F., CARVALHO, J.L.B. JABOR, P., Comparative hydrology and suspended matter distribution of four estuaries in Santa Catarina State – Southern Brazil, *Proceedings of Workshop on Comparative Studies of Temperate Coast Estuaries* (1996) 29–32.
- [2] GAT, J.R., MATSUI, E., Atmospheric water balance in the amazon basin: an isotopic evapotranspiration model, *J. Geophys. Res.*, vol. 96, No. D7 (1991) 13179–13188.
- [3] MARTINELLI, L.A., VICTORIA, R.L., STERNBERG, L.S.L., RIBEIRO, A., MOREIRA, M.Z., Using stables isotopes to determine sources of evaporated water to the atmosphere in the Amazon basin, *Journal of Hydrology* **183** (1996) 191–204.
- [4] CRUZ, F.W. Jr., KARMANN, I., VIANA, O. Jr., BURNS, S.J., FERRARI, J.A., VUILLE, M., SIAL, A.N., MOREIRA, M.Z., Stable isotope study of cave percolation waters in subtropical Brazil: Implications for paleoclimate inferences from speleothems, *Chemical Geology* **220** (2005) 245–262.

- [5] GUO, L., TANAKAA, T., WANGA, D., TANAKAA, N., MURATAB, A., Distributions, speciation and stable isotope composition of organic matter in the southeastern Bering Sea, *Marine Chemistry* **91** (2004) 211–226.
- [6] MAHAFFEY, C., WILLIAMS, R.G., WOLFF, G.A., ANDERSON, W.T., Physical supply of nitrogen to phytoplankton in the Atlantic Ocean, *Global Biogeochemical Cycles* **18** (2004) GB1034, doi: 10.1029/2003GB002129.

**ORIGIN AND EFFECTS OF NITROGEN
POLLUTION IN GROUNDWATER TRACED BY
 $\delta^{15}\text{N}_{\text{-NO}_3}$ AND $\delta^{18}\text{O}_{\text{-NO}_3}$: THE CASE OF ABIDJAN
(IVORY COAST)**

M.S. OGA YEI*, E. SACCHI**⁺, G.M. ZUPPI⁺⁺

*Université de Cocody,
UFR-STRM, Abidjan,
Ivory Coast

**Dipartimento di Scienze della Terra,
Università di Pavia,
Italy

⁺CNR-IGG,
Sezione di Pavia,
Italy

⁺⁺Dipartimento di Scienze Ambientali,
Università di Venezia,
Italy

Abstract

Groundwater resources of area of Abidjan are heavily impacted by nitrate pollution. A survey on 13 wells providing drinking water to the city was conducted in 2005, considering stable isotopes of the water molecule and of dissolved compounds (^{13}C and ^{15}N), and major and trace elements. Nitrogen isotopes allow definition of the origin of nitrate contamination, mainly from urban sewage, and the processes controlling its distribution. This information, coupled to hydrogeology and groundwater geochemistry highlights major changes in groundwater quality. Nitrate content is associated with increased acidity of poorly buffered solutions in a geochemically open system and therefore, is not affected by denitrification. Dissolved inorganic carbon confirms an input from organic matter decomposition, related to both pollution and diagenesis. This geochemical evolution is observed in both Quaternary and Continental Terminal aquifers, and is independent of depth. Comparison with previous hydrochemical data suggests a rapid decline in groundwater quality.

1. INTRODUCTION

Groundwater contamination by nitrates is frequently observed in West Africa, and is reported for Burkina-Faso[1] Niger [2, 3] Benin [4] and Senegal [5] and is especially prominent close to urban areas. Several origins have been suggested including urbanisation, deforestation and peri-urban agricultural development.

In the Abidjan region, high dissolved nitrate concentrations may be found at 100 m depth [6]. Numerous pollution sources and causes have been suggested, including increasing and deregulated urbanisation. In Abidjan, only 30% of the population is connected to the sewage network, discharging used water into the Ebrie lagoon [7, 8]. In addition, the system is affected by chronic malfunctioning of purification plants and by the unregulated interconnection with the rainwater drain. On the other hand, peri-urban area and peripheral cities are characterised by the total absence of a sewage network, and the diffuse presence of individual of leaking wells and septic tanks.

Aquifers from the Continental Terminal and Quaternary formations host young and vulnerable waters as indicated by bacteriological studies showing the common presence of *Escherichia coli* [9].

2. GEOLOGICAL SETTING

The Abidjan region is located in southern Ivory Coast (West Africa), facing the Guinea Gulf. This region constitutes the central part of a coastal

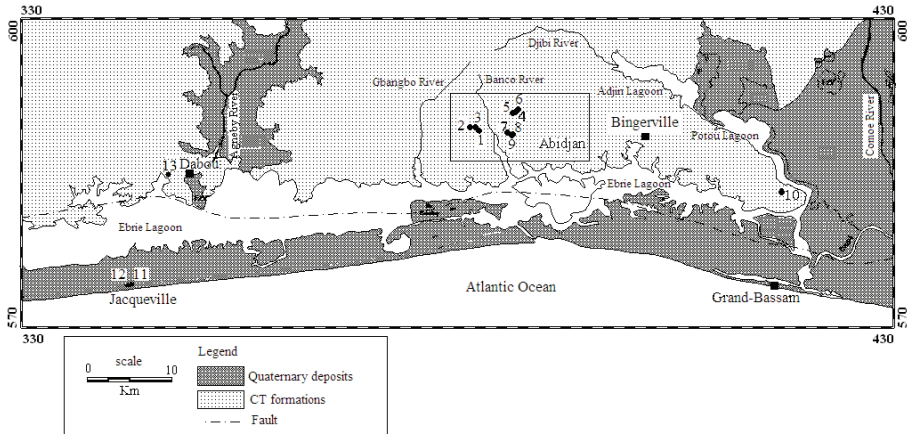


FIG. 1. Geological setting of the investigated region and sample locations.

ORIGIN AND EFFECTS OF NITROGEN POLLUTION IN GROUNDWATER

sedimentary basin, between latitudes of 5°70 and 6°00 N and longitudes of 3°30 and 4°30 W. The coastal basin represents 3% of the Ivory Coast surface.

West Africa, from the Sahel down to the Gulf of Guinea, is affected by monsoon type rainfall and squall lines. The climatic regime in the Abidjan region is humid and warm with fourth distinct seasons. The vegetation is an open forest near the coastline and becomes dense further in the continent.

Three aquifers may be distinguished within the sedimentary basin:

- The Quaternary formations (Q), located in the southern part of Ebrie Lagoon, reach a maximum thickness of 140 m and show permeability ranging from 4×10^{-5} to 10^{-3} m/s. These formations host the Oogolian and Nouakchottian aquifers, located respectively in coarse and fine-to-medium grained marine sands. These aquifers are very sensitive to pollution, their piezometric level being very close to the land surface.
- The Continental Terminal formations (CT) are Mio-Pliocenic deposits mainly constituted by sands, clays, sandstones and indurated lateritic layers. They are located to the north of Ebrie Lagoon and display a maximum thickness of 160 m. These formations host the aquifer tapped for domestic purposes in the Abidjan area. Its permeability ranges from 10^{-6} to 10^{-3} ms^{-1} and is highly transmissive, between 30×10^{-2} m^2s^{-1} and 20×10^{-2} m^2s^{-1} [10, 12]
- The Upper Cretaceous formation is constituted by poorly fractured calcareous rocks mixed with coarse sand. This reservoir is exploited by the Société Africaine d'exploitation d'Eau Minérale (SADEM) for the production of bottled water. This aquifer is poorly characterized in term of geometry, volume of pumped water and static level.

The bed rock of the studied area is constituted by the Precambrian crystalline basement.

Due to their relevance as drinking water resources for the Abidjan region, only the CT and Q aquifers have been considered in this study. Previous work has shown that unpolluted groundwater from CT displays low values of pH (3.5–5.4) and mineralization (EC between 20 and 55 $\mu\text{S} \cdot \text{cm}^{-1}$). Water from the Q aquifer also shows low pH values (3.8–6.6), but is characterised by a relatively higher mineralization (140–225 $\mu\text{S} \cdot \text{cm}^{-1}$) [6]. As a consequence of acidic pH, pCO_2 varies between $10^{-2.40}$ and $10^{-0.6}$ atm (vs atmospheric $\text{pCO}_2 = 10^{-3.5}$ atm). The comparison between $\delta^{13}\text{C}$ of DIC and $\delta^{13}\text{C}$ of soil gas has shown that dissolved carbon is acquired during transit through the unsaturated zone in an geochemically open system. Tritium and carbon-14 contents indicate that the low mineralization of groundwater is due to the short time of contact and the

total absence of carbonates in the aquifer bedrock [6]. Higher conductivities and mineralization are related to groundwater pollution by nitrates and/or chlorides.

3. MATERIALS AND METHODS

The investigation has been conducted on 12 groundwater samples which are exploited by the Société de Distribution d'Eau de Côte d'Ivoire (SODECI) for human consumption and one private well; eleven samples tap the Continental Terminal and two the Quaternary aquifers. Well depths range from 10 to 118 m. All samples have nitrate concentration higher than 10 mg/L.

The pH, redox potential, alkalinity (by HCl titration) and conductivity were in most cases measured in situ. Chemical analyses were performed at the University of Pavia, by ion chromatography and ICP-MS. All reported values have ionic balance within 5%. Samples for stable isotope analysis were collected and prepared according to standard procedures [13]. All gases were analysed on a Finningan™ MAT 250 Mass Spectrometer at ISO4 s.s., Turin, Italy.

4. RESULTS

Results confirm the general characteristics of groundwater from the Abidjan region: very low mineralization (E.C. between 69 and 331 $\mu\text{S} \cdot \text{cm}^{-1}$), acidic pH (4.0–5.3), with sodium and chloride as dominant ions. Nevertheless, nitrates range from 10 to more than 100 mg/L in samples with the highest conductivity, suggesting a major contribution to groundwater mineralisation. SiO_2 content is uniformly set at about 10 mg/L. Among trace elements, Al^{3+} is very high, and exceeds the drinking water standards for several samples. Traces of B and P were also detected. A good correlation between all chemical parameters is observed, suggesting the presence of a dominant mineralization process.

Stable isotopes of the water molecule agree with the results of previous studies, which indicate for both aquifers a local recharge from rain water. $\delta^{13}\text{C}$ values range from -15.39 to -23.08‰ vs PDB. Despite the wide range of nitrate concentrations, $\delta^{15}\text{N}$ and $\delta^{18}\text{O}$ range respectively from 9.55 to 12.55‰ vs AIR and from 6.3 to 10.7‰ vs SMOW.

ORIGIN AND EFFECTS OF NITROGEN POLLUTION IN GROUNDWATER

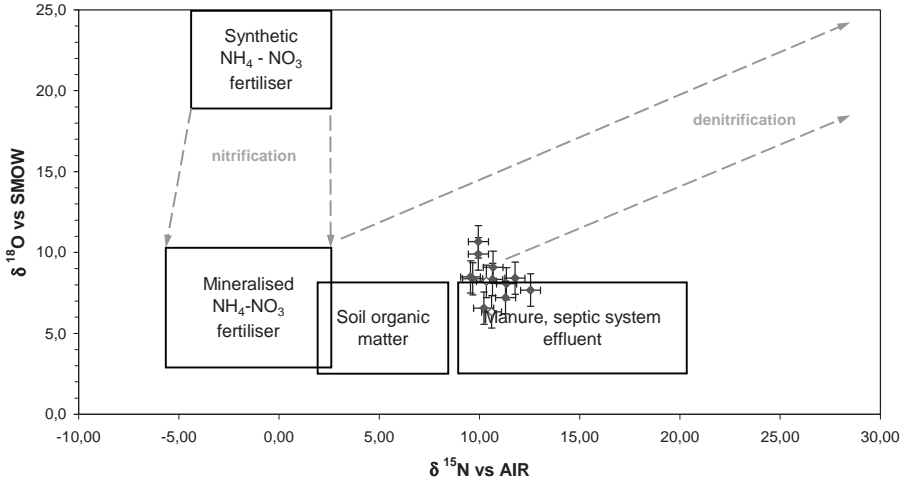


FIG. 2. Isotopic composition of dissolved nitrates (permil) in Abidjan groundwater. Empty diamonds: Q aquifer; full diamonds: CT aquifer.

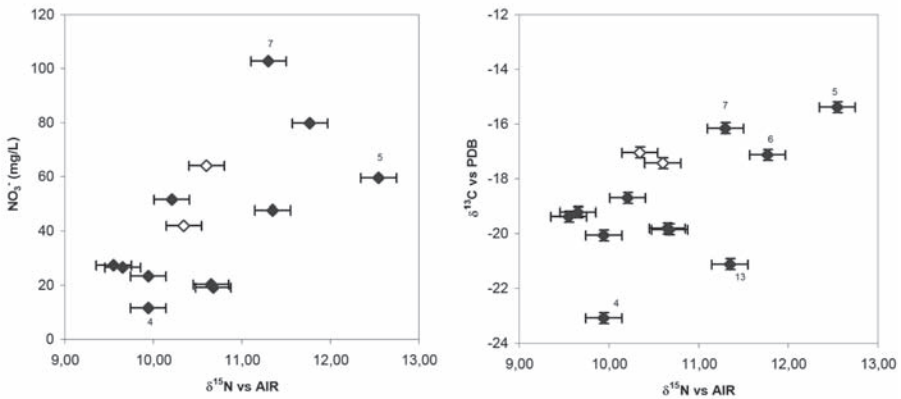


FIG. 3. Nitrate concentration (mg/L) and $\delta^{13}\text{C}$ of DIC (permil) vs $\delta^{15}\text{N}$ of DIN (permil). Empty diamonds: Q aquifer; full diamonds: CT aquifer

5. DISCUSSION

5.1. Origin of groundwater pollution

The isotopic composition of dissolved nitrates has been plotted in the classical $\delta^{15}\text{N}$ vs $\delta^{18}\text{O}$ (Fig. 2) diagram, where the position of the composition

fields has been adjusted taking into account the isotopic composition local waters ($\delta^{18}\text{O} \approx -2.6\text{‰}$). For most nitrates, interpretation of an origin from septic system effluents can be evoked. This interpretation may be further confirmed by the close relationship between dissolved nitrate content and isotopic composition (Fig. 3) which indicates that most of the contamination has a positive $\delta^{15}\text{N}$, typical of animal and human waste. Increase in dissolved nitrates is associated to an increase in sulphate, chloride, bromine and to detectable amounts of B, all typical contaminants for used water. A similar tendency is also observed for the Q aquifer.

No denitrification seems to occur despite the elevated depth of collection for most samples, around 100 m. A direct relationship between $\delta^{15}\text{N}$ of DIN and $\delta^{13}\text{C}$ of DIC is observed (Fig. 3). The more negative values of $\delta^{13}\text{C}$ in low nitrate water could correspond to a decomposition of organic matter transported from the surface, indicating that the downward migration of dissolved nitrates is very rapid and occurs in a system which is geochemically open to oxygen.

5.2. Effects of groundwater pollution

The acidity associated with nitrate pollution is generally buffered by the presence of carbonates in the aquifer matrix, this phenomenon increasing water hardness and TDS [14]. In the case of the CT and Q aquifers, the absence of carbonates and the fast infiltration rate result in a shift of groundwater towards more acidic pH, as shown in Fig. 4. The increased acidity promotes the hydrolysis of matrix silicates, releasing major and trace cations in the solution. This inference is consistent with the observed correlation between

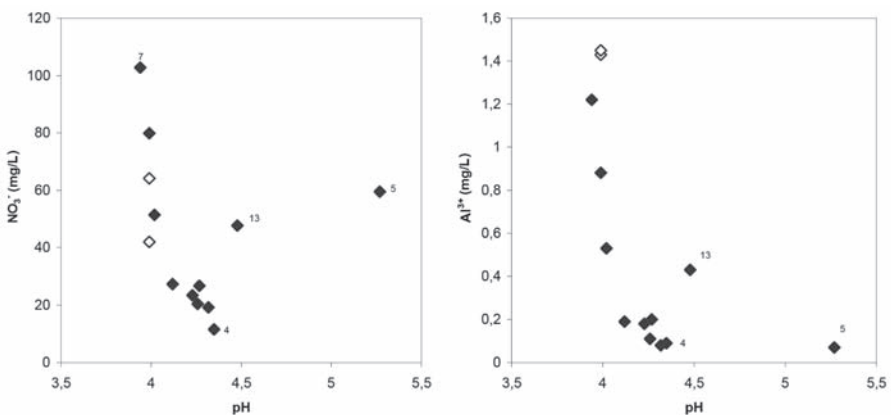


FIG. 4. Geochemical response of the water-rock system to the acidic perturbation induced by dissolved nitrates. Empty diamonds: Q aquifer; full diamonds: CT aquifer.

ORIGIN AND EFFECTS OF NITROGEN POLLUTION IN GROUNDWATER

trace elements and DIN content, even for elements which are not generally derived from the surface (e.g. Rb). The enhancement of silicate weathering is not shown by the SiO_2 content, as water is generally saturated with respect to chalcedony, but rather by Al^{3+} which is not limited in solubility, and shows a marked tendency to increase, reaching concentrations exceeding drinking water standards.

Sample 5 generally does not follow the depicted trends; it should be noted though that this sample shows the highest contents of all contaminants and the highest pH of the whole data set. Previous studies sampling from this well showed the presence of ammonia and bacterial contamination [15]. Sample 13 is a private well, only 10 m deep, and is located to the East of the main investigated area. The well is positioned at a lower altitude with respect to the village and is close to an uncontrolled landfill.

6. CONCLUSION

Stable isotopes of DIN were used to evaluate the origin of dissolved nitrates in groundwater from the Abidjan area and indicate the mechanisms of infiltration. In addition, the study demonstrated the major perturbation induced by the addition of nitrates to the water-rock equilibrium.

The comparison with previous hydrochemical and isotopic data [6] suggests that this geochemical evolution is very rapid and leading to a dramatic decline in groundwater quality.

ACKNOWLEDGEMENTS

The authors wish to acknowledge the CICOPS – Centre for International Cooperation and Development of the University of Pavia, which granted a visiting scientist scholarship to M.S. Oga, ISO4 s.s. which assisted in sample preparation and analysis, Prof. A. Profumo who performed trace element analysis and the IAEA, which granted a travel and living allowance for the presentation of this work.

REFERENCES

- [1] GROEN, J.J.B., SCHUMANN, GEIRNAERT, W., The occurrence of high nitrate concentration in groundwater in villages in Northwestern Burkina Faso, *Journal of African Earth Sciences* **7** (1988) 999–1009.

- [2] JOSEPH, A., GIRARD, P., Etude de la pollution en nitrate des aquifères du socle: exemple de la nappe de Niamey, Ministère de l'Hydraulique du Niger (1990).
- [3] GIRARD P., Techniques isotopiques (¹⁵N, ¹⁸O) appliquées à l'étude des nappes des altérites et du socle fracturé de l'ouest africain — Etude de cas: L'Ouest du Niger, Thèse, Université de Québec à Montréal (UQAM), Canada (1993) 138.
- [4] BOUKARY, M., GAYE, C.B., FAYE, A., FAYE, S., The impact of urban development on coastal aquifers near Cotonou, Benin, *Journal of African Earth Sciences*, **22** 4 (1996) 403-408.
- [5] TANDIA A.A., DIOP E.S., GAYE, C.B., Pollution par les nitrates des nappes phréatiques sous environnement semi-urbain non assaini: exemple de la nappe de Yeumbeul, Sénégal, *Journal of African Earth Sciences* **29** 4 (1999) 809–822.
- [6] OGA, Y.M-S., Ressources en eaux souterraines dans la région du Grand Abidjan (Côte d'Ivoire): Approches hydrochimique et isotopique, Thèse Univ Paris IX, Orsay, France (1998) 240.
- [7] DONGO, K., Etude de l'évolution du système d'assainissement « Eaux Usées » de la ville d'Abidjan, Mémoire de DEA des Sciences de la Terre, Université de Cocody (2001) 80.
- [8] DONGO, K., Analyse des déficiences dans la gestion du drainage urbain et des déchets solides et liquides dans les quartiers précaires de Yopougon (Abidjan, Côte d'Ivoire): approches cartographie-SIG, modélisation et socio-Anthropologie. Univer, Cocody Abidjan, UFR-STRM (2006) 229.
- [9] JOURDA J.R.P., Qualité des eaux souterraines de la nappe d'Abidjan, *Bulletin No. 4*, Juin 2004.
- [10] JOURDA, R.J.P., Contribution à l'étude géologique et hydrogéologique de la région du Grand Abidjan (Côte d'Ivoire), Thèse. Univ. Scient. Techno. et Med. de Grenoble, France (1987) 319.
- [11] SOGREA, Etude de la gestion et de la protection de la nappe assurant l'alimentation en eau potable d'Abidjan; Etude sur modèle mathématique; Rapports de phase 1 et 2, République de Côte d'Ivoire, Ministère des Infrastructures Economiques, Direction et Contrôle des Grands Travaux (1996).
- [12] SORO, N., Gestion des eaux pour les villes africaines: évaluation rapide des ressources en eau souterraine/occupation des sols, UN-HABITAT, Avril 2003 (Rapport final).
- [13] CLARK, I., FRITZ, P., *Environmental Isotopes in Hydrogeology*, Lewis Publishers, Boca Raton (1997) 328.
- [14] SPRUILL, T.B., SHOWERS, W.J., HOWE, S.S., Application of classification-tree methods to identify nitrate sources in ground water, *Journal of Environmental Quality* **31** (2002) 1538–1549.
- [15] KOUADIO, L.P., ABDOULAYE, S., JOURDA, P., LOBA, M., RAMBAUD, A., Conséquences de la pollution urbaine sur la distribution d'eau d'alimentation

ORIGIN AND EFFECTS OF NITROGEN POLLUTION IN GROUNDWATER

publique à Abidjan, Cahier de l'Association Scientifique Européenne pour l'Eau et la Santé **3/1** (1998) 61-75.

GROUNDWATER AND ITS FUNCTIONING AT THE DOÑANA RAMSAR SITE WETLANDS (SW SPAIN): ROLE OF ENVIRONMENTAL ISOTOPES TO DEFINE THE FLOW SYSTEM

M. MANZANO*, E. CUSTODIO**, H. HIGUERAS*

*Dep. of Mining, Geological
and Topographical Engineering,
Technical University of Cartagena,
Cartagena, Murcia

**Dep. of Geotechnical Engineering and Geosciences,
Technical University of Catalonia,
Barcelona, Catalonia

Spain

Abstract

Out of the largely fluctuating surface water marshes, many of the environmental characteristics of the Doñana ecosystems depend on groundwater outflow and shallow watertable. Groundwater flow in the dominantly sandy Plio-Quaternary aquifer is complex and is currently undergoing important changes due to groundwater development. The use of environmental isotopes ^{18}O , ^2H , ^3H , ^{13}C , ^{14}C , ^{34}S , ^{39}Ar and ^{85}Kr has been very successful for defining recharge areas, flow patterns, transit times and the conceptual flow model. The importance of vertical groundwater flow in unconfined areas, as well as the behaviour of pre-Holocene confined water has been assessed. Thus, mixing patterns and chemical evolution can be explained. Lagoons are mostly aquifer discharge areas in which water evaporates. Some of the solutes remain trapped in bottom sediments and some are flushed out in wet events. This pattern is being changed due to the intensive aquifer development in some areas and negative ecological impacts are appearing.

1. INTRODUCTION

The Doñana aquifer system is situated in the SW coast of Spain, between the Guadalquivir River and the Portuguese border, and covers some 2700 km²

(Fig. 1). The climate is Mediterranean with an Atlantic influence. Mean rainfall is 500–600 mm, with a very high inter-annual variability. The mean yearly temperature is around 18°C.

A large part of the area (1100 km²) is strongly protected by the Spanish law. Also, Doñana is a Ramsar Convention area since 1990. Most of the Doñana core area is inhabited, but outside the protected zones large areas have been used for intensive agriculture developed late in the 1970s. Beach-based tourism is also an important economic activity.

Several hydrodynamic studies and groundwater flow modelling at regional and local scales have been performed to understand the aquifer functioning [1] and its relationship with the many wetlands of the watertable areas [2]. Hydrochemical and environmental isotopes studies have been performed to establish a conceptual model for groundwater chemistry origin and evolution, to obtain insights into groundwater recharge, transit and residence times, and to define the role of groundwater in wetlands [3–6].

2. BACKGROUND TO AQUIFER GEOLOGY AND HYDROGEOLOGY

The aquifer system consists of detrital, unconsolidated Plio–Quaternary sediments overlapping impervious Miocene marine marls (Fig. 1). The Pliocene materials are marls and silts. The Quaternary sediment consists of deltaic and alluvial silts, sands and gravels to the north, and littoral, alluvial and eolian sands to the west. The mineralogy consists of amorphous silica with minor contents of K-, Na-feldspars, illite, chlorite and kaolinite. Carbonates are present only locally.

To the southeast, the coarse sediments are covered by a thick (50–80 m) sequence of estuarine and marshy clays separated from the ocean by a recent sand spit. The sandy area to the north and west roughly behaves as an unconfined aquifer, while under the marsh area (1800 km²), a large confined aquifer has developed.

Recharge occurs mainly by rain infiltration in the sandy areas. At a regional scale groundwater flows to the confined area and to the ocean. Discharge takes place as seepage to the ocean, to the streams and the many wetlands situated on top of the sands, as evapotranspiration and as upward flows around the marshes. The SE sector of the confined area contains old marine water not flushed out due to the low hydraulic head prevailing since the late Holocene sea level stabilisation some 6 ka BP [5, 7]. Intensive groundwater abstraction since early in the 1980s for irrigation and to supply touristic areas has induced piezometric and watertable drawdown [1, 8].

GROUNDWATER AND ITS FUNCTIONING AT THE DOÑANA RAMSAR

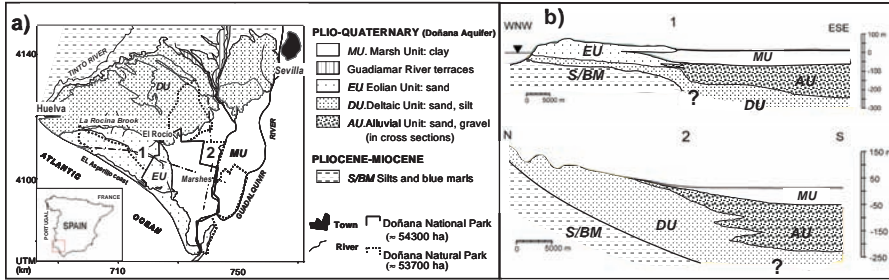


FIG. 1. Location, geology and geometry of the Doñana aquifer system. The freshwater wetlands are situated on top of the Eolian Unit (EU).

Pumping concentrates around the marshes, so it has partially depleted natural discharge to streams, phreatophytes and seepage, and has induced changes in vegetation and in wetlands hydrology [2, 8].

3. ISOTOPES AS TOOLS TO UNDERSTAND THE FLOW SYSTEM

Until 1990 the monitoring network consisted of multiscreened agricultural wells. Thus, groundwater samples and piezometric measurements integrated flow lines with different transit times and heads. As in many areas groundwater flow is mostly vertical, the information obtained did not allow insights into vertical gradients, chemical variations with depth or travel times. Early in the 1990s a dedicated monitoring network of nested boreholes was designed and built.

The study of $\delta^{18}\text{O}$ and $\delta^2\text{H}$ in rain water, surface water, phreatic and deeper groundwater samples from the whole aquifer confirmed the conceptual model for recharge origin and mechanisms:

- (1) Local rain water values fit the Mean World Meteoric Water Line (Fig. 2a).
- (2) Shallow groundwater in the watertable areas has the $\delta^{18}\text{O}$ and $\delta^2\text{H}$ signature of averaged local rain without significant fractionation: $\delta^{18}\text{O} = -4.7$ to -5.5‰ SMOW, $\delta^2\text{H} = -28$ to -33‰ SMOW. However, detailed examination of phreatic waters from the western and northern recharge areas shows that groundwater is $\sim 0.5\text{‰}$ (for $\delta^{18}\text{O}$) and $\sim 4\text{‰}$ (for $\delta^2\text{H}$) heavier in the north than in the west (Fig. 2b). This difference appears to result from higher groundwater recycling of evaporated water (due to irrigation) in the north zone, where the aquifer is much thinner than to the west [5].

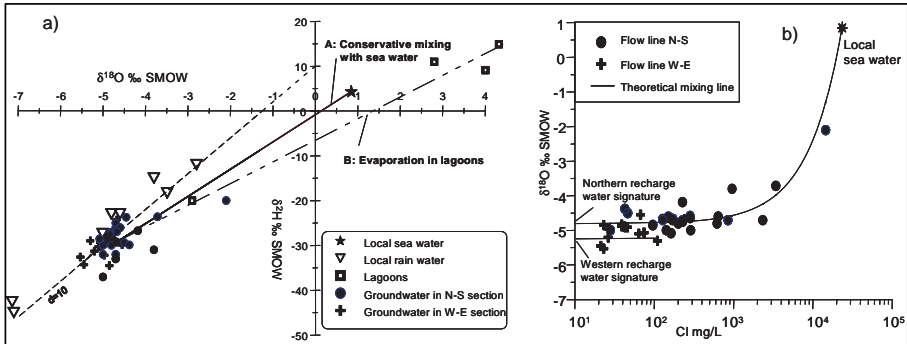


FIG. 2. a) Isotopic signature of ground and surface water showing evaporation and mixing processes. b) Observed isotopic fractionation in recharge water of the northern unconfined area.

Changes in $\delta^{18}\text{O}$ and $\delta^2\text{H}$ values along regional and local groundwater flow lines show the occurrence of three modifying processes:

- (1) A slight evaporative concentration of recharge water in the northern recharge area with respect to the western one (already mentioned).
- (2) Mixing of fresh and saline groundwater. This mixing occurs through two different mechanisms: by deep mixing of fresh and marine groundwater under the marshes, along regional flow lines; by incorporation of sea spray to very shallow groundwater and surface water around the lagoons located near the coastal sand spit. Trend A in Fig. 2a is defined by both types of samples.
- (3) Evaporative concentration of water from surface bodies in lagoons situated on certain phreatic flow lines. Trend B in Fig. 2a indicates evaporation of water prior infiltration; samples on this line are from both lagoon waters and nearby shallow groundwater [2, 5, 6].

Tritium studies helped define the groundwater flow model in different areas and to estimate transit and residence times. Studies carried out before 1990 [3, 4] had many uncertainties due to the impossibility of sampling individual flow lines. In the 1990s, the new nested boreholes allowed clarification of the groundwater flow network by measuring vertical head evolution, and establishment of flow paths through the study of flow paths that facilitate the study of chemical evolution and travel times. A significant advance was examination of different flow models to interpret ^3H data combining the different types of sampling points available, their location either in a recharge or discharge area, and the sampling methods used [9]. The work was supported by modelling (MULTIS [10]), and provided great knowledge about transit and residence times across the aquifer:

GROUNDWATER AND ITS FUNCTIONING AT THE DOÑANA RAMSAR

- **Recharge areas:** shallow groundwater (<15 m) is recent and spent between one and a few years to reach the watertable. Groundwater between 20 and 25 m depth have transit times of 15–34 years; for depths >25 m transit times are >34 years, and groundwater at >40 m depth was recharged before 1954.
- **Discharge areas:** springs in the El Asperillo coastal cliff and along La Rocina brook have short turn-over times of 6–7 years. Deeper (>30 m) groundwater close to La Rocina was recharged before 1954. Discharging groundwater along the western boundary between the marshes and the sands has transit times around 30 years at 20–25 m depth, and for depths >25 m it was recharged before 1954. The springs of El Asperillo had higher ^3H contents than expected, but the study to build-up the local input function showed that rain water contaminated with artificial ^3H and generated in 1986 in Gibraltar (to the E of Doñana) reached the area. This contaminated rain was detected in shallow coastal flows and also at shallow depths in some agricultural wells.
- **Confined area:** both the old wells and the new nested boreholes contain groundwater recharged before 1954. In spite of being pumped for cleaning several times, some new boreholes still have some remains of drilling water, as shows the presence of measurable ^3H and NO_3^- .

The ^{13}C and ^{14}C data were used to build the hydrochemical model and estimate groundwater ages. Soil gas samples indicate $\delta^{13}\text{C}$ values of CO_2 about -23 to -25‰ in the eolian sandy recharge areas, which corresponds to soil CO_2 derived from Calvin type plants ($\delta^{13}\text{C} \sim -25\text{‰}$ PDB). Groundwater may be only slightly heavier if they remain acidic and free of soil carbonates, but most often values are around -16‰ PDB. This difference can be explained as the result of isotopic equilibrium of dissolved carbonate species and soil CO_2 in an open system, whose result depends on pH. Downflow in the saturated zone conditions may change into a closed system in which there is a progressive dissolution of soil carbonates with average $\delta^{13}\text{C} = 0.0$ to -6.4‰ PDB, as measured by [3] in local sediments. These authors found that the $\delta^{13}\text{C}$ values measured in the confined area tended to be heavier the greater the salinity, and that some of the fresh waters under the marsh clays had very heavy DIC ($\delta^{13}\text{C} = -4$ to $+2 \text{‰}$). The marsh clay data can be explained explained by input of heavy C from evolved, old organic matter ubiquitous in the clay sediments, though isotopic analyses of this organic matter are not available.

The ^{14}C activity values measured in the 1980s [3] were in the range between almost 100 pMC and about 7 pMC, which means up to 15 ka according to the Fontes and Garnier model [11]. The ^{14}C ages indicated that groundwaters in the watertable areas are less than a few centuries old. Groundwater becomes much

TABLE 1. CHEMICAL AND ISOTOPIC DATA FROM THE 1997-2001 SAMPLING.

Identification (depth)	Samp. date	HCO ₃ ⁻ meq/L	NO ₃ ⁻ meq/L	³ H UT	δ ¹³ C ‰ PDB	¹⁴ C pMC	Pearson's age, years ¹	³⁹ Ar pcm	⁸⁵ Kr dpm/mL Kr	CO ₂ Vol. %	RT (°C)
SGOP8-S3 (44 m)	Nov. 00	0.7	0.03	0.00±0.14	-20.2	75.1	1852				
Mogea-SI6 (68 m)	Nov. 00	0.65	0.00	0.11±0.15	-21.1	76.9	2017				
Vetalengua S56 (80 m)	Nov. 00	3.00	0.17	0.06±0.15	-13.0	46.9	2101				
M-7-1	Jul. 01	2.74	0.03	0.15±0.13	-12.5	13.2	12259				
M-1-1	Jul. 01	2.02	0.00	0.18±0.13	-12.3	12.2	12777				
M-2-6	Jul. 01	1.1	0.00	0.01±0.13	-13.0	11.5	13723				
Alamillo-S24 (108 m)	Nov. 00	2.1	0.00	2.2±0.19	-15.5	53.1	2528				
SGOP1-S4 (140 m)	Nov. 00	0.7	0.03	0.15±0.15	-19.5	73.2	1772				
P.Doñana-S49 (155 m)	Nov. 00	1.6	0.00	0.99±0.15	-14.2	14.7	12423				
P.Doñana-S50 (56 m)	Jul. 01	0.3	0.02	0.25±0.13	-19.5	60.7	3320				
L. MariLópez-S2	Jul. 01	1.92	0.00	0.44±0.14	-11.9	31.2	4740				
S. FAO	Jul. 01	0.92	0.00	0.06±0.13	-11.3	7.4	16210				
I-2-9	Jun. 97	5.24	0.27	0.39±0.26	-14.3	46.9	2889				

GROUNDWATER AND ITS FUNCTIONING AT THE DOÑANA RAMSAR

M-8-13 (55 m)	Jun. 97	6.1	0.05	0.17±0.26	-12.0	79.1	-2880	70±6	3±0.3	30.45	19.8±1.8
P. Resina-S54 (68 m)	Jun. 97	5.51	0.05	0.23±0.25	-11.6	51.7	353	34±4/30±10	0.34±0.05	27.5	15.1±1.2
AM5	Jun. 97	3.05	0.15	0.3±0.24	-13.5	27.5	6827				
AM1	Nov. 97	3.00	0.03	0.65±0.69	-14.0	33.6	5471				
Raposo-S13 (74 m)	Jun. 97	2.38	0.03	1.15±0.26	-13.0	20.9	8784	28±4	0.28±0.04	1.75	19.7±3.4
C. Bombas-S2 (72 m)	Jun. 97	4.00	0.01	0.48±0.26	-11.0	7.34	16055	<10	0.70±0.11	4.85	17.8±1.7

¹ Pearson's ages after $\delta^{13}\text{C}$ (soil CO_2) = -21.5% and $\delta^{13}\text{C}$ (calcite) = 0‰

older southward and eastward under the marshes without significant changes in water stable isotopes, except the mixing with saline water. In order to check this conceptual mixing model, to detect possible admixtures of recent and old components, and to determine the age structure of the deep mixed waters, a new sampling to measure dissolved gasses, and ^3H , ^2H , ^{18}O , ^{14}C , ^{13}C , ^{39}Ar and ^{85}Kr were carried out in 1997–2001 (Table 1). The new ^{14}C data are coherent with the previous ones, but the heavy ^{13}C values measured by [3] were not found. Also, there is no clear relationship between ^{14}C and ^{13}C and the DIC contents (Fig. 3). Thus, the dominant model for groundwater age in the confined aquifer is that the observed decrease of ^{14}C activities downward flow is mostly due to groundwater aging. However, for some samples this interpretation is not true (see below).

The presence of measurable ^3H , ^{39}Ar and ^{85}Kr in some of the oldest groundwater samples (Table 1) indicate that they are admixtures of old and recent components. For the old wells mixing can be explained by the joint sampling of recent and old flow lines, but for single screened boreholes it can only be explained by remnants of drilling water in the low permeability sediments. To explain the ^3H contents in old groundwater, assuming a maximum of 10 TU for 1999–2001 precipitation, the recent water component in all wells should be less than about 10%, even for the youngest samples showing the highest ^{39}Ar and ^{14}C activity values. An even lower limit of about 1% is estimated for boreholes S54, S13 and S2 from the low ^{85}Kr activity. The low ^{85}Kr values demonstrate that the sampling intervals of 50–70 m below surface are deep enough to prevent significant gas exchange between water and the atmosphere, thus discarding the possible increase of ^{39}Ar activity from anthropogenic sources [5].

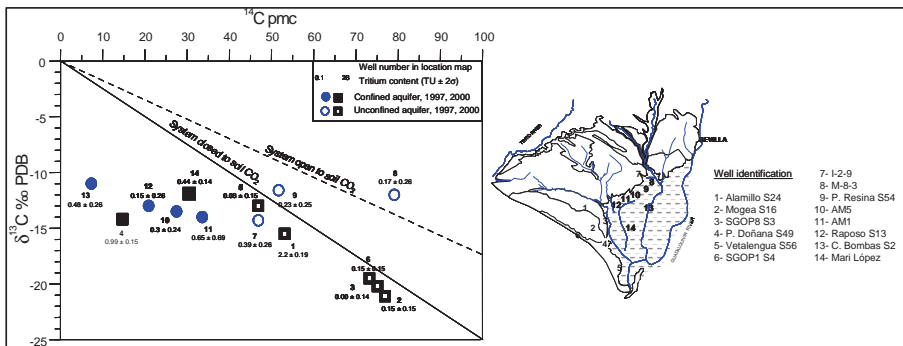


FIG. 3. $\delta^{13}\text{C}$ and ^{14}C in groundwater of the unconfined and confined areas. Values and other information are in Table 1. Tritium contents are clearly different from zero in wells 7, 9 and 18.

GROUNDWATER AND ITS FUNCTIONING AT THE DOÑANA RAMSAR

In some samples the amount of extracted gas is higher than 30% compared to air-saturated water. This excess corresponds to an equilibration pressure three orders of magnitude greater than in air and is assumed to come from organic matter in the sediments. This observation implies that in these cases most DIC is not from soil CO₂ but is sedimentogenic, and thus the calculated age is not that of groundwater, but of organic matter in the sediments. A detailed study is still lacking.

Noble gas concentrations were determined in four samples to calculate recharge temperatures of assumed palaeowaters. Evidence of CH₄ was not found. No palaeoclimatic signature was found in the freshwater component of the confined aquifer groundwater after correction of $\delta^{18}\text{O}$ and $\delta^2\text{H}$ values for marine water contribution (RT in Table 1) [5]. This result agrees with the information from a pollen record described in the coastal area of Doñana which covers the last 18 ka and suggests no major climatic changes during this period, and that during the last glacial maximum weather in the southwest of the Iberian Peninsula was humid and warm, and not very different to the present one [7].

4. THE GROUNDWATER ROLE IN WETLANDS AS INDICATED BY ISOTOPES

The numerous wetlands of Doñana have diverse geo-morphological origin and hydrology, but most of them are directly dependent on groundwater. The two most common wetland types are small erosive or eolian depressions located at the foot of stabilised dune fronts and small watercourses. Both types are mostly seasonal and their location is related to local or medium-scale groundwater flow paths. Water chemistry in those wetlands reflects mostly groundwater composition, which is highly stable in time. In general, it is of the sodium-chloride type or intermediate between sodium-chloride and calcium-bicarbonate. However, some of the lagoons show temporary changes in mineralization and ionic type which depend on modifications in the balance between water inputs and outputs and on bio-geo-chemical reactions. These reactions may produce significative temporal changes in water salinity, pH and ion composition.

Studies under way to improve the knowledge of wetlands processes include $\delta^{18}\text{O}_{\text{H}_2\text{O}}$ and $\delta^2\text{H}$ and $\delta^{34}\text{S}$ and $\delta^{18}\text{O}_{\text{SO}_4}$. The preliminary results indicate that around certain lagoons regional or local groundwater flow systems develop along the year, driven by seasonal changes in the hydraulic gradient direction between the ponds and the nearby watertable [2]. This implies that major chemical changes occurring in the wetland water bodies are transferred

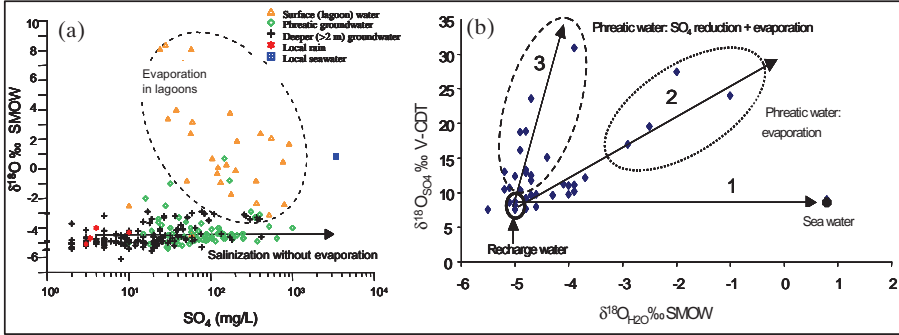


FIG. 4. a) The groundwater salinization trend without isotopic enrichment results from solid sulphur and sulphate salt dissolution. b) Groundwater samples along trend 2 show mostly evaporation; samples along trend 3 show mostly SO_4 reduction.

to the nearby shallow groundwater. In some lagoons strong evaporation in the dry season causes sodium chloride, calcium sulphate and possibly calcium carbonate precipitation and accumulation in the basin floodable zone, often accompanied by sulphate reduction and sulphur accumulation in the bottom sediments. In the next wet season, a large fraction of these salts is re-dissolved and transferred to the surrounding phreatic water along with sulphur, oxidized to sulphate (Fig. 4). This input modifies the salinity of shallow groundwater and, eventually, its ionic composition. The process is seasonal around some lagoons, but in other cases sulphate concentration in groundwater is increasing in the last years, thus pointing to enhanced oxidation of S accumulated in lake sediments.

5. CONCLUSIONS

The previous isotopic studies carried out in Doñana, combined with the improvement of the observation network and integration of chemical and hydrodynamic studies, have contributed greatly to the knowledge of the groundwater flow network, transit and residence times and the role of groundwater in the wetlands. With respect to the last subject, studies under way combining $\delta^{18}O_{H_2O}$, δ^2H , $\delta^{34}S_{SO_4}$ and $\delta^{18}O_{SO_4}$, show that although groundwater composition dominates wetlands chemistry at the regional scale, some reactions taking place within the lagoons influence the composition of the nearby shallow groundwater. Changes in water salinity, ion composition and isotopic concentration originated in the lakes can be traced downflow in the aquifer. In wetlands well connected to the groundwater flow these changes are just seasonal,

but in some areas where accumulated watertable lowering due to pumping has turned former permanent or seasonal wetlands into sporadic ones, evidence of irreversible groundwater composition changes are already noticeable. Thus, intensive groundwater abstraction is having a serious impact not only on groundwater discharge to wetlands by seepage and evapotranspiration, but also on wetlands functioning and groundwater chemistry.

REFERENCES

- [1] TRICK, TH., CUSTODIO, E., Hydrodynamic characteristics of the western Doñana Region (area of El Abalarío), Huelva, Spain, *Hydrogeology Journal* **12** (2004) 321–335.
- [2] LOZANO, E., DELGADO, F., MANZANO, M., CUSTODIO, E., COLETO, C., Hydrochemical characterisation of ground and surface waters in “the Cotos” area, Doñana National Park, southwestern Spain, In: *Groundwater and Human Development*, E.M. Bocanegra, M.A. Hernández y E. Usunoff (eds.), International Association of Hydrogeologists, Selected Papers **6** (2005) 217–231.
- [3] BAONZA, E., PLATA, A., SILGADO, A., Hidrología isotópica de las aguas subterráneas del Parque Nacional de Doñana y zona de influencia, Centro de Estudios y Experimentación de Obras Públicas, Madrid, *Cuadernos de Investigación* **C7** (1984) 1–139.
- [4] PONCELA, R., MANZANO, M., CUSTODIO, E., Medidas anómalas de tritio en el área de Doñana, *Hidrogeología y Recursos Hidráulicos* **XVII** (1992) 351–365.
- [5] MANZANO, M., CUSTODIO, E., LOOSLI, H.H., CABRERA, M.C., RIERA, X., CUSTODIO, J., Palaeowater in coastal aquifers of Spain. *Palaeowaters in Coastal Europe: Evolution of Groundwater since the late Pleistocene*, (Edmunds, W.M. y Milne, C.J., eds.), Geological Society London, Sp. Publ. **189** (2001) 107–138.
- [6] MANZANO, M., CUSTODIO, E., IGLESIAS, M., LOZANO, E., Groundwater baseline composition and geochemical controls in the Doñana aquifer system (SW Spain), In: *The natural baseline quality of groundwater*, W. M. Edmunds and P. Shand (eds.), Blackwell (in press) (2007).
- [7] ZAZO, C., GOY, J.L., LARIO, J., SILVA, P.G., Littoral zone and rapid climatic changes during the last 20,000 years: the Iberian study case, *Z. Geomorph. N.F.*; Berlin–Stuttgart, Suppl. **102** (1996) 119–134.
- [8] MANZANO, M., CUSTODIO, E., MEDIAVILLA, C., MONTES, C., Effects of localised intensive aquifer exploitation on the Doñana wetlands (SW Spain). *Groundwater Intensive Use*, Intern. Assoc. Hydrogeologists, IAH Selected Papers, 7, Balkema, Leiden (2005) 295–306.

- [9] IGLESIAS, M., Caracterización hidrogeoquímica del flujo del agua subterránea en El Abalario, Doñana, Huelva, Doctoral Thesis, Civil Engineering School, Technical University of Catalonia, Barcelona, Spain (1999).
- [10] RICHTER, J., SZYMCZAK, P., JORDAN, H., A computer program for the interpretation of isotope hydrogeologic data, Tracer Hydrology, Proceedings of the 6th Int. Symp. on water tracing, Karlsruhe (1992) 461–462.
- [11] FONTES, J.CH., GARNIER, J.M., Determination of the initial ^{14}C activity of the total dissolved carbon: a review of the existing models and a new approach, Water Resources Research **15** 2 (1979) 399–413.

RELATIONSHIP BETWEEN STABLE ISOTOPES OF PRECIPITATION AND ATMOSPHERIC CIRCULATION – CASE STUDY: APPLICATION IN A PILOT BASIN IN CENTRAL ANATOLIA

Y. INCI TEKELI

Ministry of Agriculture and Rural Affairs,
Soil and Water Resource Ankara Research Institute

A. UNAL SORMAN

Middle East Technical University,
Civil Engineering Department,
Water Resources Research Center

Ankara, Turkey

Abstract

The stable isotope values of precipitation are strongly influenced by water vapour source and trajectory. It can be used as a tool for the evaluation of atmospheric circulation. This approach requires an understanding of how atmospheric circulation influences precipitation $\delta^{18}\text{O}$. This study seeks to understand the relationship between atmospheric circulation and $\delta^{18}\text{O}$ of individual storm events for a micro-scale basin in Central Anatolia. Circulation back trajectories and $\delta^{18}\text{O}$ values for 30 precipitation samples taken from 7 individual events were also examined to determine circulation type for each event. Results indicated that precipitation $\delta^{18}\text{O}$ was related to precipitation intensity. Precipitation events originating from Siberia and Mediterranean–Africa air masses, seen high frequently in the study area, yielded relatively depleted $\delta^{18}\text{O}$ values.

1. INTRODUCTION

Spatial and temporal distributions of precipitation vary significantly in the different regions of Turkey. In general, the amount of precipitation is low in the central part of the country. There are many representative hydrologic basins established in Turkey. In the Guvenç study basin in central East Anatolia, Turkey, precipitation values are recorded continuously and have been investigated for the last 20 years. Guvenç basin is one of the representative basins in Turkey with

a drainage size of 16.125 km². In this basin five rain gauges and a streamgauging station have been installed to collect rainfall and runoff data.

The main features of the spatial and temporal variations of stable isotope ratio of oxygen and hydrogen in precipitation and atmospheric moisture are based on water vapour [1]. Factors that control $\delta^{18}\text{O}$ values of meteoric precipitation involve fractionation processes associated with evaporation and condensation of the precipitation water vapour. These factors include the temperature at which condensation occurs, the amount of precipitation, the isotope value of the water vapour source, and the degree to which the water vapour has traveled over land. These processes are related to the storm system dynamics associated with the precipitation. Many recent studies using $\delta^{18}\text{O}$ values have interpreted isotopic variability as a function of changing atmospheric circulation rather than a simple air water temperature signal [2]. All isotopic transformations of water starting from evaporation from the ocean, horizontal and vertical transfer of atmospheric water vapour, formation of rainfall should be understood. The objective of this study is to understand the relationship between atmospheric circulation and stable isotopic concentration of individual precipitation events for the Guvenc basin.

2. PRECIPITATION DATA AND METHODS

In this study, $\delta^{18}\text{O}$ and δD values derived from 30 precipitation samples collected from the Guvenc Basin are used. Samples are part of precipitation isotope record of sufficient length to study the impact of individual storm types on precipitation isotopic variability. All samples were filled to near the capacity of the container to avoid air entrapment, stoppered tightly and then labeled. The samples were sent to the Isotope laboratory for analysis at the Technical Research and Quality Control Division of the State Hydraulic Works (DSI) Ankara. Stable isotopes are measured relative to VSMOW using internal standards calibration with international standards. Sample precision is $\pm 0.1\text{‰}$ for $\delta^{18}\text{O}$ and $\pm 1.0\text{‰}$ for δD . The atmospheric circulation during each precipitation event was evaluated using a 48 – hour back trajectory approach originating from Guvenc Basin. Back trajectories were calculated using the HYSPLIT model provided by National Oceanographic and Atmospheric Administrations (NOAA), Air Resource Laboratory. Each trajectory was initiated from at 500 meters above ground level to 3000 m using archived data from the Middle East Technical University Environmental Engineering Department. Trajectory data were coupled with weather conditions for each precipitation event using synoptic-scale surface maps.

3. RESULTS AND DISCUSSION

3.1. Relationships between isotopic composition and depth-intensity of precipitation

The characteristics of precipitation (mm) collected from 7 individual storms are given in Table 1 with date, amount (mm) and intensity (mm/h). Three of seven samples (5–7) resulted from rainfall amount greater than 5 mm with intensity varying from 5 to 21.5 mm/h. The other four (1–4) produced the amounts ranging between 2.3 and 4.8 mm with intensities varying from 2.5 to 4.8 mm/h.

A scatter plot showing the $\delta^{18}\text{O}$ and δD values for each sample is presented in Fig. 1. Also shown in Fig. 1 is the global meteoric water (GMWL) line as reported by [3]. Deviations from the GMWL are found on a seasonal basis in Guvenc Basin, mainly as a result of partial evaporation, temperatures changes and small seasonal fluctuations of the deuterium excess of precipitation. The samples may also differ substantially from the GMWL in cases where the atmospheric circulation regime of the given basin area varies seasonally bringing moisture to the area from air mass sources.

In general there is a close relationship between amount of precipitation and $\delta^{18}\text{O}$ values. When precipitation amount increases, $\delta^{18}\text{O}$ values of precipitation decreases. Three storm types were observed during the period of record. From the start of sampling (23 April 2003) until (21 April 2004), spring convective storms occurred frequently in study area. These convective storms were typically

TABLE 1. PRECIPITATION AMOUNT, INTENSITY AND DURATION.

Dates	Precipitation amount (mm)	Precipitation intensity (mm/h)	Duration
1 – 8.04.2003	2.3	3.0	18:00–18:10
2 – 18.04.2003	4.7	2.5	15:00–15:10
3 – 23.04.2003	4.8	4.8	14:30–15:00
4 – 25.04.2003	2.7	3.0	14:50–15:00
5 – 25.10.2003	9.2	5.0	22:00–22:15
6 – 16.12.2003	5.3	11.6	14:15–14:20
7 – 21.04.2004	5.6	21.5	16:20–16:30

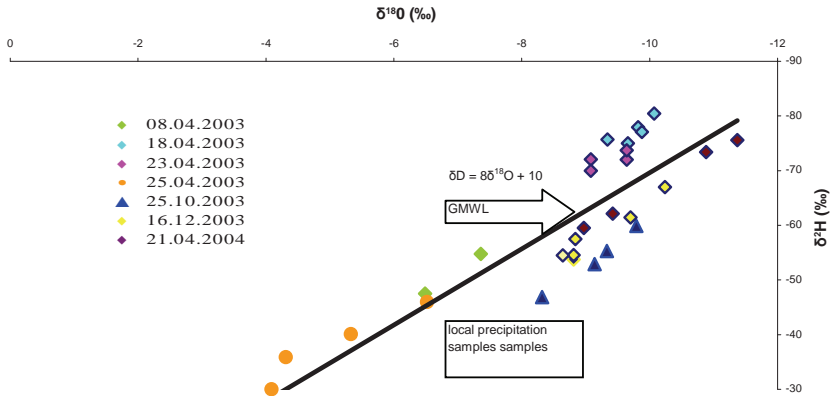


FIG. 1. $\delta^{18}O$ and δD values for each precipitation event.

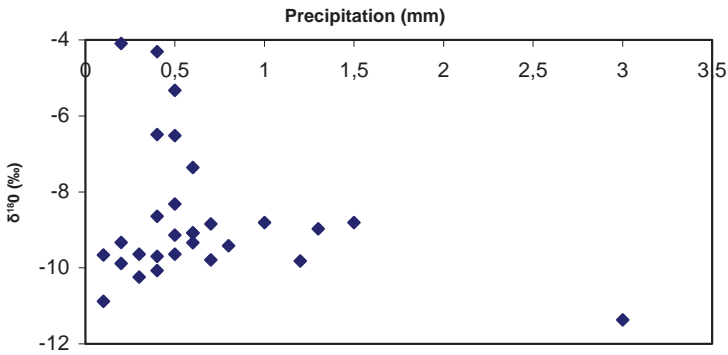


FIG. 2. Precipitation depth and $\delta^{18}O$ ‰ relationships.

small in area and of short duration. Storms in 25 April 2003 provided the most isotopically enriched precipitation, with an average $\delta^{18}O$ of -5.06 ‰ and 2.7 mm amount originating in the Siberia- Balkan. In October and December, a maritime tropical brought high amounts and intense rains to the entire basin, amounting to 9.2 mm with an average $\delta^{18}O$ of -9.16 ‰. A plot of rain $\delta^{18}O$ versus amount (Fig. 2) showed no systematic pattern except that the most enriched precipitation samples were associated with low precipitation amounts.

3.2. Relationships between isotopic composition of precipitation and back trajectories

The circulation analysis produced one, two or three centers originating from different sources. Trajectories of individual storms are shown in Table 2. The climate of Turkey, which is characterized mainly by the Mediterranean macroclimate, results from seasonal alternation of the mid-latitude frontal depressions, with the polar air masses, and the subtropical high pressures with the subsiding maritime tropical and continental tropical air masses. The results of recent studies [4] revealed that precipitation in Turkey and the North Atlantic Oscillation (NAO) are stronger in winter and autumn and weaker in spring and almost non-existent in summer. The NAO is defined as a large-scale swaying of atmospheric pressure between the dynamic subtropical anticyclone centred over the Azores region and the mid-latitude cyclone dominated over the Iceland and Greenland region in the North Atlantic. It seems that relatively wet conditions in Turkey during the negative phase of the NAO spring index are related with the cyclonic anomaly circulation over the Central Europe, although influences of the anomalous 500-hPa circulation patterns for the extreme NAO phases are getting weaker in spring compared with those in winter and autumn, due to the effects of the sub-regional and/or local physical geographic and meteorological factors [5]. Spatially and statistically, changes in precipitation amounts during NAO are more apparent in west and mid Turkey. This study provides an understanding of how different seasonal circulation types in the Guvenc Basin influence precipitation $\delta^{18}\text{O}$ and importance of atmospheric circulation.

TABLE 2. TRAJECTORIES OF AIR MASSES.

Dates	Trajectories
8.04.2003	Atlantic coastal- N. Europe (Fig. 3a)
18.04.2003	Siberia–Middle Anatolia–South East Anatolia
23.04.2003	Siberia (Fig. 3b)
25.04.2003	Siberia–Balkan
25.10.2003	Africa–Mediterranean–Europe
16.12.2003	Africa-Mediterranean- South East Anatolia (Fig. 3c)
21.04.2004	Mediterranean (Fig. 3d)

Atmospheric circulations of air masses bringing precipitation over the basin originated from Atlantic coastal, Mediterranean- Africa and Siberia centers (Table 2). Four of the seven events can be seen in the trajectory summary in Fig. 3 Atlantic coastal trajectories (Figure 3a) bring air mass across the basin with average -7.26‰ $\delta^{18}\text{O}$ and -58.29‰ δD isotopic values. On the other hand Siberia trajectories (Fig.3b) exhibit relatively low $\delta^{18}\text{O}$ and δD values with an average -9.44 and -71.96‰ respectively. These events are largely associated with easterly trajectories, although many other trajectories begin over the west before entering Turkey. Africa-Mediterranean systems (Fig. 3c) produce more negative precipitation events than that of the coastal system, with an average of -9.17‰ $\delta^{18}\text{O}$ and -58.10‰ δD values. Mediterranean effect precipitation events (Fig. 3d) are more negative, with an average of -10.16‰ $\delta^{18}\text{O}$ and -67.65‰ δD , than that of the Atlantic coastal systems. These deviations can be attributed to varying temperature conditions and source of the trajectories originating from either coastal or continental areas.

3.3. Deuterium excess

The deuterium excess is defined as $d = \delta\text{D} - 8\delta^{18}\text{O}$ [6]. It is a measure of the deviation of the given data from a line with slope 8 going through VSMOW. Deuterium excess for the precipitation collected from 7 individual storms in the basin varies between -2.58‰ and -19.46‰ . The deuterium excess offers a possibility for characterizing the interaction of different air masses and their temporal evolution.

In this study, the large range of d excess is a result of seasonal variations, with lower values in the winter season ($>-15\text{‰}$) and higher values (-2.58‰) in the spring season. These variations are found on a seasonal basis mainly because of mixing of dry-cold continental air masses and hot-humidity maritime tropic air masses over the study area.

4. CONCLUSIONS

Variation of the stable isotope contents of individual precipitation events is related with atmospheric circulation sources, trajectories and local climatic conditions. Stable isotope values of seven individual precipitation events analyzed in the Guvenc Basin deviated from the GMWL. For some dates of precipitation significant deviations from the GMWL are observed. These deviations result from different air mass trajectories such as those originating from Siberia, Atlantic and Africa-Mediterranean sources and also on the travel length of the air masses.

RELATIONSHIP BETWEEN STABLE ISOTOPES

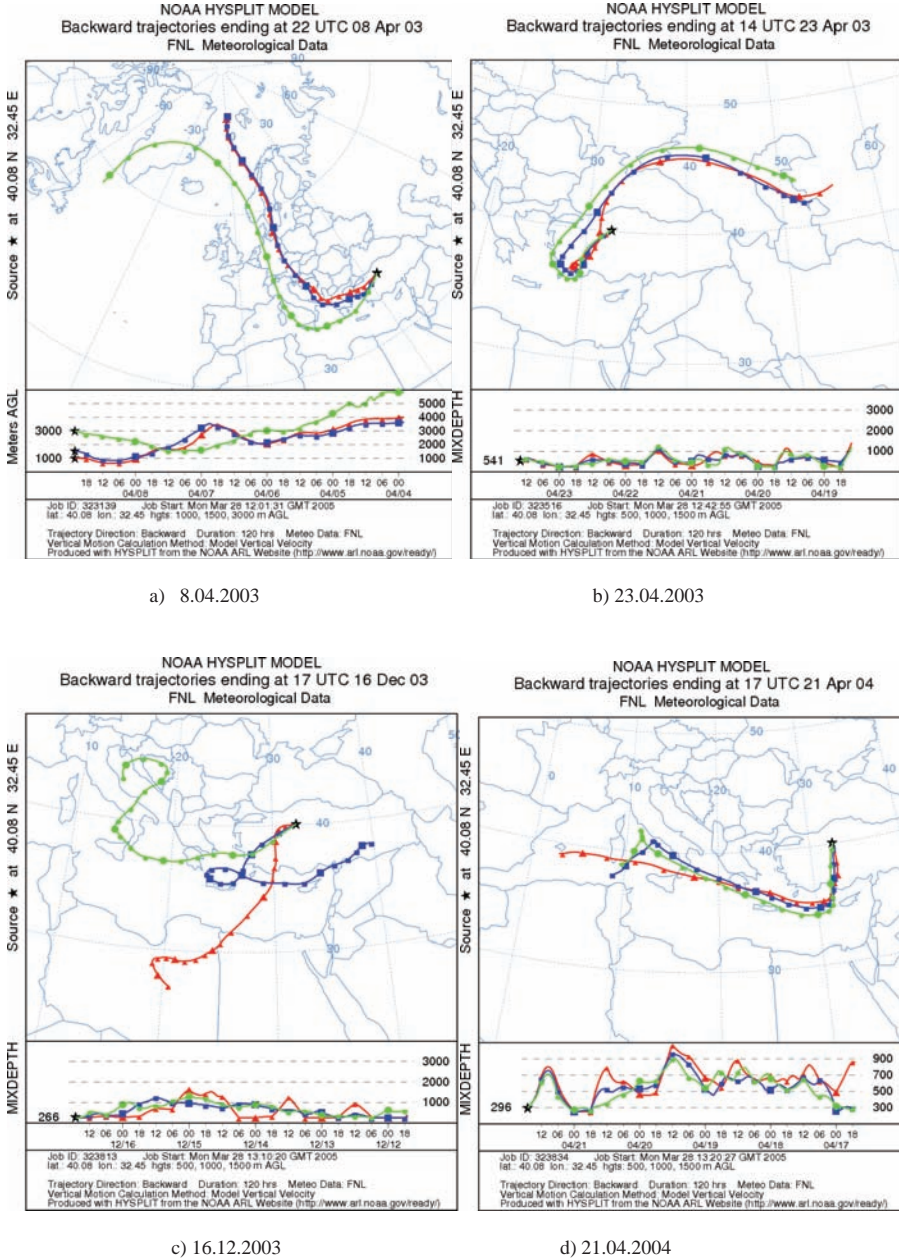


FIG. 3. Representative air mass trajectories for 4 selected events.

We hope that the ongoing efforts to document circulation-isotope relations in the Guvenc Basin not only for spring, but for all seasons will provide an important tool for better interpretation of precipitation sources and atmospheric circulation throughout the Central Anatolia region.

REFERENCES

- [1] ARAGUAS-ARAGUAS, L., et al., Deuterium and oxygen-18 isotope composition of precipitation and atmospheric moisture, *Hydrological Processes* **14** (2000) 1341–1355
- [2] KIRBY, M. E., et al., Late glacial-Holocene atmospheric circulation and precipitation in the north east United States inferred from modern calibrated stable oxygen and carbon isotopes, *Geol. Soc. Am. Bull.* **114** (2002) 1326–1340
- [3] ROZANSKI, K., et al., Isotopic patterns in modern global precipitation, *Climate Change in isotopic Records, Geophys. Monogr. Ser.*, vol. 78, AGU, Washington, D.C. (1993) 1–36,
- [4] TURKES, M., ERLAT, E., Climatological responses of winter precipitation in Turkey to variability of the North Atlantic Oscillation during the period 1930–2001, *Theor. Appl. Climatol.* **81** (2005) 45–69.
- [5] TURKES, M., ERLAT, E., Influences of the North Atlantic oscillation on precipitation variability and changes in Turkey, *Il Nuovo Cimento*, Vol.29 C, N.1 (2006),
- [6] DANSGAARD, W., “Stable isotopes in precipitation”, *Tellus* **16** (1964) 436–468

ASSESSMENT OF GROUNDWATER DYNAMICS IN UGANDA USING A COMBINATION OF ISOTOPE TRACERS AND AQUIFER HYDRAULICS DATA

C. TINDIMUGAYA*, R.G. TAYLOR⁺, K.M. KULKARNI⁺⁺,
T.C. ATKINSON⁺, J. BARKER⁺

*Water Resources Management Department,
Directorate of Water Development,
Entebbe,
Uganda

⁺Hydrogeology Group,
Department of Geography,
University College London,
London, UK

⁺⁺Isotope Hydrology Section,
International Atomic Energy Agency,
Vienna

Abstract

Groundwater is widely developed for low-cost water supplies for towns in areas underlain by weathered crystalline rock in sub-Saharan Africa, but the sustainability of abstraction is unknown. In this study, we assess groundwater dynamics in fluvial deposits and weathered – fractured crystalline rocks underlying the town of Rukungiri, Uganda using environmental tracers and aquifer hydraulics data. CFC and ³H concentrations in pumped groundwater highlight that mixing of groundwaters of different residence times has occurred. Application of lumped parameter models based on tracer concentrations and reconstructed input functions indicate that groundwater underlying Rukungiri Town is generally young (less than 50 years old). A change in groundwater flow dimension from 2 (radial) to 1 (linear) since the commencement of intensive abstraction 8 years ago combined with a steady decline in groundwater levels over the last 8 years give rise to a conceptual model of a locally bounded isotropic (gravel) aquifer. Our results suggest that current groundwater development in Rukungiri is unsustainable. To maintain current abstraction and plan for increased abstraction for rapidly growing towns, strategies to optimise groundwater abstraction and protection are therefore required to control overexploitation and possible pollution of the aquifer.

1. INTRODUCTION

Over most of sub-Saharan Africa, groundwater provides the only realistic source of water to meet the demand of dispersed rural communities and rapidly growing towns. Uganda, like many other countries in sub-Saharan Africa is developing groundwater using low-cost, simple water-supply technologies in its efforts to improve access to safe water supplies in rural areas and small towns. The availability of groundwater is, however, strongly influenced by variable climatic and geological conditions. Aquifers primarily occur in the regolith (fluvial deposits and weathered bedrock) and fractured crystalline “basement” rocks of Precambrian age. Intensive groundwater abstraction ($> 5 \text{ m}^3/\text{hour}$ per borehole), especially for town water supplies, is restricted to areas where the bedrock is highly fractured and the regolith possesses moderate to high permeability and significant storage.

Although groundwater development is on a steep rise in Uganda and elsewhere in sub-Saharan Africa, it is not known whether the current, intensive abstractions ($300\text{--}600 \text{ m}^3/\text{day}$) from wellfields within the regolith and fractured crystalline rock aquifer system is sustainable [1]. Similarly, considerable uncertainty exists regarding vulnerability of this aquifer system to contamination from local land use practices such as sewage disposal.

Understanding the dynamics of groundwater regolith and fractured basement aquifer systems is key to their sustainable development and management. In this study, we assess groundwater dynamics in the regolith and fractured crystalline rocks underlying the town of Rukungiri, Uganda from the combined application of isotope tracers and aquifer hydraulics data.

2. METHODOLOGY

Groundwater dynamics in the study area was investigated using environmental isotope tracers and hydrogeological data.

2.1. Environmental tracer data

Environmental tracers are natural or anthropogenic compounds including isotopes that are widely distributed in the near surface environment of the earth, such that variations in their abundances can be used to determine pathways and timescales of environmental processes [2]. Environmental tracers (tritium, CFC-113, CFC-12, CFC-11, and tritium-helium ratios) were used to assess groundwater residence times and investigate groundwater mixing. In this paper, a combination of anthropogenic gases (CFCs) and tritium is used

to assess mean residence times of groundwater in the regolith and fractured crystalline rock aquifer system.

2.2. Hydrogeological and hydrochemical data

Groundwater flow and hydrogeological properties of the aquifer system in Rukungiri have also been assessed using hydrogeological data. These datasets include borehole lithology, geophysical surveys, aquifer responses to imposed stress (e.g., pumping tests) and borehole hydrographs. Borehole lithological data were obtained from existing boreholes and construction of a network of 8 piezometers around a production borehole. These lithological observations were supplemented by surface geophysical survey to assess the vertical and lateral extent of the aquifer system developed for the town water supply. Furthermore, the response of groundwater levels to intensive abstraction was assessed using groundwater level data obtained from the long-term monitoring well located 100 metres from the production borehole and the piezometer network. The study site enabled, for the first time, a very detailed picture of hydraulic responses of a weathered crystalline aquifer to intensive abstraction, to be obtained.

3. RESULTS

3.1. Environmental tracer data

Where it is neither possible, nor justified to use distributed-parameter models, lumped-parameter models are particularly useful for interpreting the residence time of environmental tracers. By comparing input and output signals of the concentrations of environmental tracers in groundwater systems, residence times for groundwater in the Rukungiri aquifer were estimated by applying exponential and advection-dispersion models. Results of isotope analysis have been used to generate groundwater residence times (Table 1) for the aquifer system in Rukungiri.

Groundwater residence times determined from individual CFC species are variable. CFC -113 generates the youngest ages (7 to 35 years) while CFC-11 generates the oldest ages (8 to 47 years). The residence times generally range between 7 and 48 years. There is no marked difference between the regolith (weathered) and fractured aquifer units. Groundwater residence times determined from Tritium are, in a number of cases, higher than those from CFCs, but are in the same order of magnitude. Groundwater residence times from both CFCs and ^3H range between 7 and 48 years and the groundwater

TABLE 1. GROUNDWATER RESIDENCE TIMES FOR RUKUNGIRI.

Site code	Site name	Type of aquifer	CFC-12 (years)	CFC-11 (years)	CFC-113 (years)	Tritium (years)
UG/05/001	PW 1	Weathered -fractured	27	34	20	45
UG/05/002	PW 2	Weathered -fractured	25	31	19	14
UG/05/003	Kinyasano	Fractured	48	47	35	45
UG/05/004	Piezo 3	Weathered		8		23
UG/05/005	Piezo 1	Weathered	12	29	7	14
UG/05/006	Piezo 4	Weathered	32	35	8	45
UG/05/007	Rwarubira	Fractured	33	33	13	14
UG/05/008	Piezo 2	Weathered				23
UG/05/009	Piezo 5	Weathered	27	32	7	21
UG/05/010	Piezo 7	Fractured				24
UG/05/011	Immaculate	Fractured				26
UG/05/012	Piezo 8	Fractured		32	9	45

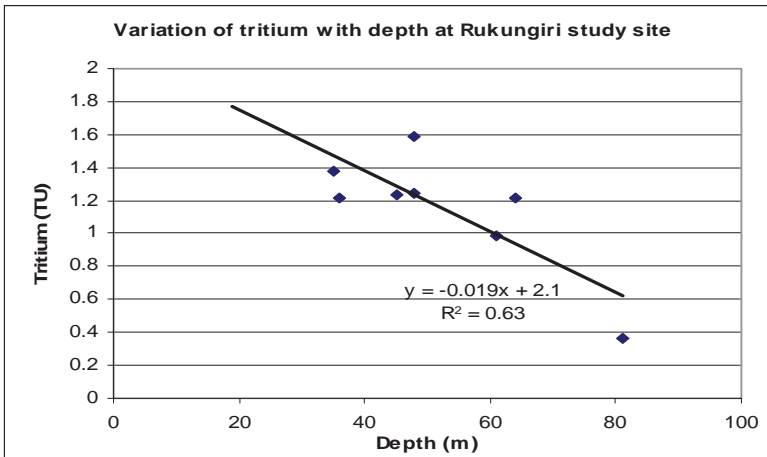


FIG. 1. Variation of Tritium with depth at Rukungiri study site.

ASSESSMENT OF GROUNDWATER DYNAMICS IN UGANDA

can thus be described as young. Tritium content is inversely proportional to aquifer depth as expected and generally decreases with depth (Fig. 1). There is no difference in tritium content between the gravel and the fractured aquifer suggesting that the two aquifer units are hydraulically connected. Groundwater is, therefore, actively recharged under current seasonally humid conditions, but is also vulnerable to pollution, particularly from rapid flow components.

3.2. Hydrogeological data

3.2.1. Site hydrogeology

Based on borehole lithology, the site hydrogeological conditions of Rukungiri wellfield have been described (Fig. 2).

Geophysical survey results indicate that the main aquifer in Rukungiri is made up of low resistivity weathered material and is bounded by high resistivity competent quartzite rock. Borehole lithology indicates that the town is underlain by a gravel aquifer which ranged between 20 and 60 m in thickness. This gravel aquifer is underlain by a fractured bedrock aquifer with which it is hydraulically connected.

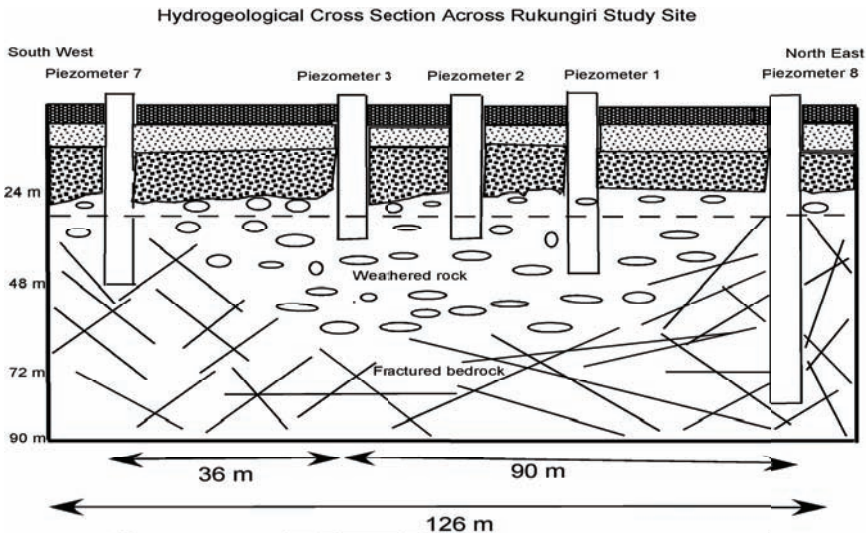


FIG. 2. Hydrogeological cross section across Rukungiri wellfield.

3.2.2. Aquifer hydraulic response

Hydraulic testing is a useful tool in determining aquifer properties, formation extent and flow mechanism. Knowledge of groundwater flow and aquifer properties is key to sustainable groundwater development. Sound analysis and interpretation of aquifer hydraulics data therefore requires good knowledge of the aquifer. In this study, diagnostic techniques were used to assess groundwater flow mechanism in the regolith and fractured bedrock aquifer systems.

Log-log & log-linear plots were used to determine flow characteristics and aquifer parameters. Based on these plots it has been found that drawdown responses of all the piezometers at Rukungiri wellfield are identical and that all the piezometers intersect the aquifer tapped by the production well. It has been found that all the piezometers exhibit slopes of between 0.5 and 0.75 on log-log plots. The high slopes suggest presence of highly permeable formation. The results further indicate that the flow in all the piezometers is one dimensional (linear).

Flow dimension analysis was used to assess the flow behavior of the aquifer [3]. The results from the production borehole indicate that the aquifer exhibited a flow dimension of 2 (radial flow) originally but this has changed to 1 (channel flow) (Fig. 3). Flow conditions at the study site are almost uniform irrespective of the distance of the piezometers from the pumping well.

3.2.3. Response of water levels to abstraction

Groundwater abstraction for Rukungiri town water supply has been ongoing since 1998 based on four high yielding deep boreholes. The abstraction rates have greatly increased over the last 3 years due to increase in demand. The average daily abstraction is about 480 m³. Based on the results of groundwater

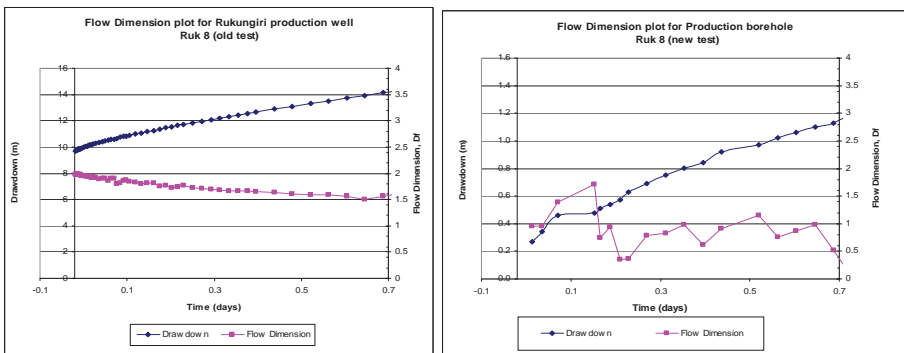


FIG. 3. Flow dimension analysis for production well in Rukungiri.

ASSESSMENT OF GROUNDWATER DYNAMICS IN UGANDA

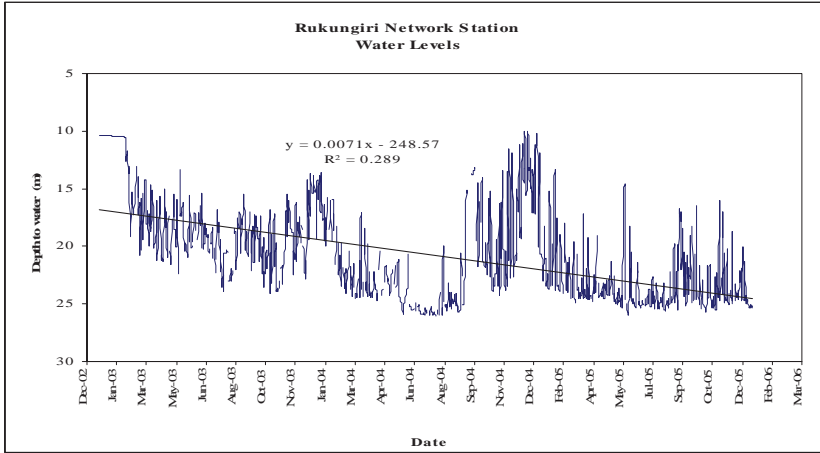


FIG. 4. Response of water level to abstraction in Rukungiri monitoring well.

monitoring in the production well and the surrounding monitoring wells, it has been found that water level in the production well has declined by 21 metres in the last 8 years of pumping. Similarly, water level in the monitoring well located 100 metres from one of the production wells has declined by 17 metres in 8 years (Fig. 4). Furthermore, groundwater monitoring in the eight piezometers drilled around the production well in 2005 indicates water level decline of about 2.5 metres in one year.

4. CONCLUSIONS

Based on residence time indicators, the groundwater in Rukungiri is young and has residence times that range between 7 and 48 years. The conceptual model of groundwater dynamics in Rukungiri suggests that the aquifer developed for town water supply is a localised isotropic gravel aquifer with very limited extent. Due to the limited extent of the aquifer, groundwater levels have continued to decline over the last 8 years and this has resulted in the change of the groundwater flow dimension from 2 (radial) to 1 (linear). Groundwater flow is one dimensional through highly permeable formations, thus exhibiting channel flow conditions. Results of this study suggest that current groundwater development in Rukungiri is unsustainable. Immediate strategies for optimal groundwater abstraction and protection are therefore required to control overexploitation and possible pollution of the aquifer.

REFERENCES

- [1] TAYLOR, R.G., BARRETT, M.H., TINDIMUGAYA, C., Urban areas of sub-Saharan Africa; weathered crystalline aquifer systems, *International Contributions to Hydrogeology* Vol. 24 (2004) 155–179.
- [2] CLARK, I., FRITZ, P., *Environmental Isotopes in Hydrogeology*, New York, Lewis publishers, by CRC Press LLC (1997) 290.
- [3] WALKER, D., DOUGLAS, A., ROBERTS, M. RANDALL., Flow dimension corresponding to hydrogeologic conditions, *Water Resources Research* vol. 39, No. 12, 1349 (2003).

ENVIRONMENTAL ISOTOPIC STUDY FOR GROUNDWATER OF THE NORTH PLAIN OF HUAI HE RIVER, CHINA¹

NIAN-JUN YE, JIAN-SHI GONG, WEI-YA GE, JIA-JU LU,
CHENG-YOU HA, WEI-ZU GU

Nanjing Centre,
China Geological Survey,
Nanjing, China

Abstract

The Huai He River, one of the seven main rivers in China, has a drainage area of 164,000 km² until Hongze Lake. The North Plain of Huai He River (NPH) covers an area of approximately 85,000 km². Due to the complex aluvial and diluvial depositional cycles, the aquifers are layered, discontinuous, connected and, leak. From hydrogeological settings and their isotopic features, shallow and deep groundwater are defined, the boundary of Lower and Middle Pleistocene is taken as the general boundary between them. Shallow groundwater is phreatic and/or slightly confined while the deep groundwater is confined. The river water line of δD and $\delta^{18}O$ is close to that of the groundwater with depths of 0–30 m. The low flow of rivers is not only recharged from the Holocene deposit/aquifers, but that of the Upper Pleistocene. From the original composition of the shallow groundwater and the monthly mean composition of precipitation, it is found that the shallow groundwater originates from local precipitation and aquifers of the Upper Pleistocene. Three recharge sources of deep groundwater are identified from uranium disequilibrium, the mixing diagram of uranium content U and $^{234}U/^{238}U$, also from that of ^{18}O versus ^{234}U excess, they are: the meteorological water from modern precipitation, the phreatic shallow groundwater and, the palaeowater. The recharge from the percolation of perched Yellow River situated to the north boundary of NPH to the deep groundwater is demonstrated by the profile of $\delta^{18}O$, the existence of tritium in groundwater even from the borehole with a depth of 1300 m. The recharge extends about 150 km from the Yellow River.

¹ Work performed within the framework of the China Geological Survey Project No.1212010340106 and, IAEA contract No.12887/RO

1. THE STUDY AREA

The Huai He River is one of the seven main rivers in China with drainage area in total of 187 000 km² (164 000 km² until Hongze Lake), it flows into the Hongze Lake first, then drains into Yangtze and Yellow Sea via four courses. It lies between two large rivers in China, the Yellow River to the north and the Yangtze River the south. Geomorphologically, about 52% of the basin is a plain, and it is situated to the north of Huai He River (Fig.1). This agricultural North Plain covers an area of 85 300 km² with a surface gradient about 1/7500 to 1/10000 towards the southeast. This plain has suffered from very serious natural disasters including floods and droughts since ancient times. Unfortunately, it has also become one of the most serious polluted areas in China over recent decades. The annual mean precipitation ranges from 600–1000 mm from north to south.

During tectogenesis during the Neogene, Pleistocene and Holocene, rifting, settling and fault movement occurred. Two important elements developed in the study area, i.e., the Yellow River formed during the Middle Pleistocene and the mountains situated to the northwest/west of study area were rifted up. These two elements dominate the geology, morphogenesis, and the fundamental hydrogeological setting.

2. HYDROGEOLOGICAL SETTINGS

The porous aquifers were formed following the depositional cycle of the aluvial fan and partly the diluvial fan, it is layered but, for individual aquifers, it is not always continuous spatially and, sometimes some layers/aquifers are connected. A typical profile of such porous aquifers is shown in Fig. 2. It is composed of Pliocene and Miocene alluvial, diluvial-alluvial, lacustrine and glacio-fluviatile deposit [1].

The deposit formed during the Pleistocene through Holocene, and has its bottom at about 40 to 140 m below the ground surface depending on location. The water bearing thickness of the aquifers range from 20–80 m, and are phreatic and/or slightly confined. The diluvial, lacustrine and glacio-fluviatile deposits formed in the Lower Pleistocene, and it's bottom is about 180–500 m below the ground surface. Water bearing sands about 20–80 m in thickness occur under confined conditions. Groundwater is grouped into so-called shallow and deep. Due to the formation complexity of the deposit and the aquifers, the boundary of these groups varies spatially. However, over the basin scale it appears possible to group it according to geological boundaries with different hydrogeochemical features. The interface of the Middle and

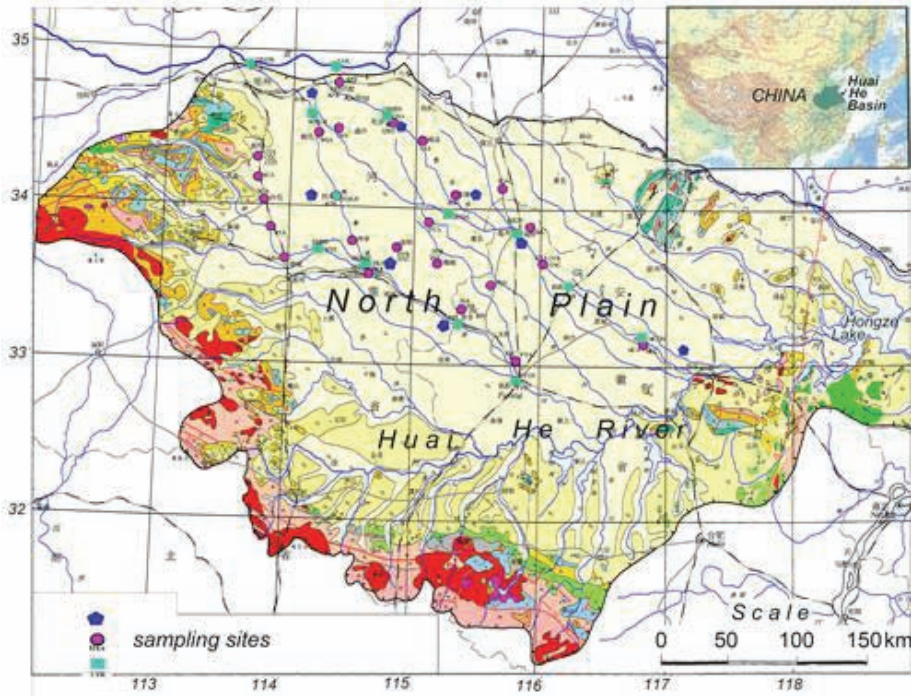


FIG. 1. The North Plain of Huai He River Basin and the sampling sites. The west and south parts of the Basin are hilly and mountainous.

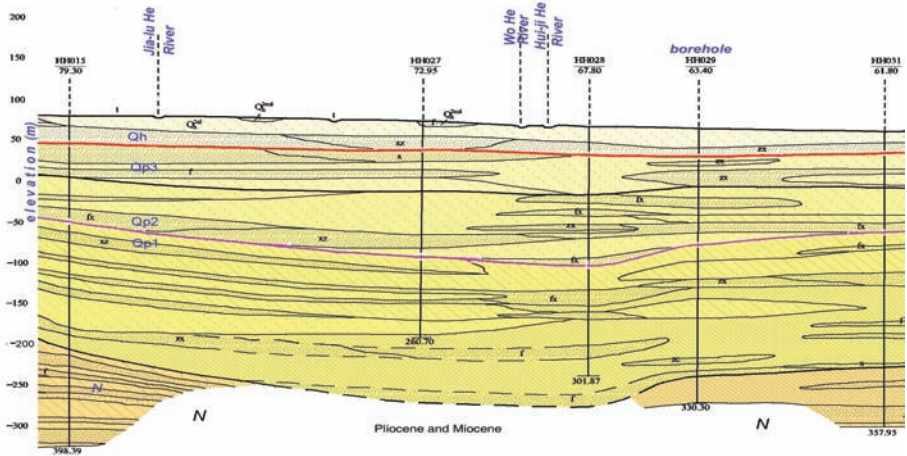


FIG. 2. A typical profile of deposit and aquifers [1].

The low flow water line seems nearly the same as that of the groundwater line of depths 0–30 m. The original composition (OC) of it can be identified from its interception with the precipitation line from 2 stations approaching the GMWL as $\delta^{18}\text{O} = -9.4\text{‰}$, $\delta\text{D} = -65.1\text{‰}$. The monthly mean precipitation has values of $\delta^{18}\text{O} = -6.6\text{‰}$ and $\delta\text{D} = -44.2\text{‰}$. It implies that the OC of it can not be formed by local precipitation/percolation alone, but requires mixing with deep groundwater. The contribution of leakage from confined aquifers would make the ^{14}C age of some shallow groundwater older, and this can be seen clearly in Fig. 5 (e.g., the JSB site with borehole depth of 44 m, has an apparent age of 14730 years BP).

4. THE SOURCE WATERS OF DEEP GROUNDWATER

4.1. ^{14}C age, mixing and leakage

The ^{14}C age shows that the palaeogroundwater seems to dominate the deep groundwater with borehole depths of more than about 100 m (Fig. 5). However, some of the deep boreholes (e.g., JSD, KFD on Fig. 5) have anomalously young ^{14}C ages, implying mixing with young water. On the contrary, groundwater from many shallow wells have ages that are older than the deposit that these wells are situated in (e.g., BZB, FYA and JSB). This discrepancy is due mainly to leakage from deep aquifers. It is also the reason that sometimes the age of low flow waters are older than what has been expected. It is surprising to see that with few exceptions, most of the wells penetrating into the Middle/Upper Pleistocene contain tritium (as shown in Fig. 6), even the deepest one, KFE, with a depth of 1300 m, contains tritium at about 3 TU. There are two possibilities for the source of tritium, mixing with percolation from surface water/precipitation or leakage from shallow aquifers.

4.2. Identification of recharge sources

Uranium disequilibrium together with stable isotopes were used to identify the recharge sources of deep groundwater. In Fig. 7, uranium content U versus the alpha activity ratio of uranium in groundwater $^{234}\text{U}/^{238}\text{U}$ shows the mixing diagram of different waters. The three end member waters can be identified from the apices of the mixing triangle [2]. The composition of source A is the MCA-type water which is the meteorological water from modern precipitation with lowest uranium content, source B is the DCB/HYC/XCB-type water, the phreatic shallow groundwater and, the source C is the KFE-type water which is palaeowater characterized by high $^{234}\text{U}/^{238}\text{U}$ produced not by chemical

ENVIRONMENTAL ISOTOPIC STUDY FOR GROUNDWATER OF THE NORTH PLAIN

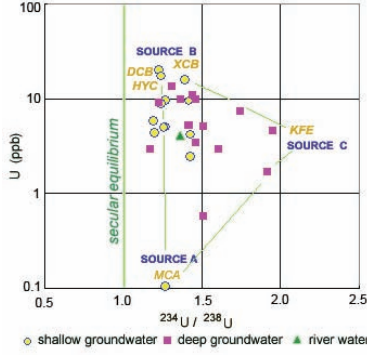


FIG. 7. Uranium content and $^{234}\text{U}/^{238}\text{U}$ of groundwaters.

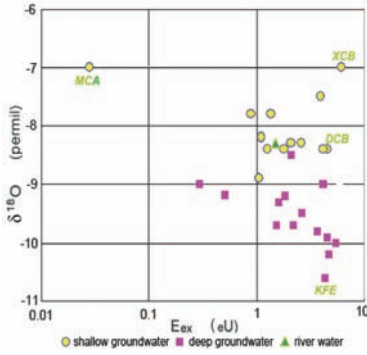


FIG. 8. ^{18}O and the ^{234}U excess of groundwaters.

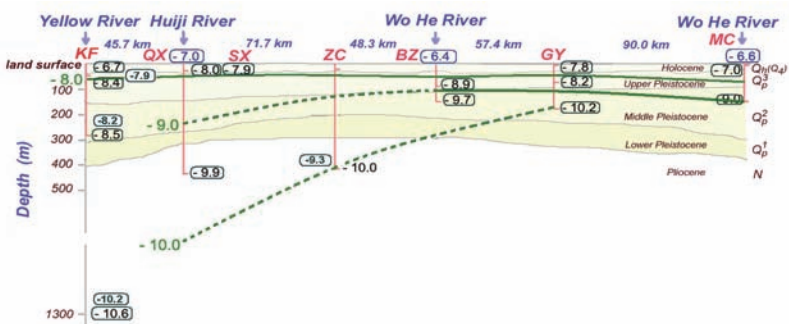


FIG. 9. Spatial distribution of ^{18}O of waters along the Wo He River.

fractionation, but from alpha recoil. As a crosscheck, ^{18}O versus ^{234}U excess E_{ex} , also shows mixing (Fig. 8). Three source waters A, B and C are also identified, however it appears the source water B will be the XCB-type if compare it with that of Fig. 7. The ^{234}U excess is defined as $E_{\text{ex}} = U (^{234}\text{U}/2^{38}\text{U} - 1)$. From the mixing diagram of Figs. 7 and 8, the proportions of these source waters for both shallow and deep groundwater and, the low flow water of rivers could be estimated [3]. It can be seen from both digrams that in general the deep groundwater is dominated by palaeowater, but the shallow groundwater is dominated by modern meteoric water

5. RECHARGE OF YELLOW RIVER TO THE DEEP GROUNDWATER

Fig. 9 shows the spatial distribution of ^{18}O of river water and groundwater along the Wo He River from upstream to the lower reaches. The low flow river water includes the Yellow River situated to the north boundary at KF, the Huiji River, the uppermost tributary of Wo He River at QX with drainage area of 4014 km², the main course of Wo He River at BZ with drainage area of 10 490 km² and that of MC of 15475 km². Groundwater profiles are sampled from different depths.

The ^{18}O of all rivers shows significant fractionation resulting from evaporative enrichment along the river course of about 300 km. Contrary to the fact that the isolines of groundwater table along the Wo He River show a big gradient towards downstream until MC because of the perched Yellow River. The isoline of groundwater ^{18}O however, shows unexpected bending towards the Yellow River. In fact, according to the hydrogeological setting it should approximately be parallel. Such bending of isolines also demonstrates mixing. The only explanation is recharge from the Yellow River which adds tritium to KFE water. The depths of percolation from the Yellow River were also estimated from the groundwater T profiles of KF, and from other places near the Yellow River. They range from 200 m to 300 m [1]. This depth reaches the Lower Pleistocene and the deep groundwater aquifers. The influence range of Yellow River recharge for the deep groundwater may extend to about 150 km until location BZ.

6. THE SIGNIFICANCE OF $^{34}\text{S}_{\text{SULPHATE}}$ IN GROUNDWATER

The $^{34}\text{S}_{\text{sulphate}}$ is helpful for identifying the origin and the fate of sulphate in groundwater [5, 6].

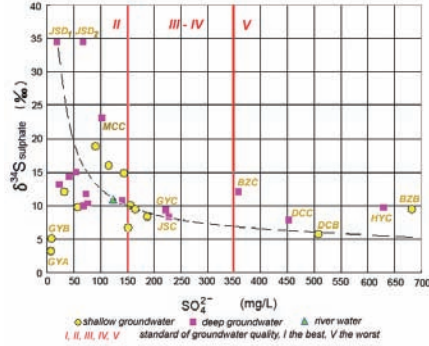


FIG. 10. $^{34}\text{S}_{\text{sulphate}}$ vs SO_4^{2-} of groundwater.

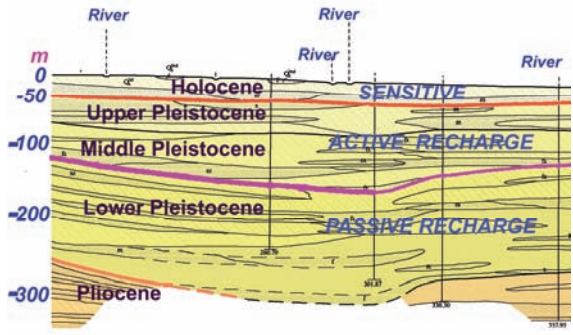


FIG. 11. The recharge zones related to rivers.

- (a) $^{34}\text{S}_{\text{sulphate}}$ values: All the $^{34}\text{S}_{\text{sulphate}}$ of groundwater are positive and higher than 5 permil except the GYs (Fig. 10). It is strongly revealed that the main source of sulphate is anthropogenic including mainly the industries. According to the current standard for the groundwater quality, for the worse water type IV and the worst type V, the $^{34}\text{S}_{\text{sulphate}}$ range of deep groundwater is about 6–10 permil while that of shallow groundwater appears wider.
- (b) River $^{34}\text{S}_{\text{sulphate}}$: It is a mixing with both the shallow and deep groundwater.
- (c) Bacterial reduction: For both the shallow and deep groundwater, it shows clearly that they have the similar trend with increasing of SO_4^{2-} accompanied by the decreasing of $^{34}\text{S}_{\text{sulphate}}$. This shift results from bacterial sulphate reduction. Such reduction causes preferential enrichment of

$^{34}\text{S}_{\text{sulphate}}$ in the residual sulphate. The trend in deep groundwater implies a pollution risk.

- (d) Multi-sources of sulphate: From Fig. 10, different sources of sulphate are revealed, they include: lithospheric sulphate from Pliocene deposit; atmospheric sulphate from meteoric deposits and industrial pollution.

7. RECHARGE ZONES RELATED TO LOW FLOW RIVER WATER

According to the relationships between low flow and groundwater recharge, sensitive, active and passive recharge zones are differentiated as shown in Fig. 11. For the study area, geological boundaries are taken as their boundaries.

ACKNOWLEDGEMENTS

The authors are deeply grateful to Dr. Pradeep Aggarwal, Dr. Tomas Vitvar of IAEA and Professors Yin Yueping, Wu Xuanmin, Wen Dongguang of CGS for their very valuable help, very kind support and encouragements.

REFERENCES

- [1] ZHAO YUN-ZHANG, et al, Groundwater Resources and the Environment of Henan Province, China Dadi Press (in Chinese), Beijing (2004).
- [2] BRIEL, L.I., An investigation of the $^{234}\text{U}/^{238}\text{U}$ disequilibrium in the natural waters of the Santa Fe River Basin of North Central Florida, PhD thesis, Florida State University (1976).
- [3] GU WEI-ZU, et al, "Uranium disequilibrium in the Cambrian-Ordovician aquifer system of southwest Datong and its application for groundwater research". Advances in Water Science (in Chinese with English abstract) **2** 12 (2001) 177–184.
- [4] OSMOND, J.K., COWART, J.B., "Theory and use of natural uranium isotopic variations in hydrology", Atomic Energy Reviews **14** (1976) 621–627
- [5] KROUSE, H.R., "Relationships between the sulphur and oxygen isotope composition of dissolved sulphate", Hydrology and Geochemistry of Sulphur Isotopes. IAEA, Vienna (1987) 19–29.
- [6] GU WEI-ZU, et al, "The use of environmental sulphur isotopes in the study of the Cambrian-Ordovician aquifer system in the south of Datong", Advances in Water Science (in Chinese with English abstract) **1** 11 (2000) 14–20.

ENVIRONMENTAL ISOTOPE AND HYDROCHEMICAL INVESTIGATION ON GROUNDWATER RECHARGE AND DYNAMICS OF THE COASTAL SEDIMENTARY AQUIFERS OF TIRUVADANAI, TAMILNADU STATE, INDIA

U. SARAVANAKUMAR, S. SHARMA, A.S. DEODHAR,
H.V. MOHOKAR, S.V. NAVADA

Isotope Hydrology Section,
Isotope Applications Division,
Bhabha Atomic Research Centre (BARC),
Mumbai

S. GANESAN

Tamilnadu Water Supply and Drainage (TWAD) Board,
Sivagangai, Tamilnadu

India

Abstract

Recharge processes and dynamics of the Tiruvadanai aquifers were investigated using environmental isotopes and hydrochemistry, in conjunction with hydrogeological data. Hydrochemical characterization of the groundwaters indicated that the shallow (<200 m) Tertiary aquifers (unconfined/semi-confined), lying below the upper Quaternary alluvial deposits, contain no-dominant (Ca–Mg–HCO₃–Cl) to saline type waters and the deeper (350–500 m) Cretaceous aquifer (confined) is a NaCl type. The concentration of various chemical species along the general groundwater flow direction (northwest to east) showed a trend with a decrease in Mg²⁺ and Ca²⁺ and an increase in Na⁺ and K⁺ in both the aquifers. This change could be attributed to ion-exchange process. Higher pH values of Cretaceous aquifer samples (7.4–8.6) could also be responsible for the lowering of Mg²⁺ and Ca²⁺ concentrations by facilitating precipitation of carbonates. A δ²H–δ¹⁸O plot shows that the Tertiary aquifer samples fall on an evaporation line. The aquifer ³H values near the ephemeral rivers range from 2 to 5 TU while those away from the rivers have <1 TU and ¹⁴C_{DIC} model ages range from 1 to 13 Ka BP. The Cretaceous aquifer samples had ³H values <1.5 TU and their ¹⁴C_{DIC} model ages are >20 ka BP, indicating palaeo-waters. Based on ¹⁴C model ages, the groundwater velocity was estimated (Tertiary aquifers: 10⁻²–10⁻³ m·d⁻¹; Cretaceous aquifer: 10⁻³ m·d⁻¹). A ¹³C_{DIC} enrichment along the flowpath of the Cretaceous aquifer was observed and could be

due to carbonate mineral dissolution. From the investigation, four types of recharge processes to the aquifer system are discerned, with the overall modern recharge component being low. The Cretaceous aquifer contains fossil groundwaters and hence, the resources may be finite and thus, their exploitation is mining. The most suitable river for implementing large-scale artificial recharge measures was also identified.

1. INTRODUCTION

Over 20 years of groundwater development of the Tiruvadanai aquifers (area >1400 km²) in the predominantly saline water bearing coastal sediments of the Ramanathapuram district, located in the Tamilnadu State (Fig. 1) in South India and known for its water scarcity, has resulted in a piezometric head decline of the order of 5 to 26 m, with the maximum at the center of basin. The possibility of seawater intrusion, quality changes due to vertical leakage and other ill effects of over exploitation are anticipated. In order to protect the aquifer system, artificial recharge measures have been implemented in the recharge area of the aquifer system. In the present study, environmental isotopes (²H, ¹⁸O, ³H, ¹³C, ¹⁴C), hydro-chemistry (major-ions) and in-situ physico-chemical parameters (EC, T, pH, etc), in conjunction with hydro-geology data, were used to investigate the recharge processes and dynamics of the coastal sedimentary aquifers of Tiruvadanai, and then to evaluate the effectiveness of artificial recharge measures to augment the aquifer system.

2. TIRUVADANAI AQUIFER SYSTEM

The aquifer system forms part of Tamilnadu Coastal Plain and has a tropical climate (Max. Temp. 41°C). The area receives rainfall from both southwest (SW) and northeast (NE) monsoons, with more than 60% of the total rainfall from the latter. The spatial distribution of rainfall in the aquifer area is non-uniform with the average annual rainfall for the last 85 years being 830 mm. Two ephemeral rivers, namely Sarugani and Manimutharu, carrying floodwater during monsoon, drain in the south and north of the aquifer area, respectively (Fig. 1).

Holocene to recent alluvial deposits (sand, clay, silt) cover most part of the region. The sedimentation over the narrow elongated basin might have taken place under fluvial, fluvio-marine, marine and aeolian environmental conditions. A small area of crystalline basement rock (granite) is exposed in the western most part of the study area. Tertiary (Miocene) sediments (sandstone, clay, gravel) are exposed on a narrow band in the western part adjoining the

ENVIRONMENTAL ISOTOPE AND HYDROCHEMICAL INVESTIGATION

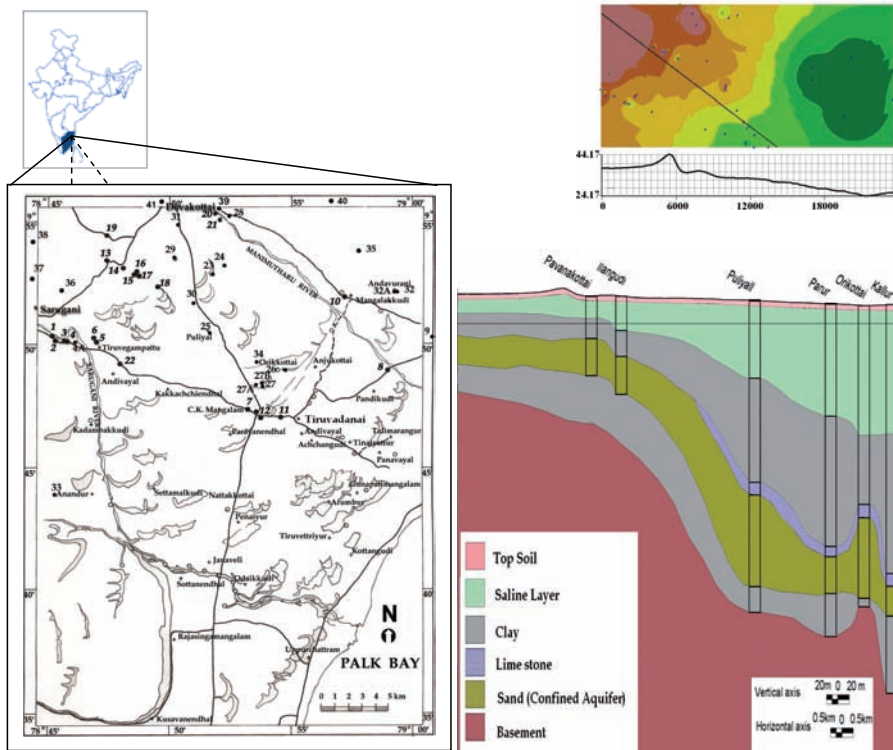


FIG. 1. Location map of Tiruvadanai Aquifer with sampling sites (1, 2, etc.) and, elevation profile and geological section along Pavanakottai (sampling site no. 14) and Tiruvadanai.

crystalline rocks. Due to unconfirmity in the geological succession of the study area, the older (Cretaceous) sedimentary rocks (sandstone) are only encountered in deep tube wells in central and eastern parts of the study area. Both the Tertiary and Cretaceous formations pinchout towards the coast with only clay deposition.

The hydrogeological data indicated that the deeper (350–500 m) Cretaceous aquifer, which lies just above the basement, contains freshwater. The shallow (<200 m) Tertiary aquifers that overlie the Cretaceous aquifer is mostly saline in the central and eastern parts of the study area and a thick sticky clay bed separates them. In the western area, the Tertiary sediments (unconfined/semi-confined) contain freshwater pockets at a few depths. These zones along with the Cretaceous aquifer have been successfully tapped over the last 20 years for drinking water supply. The present investigation deals with these freshwater zones only. The recharge area for the aquifer system is

identified in the ridge area running parallel to Sarugani-Devakottai Line, SDL (Fig. 1).

Recharge to any groundwater system depends on rainfall rate and pattern, soil type, drainage and land-use pattern, depth to water table and prevailing groundwater extraction. The rainwater collected in a number of irrigation tanks in the study area exists for 3 to 4 months only. The high evaporation losses and unfavorable sub-surface lithology lead to negligible recharge to the groundwaters. Hence, it was planned that harnessing run-off from the ephemeral rivers and the surplus from irrigation tanks during floods could improve the aquifer storage. Accordingly, a number of finger dykes and borewells (200 mm diameter, 100 m deep) were constructed on the river beds. In addition, several recharge pits inside a few selected irrigation tanks and at the ridge area running parallel to SDL were constructed. An environmental isotope and hydrochemical investigation was carried out to understand the recharge (natural, artificial) processes and dynamics of the Tiruvadana aquifers (study area: ~ 250 km²).

3. METHODS

Water-sampling programmes were carried out in November 2002 (NE monsoon), August 2003 (SW monsoon), March 2004 (summer), March 2005 (considered as post-NE monsoon due to extended NE monsoon in 2004–2005) and June 2006 (pre-SW monsoon). Water samples were collected from tube wells, irrigation tanks, ephemeral rivers (Sarugani, Manimutharu) and from the recently constructed artificial recharge structures for environmental isotopes (²H, ¹⁸O, ³H, ¹³C, ¹⁴C) and hydrochemical (major-ions) analyses (Fig. 1). T, pH, EC, etc. of the water samples were measured on site.

The stable isotope analyses were carried out using a GEO 20-20 (PDZ EUROPA) Mass Spectrometer. $\delta^{18}\text{O}$ and $\delta^2\text{H}$ were measured by the CO_2 and Pt- H_2 equilibration methods, respectively, and results are reported in the standard δ -notation relative to SMOW. (Precision: $\pm 1\text{‰}$ and $\pm 0.2\text{‰}$ for $\delta^2\text{H}$ and $\delta^{18}\text{O}$, respectively). The $\delta^{13}\text{C}_{\text{DIC}}$ analyses are reported with respect to. PDB (Precision: $\pm 0.2\text{‰}$). ^3H analyses were made by Liquid Scintillation Counter (Quantulus) after electrolytic enrichment of the water samples (Precision: ± 0.5 TU). ^{14}C activity of dissolved inorganic carbon (DIC), precipitated as BaCO_3 , was measured by CO_2 absorption technique using liquid scintillation and expressed as percentage modern Carbon (pMC) (Detection limit: 0.5 pMC), and model ages were computed. The major chemical-ions (cations, anions) in the groundwater samples were measured using Ion-Chromatography using a DIONEX 500.

4. RESULTS

4.1. Hydrochemistry

The results of the chemical analyses (major cations and anions) of the groundwater samples, and the Piper diagram of the March 2004 samples (Fig. 2), indicate presence of two distinct types of water. Tertiary aquifers (< 200 m) fall in a no-dominant (Ca–Mg–HCO₃–Cl) type to NaCl type whereas the Cretaceous aquifer (350–500 m) are predominantly NaCl type. The diagram also indicates modification of Tertiary waters from no-dominant type, to NaCl type along the flow path. In general, higher pHs (7.4–8.6) are seen in the Cretaceous aquifer compared to the Tertiary aquifer (~7). The down-gradient variations of the major-ion concentrations of the groundwater samples, indicate a general increasing trend in Na⁺ and K⁺ with decreasing Mg²⁺ and Ca²⁺ in both Tertiary and Cretaceous aquifers. The Cretaceous aquifer has low SO₄²⁻ and NO₃⁻ concentrations compared to Tertiary aquifers. In Tertiary aquifers there is no change seen in HCO₃⁻ along the flow path, whereas in the Cretaceous aquifer slight increase in HCO₃⁻ is seen along the flow path after an initial decrease. [In Figs. 2 and 3, the x-axis represents the distances of sampling sites measured from the ridge area along the groundwater flow direction].

4.2. Environmental isotopes

The results of environmental isotopes (²H, ¹⁸O, ³H, ¹³C, ¹⁴C) analyses of the water samples are shown in Fig. 3. The results of November 2002 samples indicated that the Cretaceous aquifer waters fall above the Global Meteoric Water Line (GMWL) on a δ²H–δ¹⁸O plot, with a regression equation: δ²H = 8.4 (±0.6) × δ¹⁸O + 16.1 (±3.7). The un-confined and semi-confined groundwater samples of the Tertiary aquifers showed a clear evaporation effect [Evaporation Line, EL: δ²H = 4.3 (±0.8) × δ¹⁸O – 9.7(±3.6)]. The Tertiary aquifer samples showed seasonal stable isotope variation but not the Cretaceous aquifer.

Most of the groundwater samples (Tertiary, Cretaceous) had very low ³H (0.7–1.8 TU) in August 2003, with no difference between August 2003 and March 2004 results. However, a few un-confined and semi-confined groundwater samples of the Tertiary aquifers near the rivers had ³H in the range 2.0 to 3.6 TU in August 2003. The surface water in March 2004 and the November 2003 rainwater had 5.4 and 6 TU, respectively. The δ¹³C_{DIC} values of the Tertiary and Cretaceous aquifers ranged from –22.9 to –10.1‰ PDB and –23.6 to –11.1‰ PDB, respectively. The ¹⁴C_{DIC} values of the Tertiary and Cretaceous aquifers, respectively, were 19.3 to 97.7 pMC and 0.6 to 4.1 pMC.

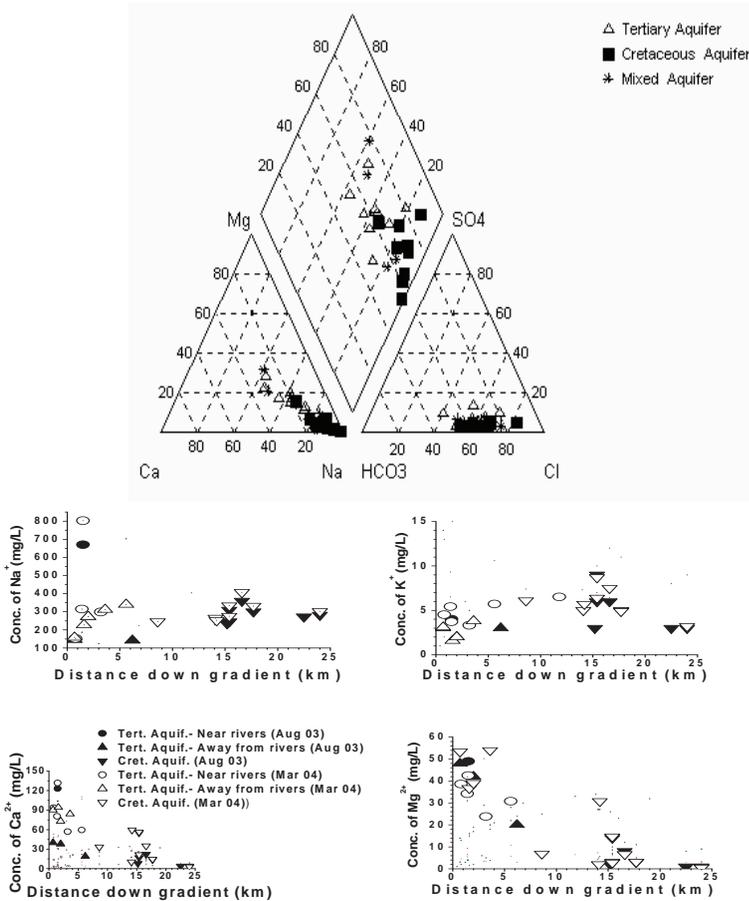


FIG. 2. Chemical results (legends for down gradient variation of chemical species is same for all).

5. DISCUSSION

5.1. Hydrochemical evolution of groundwaters

In the Cretaceous aquifers, the seasonal variation in hydro-chemistry is almost negligible (Fig. 2), whereas the Tertiary aquifers near ephemeral rivers exhibit some variation with higher, intermediate and lowest values occurring during NE monsoon, SW monsoon and summer periods, respectively. The lowest values during summer indicate the presence of a delayed recharge component. The observed general increasing trend in Na⁺ and K⁺ with decreasing Mg²⁺ and

Ca^{2+} along the flow direction in Cretaceous aquifer, apart from ion-exchange process, could be due to precipitation of carbonates of Mg^{2+} and Ca^{2+} with the rise in pH (7.4–8.6). Also, general low SO_4^{2-} and NO_3^- concentration in the Cretaceous aquifer compared to Tertiary aquifers could possibly be due to bacterial reduction of long standing waters. The observed slight increase in HCO_3^- along the flow path after an initial decrease in the Cretaceous aquifer could be attributed to dissolution of carbonate bearing minerals as well as redox processes occurring in the system, possibly by oxidation of organic matter present in the matrix to HCO_3^- , along with simultaneous reduction of SO_4^{2-} and NO_3^- which has consisted with Fig 2. This finding is also supported by slight enrichment in $\delta^{13}\text{C}_{\text{inorg}}$ along the flow path as discussed in a later section on environmental isotopes. The change in pH from almost neutral in Tertiary aquifers to slightly alkaline in Cretaceous aquifer (7.4–8.6) seems to be associated with bacterial reduction.

5.2. Groundwater age, dynamics, recharge (natural, artificial)

The slope and intercept obtained for the Cretaceous aquifer ($\delta^{18}\text{O}$ – $\delta^2\text{H}$ plot, Fig. 3) are higher compared to that of the Local Meteoric Water Line (LMWL) reported for the area [1] indicating its recharge by meteoric water during a different climatic condition than that prevailing at present. An evaporation effect in stable isotopes ($\delta^2\text{H}$, $\delta^{18}\text{O}$) is seen for the Tertiary aquifer samples (unconfined, semi-confined) and the isotope values of surface water samples fall on the evaporation line indicating possible surface water contribution (rivers, artificial recharge structures, irrigation tanks, ponds etc) to the aquifers. The evaporation effect could also be due to near-surface evaporation during the natural recharge processes.

A few Tertiary aquifer samples located near the ephemeral rivers showed some seasonal variation in $\delta^2\text{H}$ and $\delta^{18}\text{O}$, with comparatively enriched values in August 2003 ($\delta^{18}\text{O}$ -Distance downstream, Fig. 3) which reflects relatively faster recharge along the rivers. But in regions away from the river courses and lying along the ridge, the seasonal variations in the isotope values were insignificant. This indicates that the movement of water in the unsaturated zone during the recharge process in these regions is slow and thereby, the possible isotopic seasonal variations in the recharging waters get reduced and/or recharge to the aquifer at these regions is negligible. A similar seasonal change in the EC and chemistry of groundwater samples from the above two regions were observed and thus corroborating the isotope findings. The Cretaceous aquifer did not show any significant change in the isotope values indicating long residence time of the groundwaters.

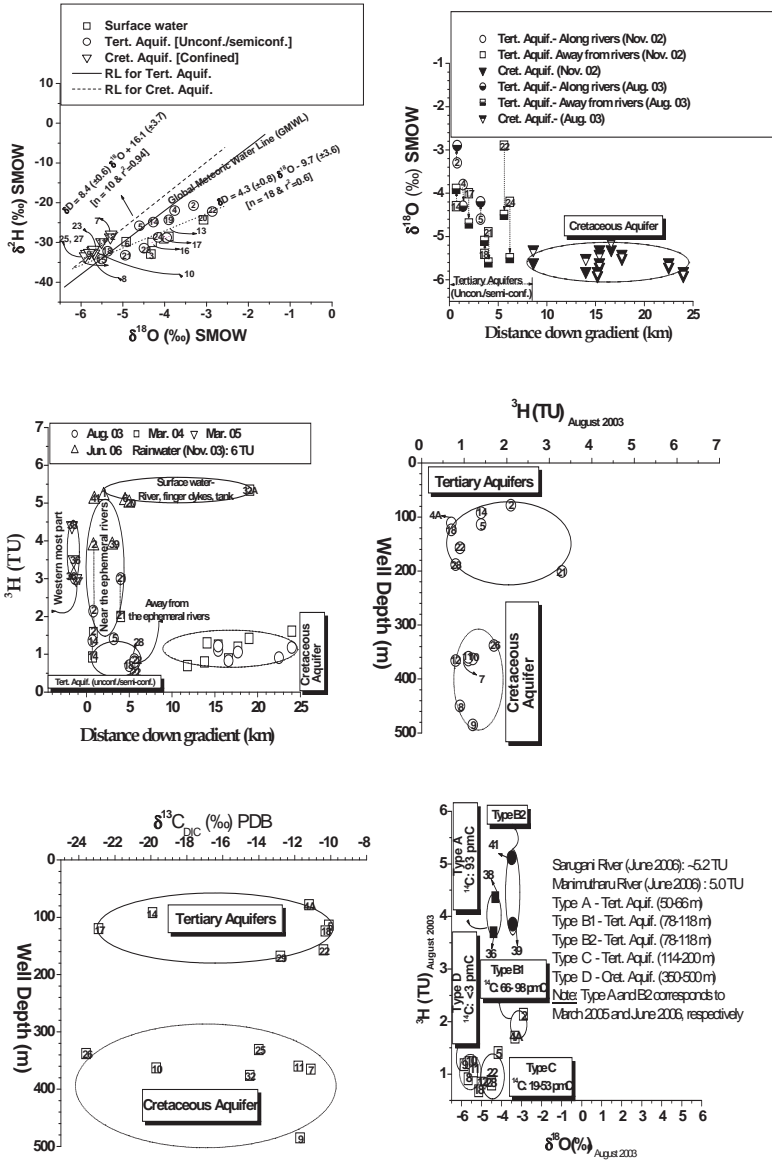


FIG. 3. Isotope results (sampling site numbers are given inside the symbol).

ENVIRONMENTAL ISOTOPE AND HYDROCHEMICAL INVESTIGATION

Generally low environmental ^3H concentration in groundwater samples away from the ephemeral rivers (<1 TU) were observed during SW monsoon and summer periods (^3H -Distance downstream, Fig. 3), whereas near the rivers the respective values were in the range 1 to 3 TU and 1.5 to 2 TU. In June 2006, the groundwater samples near the rivers had values of 1.5 to 5 TU indicating a certain amount of modern recharge through the artificial recharge borewells constructed on the rivers bed (possibly as a result of the extended and heavy NE monsoon in 2005). (The lithologs of the tube wells near the ephemeral rivers do not favour direct rainwater recharge through the sandy tracts of the rivers and/or from the surface methods of artificial recharge measures like recharge pits, irrigation tanks, etc. owing to intervening clay lens above the screens of the tube wells.) Between the groundwater samples located near the rivers (those located near to the north-bounded river) had comparatively higher ^3H values (^3H - ^{18}O , Fig. 3) indicating larger contribution from the recharge borewells constructed on the north-bounded river bed. The Cretaceous aquifer samples had very low tritium values (<1.5 TU) with no seasonal variation, indicating that they are old waters.

In the Tertiary aquifers, a slight difference in the $\delta^{13}\text{C}_{\text{DIC}}$ values of the groundwaters near and away from the ephemeral rivers was seen, with depleted values near the rivers (-20 to -23%). The $\delta^{13}\text{C}$ values of the Cretaceous aquifer indicated a slight enrichment along the general groundwater flow direction. The chemical analyses results (Fig. 2) suggest that enrichment possibly results from two simultaneous processes, namely dissolution of carbonate minerals (calcite, aragonite, dolomite etc) and bacterial reduction of oxygen bearing anions. While the first process enriches $\delta^{13}\text{C}_{\text{DIC}}$, the second depletes it by producing HCO_3^- (depleted in ^{13}C) from the oxidation of C_{org} . Since the concentration of NO_3^- and SO_4^{2-} of water in the initial stages of flow path itself is less, the effect on overall value of $\delta^{13}\text{C}_{\text{DIC}}$ is dominated by $\delta^{13}\text{C}_{\text{DIC}}$ of HCO_3^- produced from dissolution of carbonate minerals.

From $^{14}\text{C}_{\text{DIC}}$ model (Pearson, IAEA, Vogel, based on $^{14}\text{C}_{\text{DIC}}$ of a groundwater sample near the south-bounded river with a value 98 pMC as the initial activity) ages, it is observed that in the Cretaceous aquifer the groundwater ages range from ~ 20 – 40 ka, BP. A higher groundwater age along with higher δ -excess is a typical characteristic of a palaeo-climate recharge, mostly in an arid phase. Therefore, it appears that the potential and freshwater bearing deeper Cretaceous aquifer of the Tiruvadanai aquifer system contains palaeo-groundwaters i.e., not part of actively recharged flow systems, and hence the resources may be finite and their exploitation is considered mining. The $^{14}\text{C}_{\text{DIC}}$ and ^3H of the groundwater samples suggest that the Tertiary aquifers in the northwestern part of recharge area contain mostly old waters ($^{14}\text{C}_{\text{DIC}}$ model ages: 1–13 ka, BP). Based on the $^{14}\text{C}_{\text{DIC}}$ model ages, the groundwater

velocity of the Tertiary aquifers near and away from the south-bounded river was estimated to be 10^{-2} and 10^{-3} m·d⁻¹, respectively. In the Cretaceous aquifer, the groundwater velocity at the centre of the basin is 10^{-3} m·d⁻¹.

The ³H, δ¹³C_{DIC} and ¹⁴C_{DIC} of the groundwater samples of the Tertiary aquifers did not show any correlative trend with depth of wells, reflecting the multi-aquifer nature of the system and possibly the difference in their sources and processes of recharge. (However within a freshwater zone of the Tertiary aquifers, decrease in ³H and ¹⁴C_{DIC} and enrichment in δ¹³C_{DIC} was observed along the flow path). The δ¹³C_{DIC} of a few Cretaceous aquifer samples had highly depleted values and relatively low SO₄²⁻ (~18 mg·L⁻¹), indicating a reducing environment where SO₄²⁻ is reduced with simultaneous oxidation of the locally present organic matter. In the Cretaceous aquifer, since the concentrations of ³H and ¹⁴C are very low (near to detection limits), correlation between ¹⁴C/³H and the well depths could not be made. The ¹⁸O and ³H values are evidence of possibly different sources and processes of recharge.

6. CONCLUSIONS

Based on the hydrogeological, hydrochemical and environmental isotopic evidence, four types of recharge processes to the Tiruvadanai aquifer system are discerned (vide, ³H-¹⁸O plot, Fig. 3):

- (a) Modern natural recharge from the western most part of the aquifer system to the Tertiary aquifer having depth 50–66 m (Type A);
- (b) Lower and, a relatively higher modern recharge, respectively through the artificial recharge measures (recharge borewells) at the south-bounded river (Sarugani) and north-bounded river (Manimutharu) to the Tertiary aquifer having depth 78–118 m (Type B1 and Type B2, respectively);
- (c) Paleo-recharge to both the Tertiary aquifer (depth 124–200 m) and the Cretaceous aquifer (depth: 350–500 m), (Type C and Type D, respectively).

Since the modern recharge is only through the recharge borewells of the ephemeral rivers and from the narrow western area, it can be concluded that the recharge to the aquifer system is not substantial, which is also suggested by falling piezometric heads over the last 20 years. In addition, the most suitable river for planning large-scale artificial recharge measures could be the north-bounded ephemeral river (mostly using recharge borewells), rather than the south-bounded ephemeral river.

ACKNOWLEDGEMENTS

The authors express their gratitude to Mr. U. K. Sinha, Mr. K. Tirumalesh and Mr. G.N. Mendhekar from BARC, Mumbai, and Mr. K. Sobburaj, Mr. V. Arumugam and Dr. T.P. Natesan from TWAD Board for extending their various help during the investigation. Also, sincere thanks to Dr. Gursharan Singh, Head Isotope Applications Division, BARC for his encouragement during the investigation.

REFERENCE

- [1] DESHPANDE, R.D., BHATTACHARYA, S.K., JANI, R.A., GUPTA, S.K., Distribution of oxygen and hydrogen isotopes in shallow groundwaters from southern India: Influence of a dual monsoon system, *Jl. Hydrol.* **271** (2003) 226–239.

GROUNDWATER FLOW FUNCTIONING IN ARID ZONES WITH THICK VOLCANIC AQUIFER UNITS: NORTH-CENTRAL MEXICO

J.J. CARRILLO-RIVERA

Institute of Geography,
National Autonomous University of Mexico,
Coyoacán, México

A. CARDONA

Earth Sciences,
University of San Luis Potosí, México

W.M. EDMUNDS

Centre for the Environment,
Oxford University, UK

Abstract

Population increase in arid zones of Mexico has created the presence of 450 % new cities with more than 50,000 inhabitants, as related to the 1950s. Due to the arid nature of the environment, the once sufficient spring and shallow water are becoming inadequate for the supply of those cities. An answer to this problem lies with the sustainable development of deep groundwater. The geological features of the country include fractured volcanic aquifer units that are more than 1,500 m thick, and are regionally continuous over several hundred thousands of square kilometres. Groundwater development decisions need to consider, in the long span, inter-basin groundwater flow and the need to prevent environmental impacts in distant sites hydraulically connected with extraction centres. Radiocarbon is an excellent tool that initially has been applied to characterize groundwater in thick aquifer units in central Mexico to provide evidence on the hierarchy of flow (local/regional) and water age from where the distance of regional recharge was inferred. Radiocarbon also helps constrain flow path length which can then be used to characterize inter-basin groundwater communication. Radiocarbon has a large potential for future expansion of research and water management application.

1. INTRODUCTION

Population increase in arid zones of Mexico has created the presence of 45 cities with more than 50,000 inhabitants in the last 50 years; in fact, the increase

has gone from 10 to 28 cities for 1950 to 1970, respectively [1]. Due to the arid and semi-arid nature in about 65% of the territory, predictions on the increasing insufficiency of drinking water supply from the once sufficient spring and shallow groundwater has proved to be accurate [2]. A practicable option may be the sustainable development based on deep regional groundwater sources. The geological features of the country include fractured volcanic aquifer units that are more than 1,500 m thick, and are regionally continuous over of hundreds of kilometres. They also form the prominent highland topographic features.

Studies used at the government level often discuss availability of groundwater from the water balance perspective, a bulk-parameter method applied on a basin or with hydraulic boundaries at both administrative limits on the surface plane and horizontally to the depth of existing boreholes. This, and its methodological simplifications neglect the presence and importance of deep groundwater flow, which under prevailing geological conditions usually permit intra-basin flow [3, 4]. The acknowledgement of this connection and its application to prevent environmental impacts in distant sites hydraulically connected (e.g. wetlands), requires further understanding. Reference [4] reports the presence of intermediate and regional groundwater flows in the south of Mexico city, but their description and usage in defining inter-basin flow is required to further characterize groundwater development.

Therefore, the objective of this paper is to highlight the presence of regional groundwater flow systems in a thick aquifer and inter-basin groundwater flow as suggested by temperature (at borehole-head) and Lithium as a proxy of residence time with the support of radiocarbon dating as a potential tool to identify future research a sustainable groundwater development.

2. MATERIALS AND METHODS

A set of samples was collected from active water supply boreholes located on the southern part of the plane of Mexico City (Fig. 1). Prior to sampling boreholes had been pumping continuously for more than six months, and have been in operation for several years. Related physical data (temperature) was measured as well as other standard parameters not presented in the field using an in-line flow cell to ensure the exclusion of atmospheric contamination and to improve measurement stability. Two filtered (0.45 μm) samples were collected at each site in acid-washed, well rinsed low density polyethylene bottles. One sample for trace element determination was acidified to make 1% in HNO_3 , producing a pH around 1.5 sufficient to stabilise trace metals; unacidified samples were collected for anion analysis.

GROUNDWATER FLOW FUNCTIONING IN ARID ZONES

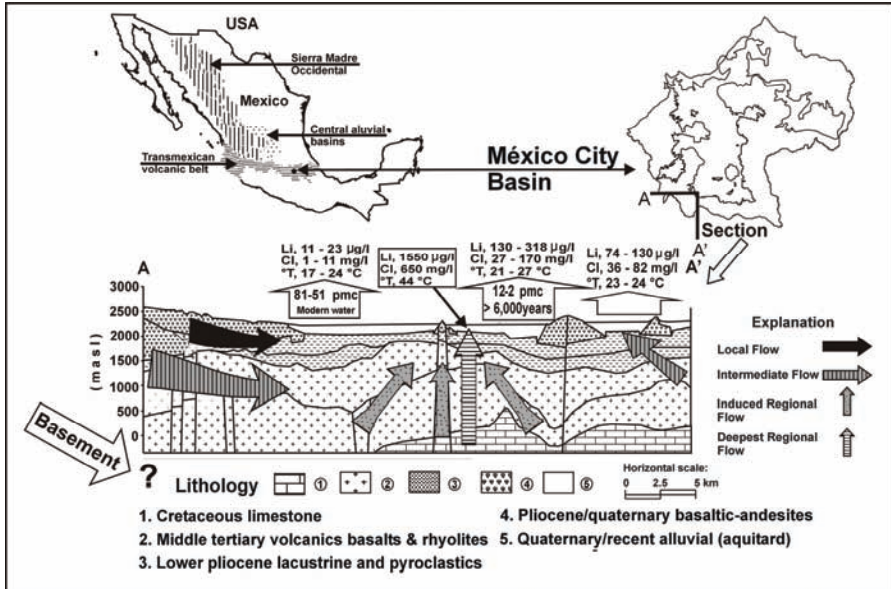


FIG. 1. Location map of study area and vertical section of geological framework of Mexico City Basin.

All inorganic analyses were carried out at the British Geological Survey (Wallingford). Chloride was analysed by automated colorimetry, Li by ICP-MS (Fison PQ1 instrument). Inter-comparisons were also made for certain elements (e.g. Li) by comparing results produced both by ICP-AES and ICP-MS. The ICP-MS data are used here in preference, because of the lower quantitation limits as compared with ICP-AES. Radiocarbon analyses were made by AMS (accelerator mass spectrometry) at Tucson, Arizona following sample preparation by the NERC Radiocarbon Laboratories at East Kilbride, Scotland. Results are reported as pmc (per-cent modern carbon) where the errors are well within 1%.

A groundwater flow system analysis was incorporated with the method fully described in reference [5] this agreeable method postulates the hierarchical arrangement of local, intermediate and regional flows according to chemical, physical, geological and hydraulic evidence; information that is used in standard groundwater studies. Such data may also be used in conjunction with the surface manifestation of each flow in terms of topography, soil and vegetation cover.

3. REFERENCE TO STUDY AREA

Relevant data from well documented study cases were used to develop evidence on the importance of the effects related to the presence of a thick aquifer unit (i.e., >1500 m) in the interpretation of observed hydrogeological response; among them, the Mexico City basin (MCB) is considered an excellent example [4]. This site is located in a topographic basin in a physiographic province of Mexico where fractured volcanic rocks prevail. The MCB is situated in the centre of the Mexican Trans-volcanic Belt (≈ 300 km wide and ≈ 900 km in length) in which major outcrops belong, mainly, to mafic extrusive rocks (inset, Fig. 1). This basin has strong hydrogeological similarities to, for example: (i) the Sierra Madre Occidental (≈ 400 km wide and ≈ 1600 km in length) where felsic flow materials prevail, and (ii) the Central Aluvial Basins (≈ 200 km wide and ≈ 500 km in length). The main similarity, among others, is characterized by boreholes initially withdrawing water from local or intermediate system and next they induce flow with high Li content and temperature values.

The MCB incorporates a geological framework in the vertical section, as presented in Fig. 1. Subsurface lithological features were obtained from direct drilling results and seismic data suggesting an aquifer thickness in excess of 2,000 m in Tertiary to Quaternary volcanic units (basaltic, andesite and rhyolite) and related sediments and pyroclastics. The volcanic units are extensively fractured and crossed by fault (graben) systems that result from tensional tectonic regional forces; these units partially cover an excess thickness of 1,000 m of limestone strata, Cretaceous in age; drilling carried out through these strata reported karstic features [6] and show that the limestone is laying on an undifferentiated basement rock. Quaternary to Recent fine-grain deposits form a 30 m to >200 thick aquitard unit [4] that is a remnant of a lake feature that almost fully covers the plane and is highly compressible. The original hydrological setting within this surface basin, as reported in the XVI Century, was that of lakes with the presence of discharge conditions that belong to local, intermediate and regional flows. Some local discharge features still remain in the surrounding mountains. However, the steady state condition evident by a continuous discharge of local, intermediate and regional flows has been disturbed. Discharge conditions that gradually changed over the last half of the XX century, time in which industrial development in Mexico city and neighbouring towns made a significant increased not only from an economic perspective (having about 50% of the productive power of the country), but also impacted groundwater withdrawal (especially in the southern part of the basin). An example of the severe stress on discharge areas of intermediate systems is the disappearance of the natural conditions of the wetland of

Xochimilco in the south of the basin, which now survives on sewage inflow from a secondary treatment plant.

Initial pumping-test results carried out in 1970s in water supply boreholes indicated the expected semi-confined conditions resulting from an inflow of the aquitard unit above. Withdrawal in the basin at that time was claimed to be about 27 m³/s. A current estimate of water needed to supply the City is about 70 m³/s. More than 50 m³/s of groundwater are obtained through 100–400 m deep boreholes located on the plain. This heavy withdrawal induces different proportions of thermal water from beneath into the withdrawal level. Thermal inflow and its effect on pumping-tests are usually ignored and often mistaken as a leaky-effect from the aquitard above. The heavy withdrawal has turned the classical semi-confining conditions into an additional inflow from beneath [4].

Intensive pumping in the last 50 years has changed local hydraulic gradients resulting in some instances in a groundwater velocity increase along the same flow direction; current regional horizontal velocity is of about 20–25 m/y ($dh/dl = 0.00159$; $K = 0.000004$ m/s; $n = 0.01$). Hydraulic parameters suggest that maximum advective displacement (up-gradient) has been of the order of 2 km in view of the length of the section in Fig. 1 (≈ 25 km) and the distance between boreholes of ≈ 1 km. Samples are expected to represent those of the original horizontal flow conditions and indicate any influence of vertical (downward or upward) flow.

4. RESULTS AND DISCUSSION

4.1. Flow system definition

The chemical response of groundwater is considered to include a memory of the characteristics of its flow path, and this is required for incorporation in hydrogeological investigations. Elements such as Li, are considered to provide a proxy on the residence time [7]. In this regard, Table 1 shows relevant values for concentrations of Li of 10.5–29.3 $\mu\text{g/L}$ (Cl, 1.0–11.8 mg/L; temperature, 17.3–24.7°C) suggesting the presence of a local flow. Values of Li of 74.0–120.0 $\mu\text{g/L}$ (Cl, 36.0–82.0 mg/L; 23.0–24.0°C) suggest a comparatively older water (intermediate flow). Concentrations of Li of 130.0–318.0 $\mu\text{g/L}$ (Cl, 27.2–170.0 mg/L; temperature, 21.2–27.2°C) suggest the presence of water with a larger residence time than the two previous identified groups, and imply the presence of a flow system of regional nature. Considering the geological framework where the MCB is located, the highest Li and Cl content of 1550 $\mu\text{g/L}$ and 650 mg/L, respectively, and the hottest discharge water temperature of 44°C

TABLE 1. CHLORIDE, TEMPERATURE, Li, ^{14}C AND $\delta^{13}\text{C}$ FOR EXTRACTION BOREHOLES, SOUTH OF THE MEXICO BASIN.

	1	2	3	4	5	6	7	8	
Cl	9.9	5.3	5.0	5.3	9.4	11.8	9.5	11.5	
Temp	19.4	17.9	18.3	18.3	19.1	18.7	20.3	18.8	
Li	15.6	22.0	15.9	16.1	11.1	24.8	11.5	10.5	
^{14}C							81.1		
$\delta^{13}\text{C}$							13.7		
	9	10	11	12	13	14	15	16	17
Cl	21.9	5.3	2.0	6.5	1.0	27.2	650.0	162.0	129.0
Temp	19.1	18.8	24.0	20.4	24.8	27.2	44.0	26.9	23.7
Li	10.8	18.4	29.7	22.9	29.3	196.0	1550.0	318.0	130.0
^{14}C		50.9			53.8	13.1	1.9		13.4
$\delta^{13}\text{C}$		13.8			13.0	6.3	0.8		4.6
	18	19	20	21	22	23	24	25	26
Cl	170.0	62.0	57.0	72.0	82.0	36.0	28.0	70.0	68.0
Temp	21.2	24.0	24.0	23.7	23.1	23.4	23.0	23.5	23.4
Li	229.0	116.0	85.0	107.0	120.0	89.0	55.0	116.0	74.0
^{14}C	12.7								
$\delta^{13}\text{C}$	6.3								

Note: Cl in mg/L, Li in $\mu\text{g/L}$, Temp in $^{\circ}\text{C}$, ^{14}C in pMC, $\delta^{13}\text{C}$ in ‰; borehole number also indicates, roughly, the distance in km from the start of the section.

of borehole 15 are considered evidence of a deepest regional flow that has travelled along the limestone strata.

Lithium, Cl and temperature data seem to be in agreement with radiocarbon corrected ages suggesting that local flows are responding to modern water (^{14}C , 81.1–53.8 pMC; $\delta^{13}\text{C}$, –13.0 to –13.8‰). The regional flow is represented by water that has a residence time between 3300 to 6000 years BP (^{14}C , 12.7–13.4 pMC; $\delta^{13}\text{C}$, –4.6 to –6.3‰). The positive value of $\delta^{13}\text{C}$ for the deepest regional flow shows a near water-rock equilibration (^{14}C , 1.9 pMC; $\delta^{13}\text{C}$, 0.8‰) with the heavy carbon source suggesting that this water travelled to the deepest part of the geological section through the Cretaceous limestone

present above the basement rock. There is a lack of radiocarbon analysis for the intermediate flow system; however Li, temperature and Cl values suggest an agreement with the proposed hierarchy of this flow.

4.2. Hydraulic continuity beyond the surface basin limit

Water budget computations often use boundaries other than those consistent with by groundwater flow systems. The presence of regional flows in thick aquifer units may provide an opportunity for hydraulic communication between surface basins. The radiocarbon age of the regional flow of 6000 years BP since it entered the flow path, and the average regional horizontal velocity of about 20–25 m/y, allowed calculation of the approximate distance between the recharge area to the extraction site (120–150 km) located almost at the southern limit of the MCB. The topography of the terrain shows that related recharge sites are located well beyond the MCB, which suggest regional flow results in inter-basin flow. Evidently, the deepest regional flow suggests a recharge site beyond the 120–150 km boundary of the regional flow. These general calculations are in agreement with the radiocarbon flow velocities of 4 m/y as reported by reference [4], the prevailing geological framework, and the flow system analysis perspective.

5. CONCLUSIONS

The presence of regional groundwater flow systems is highlighted in one thick aquifer unit in central Mexico. The use of radioisotopes provided with the additional required evidence to the one already obtained from Li and temperature (at borehole-head) about the presence of regional flows. The question about the possibility of inter-basin groundwater flow also suggested by water temperature and Li, was also suggested by the modelling of radiocarbon based water ages (derived from the Pearson Model indicated in reference [4]). This result was only possible using joint interpretation of radioisotopes, basic hydrochemistry, groundwater hydraulics, topography and the prevailing geological framework. This interpretation was reached through an understanding of the characteristics of flow systems of diverse hierarchy. As development of economic activities and related population increase become paramount in arid and semi-arid regions, the definition of the extent of regional flow systems becomes more important in thick aquifer units as those present in central and northern Mexico, and in other parts of the world. However, water quality must also be considered as Cl concentrations in regional flow suggests limitations for drinking water supply, for example. This study suggests radiocarbon dating

as a potential tool to identify a sustainable groundwater development when interpreted within the prevailing hydrogeological functioning as suggested by the flow system analysis.

ACKNOWLEDGEMENTS

The authors wish to thank the International Atomic Energy Agency for its support to present this study in the International Symposium on Advances in Isotope Hydrology and its Role in Sustainable Water Resources Management (IHS-2007).

REFERENCES

- [1] GUTIÉRREZ DE MACGREGOR, M.T., GONZÁLEZ, J.S., Dinámica y distribución espacial de la población urbana en México (Dynamics and spacial distribution of urban population in Mexico), Instituto de Geografía, UNAM (2004) 158.
- [2] GUTIÉRREZ DE MACGREGOR, M.T., et al., Impact of Mexican and USA policies in urban growth and natural resources in the notherm border of Mexico, Latin American Studies, Nihon-Burajiru Chou Kyokai, Tokio, Japan. **15** (1997) 49–62.
- [3] CARRILLO-RIVERA, J.J., Application of the groundwater-balance equation to indicate interbasin and vertical flow in two semi-arid drainage basins, Mexico, Hydrogeology Journal **8** 5 (2000) 503-520.
- [4] EDMUNDS, W.M., et al., Geochemical evolution of groundwater beneath Mexico city, Journal of Hydrology **258** (2002) 1–24.
- [5] TÓTH, J., Groundwater as a geologic agent: an overview of the causes, processes, and manifestations, Hydrogeology J. **7** 1 (1999) 1–14.
- [6] SECRETARÍA DE HACIENDA Y CRÉDITO PÚBLICO, El hundimiento de la ciudad de México, Proyecto Texcoco (The sinking of Mexico City, Texcoco Project), Vol Nabor Carrillo, México (1969) 187.
- [7] EDMUNDS, W.M., SMEDLEY, P.L., Residence time indicators in groundwater in the East Midlands Triassic sandstone aquifer, Applied Geochemistry **2** (2001) 251–274.

POSTER PRESENTATIONS

PRECIPITATION
AND ATMOSPHERIC PROCESSES

ISOTOPIC STUDY OF THE WATER EXCHANGE BETWEEN ATMOSPHERE AND BIOSPHERE AT SELECTED SITES IN PAKISTAN

M. ALI, Z. LATIF, M. FAZIL, M. AHMAD

Isotope Application Division,
Pakistan Institute of Nuclear Science
and Technology,
P.O. Nilore, Islamabad, Pakistan

Abstract

Study of water exchange between atmosphere and biosphere was initiated to understand the ties between these two spheres. This paper presents the isotope (^{18}O , ^2H) results of moisture in the soil and plants (root, stem and leaf samples). Non woody plants (wheat, grass) and soil samples from wheat and grass fields (from the surface and 7 cm below the surface) were collected during January 2005 to April 2005. Woody plants of many species were sampled from two sites near Islamabad and Lahore. Air moisture was also collected in the field. Moisture contents from these samples were extracted using the vacuum distillation method and analysed for ^{18}O , ^2H isotope contents. Data depicts that the ^{18}O and ^2H of moisture in the leaves of non-woody and woody plants are much more enriched than those of stems and follow the evaporative enrichment trend originating from the soil moisture in the active root zone. Degree of enrichment depends on the size of leaves. Significant evaporation effect in the moisture of grass stems indicates alteration during water transport through the stem of tiny/thin plants. Reflection of typical isotopic values of individual rain events in the soil and stem and the corresponding values in the leaves shows that these isotopes can identify the source of moisture uptake, which can be used for studying water-use efficiency. Leaves of woody plants have relatively depleted ^{18}O values during wet (monsoon) period mainly due to retardation of fractionation resulting from higher humidity.

1. INTRODUCTION

Stable isotopes of oxygen, hydrogen and carbon that exchange between atmosphere and biosphere help understand the ties between these two spheres. The exchange of water and carbon dioxide between the biosphere and atmosphere in many arid and semiarid environments is temporally and spatially heterogeneous. The describes research on environmental isotopes in

the water cycle dynamics in selected areas of Pakistan in order to contribute to the IAEA programme MIBA for the development of regional scale model on ecosystem which will be integrated with existing global scale programs such as IGBP, BASIN, BAHC, AMERIFLUX and EUROCARBONFLUX. Isotopic investigations (^{18}O , ^{13}C , ^2H , etc.) help evaluate the major processes such as photosynthesis, respiration and evapotranspiration through a unique simultaneous isotopic analysis of water in vegetation and the adjacent components of the water cycle [1].

Fractionation of hydrogen and oxygen isotope ratios does not occur during uptake of soil water through the root and the stem up to the leaf [2]. Isotope ratios of oxygen and hydrogen in leaf water increase because of evapotranspiration effects [3, 4]. Extent of enrichment in oxygen and hydrogen isotope ratios of water in evapotranspiring surfaces of plants depends on, among other factors, the particular physiological characteristic of each specie [5].

1.1. Site Description

Three sites were investigated. Site-1 is located approximately 22 km in the south-east of Islamabad, the second site is about 2 km away in the north-west of the first site while the third one (Changa Manga area) is situated approximately 350 km. south of Islamabad. Climate of the study sites is arid to semiarid with a bimodal distribution of precipitation. Windblown silt, clay and subordinate amounts of alluvial gravel are present through out the area surrounding site 1 and 2. Sediment is light brown to grey, very fine grained, hard, compact and calcareous. The windblown sediments average 71 to 74 percent silt-size and 15 to 16 percent clay-size material. Mineral composition is predominantly quartz with subordinate amounts of feldspar and clay minerals, including kaolinite and illite. Quaternary sedimentary rocks which are moderately bedded and sorted having immature sandstone, unconsolidated to weakly consolidated mudstone and conglomerates are also present in this area [6]. Alluvial deposits are present all around the third site. The alluvial complex consists, principally, of grey to greyish brown, fine to medium sand, silt and clay. The chief constituent minerals are quartz, muscovite, biotite and chlorite, in association with a small percentage of heavy minerals. Quartz, being resistant to the abrasive action of water, is the major constituent of sand and determines its coarseness and assortment [7].

2. METHODOLOGY

2.1. Sampling

Root, stem and leaf samples of non-woody plants (wheat, grass) and soil samples from wheat and grass fields (from the surface and 7cm below the surface) were collected from Site-1 on monthly basis from January 2005 to April 2005. Samples from leaves and stems of woody plants consisting of eucalyptus, pine, delbergia sisso, melia azedarch were sampled from Site-2 near Islamabad on monthly basis from November 2005 to February 2006. Similarly, more than 150 samples (leaves and stem) of woody plants of about seventeen species were collected from Site-3 located near Lahore. The plant samples were preserved in airtight plastic jars and these jars were placed in a freezer ($\sim 5^{\circ}\text{C}$).

Air moisture was collected during each field campaign from site 1 and fortnightly at site 2. At site 1, water vapour samples were collected for the period of two hours between 1100 to 1500 hours using aluminum plates dipped in liquid nitrogen flask. At site 2, samples were collected using a vacuum pump and cold traps. Air flow was controlled with the help of a needle valve and the air was sucked through a set of three long (25 cm) glass traps submerged in a -85°C slush bath.

2.2. Extraction of Plant/Soil Water

Moisture contents from leaves, stems and soil were extracted using the vacuum distillation method (as shown in Fig. 1). Vein of the leaf sample and bark of stem samples are removed at the time of distillation. Sample of leaf/stem (15–20 gm) or soil (60–100 gm) is placed in a round flask connected to the vacuum line. Two cold traps incorporated with the vacuum line are used to collect the moisture. The air in the flask is slightly removed and the whole



Fig. 1. Moisture extraction system from plants and soil.

system is evacuated isolating the sample flask. Whole line is evacuated. The flask is dipped in water bath kept at 85°C. Traps are kept at liquid air/nitrogen temperature. Approximately after every half an hour, the gasses accumulated in the line are expelled out. About 8–12 mL moisture is collected in the traps in five hours.

2.3. Mass Spectrometric Analysis

For measurement of $\delta^{18}\text{O}$, the moisture extracted from the plant samples or collected from air was equilibrated with CO_2 gas [8] and subsequently the equilibrated gas was measured on a mass spectrometer for $^{18}\text{O}/^{16}\text{O}$ ratio. The isotopic results were first calculated using internal standards and then against VSMOW. Zinc reduction method [9] was used to produce hydrogen gas for the subsequent analysis on mass spectrometer. Zinc shots of size ranges: 1.0–1.5 mm (250 mg) or 1.5–2.2 mm (300 mg) were introduced at the bottom of glass ampoules attached to manifold, which were evacuated. Water samples (8 μL) were added to each container in the presence of flowing argon gas. The ampoules were cooled to -196°C to freeze the water. After removing air, these ampoules were isolated and placed in specially designed aluminum furnace at 480°C for 30 minutes. After completion of the reaction, the ampoules were cooled to room temperature and the hydrogen gas was analyzed by mass spectrometric for $\delta^2\text{H}$. The measurement uncertainties of $\delta^{18}\text{O}$ and $\delta^2\text{H}$ are 0.1‰ and 1.0‰, respectively.

3. RESULTS AND DISCUSSION

Plots of $\delta^{18}\text{O}$ vs. $\delta^2\text{H}$ of moisture extracted from root, stem and leaf samples collected from Sites 1, 2 and 3 are shown in Fig. 2, 3 and 4, respectively. All these plots show that the leaves of the non-woody and woody plants are more enriched in ^{18}O and ^2H than their respective stems. Fig. 2 shows that the moisture of wheat leaves is much more enriched in both the isotopes than that of grass leaves. This suggests that the enrichment is caused by the process of evapotranspiration which is higher from the wider leaves as compared to the leaves having less surface area. Although it is well known that during water transport between the root and the shoot, the isotope composition of xylem water remains unaltered from that in the soil [2, 10], but in this case the grass stem samples are much more enriched in both the isotopes than the soil moisture samples and they are plotted much below the LMWL showing significant evaporation. While the wheat stem samples plotted in the cluster of soil moisture, they do not show any significant evaporation. These results

ISOTOPIC STUDY OF THE WATER EXCHANGE

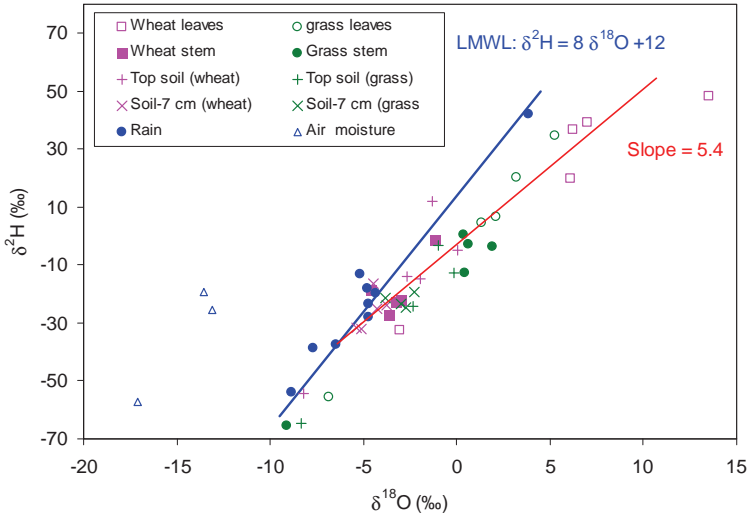


FIG. 2. Isotopic data of plants from site 1 (January 2005–April 2005).

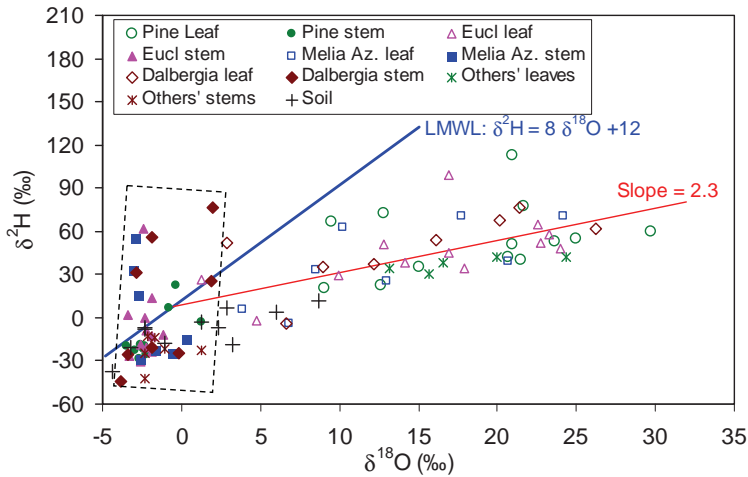


FIG. 3. Isotopic data of plants from site 2 (November 2005–February 2006).

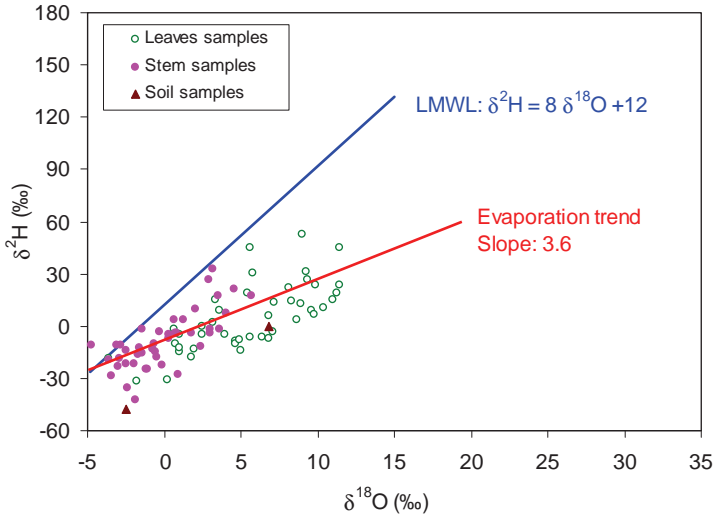


FIG. 4. Isotopic data of plants from site 3 (March 2006–June 2006).

indicate that the very thin stems like grass undergo significant evaporation resulting in enrichment of ^{18}O and ^2H isotopes. Values of $\delta^{18}\text{O}$ and $\delta^2\text{H}$ of the wheat and grass samples collected on 24th January 2005 are relatively more depleted as compared to that of the samples collected before and after this date. These values reflect the rain event that took place just two days before the samples were collected. Isotopic values of this rain water were more negative ($\delta^{18}\text{O}$: -8.87‰ , $\delta^2\text{H}$: -53.9‰) as compared to other rain events that took place during this season mainly, which were also followed by the soil moisture.

The $\delta^{18}\text{O}$ vs. $\delta^2\text{H}$ plot of leaf and stem samples of pine, eucalyptus, melia azedarch, dalbergia sissoo, cassia fistula linn, nerium oleander linn and soil under these plants collected from Site 2 is depicted in Fig. 2. Generally the leaf samples are much more enriched in both the isotopes and follow evaporation trend. It also shows that the degree of enrichment in the leaves of woody plants at this site is much higher than that in non-woody plants of the nearby site. Some of the stem samples have very high d-excess which needs further investigation. In the $\delta^{18}\text{O}$ vs. $\delta^2\text{H}$ plot of leaf and stem samples of many species of woody plants at Site 3 (Fig. 4), the data points follow the evaporation trend like in case of Site 2 but are less scattered. The degree of enrichment is less as compared to Site 2 maybe due to difference in climate.

In the temporal variation of $\delta^{18}\text{O}$ in plant samples of Site 2 (Fig. 5), it is observed that leaves of all the species show depleted ^{18}O during the months of

ISOTOPIC STUDY OF THE WATER EXCHANGE

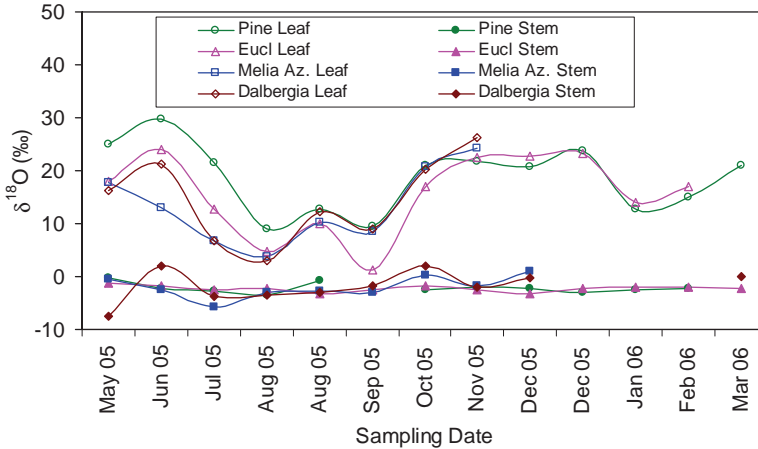


FIG. 5. Temporal variation of $\delta^{18}\text{O}$ in the leaf moisture (Site 2).

July to September, while the stem samples do not show any significant change. are which seems due to low evaporation rate due to very high humidity in the rainy season.

4. CONCLUSIONS

The following preliminary conclusions are drawn from the current study:

- ^{18}O and ^2H of moisture in the leaves of non-woody and woody plants are much more enriched than those of stems and follow the evaporative enrichment trend originating from the soil moisture in the active root zone. Degree of enrichment depends on the size of leaves.
- Significant evaporation effect in the moisture of grass stems indicates evaporation through the stem of tiny/thin plants also.
- Reflection of typical isotopic values of individual rain events in the soil and stem and the corresponding values in the leaves confirm that these isotopes can identify the source of moisture uptake, which can be used for studying water-use efficiency.
- Leaves of woody plants have relatively depleted ^{18}O values during wet (monsoon) period mainly due to retardation of fractionation resulting from higher humidity.

ACKNOWLEDGEMENTS

The authors are grateful to the International Atomic Energy Agency (IAEA)-Vienna, Austria for provision of financial support under IAEA Research Contract Pak-13064. Helpful discussions with Mr. Luis Araguas, Technical Officer, Isotope Hydrology Section, IAEA and Qazi Mudassir Hussain are thanfully acknowledged. Thanks are also due to M/S Abdul Razzaq, Bashir Ahmad, Imtiaz Ahmad and Muhammad Bashir for isotopic analysis of soil and water samples. Thanks are also due to the management of PINSTECH/Pakistan Atomic Energy Commission for providing technical support and financial assistance to materialize this research work.

REFERENCES

- [1] BRENT HELLIKER, Report of 1st RCM and general status for the IAEA CRP on Moisture Isotopes in the Biosphere and Atmosphere (IAEA-MIBA) Network (2005).
- [2] ZUNDEL, G., et al., The ^2H , ^{18}O enrichment in the leaf water of tropic trees: comparison of species from the tropical rain forest and the semi-arid region of Brazil. *Rad. Environ. Biophys* **15** (1978) 203–212.
- [3] GONFIANTINI, R., et al., Oxygen isotopic composition of water in leaves, In *Isotope and Radiation in Soil-Plant-Nutrition Studies*, IAEA, Vienna (1965) 405–410
- [4] FERHI A., LETOLLE R., Transpiration and evaporation as the principal factors in oxygen isotope variations of organic matter in aland plants, *Physiol. Veg.* **15** (1977) 363–370.
- [5] STERNBERG, L.S.L., et al., Oxygen and hydrogen isotope ratios of water from photosynthetic tissues of CAM and C₃ plants. *Plant Physiol.* **82** (1986) 428–431.
- [6] WILLIAMS, V.S., et al., Preliminary report on the environmental geology of the Islamabad–Rawalpindi area, Pakistan, *Proceedings of the First South Asia Geological Congress Islamabad, Pakistan* (1992) 358–377.
- [7] NATIONAL ENGINEERING SERVICES PAKISTAN LTD, BINNIE & PARTNERS CONSULTING ENGINEERS, Final Report on Groundwater Resources Evaluation and Study of Aquifer Under Lahore, Submitted to Water and Sanitation Agency, Lahore (1991).
- [8] EPSTEIN, S., MAYEDA, T., Variation of ^{18}O content of waters from natural sources, *Geochem. Cosmochem. Acta* **4** (1953) 213–224.
- [9] COLEMAN, M.L., SHEPHERD, T.J., DURHAM, J.J., ROUSE, J.E., MOORE, G. R., Reduction of water with zinc for hydrogen isotope analysis, *Anal. Chem.* **54** (1982) 993–995.

ISOTOPIC STUDY OF THE WATER EXCHANGE

- [10] EHLERINGER, J.R., DAWSON, T.E., Water uptake by plants: perspectives from stable isotope composition, *Plant, Cell and Environment* **15** (1992) 1072–1082.
- [11] INTERNATIONAL ATOMIC ENERGY AGENCY, Guidebook on Nuclear Techniques in Hydrology, Technical Report Series No. 91, IAEA, Vienna (1983).

GEOSTATISTICAL METHODS FOR PRODUCING STABLE ISOTOPE MAPS OVER CENTRAL AND EASTERN MEDITERRANEAN

A.A. ARGIRIOU

Laboratory of Atmospheric Physics,
Dept. of Physics,
University of Patras,
Patras

S.P. LYKLOUDIS

Institute for Environmental Research
and Sustainable Development,
National Observatory of Athens,
Athens

Greece

Abstract

Stable isotopes of water, namely ^{18}O and ^2H , have been extensively used during the last decades to address key aspects of the water cycle. Several scientific disciplines, such as hydrology, meteorology, palaeoclimatology or ecology have adopted isotopes as powerful tracers characterizing certain systems and processes. As a result several isotope databases have been created yet in most cases, the use of the data has been restricted to specific applications, possibly due to their spatial coverage. Using geostatistical methods to develop isotope maps would allow for a much broader use of isotopic data in many countries. To that end GNIP-ISOHIS isotopic precipitation data were used to generate isotopic maps of the precipitation over the Central and Eastern Mediterranean. The monthly data set was checked for outliers and then local meteoric water lines were used to complete missing values wherever possible. Simple regression models were developed to relate monthly weighted average, annual and seasonal, point isotopic values with corresponding meteorological data extracted from the CRU CL 2.0TS 2.1 gridded climatologies. The empirical models were then applied to the full gridded data sets to produce gridded isotopic datasets. Finally the residuals of the empirical models were gridded using ordinary kriging and added to the isotopic grids. The resulting grids appear to reproduce the known isotopic patterns of the area. A crosschecking was attempted with gridded data obtained by objective analysis, yet a more detailed assessment of the performance of this methodology is needed.

1. INTRODUCTION

Stable isotopes have long been used to determine and origin and history of water masses. Precipitation is a very significant part of the hydrological cycle and one of the most readily accessible for direct observation, thus its stable isotopic composition is of great importance to the correct representation of the water cycle over an area [1]. Meteorological and geographical conditions affect the isotopic composition of precipitation [2]. This renders stable isotopes powerful proxies for past climatic conditions, but also generates significant variations of modern the isotopic composition of waters on a global as well as a local scale [3]. Thus adequate stable isotopic information requires a measurement network far denser than that currently existing in most areas of the globe.

Current needs, and of course information on the past, can be addressed by modeling. Several global circulation models (GCMs) have been equipped with isotopic modules with considerable success [4, 5]. Their resolution is rather coarse though, so regional models (RCMs) incorporating isotopic modules have emerged [6]. Numerical models provide consistent global scale estimates, but their validation relies on measurements. Another alternative is statistical modeling. Several recent studies have dealt with the generation of high-resolution gridded isotopic data sets using a combination of empirical relationships and geostatistical methods to minimize interpolation errors. Some of them use direct interpolation of the data [7, 8], while others use empirical models based on geographical and/or meteorological parameters combined with gridded or other data sets [8–12].

In this work we follow the methodology proposed by Bowen and Wilkinson [9] using a set of models and interpolation methods to obtain monthly gridded isotopic climatologies for the central and eastern Mediterranean.

2. DATA AND METHODS

The domain of interest lays between 30°N–50°N and 05°E–40°E. Stable isotopic composition of precipitation, and basic meteorological parameters, covering the area between 25°N–55°N and 05°E–45°E were obtained from ISOHIS and GNIP databases, and the literature [13–16], while the the CRU CL 2.0 10°×10° data set of mean monthly surface climate over global land areas [17] provided the necessary gridded data. The length and the period represented in the time series of the various stations is both limited and quite variable. Since no consistent trend patterns could be identified [18] all available data were considered suitable for use. Local water meteoric lines (LWML) were

GEOSTATISTICAL METHODS FOR PRODUCING STABLE ISOTOPE MAPS

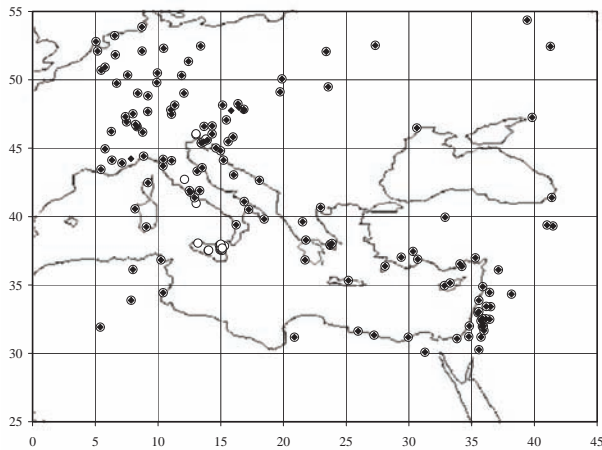


FIG. 1. Stations with monthly $\delta^{18}\text{O}$ (open circle) and $\delta^2\text{H}$ (black diamond) data.

estimated, and whenever one of the $\delta^{18}\text{O}$ and $\delta^2\text{H}$ was missing while the other was present, the LWML was used to fill the missing value. After checking the data for outliers, aggregate weighted mean values were calculated for the twelve calendar months. The final monthly set contained $\delta^{18}\text{O}$ data from 154 stations (14992 records) and $\delta^2\text{H}$ data from 136 stations (14302 records) (FIG. 1).

The methodology used herein involves building an empirical model to capture the major dependencies of isotopic composition. Then, the model residuals, considered to represent the rest of the isotopic content associations are interpolated over a normal grid. Finally the empirical model is used, with appropriate gridded data, to calculate the isotopic component on the same grid and the two fields are added to provide the final gridded isotopic composition data set.

We have developed models using five combinations of geographical and meteorological parameters, using the CRU data both for the model development and the estimation of the gridded data (Table 1). Stepwise linear regression was used to sort out statistically insignificant regressors. Two methods were tested for the interpolation of the residuals, namely triangulation with linear interpolation, and point kriging with an exponential variogram model. Actual point measurements were compared to nearest grid cell values to assess the success of the produced grid. Mean bias error (MBE) and root mean square error (RMSE) relative to the absolute, spatially averaged, observed value, hence MBE% and RMSE%, were used as goodness of fit indices. The uncertainty of the final gridded isotopic values is calculated as the root sum of

squares of the linear regression prediction error and the residuals' interpolation standard deviation.

Finally a comparison is attempted with a $1^\circ \times 1^\circ$ gridded $\delta^{18}\text{O}$ dataset obtained with objective analysis [19]. In order to reduce the resolution of our data set we used arithmetic averaging, requiring at least 75% of non blank grid points, while the realated uncertainty was obtained as the root sum of the squared combined uncertained of the gridded values and the standard error of each 1° average value.

3. RESULTS AND DISCUSSION

Model 1 (M1) is the same one used in [9], while for model M5 we included only parameters that were consistently identified as statistically significant by the stepwise regression procedure. As expeced the larger the number of parameters introduced into the model, the higher the derived correlation coefficient is.

Models using meteorological variables outperform those based solely on geographical parameters during the cold and wet months, while the opposite is true for warm and dry months. The combination of parameters provides the best models in terms of corellation coefficient. From the constitution of M5, it seems that atmospheric moisture is more important than precipitation amount, while using temperature covers the effect of altitude, and partly that of latitude, on isotopic content. On the other hand longitude is still needed, accouting

TABLE 1. MODELS' VARIABLES AND $r^2_{\text{adj}} \times 100$, RANGE FOR MONTHLY AGGREGATED DATA.

	$\delta^{18}\text{O}$ Model parameters*	$\delta^{18}\text{O}$				$\delta^2\text{H}$			
		Jan	Apr	Jul	Oct	Jan	Apr	Jul	Oct
M1	gl, gl^2, ga	0.59	0.54	0.41	0.65	0.66	0.59	0.47	0.69
M2	$gl, gl^2, gl^3, gn, gn^2, gn^3, ga, ga^2, ga^3$	0.70	0.59	0.56	0.68	0.75	0.63	0.62	0.69
M3	$gt, gt^2, gt^3, gv, gv^2, gv^3, gp, gp^2, gp^3$	0.70	0.53	0.47	0.72	0.80	0.59	0.44	0.77
M4	$gl, gl^2, gl^3, gn, gn^2, gn^3, ga, ga^2, ga^3, gt, gt^2, gt^3, gv, gv^2, gv^3, gp, gp^2, gp^3$	0.75	0.56	0.58	0.73	0.80	0.64	0.62	0.77
M5	$gl, gn, gn^3, gt, gt^2, gv, gv^2$	0.72	0.58	0.58	0.74	0.80	0.62	0.64	0.78

* gl : latitude, gn : longitude, ga : altitude, gt : temperature, gv : vapour pressure and gp : precipitation amount.

TABLE 2. GOODNESS OF FIT STATISTICS OF THE GENERATED GRIDDED DATA SETS.

		$\delta^{18}\text{O}$					$\delta^2\text{H}$				
		M1	M2	M3	M4	M5	M1	M2	M3	M4	M5
Jan	MBE%	0.0	0.0	0.0	0.0	1.0	0.0	0.0	0.0	0.0	0.1
	RMSE%	4.1	4.1	4.1	4.1	6.6	3.0	3.0	3.0	3.0	3.4
Apr	MBE%	0.0	0.0	0.0	0.0	0.9	0.0	0.0	0.0	2.0	-0.2
	RMSE%	2.4	2.4	2.4	2.4	6.8	1.8	1.8	1.8	7.6	2.4
Jul	MBE%	0.0	-22.8	0.0	0.0	-0.3	0.0	-6.6	0.0	-0.1	-0.1
	RMSE%	9.0	70.4	9.0	9.0	12.4	4.3	21.3	4.3	4.4	4.4
Oct	MBE%	0.0	0.0	0.0	0.0	-0.4	0.0	0.0	0.0	0.0	-0.1
	RMSE%	7.2	7.2	7.2	7.2	9.8	3.4	3.4	3.4	3.4	3.7

along with latitude for the observed tilt of the isotopic isopleths towards the southeastern part of the study area, as a result of the enhanced role of the Mediterranean sea as a vapour source [20].

As mentioned above the produced gridded data sets are evaluated in terms of MBE% and RMSE% calculated point wise, using the same data that were used for the model development. Kriging and triangulation provide grids with almost identical statistics, yet triangulation did not do very well at areas far away from the data points, thus only kriging results will be presented. Table 2 presents the goodness of fit statistics of the grids obtained using the five models, for four representative months.

The overall performance of all gridded data sets is very good, except for July grid with model M2, that fails to reproduce the Swiss stations of Grimsel (1950 m) and Guttannen (1055 m), that fall into the the same grid cell represented by an altitude of 2342 m. Should these points be removed the statistics would still remain about twice the values of the rest of the models for July. Apparently $\delta^{18}\text{O}$ grids are less successful in representing the observed values, and the same applies to dry and hot months for both isotopes for all models.

Based on the above models M1, that is the original model used by Bowen and Wilkinson [9] and model M3 based solely on meteorological parameters are equally potent to reproduce the observed isotopic patterns. The isotopic grids produced with model M3:for January, April, July and October are presented in FIG 2.

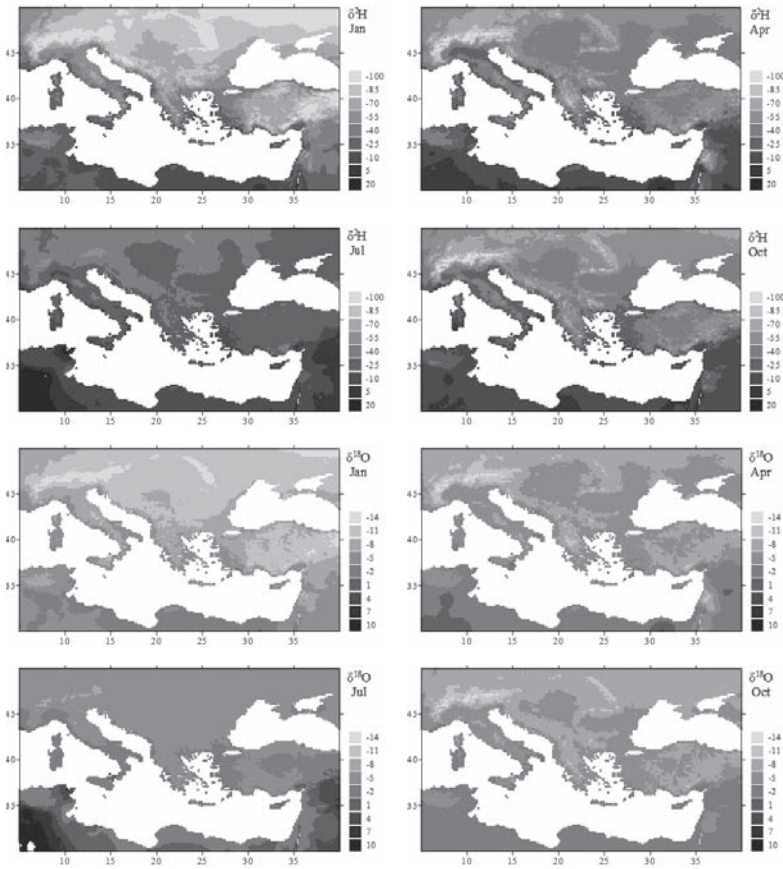


FIG. 2. Stable isotopes in precipitation, grids for model M3.

As expected, the produced distributions seem to capture the major characteristics of the isotopic composition of precipitation that are associated with temperature changes. Topography induced isotopic depletion is fairly well represented, even though somewhat lower than the actual, probably due to the smoothing and homogenization of the gridded data sets used to drive the model.

The $\delta^{18}\text{O}$ model prediction uncertainty is, on average, $\pm 1.87\text{‰}$ for M1 and $\pm 1.74\text{‰}$ for M3, while the respective values for $\delta^2\text{H}$ are $\pm 14.4\text{‰}$ and $\pm 13.2\text{‰}$, while combined model and kriging average $\delta^{18}\text{O}$ uncertainties are $\pm 2.09\text{‰}$ for M1 and $\pm 1.97\text{‰}$ for M3. Combined $\delta^2\text{H}$ average uncertainties are practically the same as the models' single kriging uncertainties are small compared to them. Winter and transient months present up to 50% higher average prediction

GEOSTATISTICAL METHODS FOR PRODUCING STABLE ISOTOPE MAPS

errors compared to summer months. The prediction errors are higher across areas with extreme conditions: Russia during January, the southern part of the study area during July, parts of the previous two areas along with alpine regions during transient months. On the other hand kriging standard deviations are higher at areas where no data are available, that is northern Balkan and central Ukraine, as well the area of Libya.

Finally, the comparison between our data set and that obtained by objective analysis interpolation, shows that during January, July and October, our method estimates more depleted $\delta^{18}\text{O}$ values (MBE% from -3% to -10%). The general fit is not so bad even though there are significant deviations in the order of 40% especially over Turkey. The RMSE% varies between 17% and 23% for the three months. For July the situation is very different. Our method grossly overestimates $\delta^{18}\text{O}$ (MBE% $+26\%$ and RMSE% $+69\%$). This behaviour though is only observed at the southern and southwestern corners of the domain, where our method estimates more positive $\delta^{18}\text{O}$ values while the objective analysis gives small negative (-3.3‰ to -3.6‰) almost constant values.

4. CONCLUSIONS

The procedure used for the generation of gridded isotopic composition of precipitation data with a resolution of $10' \times 10'$, across the Central and Eastern Mediterranean, seems to be able to reproduce the observed spatial variation of the isotopic parameters successfully, both in terms of general patterns and in terms of absolute values. Both interpolated residuals and empirical model results contribute significantly to the finale gridded values, even though the model derived is on average larger. Models using meteorological parameters present better correlation coefficients than those using only geographical data, and this not always confirmed by the goodness of fit statistics of the final grids. Grids from some models using meteorological data are not very successful when conditions become warm and dry. This is also observed when our data sets are compared to gridded $\delta^{18}\text{O}$ obtained with objective analysis interpolation. A possible remedy, and a point of future work, would be the addition of circulation patterns, or the partitioning of the study area to sub-sections and the development of models for each sub-section.

ACKNOWLEDGEMENTS

This work has been partly financed through the IAEA Coordinated Research Project #13931/R0: Geostatistical analysis of spatial isotope variability to map the sources of water for hydrology and climate studies.

REFERENCES

- [1] GAT J.R., Oxygen and hydrogen isotopes in the hydrologic cycle, *Annual Reviews of Earth Planetary Sciences* **24** (1996) 225.
- [2] DANSGAARD W., Stable isotopes in precipitation, *Tellus* **16** 4 (1964) 436.
- [3] ROZANSKI K. et al., Isotopic patterns in modern global precipitation, *Climate Change in Continental Isotopic Records*, *Geophysical Monograph AGU* **78** (1993).
- [4] HOFFMANN G. et al., Water isotope module of the ECHAM atmospheric general circulation model: A study on timescales from days to several years, *J. of Geophysical Research* **103** (1998) 16871.
- [5] NOONE D., SIMMONDS I., Associations between delta O-18 of water and climate parameters in a simulation of atmospheric circulation for 1979–95, *J. of Climate* **15** (2002) 3150.
- [6] STURM K. et al., Simulation of $\delta^{18}\text{O}$ in precipitation by the regional circulation model REMO iso, *Hydrological Processes* **19** (2005) 3425.
- [7] BIRKS S.J. et al., Maps and animations offer new opportunities for studying the global water cycle, *EOS Transactions AGU Electronic Supplement* **83** (2002) 37
- [8] BOWEN G.J., REVENAUGH J., Interpolating the isotopic composition of modern meteoric precipitation, *Water Resources Research* **39** (2003) 1299.
- [9] BOWEN G.J., WILKINSON B., Spatial distribution of delta O-18 in meteoric precipitation, *Geology* **30** (2002) 315.
- [10] MEEHAN T.D. et al., GIS model of stable hydrogen isotope ratios in North American growing-season precipitation for use in animal movement studies, *Isotopes in Environmental and Health Studies* **40** (2004) 291.
- [11] LIEBMINGER A. et al., Modeling the oxygen 18 concentration in precipitation with ambient climatic and geographic parameters, *Geophysical Research Letters* **33** (2006) L05808.
- [12] LeGRANDE A.N., SCHMIDT G.A., Global gridded data set of the oxygen isotopic composition in sea water, *Geophysical Research Letters* **33** (2006) L12604.
- [13] IAEA, Isotope Hydrology Information System. The ISOHIS Database v.12/2005, (2004), <http://isohis.iaea.org>

GEOSTATISTICAL METHODS FOR PRODUCING STABLE ISOTOPE MAPS

- [14] IAEA/WMO, Global Network of Isotopes in Precipitation. The GNIP Database v.12/2005, (2004), <http://isohis.iaea.org>
- [15] d' ALESSANDRO W. et al., Oxygen isotope composition of natural waters in the Mt. Etna area, *J. of Hydrology* **296** (2004) 282
- [16] KITA I. et al., Neutral rains at Athens, Greece: A natural safeguard against acidification of rains, *Science of the Total Environment* **327** (2004) 285.
- [17] NEW M. et al., A high-resolution data set of surface climate over global land areas, *Climate Research* **21** (2002) 1.
- [18] LYKLOUDIS S.P., ARGIRIOU A.A., Tendencies of stable isotopic content of rainfall in Central and Eastern Mediterranean, *Theoretical and Applied Climatology* (2006) submitted.
- [19] ALDUCHOV O.A., Objective analysis producing of regular fields of GNIP data, IAEA CRP: Geostatistical analysis of spatial isotope variability Meeting, Vienna (2006).
- [20] GAT J.R. et al., Isotope composition of air moisture over the Mediterranean Sea: an index of the air-sea interaction pattern, *Tellus* **55B** (2003) 953.

ISOTOPIC COMPOSITION OF METEORIC WATER IN SICILY

M. LIOTTA, R. FAVARA, M. FONTANA, E. GAGLIANO,
A. PISCIOTTA, C. SCALETTA
Istituto Nazionale di Geofisica e Vulcanologia,
Sezione di Palermo, Italy

Abstract

The isotopic composition of meteoric water in Sicily (Italy,) was investigated from May 2004 until Jun 2006; a rain gauge network (50 sites) was installed and sampled monthly. During this same period most of the circulating groundwater in the investigated area was sampled from more than 560 springs and wells related to the main aquifers. The mean weighted precipitation values were used to define the weighted local meteoric water line (WLMWL) for several sectors of Sicily. The use of GIS tools, coupled with isotopic vertical gradients, allowed us to design an isotopic contour map of precipitation in Sicily. The defined meteoric compositions fitted well with most of the groundwater samples for each sector. However, in some areas fractionation processes occurring during and after rainfall, slightly modified the isotopic composition of the groundwater.

1. INTRODUCTION

Natural waters are characterized, worldwide, by a wide range of isotope ratios, differences mainly depend on the geographical coordinates and climatic features. On a local scale, the morphological setting of the environment can significantly influence the isotopic ratios of meteoric waters. Such effects can be quantified by using local isotopic vertical gradients and can also be a useful tool when investigating hydro-geological paths. The isotopic composition of precipitation has been the object of numerous studies regarding North Western Sicily, Stromboli and Pantelleria Islands, Mount Etna and the Hyblean Mountains [1–5]. Although detailed models have been developed for each area, a synchronous comprehensive study of the isotopic composition of meteoric waters all over Sicily is non-existent. The aim of this work is to define the first isotopic precipitation map that covers all Sicily; compare it with the isotopic composition of groundwater and evaluate the relationships between the two in order to provide a useful tool for groundwater management.

2. CLIMATIC AND MORPHOLOGICAL SETTING

The various areas of the Mediterranean are characterized by a similar climate. In summer, the subtropical high-pressure cells drift toward the northern hemisphere (from May to August), whereas in winter the high-pressure cells drift back toward the equator and the weather is dominated by cyclonic storms [6]. The island of Sicily is characterized by very different morphological environments with mean yearly precipitations ranging between 400 and 1,200 mm, while the mean yearly temperature ranges between 6 and 18°C. On the north side, the mountain chain favours higher precipitation and colder temperatures. On the south side, the landscape is mainly hilly, having the lowest precipitation in Sicily, and high temperatures. The south east is a typical plateau with high temperatures and intermediate precipitation. Mount Etna is the main orographic anomaly (3300 m a.s.l.), and has the highest precipitation and the lowest temperature.

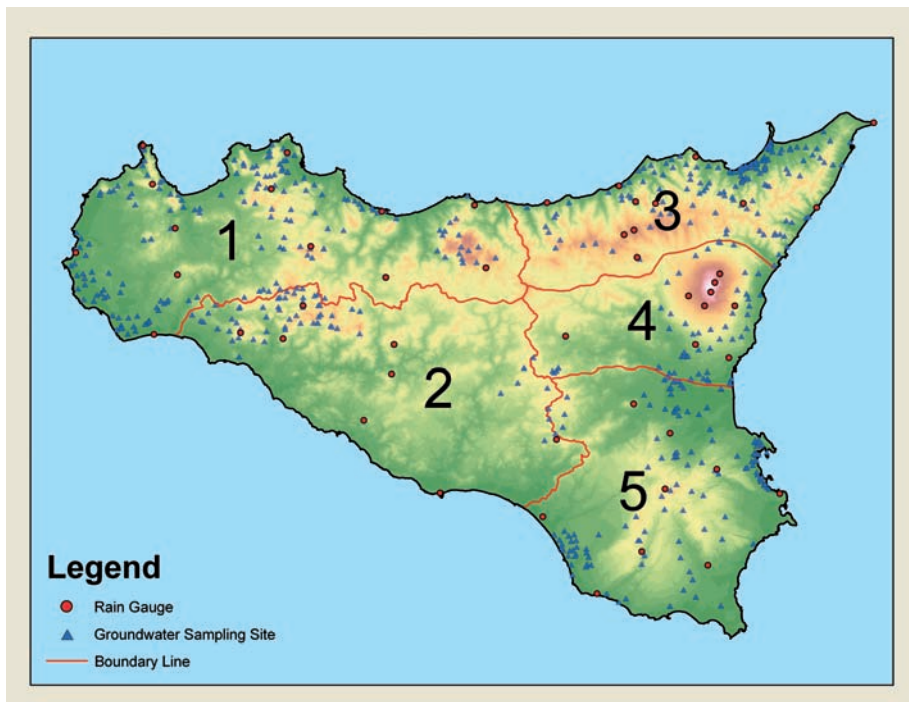


FIG. 1. Basic map of the studied area. The rain gauge network (red circles) and groundwater sampling sites (blue triangles) are also plotted.

3. METHODS

3.1. Sampling and analytical techniques

A rain gauge network (50 sites) was installed and sampled monthly from May 2004 until June 2006. During the same period, most of the circulating groundwater in the investigated area was sampled from more than 560 springs and wells related to the main aquifers. The water samples were analyzed for their oxygen and hydrogen isotopic compositions, using Analytical Precision AP 2003 and FinniganMAT Delta Plus spectrometers respectively. The isotope ratios are expressed as the deviation permil ($\delta\text{‰}$) from the reference V-SMOW. The uncertainties are $\pm 0.1\%$ for $\delta^{18}\text{O}$ and $\pm 1\%$ for δD (one standard deviation).

3.2. GIS mapping

A Geographical Information System was carried out by using ESRI-ArcGis software, the aim of which was to map the isotopic composition

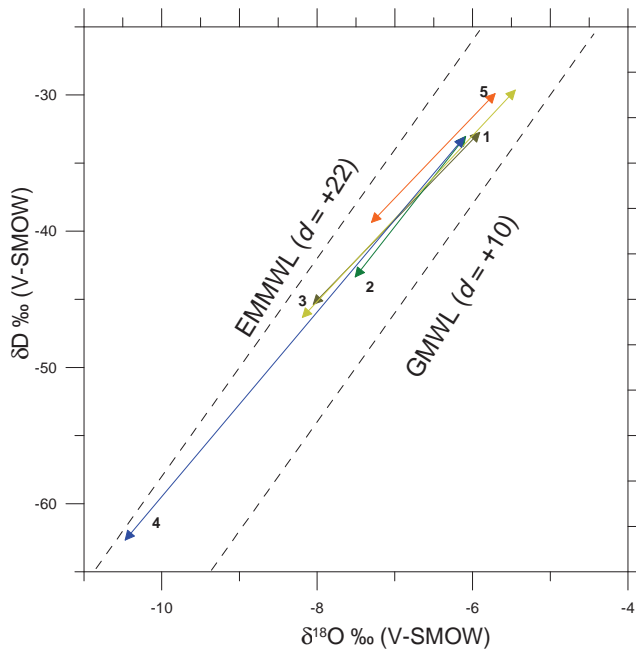


FIG. 2. $\delta\text{D} - \delta^{18}\text{O}$ diagram. Weighted Local Meteoric Water Lines (LMWL) of each sector are plotted.

of Sicilian rains; hydro-graphical and hydro-geological frameworks of this area were also used. Sicily was divided into five main sectors, using the GIS database. This was created by collecting already existing data regarding the hydro-geological and hydro-graphical characteristics of the examined territory. A Digital elevation model (DEM) was used during the raster processing of the isotopic layers. The GIS Map Calculator was used to evaluate the isotopic surface of each sector. This process generated a new raster surface; the output grid cell size was defined according to dem data resolution and the results expected from the study. A resolution of 1,000 m was selected, as it was the highest resolution possible for the spatial distribution of data. The Raster data layers developed for each sector were overlaid and a first Sicily Isotopic map was drawn up. The last step in the procedure was the re-sampling and interpolating of this map using the Inverse Distance to Power gridding method to smooth the variability effect between neighbouring data areas. Weighting was assigned to data through the use of a weighting power that controls how the weighting factors drop off as distance from a grid node increases.

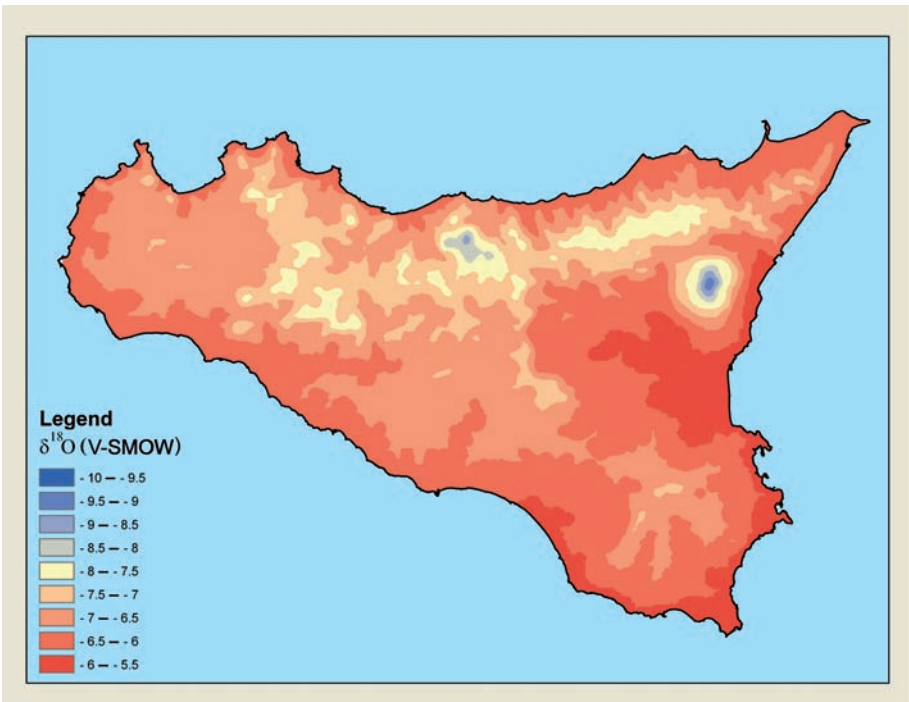


FIG. 3. Contour map of the isotopic composition (permil) of rainwater.

4. RESULTS AND DISCUSSION

In order to evaluate the average isotopic composition of the meteoric recharge, mean weighted values regarding the whole period were taken into account. Since each sector is characterized by peculiar climatic features, five Weighted Local Meteoric Water Lines (LMWL) were computed. As shown in Fig. 2, the LMWL computed for sectors 1, 2, and 3 cover similar ranges, while sectors 4 and 5 are significantly different, as they are characterized by a larger range and higher deuterium excess values respectively. With regard to the Hyblean Mountains (sector 5), the high deuterium excess values have been explained as due to the origin, in the Mediterranean, of moisture producing precipitation (Grassa et al., 2006), while the wide range found in sector 4 depends on the effect of altitude, as Mount Etna (3300 m a.s.l.) is included in this sector. The $\delta^{18}\text{O}$ -altitude relationships indicate a depletion ranging from -0.13 ‰ to -0.16 ‰ per 100m, which are lower than the gradients calculated by Longinelli and Selmo (2003) of $-0.2 \text{ ‰}/100\text{m}$ for Italy and by Poage and Chamberlain(2001) of $-0.21 \text{ ‰}/100\text{m}$ for Europe. Using the vertical isotopic gradient, in accordance with the method described in the

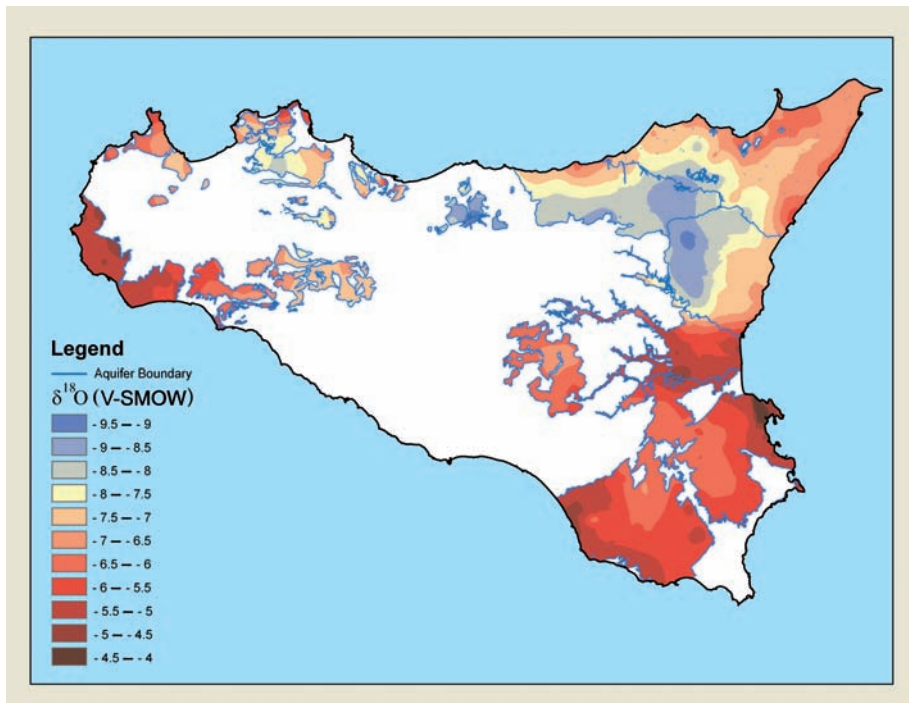


FIG. 4. Contour map of the isotopic composition (permil) of groundwater.

previous section, the isotopic contour map was drawn up (Fig. 3). It highlights the role of morphological and climatic features in determining the marked differences in the local mean isotopic compositions. The most positive values fall in sector 5 while the negative values (lower than -7.5) fall in sectors 4, 1 and 2. More precisely, the most depleted rain waters were collected on Mount Etna, in the Madonie Mountains and along the northern mountain chain. The contour map of the groundwater isotopic composition has also been drawn up (Fig. 4). It shows the main water bodies identified in Sicily. Based on the isotopic composition of the meteoric recharge, the most depleted samples fall in the mountainous areas (Mount Etna, Madonie Mountains and north mount chain). Groundwater is sometimes depleted with respect to the isotopic composition of the recharge area. This may depend on the fact that, as a consequence of the high residence times of large water bodies, the groundwater reflects the isotopic composition of rainwater that infiltrated before the observation period. In sector 5 groundwater is often enriched in respect of the meteoric recharge. Grassa et al. (2006) stated that the original isotopic composition of the meteoric recharge is probably altered by evaporation before and/or during infiltration.

REFERENCES

- [1] LIOTTA, M., FAVARA, R., VALENZA, M., Isotopic composition of the precipitations in the central Mediterranean: Origin marks and orographic precipitation effects, *Journal of Geophysical Research* **111** (D19) (2006) doi: 10.1029/2005JD006818. issn: 0148-0227.
- [2] LIOTTA, M., BRUSCA, L., GRASSA, F., INGUAGGIATO, S., LONGO, M., MADONIA, P., Geochemistry of rainfall at Stromboli volcano (Aeolian Islands): Isotopic composition and plume-rain interaction, *Geochemistry, Geophysics, Geosystems* **7** 7 (2006) doi: 10.1029/2006GC001288. issn: 1525-2027.
- [3] FAVARA R., GAGLIANO CANDELA, E., INGUAGGIATO, S., PECORAINO, G., The isotopic composition of precipitation and groundwater at Pantelleria Island (Italy), 8th International Conference on Gas Geochemistry, ICGG8, Palermo & Milazzo, Italy 2th–8th October 2005, poster section, abstr. Book pg 33 (2005).
- [4] D’ALESSANDRO, W., FEDERICO, C., LONGO, M., PARELLO, F., Oxygen isotope composition of natural waters in the Mt. Etna area, *J. Hydrol.* **296** 1–4, (2004) 282–299.
- [5] GRASSA, F., FAVARA, R., VALENZA, M., Moisture source in the Hyblean Mountains region (south-eastern Sicily, Italy): Evidence from stable isotopes signature *Applied Geochemistry* Volume: 21, Issue: 12, December, 2006 (2006). 2082–2095

ISOTOPIC COMPOSITION OF METEORIC WATER IN SICILY

- [6] BOLLE, H.-J., *Mediterranean Climate: Variability and Trends*, Springer-Verlag, Berlin (2003).
- [7] LONGINELLI, A., SELMO, E., Isotopic composition of precipitation in Italy: A first overall map, *J. Hydrol.* **270** (2003) 75–88.
- [8] POAGE, M.A., CHAMBERLAIN, C.P., Empirical relationships between elevation and the stable isotope composition of precipitation and surface waters: Considerations for studies of paleoelevation change, *Am. J. Sci.* **301** (2001)1–15.

FACTORS CONTROLLING THE STABLE ISOTOPIC COMPOSITION OF RECENT PRECIPITATION IN SPAIN

M.F. DÍAZ,* ++ J. RODRÍGUEZ,** ++, E. PÉREZ* ++, S. CASTAÑO,**,
L. ARAGUÁS-ARAGUÁS⁺

*Centro de Estudios de Técnicas Aplicadas
(CETA-CEDEX),
Ministry of Public Works,
Madrid, Spain

**Geological Survey of Spain,
Madrid, Spain

⁺Isotope Hydrology Section,
International Atomic Energy Agency,
Vienna

⁺⁺Joint Laboratory of Isotope Hydrology
IGME/CEDEX,
Madrid, Spain

Abstract

Composite monthly samples of precipitation were collected for the period 2000-2004 at 16 meteorological stations included in the “*Red Española de Vigilancia de Isótopos en la Precipitación*” (REVIP), the Spanish Network for Isotopes in Precipitation. Oxygen-18 and deuterium results were used to review previous maps showing the spatial distribution of isotope contents over the Iberian Peninsula. Long-term mean weighted values of $\delta^{18}\text{O}$ over the Iberian Peninsula range from ca. -4.0‰ in stations from Andalusia to ca. -10.0‰ in the stations located in the northern plateau. The $\delta^2\text{H}-\delta^{18}\text{O}$ relationship of the long-term weighted means is in good agreement with the GMWL, showing d-excess values only slightly above 10‰, indicating the relevance of air masses of Atlantic origin, as the main source of water vapour over the Iberian Peninsula. The spatial distribution of $\delta^{18}\text{O}$ and $\delta^2\text{H}$ in precipitation over the Iberian Peninsula can be explained by a simple multiple regression model, based on two geographic factors: latitude and elevation. This polynomial model

reproduces reasonably well the observed spatial distribution of the stable isotope composition of precipitation over Spain, facilitating the use of stable isotopes as a tool to trace the origin of surface and ground waters. Differences between measured and predicted $\delta^{18}\text{O}$ values with both global and local scale models are explained by other regional and local factors that influence the isotopic composition of precipitation.

1. INTRODUCTION

The study of the spatial and temporal changes of the isotopic composition of atmospheric water vapour, precipitation, surface water and groundwater, and the understanding of the processes controlling its spatial variability, have greatly contributed to a better knowledge of the water cycle in the last decades. Environmental isotopes have contributed to make more precise quantitative assessments of the water fluxes occurring within the different components of the hydrologic cycle at local, regional and global scale and to gain a better understanding of the governing processes. The importance of these achievements has been shown in many studies directed to the assessment of water resources and the quality of these resources, research programmes in global change, studies of ecosystems, regulatory developments and quality control in human diet.

Research on the atmospheric part of the hydrologic cycle (precipitation and surface waters) was initiated in the early 1950s. Isotope monitoring of precipitation at global scale was launched in the 1960s under the auspices of a joint collaboration between the IAEA and WMO under the programme Global Network for Isotopes in Precipitation (GNIP). In Spain, the *Centro de Estudios y Experimentación de Obras Públicas* (CEDEX) maintained the operation of the meteorological station of Madrid – Retiro since 1970, as well as some other stations with a shorter record since 1980, until the *Red Española de Vigilancia de Isótopos en la Precipitación* (REVIP) was created in 2000. Nowadays REVIP is managed by the *Centro de Estudios y Técnicas Aplicadas* (CETA–CEDEX), in collaboration with the Spanish Meteorological Survey (INM).

A first study of the factors controlling the isotopic composition of precipitation and groundwater in Spain covering the national territory in the Iberian Peninsula [1] provided a general framework for the interpretation of isotopic analyses for hydrogeology and related fields in this country. The lack of systematic isotope analyses of samples collected in meteorological stations evenly distributed through the whole national territory was pointed out though. More recently, CEDEX has presented an assessment of the results of the first two years of operation of REVIP [2], including information on the isotope

FACTORS CONTROLLING THE STABLE ISOTOPIC COMPOSITION

variability of precipitation and water vapour, and also including samples collected in stations located in the Balearic and Canary islands. This paper presents the first analysis of the information gathered during the first five-year period of the Spanish Network, which is the result of the collaboration between the Geological Survey of Spain (IGME) and CEDEX.

2. THE SPANISH ISOTOPE NETWORK: REVIP

2.1. Objectives and design of REVIP

Main objectives of REVIP, the Spanish Network of Isotopes in Precipitation, are: (1) to study the meteorological and geographic factors controlling the isotopic composition of precipitation; (2) to define a simple model to assess and predict the local isotope index of precipitation over the entire country as a tool to trace the origin of surface water and ground waters;



FIG. 1. Meteorological stations included in REVIP and GNIP database (operative since 2000).

TABLE 1. METEOROLOGICAL DATA AND WEIGHTED MEAN ($\delta^{18}\text{O}$, $\delta^2\text{H}$, AND D-EXCESS) FOR REVIP STATIONS DURING THE 2000–2004 PERIOD.

Station	Long. (°)	Lat. (°)	Elevation (m.a.s.l.)	Mean annual rainfall (mm)	Mean annual temp (°C)	Relative humidity (%)	$\delta^{18}\text{O}$ (‰)	$\delta^2\text{H}$ (‰)	d (‰)
1. Atlantic basin									
1.a. Island									
Santa Cruz de Tenerife	16 14 56 W	28 27 18 N	36	239.7	22.0	63	-1.74	-8.3	5.7
1.b. Coastal									
La Coruña	08 25 10 W	43 22 02 N	57	1070.7	15.0	77	-5.58	36.0	8.6
Santander	03 47 59 W	43 29 30 N	52	1003.4	14.8	75	-5.79	-33.4	13.0
1.c. Continental									
Morón	05 36 57 W	37 09 30 N	88	570.4	18.2	61	-4.77	27.7	10.4
Cáceres	06 20 22 W	39 28 20 N	405	577.6	16.3	58	-6.53	-42.9	9.4
Ciudad Real	03 56 11 W	38 59 22 N	627	413.9	16.0	63	-7.63	-50.9	10.2
Madrid	03 40 41 W	40 24 40 N	667	471.8	15.2	57	-6.80	-47.1	7.0
Valladolid	04 46 27 W	41 38 40 N	735	466.8	12.9	65	-7.93	-54.6	8.6
León	05 39 07 W	42 35 10 N	913	539.2	11.0	68	-9.02	-63.5	8.7
2. Mediterranean basin									
2.a. Island									
Palma de Mallorca	02 37 35 W	39 33 18 N	3	440.2	18.7	70	-5.57	-34.4	10.1
2.b. Coastal									
Almería	02 23 17 W	36 50 35 N	21	184.6	9.3	66	-4.81	-27.7	10.8

FACTORS CONTROLLING THE STABLE ISOTOPIC COMPOSITION

Valencia	00 22 52 W	39 28 48 N	13	509.3	18.9	65	-4.73	-27.3	10.5
Tortosa	00 29 29 W	40 49 14 N	48		18.1	63	-5.04	-30.8	9.5
2.c. Continental									
Murcia	01 10 10 W	38 00 10 N	62	290.8	18.9	59	-5.70	-36.7	8.9
Zaragoza	01 00 29 W	41 39 43 N	247	367.5	15.9	62	-6.31	-42.0	8.5
Gerona	02 45 37 W	41 54 05 N	129	622.0	15.0	72	-5.66	-37.3	7.9.

(3) to enhance the practical applications of stable isotope tracing to hydrological problems; (4) to provide information for the assessment of climatic changes; and (5) to contribute to the efforts of the IAEA to provide a better coverage of the GNIP network.

REVIP consists of 16 meteorological stations where composite monthly samples of precipitation are collected and analysed following the protocols established by the IAEA for GNIP. Particular care was taken in the design of REVIP in order to have wide geographic (N–S and E–W, different physiographic setting and topographic height) and climatic (stations representative of semiarid and humid areas, continental and littoral, Atlantic and Mediterranean) coverage. All main River Basin Districts defined at national level are represented in REVIP (Fig. 1). Table 1 presents the main geographic, meteorological and summary isotope characteristics of the REVIP stations for the period 2000–2004.

2.2. Sampling and analytical methods

REVIP sampling programme is organized according to the protocols issued by the IAEA: monthly collection of precipitation samples and compilation of the isotope ($\delta^{18}\text{O}$, $\delta^2\text{H}$) and meteorological data in a database maintained by CEDEX. Deuterium and oxygen-18 analyses have been undertaken at CEDEX Isotope Hydrology Laboratory using a double-inlet IRMS, Delta Plus Advantage, following the usual procedures for deuterium and oxygen analysis and referring the results to the VSMOW–SLAP scale. The uncertainty is $\pm 0.1\%$ for $\delta^{18}\text{O}$ and $\pm 1.0\%$ for $\delta^2\text{H}$.

3. PATTERNS OF THE ISOTOPIC COMPOSITION DISTRIBUTION OF PRECIPITATION IN SPAIN

Previous studies on the isotopic composition of precipitation at a global scale have shown the relationship between the degree of depletion in heavy isotopes and latitude, altitude, continentality, and intensity of precipitation [3–5]. The multiple interplay of these factors is favoured at local scale in Spain, due to the great variety of geographic and climatologic features, such as: (1) interplay of several oceanic and continental air masses, but mainly of Atlantic and Mediterranean origin; (2) topographic elevations of more than 3,000 m.a.s.l. are found both in the Iberian Peninsula and in the Canary Islands; and (3) the presence of an extensive plateau, with a mean elevation between 700 and 900 m a.s.l. in the innermost part of the Iberian Peninsula.

FACTORS CONTROLLING THE STABLE ISOTOPIC COMPOSITION

The LMWL for Spain, for the 2000–2004 period, basically coincides with the Global Meteoric Water Line, when all stations are considered together, giving a general indication about the overall quality of the results of REVIP. The partitioning of isotopes between stations located on cold (León, Valladolid, Madrid) and warm regions (Tenerife, Valencia, Almería) in Spain is clearly observed, shown the relevance of temperature as the main factor controlling the isotope composition of precipitation at the latitude of the Iberian Peninsula [6]. Deuterium-excess values are only slightly above +10‰ (Table 1), indicating the relevance of air masses of Atlantic origin as the main source of water vapour over the Iberian Peninsula.

A summary statistical analysis of the results obtained from the REVIP for the period 2000–2004 is presented in Figs. 2a and 2b. Depletion in $\delta^{18}\text{O}$ and $\delta^2\text{H}$ is shown for the Mediterranean stations as the latitude increases (left side of the plots). A similar tendency is seen for the Atlantic stations as the latitude, altitude and continentality increase (right side of the plots). However, two stations located at the Northern most part of Spain (La Coruña and Santander) make this trend to reverse due to their location at the coast and consequently at a lower altitude, showing that elevation also is an essential factor controlling isotope composition in the stations located on the Atlantic coast.

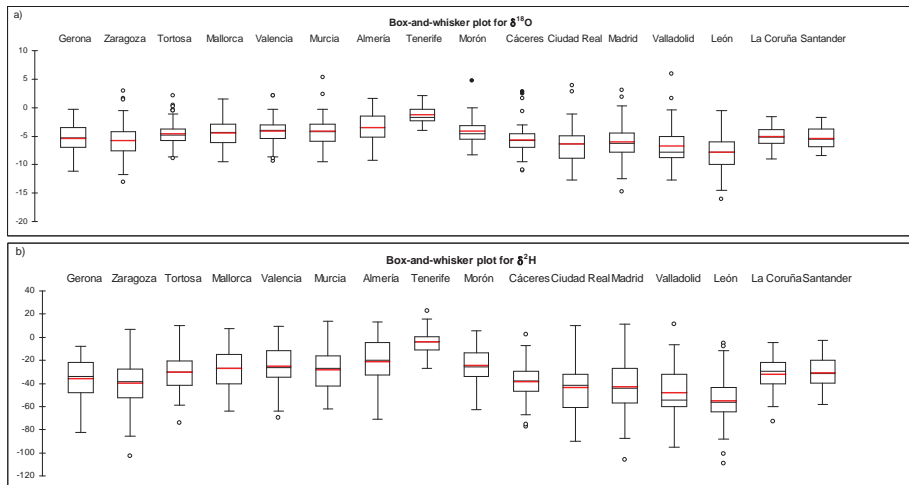


FIG. 2. (a) Box-and-whisker plots for $\delta^{18}\text{O}$. (b) Box-and-whisker plots for $\delta^2\text{H}$. Monthly averages for all REVIP stations during the 2000-2004 period are used.

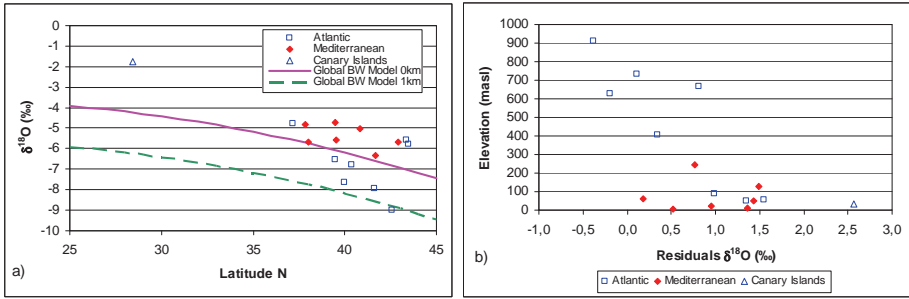


FIG. 3. (a) Global model lines obtained for 0 and 1 km elevation for the $\delta^{18}\text{O}$ contents of meteoric precipitation with increasing latitude and elevation for GNIP stations (Bowen and Wilkinson model [7] referred to as global BW model), and comparison with REVIP stations. (b) Residuals between measured isotope values of REVIP stations and global BW model $\delta^{18}\text{O}$ versus elevation.

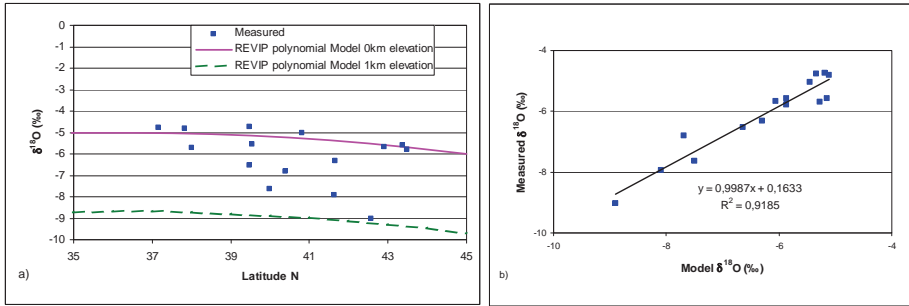


FIG. 4. (a) Local model lines obtained for 0 and 1 km elevation for the rate of depletion in ^{18}O of meteoric precipitation with increasing station latitude and elevation for REVIP stations. (b) Difference between measured and predicted $\delta^{18}\text{O}$ by the second-order polynomial for REVIP stations.

4. DERIVATION OF A MODEL FOR THE LATITUDE AND ELEVATION DEPENDENCE OF $\delta^{18}\text{O}$

In this study, the model approach used in [7–8] was adopted in first instance to predict the spatial distribution in the isotopic composition of recent precipitation in Spain. A first approximation of the spatial variation in $\delta^{18}\text{O}$ in REVIP stations is presented in Fig. 3a, using the long/term isotope compositions of global precipitation from the IAEA/GNIP database and the equation that describes $\delta^{18}\text{O}$ as a function of latitude and altitude determined in [7]. Fig. 3b shows that the isotope composition of REVIP stations are more positive than

FACTORS CONTROLLING THE STABLE ISOTOPIC COMPOSITION

those for GNIP stations located at similar latitudes, particularly in the case of REVIP coastal stations. These differences may derive from the influence of the positive $\delta^{18}\text{O}$ signature that the warm Gulf Stream may imprint to European precipitation, as suggested in [8].

A second approximation was attempted in order to better assess the combined influence of both latitude and elevation on the composition of precipitation over Spain. The equation that describes the $\delta^{18}\text{O}$ values as a function of latitude and altitude, represented in Fig. 4a, was derived using a two-step approach: first the dependence on latitude was obtained for all REVIP stations except Tenerife (Canary Islands) which belongs to a different climatic region, and later the effect of elevation was quantified. Adding the two equations, the combined dependence of isotope composition on latitude and elevation can be described as follows:

$$\delta^{18}\text{O} = -0.013 \times \text{LAT}^2 + 0.9507 \times \text{LAT} - 0.0037 \times \text{ALT} - 22.253 \quad (1)$$

where LAT is the latitude in decimal degrees and ALT the elevation of the sampling station in metres. Equation 1 provides a good first-order estimate of observed $\delta^{18}\text{O}$ in Spain ($r^2 = 0.92$; Fig 4b). The highest difference between measured and modelled data is found for Madrid-Retiro station. This positive residual (Fig. 5) may be explained as a consequence of the effect of higher evaporation rates of falling raindrops, since this is the REVIP station with the lowest mean annual relative humidity (Table 1).

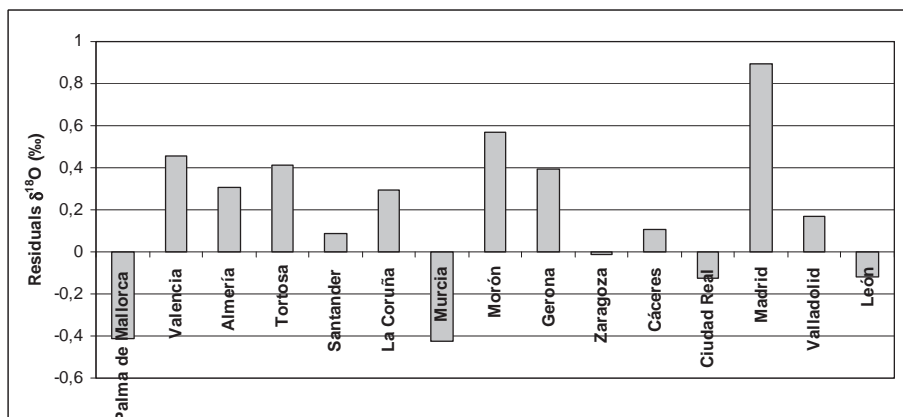


FIG. 5. Residuals between measured isotope values and the REVIP polynomial model $\delta^{18}\text{O}$.

5. CONCLUSIONS

Oxygen-18 and deuterium analyses are being performed as a contribution to GNIP, for composite monthly samples of precipitation collected at the 16 meteorological stations of the “*Red Española de Vigilancia de Isótopos en la Precipitación*” (REVIP), the Spanish Network for Isotopes in Precipitation. The $\delta^2\text{H}$ – $\delta^{18}\text{O}$ relationship of the long-term weighted means (for the period 2000-2004) is in good agreement with the GMWL, showing d-excess values only slightly above 10‰, indicating the relevance of air masses of Atlantic origin as the main source of water vapour over the Iberian Peninsula.

The spatial distribution of $\delta^{18}\text{O}$ and $\delta^2\text{H}$ in precipitation in Spain can be explained in a simplistic form by a simple regression model, based on geographic factors (latitude and elevation). This model reproduces reasonably well the observed main features of the spatial distribution of the stable isotope composition of precipitation over Spain, facilitating tracing of the source of surface and ground waters.

ACKNOWLEDGEMENTS

The cooperation and support of the staff of the Spanish Meteorological Survey (INM), for sample collection and provision of meteorological information, as well as CEDEX for carrying the isotope analysis are gratefully acknowledged.

REFERENCES

- [1] PLATA, A., Composición isotópica de las precipitaciones y aguas subterráneas de la Península Ibérica, Monografías, CEDEX, Madrid (1994) (in Spanish).
- [2] ARAGUÁS, L., DÍAZ, M., Isotope composition of precipitation and water vapour in the Iberian Peninsula. First results of the Spanish Network of Isotopes in Precipitation, In Isotopic composition of precipitation in the Mediterranean Basin in relation to air circulation patterns and climate, IAEA-TECDOC-1453, Vienna (2005) 173–190.
- [3] DANSGAARD, W., Stable isotopes in precipitation, *Tellus* **16** (1964) 436–468.
- [4] YURTSEVER, Y., GAT, J., Atmospheric waters, In *Stable Isotope Hydrology: Deuterium and Oxygen-18 in the Water Cycle*, Gat, J., Gonfiantini, R. (Eds.) IAEA, Vienna (1981) 103–139.
- [5] ROZANSKI, K., ARAGUÁS, L., GONFIANTINI, R., Isotopic patterns in modern global precipitation, Chap. 1. In: *Climate change in Continental Isotopic Records*.

FACTORS CONTROLLING THE STABLE ISOTOPIC COMPOSITION

Vol. 78 (Eds: Swart, P.K., Lohmann, K.C., McKenzie, J., Savin, S.), Geophysical Monograph, American Geophysical Union, Washington (1993).

- [6] CRAIG, H., Isotopic variations in meteoric waters, *Science* **133** (1961) 1702–1703.
- [7] BOWEN, G.J., WILKINSON, B.H., Spatial distribution of $\delta^{18}\text{O}$ in meteoric precipitation, *Geology* **30** 4 (2002) 315–318.
- [8] DUTTON, A., et al., Spatial distribution and seasonal variation in $^{18}\text{O}/^{16}\text{O}$ of modern precipitation and river water across the conterminous USA, *Hydrol. Processes* **19** (2005) 4121–4146.

APPLICATION OF ENVIRONMENTAL ISOTOPE TECHNIQUES TO SELECTED HYDROLOGICAL SYSTEMS IN PAMPEAN, ARGENTINA

C. DAPEÑA, H.O. PANARELLO
Instituto de Geocronología y Geología Isotópica
(INGEIS-CONICET-UBA),
Argentina

Abstract

The isotopic composition of precipitation in Buenos Aires station is of great importance to understand the Pampean hydrological Systems. The rain isotope content (^2H , ^{18}O and ^3H) is being recorded since 1978 at Ciudad Universitaria Station, belonging to the Red Nacional de Colectores constitutes the main recharge factor for most of local and regional hydrologic system. The knowledge and characterization of their isotope content is of fundamental importance for a hydrological investigation, so we need a historical updated record. For this reason the International Atomic Energy Agency (IAEA) in co-operation with the World Meteorological Organization (WMO) developed an international network devoted to the measurement of isotope contents in precipitation named as GNIP (Global Network for Isotopes in Precipitation) which started in 1960. The main objective of the network is to evaluate on a global scale the spatial and temporal distribution of isotope contents in precipitation and their dependence to relevant meteorological parameters [1]. In this framework, the "Instituto de Geocronología y Geología Isotópica" (INGEIS) established a National Collector Network for Isotopes in Precipitation (RNC) which integrates with the GNIP. The operation of the network in Argentina began in November 1978 with one station located in Buenos Aires City. At present, INGEIS is operating 17 stations at different altitudes and latitudes, covering a wide range of temperatures and a large variety of climates. This information allows us to know the input functions (rain isotope content) at different regions of the country [2].

Signatures of isotopes in precipitation are not static. They respond to both, synoptic and climatology and global climate change. Attracted by this issue, a new community, interested in palaeoclimate and atmospheric circulation modelling, started to use the GNIP data. However, it becomes apparent soon that the collected data were also useful in other water-related fields such as oceanography, hydrometeorology and climatology. The meteorological analysis

of the GNIP data suggests that the large scale synoptic history of the air masses (rainout history, moisture) is the major factor controlling the variability of the isotope content from one rain event to other and also the seasonality, and in tropical zones the amount of precipitation [3]. The strong linear correlation between ^{18}O and ^2H concentrations was shown by several authors [4,5] and it reflects the mass-dependent partitioning of the water isotopes in the hydrological cycle. This coupling is represented by the global meteoric water line (GMWL), *i.e.*: $\delta^2\text{H} = 8 \times \delta^{18}\text{O} + 10\text{‰}$ [4].

The isotope composition of groundwater in temperate climates reflects with a good approximation that of the average precipitation at the locality. On the other hand, some processes could modify the isotope composition during recharge mechanisms, like evaporation prior to infiltration or precipitation seasonality variations marked by a selective infiltration [6]. In addition, individual rains exhibits an isotope composition with an extended dispersion, but they join into the annual average precipitation within the normal climate variations from one year to other. A homogeneous isotope distribution indicates the water origin, while changes along groundwater paths reflect the history of the water [7].

2. ISOTOPE COMPOSTION OF BUENOS AIRES STATION

The precipitation's isotope composition of Buenos Aires station was a useful tool to complement the interpretation of some Pampean hydrologic systems. The first analyses were published by [8] and [9]. The rain isotope content (^2H , ^{18}O and ^3H) is recorded since 28 years at Ciudad Universitaria station (CUS) in Buenos Aires city. This station belongs to RNC of Argentina and to GNIP [2, 10]. The annual weighted average of Buenos Aires isotopic composition is $\delta^{18}\text{O} = -5.5\text{‰}$, $\delta^2\text{H} = -30\text{‰}$ from the period 1979–2001 and the local meteoric water line ranges from $\delta^2\text{H} = 8 \times \delta^{18}\text{O} + 12\text{‰}$ to $\delta^2\text{H} = 8 \times \delta^{18}\text{O} + 14\text{‰}$ [11, 12] These data let us to use the record like input function to the Pampean hydrologic systems. The ^3H concentration ranges between 0 TU and 17.7 TU with some values up to 40 TU, which probably responds to the spring-summer peak. At present it has been measured some values which exceed that concentration, due to non natural factors.

Dansgaard [5] established a lineal correlation between mean surface annual air temperatures and $\delta^{18}\text{O}$ – $\delta^2\text{H}$ for mean annual precipitation on global basis, where ^{18}O slope is $\theta = 0.5\text{--}0.7\text{‰}/^\circ\text{C}$. Yurtsever and Gat calculate this relation for monthly averages [13]. In view of that, the medium and high latitude stations exhibit ^{18}O and ^2H contents more depleted in winter than in summer and on a general global scale it corresponds to lower the temperature

APPLICATION OF ENVIRONMENTAL ISOTOPE TECHNIQUES

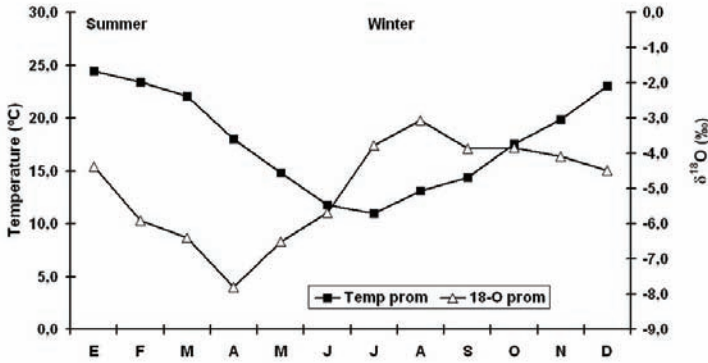


FIG. 1. Mean monthly temperature and $\delta^{18}O$ vs. time.

higher the depletion. Buenos Aires precipitation shows a good correlation between temperature and mean monthly isotope composition (Fig. 1) during January to April, where $\theta = 0.53 \pm 0.15\text{‰}/^{\circ}\text{C}$. Nevertheless, it can observe an inversion of the slope during coldest months (May-August). In addition, the most depleted values are recorded during February to March (summer season at South Hemisphere).

This pattern is also observed at Azul, Santa Fe and Corrientes stations, and some years is marked by more depleted contents with $\delta^{18}O$ values lower than -10‰ , certainly linked to the air masses source. This seasonal effect could be used like a good tracer for the hydrologic systems [12].

3. MATERIALS AND METHODS

The operation of the RNC is based on the sampling of monthly composite precipitation at selected locations. The stable isotope ratios of deuterium ($^2\text{H}/^1\text{H}$) and oxygen-18 ($^{18}\text{O}/^{16}\text{O}$) and the tritium concentration (^3H) are measured at INGEIS' Stable Isotope Laboratory. These measurements are supplemented by meteorological information such as mean surface air temperature, mean water vapour pressure at the ground water level and amount of precipitation. The INGEIS interacts with the isotope stations providing sampling instructions and bottles. The operation of the network was and still is based on the support of INGEIS stations, voluntary contributions of many Research National Institutions and private organizations, as well as individuals, who provide precipitation samples and relevant meteorological data [2]. Samples are treated following established techniques and measured in a of triple collector, multiport

inlet system, Finnigan MAT Delta S mass spectrometer. Results are expressed in the usual way as δ [‰]. Values are referred to Vienna Standard Mean Ocean Water (V-SMOW) [14]. Uncertainties are $\pm 0.1\%$ for $\delta^{18}\text{O}$ and ± 1.0 for $\delta^2\text{H}$. For tritium analyses water sample are enriched by electrolysis and measured by liquid scintillation counting. The ^3H concentrations are expressed as tritium units. The average uncertainties are *ca.* ± 1.0 TU [15].

4. PAMPEAN HYDROLOGICAL SYSTEMS

4.1. Background

The Pampean systems belong to the Humid Chaco Pampeana hydrogeological region (Fig. 2) [16]. This region covers around 350,000 km² and encloses the Buenos Aires province, where several hydrogeological investigations were made with the support of isotope techniques [2].

The Pampean plain is not homogeneous and it can be differentiated by topographic-morphological, hydrogeological peculiarities and also variations in the distribution of surface bodies and drainage networks. The landscape is distinguished by little tectonic deformation, low topographic slopes, low drainage density, the presence of materials relatively permeable on terrain surface with predominance of fine-grained sediments over coarse-grained ones, and continuity and areal extension of the geological units [17]. It is also characterized by humid and dry cycles which result on the alternance between periods with positive to negative water balance. From a hydrological point of view it is characterized by a predominance of water vertical movements (evaporation-infiltration) over horizontal flow and it shows a strong relationship between groundwater and surface water [17]. Modular annual infiltration, including zones with a well developed drainage network reaches values up to 10% of the annual precipitation [17]. The Pampean system works like a multilayered aquifer and it is possible to distinguish two units, Puelche and Pampeano. These water bearing layers make up a single hydraulic system, which extends from the water table down to the base of the Puelche's fluvial sands. The different interbedded aquifer layers are recharged locally by infiltration of rain water. The Puelche aquifer top is between 25 m to 50 m depth and its thickness ranges between 30 m and 80 meters. It is separate from the loessic Pampeano aquifer by a silty clayed level (aquitard). The Pampeano includes the phreatic layer. These water bearing layers make up a single hydraulic system, which extends from the water table down to the base of the Puelches Sands. Both aquifers are exploited for domestic, municipal, industrial and commercial use [18].

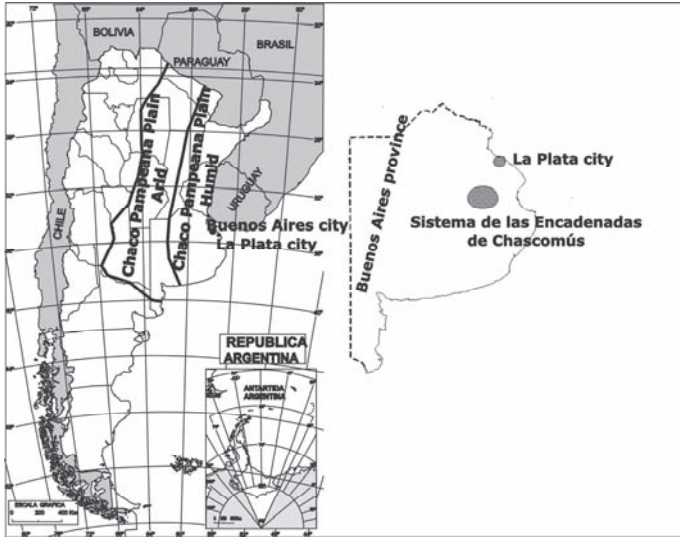


FIG. 2. Argentina country, Buenos Aires province with studied localities.

The pampean environments selected for this article are two regions of the NE Buenos Aires province: La Plata city and its surroundings and the Sistema de las Encadenadas de Chascomús in Salado River Basin (Fig. 2).

4.2. La Plata

Recharge dynamic and salinization were studied by means of stable and radioactive environmental isotopes as well as chemical analyses at La Plata City [11]. In this framework, Puelche and Pampeano aquifers were sampled in more than 100 wells during 1990 and 1991. Figure 3 shows the isotopic values obtained from groundwater samples, ocean water, de la Plata River and the local meteoric water line (LMWL) from CUS. For a best understanding samples named P represent a good summary of groundwater type found at La Plata zone. Wells P1 and P3 are located on the city SW in the recharge area (high plain) and they have filters on the two aquifers. P2 is a phreatic sample located in the south part, nearest de border of the basin. P6 and P7 belong to the well battery providing water to population and their filters are on the Puelche. Wells L1[19] and P4 are placed in the low plain, near the de la Plata River shore and they produce from salinized Puelche. These waters are not suitable for human and industrial use, and they are only used for swimming pools. These waters are

sodium chloride type, similar to sea water, with electric conductivities higher than 20 mS/cm.

Figure 3 exhibits the mixing between Puelche recharge in the low plain, de la Plata River water and old waters belonging to a sea ingression ($\delta^{18}\text{O} \approx \delta^2\text{H} \approx 0\text{‰}$, similar to SMOW). Fluctuations in the obtained groundwater values are probably due to evaporation of local precipitation prior to infiltration, selective percolation through “tosca” levels (Calcium carbonate as calcite concretions, veins and hardpan) with secondary permeability.

^3H contents range between 0.7 TU and 2.6 TU. All samples have values lower than the input function estimated for that time, suggesting transit or mixing with older groundwater flows. It is known the effect of selective percolation through tosca levels which are discontinuously interbedded and some times acting as an aquitard. The saline contents of Pampeano and Puelche at the high plain do not show any correlation with isotope content, suggesting that the main salinization mechanism is by transit, and in this particular case the salts dissolution.

4.3. Sistema de las Encadenadas de Chascomús

The relation between the surface water and shallow groundwater was evaluated at the “Sistema de las Encadenadas de Chascomús”. The water level of the lakes depends on hydrological cycle, being the inputs: precipitation, stream flow, groundwater inflow and surface runoff and the outputs: evaporation and stream outflow. The local groundwater drainage supplies the base discharge of pampasic lake’s waters and holds the perennial discharge of stream beds [17].

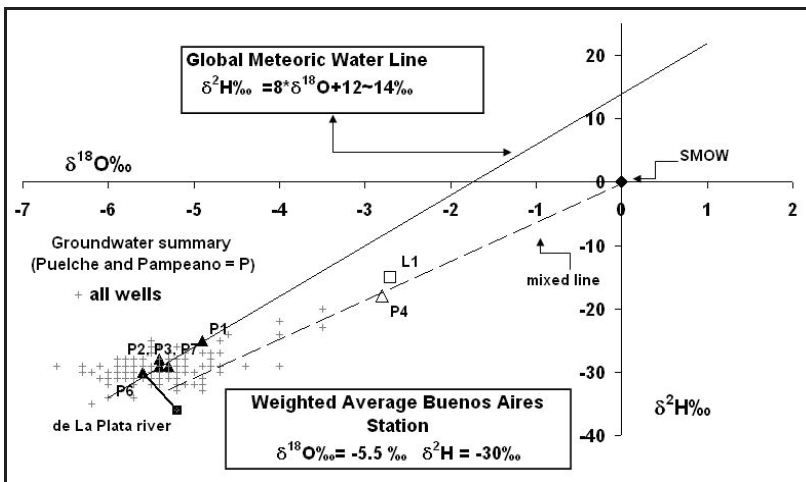


FIG. 3. $\delta^2\text{H}$ vs. $\delta^{18}\text{O}$ in La Plata city and its surroundings.

APPLICATION OF ENVIRONMENTAL ISOTOPE TECHNIQUES

During flood periods precipitation reaching the surface is stored in depressions forming shallow lakes and marshes. The water exceeding the storage capacity of the depressions moves very slowly on the surface as sheet flow. Infiltration is very high due to regional lack of slope (3×10^{-4}) and soil characteristics, and the water table is near surface at most places. As a consequence, groundwater and surficial water are strongly interrelated.

During December, 2000 and August, 2001 were taken 33 samples from Vitel, Chascomús and Adela lakes and from Vitel N, Portela, Vitel S, Valdez, Girado, San Felipe, Monte Brown and Las Tamberas streams. Groundwater was sampled from 16 phreatic wells in Pampeano aquifer [20]. Figure 4 exhibits the isotopic values obtained from surficial and groundwater samples in the 2 sampling periods, and the local meteoric water line (LMWL) from CUS.

The isotopic composition of groundwater is relatively constant for all samples. The mean summer values are -5.0‰ and -30‰ for $\delta^{18}\text{O}$ and $\delta^2\text{H}$, respectively and -5.3‰ and -32‰ for winter (Fig. 4). They are close to the average annual precipitation established in CUS ($\delta^{18}\text{O} = -5.5\text{‰}$, $\delta^2\text{H} = -30\text{‰}$) indicating their meteoric origin. Nevertheless, small fluctuations in the obtained groundwater values are probably due to evaporation of local precipitation prior to infiltration, selective percolation through tosca levels with secondary permeability. It must be taken into account that recharge waters reflect the mean precipitation with reasonable fidelity [6]. The mean residence time of precipitation on the soil surface depends on the surface materials permeability.

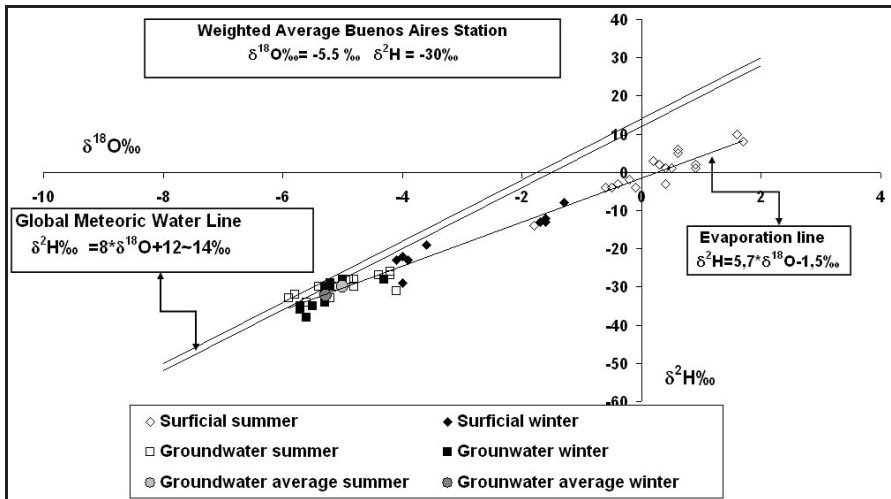


FIG. 4. $\delta^2\text{H}$ vs. $\delta^{18}\text{O}$ in "Sistema de las Encadenadas de Chascomús".

If it is high, infiltration is fast and the groundwater isotope composition could be the same or very similar to that of rains. If it is low, evaporation prior to infiltration causes isotope enriched waters. The stream and lake waters fit on an evaporation line ($\delta^2\text{H} = 5.7 \times \delta^{18}\text{O} - 1.5\text{‰}$), indicating the groundwater contribution (Fig. 4) and the fact that in summer waters are more evaporated, showing more isotope enriched values. These results are in agreement with the geochemistry.

5. CONCLUSIONS

The techniques that use environmental isotopes (^2H , ^3H , ^{18}O , ^{14}C and ^{34}S) jointly with the so-called classic procedures are a tool of great utility in hydrological and hydrogeological studies. Just now, they are included in most of the investigations carried out all over the world. Therefore, they can solve, in relatively simple form and at low cost, numerous problems in surficial waters and aquifers, related with the origin and recharge area, salinization mechanisms, processes in the unsaturated zone, as well as the determination of terms of water balance. ^3H and ^{14}C introduce the temporary variable, allowing, in favourable cases, the evaluation of groundwater residence times and flow rates. A large precipitation record at Buenos Aires station as well as others localities of Argentina is a fundamental objective to bring scientific tools for environmental isotope studies. Finally, we stand out the importance of continuing the operation of the National Collector Network of Argentina as well as the increase of stations at different latitude and altitude of the country.

REFERENCES

- [1] ROZANSKI, K., et al., Isotopic patterns in modern global precipitation. *Climate Change in Continental Isotopic Records*, Geoph. Monograph **78**, Amer. Geoph. Union (1993) 1–36.
- [2] DAPEÑA, C., PANARELLO, H.O., Evolución y estado actual de la Red Nacional de Colectores de Isótopos en Precipitación de la República Argentina, XVI Cong. Geol. Argentino, La Plata (2005) II: 635–642.
- [3] GAT, J., Variability (in time) of the isotopic composition of precipitation: Consequences regarding the isotopic composition of hydrologic systems, Symp. On the Use of the Isotope Techniques in Water Resources Development, IAEA, Vienna (1987) 551–563.
- [4] CRAIG, H., Isotopic variations in meteoric waters. *Science* **133** (1961) 1702–1703.
- [5] DANSGAARD, W., Stable isotopes in precipitation, *Tellus* **16** (1964) 436–468.

APPLICATION OF ENVIRONMENTAL ISOTOPE TECHNIQUES

- [6] GAT, J.R., TZUR, Y., Modification of the isotopic composition of rainwater by processes which occur before groundwater recharge, *Isotopes in Hydrology Symp.* IAEA, Vienna (1967) 49–60.
- [7] FONTES, J.CH., Environmental Isotopes in Groundwater Hydrology, In: Fritz and Fontes (eds.), *Handbook of Environmental Isotope Geochemistry, The Terrestrial Environment*, A. Ch. **3** (1980) 75–140.
- [8] PANARELLO, H.O., ALBERO, M.C., Tritium, oxygen 18 and deuterium contents of Buenos Aires rainwater, *Coloquio Internac. de Grandes Llanuras, Olavarría, Buenos Aires, UNESCO* (1983) II: 889–898.
- [9] PANARELLO, H.O., PARICA, C.A., Isótopos del oxígeno en hidrogeología e hidrología, Primeros valores en aguas de lluvia de Buenos Aires. *Asoc. Geol. Arg., Rev* **39** 1–2 (1984) 3–11.
- [10] IAEA/WMO, Global Network for Isotopes in Precipitation, The GNIP Database, <http://isohis.iaea.org>. (2002).
- [11] PANARELLO, H.O., et al., Mecanismos de salinización del agua subterránea de la zona de La Plata, Buenos Aires, Argentina: su interpretación por medio de los isótopos ambientales. IAEA, TEC DOC 835 (1995) 13–27.
- [12] DAPEÑA, C., PANARELLO, H.O., Composición isotópica de la lluvia de Buenos Aires, Su importancia para el estudio de los sistemas hidrológicos pampeanos, *Revista Latino-Americana de Hidrogeología*, N°4 (2004) 17–25.
- [13] YURTSEVER, Y., GAT, J., Atmospheric Waters, In: J.R. Gat and R. Gonfiantini (Eds.), *Stable Isotope Hydrology, Deuterium and oxygen-18 in the Water Cycle*, Ch. 6, IAEA Tech. Reports Series No. 210 (1981) 103–142.
- [14] GONFIANTINI, R., Standards for stable isotope measurements in natural compounds. *Nature* **271** (1978) 534.
- [15] GRÖENING, M., ROZANSKI, K., Uncertainty assessment of environmental tritium measurements in water, *Accred Qual Assur* 8:359.366. (2003).
- [16] AUGE, M., Regiones Hidrogeológicas. República Argentina y provincias de Buenos Aires, Mendoza, Santa Fe. www.gl.fcen.uba.ar/Hidrogeologia/auge/Reg-Hidrogeo.pdf (2004).
- [17] SALA, J., et al., Generalización Hidrológica de la Provincia de Buenos Aires, *Coloquio Internac. de Grandes Llanuras, Olavarría, Buenos Aires, UNESCO* (1983) III: 975–1008.
- [18] AUGE, M., et al., Actualización del conocimiento del Acuífero Semiconfinado Puelche en la Prov. de Buenos Aires, Argentina. XXXII IAH & VI ALHSUD Congress, CD ROM (2002).
- [19] LEVIN, M., et al., Uso de isótopos estables (deuterio y oxígeno-18) para determinación del origen de la salinización del “Puelchense” en la ciudad de La Plata y alrededores, I Parte, V Cong. Geol. Argentino (1973) I: 373–393.

- [20] DAPENÑA, C., et al. Environmental stable isotope of the “Sistema de las Encadenadas de Chascomús”, Buenos Aires, Argentina. III South Amer. Symp. on Isotope Geology, CD ROM. Chile (2001).

RAINWATER TRACING USING THE STABLE ISOTOPE IN THE WESTERN MEDITERRANEAN (CASE OF RIF CHAIN IN THE NORTH OF MOROCCO)

M. QURTOBI , H.MARAH
Centre National de l'Energie des Sciences
et des Techniques Nucléaires,
Rabat, Morocco

A.EL MAHBOUL
Agence du Bassin Hydraulique du Loukous,
Tétouan, Morocco

C. EMBLANCH
Université d'Avignon et des pays de Vaucluse,
Avignon, France

Abstract

Nine meteorological stations, distributed between 3 and 996 m of altitude, have been used as basis of an isotopic study of rainwater carried out in the Rif Chain (Northern part of Morocco) during the hydrological cycles 2004 to 2006. This study allowed us to examine the isotopic variations during the year and to define the relationship between ^{18}O and ^2H . The altitudinal gradient established for ^{18}O is: $\delta = -0.27\text{‰}$ per 100 m.

We have also used the relationship between emergence points altitudes of some studied springs and their ^{18}O contents to calculate the regional ^{18}O gradient. The selected springs are supposed to have nearest emergence altitudes to the ones of the neighbouring mountains. The ^{18}O content variation in the springs corresponds to an altitudinal gradient: $\delta = -0.27\text{‰}$ per 100 m. It is remarkable to note that this gradient is identical to that of the rainwater. Even if this isotopic study is reduced in time, it seems to be sustainable to establish a correct regional meteoric line at least of the slope. The constant difference related to the regression (4.25 in groundwater and 4.87 in rainwater) has to be discussed. Before having a demonstrated value, we will use the gradient and the origin ordinate determined from springs, gradient that takes into account the rains evaporation before their infiltration.

1. INTRODUCTION

The Rif Chain is situated in the north of Morocco (Fig. 1). In this region, the climate is influenced by two coasts: Atlantic Ocean and the Mediterranean Sea.

The objective of this work, starts from the stable isotope data of water acquired during an instantaneous summer season, to establish an altitudinal gradient of oxygen-18, that if it were to be refined again, could already, be used in an operational way to delimit the recharge areas, and therefore, in the protection and management of the quality of the numerous springs captured by local population.

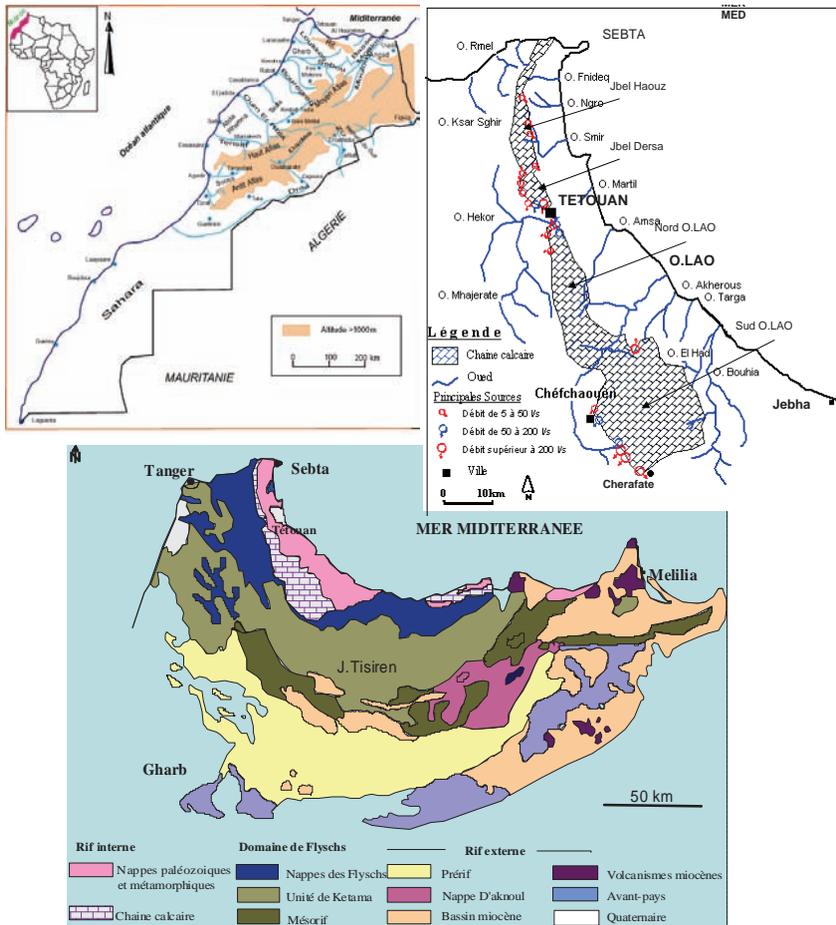


FIG. 1. Geologic map of Rif Chain [7, modified] and situation of sampling springs.

RAINWATER TRACING USING THE STABLE ISOTOPE

Seventy springs were selected during summer period (Low Water of August 2002). The sampling interested the main aquifers of the region: the Haouz Chain (mean altitude 400 m) and Jebel Dersa (mean altitude 350 m) at the north of Tétouan city, and the chalky chain in the South of Tétouan city, with a north compartment of Lao Wadi (mean altitude 800 m) and south compartment of Lao Wadi. The last, is separated by Jbel Lakrâa in west compartment Jbel Lakrâa (mean altitude 1300 m) and east compartment of Jbel Lakrâa (mean altitude 1100 m).

The selected springs are supposed to have nearest emergence altitudes to the ones of the neighbouring mountains. Analysis concerned the stable isotopes of groundwater (^2H and ^{18}O).

The use of this work was a better definition of the recharge area and therefore a better protection of two springs (Ras El Ma and Cherafate) essential in drinkable water of local populations.

Finally, this work is an example of the interest of the low water instantaneous in oxygen-18, for the establishment of the altitudinal gradients and their use in the management of the karstic aquifer. From a reduced number of measures in a zone deprived of previous data, the results are an immediate use in practical hydrogeology.

2. ALTITUDE GRADIENT OF OXYGEN-18

In order to improve the management of the numerous springs of the Rif chain used by the local population, it's necessary to establish the altitudinal gradients for the oxygen-18 to define the recharge area.

The altitude gradients of oxygen-18 contents, must be established by measures from the rainwater samples collected on several years, at different altitudes in the region supposed to be the recharge [1]. However, the absence of these data, doesn't allow us to estimate the mean altitude's recharge area with a reasonable uncertainty.

We suggest to establish this gradient with numerous springs selected from geological observations. This one allows us to approach the mean altitude's recharge area [4]. The nearest altitude of emergence to the one of the neighbouring summits was an important criteria of selection: difference between the mean topographic altitude of the neighbouring summits and those of the springs selected is not more than 100 m (Tab. 1). Consequently, for these springs there will be a little difference between the mean altitude of recharge area and that of the emergence (maximum 50 m). That will allow us to take the altitude of emergence as a reference.

TABLE 1. DETERMINATION OF RECHARGE AREA OF STUDIED SPRINGS

	Name of spring	Z (m) spring	$\delta^{18}\text{O}_{\text{‰}}$	estimated recharge area altitude
	Onsar Aherarisse	355	-5.12	321
	Ain Dailen n°1	360	-5.24	371
	Onsar Aghdir	350	-5.02	279
Chaîne	S.de Tleta Trhmat	375	-5.09	308
El Haouz	Ain Alaoui	410	-4.78	179
	Ain Feouaouare	355	-6.41	858
	Ain Meskhla 2	300	-4.96	254
Altitude moy.	Onsar Hzainane	275	-5.18	346
Zmoy = 400 m	Onsar Dchar	363	-5.22	363
	Ain El Keddane	395	-5.18	346
	Aïn Gh'ballou	265	-5.29	392
	Aïn Debbagh	280	-5.29	392
	Aïn Sidi Nejjuzi	220	-5.12	321
Jbel	Aïn Dahdah	220	-4.83	200
Dersa	Onsar Saddina	340	-5.45	458
	Aïn Ah'Nacha	300	-5.22	363
	Aïn Jemâa	310	-4.85	208
Zmoy = 350 m	Aïn Mekhysa	280	-5.22	363
	Onsar Abssir	290	-5.17	342
	Ain Sembel	285	-5.19	350
	Taliwane	870	-6.48	888
	Agourer	680	-6.64	954
	Onsar Mimossa	500	-6.56	921
Zone	El Fouara	660	-6.86	1046
Oued LAO	Onsar Arozane	820	-6.71	983
	Onsar Ighboula	800	-6.15	750
Zmoy = 800 m	Aghbalou	840	-6.08	721
	Aghbalou	380	-6.21	775

RAINWATER TRACING USING THE STABLE ISOTOPE

	El Hamma	300	-6.06	713
	O.Khzanat Melhia	400	-6.07	717
	Aïn Tazka	180	-6.44	871
	Aïn Keltoum	210	-5	271
	Aïn Bousmlal	300	-5.78	596
	El Anissar	600	-5.69	558
	A.dar Ben Yamoun	200	-6.04	704
	Torreta	280	-5.47	467
	Elhama Foukia	840	-5.97	675
	Onsar Metahar	630	-7.25	1208
	Onsar El Gaouza	640	-6.68	971
	Aïn Tissmlane	1080	-7.07	1133
Zone	Aïn Tayerset	1200	-7.45	1292
Est	Onsar Afeska	1260	-7.44	1288
Jbel	Onsar Imizaene	680	-7.4	1271
Lakrâa	Onsar Daroua	610	-6.66	963
	Ras El Ma	700	-7.02	1113
Zmoy = 1100 m	Onsar Aghermane	1000	-7.23	1200
	Onsar Aayaden	1100	-7.18	1179
	Aïn Chrafate	960	-7.12	1154
	Onsar Zaouia	350	-6.93	1075
	Onsar Taounshicht	380	-6.57	925
	Aïn Souyah	210	-6.99	1100
Zone	Onsar Anefzi	1100	-7.5	1313
Ouest	El Ma Taria	1380	-7.44	1288
Jbel	O. El Khwa	1260	-7.45	1292
Lakrâa	Onsar Asaki	970	-6.98	1096
	El Menbae	1140	-7.25	1208
Zmoy = 1300 m	Onsar Rahmanio	760	-7.17	1175
	Onsar Taria Seflia	930	-6.84	1038
	Aïn Majra	860	-7.33	1242
	Onsar Taourart	460	-7.35	1250

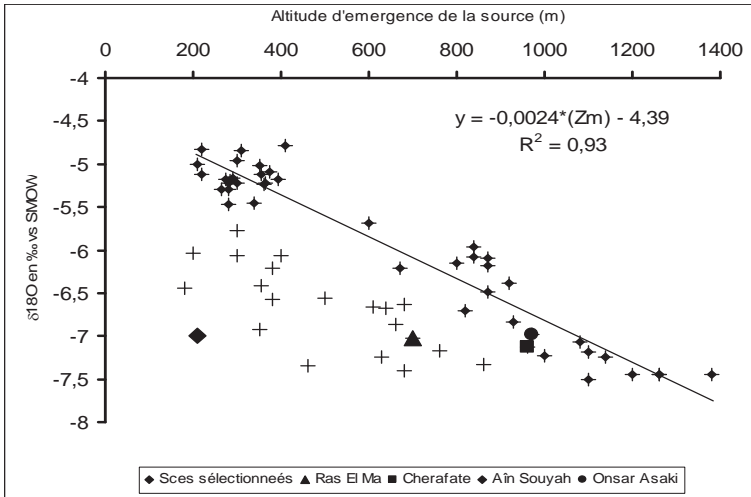


FIG. 2: Relationship oxygen-18 vs. altitude emergence of springs.

The oxygen-18 variation according to the altitude of emergence's spring corresponds to an altitudinal gradient of -0.27‰ per 100 m (Fig. 2). This gradient is almost equivalent to the one established by [6]. Indeed, by the survey of the rainwater in Morocco to different altitudes of the Atlas chain, this author found an altitudinal gradient of $-0.3\text{‰ }^{18}\text{O} / 100 \text{ m}$. On another work [2, 3] studied the karstic springs on the Atlas of Beni-Mellal, established an altitude gradient -0.26‰ per 100 m for oxygen-18.

3. DELIMITATION OF RECHARGE AREAS OF OTHER SPRINGS

While adopting the altitude gradient calculated (-0.27‰ per 100 m), we could determine the mean altitudes of the recharge areas for different springs of the north and south compartment of the Lao wadi and the Jebel Dersa and the chain of El Haouz, sampled during this work (Table 1).

In the north compartment of Lao Wadi, the altitude of recharge areas of springs (Torreta, Zerka, Yarghist and Ben Karrich) oscillate between 400 to 800 m.

Springs of the south compartment of Lao wadi (Ras El Ma and Cherafate) are supplied by mean altitudes of the recharge areas between 1000 m and 1200 m. This is in conformity with the observations of the relief's Jbel Tissouka, Jbel Bou Slimanes and Jbel Lakrâas.

RAINWATER TRACING USING THE STABLE ISOTOPE

We notice a big difference between the altitude of spring and the altitude average of the recharge area, which translates the diversity of topographic, geomorphologic and geologic contexts of the Rif chain. However these data are very useful, for example we underlined in the Table two springs whose altitudes of emergences are different (210 m for Ain Souyah and 970 m for Onsar Asaki) and situated in the same geographical sector, the West zone of the Jbel Lakrâa. Despite the different emergence altitude, the content of oxygen-18 ($\delta^{18}\text{O} = 6.99\text{‰}$) indicate some identical altitudes of recharge and the gradient allows to estimate the mean altitude of recharge area up to 1150 m. This result has an immediate repercussion on the functioning of these systems: indeed, in the Onsar Asaki case, the unsaturated zone will be relatively reduced, whereas in the Ain Souyah case it will be very developed and, it's known that, when it's thick, the unsaturated zone of karstic aquiferous can play an important role in the regularization of flow low-water [4]. Moreover it is what we notice at the spring Ain Souyah (debit flow of low-water is in the order 200 L/s).

Moreover this spring come up from the base of a cliff, more than 500 m high, which explains the average altitude of recharge calculated for this spring (1100 m).

In the same order of idea, the Ras El Ma spring (main resource of drinkable water supply of the population Chéfchaouen city, 10000 inhabitants).

For this one, the topographic basin spreads on a surface of 7 km² that overhangs the city of Chéfchaouen by an abrupt cliff that makes more than 300 m.

The average altitude of the definite recharge area for this spring is about 1100 m, which is in conformity with the geomorphologic observations and explain the flows even sustained in low-water (existence of a thick infiltration zone that maintains these flows).

For Cherafate spring, the unique source of drinkable water of the municipality of Cherafate, the area of recharge calculated for this spring is about 1150 m and corresponds to the Jbel Bouslimane's south part.

4. CONCLUSION

Due to this immediate of low-water mark we were able to establish an altitudinal gradient of oxygen-18, which if refined, can be used in an operational way in the demarcation of the recharge areas, and so, the protection and the management of the quality of numerous springs captured by the population.

A first practical use of this work is a better definition of the recharge area and so for immediate protection of two springs (Ras El Ma and Cherafate) essential in supplying water for the local population.

Finally, this work is an example of the interest of the immediate low-water mark in oxygen-18, for the establishment of altitudinal gradients and of their use in karstic aquifers management.

With a reduced number of measurements on a zone deprived in previous data, these results are immediately applicable in practical hydrogeology.

REFERENCES

- [1] BLAVOUX, Etude du cycle de l'eau au moyen de l'oxygène 18 et du tritium. Possibilités et limites de la méthode des isotopes du milieu en hydrologie de la zone tempérée. Thèse d'état, Paris VI (1978) 333.
- [2] BOUCHAOU, L., MICHELOT, J.L., CHAUVE, P., MANIA, J., MUDRY J., Apports des isotopes stables à l'étude des modalités d'alimentation des aquifères du Tadla (Maroc) sous climat semi-aride, C. R. Acad. Sc. Paris, tome 320, No. 2a, janvier 95 (1995) 95–101.
- [3] BOUCHAOU, L., MICHELOT, J.L., Isotopic investigation on the recharge of the Beni Mellal region aquifers (Tadla, Morocco), IAHS Publication, No. 244 (1997) 37–44.
- [4] EMBLANCH, C., ZUPPI, G.M., MUDRY, J., BLAVOUX, B., BATIOU, C., Carbon-13 of TDIC to quantify the role of the Unsaturated Zone: the example of the Vaucluse karst systems (Southeastern France), J. of Hydrology **279** (2003) 262–27.
- [5] LASTENNET, R., Rôle de la zone non saturée dans le fonctionnement des aquifères karstiques, approche par l'étude physico-chimique et isotopique du signal d'entrée et des exutoires du massif du Ventoux, Thèse Sciences de la terre, Hydrogéologie, Univ. Avignon (1994) 239.
- [6] MARCE, Contribution des méthodes isotopiques à l'étude des modalités d'alimentation et de renouvellement des réserves de quelques nappes souterraines du Maroc. Ed. BRGM, Orléans, 75 SGN, 447 LAB. (1975) 131.
- [7] MICHARD A., Eléments de la géologie marocaine, Notes et mém. Service géol. Maroc **252** (1976).

MODELING THE ALTITUDE ISOTOPE EFFECT IN PRECIPITATIONS AND COMPARISON WITH THE ALTITUDE EFFECT IN GROUNDWATER

F. GHERARDI*, P. BONO**, C. FIORI**, M.F. DIAZ TEJEIRO⁺,
R. GONFIANTINI*

*Institute of Geosciences and Georesources,
CNR, Pisa, Italy

**Department of Earth Sciences,
University “La Sapienza”,
Rome, Italy

⁺Centre of Studies and Applied Techniques,
Ministry for Development,
Madrid, Spain

Abstract

A numerical model has been developed to account for the altitude effect on the isotopic composition of precipitation. The model allows to predict the isotope variations in rains produced by a marine air mass which moves inland, climbs up along a mountain slope and undergoes cooling and condensation under pseudo-adiabatic and pseudo-Rayleigh conditions. It is assumed that the isotopic fractionations between liquid water and vapour occurs at equilibrium and the evaporation effects during the raindrop fall are negligible. Generally, the isotopic values observed in precipitation are in good agreement with those predicted by the model. For groundwater, the best agreement between model predictions and field observations is obtained for springs fed by small perched aquifers. The following relationships are obtained: (i) mean altitude gradients: $d(\delta^{18}\text{O})/dz = -1.8\text{‰ km}^{-1}$ and $d(\delta^2\text{H})/dz = -14.2\text{‰ km}^{-1}$ (model: -1.7 and -13.9‰ km^{-1} , respectively); (ii) local meteoric water line (valid up to an altitude of 2500 m a.s.l.): $\delta^2\text{H} = 7.53 \times \delta^{18}\text{O} + 13.5$ (model: $\delta^2\text{H} = 7.83 \times \delta^{18}\text{O} + 16.2$).

1. INTRODUCTION

During 1999–2001 water samples from springs fed by small perched aquifers have been collected along a SW-NE transect in Central Italy, and their stable isotope composition was determined. In all the aquifers selected for this

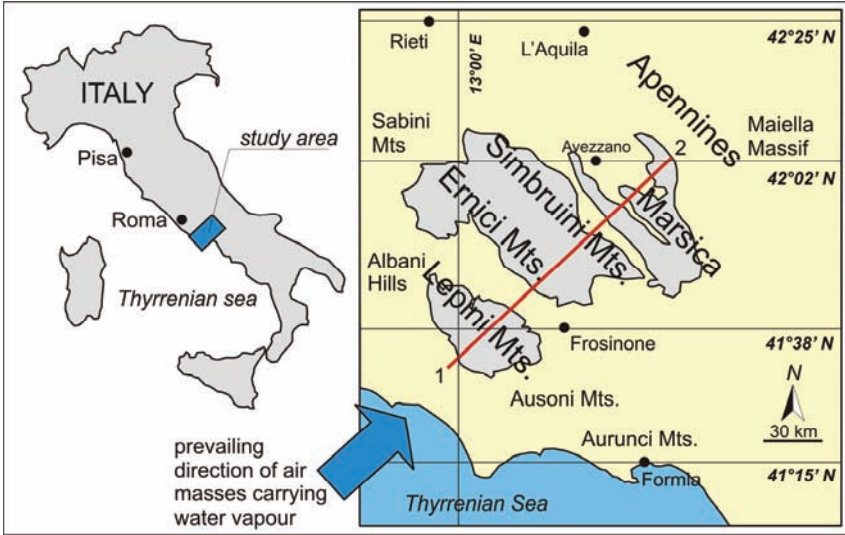


FIG. 1. Geographic sketch map showing the location of the hydrostructures (gray areas) and the SW–NE sampling transect (track 1–2) investigated in this study. Air masses coming from Tyrrhenian Sea bring moisture inland and cause most of the local precipitations.

study, the difference between recharge and discharge altitudes is small (no more than 100 m). The hydrogeological structures monitored are located south of Rome, approximately between 41° and 42°N, and include the mountain ranges of Lepini Mts. (mean altitude about 1500 m), Simbruini Mts. (about 2000 m), and Apennino Abruzzese (about 2200 m).

These mountain ranges are all NW-SE oriented, parallel to, and at increasing distance from, the Tyrrhenian coast, as shown in Fig. 1. The stable isotope compositions and sampling site elevations have been correlated with the objective of extracting information on the local vertical isotopic gradients.

2. METHODS

A simplified, Rayleigh-type numerical condensation model has been developed and applied to field data to obtain a theoretical basis for the isotopic patterns recognized in the field. The model includes some basic capabilities to predict the variations expected for the isotope concentrations in both liquid and vapour phases, assuming that air masses move inland from the sea, climb up along the mountain slopes undergoing adiabatic expansion and cooling,

MODELING THE ALTITUDE ISOTOPE EFFECT IN PRECIPITATIONS

and start to condensate as liquid water. The model application is backed up by the following considerations (i) the atmospheric vapour has a predominant source: the sea, (ii) the prevailing mechanism of formation is that of the so-called “orographic precipitations” implying a progressive vapour condensation [1], (iii) at the latitude of the study area, the precipitation generation is not dominated by large convective systems [2], whose dynamics is not adequately described by the model. Among other effects, the amount effect is actually incorporated in the model, while the shadow effect, which in principle may play a role on the north-eastern slopes of mountains, and the continentality effect seem to have a negligible influence on the isotopic signal of precipitations. Mixing of air masses with different isotopic composition and moisture content is not considered, although the model allows to take it into account [3].

The model sensitivity is tested with respect to the (i) isotopic composition of vapour, (ii) initial temperature and relative humidity of air masses, (iii) wet lapse rate, and (iv) fraction of condensed water removed from clouds. The best fitting conditions are achieved with a trial and error procedure.

The comparison between model predictions and field observations is extended also to groundwater systems, included some from other regions of Italy. Data inspection reveals that despite the general validity of the model, the agreement between field data and numerical predictions is worsening in systems characterized by hydroclimatological conditions more complex than those occurring in our study area. In particular, our model fails to reproduce the natural isotopic patterns when large karstic structures and aquifers characterized by large differences between recharge and discharge altitudes are present.

3. THE NUMERICAL MODEL

The numerical model utilized in this study is derived from that one presented in [4]. Energy and mass balances have been incorporated in a zero-dimensional model which takes into account liquid-vapour phase transition, with the isotopic equilibrium occurring continuously between the co-existing phases through isotopic exchange.

Liquid water starts to form when the vapour partial pressure in the cooling-expanding air masses equates the vapour saturation pressure at the system T, P conditions. The amount of liquid water effectively removed from clouds can be arbitrarily varied. If all the condensed water is precipitating as soon it is formed, the process is pseudo-adiabatic because a small fraction of energy is removed as well, and the isotopic effects are described by a Rayleigh condensation process. If only a part of the liquid water formed is removed as

rain (pseudo-Rayleigh conditions), it is assumed that the isotopic equilibrium between the co-existing phases is continuously assured through isotopic exchange.

During a pseudo-Rayleigh condensation, the fraction Fr_w of residual liquid water remaining in clouds progressively diminishes, following a law of the type:

$$Fr_{w(T-1)} = Fr_{w_T} \times (1 - k) \tag{1}$$

where k is the rainout rate, i.e. the steady relative decrease of the liquid water fraction in clouds for 1°C cooling. In Fig. 2 the repartition of liquid water between the rising air mass and the falling rain is shown in terms of residual liquid water in clouds as a function of the condensation altitude, with different values of k . For the sake of simplicity, k is assumed constant during the precipitation event, although it may change even drastically depending on turbulence and instability of the air mass. Under the conditions described in figure caption, at the altitude of 2000 m (ambient temperature of 5.6°C), the numerical model predicts a decrease

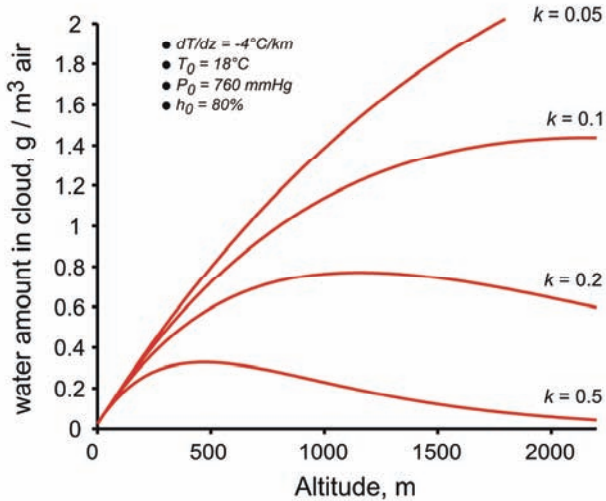


FIG. 2. Amount of residual liquid water remaining in clouds ($\text{g } H_2O_{Liq} / \text{m}^3 \text{ air}$) during the air mass adiabatic expansion, as predicted by the numerical model. Constraint parameters: T_0 (initial air mass temperature) 18°C ; h_0 (initial relative humidity) 80%; Fr_{w_0} (fraction of residual liquid initially remaining in cloud) 0.8; L/V (maximum molar liquid-vapour ratio in cloud during precipitation) 0.3. Curves describe conditions for different values of k parameter.

MODELING THE ALTITUDE ISOTOPE EFFECT IN PRECIPITATIONS

in the residual liquid water in clouds from about 1.4 to about 0.06 g H₂O_{LIQ} per m³ of air for k ranging between 5 and 50%.

The model allows also to use a pre-fixed liquid-vapour ratio in clouds according to the user's requirements. Relevant parameters have been calibrated as to let the maximum amount of liquid water in clouds to vary between 1 and 4 g H₂O/m³ air, depending on the value of k (see equation 1), and in agreement with data reported in literature for convective storm clouds (e.g. [5] and [6]).

Several simplifying assumptions are implicit in the model implementation shown here. In particular: (i) the condensed phase consists of liquid water only, i.e. super-cooled water when the temperatures drops below 0°C; (ii) the isotopic fractionations between liquid and vapour are assumed to occur at equilibrium; (iii) partial re-evaporation during raindrop fall is neglected.

The assumption (i) appears reasonable because super-cooled liquid is known to occur in clouds between 0 and -10 °C ([7] and references cited therein) and our computations were not extended below -10 °C. Nevertheless, the model can be adapted also for systems where ice and vapour co-exist, but the isotopic re-equilibration between ice crystals and vapour in clouds may become too slow [8].

4. APPLICATION OF THE NUMERICAL MODEL TO FIELD DATA FROM SW-NE TRANSECT: SENSITIVITY ANALYSIS

Isotope data on precipitation and/or groundwater allow to establish δ -altitude relationships. However, any given data set may satisfy more than one combination of meteorological and isotopic parameters.

The solution of this inverse problem is inherently non-unique. Therefore, a sensitivity analysis has been performed by varying the input parameters of the numerical model in order to circumscribe the problem. The input values have been calibrated on the basis of available meteorological and climatological data. Thus, the initial temperature, T_0 , and the relative humidity, h_0 , of the rising air masses have let to vary between 14 to 22°C, and between 60 to 95%, respectively. The ambient lapse rate, dT/dz , has let to vary between -4 to -6 °C/km, which is the range commonly adopted for wet air. Fig. 3 displays the sensitivity tests with respect to T_0 and h_0 .

Inspection of isotopic parameters reveals that the correlation between vertical isotopic gradients and altitude (which, in turn, is linearly correlated with temperature) depends also on the selected initial conditions. For instance, a $d(\delta^{18}\text{O})/dz$ value ranging between -1.5 to -2.8‰ km⁻¹ can be attained during a rise of about 2500 m along a mountain slope. Also, the slope and intercept of

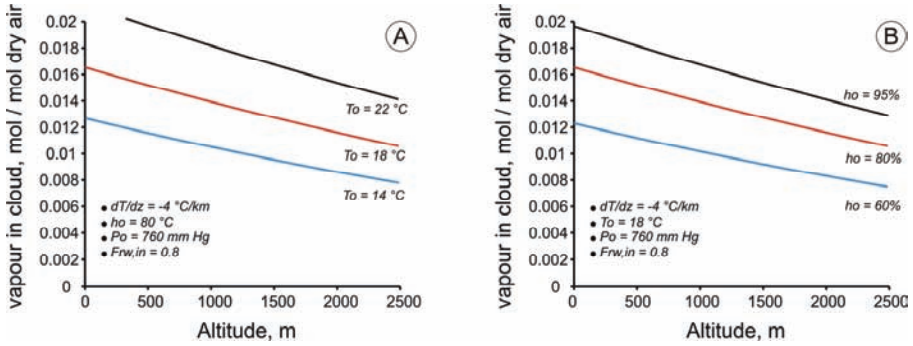


FIG. 3. Variation of the amount of vapour present into a rising air mass as a function of altitude for different initial temperature (T_0 ; box A) and relative humidity (h_0 ; box B) values of the air mass.

the meteoric water line predicted by the model are sensitive to variations in temperature and humidity only.

With reference to the initial conditions tested in this study, an increase of temperature from 14 to 22°C and an increase in h_0 from 60 to 95%, produces to the following changes of the $\delta^2\text{H}$ - $\delta^{18}\text{O}$ correlations:

$$\begin{aligned} \delta^2\text{H} &= 8.16 \times \delta^{18}\text{O} + 19.5 \quad (T_0 = 14^\circ\text{C}) \text{ to} \\ \delta^2\text{H} &= 7.61 \times \delta^{18}\text{O} + 13.1 \quad (T_0 = 22^\circ\text{C}), \text{ and} \\ \delta^2\text{H} &= 8.25 \times \delta^{18}\text{O} + 20.7 \quad (h_0 = 60\%) \text{ to} \\ \delta^2\text{H} &= 7.66 \times \delta^{18}\text{O} + 13.6 \quad (h_0 = 95\%). \end{aligned}$$

The slope $\delta^2\text{H}/\delta^{18}\text{O}$ and the deuterium excess $d = \delta^2\text{H} - 8 \times \delta^{18}\text{O}$ vary appreciably with T_0 and h_0 (overall range 15 to 18), and their numerical values are inversely correlated with initial temperature and relative humidity of air masses. This is in agreement with the observation that both slope and d are generally higher in winter precipitation than in summer rains (see for instance [9]).

5. APPLICATION OF THE NUMERICAL MODEL TO FIELD DATA FROM SW-NE TRANSECT: BEST FITTING PARAMETERS

The application of the above numerical model to isotopic data from springs on SW-NE transects in Central Italy, has provided the theoretical basis

MODELING THE ALTITUDE ISOTOPE EFFECT IN PRECIPITATIONS

for the isotopic patterns observed in the field. The model-derived values for the mean altitude gradients, $\delta^2\text{H}$ - $\delta^{18}\text{O}$ correlation, and deuterium-excess are:

- (i) mean altitude gradients: $d(\delta^{18}\text{O})/dz = -1.7 \text{‰ km}^{-1}$ and $d(\delta^2\text{H})/dz = -13.9 \text{‰ km}^{-1}$;
- (ii) local meteoric water line (valid up to an altitude of 2500 m a.s.l.): $\delta^2\text{H} = 7.83 \times \delta^{18}\text{O} + 16.2$;
- (iii) deuterium excess: 17‰.

The model predictions are in reasonable agreement with field data (Fig. 4), for which we derive:

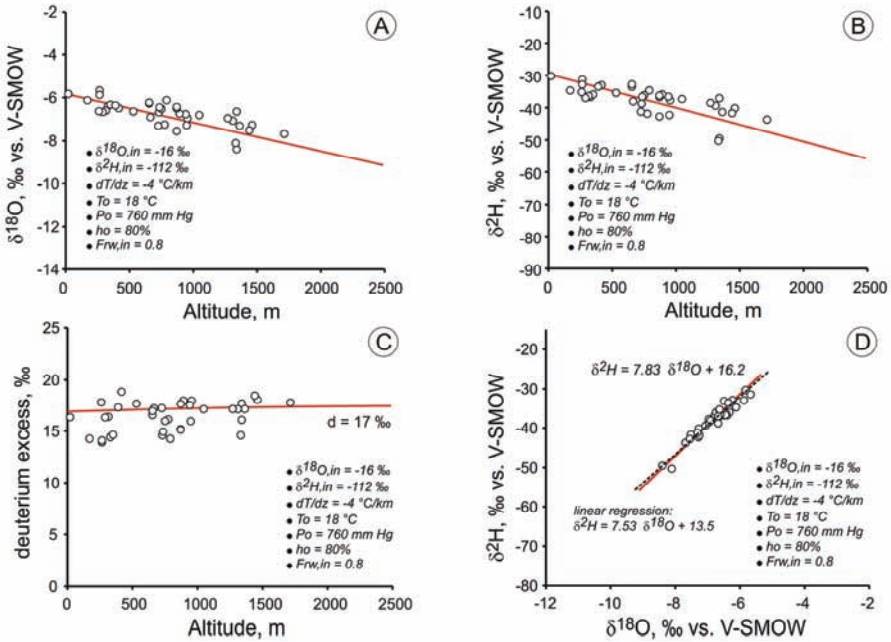


FIG. 4. Model fitting of spring data along the SW-NE transect in Central Italy. The diagram shows the $\delta^{18}\text{O}$ (box A), $\delta^2\text{H}$ (box B), d -excess (box C) vs. altitude and the $\delta^2\text{H}$ - $\delta^{18}\text{O}$ (box D) correlations. Best fitting parameters: $\delta^2\text{H}, \text{in}$ and $\delta^{18}\text{O}, \text{in}$ (initial isotopic composition of vapour mass) -112 and -16‰ , respectively; T_0 (air mass initial temperature) 18 °C , h_0 (initial relative humidity) 80% ; Frw, in (fraction of residual liquid initially remaining in cloud) 0.8 ; dT/dz (wet lapse rate) -4 °C/km .

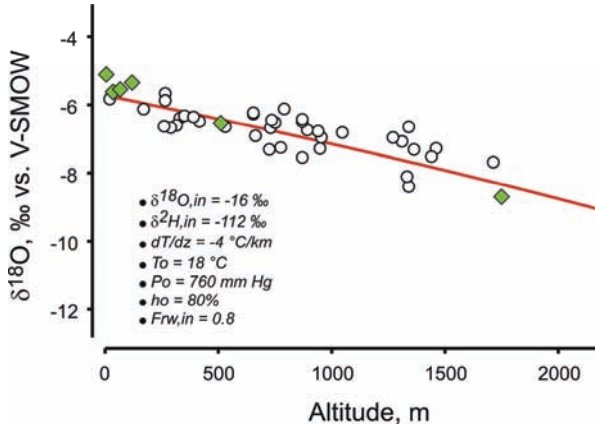


FIG. 5. Model fitting of spring (empty circles) and precipitation (full diamonds) data along the SW–NE transect in Central Italy. The diagram shows the $\delta^{18}\text{O}$ vs. altitude correlation. Rain data are weighted means of monthly average values of samples collected in the period 1999–2003 in 6 rain gauges along the same transect at elevations ranging between 5 and 1750 m a.s.l.. Best fitting parameters are as in Figure 4.

- (i) mean altitude gradients: $d(\delta^{18}\text{O})/dz = -1.8\text{‰ km}^{-1}$ and $d(\delta^2\text{H})/dz = -14.2\text{‰ km}^{-1}$;
- (ii) local meteoric water line (valid up to an altitude of 2500 m a.s.l.): $\delta^2\text{H} = 7.53 \times \delta^{18}\text{O} + 13.50$ (orthogonal regression);
- (iii) deuterium excess: 16.5‰.

For comparison, the orthogonal regression of precipitation data reported in [10] for Thyrennian stations is: $\delta^2\text{H} = 7.21 \times \delta^{18}\text{O} + 9.44$

A good agreement between numerical predictions and field data is obtained also for precipitation. Monthly precipitation samples were collected in six stations located along the same transect shown in Fig. 1, at elevations ranging between 5 and 1750 m a.s.l. In Fig. 5, the weighted monthly average $\delta^{18}\text{O}$ values calculated for these stations over the period 1999–2003 have been compared with theoretical trend and springs data already shown in Fig. 4A. A linear regression over rain data gives an altitude gradient, $d(\delta^{18}\text{O})/dz$, of -1.9‰ km^{-1} almost coincident with that of local groundwaters (-1.7‰ km^{-1}).

5. CONCLUSIONS

A satisfactory agreement between theoretical predictions and field observations has been obtained for all the sets of data taken into consideration, suggesting that the Rayleigh-type approach utilized in this study is adequate to describe the stable isotope correlation with altitude observed for meteoric waters.

Springs fed by small perched aquifers show the best fitting with theoretical patterns. For these hydrologic systems, the variation of the stable isotope composition with altitude occurs in a theoretically predictable manner, obeying a good linear correlation. On the contrary, springs fed by large aquifers whose recharge area extends over a wide altitude span, exhibit larger discrepancies and spreading of values. Moreover, because of mixing between waters recharged at different elevations, and/or large difference between the mean recharge elevation and that discharge, large springs usually show lower and irregular isotopic gradients with altitude. Thus, an in-depth knowledge of the geologic and hydrogeologic setting is crucial for a proper selection of sampling sites in order to obtain the best agreement with the theoretical predictions isotopic values.

The use of small springs to establish the isotopic altitude gradients is particularly appealing in areas where an appropriate network for rain water collection is not available, nor its implementation is feasible. In the Mediterranean climatic conditions, with prevailing fall-winter rains, the isotopic composition of springs well reflect the mean isotopic composition of precipitation. Another advantage is that springs do not require long monitoring periods, as the seasonal isotopic variations are normally smoothed. This makes springs suitable observation sites for monitoring the long term effects of the announced climatic changes on the isotopic composition of water.

REFERENCES

- [1] BRAS, R.L., Hydrology. An Introduction to Hydrology Science. Addison-Wesley Publishing Company (1990) 643.
- [2] JOUZEL, J., HOFFMANN, G., KOSTER, R.D., MASSON, V., Water isotopes in precipitation: data/model comparison for present-day and past climates, *Quat. Sci. Reviews* **19** (2000) 363–379.
- [3] CELLE-JEANTON, H., GONFIANTINI, R., TRAVI, Y., SOL, B. Oxygen-18 variations of rainwater during precipitation : application of the Rayleigh model to selected rainfalls in Southern France, *J. Hydrology* **289** (2004) 165–177.

- [4] GONFIANTINI, R., ROCHE, M-A., OLIVRY, J-C., FONTES, J-C., ZUPPI, G.M., The altitude effect on the isotopic composition of tropical rains, *Chem. Geol.* **181** (2001) 147–167.
- [5] KYLE, T.G., SAND, W.R., Water content in convective storm clouds. *Science* **180** (1973) 1274–1276.
- [6] ACKERMAN, B., WESTCOTT, N.E., Midwestern convective clouds. *J. Weather Modif.* **18** (1986) 87–94.
- [7] JOUZEL, J., Water stable isotopes: atmospheric composition and applications in polar ice core studies, In: *Treatise in Geochemistry* (H.D. Holland, K.K. Turekian Eds.), Vol. 4, *The Atmosphere* (R.K. Keeling Ed.) (2004) 213–243.
- [8] GONFIANTINI, R., GHERARDI, F., Modelling the isotope composition of precipitation. *International Workshop on Isotopic Effects in Evaporation*, Pisa, 3–5 May 2006, *Extended Abstracts* (2006) 86–89.
- [9] ROZANSKI, K., ARAGUÁS-ARAGUÁS, L., GONFIANTINI, R., Isotopic patterns in modern global precipitation, In *Continental Isotope Indicators of Climate*, AGU Geophys. Monograph, Am. Geophys. Union, Washington, D.C. (1993) 1–36.
- [10] LONGINELLI, A., SELMO, E., Isotopic composition of precipitation in Italy: a first overall map. *J. Hydrology* **270** (2003) 75–88.

ISOTOPES IN PRECIPITATIONS OF KINSHASA AREA: MOISTURE SOURCES AND GROUNDWATER TRACING

L. NDEMBO*, Y. TRAVI**, L.M. MOYENGO*,
J.N. WABAKAGHANZI*

*Commissariat Général à l'Energie Atomique,
République Démocratique du Congo

**Laboratoire d'Hydrogéologie,
Université d'Avignon et des Pays de Vaucluse,
Avignon, France

Abstract

Event samples of rains have been collected for stable and radioactive isotopes data (^{18}O , ^2H and ^3H) on Kinshasa area (Democratic Republic of the Congo) from September 2003 to November 2005 (IAEA TCP ZAI/8/013). Stable isotopes values for rainy seasons as a whole (September to May) shows a relatively narrow range of variation (-0.05 to -7.79‰ for ^{18}O) compared with that is generally observed in tropical areas. The local meteoric line ($\delta^2\text{H} = 8,12 \times \delta^{18}\text{O} + 15$) is distinct from World Meteoric Line. Mean values of deuterium excess are quite different in the main rainy season period (October–November in particular) with Deuterium excess (d) close to 10 associated with more depleted values, and in the more scarce rainfall event period (d up to 22). These later data may be linked to significant local recycling of air moisture from equatorial forest and/or surface water (Pool Malebo on the Congo River). In the context of siliceous and non carbonate aquifer with short renewal time, these data may be used, together with tritium and post nuclear radiocarbon, for tracing groundwater recharge.

1. INTRODUCTION

The Democratic Republic of the Congo, extending from Atlantic Ocean to the Eastern plateaus (longitude 32°E), covers the major part of the Congo basin. Within the Kinshasa area, western part of the territory, from latitude 3.9°S to 5.1°S , and longitude 15.2°E to 16.6°E , the Mont Amba aquifer has recently been studied with the IAEA support (TC project ZAI/8/013) using for the first time environmental isotopes (^{18}O , ^2H , ^3H , ^{13}C and ^{14}C). Rainfall isotope

composition has been determined, at individual event scale, from September 2003 to November 2005 (n = 150); groundwaters have also been investigated during the same period (8 campaigns on 20 sites). Data from former analyses, related to monthly rainfall (total rainfall accumulated during any given month, 1961 to 1968, n = 59) are available as data stored in the IAEA database (GNIP); Samples were collected at the meteorological station of Binza, located about 4 km far from the current Mont Amba station.

11 rainy season samples are then available in the studied area, including 3 from Mont-Amba station (event scale), and 8 from Binza station (monthly scale), the last 3 rainy seasons showing some incomplete data.

The aim of this paper is mainly to present isotopic data from rainfall with two goals: -firstly characterizing the input signal and its spatial and temporal variability for their use in hydrogeological investigations. In a preliminary approach, the rainfall signature is compared to groundwater isotope contents. And, - secondly, briefly discussing this spatial and temporal distribution pattern in the context of regional atmospheric circulation.

With the exception of some more localized convective rains, the pluviometric regime of Southern part of Democratic Republic of the Congo is determined by the seasonal displacement of the Inter tropical Convergence Zone and the Inter Oceanic Confluence (IOC). The later results from the front of the trade winds originated by the Mascareignes anticyclone (South-East) and those from the "Sainte Helène" deflected to South East. In this context, the CIO is of convergent nature and determines the rainy season in Kinshasa [1].

Isotopic and chemical studies of precipitation for hydrogeologic and hydrologic purposes need average, annual or monthly approaches [2, 3] and [4]. With these time scale, the long term data sampling offers the means to describe global process, without apprehending the mechanism inducing local precipitation composition. In a more reduced time scale, this data allow to show off the effect of meteorological parameters on the isotopic composition of precipitations [5].

In this paper, the typical isotopic values of rains and their evolution during the rainy season are at first examined in term of local meteorological parameters: temperature, atmospheric humidity and height of precipitation. The local meteoric line is also defined, which constitute the reference for the determination of the origin and the evolution of natural waters with the isotopic data [6 and 7].

Secondly, seasonal characteristics and long term evolution of isotopic composition of precipitation are examined within the context of Southern Africa.

2. RESULTS AND DISCUSSIONS

2.1. Rainfall isotopic composition: climatic parameters and seasonality

The data sampled between 2003 and 2005 at Mont-Amba shows that the ^{18}O (‰) contents of the rain, on an event-driven scale, vary between -7.99 and -0.05 ‰ (median 3.43 ‰), and from -52.44 to 15.54 ‰ (median -12.40 ‰) for deuterium. Deuterium excess (d) varies between 7.56 and 22.36 ‰ (median 14.83 ‰). Considering the 3 rainy seasons, the ^{18}O and ^2H weighted means values are -4.5 and -22.24 ‰, respectively.

Over the same period, the extreme values of the climatic parameters are 6.50 and 106.50 mm for the monthly precipitation (median 31.97 mm), 24 and 30.5°C (median 28.5°C) for the air temperature, and 70.25 and 97.50% for the relative humidity (median 81.27%).

For the Binza station, the monthly weighted means contents of stable isotopes are included between -8.5 and -0.1 ‰ (median 3.90 ‰) and, -57.6 and 15.60 ‰ (median -12.40 ‰), respectively for ^{18}O and ^2H . For the whole rainy seasons, the weighted means contents are -3.44 ‰ ^{18}O and -12.11 ‰ ^2H .

Deuterium excess (d) varies between 3.8 and 28.4 ‰ (median 13.3 ‰). The extreme values of the climatic parameters are: 10 and 404 mm (median 144.9 mm) for the monthly precipitation and 20.7 and 25.9° (median 24.55°C) for the average temperature. Data of the relative humidity were not available for this period.

Figures 1a and 1b present the evolution of the ^{18}O contents and deuterium excess (d) versus precipitation for the two stations, during the rainy season. Data for Mont Amba (monthly weighted means O-03/04, O-04/05) are compared with that of Binza (monthly weighted means over the period 61-65, indicated O-60). It is noted that, (i) ^{18}O and d excess vary seasonally with an isotopic enrichment at the beginning of rainy season, and also during the small dry season which is spread out between mid January and mid February; (ii) a good relation seems to exist with the precipitation (amount effect), except at the end of the season for the years 2000 (Amba station) where one observes a net enrichment compared to the values of the Binza station which appear more in agreement with the precipitation; (iii) deuterium excess appears to increase during the rainy season, with a peak more peak marked during the driest period, in particular for the years 2000.

At event and monthly scale (table 1) the correlation (Pearson) of isotope contents with amount of rainfall, air temperature and relative humidity is generally poor or inexistent (coeff. below 0.5). It could be noted a better correlation with temperature at event scale (Mt Amba) during the rainy period (whereas temperature represent average of the given month), and a better

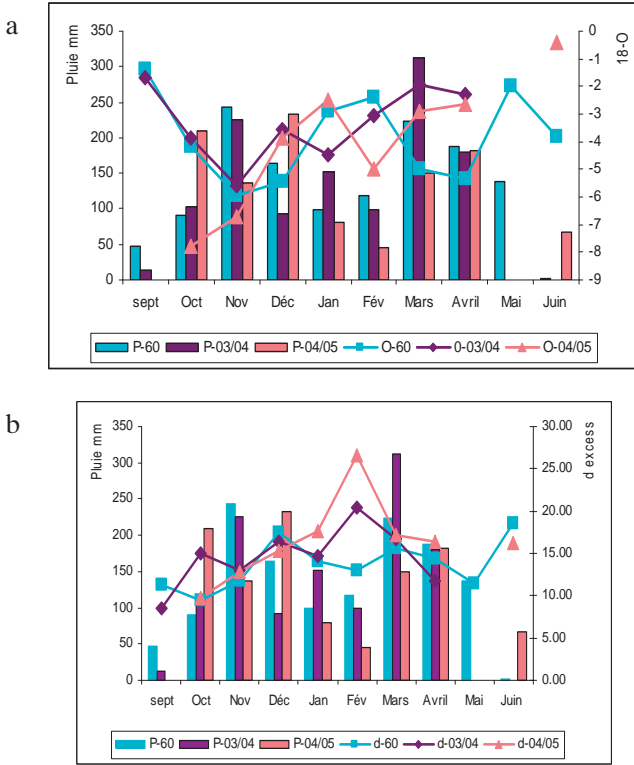


FIG. 1. a). $\delta^{18}O$ evolution during the rainy season. b). d -excess evolution during the rainy Kinshasa – DR Congo season, Kinshasa – DD Congo.

monthly correlation with the rainfall amount for Binza (sixties) whereas there is no correlation for the Amba station ($r^2 \text{ }^{18}O = 0.086$ for Mont Amba et -0.619 for Binza), mainly related to the last part of the rainy season.

The relatively good correlation between amount effect and isotope content for the Binza station is illustrated on Fig. 2.

If we except the amount effect, the rainfall isotope content and deuterium excess (Fig. 1a and 1b) seem to be strongly influenced by the regional atmospheric circulation process. Seasonally, depleted values regularly observed in November/December could be linked to the ITCZ control, associated with the grains lines which moving from east to west while producing strong stormy precipitations [8]. The reduction of the rains of the small dry season, between January and February, most likely associated with the influence of the North-

ISOTOPES IN PRECIPITATIONS OF KINSHASA AREA

TABLE 1. CORRELATION ARRAY (PEARSON) : RAINFALL, ^{18}O , ^2H , d-EXCESS, RH AND T°C

Variables	Site	T($^\circ\text{C}$) air	^2H	^{18}O	HR	Lame	d excess
t($^\circ\text{C}$) air	Amba	1					
	Binza						
^2H	Amba	0.458	1				
	Binza	-0.296					
^{18}O	Amba	0.513	0.981	1			
	Binza	-0.253	0.961				
RH	Amba	-0.572	-0.494	-0.521	1		
	Binza	nd	nd	nd			
Rain	Amba	-0.017	0.139	0.086	-0.067	1	
	Binza	0.376	-0.597	-0.619	nd		
d-excess	Amba	-0.194	0.266	0.074	0.052	0.287	1
	Binza	-0.16	0.156	-0.123	nd	0.07	

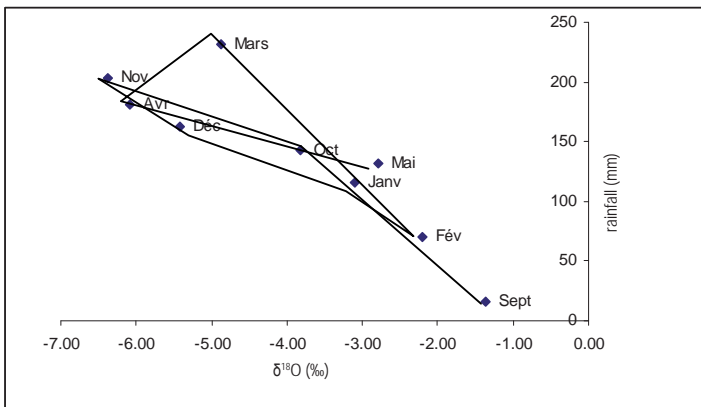


FIG 2. Amount effect observed at Binza station.

East “Alizé”, heat and dry, is accompanied by the enrichment of the ^{18}O and ^2H contents and higher values of d ; these last suggest a local vapour recycling

2.2. $\delta^2\text{H}$ vs ^{18}O relationship

The dispersion of points around the meteoric line reflects space and temporal variability of climatic parameters (origin and history of the masses of vapour, secondary evaporation of the rains in the event, vapour recycling,) which locally affects the slope as well as deuterium excess of the local meteoric line.

The local meteoric water lines, $\delta^2\text{H}$ vs ^{18}O (Fig. 3), derived from monthly data (Binza) and individual event are defined by the equations: $\delta^2\text{H} = 7.7 \times ^{18}\text{O} + 12.3$ ($r^2 = 0.96$; $n = 59$) with monthly weighted means related to the sixties (LML Binza), and $\delta^2\text{H} = 8.11 \times ^{18}\text{O} + 15$ ($r^2 = 0.94$; $n = 129$) with individual event data from 2003 to 2005 (LML Amba).

The slope of regression lines, close to 8, is slightly different; this difference is probably due to measurement and sampling conditions. This also indicates that the influence of droplets evaporation is not significant and that more enriched values observed in the middle (short drier period) and the end of rainy season (Mt Amba station), are, most probably, associated with the regional circulation patterns (see also Fig. 1).

As already observed, the deuterium excess, defined as $d = \delta^2\text{H} - 8 \times \delta^{18}\text{O}$ is, in most cases, greater than 10 [14], and the local lines are clearly above the so-called Global Meteoric Water Line (GMWL) $^2\text{H} = 8 \times \delta^{18}\text{O} + 10\text{‰}$ [9].

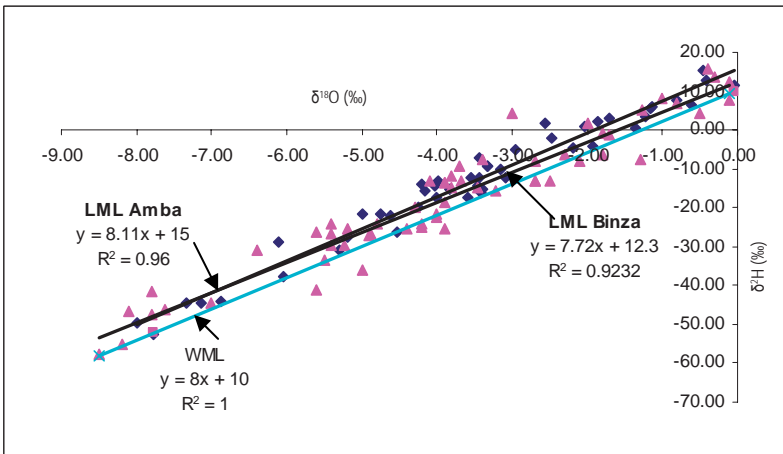


FIG. 3. The $\delta^2\text{H}$ vs. ^{18}O diagram based on monthly (Binza) and event (Amba) precipitations for Kinshasa stations.

ISOTOPES IN PRECIPITATIONS OF KINSHASA AREA

These results suggest that, especially in the short rain period middle of the rainy season, rain is produced with a substantial contribution of recycled moisture; such observation has already been suggested by meteorological studies [10], considering strong evapotranspiration in this region [11] and large stretch of water of more than 400 km² associated with the Congo River (Pool Malebo).

For hydrogeological investigations, taking into account the large annual variation of isotope contents in tropical regions [12, 13], the local meteoric water line related to recent event data (2003-2005, n = 129) will be chosen as input signature: $\delta^2\text{H} = 8.11 \times \delta^{18}\text{O} + 15$

2.3. Rainfall signature and groundwater isotope content

Figure 4 and Fig. 5 illustrate the groundwater response to seasonal variability of the isotopic signal in precipitation, and the $\delta^2\text{H} - \delta^{18}\text{O}$ plot of the groundwater isotope data. The groundwater isotopic means values appear to be slightly enriched when compared to rainfall isotope weighted mean value. This implies a significant evaporation on the ground, before or during infiltration. The data points presented on Fig. 5 lie under the Local meteoric line, suggesting an evaporative enrichment. All along the rainy season, the variability of the input signal does not produce a significant variability in the groundwater

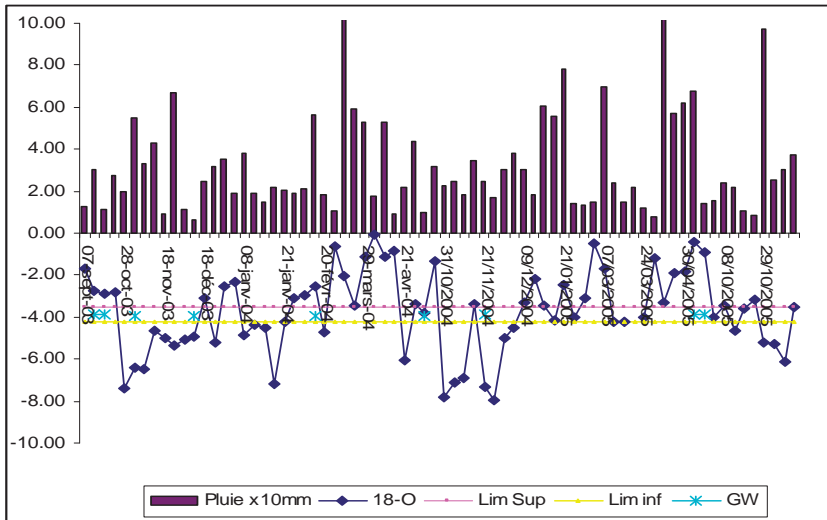


FIG. 4. Variability of the isotope signal in precipitation on event basis, compared to isotope signature evolution in groundwater.

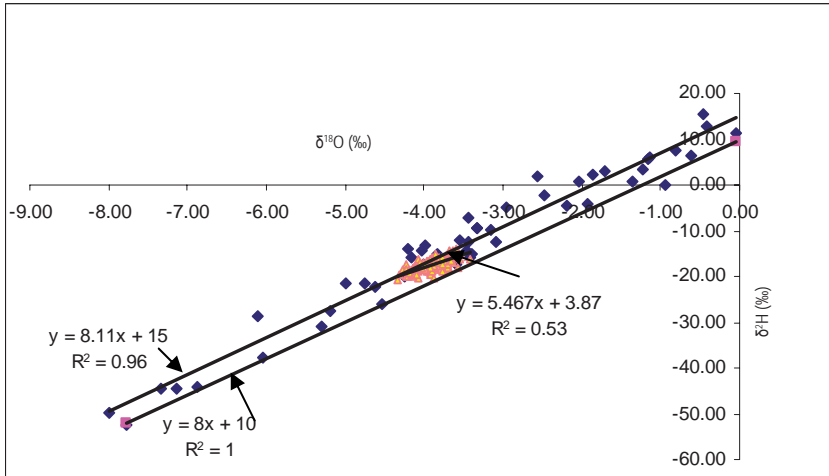


FIG. 5. Isotope composition of groundwater plotted on the $\delta^2\text{H} - \delta^{18}\text{O}$ diagram.

signature, suggesting that infiltrating water is submitted to substantial mixing before reaching the aquifer, and also a low aquifer renewal rate at event scale.

2.4. Long term trends and regional context

At yearly scale, the correlation ^{18}O with cumulative rainfall is very poor, as already observed in these regions [6] highlighting that the control on long term fluctuation in isotope content in precipitation is mainly due to the regional processes.

Comparing the data from Binza station (sixties) to that of Mt Amba (200–2005) one can observe an apparent shift towards more positive ^{18}O values during the third part of the rainy season. The reasons may include changes in the source of vapour, varying contribution of moisture from different origins or a modification of air mass circulation patterns. Unfortunately, the available record is too short and incomplete to allow any definite conclusion with regard to the significance of this evolution in a zone climatically poorly understood. This highlights the necessity to continue a regular rainfall sampling.

REFERENCES

- [1] LEROUX M., Le climat de l'Afrique tropicale, tomes 1 et 2, Edit Slatkine, Genève -Paris (1983) 633.
- [2] YURTSEVER, Y., GAT, J.R., Atmospheric waters. Stable isotope hydrology: deuterium and oxygen in the water cycle. IAEA, Technical Report, Serie n° 210. (1981) 103–143.
- [3] ROZANSKI, K., ARAGUAS ARAGUAS, L., GONFIANTINI, R., Relation between long-term trends of oxygen-18 isotope composition of precipitation and climate. *Science* **258** (1992) 981–985.
- [4] GONFIANTINI, R., On the isotopic composition of precipitation. Proceedings, International symposium. *European Geologist* **2** (1995) 5–8.
- [5] INGRAHAM, N.L., Isotopic variations in precipitation. *Isotopes tracers in Catchment Hydrology* (C. Kendall, C., J.F. Mc Donnel, Eds) Elsevier, Amsterdam. (1998) 87–118.
- [6] ROZANSKI, K., ARAGUAS ARAGUAS, L., GONFIANTINI, R., Isotopic patterns in modern global precipitation, In: *Continental Isotopes Indicators of Climate*, American Geophysical Union Monograph (1993).
- [7] CLARK, I., FRITZ, P., *Environmental Isotopes in hydrogeology*, CRC Press LLC (1997) 328.
- [8] QUOIDBACH, J., GOLBERT, G., Vents en altitude au Congo, Institut Royal Météorologique de Belgique (1971).
- [9] CRAIG, H., Isotopic variations in meteoric water, *Sciences* **133** (1961) 1702–1703.
- [10] GONG, C., ELTAHIR, E. A. B., Sources of Moisture for Rainfall in West Africa, *Water Resources Research* **32** (1996) 3115–3121.
- [11] NDEMBO, L., MAKOKO, M., Flux d'eau et transfert des solutés dans les horizons profonds des sols du Mont Amba, *Annales de la Faculté des Sciences Agronomiques de l'Université de Gand / Belgique* (2001) 115–122.
- [12] LE GAL LA SALLE, C., Circulation des eaux souterraines dans l'aquifère captif du Continental Terminal – Bassin des Iullemeden, Niger, *Méthodologie et applicatipons: isotopes stables de la molécule de l'eau, carbone-14, chlore-36, uranium et gaz noble*, Thèse de doctorat, Université de Paris sud (1994) 174.
- [13] TAUPIN, J. D., GALLAIRE, R., ARNAUD, Y., Analyses isotopiques et chimiques des précipitations sahéliennes d la région de Niamey au Niger: implications climatiques, *Hydrochemistry: proceedings of the Rabat Symposium*, IAHS. Publication No. 244 (1997).

NON-MASS DEPENDENT OXYGEN ISOTOPE EFFECT OBSERVED IN WATER VAPOUR FROM ALERT, CANADA

Y. LIN*¹, L. HUANG**, R.N. CLAYTON**^{‡§}

*The Department of the Geophysical Sciences,
The University of Chicago,
Chicago, Illinois, USA

**Atmospheric Science and Technology Directorate
Science and Technology Branch,
Environment Canada,
Toronto, Ontario, Canada

[‡]The Enrico Fermi Institute,
The University of Chicago,
Chicago, Illinois, USA

[§]Department of Chemistry,
the University of Chicago,
Chicago, Illinois, USA

Abstract

Twenty-six precipitation samples from Chicago, IL and northwest part of Indiana were collected from 2003 to 2005. Twenty-five water vapour samples were collected at Alert, Canada (82.5°N, 62.3°W) from 2002 to 2005 by Environment Canada. Seven ice core samples from Dasuopu glacier, Chinese Himalayas (28.2°N, 85.4°E) were drilled by Lonnie G. Thompson and prepared by Mary E. Davis. Sample of Standard Light Antarctic Precipitation (SLAP) is available in the laboratory. Water samples were reacted with bromine pentafluoride to produce oxygen, which was then purified and measured by Delta E gas source mass spectrometer. Oxygen isotopic compositions are reported in delta notations and relative to VSMOW. A $\lambda_{\text{MDF}}(\text{H}_2\text{O}) = 0.5292 \pm 0.0031$ (2σ) is determined from three-isotope plot of local precipitation samples. No oxygen isotopic anomaly is found in ice core samples from Dasuopu glacier, Chinese Himalayas. $\Delta^{17}\text{O}$ of $0.076 \pm 0.075\text{‰}$ (2σ) is observed in water vapour from Alert, Canada. Standard

¹ Present address: 5734 S. Ellis Ave., The Department of the Geophysical Sciences, The University of Chicago, Chicago, Illinois 60637, USA

Light Antarctic Precipitation (SLAP) possesses a positive anomaly of 0.059‰. Stacked seasonal trend of $\Delta^{17}\text{O}$ observed at Alert, Canada points toward a maximal value in late spring, which may be due to the lowering of the tropopause level, increasing tropopause folding events, and lowering the Planetary Boundary Layer (PBL) mixing height at the Arctic during spring time. Thus, the intrusion of stratospheric air is at its maximum.

1. PURPOSE AND LAYOUT

Positive oxygen isotopic anomalies (^{17}O excess) have been observed in atmospheric O_3 , CO_2 , N_2O , CO , sulfate aerosols, and H_2O_2 in natural water. Ref. [1] and [2] predicted positive anomalies up to 13‰ and 10‰ in stratospheric water. Ref. [3] predicted a maximum of 30 ‰ in $\Delta^{17}\text{O}$ of stratospheric water vapour. Direct cryogenic sampling of water vapours from the upper troposphere and the lower stratosphere over New Zealand did not yield a significant oxygen isotopic anomaly with large uncertainties involved as in [4].

The goal of this study is to identify oxygen isotopic anomalies in high latitude or high altitude tropospheric water vapour.

Based on the knowledge of variation of the height of the tropopause and general global circulation, two sites were chosen to observe the signals of oxygen isotopic anomalies from the stratosphere. The first site is Alert, Canada (82.5°N, 62.3°W), where the tropopause height is low and where there is downward intrusion of stratospheric air. The second site is Dasuopu glacier in the Chinese Himalayas (28.2°N, 85.4°E), where the altitude is high (7.2 km), yet is close to the tropics.

2. SAMPLE COLLECTION

Four different sample sets — local precipitations, water vapour from Alert, Canada, ice core samples from Dasuopu glacier, Chinese Himalayas, Standard Light Antarctic Precipitation (SLAP) — are involved in this study. Detailed sample collection procedures are in [5].

Twenty-one rain water and five snow samples were collected in Chicago, IL and northwest Indiana from 11/03/2003 to 03/25/2005. Air samples were collected at ground level from 7/02/2002 to 8/08/2005 at Alert, Canada by Environment Canada personnel (coordinated by Lin Huang). Alert is located at the northeastern tip of Ellesmere Island in the Canadian Arctic. The area is approximately 100 m above sea level. Alert is in complete darkness from November to April. Collection periods were variable, ranging from one to three months. Twenty-five water vapour samples were trapped as a by-product

NON-MASS DEPENDENT OXYGEN ISOTOPE EFFECT OBSERVED IN WATER

of air collection for *in situ* measurements in CO₂. Seven ice core samples from Dasuopu glacier, Chinese Himalayas were obtained from the Ohio State University (courtesy of Mary E. Davis and Lonnie G. Thompson). The Himalayas contain the largest volume of ice outside the Polar Regions. Three cores, each 159.9 m, 149.2 m, 167.7 m long, were recovered from different sites on the relatively flat portion of the Dasuopu Glacier at an elevation of 7200 m in 1997 by Lonnie G. Thompson. All seven ice core samples obtained for this study are from the third core. The samples were cut between dry season dust peaks by Mary E. Davis. For example, Icecore-1975 was cut between the 1974/1975 dust layer and the 1975/1976 dust layer. Half of each of the dust layers was included, so Icecore-1975 would contain late dry season of 1974/1975 plus wet season (summer) 1975 plus early dry season of 1975/1976.

3. SAMPLE ANALYSIS

In this study, water samples were reacted with BrF₅ following the method of [6] as reaction:



Milligram-sized samples of water were reacted with bromine pentafluoride in a nickel vessel to liberate oxygen in 100% yield. The temperature of the Ni reaction tube is 200°C rather than 80°C in the original method. The higher temperature would decompose metastable reaction products, such as O₃ and H₂O₂, which form in the explosive reaction of BrF₅ and H₂O. After fluorination, each water sample was further purified through a 15× molecular sieve, before being introduced into the mass spectrometer.

All mass spectrometric analyses were done with Delta E gas source isotope ratio mass spectrometer and the results are reported in delta notation relative to VSMOW.

External precisions of δ¹⁸O, δ¹⁷O, and Δ¹⁷O for the entire fluorination and mass spectrometric analysis are taken from 2σ standard deviations of δ¹⁸O, δ¹⁷O, Δ¹⁷O of ten analyses of VSMOW. 2σ external precisions determined in such a way are 0.352‰, 0.674 ‰, and 0.045‰ for δ¹⁷O, δ¹⁸O, and Δ¹⁷O respectively.

4. RESULTS AND DISCUSSION

Table 1, 2, and 3 in [5] showed the date of sample collection, the date of fluorination, O₂ preparation number, yield (%) of fluorination, the date of mass

spectrometer analysis, working standard used in mass spectrometer analysis, $\delta^{18}\text{O}$, $\delta^{17}\text{O}$, their 1σ standard errors (internal precisions of mass spectrometer), and $\Delta^{17}\text{O}$ of twenty-six local rain and snow samples, one SLAP, twenty-five water vapour samples from Alert, Canada, and seven ice core samples from Dasuopu glacier, Chinese Himalayas.

4.1. Laboratory-specific $\lambda_{\text{MDF}}(\text{H}_2\text{O})$

For a small deviation from the mass-dependent fractionation line, as in the case of atmospheric water, it is important to determine the precise λ value of mass-dependent fractionation (MDF), $\lambda_{\text{MDF}}(\text{H}_2\text{O})$. This $\lambda_{\text{MDF}}(\text{H}_2\text{O})$ varies with the mass spectrometers used. A laboratory-specific $\lambda_{\text{MDF}}(\text{H}_2\text{O})$ was determined by analyzing local precipitation samples.

Oxygen isotopic compositions of local precipitation samples are plotted on a three-isotope plot as in Fig. 1 with a slope of 0.5292 ± 0.0031 and an intercept of 0.071 ± 0.034 through model-2 fit of Isoplot 3.00 (courtesy of Ken R. Ludwig, the University of California, Berkeley). Model-2 fit of Isoplot 3.00 assigns equal weights and zero error-correlations to each point. This regression avoids the mistake of weighting the points according to analytical errors when some other causes of scatter are involved, as in the case of local precipitation samples, temperature and sources of moisture could likely generate additional

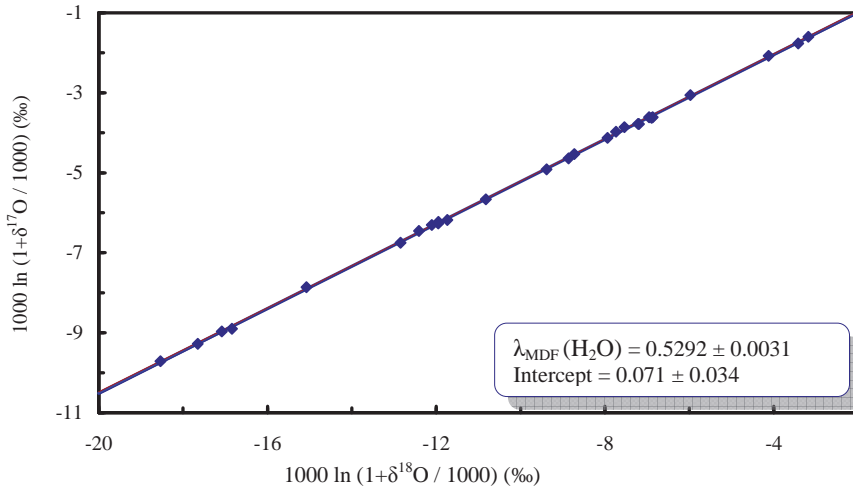


FIG. 1. Oxygen isotopic compositions of rain and snow samples collected in the Chicago area, reported relative to VSMOW.

scatter in the data. As a result of this regression, the uncertainties of the fit shown are the lower limits.

4.2. Oxygen isotopic anomalies observed

With this laboratory-specific $\lambda_{MDF}(H_2O) = 0.5292$, an average $\Delta^{17}O$ ($\Delta^{17}O = [\ln(1 + \delta^{17}O) - 0.5292 \times \ln(1 + \delta^{18}O) - 0.071] \times 1000\text{‰}$) of 0.076‰ for water vapour samples from Alert, Canada is observed with a 2σ standard deviation 0.075‰ and a 2σ uncertainty of 0.045‰ as in Fig. 2. $\Delta^{17}O$ is 0.059‰ in Standard Light Antarctic Precipitation (SLAP). The average $\Delta^{17}O$ is 0.009‰ for ice core samples from Dasuopu glacier, Chinese Himalayas. These ice core samples are mass-dependently fractionated. Local precipitation samples, although scattered, have a mean of zero in $\Delta^{17}O$. This scatter in $\Delta^{17}O$ of local precipitation samples is likely caused by other factors in addition to sample analysis since the 2σ standard deviation of 0.066‰ is larger than the 2σ external precision of 0.045‰. Possible factors are kinetic fractionations such as kinetic evaporation and kinetic diffusion occurring during precipitation, re-evaporation of raindrops and sublimation of snow.

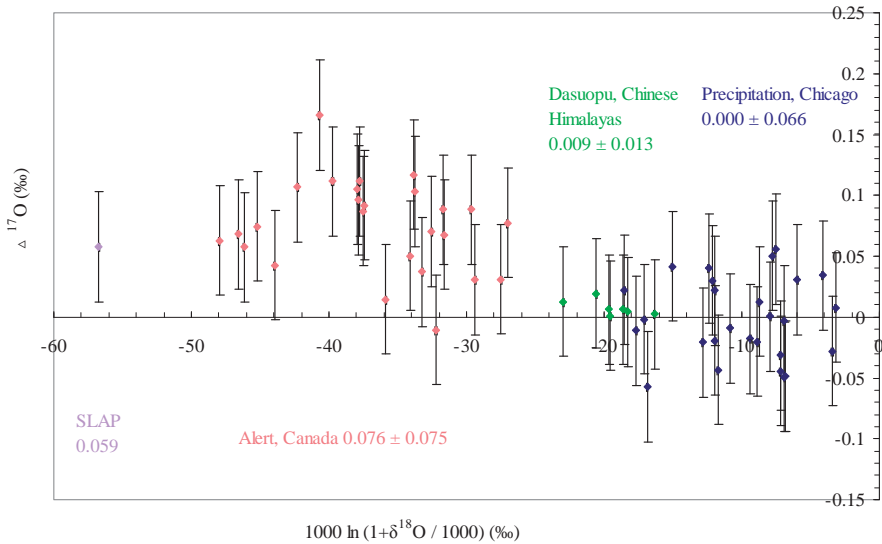


FIG. 2. Oxygen isotopic anomalies observed in water samples determined by a $\lambda_{MDF}(H_2O) = 0.5292 \pm 0.0031$ (2σ). Coral diamonds denote water vapours from Alert, Canada; Green diamonds denote ice core samples from Dasuopu glacier, Chinese Himalayas; Lavender diamonds denote Standard Light Antarctic Precipitation (SLAP); and blue diamonds denote local precipitation samples. The means of the oxygen isotopic anomalies are shown in texts with their 2σ standard deviations. 2σ error bar is shown for each datum.

4.3. Seasonal trend observed in $\Delta^{17}\text{O}$ of water vapour samples from Alert, Canada

Stacked seasonal variation in $\Delta^{17}\text{O}$ in water vapour samples from Alert, Canada as shown in Fig.3 could be explained by the seasonal trend of the downward mass flux in the northern hemisphere and in the seasonal trend of the height of Arctic tropopause and the height of Planetary Boundary Layer (PBL) at Alert. The maximum of downward mass flux of the northern hemisphere occurs in late spring months and the minimum occurs in winter months as in [7]. The height of Arctic tropopause is at its maximum in late spring months and at its minimum in summer months as in [8]. With the maximum of the downward mass flux and the minimum height of Arctic tropopause occurring in late spring, the maximum of $\Delta^{17}\text{O}$ would reasonably occur in late spring.

5. SUMMARY

This study addresses the question of whether there is an oxygen isotopic anomaly in stratospheric water by measuring water vapour samples from the North Pole and the South Pole, where downward air transports from the stratosphere into the troposphere take place.

By measuring twenty-six local rain and snow samples in the Chicago area, $\lambda_{\text{MDF}}(\text{H}_2\text{O})$ is determined to be 0.5292 ± 0.0031 . Positive anomalies with a maximum value of 0.167‰ and a mean of 0.076‰ with a 2σ standard

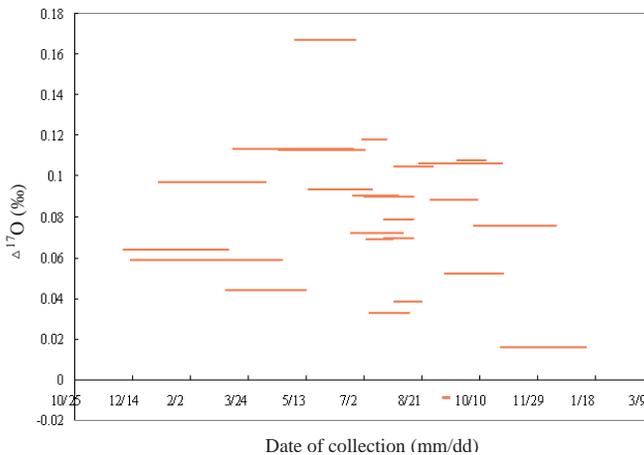


FIG. 3. Stacked seasonal variation of $\Delta^{17}\text{O}$ in water vapour samples from Alert, Canada, with a maximum in late spring.

deviation of 0.075‰ are observed in water vapour samples from Alert, Canada. Stacked seasonal trend of $\Delta^{17}\text{O}$ has a maximum in spring time, during which the height of Arctic tropopause is at its minimum and the intrusion of air from the stratosphere is at its maximum. These are strong evidence that non-mass dependent (NMD) oxygen isotope fractionation does occur in the stratosphere and gets transferred into water vapour.

These anomalies could be explained by the transfer of positive oxygen isotopic anomalies through $\text{O}_3 \rightarrow \text{NO}_x \rightarrow \text{HO}_x \rightarrow \text{H}_2\text{O}$ chain in the stratosphere as in [9], [2], and [3], and the subsequent mixing of this anomalous stratospheric water with tropospheric water vapour at Alert, Canada or Antarctica where the tropopause heights and PBL heights are low and where downward mixing of stratospheric air with tropospheric air takes place and reaches the surface.

ACKNOWLEDGEMENT

Authors sincerely thank Tim Christie, Kevin Anderson, Maria Vavro and Brad Hansen, as the contractors at Alert Observatory (2002–2003), and Andrew Platt, Alina Chivulescu and Kessler Robert, at Environment Canada, for water vapour samples collections, logistic support and technical advice.

REFERENCES

- [1] LYONS, J.R., Mass-independent fractionation in stratospheric water: a potential new indicator of provenance, *Geophysical Research Abstracts* **5** (2003) 13565.
- [2] BECHTEL, Ch., ZAHN, A., The isotope composition of water vapour: a powerful tool to study transport and chemistry of middle atmospheric water vapour, *Atmos. Chem. Phys. Discuss.* **3** (2003) 3991–4036.
- [3] ZAHN, A., FRANZ, P., BECHTEL, C., GROOSZ, J.U., RÖCKMANN, T., Modeling the budget of middle atmospheric water vapour isotopes, *Atmos. Chem. Phys.* **6** (2006) 2073–2090.
- [4] FRANZ, P., RÖCKMANN, T., High-precision isotope measurements of H_2^{16}O , H_2^{17}O , H_2^{18}O , and the $\Delta^{17}\text{O}$ -anomaly of water vapour in the southern lowermost stratosphere, *Atmos. Chem. Phys. Discuss.* **5** (2005) 5373–5403.
- [5] LIN Y., HUANG, L., LYONS, J.R., CLAYTON, R.N., Possible evidence for non-mass dependent oxygen isotope effects in water vapours from Alert, Canadian Arctic, *Isotopes Environ. Health Stud.* (2007) submitted.
- [6] O'NEIL, J.R., EPSTEIN, S., Oxygen isotope fractionation in system dolomite-calcite-carbon dioxide, *Science* **152** (1966) 198–201.

- [7] APPENZELLER, C., HOLTON, J.R., ROSENLOF, K.H., Seasonal variation of mass transport across the tropopause, *J. Geophys. Res.* **101** (1996) 15071–15078.
- [8] NAGURNY, A.P., Climatic characteristics of the tropopause over the Arctic Basin, *Ann. Geophys.* **16** (1998) 110–115.
- [9] LYONS, J.R., Transfer of mass-independent fractionation in ozone to other oxygen-containing radicals in the atmosphere, *Geophys. Res. Lett.* **28** (2001) 3231–3234.

SURFACE WATER DYNAMICS

DYNAMICS OF WATER TRANSPORT THROUGH THE VELIKA MORAVA CATCHMENT

N. MILJEVIC, D. GOLOBOCANIN, A. MILENKOVIC
Vinča Institute of Nuclear Sciences

M. NADEZDIC
Republic Hydrometeorological Service of Serbia

Belgrade, Serbia

Abstract

The Velika Morava (tributary of the Danube) is the largest river entirely situated in Serbia with an average annual outflow of 220 m³/s. Environmental isotopes (deuterium, tritium, oxygen-18) together with hydrochemical parameters (water temperature, pH value, electrical conductivity, major ions, and flow measurements) were applied to study dynamics of hydrological cycle in this macro-scale catchment (37.4 km² area). Used data are spanned during a two-year period, September 2004 to December 2006. Stable water isotope composition of analysed samples from three meteorological stations, seven sites for water quality and 25 piezometers followed the Global Meteoric Water Line (GMWL) indicating a common water origin and a relation between the flows of surface and shallow underground waters in the basin. Precipitation isotope composition exhibited strong seasonal variations, which although significantly damped within the catchment, were reflected in stream water at analysed sampling sites. Using the sinusoid curve-fitting method for variations of oxygen-18 content in precipitation and stream water, the mean transit time of water in the catchment was estimated.

1. INTRODUCTION

Isotope methods were introduced into catchment hydrology research in the 1960s as complementary tools to conventional hydrological methods for addressing questions of where water goes when it rains, what pathways it takes to the stream and how long water resides in the catchment [1]. Naturally occurring stable (²H, deuterium and ¹⁸O) and radioactive (³H, tritium) isotopes of the water molecules have been common tools for assessing relative contributions of flow derived from uniquely labelled geographical sources or distributed components such as direct precipitation runoff, shallow and deep groundwater, surface waters including lakes and wetlands and water dating

up to about fifty years of age. River discharge consists mainly of two principal components, surface run off of precipitation and groundwater seepage. Isotope signals in river discharge can potentially contribute to better understanding of the continental portion of the hydrological cycle, including information such as water origin, mixing history, water balance, water residence times, surface-groundwater exchange and renewal rates, and evaporation-transpiration partitioning.

Hydrochemistry of the Velika Morava catchment has been studied extensively over the last 15 years.

The aim of this investigation is to use isotope techniques for better understanding of dynamics of surface water systems and their interaction with groundwater through the Velika Morava catchment.

2. STUDY AREA

2.1. Hydrogeological settings

The Velika Morava catchment, entirely situated in Serbia (Balkan Peninsula), drains a total inland basin of 37 400 km² with an altitude range from 70–1500 m asl (Fig. 1). The river formed at town Stalac by the junction of two rivers, the Zapadna Morava (15.680 km², 295 km) and the Juzna Morava (15.400 km², 308 km) is 185 km long and flows up north to the Danube River. The discharge measured at the outlet of the watershed at Ljubicevski station, near its confluence (21.75 km) is 240 m³/s annually with maximum in the spring (March–April, 430 m³/s) and minimum in late summer (August–September, 90 m³/s) based on the 1946–1984 period record.

The region falls in the European moderate continental climate zone with four seasons (cold winter and hot summer) with mean annual temperature of around 11°C and humidity of 74%. The annual precipitation amount, which mainly falls as rain, though snow does occur during the winter months, varies from 590 mm (south-east part) to 761 mm (west part) for the 1961–1990 period. The highest precipitation period is May–July (up to 90 mm monthly) and the period January– March (down to 40 mm monthly) is with the lowest precipitations.

The catchment is presented by the mountainous regions of Rhodopian system, igneous rocks, serpentinites, Proterozoic and Paleozoic crystalline schist complex (mica shists, gneisses, marbles, quartzites), limestone and weakly coherent Neogene sediments of intergranular porosity. The latter begin with basaltic conglomerates overlying the Cretaceous sediments and crystalline schists [2]. The non-uniform alluvium deposits (approximately 7–17 m thickness)

DYNAMICS OF WATER TRANSPORT THROUGH THE VELIKA MORAVA

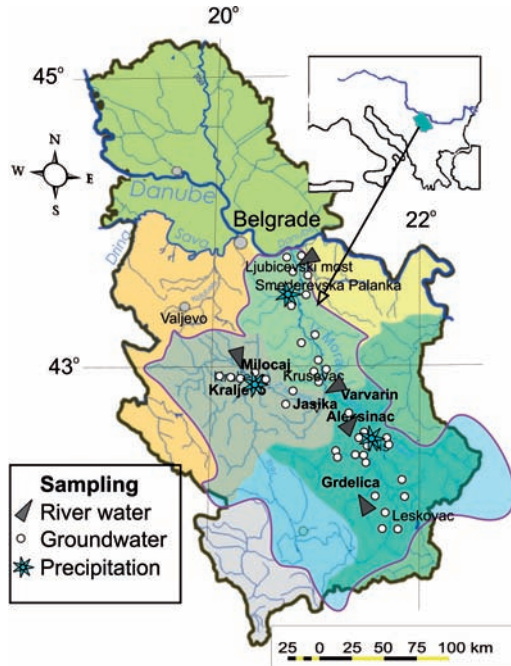


FIG. 1. Map of the Velika Morava catchment with locations of isotopic sampling network: precipitation meteorological stations (stars), hydrogeological stations (triangles) and groundwater (piezometers – open circles).

are composed by Quaternary sand-gravel (hydraulic conductivity $2-7 \times 10^{-3}$ m/s) in crossing with silt and silty clays with a saturated thickness of as much as 7 m and well yields of as much as 10 L/s. Water bearing strata consist of sands from Miocene-Pliocene, Quaternary gravelly-sand deposits and alluvial planes of the rivers Velika Morava, Južna Morava and Zapadna Morava. In the southern part of the region, water bearing strata of a fracture porosity is widely spread. Groundwaters accumulated in alluvial water bearing deposits are hydraulically connected with surface waters. Recharge to the aquifer is assumed to occur as percolation of water from precipitation to the water table, as movement of water from the Velika Morava River and tributaries into the aquifer, and as discharge of groundwater from underlying or lateral deposits into the valley deposits. Soil coverage in the catchment is mainly cambisol and luvisol while the alluvial plane land is dominated by fluvisol [3] and mainly used as agricultural cropland.

2.2. Sample collection

The field activities for precipitation, river water and groundwater sampling have been carried out since September 2004 via cooperation with regular long-term governmental monitoring conducted by the Republic Hydrometeorology Service of Serbia. The cumulative monthly precipitation samples for isotopic analyses were collected at three meteorological rain gauge stations, Smederevska Palanka (20°57E, 44°22N, 121 m asl), Nis (21°54E, 43°20N, 202 m asl), and Kraljevo (20°42E, 43°42N, 215 m asl) (Fig. 1) assuming they were representative of catchment-average inputs. Grab river water samples on a quarterly basis were collected on the same day at seven stream hydrological gauging stations (one near the confluence of the river and the other high away upstream) since September 2004 and sampling program is still underway. Collection of shallow groundwater samples was performed once a year from 25 piezometers (3–21 m depth, diameter 50 to 105 mm) installed in the sections perpendicular to the direction of surface water flow in the distance between 0.2 and 13 km from the river.

3. Materials and methods

Samples for isotopic analyses were collected and stored according to standard procedures [4] while sampling, preservation and analytical protocols for chemical analyses were conducted in accordance with standard methods for surface waters [5]. The samples were analysed for stable isotopes (deuterium and oxygen-18) and radioactive isotope tritium as well as hydrochemical parameter, water temperature, pH value, electrical conductivity and major anions (CO_3^{2-} , HCO_3^- , NO_3^- , SO_4^{2-} , Cl^-) and cations (K^+ , Na^+ , Ca^{2+} , Mg^{2+}).

The isotopic composition of $^2\text{H}/^1\text{H}$ and $^{18}\text{O}/^{16}\text{O}$ are expressed in δ values (‰, as permil) relative to V-SMOW (Vienna Standard Mean Ocean Water). The oxygen isotopic composition was determined by means of the water– CO_2 equilibration technique [6] and the isotopic composition of hydrogen was performed using H_2 generated by reduction of water over hot zinc metal [7] using the SIRA 12, VG Isogas mass spectrometer. The analytical precision was better than $\pm 0.5\text{‰}$ for $\delta^{18}\text{O}$ and $\pm 2\text{‰}$ for $\delta^2\text{H}$. Tritium activity was measured by a liquid scintillation spectrometer (1219 Rack Beta Spectral) after enrichment by electrolysis [8]. Tritium concentrations are reported in TU units with analytical precision of 10–100%.

Seasonal trends in $\delta^{18}\text{O}$ values in precipitation and stream waters were modelled using sine functions of appropriate amplitude and frequency (Eq. (1)) [9] to fit seasonal sine wave curves to annual $\delta^{18}\text{O}$ variations

DYNAMICS OF WATER TRANSPORT THROUGH THE VELIKA MORAVA

$$\delta^{18}O = X + A \times [\cos(ct - \theta)] \tag{1}$$

where X is the weighted mean annual measured $\delta^{18}O$ (‰), A is the estimated ^{18}O annual amplitude (‰), c is the radial frequency of annual fluctuations ($0.017214 \text{ rad d}^{-1}$), t is the time in days after the start of the sampling period, and θ is the phase lag or time of the annual peak $\delta^{18}O$ in radians. Sine wave models fitted to precipitation and stream water $\delta^{18}O$ variations were used to calculate mean resident time (T in month) of water on a catchment scale expressed mathematically for a well-mixed model as:

$$T = \frac{6}{\pi} \sqrt{\left(\frac{A_p}{A_r}\right)^2 - 1} \tag{2}$$

where A_p is the amplitude of precipitation $\delta^{18}O$ (‰), and A_r is the amplitude of the river water $\delta^{18}O$ (‰). In general, the amplitude of any sinusoidal function is proportional to its standard deviation, and in applied rapid method [10] the ratio A_p/A_r is replaced with their standard deviation ratio (σ_p/σ_r).

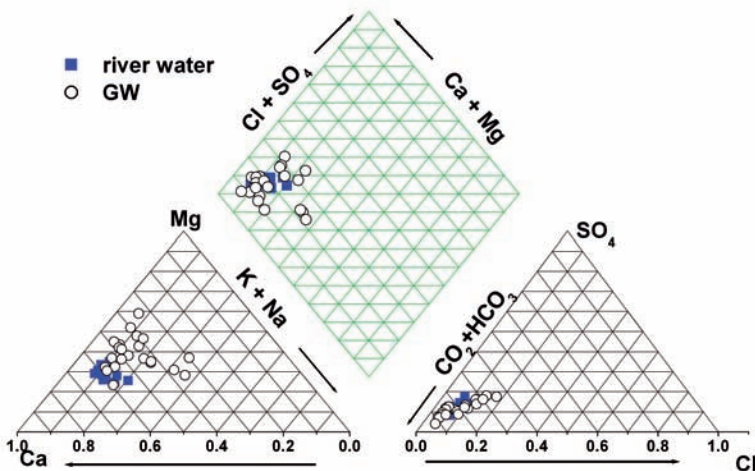


FIG. 2. The Piper trilinear diagram for river water and groundwater in the Velika Morava catchment.

4. Results and discussion

The Piper trilinear plot (Fig. 2) for fresh and groundwaters showed similarity in their chemical composition dominated by the Ca-Mg facies for cations and the bicarbonate-chloride-sulfate for anions. The shallow groundwater composition (electrical conductivity 517 to 1930 $\mu\text{S}/\text{cm}$) was rather homogeneous and characterized by low concentrations of solutes (total dissolved solids TDS < 620 mg/L) and HCO_3^- as the major anion ($\text{HCO}_3^- \gg \text{Ca}^{2+} > \text{SO}_4^{2-} > \text{Mg}^{2+} > \text{Na}^+$). The cations were mainly calcium, sodium, and magnesium type while the anions were mainly chloride and sulfate type. Quite good correlations were found between bicarbonate to Ca^{2+} , Mg^{2+} , and Na^+ ($r = 0.69, 0.66,$ and 0.60 , respectively) suggesting that these three cations were balanced mainly by bicarbonate anion, and originated from dissolution of sedimentary rocks dominated by calcite and dolomite minerals. The major anions, SO_4^{2-} , Cl^- , and NO_3^- , which originate from juvenile rainwater (washout) or anthropogenic influences (agricultural activities), with exception for SO_4^{2-} ($r = 0.60$) do not show any correlation to HCO_3^- .

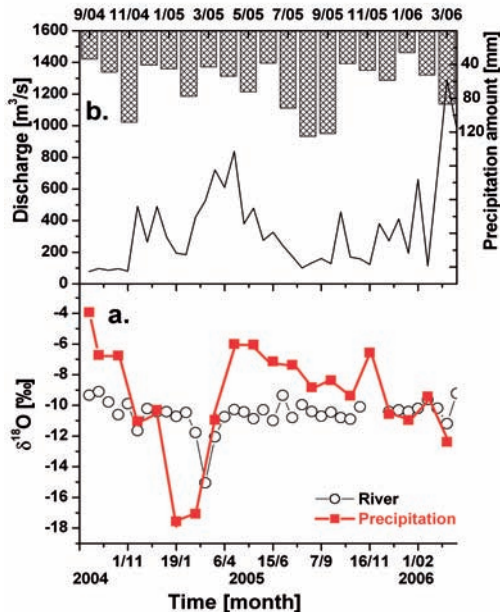


FIG. 3. Temporal variations of isotopic composition in precipitation and river water $\delta^{18}\text{O}$ (a), and discharge and precipitation amount (b) for the Velika Morava catchment (profile – Ljubicevski most) for the period September 2004 – March 2006.

DYNAMICS OF WATER TRANSPORT THROUGH THE VELIKA MORAVA

The variations in the stable isotope composition in the catchment for precipitation, river water, and groundwater throughout the time of observation expressed as the coefficient of variation (CV = standard deviation/mean 100%) [11] were 37.9%, 6.0, 7.9 and respectively. Precipitation showed a clear seasonal pattern with increasing depletion of heavy isotopes in cold winter months (November-April: mean $-11.9 \pm 3.7\text{‰}$ for $\delta^{18}\text{O}$, and $-83 \pm 29\text{‰}$ for $\delta^2\text{H}$) and the enriched isotope composition in summer rainfall (May to October: mean $-7.4 \pm 1.8\text{‰}$ for $\delta^{18}\text{O}$, and $-48 \pm 12\text{‰}$ for $\delta^2\text{H}$). For the study period, mean weighted precipitation for $\delta^{18}\text{O}$ was similar for the three locations, Kraljevo (-9.7‰), Nis (-9.3‰), and Smederevska Palanka (-9.1‰). The local meteoric water line, $\delta^2\text{H} = 7.4 (\pm 0.2) \times \delta^{18}\text{O} + 6.1 (\pm 4.1)$ ($r^2 = 0.99$, $\sigma = 0.60$) calculated on the basis of $n = 45$ monthly values for the whole observation period over the catchment using the orthogonal regression was close to the GMWL.

In comparison to precipitation, isotopic composition of river waters was highly damped and similar at all sites exhibiting seasonal differences (Table 1). Generally, δ values were depleted during the winter months (minimum in March) when rainfall and snowmelt generate the highest flows and more enriched in summer stream water. Most of data points for river waters lie above the GMWL. The flow weighted mean of $-10.4 \pm 0.2\text{‰}$ reflects the influence of

TABLE 1. PRECIPITATION AND FLOW-WEIGHTED MEAN $\delta^{18}\text{O}$, MEAN MODELLED $\delta^{18}\text{O}$ AND AMPLITUDE, APPROXIMATE MEAN RESIDENCE TIMES

Subcatchment	Location	Mean	Volume/Flow Weighted Mean	Amplitude	MRT
		$\delta^{18}\text{O} (\text{‰})$		(months)	
Juzna	Nis	-9.6	-9.3	2.00	
Morava	Aleksinac	-10.2	-10.3	0.39	9.7
	Grdelica	-10.4	-10.7	0.49	7.5
Zapadna	Kraljevo	-9.6	-9.7	1.73	
Morava	Jasika	-10.5	-10.4	0.52	6.1
	Milocaj	-10.5	-10.6	0.47	6.8
	Ibar- L. lakat	-10.3	-10.3	0.24	13.6
Velika	S. Palanka	-9.1	-9.1	2.00	
Morava	Lj. most	-10.4	-10.3	1.01	3.2
	Varvarin	-10.2	-10.1	0.44	8.4

integrated seasonally variable precipitation inputs from higher elevations that fell upstream of the sample locality and longer residence time groundwater sustains baseflows.

Groundwater in three subcatchments, areas along the Velika Morava River, the Zapadna Morava River and the Juzna Morava River had quite similar isotopic signatures ($\delta^2\text{H} = -69 \pm 6\text{‰}$ and $\delta^{18}\text{O} = -9.9 \pm 0.8\text{‰}$). Rate of depletion in ^{18}O with increasing latitude gave from the slope of the regression line value for the gradient of $-0.4\text{‰}/100\text{ m}$ for groundwater level reduced to mean sea level that is comparable with the lapse rate found for rivers in the USA ($-0.42\text{‰}/100\text{ m}$) [12]. Tritium content varied from 3 to 24 TU, suggesting a high spatial variability of the modern recharge process throughout the basin.

The mean stream water residence times calculated using Eq. (2) are summarized in Table 1. The $\delta^{18}\text{O}$ standard deviations for stream water varied from 0.24 to 1.01‰ while standard deviations for precipitation were between 3.47 and 3.99‰. The patterns of $\delta^{18}\text{O}$ variations were well described by the seasonal sine wave model and that was reflected in the strength of correlations between observed and modelled values for all sites ($r^2 = > 0.5$). A first approximation of mean residence times ranged from 3.2 to 13.6 months with 95% confidence limits. The results provide an indication of the degree of mixing with groundwater between 45 and 76% within each subcatchment and thus offer a valuable integrated assessment of the differences in the hydrological functioning of the whole catchment. The residence times are not scale dependent whereas subcatchments with similar hydrological processes exhibited similar residence times such as Jasika and Milocaj sites (6.1 and 6.8, respectively).

5. Conclusion

Isotope technique applied the first time to study interaction between surface and groundwater will contribute to an improved conceptualization of the Velika Morava catchment hydrology. The mean annual ^{18}O composition of precipitation is enriched in ^{18}O compared to mean annual stream water and groundwater isotopic composition, and therefore it is likely that summer precipitation does not contribute significantly to recharge in this region. Estimated mean residence times should be taken as a first approximation and be compared to results from other sites. Isotopic results obtained during this project will permit the development of the resource management water model of this catchment.

ACKNOWLEDGEMENTS

We thank the Ministry of Sciences and Environmental Pollution for financial support within the project ON142039. We also wish to acknowledge the IAEA–CRP project “Isotopic age and composition of streamflow as indicators of groundwater sustainability” (F3.30.15) for supporting the research contract (SCG-12958).

REFERENCES

- [1] McDONNELL, J.J., Where does water go when it rains? Moving beyond the variable source area concept of rainfall-rainoff response, *Hydrol. Process.* 17 (2003) 175–181.
- [2] PETKOVI, K. (Ed.), *Serbian Geology*, Institute for regional geology and paleontology, Faculty of Mine and Geology, University of Belgrade, Belgrade (1978) (in Serbian).
- [3] PROTI, N., et al., The Status of Soil Surveys in Serbia and Montenegro, European soil bureau. Research report 9 (2005) 297–315.
- [4] UNITED NATIONS ENVIRONMENT PROGRAMME GLOBAL ENVIRONMENT MONITORING SYSTEM (GEMS)/INTERNATIONAL ATOMIC ENERGY AGENCY, *Analytical Methods for Environmental Water Quality* (2004), http://www.gemswater.org/quality_assurance/index-e.html.
- [5] AMERICAN PUBLIC HEALTH ASSOCIATION, AMERICAN WATER WORKS ASSOCIATION AND WATER ENVIRONMENT FEDERATION, *Standard Methods for the Examination of Water and Wastewater*, 20th Edition. American Public Health Association, Washington, DC (1998).
- [6] EPSTEIN, S., MEYEDA, T.K., Variation of ^{18}O content of waters from natural sources. *Geochim. Cosmochim. Acta* 4 (1953) 213–223.
- [7] COLEMAN, M.L., et al., Reduction of zinc for hydrogen isotopic analysis. *Anal. Chem.* **54** (1982) 993–995.
- [8] HUT, G., Intercomparison of low-level tritium measurements in water, IAEA, Vienna (1986).
- [9] RODGERS, P., et al., Using stable isotope tracers to assess hydrological flow paths, residence times and landscape influences in a nested mesoscale catchment, *Hydrol. Earth Sys. Sci.* **9** (2005) 139–155.
- [10] MILJEVIC, N., et al., “Rapid method for mean residence time determination” (Proc. Int. Sym. IHIWRM Vienna, 2003), IAEA-CSP-23, IAEA, Vienna (2004) 291–293.

- [11] O'DRISCOLL, M.A., et al., Seasonal ^{18}O variations and groundwater recharge for three landscape types in central Pennsylvania, USA, *J. Hydrol.* **303** (2005) 108–124.
- [12] DUTTON, A., et al., Spatial distribution and seasonal variation in $^{18}\text{O}/^{16}\text{O}$ of modern precipitation and river water across the coterminous USA, *Hydrol. Process.* **19** (2005) 4121–4146.

DETECTION OF WATER LEAKS IN FOUM EL-GHERZA DAM (ALGERIA)

N. HOCINI, A.S. MOULLA

Department of Applied Hydrology and Sedimentology,
Centre de Recherche Nucléaire d'Alger (CRNA),
Algiers, Algeria

Abstract

The main objective of this work was to identify the origin of water leakage in the Foug El-Gherza dam combining conventional, tracing and isotope techniques. The investigation was performed by a research team from the Algiers Nuclear Research Centre in collaboration with engineers from the National Agency for Dams. The chemical and isotopic results have shown no influence of dam water on the surrounding aquifers. Dye tracing has shown a faster water circulation through complex pathways for the right bank as compared to the left one.

1. INTRODUCTION

This work was carried out within the framework of a Regional Co-operation AFRA programme supported by the IAEA (RAF/8/028). This programme deals with the strengthening and development of scientific knowledge in African countries, mainly in the detection of dam leakage and safety. The main objective of this work was to identify the origin of water leakage combining conventional, tracing and isotope techniques. Classical methods concerned the monitoring of changes in physico-chemical parameters (conductivity, temperature and chemical composition). Isotopic and tracing techniques involved the determination of the isotopic composition of different water bodies (oxygen-18 and tritium) and the labelling of the reservoir (Rhodamine-WT fluorescent tracer), respectively.

2. DESCRIPTION OF THE STUDY AREA

Foug-El-Gherza dam is located at 18 km east of Biskra province in the south-eastern part of Algeria (Fig.1). Surface water is mainly collected for irrigation purposes.

The dam model project was designed in 1946 by the Algerian Hydraulics Laboratory (Neyrpic). The completion of the construction phase was in 1952 and first operation immediately showed leaks at the downstream part of the dam. Since then, leakage continued and the maximum water loss (20.7 Mm^3) was recorded from 1981 to 1982.

The dam regulates about 13 Mm^3 of water conveyed by Wadi El-Abiod (Fig. 2) ephemeral river and tributaries during a whole hydrological cycle for a catchments of $\sim 1300 \text{ km}^2$.

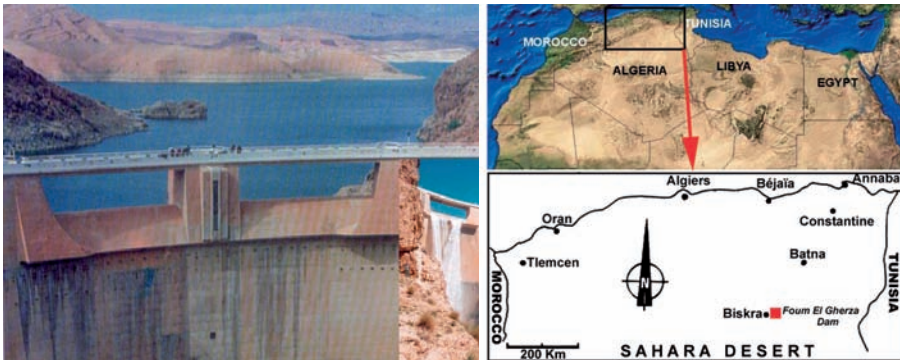


FIG. 1. Map showing the location of the dam site.

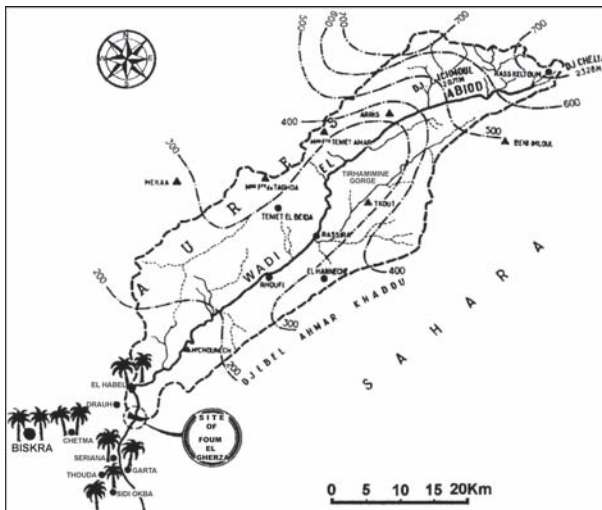


FIG. 2. The catchment area of Foum El-Gherza dam.

DETECTION OF WATER LEAKS IN FOUM EL-GHERZA DAM

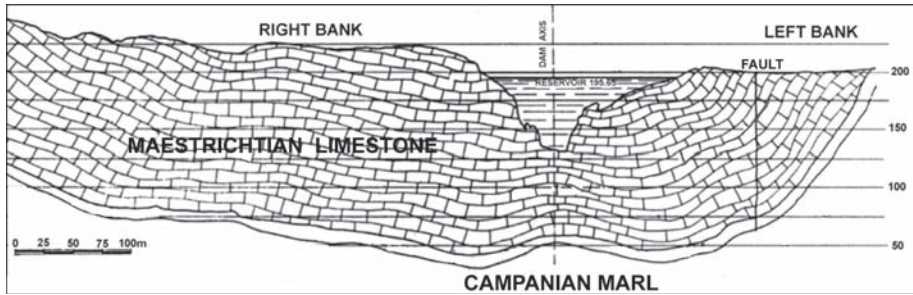


FIG. 3. Geological cross-section of the dam site and geology of site surroundings.

2.1. Geological and hydrogeological settings

The massif where the dam is founded is composed of a relatively thick fissured karstic Maestrichtian limestone laying over a Campanian marl stratum (Fig. 3).

Three main aquifers are present in the investigated region. These are from the shallowest to the deepest the following:

- The alluvial phreatic aquifer: it is contained in the alluvial deposits and is recharged by precipitation and infiltration from the riverbed and from irrigation channels.
- The Miopliocene sands and the Senonian-Eocene carbonate aquifers.
- They are deeper and both are still artesian at some locations.

2.2. History of the leakage phenomenon

The first filling and operation of the reservoir started in 1952 upon completion of the construction, which was then resumed between 1954 and 1957 by the reinforcement of the hydraulic works and the injection of a grouting curtain. Just after dam filling, leaks started to appear at the immediate downstream of the dam (1.6 Mm^3 in 1952/53, $\sim 2.0 \text{ Mm}^3$ for the next two years). The maximum value was observed for season 1981/82, during which not less than 20.7 Mm^3 was recorded (Fig. 4). Due to lack of precipitation, the leakage rate started to fall down and during summer 1994 (June 24) no more water was present in the reservoir.

Seepage takes place both at the left and the right banks. The leaks at the left bank are visible and their flow rate is rather low. They are collected within a small irrigation channel which follows the riverbed towards the irrigated areas. On the contrary, right bank leaks flow via a two-row network of drains and are directly collected within the irrigation gallery.

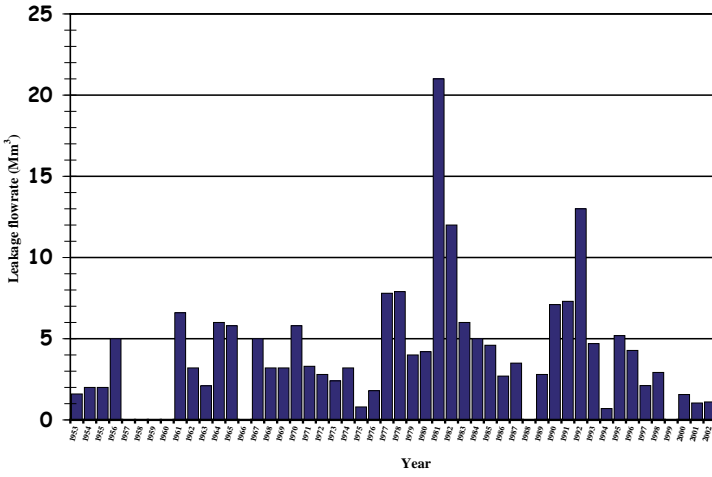


FIG. 4. History of the leakage at Foum El-Gherza since first filling of the reservoir.

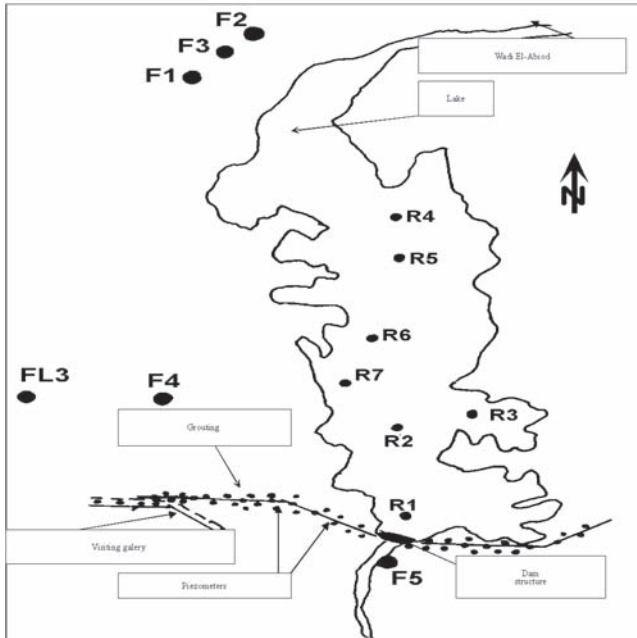


FIG. 5. Schematic location of sampling sites during field campaigns.

3. EXPERIMENTAL WORK

One evaluation mission and two field trips were carried out (Fig. 5). During the first field campaign, sampling for all water bodies that are present within the immediate vicinity of the dam were carried out. In addition, conductivity and temperature profiles were recorded for the accessible piezometers on both banks and for some points in the lake itself.

The first in situ observations have shown the existence of lateral infiltration through the massif. Land collapse and rockfall were also noticed. Excavations and large cracks were brought to sight by the decrease of water level in the lake (6.5 Mm^3 at that time). It was even possible to hear water flowing through the carbonate fractures on the left bank.

During the second field mission and in addition to recording profiles as during the first field trip, tracer experiments using Rhodamine-WT were carried out. Making use of such a tool, an estimation of the total flowrate at the outlet of the irrigation gallery was performed.

Moreover, the reservoir water was also labelled in the vicinity of the banks for the lake of interconnection experiment purposes. The volume of water in the lake was at that time about 5.9 Mm^3 .

4. RESULTS AND CONCLUSIONS

The achievements and the results gathered from the field campaigns allowed us to identify the problems affecting this dam through the overall observation of the features of the physical medium (geology) where it has been built.

The results obtained from temperature and conductivity profiles that were drawn for the probe accessible piezometers have shown the presence of very complex vertical and horizontal flows as depicted in Figs 6a and 6b. This could be due to the geological characteristics of the site.

With regard to the chemical composition, a Piper diagram (Fig. 7) showed that there is no relationship between reservoir water and groundwater that is occurring in the immediate vicinity of the reservoir. This was further confirmed by the isotopic results through oxygen-18 and tritium contents as summarized in Table 1.

An interconnection experiment using Rhodamine-WT fluorescent tracer was performed afterwards. It consisted of labelling the reservoir water at a distance of 2 m from the shores. The monitoring of tracer arrival at the downstream springs showed that Rhodamine was detected respectively after two days at the right bank and after one week at the left bank, since injection started.

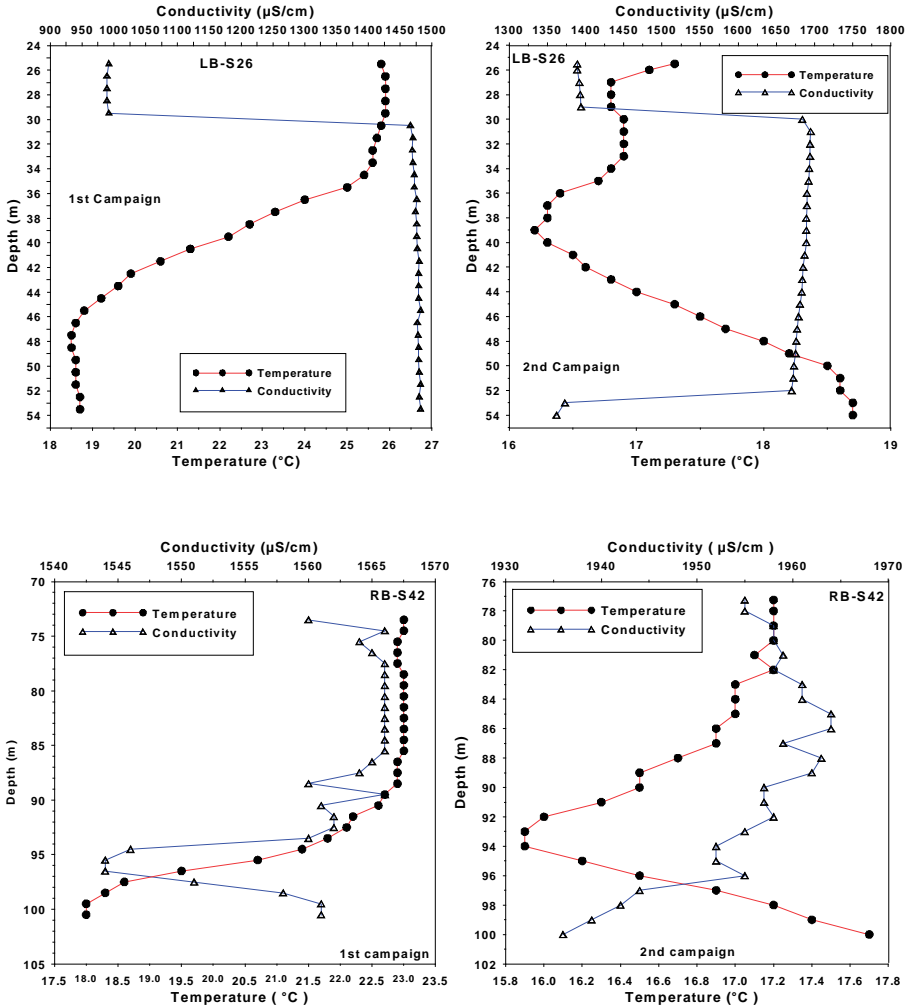


FIG. 6. (a) Comparison of left bank S-26 piezometer EC & T profiles of the two campaigns; (b) Comparison of right bank S-42 piezometer EC & T profiles of the two campaigns

The investigation described in this paper lead us to the conclusion that the implementation of such a pilot study and its associated preliminary findings seems to be satisfactory. However, according to the complexity of the geological site, more experiments need to be performed in order to better understand and better address the leakage phenomena.

DETECTION OF WATER LEAKS IN FOUM EL-GHERZA DAM

TABLE 1. ISOTOPIC COMPOSITION OF SOME SAMPLES

Sample	Tritium (TU)	$\delta^{18}\text{O}$ (‰)
Borehole F1	2.1	-7.3
Borehole F2	1.3	-7.5
Borehole F3	< 0.4	-7.5
Borehole FL3	1.4	-7.9
Borehole F4	2.0	-7.4
Borehole F4 bis	1.7	-7.5
Borehole F5	< 0.4	-7.4
Reservoir	9.7	-0.2

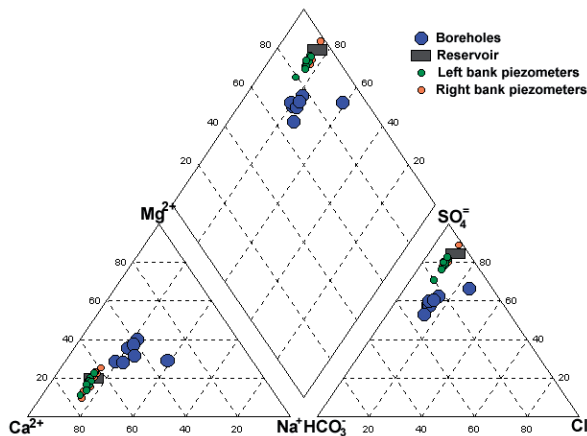


FIG. 7. Chemical classification of samples according to Piper diagram

ACKNOWLEDGEMENTS

The above investigation was carried out within the framework of IAEA-AFRA-RAF/8/028 regional cooperation project. The authors are very grateful to the staff and colleagues of the ‘Agence Nationale des Barrages’ for their fruitful co-operation and logistic assistance during field missions. All analyses were performed at the Applied Hydrology and Sedimentology Department, Algiers Nuclear Research Centre whose staff contribution is gratefully acknowledged.

REFERENCES

- [1] PLATA BEDMAR, A., "Detection of leakage from reservoirs and lakes". Use of Artificial Tracers in Hydrology, (Proc. Advisory Group Meeting), IAEA-TECDOC-601, IAEA, Vienna (1991).
- [2] REMINI, B., HOCINI, N., MOULLA, A.S. , La problématique des fuites d'eau dans le barrage de Fougues-Boudjar (Biskra). Premier Séminaire National sur le Développement des Zones Arides et Semi-arides. University of Djelfa, Algeria, (16–17 May 1999).
- [3] REMINI, B., HOCINI, N., MOULLA, A.S., Water leaks in Fougues-Boudjar dam (Algeria), *EIN-International* No. 6 (2001) 55–59.
- [4] HOCINI, N., Etude des fuites dans les barrages au moyen des techniques isotopiques. Premières Journées d'Etudes sur les Applications des Techniques Nucléaires en Ressources Hydriques et en Agriculture, COMENA/CDTN, Algiers 30/11-02/12/98.
- [5] PLATA BEDMAR, A., ARAGUAS-ARAGUAS, L., Detection and Prevention of Leaks from Dams. Balkema, Rotterdam (2002).

**ISOTOPIC AND CHEMICAL STUDY OF LAKE
MASSACIUCCOLI, TUSCANY**
*Hydrodynamic patterns, water quality and anthropogenic
impact*

I. BANESCHI*, R. GONFIANTINI*, M. GUIDI*, J.L. MICHELOT***,
D. ANDREANI*, G.M. ZUPPI**

*Institute of Geosciences and Georesources-CNR
Pisa, Italy

**Department of Environment Science,
Università Cà Foscari,
Venezia, Italy

***UMR IDES CNRS-Université Paris-Sud,
Orsay, France

Abstract

Lake Massaciuccoli (7 km², 15 km north of Pisa, Tuscany), occupies a shallow depression on a coastal marshy plain. The lake is connected to the sea by a 8 km channel with sluices flowing through an old sandpit pond. Hydrochemistry and stable isotopes are applied to investigate water, salt and nutrient inputs into the lake from drainage channels, groundwater and the sea. In general, the ion concentrations plotted versus Cl⁻ suggest mixing with seawater, but do not allow to discriminate between contributions of continental water versus seawater — which vary seasonally — nor between those from farming practices and redox processes. Vice-versa, hydrochemistry and isotopic tracers (²H, ¹¹B, ¹³C, ¹⁸O, ³⁴S) combined together, highlight the water mass dynamics and the role of continental waters, show the organic matter cycles and the anthropogenic contributions, and allow to define the main redox processes and their rates.

1. INTRODUCTION

Lake Massaciuccoli (7 km², max. depth 2.5 m, volume 15 × 10⁶ m³) occupies a shallow depression on a coastal marshy plain of approximately 25 km² located 15 km north of Pisa, Tuscany (Fig. 1). The lake, whose surface level varies seasonally from 0.5 to -0.5 m asl, is connected to the sea by a 8 km

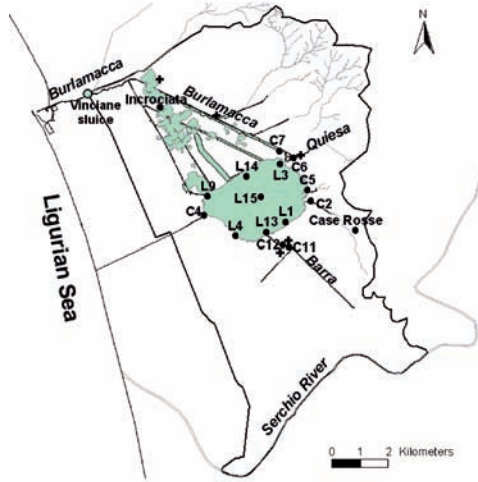


FIG. 1. Location map of Massaciuccoli basin. Sampling site (●) and pumping station (+) are shown.

channel (called *Burlamacca*) flowing through some artificial ponds (total volume of $37 \times 10^6 \text{ m}^3$), which are remains of old sandpits. A sluice, constructed two centuries ago and not well maintained, regulates the access of seawater to the whole system. The lake is kept vertically well mixed by winds throughout the whole year. On the contrary, well defined thermoclines develop in summer in the sandpit ponds, where water attains a depth up to 25 m. Some ponds are reached by seawater and therefore develop a permanent stratification.

The mean precipitation is about 1000 mm/year, falling mostly in autumn and in winter. The mean temperature ranges from 7°C in winter to 22°C in summer, with 15°C for the mean year-round value.

Starting from the 18th century, most of the plain between the sea and the Apuan Alps was reclaimed and used for intensive farming. Part of the plain lies below sea level (-1 to -3 m), and five pumping stations are used to remove the drainage water and pour it into the lake. Sand deposits and dunes occupy the coastal belt, while to the east the cover consists mainly of several meters thick peat deposits.

As a consequence of collecting the irrigation drains, eutrophication is increasing in the lake, in spite of the natural conditions preserved in the surrounding marsh – a sanctuary for aquatic birds. It is therefore necessary to investigate the lake balance and the organic carbon cycle in order to evaluate the anthropogenic impact and modifications of the natural conditions, as mandatory for setting up adequate plans to protect the lake and its environment. These are

ISOTOPIC AND CHEMICAL STUDY OF LAKE MASSACIUCCOLI

the main objectives of a series of investigations based on hydrochemical and isotopic tracers, which have been undertaken at the Institute of Geosciences and Georesources in collaboration with the universities of Venice and Paris-Sud. The isotopic ratios measured include $^2\text{H}/^1\text{H}$, $^{18}\text{O}/^{16}\text{O}$, $^{13}\text{C}/^{12}\text{C}$, $^{11}\text{B}/^{10}\text{B}$, and $^{34}\text{S}/^{32}\text{S}$. The preliminary results are reported in this paper. Last but not least, the problems described here are common to many wetlands, for which our investigations can be of interest.

2. FIELD MEASUREMENTS AND SAMPLING

Lake water was sampled at seven stations. All the major inflowing streams were also sampled. The samplings campaigns were conducted in July-August 2004, February-March 2005, May 2005 and November 2006. A sandpit, named *Incrociata*, was sampled at different depths in May 2005.

The field measurements included temperature, pH, salinity, dissolved oxygen, depth — using an automatic multi-parametric probe and alkalinity. Chemical and isotopic analyses were performed in the laboratory with the usual techniques.

3. RESULTS AND DISCUSSION

3.1 Lake water balance

The water balance of Lake Massaciuccoli is quite complex. The inflow is provided by precipitation over the lake, drainage water from the adjacent marsh and the pumping stations, and possibly some seawater through the Burlamacca channel (mainly in summer). It is possible, however, that most of seawater is stored in the sandpit ponds, where it sinks because of its higher density and push out fresh water floating on the surface which eventually reaches the lake. The outflow is given by evaporation from the lake (including plant transpiration from reeds), and the water discharged into the sea through the Burlamacca channel (mainly in winter). Furthermore, water exchanges with groundwater can provide some additional inflow and outflow, which however are practically impossible to estimate.

The chloride concentration of lake water, ranging from 730 mg/L in winter (i.e. after the major rain period) to above 1220 mg/L in autumn (after the major evaporation period, with lake surface at -0.20 m asl), confirms that seawater does not reach the lake in significant amount. The stable isotope composition of lake water (approximately $\delta^{18}\text{O} = -3.5$ and $\delta^2\text{H} = -20$ ‰ in winter, and -0.5

and -10% , respectively, in summer) leads to the same conclusion. Note that drain channels carry water with considerably more negative δ -values.

A rough computation based on the water isotopic composition, indicates that in summer the lake is losing about $20 \pm 10\%$ of its water. In spite of the large uncertainty, this estimate indicates that the lake level decrease in summer is largely due to evaporation, possibly combined with some losses to groundwater because of the water table which is below the lake level.

3.2. Human impact and biotic processes

The drainage channels, and in particular the *Barra* channel draining the southern part of the lake catchment area, carry water rich in nutrients derived from the farming practices and, to a limited extent, domestic drains. Isotopes and hydrochemistry help in studying the effects of these contaminants on water and life of Lake Massaciucoli.

3.3.1. The carbon isotopes and the carbon cycle

The $^{13}\text{C}/^{12}\text{C}$ ratio and concentration of dissolved inorganic carbon (DIC), monitored during a full year in the lake and channel water, exhibit seasonal variations determined by the inflow of organic carbon, its oxidation to CO_2 , and its exchanges with the atmosphere.

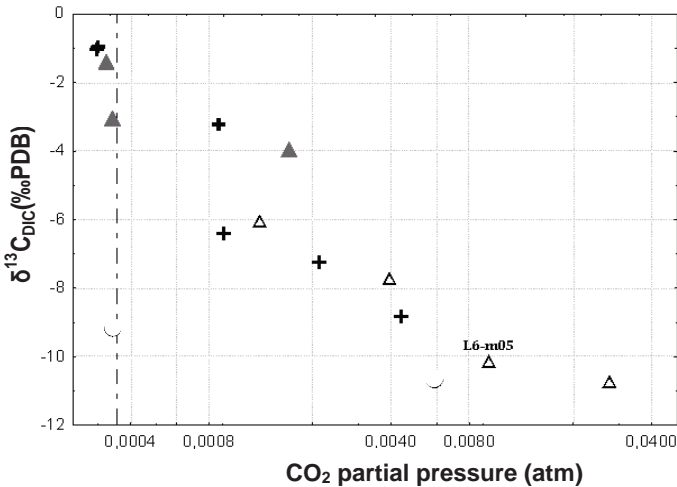


FIG. 2. Correlation between $\delta^{13}\text{C}_{\text{DIC}}$ and CO_2 for samples collected in channels (Δ), lake (\blacktriangle) and Incrociata sandipit (+).

ISOTOPIC AND CHEMICAL STUDY OF LAKE MASSACIUCCOLI

The most negative $\delta^{13}\text{C}_{\text{DIC}}$ values observed in the Lake Massaciuccoli system are about -10% . The negative correlation between $\delta^{13}\text{C}_{\text{DIC}}$ and dissolved CO_2 (Fig. 2) implies that $^{12}\text{CO}_2$ is preferentially released during respiration and decomposition of organic matter. In effect, oxidation of organic matter produces ^{13}C -depleted CO_2 , i.e. with a $\delta^{13}\text{C}$ close to that of organic carbon (-15 to -25% , depending on the photosynthetic path), while disproportion reactions produce less depleted CO_2 because the oxidized carbon is enriched in ^{13}C with respect to the reduced carbon species co-generated in the process [1].

The $\delta^{13}\text{C}_{\text{DIC}}$ of channels draining the farmed land ranges from -8 to -11% . Although the natural vegetation mainly follows the C3-photosynthetic pathway, in the farmed land the dominating crop (70%) is corn (C4). Thus, the $\delta^{13}\text{C}_{\text{DIC}}$ of drainage channels is mainly controlled by the C4-plant decay, as drainage water from farmed land is supersaturated in CO_2 with respect to air CO_2 .

In summer, photosynthesis is prevailing and thus the concentration of dissolved CO_2 is low, the $\delta^{13}\text{C}_{\text{DIC}}$ increases because of the preferential uptake of isotopically light CO_2 from the DIC pool and the consequent ^{13}C enrichment of remaining DIC, as observed for algae. This process is accompanied by partial re-equilibration with the air CO_2 producing $\delta^{13}\text{C}_{\text{DIC}}$ ranging from $+1$ to -3% [2–4]. As a consequence, the lake, where photosynthesis prevails, exhibit the highest $\delta^{13}\text{C}_{\text{DIC}}$ values.

3.2.2. Boron isotopes in surface waters

The isotopic composition of dissolved boron ranges from $+37$ to $+17\%$ (in $\delta^{11}\text{B}$). The highest values ($+30$ to $+37\%$) are observed in the Burlamacca canal close to the sea, values which are consistent with the $\delta^{11}\text{B}$ mean value for seawater ($+39.5\%$, [5]). The $\delta^{11}\text{B}$ values decrease progressively as the distance from the sea increases. In Lake Massaciuccoli and in channels draining the farmed land, the $\delta^{11}\text{B}$ can be as low as $+15\%$ and the values decrease as the B/Cl ratio increases, that is with the increase of boron of non-marine origin released in the system by the drainage water. A $\delta^{11}\text{B}$ ranging from $+15$ to $+20\%$ is probably typical of boron. The only exception is a sample from a drain channel (L12) with high B/Cl ratio and intermediate $\delta^{11}\text{B}$ value.

Different types of water usually exhibit different isotopic compositions of dissolved boron. For the Massaciuccoli basin, however, isotopic data of boron for sediments, soils, fertilizers, manure, and farming and domestic drains, are not yet available. Therefore, literature values have been used in Fig. 3. At this stage of our investigation, boron isotopes show once more the penetration of seawater in the whole system lake-ponds-Burlamacca, but it is hoped that they will help in identifying the major sources of boron released in the basin. The isotope geochemistry of dissolved boron, however, is quite complex because of

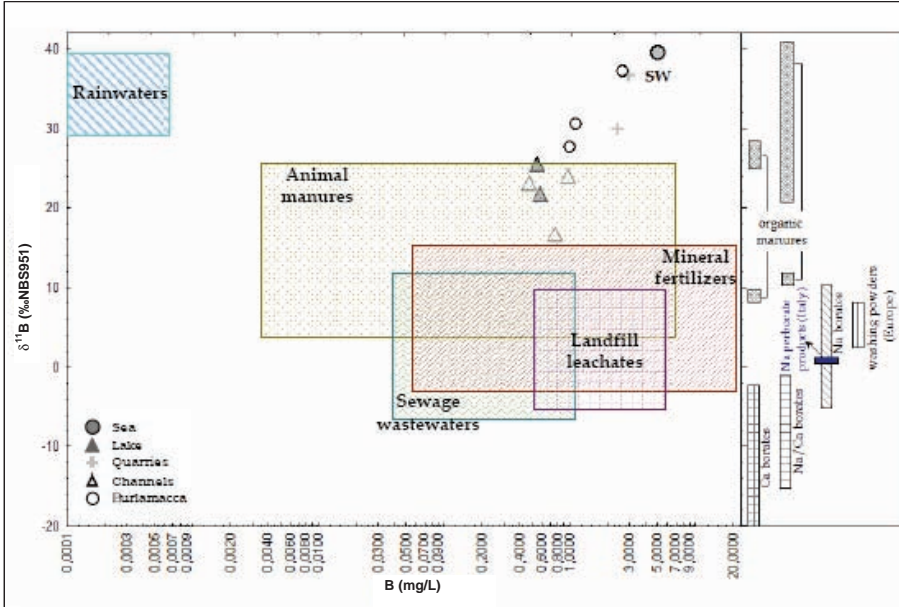


FIG. 3. $\delta^{11}B$ vs B content. Typical values for different materials are underlined.

the isotopic fractionations occurring in adsorption/desorption processes with clay minerals of soil and aquifer matrix [6–8].

3.3.3 Sulphur isotopes in sandpit ponds

Vertical profiles of sandpit pond indicates the occurrence of strong redox gradients. The oxygen concentration decreases within the first 4–5 m from saturation with air to virtually nil, because the water stratification acts as a barrier, preventing mixing between superficial waters rich in oxygen and deep anoxic waters. In addition, a regular increase of CO_2 with depth can be observed in the Incrociata pond, together with chloride and sulphate variations. The alkalinity and Eh trend, and the presence of H_2S suggest the occurrence of bacterial SO_4^{2-} reduction at depth. These trends are paralleled by a $\delta^{13}C_{DIC}$ decrease and an increase of $\delta^{34}S(SO_4^{2-})$, suggesting a biogenic production of CO_2 together with sulphate reduction.

Depending on environmental conditions, sulphur isotope fractionation between SO_4^{2-} and H_2S can be quite variable, with enrichment factors between less than 4 to more than 46‰ [9-12]. However, Canfield [13] observed that S isotope fractionation ranges only from 8 to 21‰ in situations where sulphate-reducing bacteria are supported by high concentrations of amended substrate

ISOTOPIC AND CHEMICAL STUDY OF LAKE MASSACIUCCOLI

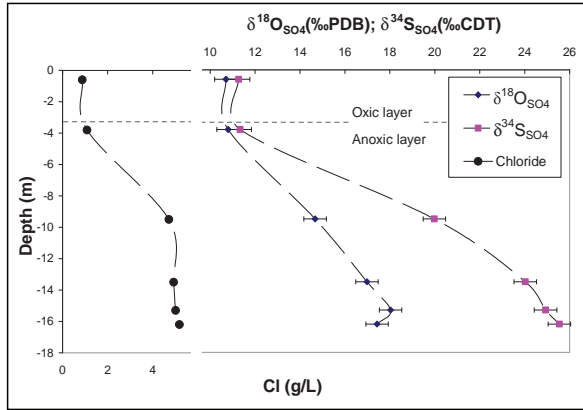


FIG.4. $\delta^{34}S_{SO_4}$ and $\delta^{18}O_{SO_4}$ vertical profiles in Incrociata sandpit.

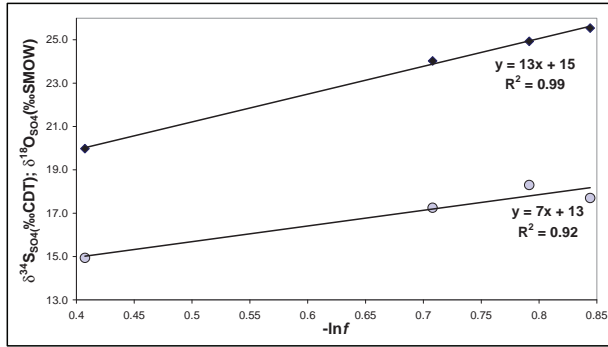


FIG. 5. Correlation between $\delta^{18}O(SO_4^{2-})$ and $\delta^{34}S(SO_4^{2-})$

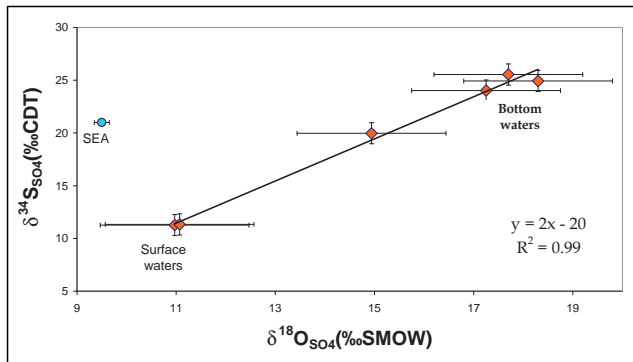


FIG. 6. $\delta^{34}S_{SO_4}/\delta^{18}O_{SO_4}$ diagram for Incrociata sandpit waters.

such as acetate, ethanol, and lactate. Since bacteria break down faster ^{32}S - ^{16}O bonds than those involving ^{34}S or ^{18}O , as reduction proceeds the residual SO_4^{2-} becomes progressively enriched in ^{34}S and ^{18}O [14, 15]. Hence, the increase of $\delta^{34}\text{S}$ and $\delta^{18}\text{O}$ values and the simultaneous decrease of SO_4^{2-} concentration in the water column are expected, as shown in Fig. 4. If sulphate is not added to, or removed from, the system by an independent mechanism, the ^{34}S or ^{18}O enrichment of residual sulphate obeys a Rayleigh model, and the slope of $\delta^{34}\text{S}$ and $\delta^{18}\text{O}$ vs. $\ln f$ (with f being the fraction of the residual sulphate) gives the fractionation factors of the reduction process (Fig. 5).

The slope of the linear correlation between $\delta^{18}\text{O}(\text{SO}_4^{2-})$ vs. $\delta^{34}\text{S}(\text{SO}_4^{2-})$ of Fig. 6 is close to 0.5, which falls almost exactly in the middle of the range reported [16] — 0.25 to 0.71 — for the microbial reduction of sulphate.

4. CONCLUSION

This work gives underline that the distribution in the system of trace elements depends on the presence and intensity of biotic activity. Photosynthesis and degradation of organic matter are key processes. In particular, low $\delta^{13}\text{C}_{\text{DIC}}$ values, approaching the typical isotopic signal of C4 vegetation, are measured within channels with high pCO_2 . In fact corn is the main cultivation in the southern basin. In the lake $\delta^{13}\text{C}$ values correspond to the value expected for equilibrium with the atmosphere. In the excavation area, which represent a meromictic system, a significant increase in alkalinity is detected in the deepest anoxic part, together with a decrease in pH and SO_4 and NH_3 and H_2S production. At the same time, $\delta^{13}\text{C}_{\text{DIC}}$ and $\delta^{34}\text{S}_{\text{SO}_4}$ signals decrease, suggesting occurrence of oxidation of organic matter and reduction of SO_4 mediated by sulphate-reducing bacteria.

The high boron concentrations in the agricultural network are higher than the mean value of lake water. Indeed, the B/Cl correlation plot underlines three compartments within the studied area: (1) waters draining the agricultural network, (2) lake waters and (3) waters from the Burlamacca channel and the excavation area. Samples with highest B/Cl values are characterized by lowest $\delta^{11}\text{B}$ values. These anomalies have been ascribed to contamination by manure.

We can conclude that isotopical research allowed us to underline the influence of agricultural activity on the chemical composition of lake water, the hydrodynamic equilibrium and surficial sediment composition.

REFERENCES

- [1] ROMANEK, C.S., et al., Carbon isotope fractionation in synthetic aragonite and calcite: effects of temperature and precipitation rate, *Geochim. Cosmochim. Acta* **56** (1992) 419–430.
- [2] BARTH, J.A.C., VEIZER, J., Carbon cycle in St. Lawrence aquatic ecosystems at Cornwall (Ontario) Canada: seasonal and spatial variations, *Chem. Geol.* **159** (1999) 107–128.
- [3] TELMER, K., VEIZER, J., Carbon fluxes, pCO₂ and substrate weathering in a large northern river basin, Canada: carbon isotope perspectives, *Chem. Geol.* **159** (1999) 61–86.
- [4] AUCOUR, A.M., et al., Use of ¹³C to trace origin and cycling of inorganic carbon in the Rhone river system, *Chem. Geol.* **159** (1999) 87–105.
- [5] GONFIANTINI, R., et al., Intercomparison of Boron Isotope and Concentration Measurements. Part II: Evaluation of Results, *Geostandards Newsletter* **27** (2003) 41–57.
- [6] TONARINI, S., et al., Intercomparison of boron isotope and concentration measurements. Part I: Selection, preparation and homogeneity tests of the intercomparison materials, *Geostandards Newsletter* **27** (2003) 21–39.
- [7] PENNISI, M., et al., The utilization of boron and strontium isotopes for the assessment of boron contamination of the Cecina river alluvial aquifer (central-western Tuscany, Italy). *Applied Geochem.* **21** (2006) 643–655.
- [8] PENNISI, M., et al., Behaviour of boron and strontium isotopes in groundwater-aquifer interactions in the Cornia plain (Tuscany, Italy), *Applied Geochem.* **21** (2006) 1169–1183.
- [9] HARRISON, A.G., THODE, H.G., Mechanisms of the bacterial reduction of sulfate from isotope fractionation studies, *Trans. Faraday Soc.* **53** (1958) 84–92.
- [10] REES, C.E., A steady-state model for sulphur isotope fractionation in bacterial reduction processes, *Geochim. Cosmochim. Acta* **37** (1973) 1141–1162.
- [11] CHAMBERS, L.A., TRUDINGER, P.A., Microbial fractionation of stable sulphur isotopes: a review and critique, *Geomicrobiol.* **1** (1979) 249–293.
- [12] CANFIELD, D.E., et al., Isotope fractionation and sulfur metabolism by pure and enrichment cultures of elemental sulfur disproportionating bacteria, *Limnol. Oceanogr.* **43** (1998) 253–264.
- [13] CANFIELD, D.E., Isotope fractionation by natural populations of sulfate-reducing bacteria”, *Geochim. Cosmochim. Acta* **65** (2001) 117–124.
- [14] MIZUTANI, Y., RAFTER, T.A., Isotopic behaviour of sulphate oxygen in the bacterial reduction of sulphate, *Geochem. J.* **6** (1973) 183–191.
- [15] HOLT, B. D., KUMAR, R., Oxygen isotope fractionation for understanding the sulphur cycle, In: KROUSE, H. R., GRINENKO, V.A., *Stable isotopes in the*

assessment of natural and anthropogenic sulphur in the environment, John Wiley & Sons, New York (1991) 27–41.

- [16] AHARON, P., FU, B., Microbial sulfate reduction rates and sulfur and oxygen isotope fractionations at oil and gas seeps in deepwater Gulf of Mexico — Its origin and evolution, *Geochim. Cosmochim. Acta* **64** (2000) 233–246.

MEAN RESIDENCE TIME OF WATER FROM SPRINGS OF THE PLITVICE LAKES AND UNA RIVER AREA

S. BABINKA*, B. OBELIĆ**, I. KRAJCAR BRONIĆ**,
N. HORVATINČIĆ**, J. BAREŠIĆ**, S. KAPELJ***, A. SUCKOW*¹

*Leibniz Institute for Applied Geosciences,
Hannover, Germany

**Rudjer Bošković Institute,
Zagreb, Croatia

***University of Zagreb,
Faculty of Geochemical Engineering,
Varaždin, Croatia

Abstract

Within the FP5 project ICA2-CT-2002-10009 several tracers from springs that feed the Plitvice Lakes (Croatia) and springs in Una River valley (Bosnia and Herzegovina), as well as stable isotopes and tritium activity of precipitation from the Plitvice Lakes area were measured in the period 2003-2005. The aim of this work is to model the Mean Residence Time (MRT) by comparative measurements of concentrations of stable isotopes (^2H , ^{18}O), helium isotopes ($^3\text{He}/^4\text{He}$), chlorofluorocarbons (CFC-11, CFC-12, CFC-113), SF_6 and hydrochemical analyses. The complexity of the karst system required a multi-tracer approach, since one environmental trace substance alone leaves too much ambiguity in interpretation.

1. INTRODUCTION

Study area is the transboundary region that encompasses catchment areas of the upper flow of the Korana River in Croatia, which belongs to the Plitvice Lakes National Park, and the Una River in Bosnia and Herzegovina (Fig. 1). Dyeing experiments performed in the period 1973–1989 [1] showed that the water infiltrated from the Croatian side, including Plitvice Lakes and

¹ Now at: International Atomic Energy Agency, Vienna, Austria

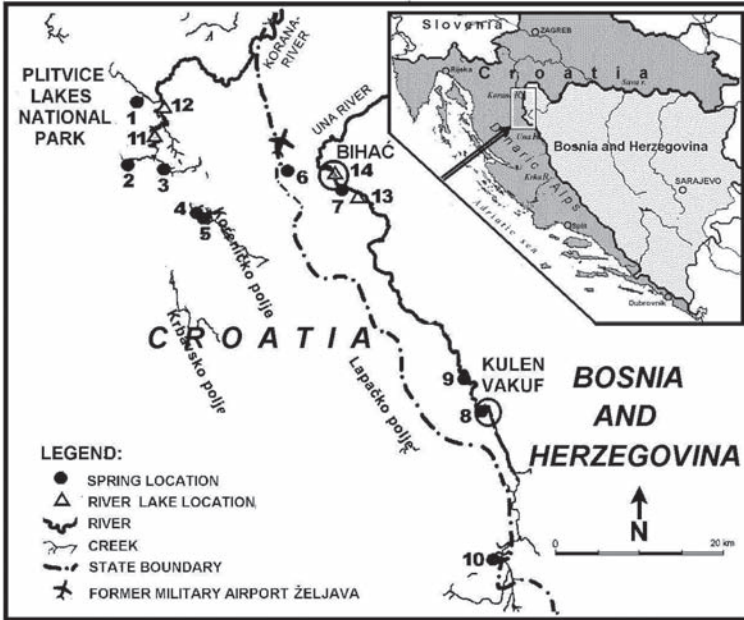


FIG. 1. Sampling sites at the Plitvice Lakes National Park and Una River. Springs: 1 – Plitvica; 2 – Bijela Rijeka; 3 – Crna Rijeka; 4 – Stipinovac; 5 – Koreničko Vrelo; 6 – Klokot; 7 – Privilica; 8 – Ostrovica; 9 – Toplica; 10 – Spring of Una R.. Lake and river water: 11 – Lake Prošće; 12 – Lake Kozjak; 13 – Una River near restaurant “Sunce”; 14 – Una River at Bakšaiš. Open circles denote larger settlements (Bihać and Kulen Vakuf).

the karstic fields (poljes) Koreničko Polje, Lapačko Polje and Krbavsko Polje, and discharges in the springs Privilica and Klokot. These springs are important for water supply of the town Bihać and other settlements the Una River catchment area. For determination of mean residence times in ten springs in the area and to assess the response of the springs in the Una River area to the recharge on the Croatian side comparative measurements of stable isotopes (^2H , ^{18}O), tritium (^3H), noble gases helium (He) and neon (Ne), helium isotope ratio ($^3\text{He}/^4\text{He}$) as well as chlorofluorocarbons (CFC-11, CFC-12, CFC-113) and sulphur hexafluoride (SF_6) were applied. Dating groundwater by means of environmental tracers and lumped parameter models requires a conceptual model of groundwater flow. Here the karst reservoir is approximated by two interconnected parallel flow systems of a conduit network with a quick flow component and a matrix of a fissured-porous aquifer (karst massif) with a slow flow component.

2. SAMPLING AND MEASUREMENT

Monthly precipitation samples for isotope (^2H , ^{18}O , ^3H) measurements were collected at the Plitvice Lakes in the period from July 2003 to December 2005. Sampling of spring and surface waters was performed monthly between April 2003 and June 2005 at the sites shown in Fig. 1. Noble gases and CFC/SF₆ in ten springs were taken twice, in November 2003 during a wet and high-discharge season and in July 2004 during the dry and low-discharge period. Four samples were taken from surface water for CFCs and SF₆: from Prošće and Kozjak Lake of the Plitvice Lakes and from the Una River upstream (“Sunce”) and downstream (Bakšaiš) of Bihać.

For $\delta^2\text{H}$ measurement a chromium reactor was used to reduce 1 μL of a water sample to hydrogen (Finnigan H/Device). The deuterium in the hydrogen gas was analyzed using a dual inlet mass spectrometer (Finnigan Delta-S) at the Leibniz Institute for Applied Geosciences. The analytical precision is 0.8‰. The determination of $\delta^{18}\text{O}$ was performed following the equilibration method with CO₂. The analytical precision for oxygen is 0.1‰. The $\delta^{18}\text{O}$ and $\delta^2\text{H}$ data are normalized to the VSMOW standard.

Tritium in water was measured at the Rudjer Bošković Institute using gas proportional counter with a detection limit of 2 T.U. [2]. Samples from the two sampling campaigns involving CFC/SF₆ and noble gases were measured by the ^3He ingrowth technique [3][4]. Noble gas concentrations for ^3He and ^4He were determined on a MAP 215-50 noble gas mass spectrometer using the methods outlined in [4]. ^{20}Ne and ^{22}Ne were measured in a quadruple mass spectrometer (Balzers QMG112). The system was calibrated using defined quantities of air. Absolute concentrations of the noble gases were determined with a precision of $\pm 1\%$, $^3\text{He}/^4\text{He}$ ratios to better than 0.5%. Measurements of CFCs and SF₆ were performed by using purge and trap gas chromatography with electron capture detection [5][6]. The reproducibility of the whole procedure is about 1% in air and 3% in water [7].

3. HYDROLOGICAL CONNECTION

Stable isotope composition ($\delta^2\text{H}$ vs. $\delta^{18}\text{O}$) of precipitation at the Plitvice Lakes is shown in Fig. 2A. The local meteoric water line (LMWL) is shifted with respect to both the global MWL and the local MWL for station Zagreb ($\delta^2\text{H} = 7.8 \times \delta^{18}\text{O} + 5.7$) [8]. ^2H excess in Plitvice is higher than 10‰ (mean 13.5‰), showing the influence of the Mediterranean water masses, although in the area a continental type of climate prevails. Two clusters of spring and surface waters can be discerned in the $\delta^2\text{H}/\delta^{18}\text{O}$ plot (Fig. 2B) with values

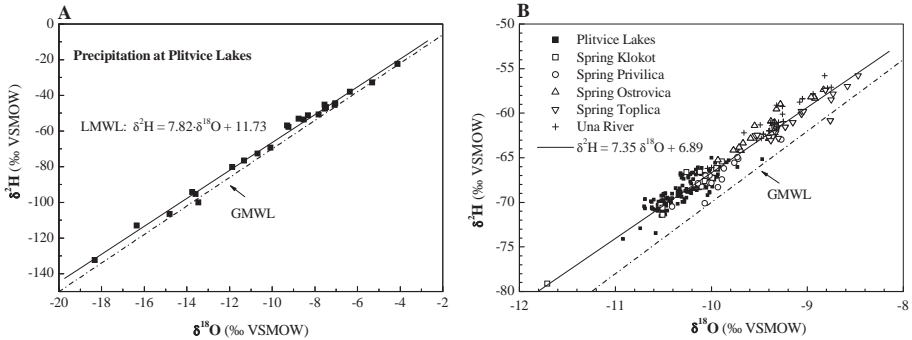


FIG. 2. $\delta^{18}\text{O}$ and $\delta^2\text{H}$ plot of precipitation at Plitvice Lakes (A) and of spring and surface water at Plitvice Lakes and the Una River (B).

lower and higher than $\delta^{18}\text{O} = -9.7\text{‰}$: more positive values ($\delta^{18}\text{O} = -9.5 \pm 0.5\text{‰}$) indicate lower mean altitude of the recharge area of Una River (average altitude 230 m asl) than that of the Plitvice catchment (average altitude 700 m asl; $\delta^{18}\text{O} = -10.3 \pm 0.2\text{‰}$).

The springs Klokot and Privilica near the Bihać municipality have the stable isotope signature of the Plitvice catchment, suggesting a hydrologic connection of these two systems and the same infiltration area from Croatia, which was also determined by former dyeing experiments: water infiltrating from Kravsko Polje, Koreničko Polje and Prijeboj near Plitvice Lakes was discharged into springs Klokot and Privilica near Bihać, while springs Una, Toplica and Ostrovica are fed from a different recharge area.

4. CALCULATION OF MEAN RESIDENCE TIMES (MRT)

4.1. Results of ^2H and ^3H

The seasonal variation (Fig. 3) of $\delta^2\text{H}$ in all springs at the Una River catchment area and some springs at Plitvice is a strong indication that the springs contain a component with MRT <5 yr. However, no seasonality within a detection limit of 0.8‰ was found for the springs Bijela Rijeka, Stipinovac and Koreničko Vrelo, indicating MRT of spring waters >5 yr.

For some springs in the Plitvice Lakes catchment MRT were determined earlier [9]. By applying the exponential model it was concluded that MRT in all major springs, including Crna Rijeka and Bijela Rijeka, ranged between 1 and 4 years.

MEAN RESIDENCE TIME OF WATER FROM SPRINGS OF THE PLITVICE LAKES

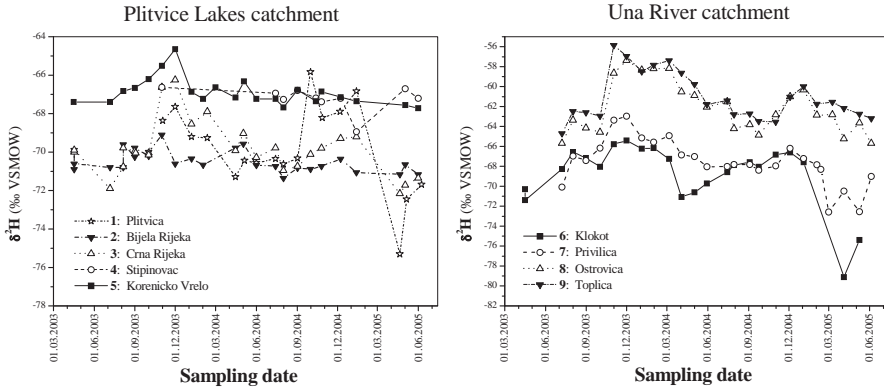


FIG. 3 Seasonal variations of deuterium in springs.

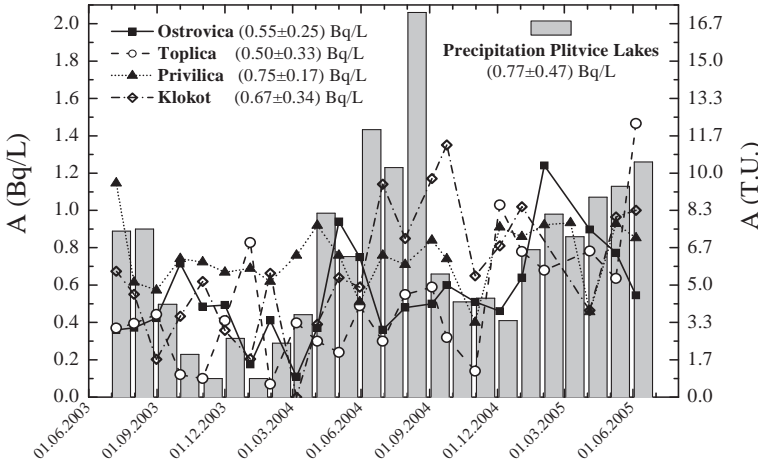


FIG. 4 Comparison of tritium activity in precipitation of the Plitvice Lakes and four springs from Una River. The mean values and standard deviations during the measurement period are also given.

Time series of tritium were measured for the Una River springs 6, 7, 8, and 9 (Fig. 4). The seasonal variation of spring Privilica (2.3–9.5 TU) is the smallest compared with the other three springs (2.0–12.2 TU), indicating the longest MRT for the spring water mixture (compare Table 1). On the other hand, the stronger tritium fluctuations in the springs Toplica, Ostrovica and Klokot indicate the greater influence of short-term components in the springs.

Tritium in precipitation at the Plitvice Lakes compares better with mean tritium values in the springs Klokot and Privilica near Bihać than with the springs Ostrovica and Toplica near Kulen Vakuf, which confirms the stable isotope results (Fig. 3).

4.2. CFC and SF₆

Fig. 5 summarizes measured concentrations of CFC-11, CFC-12, CFC-113, and SF₆ in spring and surface waters for the sampling campaigns in November 2003 and July 2004. Concentrations of CFCs and SF₆ in water at all sampling locations except CFC-11 in spring Privilica were higher in November 2003 (wet period) than in July 2004 (dry period). These systematic differences can be explained by different mixing ratios of young and old water during high and low discharge conditions. On average spring water collected in July 2004 contained components with higher MRT than the spring water sampled in November 2003. During the dry summer months in spring base flow prevails, which is older and contains less CFCs and SF₆. On the other hand, the rain-rich autumn causes more young water in the springs. These hydrological states were modelled separately.

4.3. Noble gases (He, Ne)

Dating with tritium/tritiogenic helium needs knowledge about recharge conditions like altitude and infiltration temperature. These are not sufficiently known and — according to the helium and neon concentration data — temperature seems to show great variations. From the measured values the amount of excess air and its fractionating have to be deduced. To do this, especially in karst systems the heavy noble gases Ar, Kr and Xe should be measured [10], which was not possible within the framework of our project. As a consequence, recharge temperatures cannot be determined with the necessary unambiguity and loss of tritiogenic helium (³He_{trit}) cannot be excluded. For this reason, it is not possible to deduce reliable MRTs of karst spring water based on the only He and Ne concentration and the ³He/⁴He ratio in our study. Future studies dedicated to karst groundwater therefore should make sure that not only helium and neon, but also heavy noble gas concentration, are measured.

4.4. Computing of MRT

Data processing was performed using the LabData Database and Laboratory management system. This includes a module called “Lumpy” for MRT calculations [11, 12] (Table 1). The module is able to fit time series of

MEAN RESIDENCE TIME OF WATER FROM SPRINGS OF THE PLITVICE LAKES

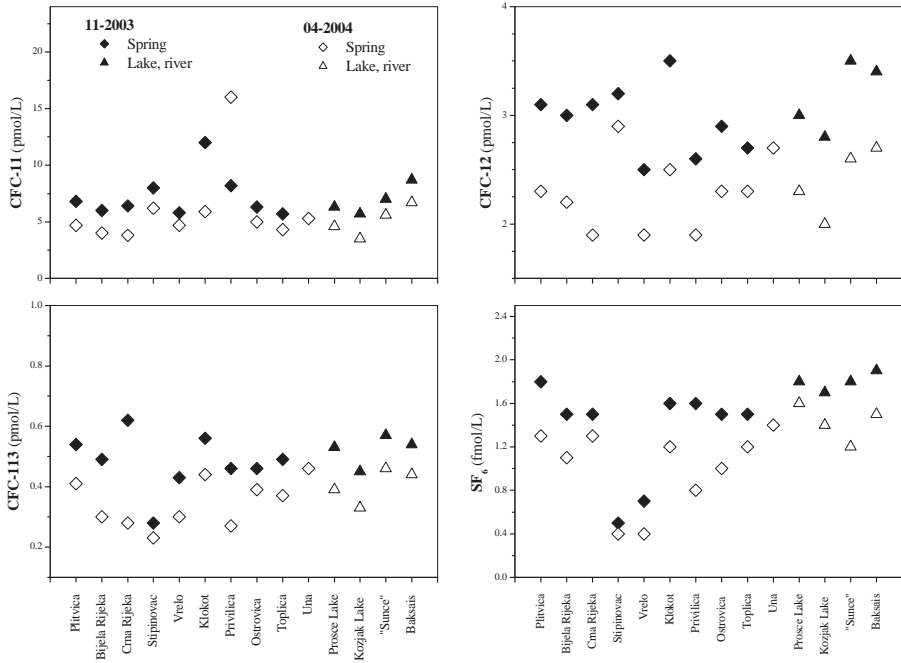


FIG. 5. Concentrations of CFC-11, CFC-12, CFC-113 and SF₆ from the springs and surface waters collected during sampling campaigns in November 2003 and July 2004.

several tracers at one site simultaneously. To compute the MRT for ten springs either a one-component model (exponential model: EM, dispersion model: DM) or a two-component model (piston flow-dispersion model: PMDM, piston flow-exponential model: PMEM) is used. PMDM describes a mixture between two water components with different MRTs and describes the “young” component in the karst conduit network (t_c), while the DM describes the “old” component in the karst matrix (t_m). Since long input time series for tritium and stable isotopes in precipitation are not available for Plitvice, the time series of Zagreb [8, 9] is used for modelling. The difference in the annual average of stable isotope values between the existing 2-years time series in Zagreb and Plitvice numerically is handled using a shift to the input tracer data that can be defined in Lumpy. This takes differences in altitude and continentality between input station and modelled system into account. Due to systematic differences in the CFCs and SF₆ concentrations during the sampling campaigns in November 2003 and July 2004, these states were computed separately (State I and II). For the PMDM this means the combination of a piston flow model

TABLE 1. RESULTS OF LUMPED PARAMETER MODELS (LPM) FOR TEN SPRINGS IN CROATIA AND BOSNIA-HERZEGOVINA.

$\delta^2\text{H}$ shift describes the shift parameter in Lumpy to adapt the Zagreb input function to the infiltration area. The Péclet number is one modelling parameter of the DM. State I refers to sampling in November 2003 and State II in July 2004. t_c – the “young” component in the karst conduit network (PMDM); t_m – the “old” component in the karst matrix (DM). r_c – fraction of the “young” water component in the conduit network; r_m – the “old” water component in the karst matrix.

Spring	LPM	$\delta^2\text{H}$ shift (‰)	Peclet Number	MRT State I (yr)		MRT State II (yr)		Admixture (%)	
				t_c	t_m	t_c	t_m	r_c	r_m
Plitvica	EM	-7.8	–	0	4	0	13.5	0	100
Bijela Rijeka	DM	-9.5	3	0	6	0	20	0	100
Crna Rijeka	PMDM	-7.9	2.5	0.4	3	0.4	28	10	90
Stipinovac	DM	-5.2	6.5	0	13	–	–	0	100
Kor. Vrelo	DM	-5.2	7	0	11	0	17	0	100
Klokot	PMDM	-5.6	1	0.1	2.5	0.1	12	10	90
Privilica	PMDM	-5.3	3	0.2	1.5	0.2	27	10	90
Ostrovica	DM	0	2.5	0	2.5	0	17	0	100
Toplica	DM	1	1	0	3	0	20	0	100
Una	PMDM	–	10	–	–	0.5	15	50	50

for the “young” component (up to 0.5 years) in the karst conduit network and a dispersion model for the “old” component (up to 28 years) in the karst matrix.

5. CONCLUSIONS

Stable isotope (^2H , ^{18}O) and tritium measurements confirmed the hydrological connection between surface and groundwater from the Croatian side (Plitvice Lakes catchment) and the Una River catchment area. Their seasonal variation is a strong indication that MRT of most springs is less than 5 years.

To obtain MRTs a multi-tracer lumped parameter modelling approach was applied using the model code “Lumpy”. Time series of stable isotopes (^2H and ^{18}O) and tritium (^3H) were used with monthly resolution as well as

MEAN RESIDENCE TIME OF WATER FROM SPRINGS OF THE PLITVICE LAKES

chlorofluorocarbons (CFC), sulphur hexafluoride (SF₆) and noble gases (He, Ne) from sampling campaigns in November 2003 and July 2004. The two campaigns were modelled separately, because they present two different hydrological states: a high-discharge state in the rainy autumn and the base flow conditions with low discharge in summer. Using the multi-tracer approach, two components of the groundwater flow could be distinguished: the quick flow in the conduit network with a MRT up to 0.5 years and the slow component in the matrix of a fissured-porous aquifer with a MRT up to 28 years. Groundwater dating with T³He using only the ³He/⁴He ratio and helium and neon concentrations gave no unique results in our study due to the variable infiltration temperatures typical for karst systems. With helium and neon concentrations only in these systems it is not possible to deduce any fractionation of excess air and possible gas loss. For this reason in karst studies also the heavy noble gases argon, krypton and xenon should be measured.

ACKNOWLEDGEMENTS

Work funded by the EU project ICA2-CT-2002-10009 and by the Projects 098-0982709-2741 and 160-0982709-1709 of the Ministry of Science, Republic of Croatia. δ¹⁸O measurements were performed in the laboratories of Umweltforschungszentrum Leipzig-Halle (UFZ), Germany and the International Atomic Energy Agency (IAEA), while noble gas mass spectrometric measurements were performed at the Institute of Environmental Physics/Oceanography, University of Bremen, Germany. We wish to thank G. Zwicker for collecting precipitation and water samples at Plitvice Lakes and to H. Merdanić and the staff of the Biotechnical Faculty in Bihać for collecting samples at Una River area.

REFERENCES

- [1] KAPELJ, S., KAPELJ, J., SINGER, D., OBELIĆ, B., HORVATINČIĆ, N., BABINKA, S., SUCKOW, S., BRIANSO, H.L., Risk assessment of groundwater in the area of transboundary karst aquifers between the Plitvice Lakes and the Una River catchments, 2nd International Conference "Waters in protected areas", Dubrovnik, 25th to 27th April 2007.
- [2] HORVATINČIĆ, N., Radiocarbon and tritium measurements in water samples and application of isotopic analyses in hydrology, *Fizika (Zagreb)* **12** (S2) (1980) 201–218.

- [3] CLARKE, W.B., JENKINS, W.J., TOP, Z., Determination of tritium by means spectrometric measurements of ^3He , *Int. J. Appl. Isot.* **27** (1976) 515–522.
- [4] BAYER, R., SCHLOSSER, P., BÖNISCH, G., RUPP, H., ZAUCKER, F., ZIMMEK, G., Performance and blank components of a mass spectrometric system for routine measurement of helium isotopes and tritium by the ^3He ingrowth method, *Sitzungsberichte der Heidelberger Akademie der Wissenschaften, Mathematisch-naturwissenschaftliche Klasse* **5** (1989) 241–279, Springer Verlag.
- [5] BULLISTER, J.L., WEISS, R.F., Determination of CFC3F and CCl₂F₂ in seawater and air, *Deep Sea Res.* **35** (1988) 839–854.
- [6] OSTER, H., Datierung von Grundwasser mittels FCKW: Voraussetzungen, Möglichkeiten und Grenzen – Dissertation, Institut für Umwelphysik, Universität Heidelberg (1994).
- [7] OSTER, H., SONNTAG, C., MÜNNICH, K.O., Groundwater age dating with chlorofluorocarbons, *Water Resour. Res.* **32** (1996) 2989–3001.
- [8] VREČA, P., KRAJCAR BRONIĆ, I., HORVATINČIĆ, N., BAREŠIĆ, J., Isotopic characteristics of precipitation in Slovenia and Croatia: Comparison of continental and maritime stations, *Journal of Hydrology* **330** (2006) 457–469.
- [9] HORVATINČIĆ, N., KRAJCAR BRONIĆ, I., PEZDIČ, J., SRDOČ, D., OBELIĆ, B., The distribution of radioactive (^3H , ^{14}C) and stable (^2H , ^{18}O) isotopes in precipitation, surface and groundwaters during the last dDecade in Yugoslavia, *Nuclear Instrum. Meth. in Physics Research* **B17** (1986) 550–553.
- [10] AESCHBACH-HERTIG, W., PEETERS, F., BEYERLE, U., KIPFER, R., Paleotemperature reconstruction from noble gases in ground water taking into account equilibrium with entrapped air, *Nature* **405** (2000) 1040–1044.
- [11] SUCKOW, A., DUMKE, I., A database system for geochemical, isotope hydrological and geochronological laboratories, *Radiocarbon* **43** (2001) 305–317.
- [12] SUCKOW, A., LabData: A database and laboratory management system for isotope hydrology, geochronology and geochemistry. International Symposium on Isotope Hydrology and Integrated Water Resources Management, 19–23 May 2003, IAEA-CN-104/P-81; IAEA, Vienna (2003).

THE USE OF TRITIUM IN RIVER BASE FLOW TO UNDERSTAND LONG-TERM CHANGES IN WATER QUALITY

R.L. MICHEL
US Geological Survey,
Menlo Park, USA

P.K. AGGARWAL, T. KURTTAS, L. ARAGUAS ARAGUAS,
K.M. KULKARNI
International Atomic Energy Agency,
Vienna

Abstract

To study the impact on water quality of changes in land-use, climate, or other factors, the residence times of water within the watershed must be understood. One manner of addressing this issue is through the use of tritium data. It has been over 50 years since thermonuclear weapons began producing tritium in large quantities, and over 40 years since the peak production of tritium by weapons testing in 1962. Since then, the tritium concentrations in the atmosphere have decreased and leading to a perception that tritium is no longer useful for determining physical parameters of surface waters. However, surface waters are frequently composed of a mixture of recent precipitation and baseflow, the latter of which can have residence times on the order of weeks to decades, or higher. The fraction of groundwater in surface flow and its age impacts the tritium concentrations of the surface flow. If the residence time of the waters composing base flow is decadal or longer, it is frequently possible to estimate the age of the active groundwater component in the river basin. Data from the Rocky Mountain area of Colorado is analyzed during three timespans: 1. The four years immediately after the bomb tests; 2. the decades after the tests (1970–2000); 3. 2000 to the present. The early time period is found to be the best time to estimate the fraction of base flow in a system. Using the ratio of tritium concentration in precipitation/tritium concentration (C_p/C_r) in surface water, it is possible to estimate the residence times of water within watersheds both on historical and recent data.

1. INTRODUCTION

The need to understand the changes in water quality brought about by changes in land-use or climate is one of the greatest issues in hydrology. To accomplish this, the residence times within a watershed must be known. One method of addressing the issue is through the use of the tritium transient produced by the large-scale atmospheric nuclear weapons in the early 1960s. The value of this transient for the study of physical processes in water science was quickly recognized [1]. Collection of long-term data sets was begun at that time, many of which have been analyzed [2, 3]. However, a large number of monitoring stations were established in the mid-1960s but discontinued after a few years due to funding considerations. Many large numbers of river basins were never sampled in a rigorous manner at any time. Recently, the International Atomic Energy Agency (IAEA) began a program designed to collect and compile isotope data for river systems throughout the world [4]. The IAEA has also compiled a data set of over 8000 surface water measurements of tritium from the 1940s to the present. One question is what information can be gained from any of the shorter tritium data sets. This issue is investigated by looking at measurements made of rivers and streams in the Colorado Rocky Mountains from the 1960s to the present.

2. TRITIUM TRANSIENT IN BASIN OF THE UPPER COLORADO RIVER

Tritium concentrations in the Upper Colorado River above Cisco, Utah, whose basin is mostly on the western slope of the Rocky Mountains in Colorado, have been measured since the early 1960s. The long-term tritium data base has been analyzed and a residence time of 14 years was obtained. Baseflow was found to constitute about 60% of all flow in the long-term tritium data set. However, many shorter term data sets within the area have not been studied in any detail. Below we detail the use of tritium to study the issue of the age and quantity of baseflow from both historical and recent data sets.

2.1. Concentration fluxes in the years after the bomb-peak (1962–1967)

Figure 1 shows tritium concentrations in water from the Upper Colorado River and basin precipitation as well as flow rates for the years immediately following the bomb peak to 1967. The flow in this system is snow-melt driven with the largest flow found during the late spring and early summer. In the early years of the tritium transient, snow melt results in an increase in tritium

THE USE OF TRITIUM IN RIVER BASE FLOW

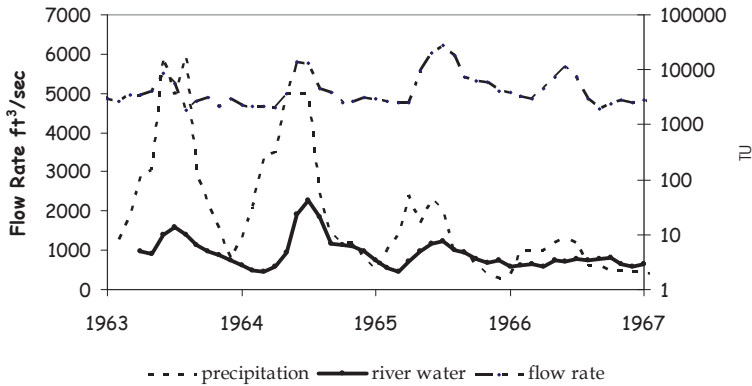


FIG. 1. Monthly tritium concentrations in the Upper Colorado River at Cisco, Utah during the beginning of the major tritium peak. Also shown are flow rates and tritium concentrations in precipitation in the basin and flow rates in ft³/sec.

concentrations in river water. An estimate of the percentage of recent snowmelt in the runoff can be obtained from the monthly tritium data if it is assumed that the tritium concentrations at low flow are representative of baseflow. The increase in tritium concentrations in the river water during spring melt in the early part of the transient can be attributed to tritium derived from the melting snow which has high (>1000 TU) concentrations during the height of the transient. This method only works until about 1965 when falling atmospheric concentrations drop to near the level of the base flow.

Using this approach, the percentage of recent precipitation is calculated to be about 30% during the period 1963–65. This is lower than the percentage calculated by the analyses of the long-term tritium data. However, it can be assumed that some of the baseflow also has a fraction of recent precipitation so the slight underestimate is not surprising. This approach does give a reasonable estimate for the fraction of recent water flowing out of the basin for rivers such as the Upper Colorado where monthly data are available during the beginning of the major bomb peak.

2.2. Measurements of rivers and streams; 1970–2000

Following the halt of atmospheric nuclear testing by the major powers in 1962, tritium research in hydrology began to focus more on recharge and groundwater studies. During this period, there were many cases where a small number of surface water samples were measured, generally as part of a larger

study on recharge. These data tend to be of limited duration but can still provide information about the residence times of the surface water systems studied.

The response of streams and rivers to the tritium transient can be calculated for different timescales in a given area. These responses can be compared to available measurements of tritium concentrations in surface waters to determine what timescales most closely fit measured data. For this presentation, a simple lumped-sum parameter model will be used where the change in concentration with time of baseflow is given by

$$dC_{\text{base}}/dt = k(C_p - C_{\text{base}}).$$

In this equation C_{base} = tritium concentration of the base flow, C_p = tritium concentration of precipitation, and k is the rate constant for replacement of water in the baseflow reservoir and the reciprocal of the residence time of the water in the reservoir. The tritium concentration measured in the river water (C_r) is a function of both C_p and C_{base} .

$$C_r = m \times C_{\text{base}} + n \times C_p$$

where

$$n + m = 1.$$

The calculation for C_{base} is carried out from the beginning of the bomb transient to the time period of interest. A range of values for k is used to obtain the dependence of tritium concentrations in baseflow with different residence times. The values for the tritium concentration in precipitation are obtained from the IAEA web site or other data sets if available. To normalize the response of a system over time, the ratio of tritium concentration in precipitation to the tritium concentration in baseflow (C_p/C_{base}) is used.

This approach has been applied to the Colorado Rocky Mountains which includes the basin of the Upper Colorado River. The results of these calculations for different residence times are given in Fig. 2 as the ratio of C_p/C_{base} over the bomb transient. In the early part of the transient when atmospheric concentrations are high relative to surface water, the ratio can be much greater than one. As the transient progresses, concentrations in precipitation drop quickly, but the concentrations in baseflow can show a lagging effect depending on the residence times of water within the basin. Thus, the ratios drop to less than one by the late 1960s, with the response of the ratios depending on the timescale for retention of water in the basin. For short timescales (< 5yrs) the ratios decline initially but return close to one in about a decade. For longer

THE USE OF TRITIUM IN RIVER BASE FLOW

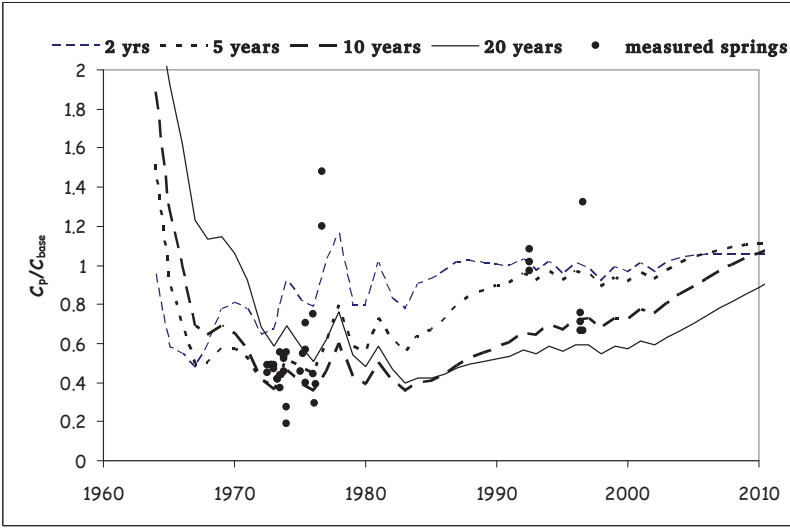


FIG. 2. Response of the ratio C_p/C_r for the Rocky Mountains of Colorado during the tritium transient for four residence times. Superimposed on the graph are the ratios for samples of springs and small lakes measured during the same period.

timescales (> 10yrs), the ratio is less than 0.7 into the 1980s and is still less than one in the present decade. Measurements made of tritium concentrations in surface water during the tritium transient can be used to estimate residence times for these waters within the respective basins. The concentration measured can be divided into the tritium concentration of precipitation to come up with a ratio of C_p/C_{base} . For this approach, it is best to use the yearly tritium concentration in precipitation because of the large variations seen in monthly tritium concentration in wetfall.

Between 1970 and 2000, a small number of measurements were made of surface waters in the Colorado Rocky Mountains including the basin of the Upper Colorado River. Tritium concentrations were measured on a number of streams and seeps sampled in the Colorado Rocky Mountains in the mid-1970s, small lakes and springs in the Flattops Wilderness area on the western side of the Rockies in the early 1990s, and streams and tributaries on the eastern side of the Rocky Mountains in the late 1990s. No long-term series are available for these systems, but it is still -useful to obtain information about the residence times of the waters that make up these outflows. All the headwaters for these sites can be assumed to have a very similar input function for tritium in precipitation. Using the above approach, estimates of residence times for

waters that compose these systems can be determined. It is not possible with these data to separate out the baseflow component from the total stream flow, so the points are plotted as C_p/C_r where C_r is the tritium concentration of the surface water composed both of baseflow and recent precipitation.

The ratios of C_p/C_r for the individual springs and lakes are plotted on Fig. 2. Some of the ratios are found to be well above one. These waters are composed of mostly old, possibly pre-bomb water, which has a tritium concentration much lower than the concentration in precipitation. Thus, the concentrations of C_r are a mixture of near zero water with recent precipitation, giving a ratio of $C_p/C_r > 1$. The samples from the Flattops Wilderness Area, collected in the early 1990s, have ratios very close to one, indicating that the waters are on the order of a few years old at most. The age range determined from tritium is supported by other measurements [5] which indicate that the water in these lakes and springs is replaced almost yearly by snowmelt. Most of the spring and river samples in the study area have ratios of C_p/C_r less than one. The ratios indicate that the baseflow components of the surface flows measured have a finite residence time in the system. In the case of most of these surface waters, the age of the baseflow component appears to be on the order of a decade or more. Thus, even with a small number of measurements widely spaced over time, it is possible to obtain information on residence times in these systems.

2.3. Tritium concentrations in surface water at the present day

Present day measurements of tritium concentrations in rivers and streams can still be of value, especially if the residence times of waters within the system are on the order of a decade or greater. Figure 3 is a graph of the ratio of C_p/C_{base} for a range of different residence times in a system. For comparison, the same ratio is given if there had been no tritium transient, ie the steady-state condition. It can be seen that for residence times in the range of 1–10 years there is very little difference in the ratio which is close to one. However, beyond about a residence time of about 10 years, the ratio starts to decline and reaches a minimum of about 0.5 at a residence time of about 40 years. Thus, for springs and rivers where the residence time of baseflow within the system is decadal or greater, the impact of the tritium transient can still be seen. As noted in studies of long-term data sets, residence times of this magnitude are common. Using this approach requires a series of high-quality measurements of the surface water and knowledge of the concentration of the precipitation in the basin. An example of this approach is shown in a paper in this session [6] for the Yukon River in Alaska, where a series of tritium measurements were made during 2002–2005. This approach works best for mid-latitude Northern Hemisphere

THE USE OF TRITIUM IN RIVER BASE FLOW

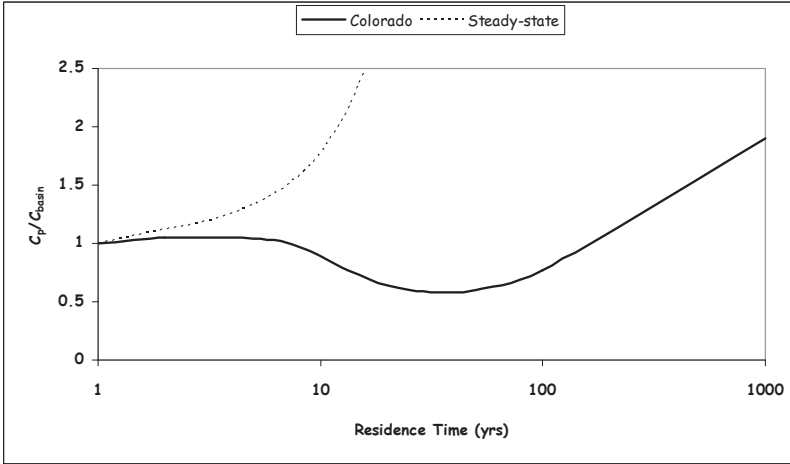


FIG. 3. The ratio C_p/C_{basin} for surface waters of residence times of 1–1000 years for the Colorado Rocky Mountains in 2007.

regions where the impact of the tritium transient on tritium concentrations in atmospheric moisture was greatest.

3. CONCLUSIONS

A lumped-sum parameter model has been applied to estimate residence times of baseflow that flows into surface waters in the range of the Colorado Rocky Mountains including the basin of the Upper Colorado River. To normalize concentrations over time and facilitate interpretation, the ratio of the yearly concentration in precipitation divided by the concentration measured in surface water is used. Using this ratio, measurements of surface waters in the study area are compared to possible responses to the tritium transient to estimate residence times for waters to reside within watersheds. Tritium measurements of springs and rivers carried out between 1970–2000 suggest a decadal residence time in most watersheds, similar to residence times determined from long-term studies of most river basins. At the present time, this ratio can still give estimates of residence times within a system for timescales of 10 or more years for this particular area. Thus, tritium measurements of surface waters can still provide important information for this part of the United States.

REFERENCES

- [1] SUESS, H.E., Tritium geophysics as an international research project, *Science* **163** (1969) 1405–1410.
- [2] MICHEL, R.L., Residence times in river basins as determined by analysis of long-term tritium records, *J. of Hydrol.* **130** (1992) 367–378.
- [3] RANK, D., ALDER, L., ARAUGUAS, L.A., FROEHLICH, K., ROZANSKI, K., AND STICHLER, W., Hydrological parameters and climatic signals derived from long-term tritium and stable isotopes time series of the River Danube, in: *Isotopic Techniques in the Study of Environmental Change*, International Atomic Energy Agency, Vienna, Austria (1998) 191–205.
- [4] GIBSON, J.J., AGGARWAL, P., HOGAN, J., KENDALL, C., MARTINELLI, L.A., STICHLER, W., RANK, D., GONI, I., CHOUDHRY, M., GAT, J., BHATTACHARYA, S., SUGIMOTO, A., FEKETE, B., PIETRONIRO, A., MAURER, T., PANARELLO, H., STONE, D., SEYLER, P., MAURICE-BOURGOIN, L., HERZEG, A., Isotope studies in large river basins: A new global research focus, *EOS* **83** (2002) 613–617.
- [5] MICHEL, R.L., TURK, J.T., CAMPBELL, D.H., MAST, A., Use of natural ³⁵S to trace sulphate cycling in small lakes, Flattops Wilderness Area, Colorado, USA, *Water, Air and Soil Pollution Focus* **2** (2002) 5–18.
- [6] MICHEL, R.L., SCHUSTER, P., WALVOORD, M. Tritium concentrations in the Yukon River Basin and their implications, this proceedings.

DEUTERIUM AND OXYGEN-18 RATIOS IN RAINFALL AND STREAMFLOW IN A MAJOR DRINKING WATER CATCHMENT NEAR SYDNEY, AUSTRALIA DURING DROUGHT

C.E. HUGHES, M.J. FISCHER, D.M. STONE, S.E. HOLLINS

Institute for Environmental Research,
Australian Nuclear Science and Technology Organisation,
Sydney, Australia

Abstract

The Warragamba catchment near Sydney, Australia, is in the midst of a major drought that is threatening water supplies for Australia's largest city. Over a period of 18 months 227 event based rainfall samples were collected at four locations, 74 streamflow samples were collected from the four major inflowing rivers and their tributaries and 45 reservoir samples were collected at various depths from Warragamba dam. The samples were analysed for δD and $\delta^{18}O$. These data provide a baseline dataset for establishment of a local meteoric water line for the Sydney region and for use in modelling of flow pathways and weather patterns in the Warragamba catchment.

1. INTRODUCTION

With a population of more than 4.2 million people, Sydney is Australia's largest city. It depends on surface water for its drinking water with 11 reservoirs providing 2584 GL storage capacity. The largest reservoir is Warragamba Dam or Lake Burragorang with a storage capacity of 2027 GL. Warragamba Dam's catchment area has an area of 9051 km² and an average rainfall of 840 mm/yr [1]. Four rivers flow into the dam from three distinct areas of the catchment. The Cox's and Kowmung Rivers drain the Blue Mountains western side of the catchment which has the highest rainfall. The Nattai River drains the southern highlands on the eastern side of the catchment which received more coastal rainfall. The Wollondilly River drains the largest southern portion of the catchment which has the lowest rainfall. Since the reservoir was last filled in Aug 1998 and October 1999 the storage levels have declined to a current level of 35% despite continuous transfers from an adjacent catchment.

Few stable isotope studies or measurements have been conducted in this catchment and the nearest GNIP sites are ~1000 km away. This extended

dry period provides an opportunity to conduct baseline isotopic studies to contribute to an analysis of the hydrological behaviour of the local climate catchment during drought.

2. METHOD

Rainfall composite samples were collected on an event basis at four sites: Lithgow in the Cox's River catchment; Mt Werong in the Kowmung River catchment; Big Hill in the Wollondilly catchment and Mittagong in the Nattai River catchment. A total of 227 rainfall samples were analysed for δD and $\delta^{18}O$ from the four sites for 18 months from February 2005 to August 2006.

During the same period 74 streamflow samples from major rivers and tributaries and 45 reservoir samples from multiple depths have been collected and analysed.

3. RESULTS

Initial observation indicates that there is little difference between the local meteoric water lines for the 4 sites. Overall the sites exhibit predictable variations – rainfall at the higher elevation and cooler Blue Mountains sites

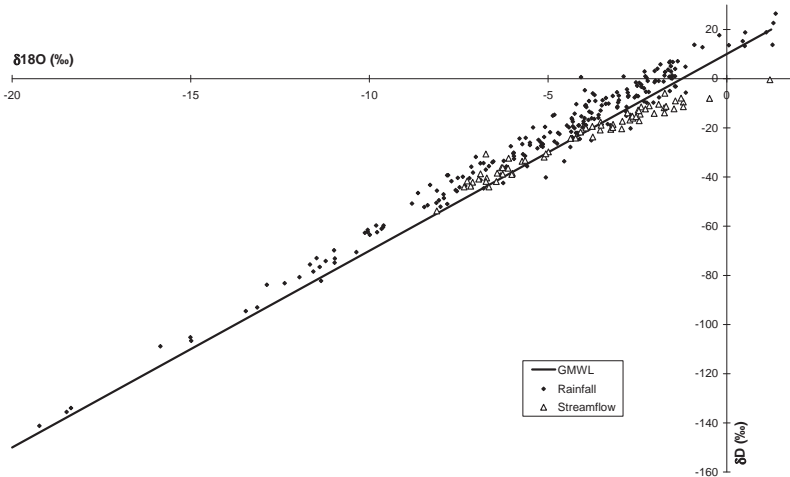


FIG. 1. Deuterium and oxygen-18 ratios in rainfall and streamflow in the Warragamba catchment from Feb 2005 to August 2006.

DEUTERIUM AND OXYGEN-18 RATIOS IN RAINFALL AND STREAMFLOW

is more depleted rainfall than rainfall nearer to the coast and some seasonal pattern is evident. In comparison with the global meteoric water line Sydney waters have a higher deuterium excess. Many of the river samples and all of the reservoir samples show a marked evaporative enrichment (Fig. 1).

The results provide baseline data for the Sydney Region and will be applied to catchment water balance and runoff process studies, groundwater recharge studies and to understanding the relationship between climate patterns and stable isotopes in precipitation in the Sydney region.

ACKNOWLEDGEMENTS

We would like to acknowledge the following people for assistance with sampling and data collection: Stuart Hankin from ANSTO; James Ray and Martin Gilmore from the Sydney Catchment Authority; and Judy Blair, Brian and Ina Casburn, Bob Cullen, Peter Davy, Stan Philips, Doug Sewell and Dave Villiers who tirelessly collect samples for us at their homes.

REFERENCE

- [1] SYDNEY CATCHMENT AUTHORITY, Dams of Greater Sydney and Surrounds – Warragamba. SCA Brochure Nov 2002. http://www.sca.nsw.gov.au/publications/files/WARRA_FIN.pdf

NEW APPROACHES FOR THE DETAILED ASSESSMENT OF MEROMICTIC LAKES BY USING STABLE ISOTOPES

A. SEEBACH, K. KNÖLLER

UFZ – Helmholtz Centre for Environmental Research,
Department of Isotope Hydrology,
Halle (Saale), Germany

Abstract

In recent years many approaches have been established in calculating lake water balances basing on meteorological/hydrological information supplemented with isotope data sets according to the mass and isotope balance equations. All of them have in common that the most important parameter – the evaporation flux – can only be obtained with an equation derived from the resistance model of the evaporation process introduced by Craig and Gordon in 1965. The preparation of field sampling systems for water vapour combined with in-lake evaporation pans shall improve the accurate determination of net evaporation fluxes. Therefore, two study sites within the Lusatian Lignite Mining District had been chosen to investigate lake-groundwater interactions and mixing dynamics of meromictic acidic mining lakes. A two-year data set of lake water, precipitation and air moisture sampled 10 cm and 100 cm above lake surface will be calibrated with pan evaporation and linked to meteorological data and groundwater samples of the lake's catchment area.

1. INTRODUCTION

In Lower Lusatia, Germany, extensive surface mining activities caused significant changes to the aquatic systems. The flooding of former opencast pit areas subjected the lakes to continuous ion inflow and acidification. The pyrite minerals that occur in the lignite bearing sediment strata are aerated and oxidized when the surrounding sediment layers are removed and mixed. Seeping rainwater and / or the rising groundwater table mobilizes the oxidation products and carries them into the mining lakes leading to acidic conditions and high density gradients. In this cases the lakes may establish a permanent stratification.

In this context, the mixing dynamics of mining lakes ought to be investigated. A present joint research project is concerned with the stratification

of water bodies, in particular of meromictic mining lakes. The application of stable oxygen isotope methods was used to understand the mixing dynamics within the lakes and the connection between groundwater and lake water.

Oxygen-18 and deuterium are considerable environmental tracers that allow following the hydrological cycle at different scales [1]. The applicability of the isotope mass balance approach has been well proven within the last decades for the estimation of water balances of lakes and catchments all over the world [2]. The range of study sites contains artificial lakes [3, 5] as well as natural lakes like sinkholes [2] or wetland-dominated river basins [6]. Since the appliance of that tool has been growing so successfully, many different approaches of sampling methods have been established both on different spatial and time scales (e.g. daily [7, 8] to monthly [5] time steps). The combination of diverse conventional attempts (e.g., chemical mass balance) with the isotope water balance [4, 5] may help to evaluate both water budgets and environmental impacts like the contamination or acidification of water bodies. However, for all that, there are still limitations to the isotope mass balance model in particular for determining the isotopic composition of atmospheric water vapour [9]. Therefore a new approach for collecting and analyzing atmospheric water vapour will be presented.

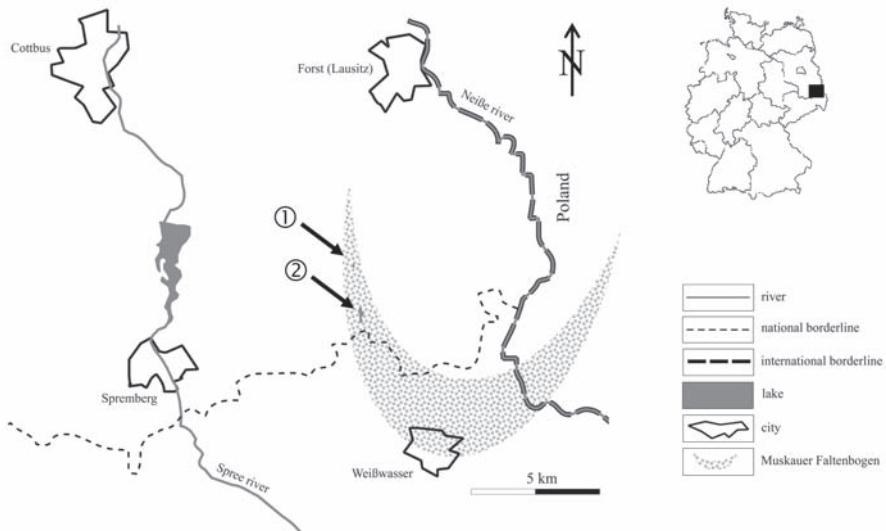


FIG. 1. Generalized map of the study area and its location in Germany. The arrows indicate Lake Waldsee (①) and Lake Moritzteich (②).

2. STUDY SITE

The study site is located within the Lower Lusatian Lignite Mining District, Germany. This region is an ice-pushed ridge of a moraine formed by the Middle Pleistocene Elster-glacial, called Muskauer Faltenbogen. Horizontal Tertiary deposits have been deformed and straightened up glaciotectonically. The exploration of the uplifted lignite layers started during the early 1860s and lasted until the late 1950s [10]. The resulting mining lakes are located in a linear order that shows the geomorphological structure of the moraine. Two lakes have been chosen to carry out the investigations.

Lake Waldsee (⊙ in Fig. 1) is a meromictic pond with a surface area of approximately 3400 m², a volume of 7500 m³ and a maximum depth of 4.9 m. The mining activities lasted from 1941 until 1948. Lake Moritzteich (⊙ in Fig. 1) has a volume of 1,2 × 10⁶ m³ and a surface area of 160 × 10³ m². The maximal depth is 17.5 m. The mine drainage ended 1960, today's lake water level had been reached in 1978.

3. METHODS

Based on the general hydrologic water balance (Equation (1)):

$$dV/dt = I_G + I_Z + P - E - O \tag{1}$$

the equation of the isotope water balance (Equation (2)) can be written as:

$$\frac{Vd\delta^{18}O_L + \delta^{18}O_L dV}{dt} = \delta^{18}O_P(I_Z + P) + \delta^{18}O_G I_G - \delta^{18}O_E E - \delta^{18}O_O O \tag{2}$$

where V is the volume of the lake, I_G the groundwater inflow, I_Z the surface inflow, P the precipitation, E the evaporation and O the outflow while the δ terms $\delta^{18}O_L$, $\delta^{18}O_P$, $\delta^{18}O_G$, $\delta^{18}O_E$ and $\delta^{18}O_O$ refer to the oxygen isotope composition of the lake water, the precipitation, the groundwater, the evapourate and the subsurface outflow relative to Vienna Standard Mean Ocean Water (VSMOW), respectively. Except $^{18}O_E$, all parameters are easily ascertainable. The isotope signature of the evapourate can conventionally be calculated according to Equation (3) derived from the resistance model of the evaporation process proposed by Craig and Gordon (1965) [11]:

$$\delta^{18}O_E = \frac{1}{1-h-\Delta\varepsilon} \left(\frac{\delta^{18}O_L - \alpha + 1}{\alpha} - h \delta^{18}O_A - \Delta\varepsilon \right) \tag{3}$$

with the equilibrium isotopic fractionation factor α for $\delta^{18}\text{O}_{\text{water}}/\delta^{18}\text{O}_{\text{vapour}}$ [12], the ambient relative humidity h and $\Delta\epsilon$ as the kinetic enrichment of $\delta^{18}\text{O}_{\text{bl-v}}$ from the boundary layer to the free atmosphere during the evaporation of surface water. The calculation of $\Delta\epsilon$ follow Equation (4) [13]:

$$\Delta\epsilon \delta^{18}\text{O}_{\text{bl-v}} = 14.2 (1 - h) \quad (4)$$

The isotopic content of the atmospheric moisture $\delta^{18}\text{O}_A$ can be calculated by supposing isotopic equilibrium between local precipitations and atmospheric water vapour following Equation (5) [9]:

$$\delta^{18}\text{O}_A = \delta^{18}\text{O}_P (1 - 1/\alpha) \quad (5)$$

Applying equation (3) in areas with high air humidity may induce uncertainties as it was established for humidity values close to 25%. In the following a method is presented, that allows the calibration of equations (3) and (5). In the first place a water vapour sampling unit has been constructed to allow the direct determination of the isotopic composition of atmospheric water vapour. Furthermore in-lake evaporation pans have been installed to document the isotopic enrichment of the pan water with progressing evaporation [14]. Apart from that rain gauges have been positioned at both study sites.

3.1. Water vapour sampling unit

For collecting and sampling atmospheric water vapour a construction (Fig. 2) has been designed that affords average samples on a monthly basis. The

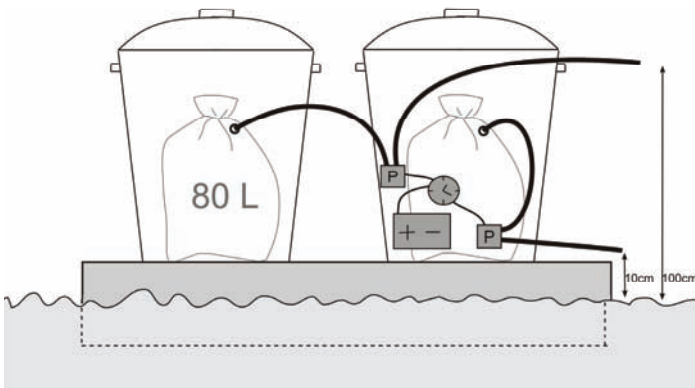


FIG. 2. Outline of the water vapour sampling unit.



FIG. 3. Photograph of the water vapour sampling unit at Lake Moritzteich.

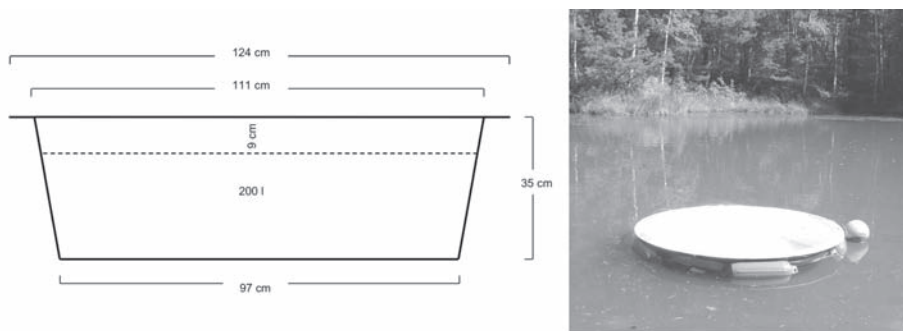


FIG. 4 Outline and photograph of the in-lake evaporation pan at Lake Waldsee.

water vapour sampling unit is positioned on a floating platform (Fig. 3) and placed into two plastic rain barrels. A car battery is linked to a clock timer that operates two peristaltic pumps which inlet adjacent air in 10 cm and 100 cm height above lake surface, respectively. The air is piped into gas sampling bags that are stored into the rain barrels. The pumps work every four hours for for 20 minutes. The sample bags contain 80 L. The evacuation of the sample bags takes place by using cold traps connected to vacuum exhaust. Measurements of the isotopic composition of the humidity samples is conducted by pyrolysis method, that allows very small sample sizes of 0.8 mL. The isotope ratios of $^2\text{H}/^1\text{H}$ and $^{18}\text{O}/^{16}\text{O}$ are conventionally expressed in delta notations of their

relative abundances as deviations in permil (‰) from the Vienna Standard Mean Ocean Water (VSMOW).

3.2. In-lake evaporation pans

In-lake evaporation pans (Fig. 4) have been installed at the two study sites, respectively. Fountain basins have been filled with 200 L of lake water. To prevent the pans from subsiding, a belt of buoys has been bonded around them. Sampling of the pan water takes place every month. Depending on precipitation and evaporation rate, the pans are refilled with lake water or decanted to obtain their initial volume. In case of replenishment, the new water composition within the evaporation pan as well as the refilled water is measured for isotope ratios. The amount of the refilled or decanted water is documented to calculate evaporation rates. Stable isotope analysis of deuterium and 18-oxygen in the pan water is carried out using a CO₂ equilibration unit coupled with an IRMS (Finnigan MAT Delta S). The analytical uncertainty of the δD and $\delta^{18}O$ measurements are 0.1‰ and 0.8‰, respectively.

4. CONCLUSIONS

The operation of the in-lake evaporation pan and the water vapour sampling unit are still in testing phase, therefore no results are currently available. Higher-than-average rainfall may effect flooding of the evaporation pans and/or swashing lake water into the pans. The evacuation of the gas sampling bags is still in practice

ACKNOWLEDGEMENTS

We would like to thank the German Research Foundation (DFG) and the Helmholtz Centre for Environmental Research – UFZ for the financial support of this work.

REFERENCES

- [1] GIBSON, J.J., EDWARDS, T.W.D., BIRKS, S.J., ST AMOUR, N.A., BUHAY, W.M., MCEACHERN, P., WOLFE, B.B., PETERS, D.L., Progress in isotope tracer hydrology in Canada, *Hydrol. Process.* **19** (2005) 303–327.

NEW APPROACHES FOR THE DETAILED ASSESSMENT OF MEROMICTIC LAKES

- [2] SACKS, L., Estimating ground-water inflow to lakes in Central Florida using the isotope mass balance approach, U. S. Geological Survey Water-Resources Investigations Report 02-4192, Florida (2002).
- [3] ZIMMERMANN, U., Isotopenhydrologie von Baggerseen, Steir. Beitr. Z. Hydrogeologie **30** (1978) 139–167.
- [4] YEHDEGHO, B., PROBST, G., Chemical mass budget of two dredged lakes embedded in shallow Quaternary aquifers in southern Austria, Environmental Geology **40** (2001) 809–819.
- [5] KNOELLER, K., STRAUCH, G., The application of stable isotopes for assessing the hydrological, sulfur, and iron balances of acidic mining lake ML111 (Lusatia, Germany) as a basis for biotechnological remediation, Water, Air, & Soil Pollution: Focus 2 (2002) 3–14.
- [6] STADNYK, T., ST. AMOUR, N., KOUWEN, N., EDWARDS, T.W.D., PIETRONIRO, A., GIBSON, J.J., A groundwater separation study in boreal wetland terrain: The WATFLOOD hydrological model compared with stable isotope tracers, Isotopes in Environmental and health Studies **41** (2005) 49–68.
- [7] VALLET-COULOMB, C., GASSE, F, ROBISON, L., FERRY, L., Simulation of the water and isotopic balance of a closed tropical lake at a daily time step (Lake Ihotry, South-West of Madagascar), Journal of Geochemical Exploration **88** (2006) 153–156.
- [8] GIBSON, J.J., EDWARDS, T.W.D., PROWSE, T.D., Development and validation of an isotopic method for estimating lake evaporation, Hydrol. Process. **10** (1996) 1369–1382.
- [9] YEHDEGHO, B., ROZANSKI, K., ZOJER, H., STICHLER, W., Interaction of dredging lakes with the adjacent groundwater field: An isotope study, Journal of Hydrology **192** (1997) 247–270.
- [10] KULKE, M., SCHOSSIG, W., Aus der Geschichte der Braunkohlengrube ‘Conrad’ bei Groß Koelzig, Beiträge zur Geschichte des Bergbaus in der Niederlausitz Bd. 6, Förderverein Kulturlandschaft Niederlausitz e. V. (Ed.), Cottbus (2006).
- [11] CRAIG, H., GORDON, L.I., Deuterium and oxygen-18 variations in the ocean and the marine atmosphere, Stable Isotopes in Oceanographic Studies and Paleotemperature: Spoleto, E. Tongiorgi (Ed.), pp. 9-130, Consiglio Nazionale delle Ricerche, Laboratorio di Geologia Nucleare, Pisa (1965).
- [12] MAJOUBE, M., Fractionnement en oxygène-18 et deutérium entre l’eau et sa vapeur, J. Chim. Phys. **10** (1971) 1423–1436.
- [13] GONFIANTINI, R., Environmental Isotopes in Lake Studies, Handbook of Environmental Geochemistry, Bd.2: The Terrestrial Environment, Fritz, P., Fontes, J.C. (Eds.), Elsevier, New York (1986) 113–168.
- [14] FROEHLICH, K., Evaluating the water balance of inland seas using isotopic tracers: the Caspian Sea experience, Hydrol. Process. **14** (2000) 1371–1383.

DO WATER ISOTOPES REFLECT DIFFERENCES IN TIMBER HARVEST PRACTICES? ISOTOPE ECOHYDROLOGY IN THE MICA CREEK WATERSHED, IDAHO USA

P. KOENIGER, T.E. LINK, J.D. MARSHALL

Department of Forest Resources,
College of Natural Resources,
University of Idaho,
Moscow, ID, USA

Abstract

The impacts of timber harvesting techniques on the water balance and flow regime were studied at the catchment scale at the Mica Creek Experimental Watershed (97 km², 975–1,750 m a.s.l.) in northwestern Idaho, USA. These studies relied on stable isotopic techniques to assess the variation in water isotope fluxes of clear-cut, partial-cut (thinned), and unimpacted forest sites. Precipitation, stream flow, soil water, and sap flow, and stable isotope concentrations (deuterium and oxygen-18) of these components were measured on a monthly basis starting in fall 2004. The isotopic composition of sap flow appeared to reflect differential canopy interception losses, with greater enrichment under the densest canopies.

1. INTRODUCTION

Forest management has profound impacts on watershed hydrology, hydrochemistry and sediment mobilization. Discharge yield from clear-cuts are higher due to decreasing transpiration and interception loss in comparison to control forests [1]. Higher amounts of organic compounds (DOC) are expected from forested sites and nutrient loss is higher after deforestation. Road construction and tree harvest also increase sediment transport and lead to higher sediment load after deforestation. Impacts of deforestation are well investigated and clearly shown in paired watershed studies. Investigations on the isotope composition of water components due to changes in forest cover are rare. We studied differences in isotope composition in relation to forest cover. Isotope composition was measured in the snow layer, soil water, sap flow, and

stream flow. Our goal was to apply stable isotope measurements to improve estimates of the components of the water budget for forested watersheds.

2. STUDY SITE AND METHODS

The Mica Creek Experimental Watershed (MCEW) is located in the Northern panhandle of Idaho approximately 80 km northeast of Moscow (latitude 47.150, longitude -116.266, elevation 975–1725 m). Mica Creek is a

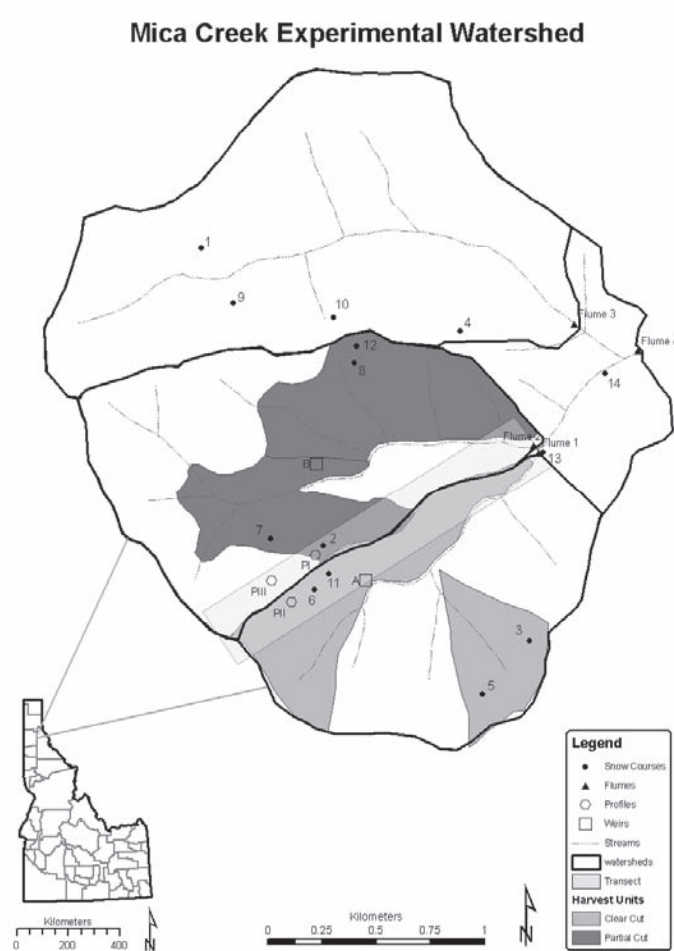


FIG. 1. Location of the Mica Creek Experimental Watershed (MCEW) in Northern Idaho (insert), forest treatments (clear-cut, partial-cut and control forest) and sampling sites for meteorological data, soil and plants and stream flow (flume-1 to 4).

DO WATER ISOTOPES REFLECT DIFFERENCES IN TIMBER HARVEST PRACTICES?

tributary of the St. Joe River and predominantly drains forested mountainous terrain. The watershed size is 97 km² and comprises three smaller study watersheds with total area of 27 km² (Fig. 1). Hill slopes in this area range from 20 to 40% and stream gradients range from approximately 5–15%. The climate of the region is continental maritime. Hill slope soil layers in the MCEW are approximately 1 m deep with a moderate (~3 cm) humus layer. The first 50 cm is silt loam, with field capacity of 0.33 cm³ cm⁻³, and wilting point 0.13 cm³ cm⁻³ of volumetric soil water content. The dominant bed rock is the Wallace gneiss with some areas of Prichard quartzite.

Vegetation on the site consists of 65 to 75 year old naturally regenerated conifer stands; remnant old-growth western red cedar (*Thuja plicata*) remains along the upper tributaries of the West Fork of Mica Creek.

The current vegetation community status resulted from extensive logging that took place during the 1920s and 1930s. Since that time, there have been no major anthropogenic disturbances until logging began in 2001 in the watershed. Dominant canopy vegetation within the watershed includes western larch (*Larix occidentalis*), grand fir (*Abies grandis*), western red cedar (*Thuja plicata*), western white pine (*Pinus monticola*), western hemlock (*Tsuga heterophylla*), and Engelmann spruce (*Picea engelmannii*). Understory vegetation is largely comprised of grasses, forbs, and shrubs. The study site is comprised of three sub-catchments. In 2001, harvesting of timber took place with a combination of line and tractor skidding. Clear-cut harvest took place on a north- (~23 ha) and a southeast- (~43 ha) facing slope, while partial cut harvests (50 % canopy removal) took place on a northeast- (~34 ha) and a southeast- (~49 ha) facing slope (Fig. 1). The clear-cut site was broadcast-burned and planted following harvest.

Four Parshall flume gauge stations were installed in the Mica Creek catchment in 1990 and 1991. Stations 1 and 2 monitor flow from the clear-cut and partial-cut catchments, respectively, while station 3 monitors stream flow from the untreated control catchment. Station 4 monitors the cumulative effects of treatments in catchments 1 through 3.

Precipitation, air temperature, and snow water equivalent (SWE) were derived from the Mica Creek Snotel site on daily resolution. Precipitation samples for isotope analyzes were collected as weekly totals in Moscow beginning in October 2005 and extrapolated to the MCEW because the collection of precipitation during winter is difficult in the remote field site. Snow samples were collected in February, March and April 2006 as snow integral samples on snow courses and from transect sampling (Fig. 1) and analyzed for $\delta^2\text{H}$ and $\delta^{18}\text{O}$. Soil samples were taken in 10 cm intervals from profiles to a depth of 1 m in the clear-cut, partial-cut and control site once a month during the summer period. At the same time sap flow isotope concentrations were analyzed

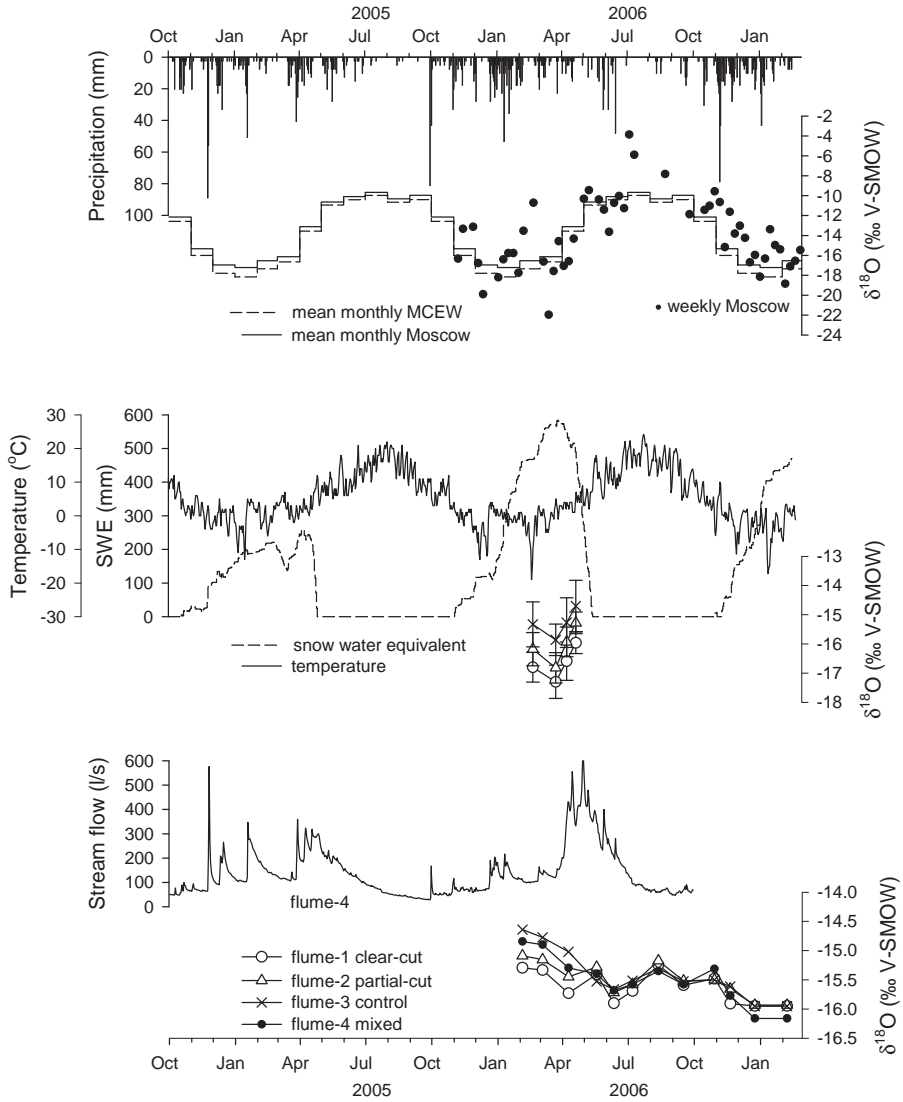


FIG. 2. Precipitation, air temperature, snow water equivalent and stream flow as well as $\delta^{18}\text{O}$ values of this components during the period of October 2004 to February 2007. Isotope values in precipitation were collected in Moscow-Idaho and are shown in relation to monthly mean values for Moscow and Mica Creek (see [2, 3]).

DO WATER ISOTOPES REFLECT DIFFERENCES IN TIMBER HARVEST PRACTICES?

from tree core samples taken from three trees at each site. Soil water and tree sap flow samples were analyzed by direct equilibration after irradiation with a gamma radiation source. All isotope analyses were conducted at the Idaho stable isotope laboratory (ISIL), located at the University of Idaho, Moscow. For oxygen-18 a headspace-equilibration technique was used (26°C for 20 h with a GasBench II). The equilibrated CO₂ was transferred by continuous flow technique into a Finnigan Delta XP IRMS. Deuterium was measured using a Finnigan H-Device (chrome reduction at 900°C) connected to a Finnigan Delta Plus in dual inlet mode. All isotope concentrations were expressed as δ-values in ‰ against the international standard V-SMOW. Precision of δ¹⁸O and δ²H analyses was approximately 0.2‰ and 1‰ respectively.

3. RESULTS AND DISCUSSION

Mean yearly precipitation at the MCEW is about 1450 mm. Precipitation occurs mainly during the period of November through May (Fig. 2) and the summer is relatively dry. δ¹⁸O values in precipitation, derived from weekly samples in Moscow, are plotted against mean monthly values for Moscow and Mica Creek (derived from the website www.waterisotopes.org after [2, 3]). The unweighted values are in good agreement with the long-term mean monthly values. Spring snowmelt is the main water input for the soil storage and also dominates stream flow dynamics. We intensively measured snow cover and isotope contents of snow integral samples during late winter and early spring 2006 and found a distinct spatial variability of snow input related to forest cover density [4]. Snow samples collected at snow courses and at a transect (see Fig. 1) showed relative enrichment in the control in comparison to the partial-cut and clear-cut sites (Fig. 2). This enrichment can be explained by interception of snow in the tree crowns and adjacent evaporative enrichment of throughfall [5, 6].

Stream flow δ¹⁸O values of the control and partial-cut sites are relatively enriched in comparison to the clear-cut site during February, March and April 2006 and are in the same order of magnitude from mid May through the summer months (Fig. 2). The δ¹⁸O values observed at the flume sites seem to represent the winter precipitation and the differences in isotope composition due to snow interception. Base flow samples collected in September 2006 represent isotope compositions of winter precipitation. δ¹⁸O values of soil water from the upper 30 cm and sap flow from October 2004 until October 2005 and from November 2006 are plotted in Fig. 3. The isotope samples for 2006 are soon to be analyzed. The time series shows tendencies of higher enrichment of soil water from control and partial-cut sites in comparison to the clear-cut site. The plotted sap flow values represent a mean of three tree core samples that were collected at

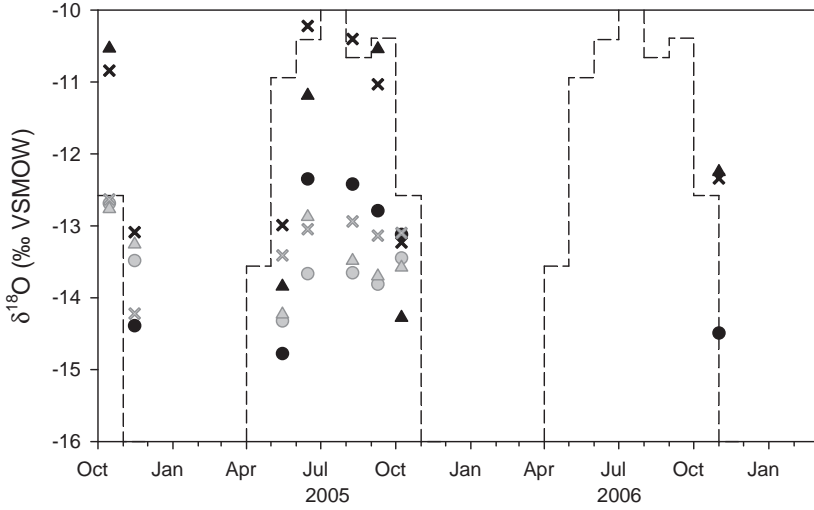


FIG. 3. $\delta^{18}\text{O}$ values in soil water of the upper 30 cm soil layer (black symbols) and sap flow (grey symbols) at the clear-cut (circle), partial-cut (triangle) and control site (cross) of the Mica Creek Experimental Watershed (MCEW) collected during June–October 2005 and November 2006 in relation to calculated mean monthly values of precipitation (see Fig. 2).

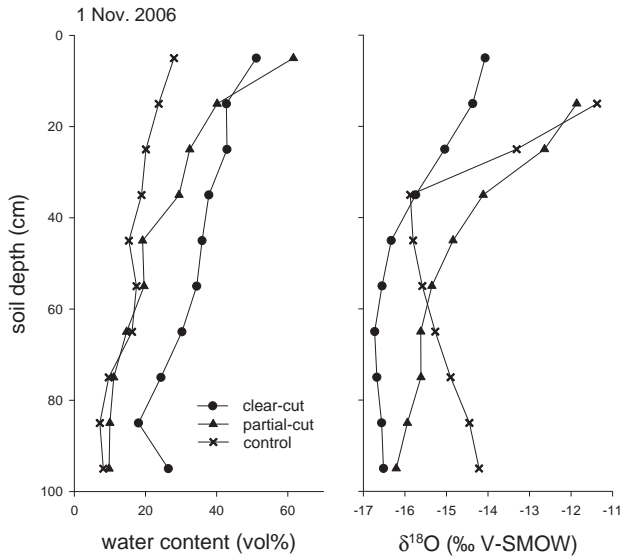


FIG. 4. Water content and $\delta^{18}\text{O}$ values of soil water collected from soil profiles in November 2006 at the clear-cut, partial-cut and control site of the Mica Creek Experimental Watershed (MCEW).

DO WATER ISOTOPES REFLECT DIFFERENCES IN TIMBER HARVEST PRACTICES?

each site. The sap flow $\delta^{18}\text{O}$ values are usually more depleted than soil water values collected in the upper 30 cm. This might indicate water uptake from deeper depths during the summer months. Soil water isotope concentrations are known to represent transpiration. In general root water uptake and stem water transport do not alter isotope concentrations [7].

Fig. 4. shows soil water collected from 1 m deep profiles that were taken in November 2006. The soil water content is higher in the clear-cut site and in the upper 50 cm of the partial-cut site; it decreases with depth for all three profiles. Isotope concentrations of the soil plots indicate more enriched water in the upper half due to recent precipitation and more depleted values in the lower part. Oxygen-18 values for the year 2005 as well as deuterium values are soon to be analyzed. The field sampling campaign is ongoing until July 2007.

4. CONCLUSION

We found a pronounced seasonal isotope signature in precipitation. Precipitation mainly occurs during winter and early spring with snowmelt as a main input for the soil water storage. Isotope concentrations in the snow layer were found to be impacted by isotope enrichment through snow interception. Soil water, sap flow and stream water reflected the snow enrichment patterns. The amount of enrichment reflects canopy density.

ACKNOWLEDGEMENTS

We thank John Gravelle, Jason Hubbart and Enhao Du for fieldwork assistance. This work was funded by USDA-CSREES NRI grant #2003-01264, and USFS Research Joint Venture Agreements #03-JV-11222065-068 and #04-D6-11010000-037.

REFERENCES

- [1] STEDNICK J.D., Monitoring the effects of timber harvest on annual water yield, *J. Hydrol.* **176** (1996) 79–95.
- [2] BOWEN, G. J., REVENAUGH, J., Interpolating the isotopic composition of modern meteoric precipitation, *Water Resources Research* **39** 10 (2003) 1299, doi:10.129/2003WR002086 and www.waterisotopes.org

- [3] INTERNATIONAL ATOMIC ENERGY AGENCY / WORLD METEOROLOGICAL ORGANIZATION, Global network of isotopes in precipitation, The GNIP database, <http://isohis.iaea.org> (2004).
- [4] KOENIGER, P., HUBBART, J.A., LINK, T., JOHN, D. MARSHALL, J.D., Stable isotope variability in snowcover and snowmelt reflect responses to forest management at the Mica Creek Experimental Watershed, Northern Idaho, *Hydrol. Processes*, (in review).
- [5] CRAIG, H., GORDON, L. I., Deuterium and oxygen 18 variations in the ocean and the marine atmosphere, In Tongiorgi, E. (Ed.), *Stable isotopes in Oceanographic and Paleotemperatures*, Speleto, Italy, (1965) 9–130.
- [6] GAT, J.R., Some classical concepts of isotope hydrology, In: *Isotopes in the water cycle* (Eds. Aggarwal P. K., Gat J. R., Froehlich F. O.) Springer, Amsterdam (2005) 127–138.
- [7] EHLERINGER, J.R., DAWSON, T.E., Water uptake by plants: perspective from stable isotope composition, *Plant Cell Environ.* **15** (1992) 1073–1082.

EVALUATION OF THE IMPACT OF GROUNDWATER RESOURCES ON SURFACE WATER IN CHIHUAHUA, NORTHERN MEXICO

L.G. HERNÁNDEZ-LIMÓN, J. MAHLKNECHT¹
Tecnológico de Monterrey,
Campus Monterrey, Mexico,

A. CHÁVEZ-RODRÍGUEZ
Universidad Autónoma de Chihuahua,
Chihuahua, Mexico

A. PINALES-MUNGUÍA
Estudios y Proyectos en Agua Subterránea S.A. de C.V.,
Chihuahua, Mexico

R. ARAVENA
Department of Earth Sciences,
University of Waterloo,
Waterloo, Canada

Abstract

We carried out a stream-aquifer interaction study in Rio Conchos basin, Northern Mexico, to find out the best water resources management strategy for the improvement and conservation of damaged aquatic ecosystems. A numerical finite-difference model (MODFLOW) was used to simulate groundwater flow of a sub-area of the Meoqui-Delicias aquifer system with a length of 40 km along the Rio Conchos and 10 km to both sides of this stream. A two-step calibration was achieved to increase the reliability of the model: the first step was the traditional process of adjusting hydraulic model parameters and comparing the results until calculated head values closely match the measured values at selected points of the upper aquifer; the second step included the comparison of results from a particle tracking program (MODPATH) with tracer data (origin and residence time of water) by using a backward particle tracking process in the numerical flow model. The results indicate that in the present study area evaporational enrichment processes from irrigation might have an impact on the estimation of residence times.

¹ corresponding author, Email: jurgen@itesm.mx

However environmental tracers may still be useful tools in combination with numerical flow models if the flow model is not significantly sensible to this uncertainty.

1. INTRODUCTION

In semiarid and arid regions the evapotranspiration exceeds by far the precipitation during the growing season, which has two consequence that groundwater is abstracted for irrigation. Especially irrigation districts, which according to [1] integrate the necessary infrastructure to facilitate groundwater and/or surface water flow to cultivated lands for the irrigation of crops, may extract large quantities of water, reducing natural discharges in streams and thus causing important changes that may be critical to ecosystems. Therefore, it is necessary to manage groundwater resources in such areas, to keep a reasonable quantity of stream discharge for the conservation of aquatic ecosystems. [2] observed that it is a common practice to use analytical tools (e.g. Theis, Hantush etc.) to quantify the streamflow depletion caused by groundwater extraction, and a several studies on the quantitative hydrological system are available (e.g. [3, 4]). However it is quiet uncommon to use environmental tracer technologies for groundwater-surface water management questions. We believe that quantitative hydrological systems may be improved by information obtained from environmental tracers. To test our hypothesis and to evaluate management strategies, we conducted a study on an alluvial stream-aquifer system located in arid-semiarid Chihuahua, Northern Mexico, collecting field data and applying a numerical groundwater flow model.

2. SITE DESCRIPTION AND AQUIFER CHARACTERISTICS

Meoqui-Delicias area includes some important towns (Delicias, Meoqui) and villages (Saucillo, Julimes, Rosales) (Fig. 1). The main activity is agriculture; the region is known for nut, onion and pepper production, as well as cattle farming for dairy products. Chihuahua's most important irrigation district covers a large part of this area. Furthermore, the nearness to the U.S.A. attracts manufacturing and pharmaceutical industries to settle down in this area.

The region is part of the physiographic province Mesa Central del Norte (Central Northern Highland) which comprises large parts of the State of Chihuahua in Northern Mexico. In the west it borders on the Sierra Madre Occidental. The Highland of Chihuahua rises progressively in western direction and has an approximate altitude of 800 to 2000 m above sea level. The climate in Delicias is classified as arid-semiarid with a mean annual air temperature

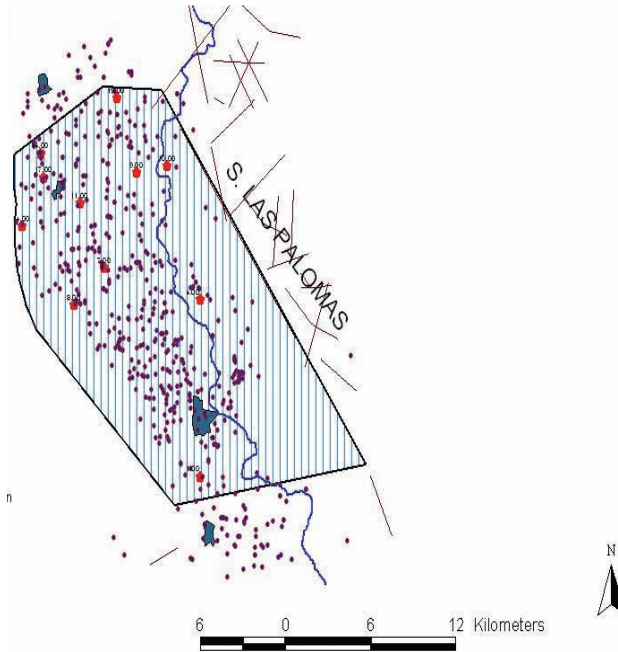


FIG. 1. Model area with Rio Conchos stream (blue line), geological structures, urban areas (the largest one is Delicias), water production wells (small dots), CFC sampling points (larger, red dots).

of 20.1°C and 294 mm precipitation. Precipitation falls primarily between July and September [5].

The area consists primarily of sedimentary and igneous rocks. The quaternary alluvial sediments cover the major part of the area. The Meoqui-Delicias aquifer is supposed to have a maximum thickness of 500 m [5] with sediments that are supposed to have a medium to high permeability but they incorporate also lacustrine deposits having a lower permeability. The conglomerates are classified as medium permeable. Tertiary igneous rocks like rhyolite, rhyolitic tuff and tuff with a relatively high permeability also show an ample distribution. Cretaceous limestone, sandstone and siltstone with low permeability are cropping out in the south of the aquifer system [6].

Two aquifer complexes are distinguishable in Meoqui-Delicias: the one who is formed by granular and clastic material filling the valleys, and the other hosted by fractured vulcanites. This investigation contemplates only the first complex of sediment constitution. The principal groundwater flow direction is

parallel to the principal stream Río Conchos from south to north [7], [6]. Only local inversion of groundwater flow is detected. The actual groundwater levels are between 6 and 80 m. Meoqui-Delicias aquifer system receives approximately 85 mm recharge per year [8]. No long-term measurements of potentiometric levels were obtainable, but [5] mention an averaged drawdown of 0.6 m since 1972 despite the water extraction restrictions imposed since 1962. The studied sub-area is supposed to have minor water table changes.

3. METHODOLOGY

Water quantity (extraction, hydrometry and water table) and aquifer data were obtained from previous investigations and two field campaigns during 2005, while field chemical parameters (temperature, pH, TDS), water chemistry, water isotopes and gaseous tracers were sampled during dry season (May 2005). Nitrate (N-NO₃) concentrations were determined at the Laboratory of Centro Calidad Ambiental, ITESM Campus Monterrey, following EPA 300.1/1999 standard. Deuterium (²H) and oxygen-18 (¹⁸O) isotopes have been analyzed at the Environmental Isotope Laboratory, University of Waterloo. Chlorofluorocarbons (CFC's) were analysed according to description of [9] at Spurenstofflabor Oster, Germany.

The USGS numerical finite-difference model MODFLOW [10] in conjunction with the particle tracking program MODPATH [11] was used to simulate groundwater flow and particle transport of a sub-area of the Meoqui-Delicias aquifer system with a length of 40 km along the Río Conchos and 10 km to both sides of the stream; the model area is limited to the east (Sierra Las Palomas) by an important fracture system considered as a no-flow boundary [12] (Fig. 1).

The selected grid consists of 244 columns and 243 rows covering a total of 590 km². Data for each cell were entered, i.e., the top and bottom of the six aquifer layers, hydraulic conductivity (horizontal and vertical). Since steady state conditions are assumed, a constant head boundary was assigned to give the amount of subsurface flow needed to maintain the water table at the observed position. A stream-routing module was used to account for the interaction between stream and aquifer, using following parameters: bottom, top, and width of river, as well as Manning's roughness coefficient.

4. CALIBRATION STRATEGY

A two-step calibration was achieved to increase the reliability of the model: the first step is the traditional process of adjusting hydraulic model parameters and comparing the results until calculated head values closely match the measured values at selected points of the upper aquifer; the second step includes the comparison of results from backward tracking calculations with results of tracer interpretation (origin and residence time of water). The following parameters were identified: recharge and discharge, rate and direction of flow, distribution of aquifer parameters, hydraulic conductivities, and boundary conditions. Permeability was adjusted by trial and error until the groundwater contours matched the water table contours. The ground-water balance (m^3/d) of the calibrated model is shown below:

Inflow:	33 676
Outflow:	7 299
Recharge:	117 946
Extraction (wells):	102 921
Movement to river:	41 402

The calibrated hydraulic conductivity is 9.5, 0.18, 0.19, and 0.2 m/d for alluvial deposits, polymictic conglomerates, volcanic rocks, and metamorphic rocks, respectively, while recharge flux has been estimated 219, 10.9, 3.7, and 1.9 mm/yr for irrigated land, brushes, urban areas, and grassland, correspondingly.

The numerical finite-difference model was then used to simulate ground-water flow and interaction with Rio Conchos as a consequence of different water management alternatives with the scope to find out best water resources management practice for improvement of aquatic ecosystems. This paper concentrates on the calibration with environmental tracers.

5. CALIBRATION WITH TRACERS

5.1. Isotopes

Stable isotopes ^{18}O and ^2H help to establish fractionation processes and consequently also the origin of water inside the aquifer. Fortunately, local isotopic data from GNIP network (IAEA) is reported between 1962 and 1988 to construct a Local Meteoric Water Line (LMWL). Figure 2 shows the Global Meteoric Water Line (GMWL) by [13] with the equation $\delta^2\text{H} = 8.17 \delta^{18}\text{O} + 11.27$,

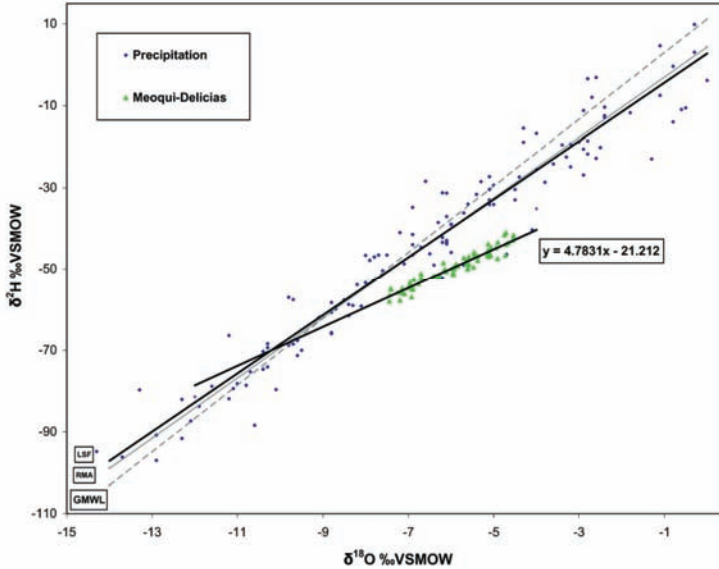


FIG. 2. Stable isotopes in rain water (data from GNIP station in Chihuahua) and groundwater from Meoqui-Delicias aquifer.

and two LMWLs of Chihuahua for different adjustment: $\delta^2\text{H} = 7.13 \delta^{18}\text{O} + 2.78$ (LSF) and $\delta^2\text{H} = 7.37 \delta^{18}\text{O} + 4.31$ (RMA) [14]. The regression line of groundwater samples ($\delta^2\text{H} = 4.78 \delta^{18}\text{O} - 21.2$) in Figure 2 indicates enrichment due to evaporation. The enrichment process most probably happens during the conduction of water through open irrigation channels and part of the irrigated water percolates to the groundwater reservoir.

Thus, the agricultural use of water most likely changed groundwater composition in Meoqui-Delicias aquifer. Using nitrate as indicator of human impact, it is possible to demonstrate that areas with N-NO_3 values above 10 mg/L correspond to isotopically more enriched samples [15].

5.2. Chlorofluorocarbons

The observed CFC concentrations in groundwater were compared to atmospheric concentrations of the monitoring station at Nivot Ridge, Colorado, USA [16]. These values are supposed to be valid in the whole world with maximum deviations of 10% [17]. Using these concentrations it is possible to establish the residence time of water in the aquifer and to have an insight into groundwater conditions.

EVALUATION OF THE IMPACT OF GROUNDWATER RESOURCES

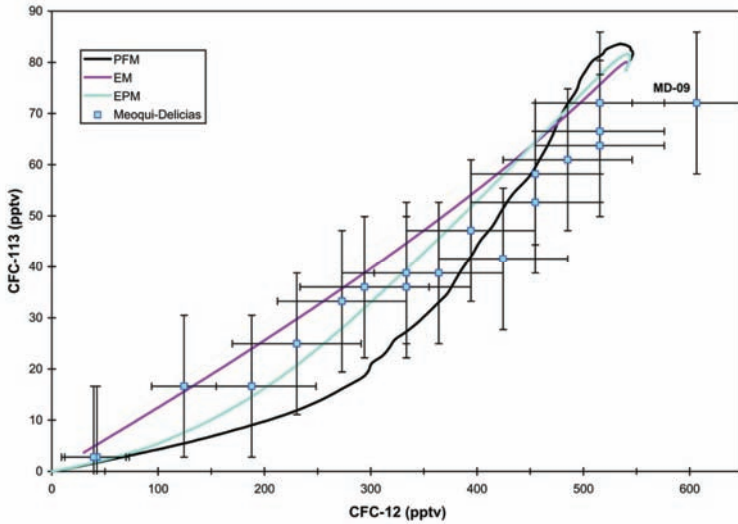


FIG. 3. CFC-12 versus CFC-113 concentration of samples from upper Meoqui-Delicias aquifer complex. PFM = piston flow model, EM = exponential model, EPM = exponential piston flow model.

The calculation was described by [18] using the equations of [19] and the constants of [20] and [21]. The obtained concentrations are in parts per trillion by volume (pptv). If the aquifer is shallow with a depth-to-groundwater less than 10 m, then the calculated concentrations describe the atmospheric CFC values during infiltration. If the vadose zone is deep, then it is necessary to apply a correction of the concentrations according to [22] and [23].

A comparison between CFC-12 and CFC-113 concentrations (Fig. 3) indicates that most sample points are within the area bounded by different curves representing three possible models: piston flow model (PFM), exponential model (EM) and a combined model of exponential and piston flow (EPM). The PFM is valid for confined aquifers with a small and distant recharge zone, while EM is applicable for perfectly mixed reservoirs, and thus receiving recharge in the whole aquifer area. The EPM is a combination between both explained models. Due to the geological settings of the plains, the exponential model seems to be most appropriate. Practically all samples were collected in the highly permeable alluvial sediments from Quaternary where conditions are generally not confined.

CFC concentrations in the Meoqui-Delicias aquifer are relatively uniform. There is only one value above atmospheric contents. According to PFM the

residence time was computed between 0 and 45 years and according to EM the mean residence time varies between 8 and 300 years (using CFC-12 and CFC-113). The latter range is more consistent with the hydrogeological settings. As shown, chemical and stable isotope results suggest enrichment due to irrigation agriculture, which may also happen with CFCs and reduce the reliability of “ages”. A sensibility analysis showed, however, that the uncertainty with respect to the residence times did not have a significant impact on the numerical flow model.

6. CONCLUSIONS

A numerical finite-difference model was used to simulate groundwater flow of a sub-area of the Meoqui-Delicias aquifer system. The calibration was achieved by (i) adjusting hydraulic model parameters and comparing the results until calculated head values closely match the measured values at selected points of the upper aquifer, (ii) comparing results from a backward tracking process of water particles with results of CFC residence times. By using stable water isotopes it could be evidenced that enrichment processes due to evaporation are present and may modify also CFC concentrations. Fortunately this uncertainty did not have a significant impact on the groundwater model.

ACKNOWLEDGEMENTS

This study could be carried out with funds received from Fondo Sectorial de Investigación Ambiental (contract FOSEMARNAT-2004-01-221) and World Wildlife Foundation Mexico (contract KE50). We acknowledge the effort of Comisión Nacional del Agua Delegación Chihuahua (Melchor Ocampo) and Secretaría de Medio Ambiente y Recursos Naturales Delegación Chihuahua (Manuel Irigoyen) for facilitating existing studies and data.

REFERENCES

- [1] CNA – COMISIÓN NACIONAL DEL AGUA, Ley de Aguas Nacionales, México (1992).
- [2] NYHOLM, T., CHRISTENSEN, S., RASMUSSEN, K.R., Flow depletion in a small stream caused by ground water abstraction from wells, *Ground Water* **40** (2002) 425–437.

EVALUATION OF THE IMPACT OF GROUNDWATER RESOURCES

- [3] SOPHOCLEOUS M.A., TOWNSEND, M.A., VOGLER, L.D., MCCLAIN, T.J., MARKS, E.T., COBLE, G.R., Experimental studies in stream-aquifer interaction along the Arkansas River in central Kansas: Field testing and analysis, *Journal of Hydrology* **98** (1988) 249–273.
- [4] LINDGREN, R.J., LANDON, M.K., Effects of groundwater withdrawals on the Rock River and associated valley aquifer, Eastern Rock Country, Minnesota, U.S. Geological Survey Water-Resources Investigations Tech. report **99-4157** (2000).
- [5] CONAGUA – COMISION NACIONAL DEL AGUA, Actualización del estudio geohidrológico del acuífero Meoqui-Delicias, Chihuahua, Report, Contract No. 75120243 (2005).
- [6] INEGI – INSTITUTO NACIONAL DE ESTADISTICA, GEOGRAFIA E INFORMATICA, Cartografía Hidrología Subterránea Delicias H13-10 (Groundwater hydrology map Delicias), Scale 1:200,000 (1999).
- [7] UACH – UNIVERSIDAD AUTÓNOMA DE CHIHUAHUA, Estudio geohidrológico del valle de Chihuahua (Primera Etapa), Tech. report (1978).
- [8] SIGE – SISTEMA DE INFORMACIÓN GEOGRÁFICA DEL SECTOR EDUCATIVO, Internet: <http://sige.seyc.gob.mx/> (2004).
- [9] OSTER, H., SONNTAG, C., MÜNNICH, K.O., Groundwater age dating with chlorofluorocarbons, *Water Resources Research* **32** 10 (1996).
- [10] HARBAUGH, A.W., BANTA, E.R., HILL, M.C., MCDONALD, M.G., MODFLOW-2000, the U.S. Geological Survey modular ground-water model – User guide to modularization concepts and the ground-water flow process, U.S. Geol. Surv. Open-File Report **00-92** (2000).
- [11] POLLOCK, D.W., User's Guide for MODPATH/MODPATH-PLOT, Version 3: A particle tracking post-processing package for MODFLOW, the U.S. Geological Survey finite-difference ground-water flow model: U.S. Geol. Surv. Open-File Rep **94-464** (1994).
- [12] ITESM/EPAS – INSTITUTO TECNOLÓGICO Y DE ESTUDIOS SUPERIORES DE MONTERREY / ESTUDIOS Y PROYECTOS DE AGUA SUBTERRÁNEA. Estudio de la Interacción del Río Conchos con el acuífero Meoqui-Delicias para fines de protección de los ecosistemas acuáticos. Tech. report (2005).
- [13] ROZANSKI, K., ARAGUÁS-ARAGUÁS, L., GONFIANTINI, R., Isotopic patterns in modern global precipitation, In: SWART P.K., LOHMANN K.C., MCKENZIE J., SAVIN S. (eds) *Climate change in continental isotopic records*. Geophysical Monograph **78**, American Geophysical Union, Washington, D.C., (1993) 1–36
- [14] INTERNATIONAL ATOMIC ENERGY AGENCY, Statistical treatment of data on environmental isotopes in precipitation (Period 1960-1997) (2002)
- [15] MAHLKNECHT et al., (in preparation)

- [16] U.S. GEOLOGICAL SURVEY, Internet site: http://water.usgs.gov/lab/software/air_curve/
- [17] CUNNOLD, D.M., FRASER, P.J., WEISS, R.F., PRIN, R.G., SIMMONDS, P.G., MILLER, P.R., ALYEA, F.N., CRAWFORD, A.J., Global trends and annual releases of CCl₃F and CCl₂F₂ estimated from ALE/GAGE and other measurements from July 1978 to June 1991, *J. Geophys. Res.* **99** (1994) 1107–112.
- [18] PLUMMER, L.N., BUSENBERG, E., Chlorofluorocarbons, In: COOK, P., HERCZEG, A.L., *Environmental Tracers in Subsurface Hydrology*, Kluwer Academic Publishers, Boston, USA (2000) 529.
- [19] WEISS, R.F., PRICE, B.A., Nitrous oxide solubility in water and seawater, *Marine Chemistry* **8** (1980) 347–359.
- [20] WARNER, M.J., WEISS, R.F., Solubilities of chlorofluorocarbons 11 and 12 in water and seawater, *Deep-Sea Res* **32** (1985) 1485–1497.
- [21] BU, X., WARNER, M.J., Solubility of chlorofluorocarbon 113 in water and seawater, *Deep-Sea Research* **42** (1995) 1151–1161.
- [22] COOK, P.G., SOLOMON, D.K., PLUMMER, L.N., BUSENBERG, E., SCHIFF SL., Chlorofluorocarbons as tracers of groundwater transport processes in shallow, silty sand aquifer; *Water Resources Research* **31** (1995).
- [23] ENGESGAARD, P., HØJBERG, A.L., HINSBY, K., JENSEN, K.H., LAIERT, LARSEN, F., BUSENBERG, E., PLUMMER, L.N., Transport and Time Lag of Chlorofluorocarbon Gases in the Unsaturated Zone, Rabis Creek, Denmark, *Vadose Zone J* **3** (2004) 1249–1261.

INTERNET GIS AND WATER RESOURCE INFORMATION

P. DEEPRASERTKUL, R. CHITRADON

Hydro and Agro Informatics Institute,
National Science and Technology Development Agency,
Bangkok, Thailand

Abstract

GIS is Geographic Information System, a computer system capable of integrating, storing, editing, analyzing, sharing and displaying geographically referenced information. At present, GIS is not only limited to cartography but also involves in various activities i.e. scientific investigation, natural resource management, environmental impact assessment, etc. Internet GIS allows more information sharing as many users can access GIS at the same time. Another progress in GIS is GIS/MIS where non-geographical information (customized to users' purposes) regarding the particular area was overlaid with GIS. Internet GIS/MIS is useful for water resource management as it gives users better understanding of the overall picture i.e. GIS: locations of rivers/basins, topography of the flooded/drought areas, linkages of geographical factors and natural disasters occurred and MIS: water demand and supply thus gives users the ability to find best solution for each area and manage water resource in a sustainable manner.

1. INTRODUCTION

GIS can be linked to location data, such as people to addresses, reservoirs to plant, or rivers within a network [1]. This information can be laid to give a better understanding of how it all works together. Internet GIS/MIS is a research and application that utilizes the Internet systems to facilitate the access, processing, and dissemination of geographic or non-geographic information and spatial analysis knowledge [4]. The Internet GIS/MIS system has become a technology to support spatial analysis and expand information representation in GIS and MIS. These display usage can also meet water demand for management, analysis, estimation, and decision.

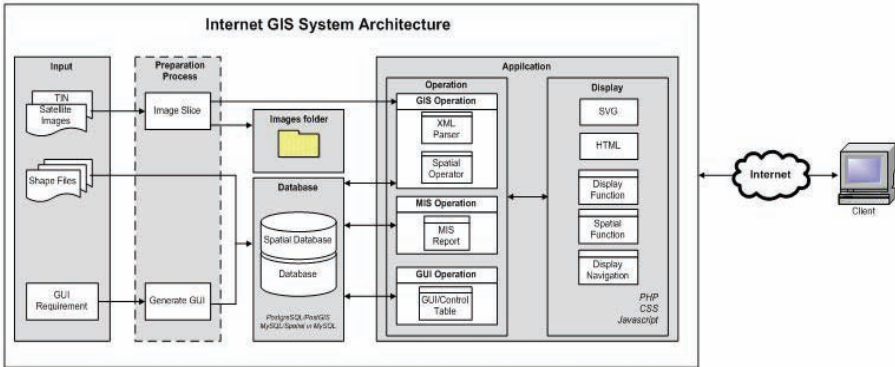


FIG. 1. Internet GIS/MIS System Architecture

2. INTERNET GIS/MIS SYSTEM ARCHITECTURE

Architecture of Internet GIS/MIS System is shown in Figure 1. **GIS:** Geographical features can be described with raster data, for example, aerial or satellite images or vector data (points, lines and polygons). For vector data, they are imported to database and spatial database, respectively. **MIS:** The output reports are created and displayed on the Internet GIS/MIS. The data are queried from databases. **GUI Generator:** Internet GIS/MIS gives users the ability to easily generate GUI. The GUI and control table are created when the system receives the requirement.

3. XMLCOMPILER

The architecture of XMLCompiler is shown in Figure 2. XMLCompiler accesses and queries the non-spatial and spatial data to produce an input file. A software tool for parsing and converting the input file to *svg* files in XMLCompiler is XMLParser. The *svg* files are compressed to the *svgz* files.

Definition 1: Let I be an input file of XMLParser and contains a lot of stream lines. $I = \{s_j \mid s_j \text{ is the input stream and } j \text{ is a number of input streams}\}$.

Definition 2: Let O be a set of XMLParser output files. $O = \{o_k \mid o_k \text{ is the output file and } k \text{ is less than or equal a number of } geocode\}$, where *geocode* is a geographical code to identify a point or area at the surface of the earth [7].

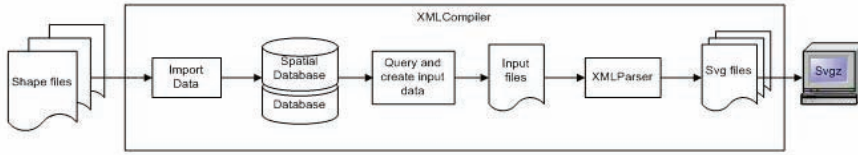
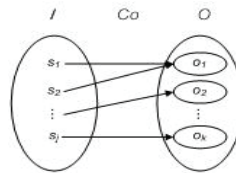


FIG. 2. A XMLCompiler architecture

Definition 3: Let Co be the mapping function from I to O : $Co: I \rightarrow O$. Co is the XMLParser processes and many-to-one function. Since many input streams containing the similar *geocode* are mapped to one output file.



The XMLParser is correct with respect to the input assertion s_j and the output assertion o_k . Suppose that s_j is true, so that s_j contains data in database and has satisfying pattern. Then XMLParser converts s_j to o_j . Hence, o_k is true [5]. However, when a number of the input streams in I are added and associate with the original, a closure occurs. Hence, the new input files I^* have both original and added input streams. Thus, $I \subseteq I^*$. In case of O , the closure of output relation is also constructed in the similar condition. Thus, $O \subseteq O^*$ where O^* is a new set of output files. Then, the assertion $s_j \in I^*$ if $s_j \in I$ and $I \subseteq I^*$. Also, the assertion $o_k \in O^*$ if $o_k \in O$ and $O \subseteq O^*$. As the correctness assertion of I , O , and closures of their relations, XMLParser can be inferred that it is the robust program.

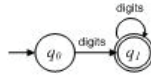
3.1. XMLParser

XMLParser is written by C programming language and applied Lex and Yacc for generating a lexical analyzer and a parser. Lex is a program generator designed for lexical processing of character input streams. The Lex source file associates the regular expressions and the input file fragments [3].

Definition 4: A *finite automaton* is a 5-tuple $(Q, \Sigma, \delta, q_0, F)$ [6], where

1. Q is a finite set called the *states*,
2. Σ is a finite set called the *alphabet*,

3. $\delta: Q \times \Sigma \rightarrow Q$ is the transition function,
4. $q_0 \in Q$ is the start state, and
5. $F \subseteq Q$ is the set of accept states.



This state diagram of finite automaton (M) accepts all strings that have at least one digit. Thus $L(M) = \{w \mid w \text{ contains at least one digit}\}$. For Yacc, the heart of source is a collection of grammar rules [2].

Definition 5: A context-free grammar is a 4-tuple (V, Σ, R, S) [6], where

1. V is a finite set called the variables,
2. Σ is a finite set, disjoint from V , called the terminals,
3. R is a finite set of rules, with each rule being a variable and a string of variables and terminals,
4. $S \in V$ is the start variable.

The structure of XMLParser is shown in Figure 3 which has two following steps.

Step 1: The *xmlparser.lex* is the source specification which specifies the regular expressions. It recognizes expressions in a stream and performs the specified actions as it is detected.

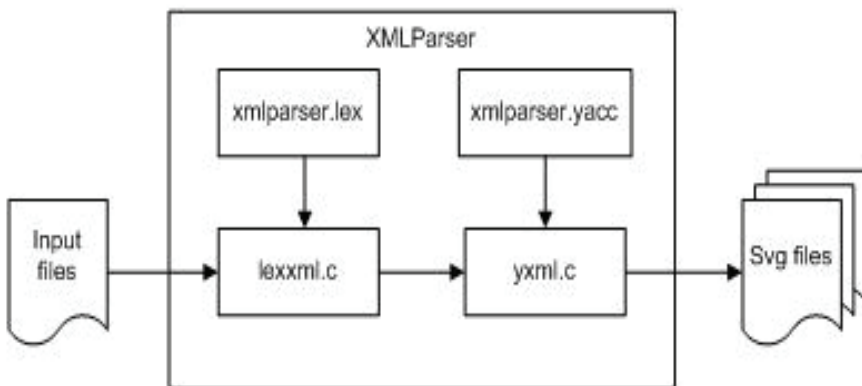


FIG.3. A structure of XMLParser.

with GIS which can perform more perfectly and support government to make decisions better.

6. FURTHER DEVELOPMENT

The user-friendly XMLCompiler interface is expected that it will be released within the next few months. The tool for generating two or more spatial data by using the spatial operation function in PostGIS and Spatial Data in MySQL is developing.

REFERENCES

- [1] ESRI, The Guide to Geographic Information Systems, GIS.com (2007), <http://www.gis.com>.
- [2] JOHNSON, S.C., Yacc: Yet Another Compiler-Compiler, Yacc Online Manual, <http://dinosaur.compilertools.net/yacc/index.html>.
- [3] LESK, M.E., SCHMIDT E., Lex-A lexical Analyzer Generator, Lex Online Manual, <http://dinosaur.compilertools.net/lex/index.html>.
- [4] PENG, Z.R., TSOU, M.H., Internet GIS Distributed Geographic Information Services for the Internet and Wireless Networks, John Wiley & Sons, Inc., New Jersey (2003).
- [5] ROSEN, K.H., Discrete Mathematics and Its Applications, Fifth Edition, the McGraw-Hill Companies, New York (2003).
- [6] SIPSER, M., Introduction to the Theory of Computation, PWS Publishing Company, Boston, United State of America (1997).
- [7] WIKIPEDIA, Geocode, Wikipedia Foundation, Inc. (2007), <http://en.wikipedia.org/wiki/Geocode>.
- [8] WIKIPEDIA, Lookup Table, Wikipedia Foundation, Inc. (2007), http://en.wikipedia.org/wiki/Lookup_table.

ENVIRONMENTAL ISOTOPES IN THE WATER CYCLE IN THE CATCHMENT OF THE QUEQUEN GRANDE RIVER, ARGENTINA

D.E. MARTÍNEZ*, C. DAPEÑA**, T. BENTACUR VARGAS***,
H.O. PANARELLO**, M. QUIROZ LONDOÑO⁺, H.E. MASSONE⁺⁺

*CONICET and Centro de Geología
de Costas y del Cuaternario,
U.N. de Mar del Plata, Argentina

**Instituto de Geocronología y Geología Isotópica
(INGEIS-CONICET-UBA)

***Universidad de Antioquia,
Colombia

⁺FONCYT and Centro de Geología de Costas
y del Cuaternario,
U.N. de Mar del Plata, Argentina

⁺⁺Centro de Geología de Costas y del Cuaternario,
U.N. de Mar del Plata, Argentina

Abstract

The catchment of the Quequen Grande River, in the Province of Buenos Aires, is about 10,000 km² occupying an important area in the Pampa Plain, the most important agricultural productive area in Argentina. The area is covered by Upper Cenozoic loess-like sediments forming an unconfined aquifer, and it is drained mainly by the streams. Most important aspects of its hydrology, like groundwater-surface relationship, recharge volume and area, etc., remain unknown at present. Moreover, before the starting of an IAEA CRP in November of 2004, no isotopic data existed in the catchment. After about two years of data collecting some results are able to be communicated. Local meteoric water lines has been obtained for three sampling sites in the catchment, presenting clear differences between coastal and inland rainfalls. A clear difference has been stated between the isotopic composition of inland precipitation and the isotopic composition of coastal precipitation. This observation is partially due to continental effect, but different precipitation sources can also be recognized. Preliminarily, the dominance of a recharge

area in groundwater composition has been established. Stable isotope composition of groundwater is very homogeneous, corresponding to a well mixed system. The surface water composition is clearly dominated by groundwater discharge, with some evaporation effect, and some temporary changes related to strong rainfall events.

1. INTRODUCTION

This study is a part of a Research Coordinated Project (CRP) of the International Atomic Energy Agency (IAEA) “Isotopic Age and composition of streamflow as indicators of groundwater sustainability”. The main hypothesis of this project is that the knowledge of the hydrochemical and isotopic composition of river water and groundwater will be very helpful to identify river water-groundwater relationship and to develop adequate water management sustainable criteria. About 15 catchments from Africa, Asia, Europe and South-America were chosen to participate in this CRP, being the catchment of the Quequén Grande river, in the Province of Buenos Aires, Argentina, one of them.

The Quequen River basin covers an area of 10,000 km², in the Province of Buenos Aires in Argentina (Fig. 1). The mean flow rate of the river near its outflow on the Atlantic Sea is about 20 m³/s, with a maximum record of 700 m³/s. The basin is an important agricultural area, and the alternation of flood and drought periods affects the economy of the population. Then, a better knowledge of how the water system works will be very important to plan land uses and economic activities. There is little knowledge of the hydrological dynamics of the catchment. Despite its large area very few flow rate measuring stations exist and there is no groundwater monitoring network operating. This need for basic information should be catered for by means of an extended surface and groundwater monitoring network and the implementation of uninterrupted records over the years. But the economy of the region needs more urgent solutions, and important actions need to be taken to achieve a sustainable agricultural development, which is strongly linked to water resources management.

The way in which hydrochemical and isotopic composition of waters reveals the flow paths and water age is a very important tool to count with basic information in a shorter time. The conceptual basis for the application of hydrochemical and isotopes measurements have been stated in many papers leading with the groundwater-stream water relationships in the hydrologic cycle [1–4]. Some important developments of the tracer studies and water age determination in catchments [5–8] constitute important antecedents for the project under development.

Then, our proposal is to develop an integrated study of surface water and groundwater applying hydrogeochemical and isotopic techniques in order to evaluate the relationship between surface water and groundwater and to assess groundwater contribution to the streamflow in the catchment of the Quequén Grande River, Argentina.

2. HYDROLOGICAL AND HYDROGEOLOGICAL BACKGROUND

The catchment is located in a plain area known as “intermountain plain”, which is a vast region among the only two existing ranges in the Province known as Tandilia and Ventania ranges (Fig. 1). Tandilia range is formed by Precambrian metamorphic rocks, mainly migmatites and granitoids, and a thick cover of Lower Palaeozoic sedimentites, mainly orthoquartzites. A block structure produced as a consequence of Andic movements during the Tertiary formed a series of table hills of low altitudes (about 400 m.a.s.l.). Ventania Range is formed by Palaeozoic rocks, mainly sandstones, conglomerates and diamictites. The structure is mainly a complex fold system. The maximum altitude is 1,100 m.a.s.l.

A thick sequence of Tertiary and Quaternary sediments overlies the Palaeozoic rocks, forming an aquifer system known as Pampeano aquifer. This system is composed by fine sands, silt and silt-sands, with clayey layers intercalated, of aeolian and fluvial origin. The maximum thickness has been determined by drilling in Necochea city, where basement rocks were found at 296 m depth. Permeability of the sediments is in the order of 10 m/day.

The climate of the area is sub-humid temperate. The average annual temperature is 14°C, being July the month of lower temperatures with an average of 7.3°C, and January the hottest month with an average temperature of 21°C [9]. The mean rainfall for the period 1961–1990 was about 800 mm. During the last 10 years, the annual precipitation values have ranged from 703 mm/year to 1400 mm/year, with an average of 943 mm/year. The highest precipitation values are recorded between September and March. As for the evapotranspiration potential values calculated for that same period with Thorthwaite method, they have been estimated between 750 mm/year and 833 mm/year, with an average of 786 mm/year

The catchment is drained by a series of streams with a general trend North-South which are intercepted by the Pesacado Castigado Creek (Fig. 1), with a Northwest to Southeast trend. The Quequén Grande river at its outlet into the Atlantic Ocean has an average flow rate in the order of 11 m³/s [9], with peaks reaching to 300 m³/s, and a maximum historical record of 758 m³/s during November 1985.

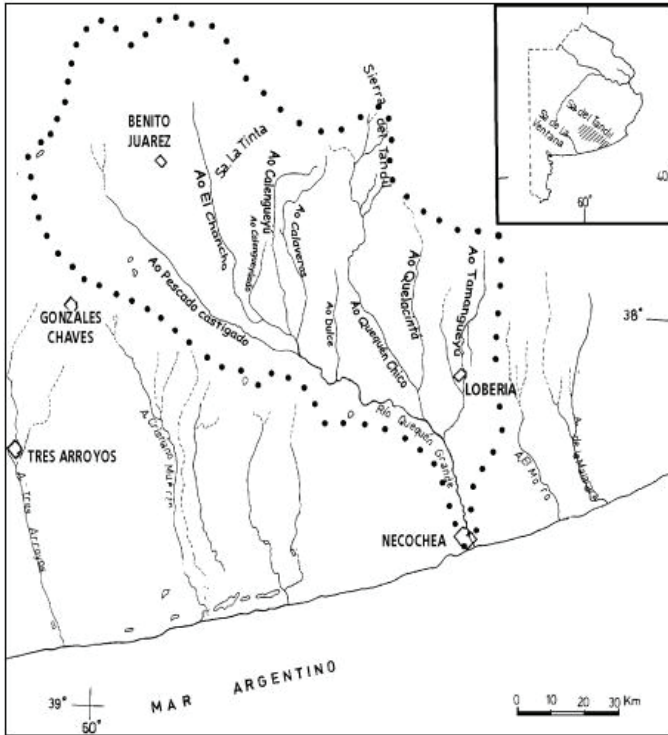


FIG. 1. Location map.

3. METHODS

In order to characterize the isotopic composition of the different components of the water cycle in the considered catchment a sampling network was designed, including four monthly composite rain water sampling points (LNE, LLO, LSM and LLN), five weekly stream water sampling points (SLC, STA, SPB, SPA and SEC) and a variable number of groundwater sampling point with a seasonal frequency (Fig. 2).

Chemical analyses were performed on stream and groundwater samples using standard techniques. Isotopes measurements were made at the laboratories of the Instituto Nacional de Geocronología y Geología Isotópica (INGEIS). Stable isotopes ^2H and ^{18}O were analyzed with a mass spectrometer Finnigan MAT Delta S. The results are expressed as isotopic deviation $\delta\%$ using as reference the Vienna Standard Mean Ocean Water (V-SMOW). Uncertainties are $\pm 0.2\%$ and $\pm 1.0\%$ for $\delta^{18}\text{O}$ and $\delta^2\text{H}$ respectively. Tritium

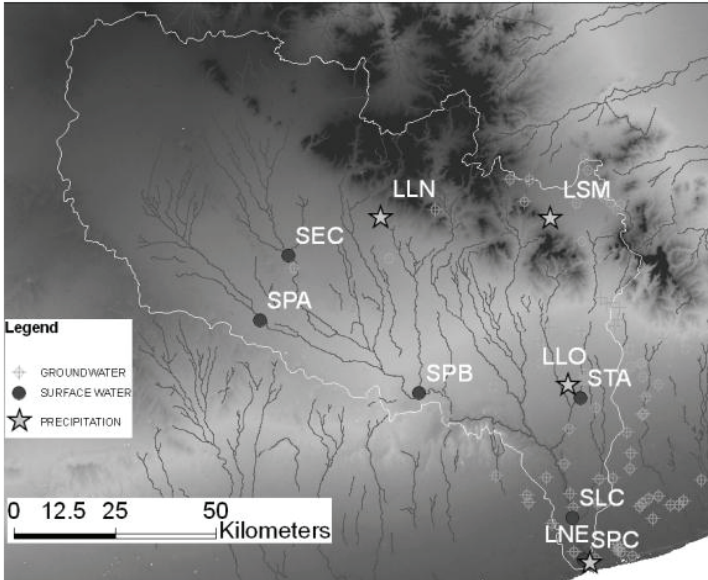


FIG. 2. Distribution of sampling points.

analysis is made by liquid scintillation. Concentrations of ^3H are expressed as Tritium Units: $1 \text{ TU} = 1 \text{ atom } ^3\text{H} / 10^{18} \text{ atoms } ^1\text{H}$ and the average uncertainty is $\pm 1.0 \text{ TU}$ [10].

4. RESULTS

4.1. Isotopes in precipitation

The most complete record of isotopes in rain water corresponds to the sampling sites LNE, LLN and LSM, covering about two years of sampling at present. The sampling site LLO has a short record. Figure 3 exhibits the distribution of the rain water composition jointly with the Global Meteoric Water Line (GMWL) [11]. This figure shows a clear difference between the inland precipitation (LSM and LLN) and coastal precipitation (LNE). Temperature effect on rain water composition can also be observed, being the winter samples (July) the most depleted samples ($\delta^{18}\text{O} < -7 \text{ ‰}$ and $\delta^2\text{H} < -40 \text{ ‰}$) and the summer ones (November–January) the most enriched ($\delta^{18}\text{O} -3 \text{ ‰}$ to -5 ‰ and $\delta^2\text{H} -10 \text{ ‰}$ to -30 ‰). Nevertheless some summer depleted values probably responds to amount effect ($\delta^{18}\text{O} -7.7 \text{ ‰}$ and $\delta^2\text{H} -51 \text{ ‰}$).

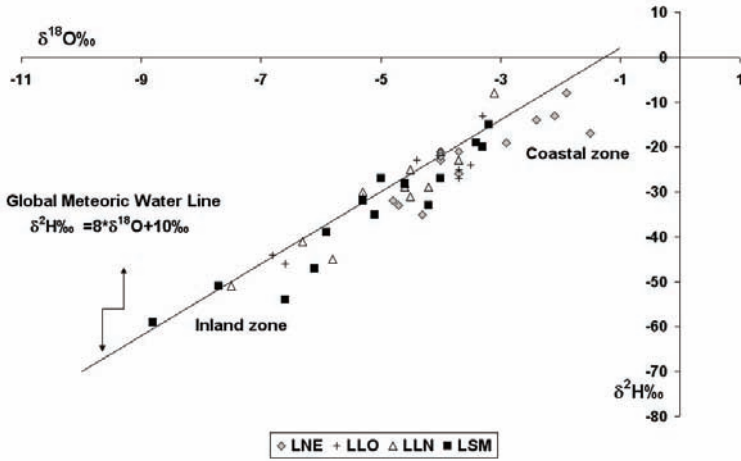


FIG. 3. δ^2H vs. $\delta^{18}O$ of precipitation at locations LNE, LLO, LLN and LSM.

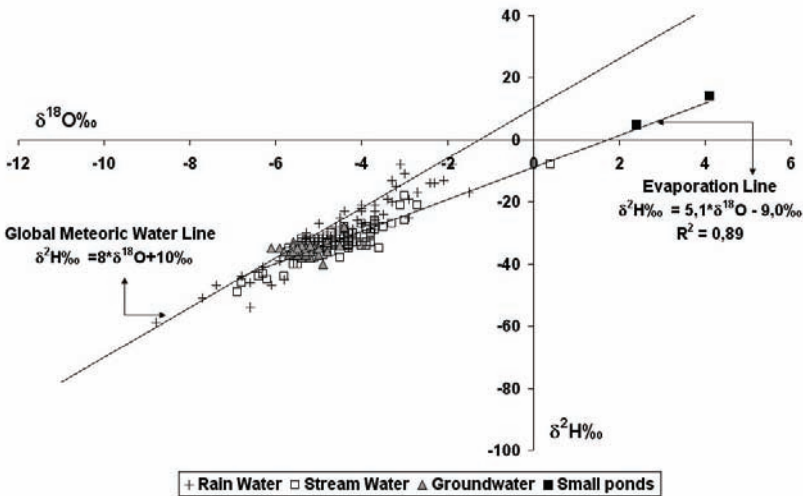


FIG. 4. δ^2H vs. $\delta^{18}O$ with Global Meteoric Water Line, rain, stream water and groundwater.

4.2. Isotopes in stream water

Stream water isotope composition for the different samplings points is also shown in Figure 4 jointly with the GMWL. It is not possible in this paper to go

ENVIRONMENTAL ISOTOPES IN THE WATER CYCLE

TABLE 1. MINIMUM, MAXIMUM AND AVERAGE VALUES OF STABLE ISOTOPES IN DIFFERENT WATER TYPES.

Water type	$\delta^2\text{H} \text{‰}$ min	$\delta^2\text{H} \text{‰}$ max	$\delta^2\text{H} \text{‰}$ average	$\delta^{18}\text{O} \text{‰}$ min	$\delta^{18}\text{O} \text{‰}$ %max	$\delta^{18}\text{O} \text{‰}$ average
Precipitation	-59	-8	-29.1	-8.8	-1.4	-4.5
Stream water	-49	-8	-33.0	-6.9	0.4	-4.7
Groundwater	-40	-28	-35.4	-6.1	-4.4	-5.3

into depth of the differences recognized in the sites, or seasonalities in changes, but at least it is easy to observe some samples that are affected by evaporation processes fitting a distinct line, and the most dispersed along the meteoric line. The most evaporated samples correspond to a couple of small evaporated ponds in the area. The wide range of values of isotopic composition for stream water is shown in Table 1.

4.3. Groundwater

Groundwater isotope composition differs from the other two elements considered (rain and streamwater), showing a very narrow variation range, around a mean isotopic composition. Most of the samples are represented little bit below the GMWL, which can indicate some evaporation prior to infiltration (Fig. 4).

5. DISCUSSION AND CONCLUSIONS

Groundwater samples presents a relatively homogenous composition, which can be interpreted as the result of a well mixed system. Stream water shows a higher degree of variation along the meteoric line and also an evaporation line. The evaporation line crossed the meteoric water line approximately where most of the groundwater samples are represented, and many of the stream water samples are placed around this area.

The observed results demonstrates that rain water is the source of most of the water in the system, and specifically it is infiltrated in the area around LSM and LLN. If well temperature and probably continental effects can be observed in rain composition, the weighted average composition in that places corresponds to groundwater isotope contents. The groundwater system is well mixed and consequently groundwater composition is very homogeneous. The

fact that most of the streamwater is around groundwater composition validates the conceptual models in the catchment suggests that most of the streamflow is baseflow. Evaporation effects on streamwater are recognized and also some depleted measurements as a consequence of sampling after rainy days.

REFERENCES

- [1] SEILER, K-P., LINDNER, W., Near-surface and deep groundwaters. *J. Hydrol.* **165** (1995) 33–44.
- [2] TÓTH, J., Hydraulic continuity in large sedimentary basins, *Hydrology Journal*, Vol. **3** 4 (1995) 4–16.
- [3] WINTER, T.C. et al., *Ground Water and Surface Water A Single Resource*, U.S. Geological Survey Circular **1139** (1998) 79, Denver, Colorado, USA.
- [4] SOPHOCLEUS, M., Interactions between groundwater and surface water: the state of the science, *Hydrogeology Journal*, Vol. **10** 1 (2002) 52–67.
- [5] MICHEL, R.L., Residence times in river basins as determined by analysis of long-term tritium record. *J. Hydrol.* **130** (1992) 367–378.
- [6] MCDONNELL, J.J., et al., A combined tracer-hydropetric approach to assessing the effects of catchment scale on water flowpaths, source and age, *International Association of Hydrological Sciences, Publication* **258** (1999) 265–274.
- [7] HOLKO, L., Stable environmental isotopes of ^{18}O and ^2H in hydrological research of mountainous catchment, *J. Hydrol. Hydromech.* **43** (1995) 249–274.
- [8] VITVAR, T., et al., A review of isotope applications in catchment hydrology, In Aggarwal et al. Edits.: *Isotopes in the Water Cycle*, Springer, The Netherlands (2005) 151–169.
- [9] KRUSE, E., et al., Caracterización de la red de drenaje para la evaluación hidrológica en la región interserrana (provincia de Buenos Aires), En actas, I Congreso Nacional de Hidrogeología y III Seminario Hispano – Argentino sobre temas actuales de hidrología subterránea, Bahía Blanca (1997) 133–145, Argentina.
- [10] GRÖENING, M., ROZANSKI, K., Uncertainty assessment of environmental tritium measurements in water, *Accred Qual Assur* **8** 359.366. (2003).
- [11] CRAIG, H., Isotopic variations in meteoric waters. *Science* **133** (1961) 1702–1703.

C-14 AND TRITIUM CONCENTRATIONS ALONG ROMANIAN DANUBE SECTOR¹

Preliminary Results

C. VARLAM*, I. STEFANESCU*, S. CUNA[†], I. FAURESCU*,
I. POPESCU*, M. VARLAM*²

*National Institute for Cryogenic
and Isotopic Technologies,
Rm. Valcea, Romania

[†]National Institute for Isotopic
and Molecular Technologies,
Cluj, Romania

Abstract

Danube River Basin is the second river basin in Europe comprising 18 countries. Lower Danube Basin covers the Romanian-Bulgarian sub-basin downstream of Cazane Gorge and the sub-basins of Siret and Prut River. Cernavoda Nuclear Power, a CANDU type reactor, is situated in this region upstream Danube Delta. Taking into account the future development of this important Romanian nuclear objective, the knowledge of the present condition of tritium and C-14 concentrations levels becomes a necessity. Therefore, an extensive monitoring program for these isotopes, along the Romanian sector of the Danube River Basin, starting with Cazane Gorge and ending with the three branches of the Danube Delta, has been started. The tributaries from this sector: Cerna, Jiu, Olt, Arges are included also in this ongoing project. Preliminary results of tritium level measured in 17 locations within the mentioned areas are presented in the paper. This tritium level is compared with the tritium concentration in precipitation during the year 2006. In order to make an isotopic evaluation of water balance, the monitoring program will run during the year 2007 extending the scope of interest on stable isotopes: ²H, ¹⁸O, ¹³C and a multivariate statistical analysis will be developed.

¹ Work performed within the Framework of AMCSIT CEEX 63/2005

² Present address: Institute for Reference Materials and Measurements, Geel, Belgium

1. INTRODUCTION

Rivers constitute an important freshwater source and much of the world's population has relied on rivers for its development. In recent years, many international and national hydrology research programmes have focused on large river basins. In humid basins, precipitation processes stand for the primary signal traced by river discharge. Evidence that precipitation input signals are not static is found from long term isotopes records of the European rivers. Inter-annual variations in these processes reflect the inherent decadal variability of precipitation processes. Comparison of tritium in Danube River with precipitation at Vienna [1] reveals that not only short term signals but also long term changes of isotope ratio in precipitation are transmitted through the catchments and can be detected in the river water. The comparison of measured and modeled ^3H contents in Danube River revealed that the best fit which could be obtained (mean residence time of 3 y) is still not satisfactory [2].

The Danube River Basin is the second largest river basin in Europe covering 801,463 km² [3]. It lies in the west from the Black Sea in Central and South-eastern Europe. Due to its geologic and geographic conditions, the Danube River Basin can be divided into 3 main parts: Upper Danube Basin, Middle Danube Basin and Lower Danube Basin. A rate of 65% of Lower Danube Basin is the natural border between Romania and Bulgaria. Two important nuclear objectives for both countries are found in this region: Kozloduy NPP and Cernavoda NPP. Nuclear energy is considered by the two countries an alternative for the future development, therefore Romania has already built a new CANDU type unit in Cernavoda, which will be placed into operation during the 2007, and Bulgaria started negotiations for a new nuclear power plant in Belene. The knowledge of tritium and C-14 levels in the Lower Danube Basin offers two important items of information: first, in the environmental radioactivity monitoring program (Cernavoda is a CANDU type reactor, where tritium and C-14 are the most important radioisotopes released in the environment) and second a primary estimation of river discharge signature for the end part of Danube by comparing the level from precipitation and river water.

2. SAMPLING LOCATIONS

The Danube typology constitutes a harmonized system developed by the countries sharing the Danube River [3]. The most important factors used for this system are mean water slope, substratum composition, geomorphology and water temperature. Lower Danube Basin contains four sections type:

C-14 AND TRITIUM CONCENTRATIONS ALONG ROMANIAN DANUBE

Iron Gates Danube, Western Pontic Danube, Eastern Wallachian Danube and Danube Delta.

Iron Gates Danube section (A, Fig. 1) has an average width of about 750 m and runs through a canyon or through valley form. This section is characterized by high current velocity (from 1.8 m/s up to 5 m/s). Sampling point chosen was Ieselnita (1, Fig.1), location with easy access to the left side of the Danube. Next sampling point was Cerna, Danube tributary, at Toplet location (2, Fig. 1). Cerna is a small mountain river without industrial activity. The end of this section was Turnu Severin (3, Fig.1) another sampling point.

Western Pontic Danube section (B, Fig. 1) contains a floodplain landscape with higher plains of terraced accumulation in a meander and floodplain valley. The main channel has an average width of 830 m and mean depth of 8.5 m. This section is characterized by moderate values of current velocity, 1.30 m/s. The diversity of water bodies in this area close to the stream is wide, but we focused on the main course and on few tributaries with significant mining industry, Jiu River (4, Fig. 1), and chemical industry Olt River (6, Fig. 1) and Arges River (8, Fig. 1). Bechet location (5, Fig. 1) from the main course is important because it is situated downstream Kozloduy NPP. Another sampling point was Turnu Magurele (7, Fig. 1) which is located downstream Olt River, approximately in the middle of this section. The end of this section is Chiciu-Silistra (9, Fig. 1) another important sampling point, before Danube splitting into two branches, Old Danube and Borcea.

The Danube changes its watercourse northward in Eastern Wallachian Danube section (C, Fig. 1). There are two large isles, Balta Ialomitei and Balta Brailei, and many natural lakes. The main channel has an average width of 650 m, and mean depth of 10.5 m. The section is characterized by slow current velocities of 0.8 m/s. The first sampling point of this section was established in Seimeni (10, Fig. 1) downstream Cernavoda NPP discharge channel and the second in Giurgeni (11, Fig. 1), a point between the two isles where Danube has one main branch for a small distance.

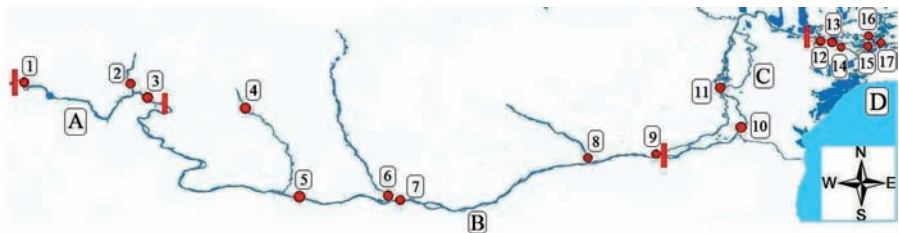


FIG. 1. Section type and sampling areas from Lower Danube Basin: A - Iron Gates Danube; B - Western Pontic Danube; C - Eastern Wallachian Danube; D - Danube Delta.

The Danube Delta section (D, Fig. 1) is the Danube's youngest territory. There are three main water channels: Chilia, Sulina and Sf. Gheorghe, with numerous canals and floating islands. This section is characterized by average current velocities of 0.7 m/s. The shape of delta is triangular, and at mean water levels, 60% of this area is covered by waters. We established six sampling points. First point was Tulcea (12, Fig. 1) on the main course before Danube splitting into Sulina and Sf. Gheorghe branches. The other five points were: Ceatal Izmail(13, Fig. 1), junction of Litcov Canal with Sf. Gheorghe Branch (14, Fig. 1), Mila 23 (15, Fig. 1), junction of Litcov Canal with Ismail Canal (16, Fig. 1) and Crisan (17, Fig. 1).

3. SAMPLING AND MEASUREMENTS

Precipitation sampling was performed on a monthly basis in a typical rain water collector [4] in Drobeta Turnu Severin location, starting from April 2006. At the end of the month the container was shaken thoroughly and a 1 liter sample was filled for shipment to the analytical laboratory. Particular attention was paid to the collection and preservation of water sample [5]. Water samples for tritium measurement were collected one meter from the left bank of Danube, 10 cm from the water surface, in brown glass bottle. pH, conductivity and temperature for water sample were measured at the sampling location using portable apparatus WTW pH/cond 340i.

As tritium is a soft beta emitter (5.72 keV mean energy), liquid scintillation is the most appropriate technique for a large number of samples. On this work, the low-background liquid scintillation spectrometer Quantulus 1220 (Wallac) was used to determine tritium in water samples. The analytical method used to determine tritium in water samples was, briefly, the following: samples were filtered through slow depth filters; 250 ml of filtrate was distilled using ISO method [6]; 8 ml of distillate was mixed with 12 ml of scintillation cocktail OptiPhase Hisafe 3 in polyethylene vials; three background samples and tritium standards were simultaneously prepared. Samples, backgrounds and tritium standards were counted using Quantulus 1220 during 1000 min/sample.

CO₂ direct absorption method for preparing samples for radiocarbon analysis by liquid scintillation counting is applied in our laboratory [7]. For this method it was estimated to be necessary a minimum of 2.6 g of CO₂ as DIC in the water sample. Due to a large amount of sample necessary for ¹⁴C measurement using direct absorption method, the precipitation of dissolved inorganic carbonate (DIC) from water samples was made on site according to the environmental protection laws. In this way, DIC presence in about 80 L of water was reduced to a volume less than 1 L. Barium carbonate from precipitate

C-14 AND TRITIUM CONCENTRATIONS ALONG ROMANIAN DANUBE

is then acidified to release carbon dioxide, which is purified. A similar procedure is applied to generate CO_2 from CaCO_3 using standard carbonate material (modern marine shell) and background carbonate material (marble). The last step of the preparation procedure is to absorb CO_2 in the form of carbamate, and to ensure that exactly the same amount stage is absorbed for each sample, standard and background. The vials are then counted via conventional C-14 analysis. Applying the validation procedure [8] it was established a mean activity for marine shell of 0.2178 ± 0.0039 Bq/g C that translate to 114.18 ± 1.82 pMC, referred to the decay corrected 95% NBS oxalic acid activity and adjusted to $\delta^{13}\text{C} = -25\text{‰}$. Each ^{14}C activity was corrected by its individual $\delta^{13}\text{C}$. The $^{13}\text{C}/^{12}\text{C}$ ratio was measured by mass spectrometry from small aliquots of CO_2 gas. Values are given relative to the VPDB standard, the overall precision is typically $\pm 0.1\text{‰}$.

4. EXPERIMENTAL RESULTS

The average fallout during the year 2006 in Romania was with 36.5 mm lower than the normal climatologic average [9]. It was recorded deficit monthly average in precipitation for January, February, May, July, September, November, and December with a notable negative deviation of 55% for December. Notable excess precipitation were recorded for March (118.9%) and August (105.8%).

The same pattern was recorded in the monitored precipitation from Turnu Severin location (Fig. 2), with maximum precipitation average in March

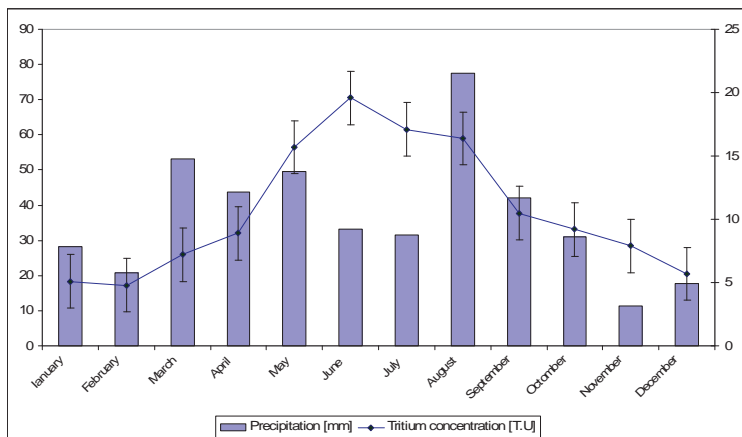


FIG. 2. Monthly average precipitation and monthly average tritium concentration in precipitation during the year 2006 at Turnu Severin location

2006 (53.6 mm) and August 2006 (77.5 mm), and a minimum precipitation average in November 2006 (11.4 mm) and December 2006 (17.8 mm). Tritium concentration during the year 2006 at Turnu Severin location had an average of 10.7 ± 2.1 TU (one Tritium Unit, TU, corresponds to 10^{18} hydrogen atoms). We recorded a minimum tritium concentration of 5.1 ± 2.1 TU in January 2006 (Fig. 2) and a maximum tritium concentration of 19.6 ± 2.2 TU in June 2006. Comparing published values for tritium in precipitation in Austria [10] with measured values for the monitored location we can conclude that annual tritium concentration average has had the same trend for the past years: 10.4 TU for 2000, 10.5 TU for 2001 and 10.46 TU for 2002. There are no other influences

TABLE 1. TRITIUM CONCENTRATION IN SAMPLING LOCATIONS ALONG LOWER DANUBE BASIN.

Location number	Location name	Section type	Water body	Tritium activity concentration [TU]
1	Ieselnita	A	Danube	17.6 ± 2.2
2	Toplet	A	Cerna	8.3 ± 2.1
3	Drobeta Turnu Severin	A	Danube	14.8 ± 2.2
4	Filiasi	B	Jiu	9.3 ± 2.1
5	Bechet	B	Danube	27.9 ± 2.3
6	Islaz	B	Olt	6.8 ± 2.1
7	Turnu Magurele	B	Danube	12.8 ± 2.1
8	Oltenita	B	Arges	11.8 ± 2.1
9	Chicciu/Silistra	B	Danube	9.7 ± 2.1
10	Seimeni	C	Danube	32.4 ± 2.3
11	Giurgeni	C	Danube	15.9 ± 2.2
12	Tulcea	D	Danube	11.6 ± 2.1
13	Ceatal Ismail	D	Danube	12.6 ± 2.1
14	Sf. Gheorghe branch and Litcov channel	D	Danube	10.7 ± 2.1
15	Litcov channel and Isac channel junction	D	Danube	8.5 ± 2.1
16	Mila 23	D	Danube	19.8 ± 2.2
17	Crisan	D	Danube	18.7 ± 2.2

C-14 AND TRITIUM CONCENTRATIONS ALONG ROMANIAN DANUBE

and tritium behavior in precipitation has the same tendency to decrease in the environment.

The tritium sampling campaigns were seasonal. Tritium concentration average in Danube water along the Lower Danube Basin was 15.7 ± 2.2 TU, Table 1. This value is near the average tritium concentration value of 10.7 ± 2.1 TU in precipitation (with respect for measurement uncertainties).

The reference location for Romanian Danube water is Ieselnita. The average tritium concentration of 17.6 ± 2.2 TU for this location are the environmental radioactivity value, even if upstream this location there are two other nuclear power plant (Paks NPP and Krcko NPP on Sava tributary). Two higher values than the average tritium concentration were recorded for Bechet and Seimeni, 27.9 ± 2.2 TU and respectively 32.4 ± 2.2 TU. The two locations have nearby two different nuclear power plant, Kozloduy and Cernavoda, respectively with important tritiated effluents discharged in the Danube. Tributaries had lower values than the average tritium concentration due to their different basins with strong groundwater components. Tritium level in Danube water is continuously decreasing from 20–25 TU in 1995 [11] to precipitation level, even if the nuclear objectives are in the monitored areas.

TABLE 2. PHYSICO-CHEMICAL CHARACTERISTICS AND C-14 ACTIVITY MEASURED ALONG DANUBE.

Location Number	Water body	pH in-situ	T (°C)	Cond (μS/cm)	HCO ₃ ⁻ (mg/L)	CO ₃ ²⁻ (mg/L)	δ ¹³ C (‰)	¹⁴ C (pMC±σ)
1	Danube	7.59	24.0	404	152.5	6.0	-7.8	95.66 ± 1.87
2	Cerna	7.94	20.3	305	125.0	3.0	-9.3	68.48 ± 1.53
4	Jiu	8.13	24.8	350	118.9	3.0	-7.6	72.36 ± 1.52
5	Danube	8.35	25.3	397	146.4	6.0	-8.2	106.03 ± 2
6	Olt	8.62	23.8	529	109.8	6.0	-10.4	74.26 ± 1.60
7	Danube	8.29	23.9	418	137.5	3.0	-8.4	98.18 ± 1.90
8	Arges	7.53	24.1	483	164.7	6.0	-11.7	78.19 ± 1.78
9	Danube	8.42	25.8	400	146.4	6.0	-9.6	99.91 ± 1.92
10	Danube	8.17	23.7	437	152.4	6.0	-9.8	110.68 ± 2.06
11	Danube	8.49	24.9	405	159.4	6.0	-8.7	99.49 ± 1.92
12	Danube	8.19	23.4	416	125.0	3.0	-10.4	96.17 ± 1.88
14	Danube	8.31	23.6	414	155.0	6.0	-11.1	97.45 ± 1.89
17	Danube	8.25	24.0	418	110.4	5.0	-10.7	96.52 ± 1.87

The ^{14}C sampling campaign was at the end of August 2006. ^{14}C levels measured along the Lower Danube Basin are presented in Table 2. pH, conductivity and temperature were measured at the sampling location. Range of pH measured in the field was between 7.53 (for Arges tributary) and 8.62 (for Olt tributary). The lowest temperature recorded was in Cerna tributary (mountain river). Conductivity along the Danube was around $400\ \mu\text{S}/\text{cm}$, and extreme values were recorded for tributaries, the lowest values of $305\ \mu\text{S}/\text{cm}$ in Cerna river and the highest values of $529\ \mu\text{S}/\text{cm}$ in Olt river. The major component of inorganic carbon in water was HCO_3^- with values varying from $109.8\ \text{mg}/\text{L}$ (Olt river) to $164.7\ \text{mg}/\text{L}$ (Arges river).

The measured $\delta^{13}\text{C}$ values varied along Lower Danube Basin between $-7.8\ ‰$ at the beginning of this areas and $-11.1\ ‰$ in Danube Delta. Lower values were recorded in Danube Delta where CO_2 derived from the oxidation of organic mater influenced isotopic composition. Measured ^{14}C activity along Danube had modern values, with two exceptions Bechet and Seimeni, which are situated downstream nuclear power plants. In fact, there are some published studies [12, 13] that indicate an increasing trend for ^{14}C atmospheric concentration in Cernavoda, within a range between $105\ \text{pMC}$ and $123\ \text{pMC}$. Each tributary had lower values indicating different contribution from different groundwater reservoirs.

5. CONCLUSIONS

In the most cases surface water systems are an intermediate step between precipitation and a given archive, such as lacustrine sediments, groundwater or organic matter. The headwaters and streams will reflect the isotopic composition of local precipitation, but in downstream areas the quantitative importance of all water resources will control the isotopic contents. In order to make an isotopic evaluation of water balance and dynamics in Lower Danube Basin it was decided to extend the monitoring program to deuterium and oxigen-18 during the year 2007. Despite the nuclear activity in the observed areas, tritium and ^{14}C activities present slightly higher values for specific locations without any influence in the catching river. Those first campaigns were a screening test for complex areas that have a $1075\ \text{km}$ distance. The long term tritium and ^{14}C monitoring activity has been set-up. The whole sampling strategy has been defined in order to provide the required data package to analyze in a quantitative way the influence of the nuclear human activities along Danube and especially those of Cernavoda NPP.

REFERENCES

- [1] RANK, D., et al., Hydrological parameters and climatic signals derived from long term tritium and stable isotope time series of River Danube, IAEA-SM-349, IAEA Vienna (1998) 191–205.
- [2] RANK, D. et al., Runoff characteristics of the upper Danube basin: conclusions from long-term environmental isotope records, Geophysical Research Abstracts, Vol. 7, 03315 (2005).
- [3] INTERNATIONAL COMMISSION FOR THE PROTECTION OF DANUBE RIVER, The Danube River Basin District Part A— Basin wide Overview (2005), <http://www.icpdr.org/DANUBIS>.
- [4] INTERNATIONAL ATOMIC ENERGY AGENCY, Measurement of Radionuclides in food and the environment, Technical Reports Series No. 295, Vienna (1989).
- [5] APHA-AWWA-WEF, Standard Methods for the Examination of Water and Wastewater, 19th Edition, American Public Health Association, Washington (1995).
- [6] INTERNATIONAL STANDARD ORGANIZATION, Water-Quality. Determination of tritium activity concentration in water sample, Liquid scintillation Method (1989).
- [7] LEANY, F., HERZEG, A., DWIGHTON, J., New developments in carbosorb method for C-14 determination, Quarter. Geochronology **13** (1994) 171–178.
- [8] VARLAM, C., STEFANESCU, I., VARLAM, M., FAURESCU, I., POPESCU, I., Optimization of C-14 concentration measurement in aqueous samples using direct absorption method and liquid scintillation counting, Advances in Liquid Scintillation Spectrometry Conference, Katowice, Poland (2005).
- [9] NATIONAL METEOROLOGY ADMINISTRATION, <http://www.inmh.ro/index.php?id=402>
- [10] KRALIK, M., HUMMER, F., STADLER, E., SCHEIDLEDER, A., TESCH, R., PAPESCH, W., Tritium Osterreich Jahresbericht 1997 bis 2002, <http://www.umweltbundesamt.at> (2005).
- [11] DIETER, R., et. al., Oxygen-18, deuterium and tritium in the Black Sea and the Sea of Marmara, J. of Environmental Radioactivity **47** (1999).
- [12] DAVIDESCU, F., PETRES, R., TENU, A., Tritium and C-14 trend in the environment for Cernavoda Power Plant (in Romanian), Mediul inconjurator, vol.II, No.1 (2002).
- [13] TENU, A., DAVIDESCU, F., CUCULEANU, V., Tropospheric CO₂ in Romania: concentration and isotopic composition measurements, IAEA-TECDOC-1269 (2002).

THE ROLE OF RIVERS IN THE SWISS NETWORK FOR THE OBSERVATION OF ISOTOPES IN THE WATER CYCLE (ISOT)

U. SCHOTTERER, M. LEUENBERGER, P. NYFELER, H.U. BÜRKI
Division of Climate and Environmental Physics,
Physics Institute,
University of Bern, Switzerland

R. KOZEL, M. SCHÜRCH
Federal Office for the Environment,
Bern, Switzerland

W. STICHLER
GSF – Institute for Groundwater Ecology,
Neuherberg, Germany

Abstract

During recent decades, Switzerland has been going through the greatest change in climate regarding temperature and the distribution of precipitation since the national climate measurement and observation network was established in 1864. Water isotopes (^2H , ^3H and ^{18}O) provide an important additional tool to evaluate the influence of these changes on the different compartments of the hydrological cycle. The Swiss network for the observation of isotopes in the water cycle (ISOT) comprises precipitation, river water, and shallow groundwater stations. The climatic trend of stable isotopes in precipitation, especially the distinct shift to more enriched values between 1985 and 1990, is also recorded in the isotopic composition of the main rivers discharging from Switzerland. However, the isotopic signature is complex, because a variety of different catchment and discharge characteristics (glaciers, snow cover, hydro-electric regulations) are superimposed on the trends. For example, the effects of the heat wave in summer 2003 resulted the following year in more negative δ -values for all main rivers. Drought at the beginning of the year and extreme heat during the summer changed the precipitation conditions and discharge ratios of winter to summer precipitation. During recent years, there has also been a change in the behaviour of deuterium excess. It has increased in the River Ticino on the south side of the Alps probably as the result of a greater influence of the Mediterranean Sea as a source of moisture to the south of the Alps. The values have remained stable in rivers on the northern side of the Alps.

1. INTRODUCTION

Since 1992, in the framework of the national groundwater observation network NAQUA, the Federal Office for the Environment has been operating the Swiss Network for the Observation of Isotopes in the Water Cycle (ISOT) in close collaboration with the Division of Climate and Environmental Physics at the Physics Institute of the University of Bern [1]. The longest time-series of measurements of isotopes in precipitation reach back to 1970. River sampling started in 1985. As more than 80% of Switzerland's drinking water comes from groundwater, the network also contains shallow groundwater stations to observe any possible influences of climate change on recharge mechanisms. The network now consists of 13 precipitation stations, 10 river stations, and 3 groundwater stations including stations of the Division of Climate and Environmental Physics and of the Federal Office for Public Health.

The precipitation stations are situated in areas that are climatologically different such as the Jura Mountains, the Central Plateau, the Alps and the southern side of the Alps. The backbone is a NW/SE transect from Bern over the Alps to Locarno. The isotopic composition of the main river waters is measured upstream and downstream of lakes and at points where water leaves

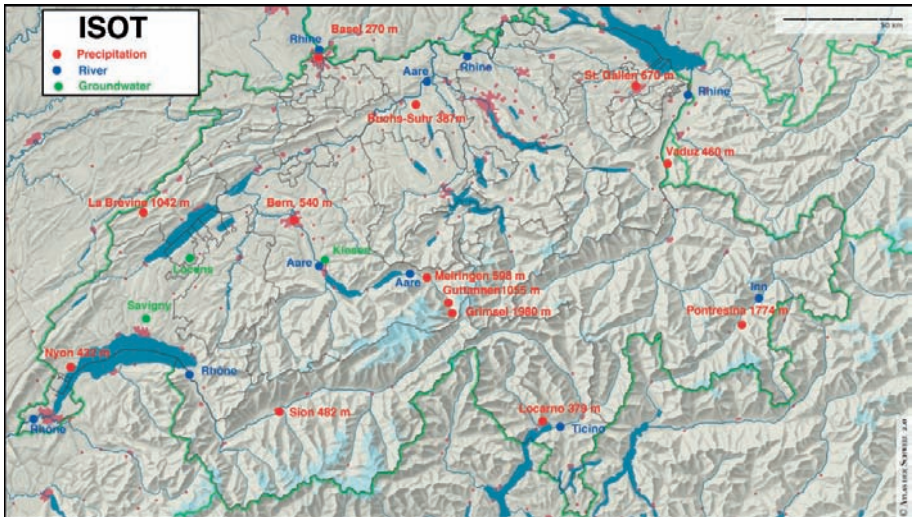


FIG 1. The station set-up in 2006 for the Swiss Network for the Observation of Isotopes in the Water Cycle. Although the small-scale differences in alpine orography cannot be sampled at sufficient density to reproduce local effects, the combined observation of precipitation, rivers and shallow groundwater reproduces a realistic picture of the recent water isotope distribution.

THE ROLE OF RIVERS IN THE SWISS NETWORK

Switzerland. The altitude of the sampled river catchments varies from 1000 to 2500 m. The groundwater stations are chosen to observe changes in small, flat catchments and in regimes governed by the interplay of river water and local groundwater. The precipitation samples are based on monthly composites, most of the river water samples are done on a 28-day composite proportional to flow rate and groundwater samples are taken twice a month. Each year the results of the previous year and the long-term trends are discussed and evaluated by a small group of experts. This group also proposes adaptations to the network when necessary. Originally the network was expected to serve hydro-geologists and engineers in water resource studies, but today most requests for data come from those studying paleo-climatology or environmental issues.

The network is of increasing importance. As a result of the probable change in climate, the pressure on water resources will also increase in Switzerland, the “water tower” of Europe. During the recent decades Switzerland has been going through the greatest climatic change since the national meteorological network was established in 1864. The marked climatic shift started at the end of the 1970s. The summer- and winter months experienced a sudden warming, amounts of precipitation temporarily increased during the winter and there was a higher frequency of heavy precipitation events during the summer [2]. Furthermore, a recent study dealing with projections of climate change in Switzerland up to 2050 expects warmer winters, hotter summers and a distinct shift in the distribution of seasonal precipitation with related consequences for society and the environment [3].

2. THE ROLE OF THE RIVERS IN THE FRAMEWORK OF THE ISOT

Water in rivers may come from many sources having different isotopic compositions depending on the source of moisture, distribution of precipitation, infiltration characteristics, residence time and the altitude of the catchments. As an example, the distribution of $\delta^{18}\text{O}$ and δD in river waters across the United States has been used successfully to classify large water catchments in terms of moisture sources and recharge composition [4].

Most of the river stations in the ISOT coincide with stations of the National River Monitoring and Survey Programme (NADUF). This programme is designed to provide the fundamental data for water protection and research. The data sets include physical, geochemical and anthropogenic influenced parameters. Thus, the observation of water isotopes in rivers adds valuable information on residence times and characteristics of individual catchments. The isotopic composition in the river water reflects changes in the

corresponding precipitation, but is damped. The $\delta^{18}\text{O}$ differences in the long-term mean of winter and summer in Switzerland are of the order of 5 to 8 ‰; in river water they hardly exceed 1 to 2 ‰ depending on the size of the catchments and the turn over of the lakes in between. If precipitation occurs as snow during the winter, the negative isotope values in rivers are shifted towards the warmer season when water from the snowmelt is the dominating component of discharge [5].

3. SELECTED RESULTS

According to the recorded changes in temperature and the distribution of precipitation in Switzerland during recent decades, the isotopic composition of precipitation has also changed. The isotopic cycle over the years was similar for all stations and was most pronounced between 1985 and 1990. Local differences in meteorological conditions along the transect over the Alps can be seen but they do not hide the general picture of the trans-regional change in climate. For instance, the effect of altitude changes with time and is not linear because the level of the clouds rises in front of the alpine barrier. A higher cloud base leads to lower temperatures and lower δ -values. On the other hand, precipitation south of the Alps in Locarno is governed by a different meteorological regime (Fig. 2, and see Fig. 1 for the geographical distribution).

There were also changes in the isotopic composition of river water. Sampling started in 1985 and the increases in isotope values were followed

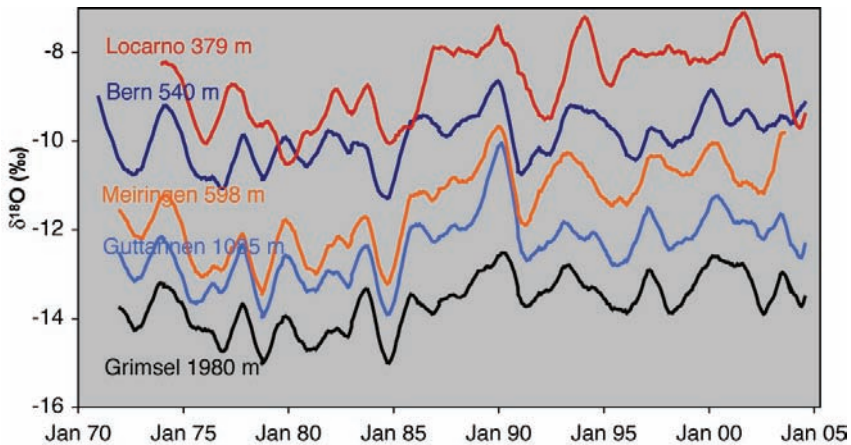


FIG 2. The climatic trend in $\delta^{18}\text{O}$ in precipitation across the Alps. A two-fold 12-month moving average reduces seasonal differences.

THE ROLE OF RIVERS IN THE SWISS NETWORK

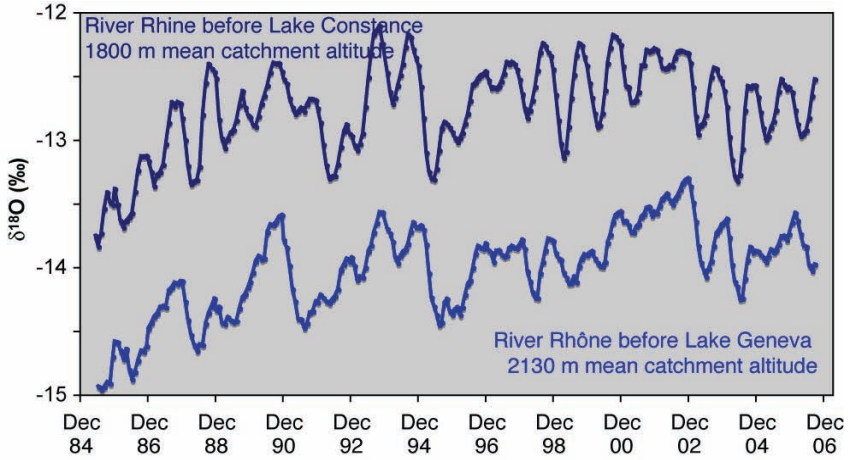


FIG 3. The climatic trend in $\delta^{18}\text{O}$ in the River Rhine and the River Rhône. A 6-month moving average was applied to emphasize the differences in seasonal changes.

from the onset of the rapid shift in climate (Fig. 3). The parallel changes in $\delta^{18}\text{O}$ for both rivers suggest that their catchment areas were affected in the same way.

Nevertheless, after 1996 the picture differs slightly. In contrast to the River Rhône the δ -values in the River Rhine increased less or stabilized. A reason for this could be regionally changing input conditions through a change from winter to summer precipitation. The proportion of winter precipitation seems to be higher in the catchment areas of the River Rhine. In general, the irregular winter/summer $\delta^{18}\text{O}$ differences confirm the meteorological findings of the increasing variability in the seasonal precipitation pattern and snow cover. Due to intensive hydropower production with numerous reservoirs in the River Rhône basin, the δ -values are more dampened or even absent in this river.

The behaviour of deuterium excess indicates a further regional difference. The deuterium excess in precipitation depends mainly on kinetic isotopic effects regarding evaporation processes. Therefore, it provides information that cannot be obtained by the individual δ -values alone. The evaporation process includes effects regarding the conditions at the marine source of atmospheric moisture and sub cloud effects when falling raindrops evaporate during local rainout. In general, both effects cause a slight seasonal difference with lower values in the first half of the year and higher values in the second half of the year. The seasonal d-excess pattern in the precipitation is also transferred to the river water although not always visible [6]. This is illustrated in Figure 4

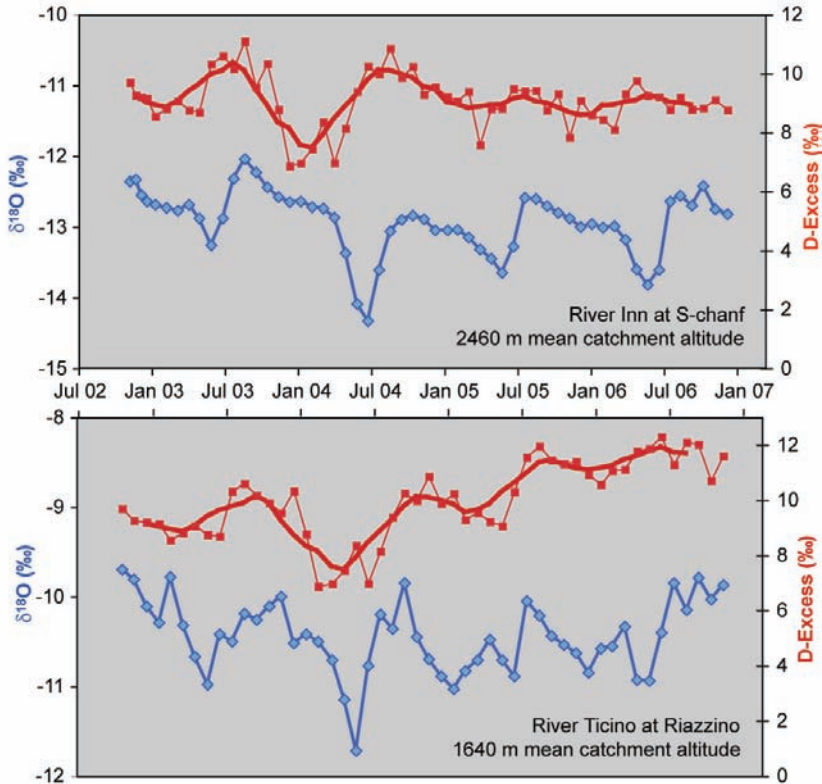


FIG 4. $\delta^{18}\text{O}$ and deuterium excess in the River Inn and the River Ticino between 2002 and 2006. The $\delta^{18}\text{O}$ of the young River Inn is clearly dominated by snowmelt; its average deuterium excess remains stable in contrast to the increase in the River Ticino, which indicates a rinsing influence of moisture from the Mediterranean Sea.

with data from two other river systems, which discharge to the North and to the South respectively.

Snowmelt marks the $\delta^{18}\text{O}$ course of the River Inn at S-chanf due to the high catchment area at nearly 2500 m mean altitude. Glaciers cover about 10% of the area. Maximum snowmelt occurs around July indicated by minimum δ -values from winter precipitation. The absence of scatter in $\delta^{18}\text{O}$ is partly due to smoothing in the snow cover during melt and probably also due to the mixing in the Engadine lakes at the source of the river. Although the scatter in the River Ticino is more pronounced, changes similar to those for the River Inn are still visible. The scatter is caused by the greater influence of rain and the widespread tributaries. The River Ticino is sampled where it flows into Lake Maggiore.

THE ROLE OF RIVERS IN THE SWISS NETWORK

The results are interesting particularly with respect to the deuterium excess. The seasonal change is distinct in 2003 and 2004. As maximum d-values are related to precipitation of the second half of the year, they are stored (in case of solid precipitation) in the lowermost part of the snow pack. Therefore, they contribute to the isotopic composition of discharge at the very end of the melting process. Depending on the precipitation distribution, the d-variation is attenuated or smoothed by rain during summer/autumn. In our example, smoothing occurred in 2005 and 2006. The trend to higher d-values in the River Ticino may be attributed to a growing influence of moisture from the Mediterranean Sea. Although originally related to the Eastern Mediterranean Sea, this effect is increasingly observed in the influence area of influence of the whole basin [7].

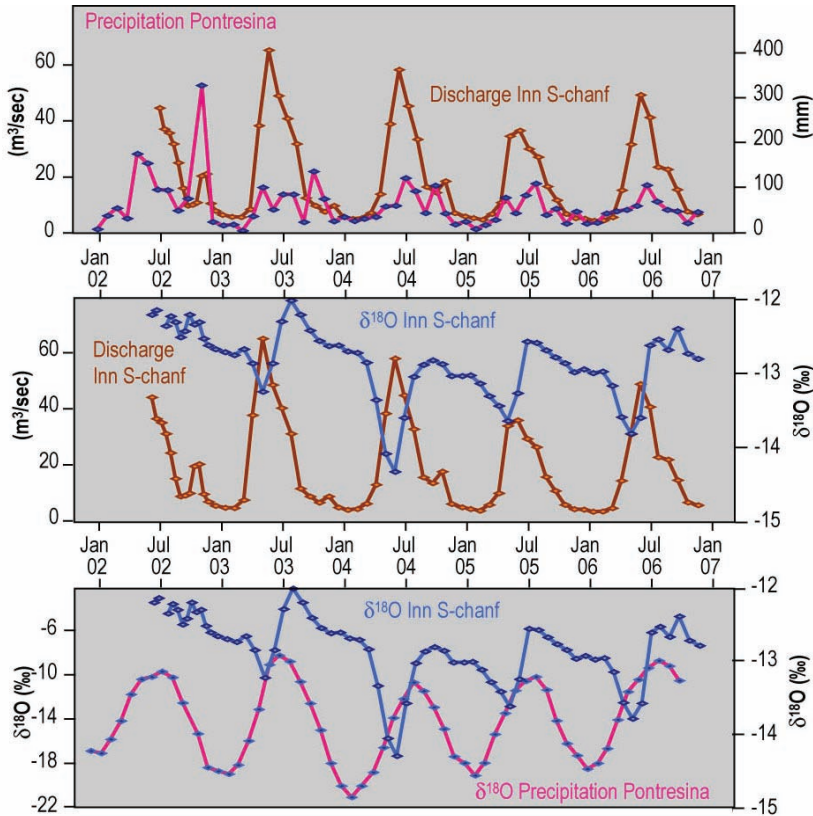


FIG 5. The combination of precipitation, discharge, and $\delta^{18}\text{O}$ data reveals the origin of water draining the River Inn basin. Although the changes in precipitation and discharge suggest a direct relation, a comparison of the $\delta^{18}\text{O}$ data shows that precipitation at that time contributes only partly to direct run off.

In both rivers the $\delta^{18}\text{O}$ values were the most depleted in 2004 after the hot, dry summer of 2003, as was the case for the Rhine and the River Rhone. This indicates a general shift in the ratio of winter to summer precipitation in the discharge. We discuss this in greater detail using data for the River Inn in Figure 5 (below).

Precipitation and discharge data in the upper part of Figure 5 suggest a direct contribution of the current precipitation to the river run off. In summer, the maximum in precipitation is increased by snowmelt. However, the isotope data give a more detailed picture of this process. The seasonal variations of δ -values in precipitation and discharge are shifted by several months, depending on snow cover distribution and temperature as a driver for the onset of the melting process (lower part of Figure 5). In general, the minimum δ -values coincide with a maximum discharge; the intermediate groundwater storage in the basin is filled up and more snowmelt contributes to direct run off obscuring the more enriched δ -values of summer precipitation. The order of magnitude of the depleted $\delta^{18}\text{O}$ (or δD) depends on the mixing ratios of the different water bodies and their respective δ -values.

The situation starting in November 2002 provides a good example: relatively high temperature (snow cover built up only in higher catchments) and heavy precipitation of more than 300 mm led to an increase in discharge with more enriched $\delta^{18}\text{O}$ values. As even the $\delta^{18}\text{O}$ in precipitation in the lower parts of the catchments was 3‰ more depleted (-15.60‰ in Pontresina at 1800 m) than the $\delta^{18}\text{O}$ in the average discharge, most of the run off was composed of infiltrated summer rain only. The following winter months were extremely cold and dry, summer precipitation during the heat wave in 2003 corresponded to the long-term average. Discharge increased early with a very high maximum already at the beginning of June. Due to the sudden warming and the fact that the ground was still frozen, the melting from the November snow cover ran off very directly. The negative $\delta^{18}\text{O}$ -snow melt peak in the discharge was less (warm November precipitation) and values increased quickly by the contribution of summer precipitation. Due to the changed infiltration conditions increased by drought and evapo-transpiration during the hot summer, groundwater levels started to drop. During the following year, the distribution of precipitation returned to normal, but the mixing ratios of the different water bodies were still disturbed, resulting in highly depleted d-values in the discharge during the summer months.

Of course, these diagnostic findings based on stable isotopes are not stand alone results; they will serve as additional boundary conditions for model experiments describing the influence of changing precipitation and temperature distribution on discharge mechanisms in alpine catchments.

ACKNOWLEDGEMENTS

We are grateful to the Swiss National Science Foundation for supporting this work.

REFERENCES

- [1] SCHÜRCH, M., KOZEL, R., SCHOTTERER, U., TRIPET, J-P., Observations of isotopes in the water cycle—the Swiss National Network (NISOT), *Environmental Geology*, **45** (2003) 1–11 .
- [2] BADER, S., BANTLE, H., Das Schweizer Klima im Trend. Temperatur- und Niederschlagsentwicklung 1864–2001. *Meteo Schweiz*. Veröffentlichung No. 68 (2001).
- [3] OCCC/PROCLIM, Klimaänderung und die Schweiz 2050. Erwartete Auswirkungen auf Umwelt, Gesellschaft und Wirtschaft. http://www.occ.ch/products/ch2050/CH2050-bericht_d.html (2007).
- [4] KENDALL C., COPLEN T. B., Distribution of oxygen-18 and deuterium in river waters across the United States, *Hydrological Processes* **15** (2001) 1363–1393.
- [5] SCHOTTERER U., STOCKER, T., BÜRKI H.U., STICHLER, W., TRIMBORN, P., KOZEL, R., The influence of floods on the water balance of river basins by means of isotopes of the water molecule. *International Conference on Flood Estimation*, March 6–8, Berne. *Reports of the Intern. Com. for the Hydrology of the Rhine Basin II-17* (2002) 229–235.
- [6] SCHOTTERER, U., FRÖHLICH, K., STICHLER, W., TRIMBORN, P., Temporal Variation of ¹⁸O and Deuterium Excess in Precipitation, River and Spring Waters in Alpine regions of Switzerland, In: *Isotope Techniques in the Study of Past and Current Environmental Changes in the Hydrosphere and Atmosphere*, IAEA, Vienna (1993) 53–64.
- [7] INTERNATIONAL ATOMIC ENERGY AGENCY, Isotopic composition of precipitation in the Mediterranean Basin in relation to air circulation patterns and climate, L.Gourcy (Ed.), IAEA-TECDOC-1453 (2005).

GROUND WATER INPUT TO A RARE FLOOD EVENT IN AN ARID ZONE EPHEMERAL RIVER IDENTIFIED WITH ISOTOPES AND CHEMISTRY

B.Th. VERHAGEN
School of Geosciences,
University of the Witwatersrand,

M.J. BUTLER
Environmental Isotope Group,
iThemba LABS (Gauteng)

Johannesburg, South Africa

Abstract

Various isotope studies in temperate climates have shown that the shallow groundwater component feeding perennial rivers during rainfall events can be more important than surface runoff. We report here on possibly unique isotopic and chemical evidence of groundwater contributions to a rare flood event of the ephemeral Auob River during the exceptional rains of 1999/2000 in the arid/semi-arid Kalahari of south-eastern Namibia. The recognition of this process was enabled by a detailed knowledge of the isotope hydrology of groundwater in the area and provided insights into aspects of the palaeo-hydrology of the Auob River catchment.

1. INTRODUCTION

In studies using stable isotope and chemical environmental tracers in hydrograph separation e.g. [1, 2] on temperate zone streams and rivers, it was discovered that a substantial proportion of what had previously been ascribed to surface runoff during storm events were in fact contributions of shallow groundwater in river bank storage, displaced by infiltration of storm rainfall. Such hydrograph separation relied on the contrast between the (variable) isotopic (e.g. $\delta^2\text{H}$, $\delta^{18}\text{O}$) and chemical (e.g. Cl^-) content of rainfall during the storm event and the values in the shallow groundwater. Groundwater contributions to ephemeral river flood events in arid/semi-arid environments, to the authors' knowledge, had never been reported.

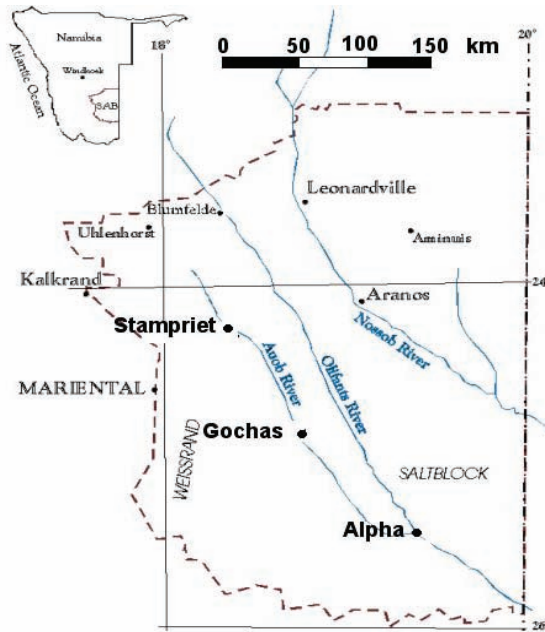


FIG. 1. Map of the area of study, showing the Auob River and other ephemeral drainages in south-eastern Namibia and three river sampling stations. (After[3]).

2. OBSERVATIONS ON AUOB RIVER FLOOD WATER

In the framework of a major water resource investigation¹ in south-eastern Namibia, numerous groundwater samples were analysed for their environmental isotope and chemical content [4]. The area (Fig. 1) is traversed by several ephemeral river beds, that flow infrequently.

The area is underlain by Carboniferous to Tertiary sediments of the Karoo formation (Fig. 2). The alternating sequence of sandstones and mudstones that constitute confined aquifers is covered by Tertiary to recent unconsolidated to semi-consolidated Kalahari sand and calcrete. Groundwater in the shallow phreatic aquifer of the Kalahari shows clear isotopic evidence of kinetic evaporation of rain water before or during infiltration into the sub-surface [3, 5]. This evaporation signal (Fig. 5) is observed also in minor springs, and to

¹ International Atomic Energy Agency Regional Project RAF8029, in cooperation with the Department of Water Affairs, Windhoek and the Council for Scientific and Industrial Research, Stellenbosch, South Africa.

GROUND WATER INPUT TO A RARE FLOOD EVENT IN AN ARID ZONE

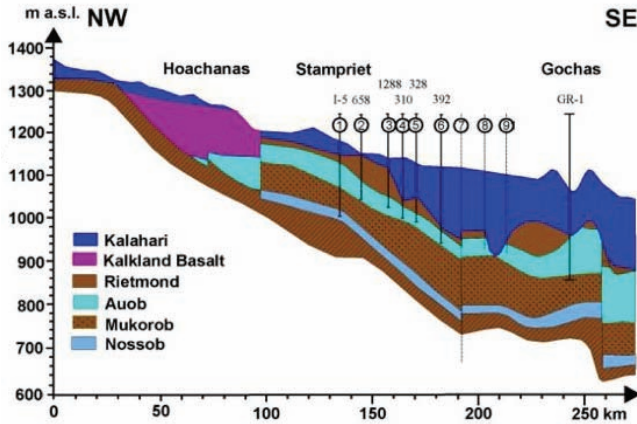


FIG. 2. Hydrogeological cross section of the geology underlying the Stampriet area.

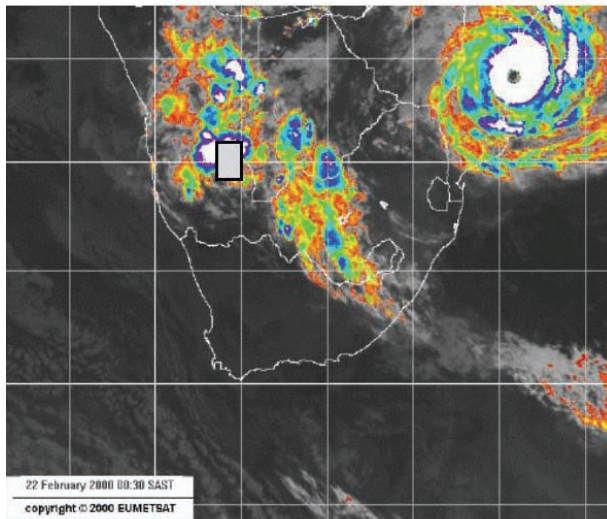


FIG. 3. Eumetsat image of southern Africa on 22 February 2000 shows study area and SE trending low pressure zone from the ITCZ and cyclone Eline making landfall over Mozambique.

various degrees also in parts of the underlying, deeper confined/semi-confined sedimentary aquifers [4, 5]

The exceptional rainfall of the 1999–2000 season (Fig. 3; up to 4 times the annual average in the study area) that was experienced also in many other parts of southern Africa, produced rare flood events of the Auob River, and other usually dry rivers in the area (Fig. 1). In the course of the groundwater investigation daily river water samples were collected at Stampriet ~100 km downstream from river upper reaches of the catchment during the most pronounced of these flood events with peak discharge rates $>50 \text{ m}^3\text{s}^{-1}$ (Fig. 6).

3. ISOTOPE DATA

A $\delta^2\text{H}/\delta^{18}\text{O}$ plot of the daily samples taken over the twelve days from the Auob River (Fig. 4) shows a near-perfect linear correlation, a wide range of values and slope of 6.2, intermediate between that of the GMWL and of the local evaporation line $s \sim 5.4$ (Fig. 5). These features suggest mixing between very depleted water and an end-member enriched by evaporation.

Rainwater collected during the project had a tritium content of 2–3 TU, a wide range of stable isotope ($\delta^2\text{H}$, $\delta^{18}\text{O}$) values often highly depleted in some storms. These are shown in Fig. 5, along with the cluster of deep and shallow groundwater values with a regression of $s = 5.4$ and the Auob River values.

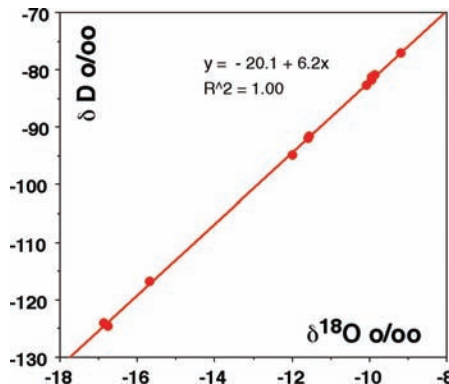


FIG. 4. Highly linearly correlated values of $\delta^2\text{H}$ versus $\delta^{18}\text{O}$ for the Auob River flood suggest mixing between depleted water and an end-member enriched through evaporation (Fig. 5).

GROUND WATER INPUT TO A RARE FLOOD EVENT IN AN ARID ZONE

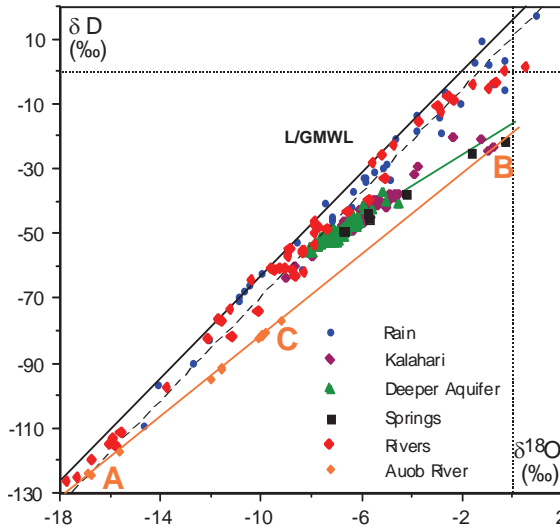


FIG. 5. $\delta^2H/\delta^{18}O$ diagram for rainfall in south-eastern Namibia for the period 1999–2001, groundwater and springs. Also shown are the Auob River data points (Fig. 4).

4. HYDROLOGICAL AND CHEMICAL DATA

The stage recorder at Stampriet where the river was sampled, ceased functioning at the onset of the flood peak, and may have malfunctioned earlier. Flow measurements 80 km downstream at Gochas provide an indication of the

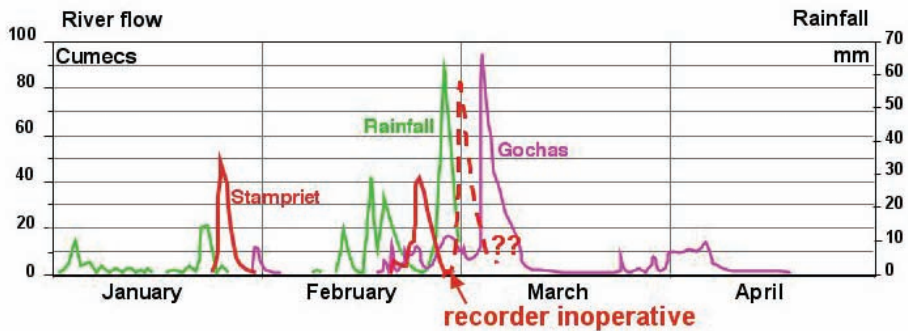


FIG. 6. Rainfall for the period January–April 2000 with flow measurements for the Auob River at stage recorders at Stampriet and Gochas. The recorder at Stampriet became inoperative during the flood peak, and probably was malfunctioning before.

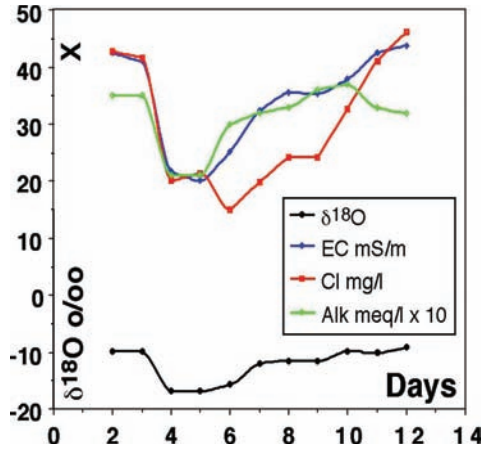


FIG. 7. Temporal variation of various parameters measured on flood water in the Auob River during the flood in February 2000. The negative excursion in all parameters suggests the addition of direct rain runoff into the ephemeral base flow.

stream response, but delayed by 2–3 days. A speculative reconstruction of the peak at Stampriet is shown in Fig. 6.

The parameters measured on the river samples ($\delta^2\text{H}$, $\delta^{18}\text{O}$, E.C., $[\text{Cl}^-]$, $[\text{HCO}_3^-]$) could therefore not be correlated accurately with flow rates, which would have allowed hydrograph separation. The temporal variation of the parameters over the 12 day period of the 2000 flood are shown in Fig. 7.

The values of $\delta^{18}\text{O}$, EC, $[\text{Cl}^-]$, Alk remained steady for the first two observations suggesting the influence of groundwater. A drop in all parameters in days 4 and 5 reflect coincided with the reconstructed flow peak at Stampriet (Fig. 6). The drop could therefore be interpreted as dilution with isotopically depleted storm runoff. The recoveries with the subsequent reduction in flow suggest different components to the input of the river upstream of Stampriet.

5. FLOOD COMPONENTS

Referring to Fig. 5 it is seen that the range of stable isotope values for the Auob River plot along a regression line $s \sim 6.2$ that originates at A near the most depleted end of the G/LMWL. When the line is extrapolated from C it is seen to intersect groundwater/spring water values at the most positive end of their range at B, i.e. very shallow groundwater components. The line is therefore interpreted as a mixing trend between evapouratively enriched

GROUND WATER INPUT TO A RARE FLOOD EVENT IN AN ARID ZONE

shallow ground water and very depleted rainwater that characterised the storm sequences observed in the period around February 2000.

The different time trajectories followed by the parameters characterising river water after the major flood event are interpreted as the various shallow ground water components, displaced by rain water infiltrating in the river catchment — in other words, the (ephemeral) base flow — once more dominating. Mixing proportions (Fig. 5) show that up to 50% of the flood was derived from groundwater early and later in the flood. These conclusions are strengthened by the fact that early in 2001 the river flowed again although rainfall was much lower than in 2000. They have led to important insights into the hydrological relationships of the shallow aquifer with surface and deeper formations, as well as recharge mechanisms in the area. As yet, the mechanism for the ubiquitous evaporation signal most pronounced in the shallow groundwater in the area is still to be investigated [5].

6. ASSESSING SURFACE EVAPORATION

It might be argued that the evaporative enrichment observed in the temporal changes of stable isotope composition of the river could be ascribed to contemporaneous evaporative losses from the open surface of the river itself.

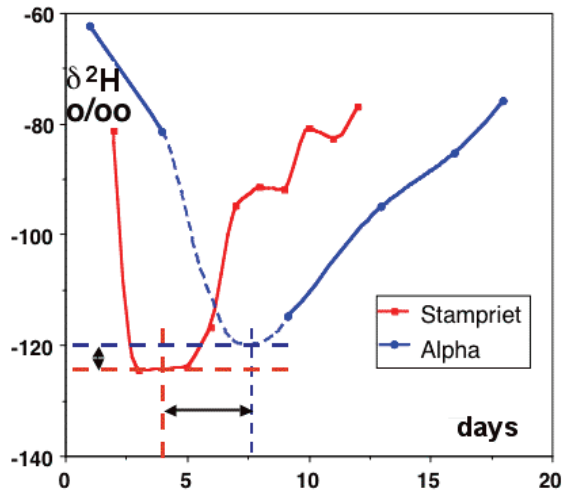


FIG. 8. Comparative variations in δ^2H for the Aoub river flood for samples taken at Stampriet and about 170 km downstream at Alpha.

Samples taken during the same period at Alpha, 170 km further downstream from the principal sampling point at Stampriet, showed a comparable, but delayed and dispersed, isotopic excursion in the flood. As the series of samples taken at Alpha was not complete, part of the $\delta^2\text{H}$ /time curve had to be interpolated. As is seen in Fig. 8, compared with an overall variation of some 55‰, the enrichment that occurred over this distance of flow is some 5‰ over a distance of flow much longer than the headwaters of the river from Stampriet. This rules out evaporative enrichment from the river surface as the cause for the major excursion in stable isotope values, and reasonably also of the various other parameters.

7. CONCLUSIONS

This is the first known instance where ground water contributions to flow in an arid zone ephemeral river have been reported. Variations in isotopic ratio and dissolved species concentrations have shown conclusively that up to 50% of flood water in the Auob River in early-2000 was “old” water – shallow ground water, accumulated over previous, more average, rainy seasons, displaced by infiltrating rain water.

This data could only be interpreted in terms of pre-existing detailed information on the aquifers in question and contributes to an understanding of aquifer behaviour in the area. It can also be speculated that, during the storm events of 2000 and 2001 we may have observed the brief re-activation of palaeo-sources that sustained river flow under earlier climatic conditions, become dormant under the present arid phase.

ACKNOWLEDGEMENTS

The authors acknowledge with thanks the contributions to this work by officials of the Namibian Department of Water Affairs, Windhoek, in particular for information on river flow rates and the collection of numerous samples. The analytical work was performed by the Environmental Isotope Laboratory, at the time in the Schonland Research Institute, University of the Witwatersrand, Johannesburg. Financial support by the International Atomic Energy Agency is gratefully acknowledged.

REFERENCES

- [1] SKLASH, M.J., FARVOLDEN, R.N., FRITZ, P., A conceptual model of watershed response to rainfall, developed through the use of oxygen-18 as a natural tracer, *Canadian Journal of Earth Sciences* **13** (1976) 271–283.
- [2] TURNER, J.V., BRADD, J.M., WAITE T.D., Conjunctive use of isotope techniques to elucidate solute concentration and flow processes in dryland salinized catchments. *Isotope Techniques in Water Resources Development*, IAEA, Vienna (1992) 33–60.
- [3] KIRCHNER, J., TREDoux, G., WIERINGA, A., CHRISTELIS, G., Assessment of the recharge to the Stampriet artesian basin to formulate a groundwater management plan for sustainable use of the resource in the southeast Kalahari of the Republic of Namibia, Final report on the project RAF/8/029 to the IAEA, Vienna, DWA, Windhoek (2002).
- [4] VERHAGEN, B.Th., Unpubl. reports to the IAEA on RAF8029 data and comments to DWA (2002).
- [5] GEYH, M.A., VERHAGEN, B.Th., BUTLER, M.J., Isotopic and Hydrochemical Data of the Stampriet Artesian Basin — a Challenge (Stampriet Revisited), *Proceedings, Hydrological Association of Namibia conference*, Windhoek, March 2007, In press (2007).

WATER FLOWPATHS IN THE MOUNTAINOUS WATERSHED TRACED BY ^{18}O ISOTOPE

Experimental approach

M. SANDA, M. SOBOTKOVA, M. CISLEROVA
Czech Technical University,
Dept. of Irrigation, Drainage
and Landscape Engineering,
Prague, Czech Republic

Abstract

Uhlirská, Jizera Mountains, Czech Republic, is a typical watershed with the crystalline bedrock forming Cambisols. It is situated in a humid mountainous region where soils are shallow and highly permeable with preferential pathways. As a result of these facts, outflow caused by storms can be of a quick response and high magnitude. Based on the observations performed since 1998, it becomes evident that soil profile plays dominant role in the rainfall-runoff transformation. Data collection of the water regime in the soil profile and the subsurface flow accompanied with the standard climatic and hydrological monitoring is performed. Due to the fact that the behavior of flow of water in the heterogeneous soil profile and hydrogeological structure is not fully understood, quantitative measurements are supplemented by the additional techniques of the tracing of stable oxygen isotope ^{18}O and silica since 2006 in rainfall, outflow and soil and groundwater.

1. INTRODUCTION

Uhlířská (1.78 km²), is a typical watershed with the crystalline bedrock forming Cambisols as 60% of the area of the Czech Basin. It is situated in a humid mountainous region the northern part of Czech Republic where soils are typically shallow and highly permeable with preferential pathways. As a result of these facts, outflow caused by storms can be of a quick response and high magnitude. Focusing on the flow processes in the subsurface, the aim of the hydrological research is to reveal the flow mechanism transforming rainfall into runoff in both variably saturated soil profile on the instrumented hillslope and within the scope of the watershed. To record also other factors of the hydrological cycle, the site is accompanied with the basic climatic

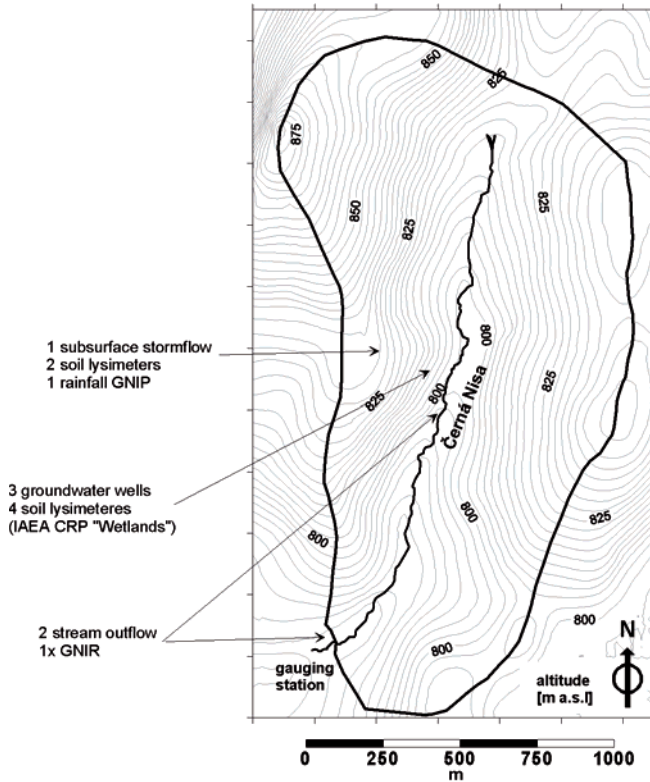


FIG. 1. Water sampling locations in the experimental watershed Uhlirská, Czech Rep.

station recording air temperature, net radiation, wind speed and humidity on a continuous basis.

Based on the observations performed, it becomes evident that soil profile plays dominant role in the rainfall-runoff transformation [1]. Flow of the water in the heterogeneous porous environment, including the soil profile and hydrogeological saturated structure can not be satisfactorily described using quantitative hydrological variables only. Quantitative measurements lack the information about the nature of the transformation in space and time. Therefore additional techniques stated to be utilized. Due to the fact that the behavior of flow of water in the heterogeneous porous media and highly heterogeneous hydrogeological structure is not fully understood, a targeted study of these phenomena in the field scale has been launched in 2006. The tracing by means of the natural substances is the only noninvasive tool available to render the

WATER FLOWPATHS IN THE MOUNTAINOUS WATERSHED

mechanisms of the outflow. Study of the water dynamics by means of natural tracers is targeted to employ effects of stable oxygen isotope ^{18}O [2] and silica as SiO_2 [3] within the elements of the hydrological cycle. Such investigation increases the quality of the present research fundamentally by adding an independent set of information for subsurface stormflow generation.

2. EXPERIMENTAL SETUP

Both of the natural elements (^{18}O and silica ions) are sampled at selected spots in the watershed since the spring of 2006. These activities cover the sample collection of rainfall, snowmelt, snowcover, subsurface stormflow, groundwater, soil water from suction lysimeters and the stream outflow at two gauging stations. Silica is not sampled in the meteoric water (snowmelt and rainfall) assuming not to be present.

Besides the most recent activities in the area of the environmental hydrological isotopes, detailed, long-term automated measurements of climatic and hydrological components have been performed within last decade. The measurements comprise rainfall, air and surface temperature, net radiation, air humidity, barometric pressure and wind speed measurements. Soil suction, soil moisture and groundwater level in chosen locations is being acquired as well. In the subsurface, stormflow is collected for the outflow measurements on the hillslope. This setup was built for the dynamics of the subsurface stormflow generation, recently utilized for the isotope content sampling as well.

3. OBSERVATIONS OF THE HYDROLOGICAL CYCLE IN 2006

During 2006, four significant snowmelt/rainfall – runoff episodes were observed – snowmelt in March-May, local rainstorm in June, and two frontal extreme storm in August. Snowmelt lasted in the period of 25.3.–18.5.06. Total amount of snow at the watershed was estimated in the range of 500–600 mm of the water equivalent. In addition, 81 mm of the rain contributed since 12.4.06. Here, there is transparent impact of the melting water at the beginning of the episode. At the last phase, the subsurface trench outflow was also sampled. Complex picture indicates the replacement of pre-melt water in the subsurface outflow and the stream outflow as well. Outflow is being transformed by the variably saturated soil profile and then in the saturated aquifer. Variation of SiO_2 prior to the snowmelt shows the range of low concentration values, however since the commencement of the snowmelt, a rapid rise is observed. Possibly, the pre-event baseflow drains the aquifer via paths, which are washed permanently,

where silica can not be dissolved into the water at higher concentration. On contrary to, the snowmelt water replaces the soil water stagnant during the winter season in the soil profile. Given a sufficient time to dissolve silica in soil water, this contributes to its rapid rise in the streamflow.

Significant storm rainfall occurred in the period of 4.8.–8.8.06 with 247 mm of rain, resulting in one of the two highest discharge intensities (estimated as 3.2–3.8 m³/s) since the establishment of the observations in 1981. Here, the quicker response of the soil profile to the change of $\delta^{18}\text{O}$ is evident. It supports the hypothesis of the partial transformation of the rainfall onto runoff within the soil profile, employing the preferential pathways. Later the differences of the oxygen isotope signatures found in the subsurface stormflow and the watershed streamflow are diminished, probably due to the extreme nature of the event, where the most of the pre-event water is already displaced with the causal rainwater. The course of the concentrations of SiO_2 at the same checkpoints is similar. The fall of SiO_2 concentration during the culmination of the flow is observed, due to the extreme amount of the outflow from the soil profile and from the watershed.

Two additional rainfall events causing the rapid outflow were tracked. Local rainstorm on 21/22.6.06 producing 29.7 mm of rain, and regional long term rainfall 23.8.06–4.9.06 of the total amount of 104.2 mm. These two events behaviour is of a similar pattern as other vegetation season events (e.g. rainfall of 4–8.8.06 described above).

4. FLOW SEPARATION, TRACING OF WATER ORIGIN

Until recent, conventional hydrograph separation techniques were applied on the limited data set only. The separation is based on the following set of Eqs (1), (2) and (3) for outflow intensity and isotope content in the water.

$$Q_t = Q_s + Q_n \quad (1)$$

$$c_t Q_t = c_s Q_s + c_n Q_n \quad (2)$$

$$R_s = \frac{Q_s}{Q_t} = \frac{c_t - c_n}{c_s - c_n} \quad (3)$$

where

Q_t is total amount of the outflow (m³/s)

Q_s is the amount of pre-event water in the outflow (m³/s),

Q_n is the amount of the event water in the outflow (m³/s),

WATER FLOWPATHS IN THE MOUNTAINOUS WATERSHED

- c_s is long term concentration of tracer ($\delta^{18}\text{O}$),
- c_n is event concentration of tracer ($\delta^{18}\text{O}$),
- R_s is instant fraction of pre-event water in the outflow (-).

Course of the isotope $\delta^{18}\text{O}$ in water is shown on the Fig. 2 for the stormflow episode of 21–24.6.06. Fig. 3 shows the separation of the hydrograph based on the Eqs (3), considering the pre-event content in stream outflow of $\delta^{18}\text{O} = -10.1\%$ (measured in the outflow prior to the event). Adequate separation is performed

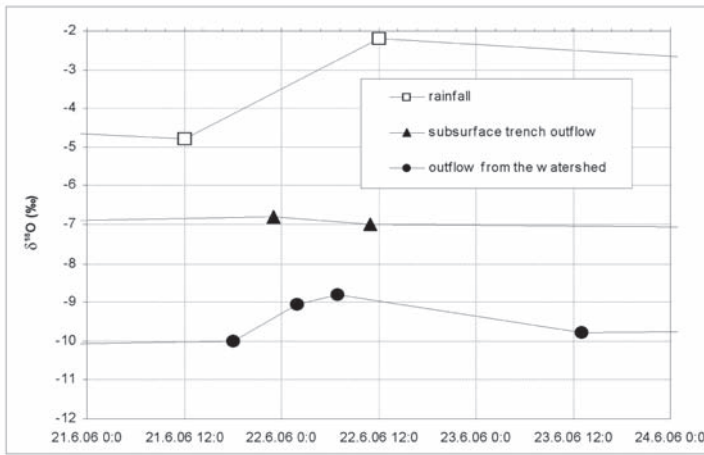


FIG. 2. Isotope $\delta^{18}\text{O}$ in rain and subsurface and stream outflow.

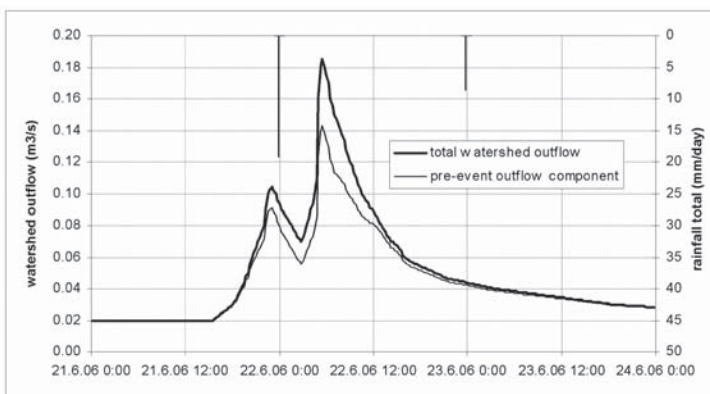


FIG. 3. Outflow hydrograph at the stream gauging profile.

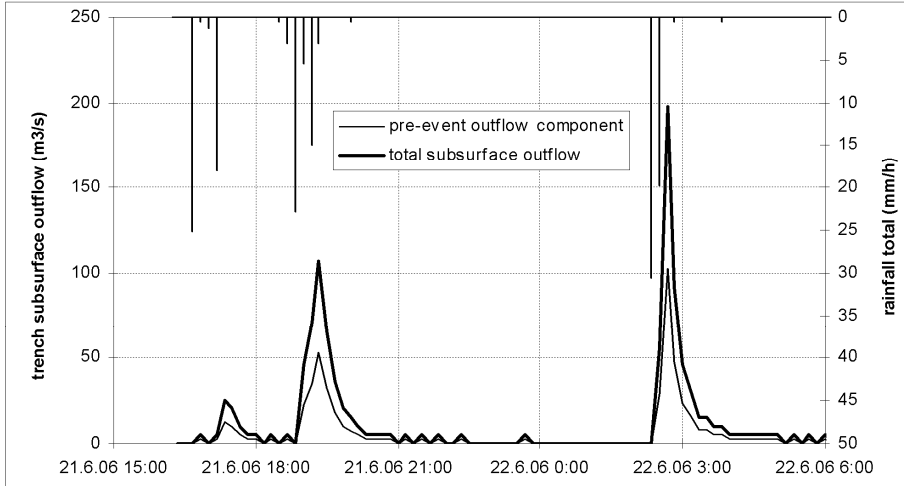


FIG. 4. Outflow hydrograph at the subsurface trench.

for experimental trench with the pre-event water content in soil (by means of soil lysimeter) of $\delta^{18}\text{O} = -10.9\text{‰}$. Separation of the watershed hydrograph shows the significant pre-event water component (not less than 75%). Subsurface outflow from the shallow soil profile shows that 46-51% of the subsurface storm flow is composed of the pre-event water. These findings indicate important role of the soil profile and the valley aquifer for the runoff generation and isotopic composition of storm outflow. Analyzing isotope data, the hypothesis of subsurface outflow dominant impact on the watershed streamflow has been supported. Quick subsurface outflow from the soil profile and the outflow from the watershed exhibit similar dynamics, analyzing both quantity and quality of selected natural tracer [4].

5. ONGOING ACTIVITIES

Experimental watershed became a member of GNIP and GNIR networks run by IAEA and is also part of the IAEA CRP “Isotopic techniques for assessment of hydrological processes in wetlands. Experimental watershed is also part of the BIOGEOMON network of experimental areas with the atmospheric deposition observations. Detailed monitoring of the chemical components in the outflow are run by Water Research Institute, Prague, CZ.

WATER FLOWPATHS IN THE MOUNTAINOUS WATERSHED

Recently, subsurface is sampled for basic environmental chemical content (such as pH, electrical conductivity and basic ions) as well.

ACKNOWLEDGEMENTS

This research has been supported by the Czech Science Foundation 205/06/0375.

REFERENCES

- [1] ŠANDA, M., HRNČÍŘ, M., NOVÁK, L., CÍSLEROVÁ M., Impact of the soil profile on rainfall-runoff process, *J. Hydrol. Hydromech.* vol. 54, No. 2 (2006) 163–182.
- [2] KENDALL, C., MCDONNELL, J.J., (Eds.) J., *Isotope Tracers in Catchment Hydrology*, Elsevier Science B.V., Amsterdam (1998).
- [3] KENNEDY, V.C., Silica variation in stream water with time and discharge, in nonequilibrium systems in natural water chemistry, *Adv. Chem. Ser.* vol. 106 (1971) 94–13.
- [4] ŠANDA, M., NOVÁK, L., HRNČÍŘ, M. AND CÍSLEROVÁ, M., Tracing of the water flowpath in the soil profile of the mountainous watershed by means of natural elements, L.Pfister, P. Maten, R. Van den Bos, L. Hoffmann (Eds.) (2006). “Uncertainties in the ‘monitoring-conceptualisation-modelling’ sequence of the catchment research. Proceedings of the eleventh biennial conference of the euromediterranean network of experimental and representative basis (ERB), 22–26 September 2006”, Luxembourg, Luxembourg (2006) 183–184.

PRELIMINARY ISOTOPE STUDIES IN POYANG LAKE

WENBIN ZHOU¹, MAOLAN WANG, CHUNHUA HU,
HUAYUN XIAO XIAO

Key Lab for Poyang Lake Ecology
and Bio-resource Utilization,
Ministry of Education,
Nanchang University,
China

Abstract

Poyang Lake is the largest fresh water lake in China, and the largest wetland protection area in Asia. The lake serves as the largest buffer for the Yangtze River as well. In order to make better understanding of the water dynamics, water balance, water chemistry, and the relations between lake, rivers and groundwater, isotope investigation has been carried out systematically for one and a half hydrological years. The paper reports the preliminary results of the study.

1. INTRODUCTION

The stable isotope of hydrogen and oxygen can be used as a naturally occurring tracer for evaluating travel times, residence times, and mixing conditions in ground water. This information can provide valuable insight regarding the movement of potential contaminants [1]. Measurements of the concentrations and carbon isotopes of dissolved inorganic carbon (DIC) in water samples are routinely used in studies of carbon geochemistry and biogeochemistry of natural waters. Values of carbon isotopes, along with other chemical measurements in rivers, have been used to evaluate the sources, sinks and fluxes [2, 3].

The water cycling and water environment of the Poyang Lake catchment has great impacts to the eco-environment of Jiangxi Province and the middle- and downstream of Yangtze River region. However, due to the lack of relevant

¹ Corresponding author. Email: wbzhou@ncu.edu.cn. Supported by International Science Cooperation project of China (2006DFB91920) and the National Natural Science Foundation of China (40672159).

fundamental data, the scientific decision-making process for the sustained development of Poyang Lake region becomes impossible. The goals of our research are to investigate the water resources and water environment, and further simulation models to predict their evolution.

2. STUDY AREA DESCRIPTION

Poyang Lake, the biggest fresh water lake in China, is located in northern Jiangxi Province, bounded by latitudes $28^{\circ}10'N$ and $29^{\circ}50'N$, and longitudes $115^{\circ}30'E$ and $117^{\circ}05'E$. The lake covers an area of ca. 3,900 km². The lake is shallow and is connected with five main rivers, namely Gan River, Fu River, Xin River, Rao River and Xiu River. Rao River is comprised of Chang River and Le'an River. Waters from these rivers run through Poyang Lake and empty into the Yangtze River through a narrow passage at Hukou except during the

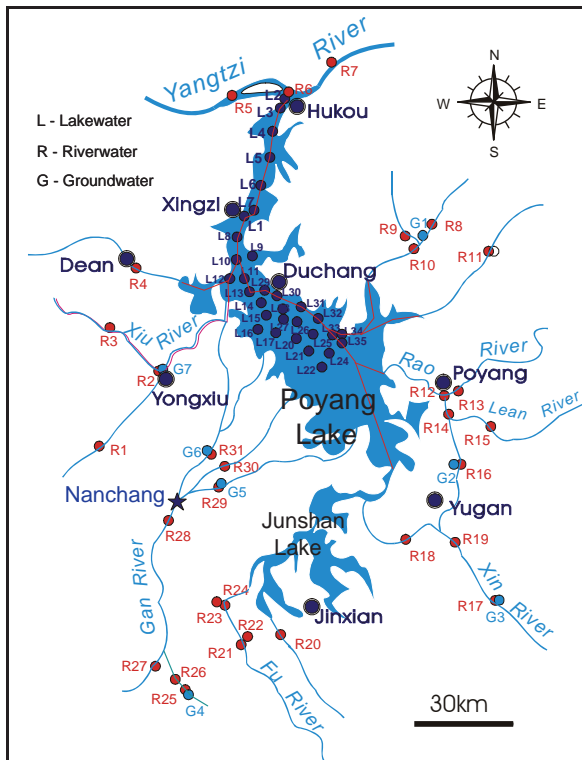


FIG. 1. Sketch map showing sampling locations in Poyang Lake catchment, China.

PRELIMINARY ISOTOPE STUDIES IN POYANG LAKE

flood stage of these rivers. Its annual afflux of water to Yangtze River exceeds the total water amount of the three rivers: Huanghe River, Huaihe River and Haihe River. The area of the watershed is 162,200 km², taking up 97% of Jiangxi provincial territory, 9% of the Basin of Yangtze River. The annual mean runoff of the watershed is 152.5 billion m³, accounting for 16.3% of that of the watershed of Yangtze River.

Annual floods, beginning in late May/June and usually ending in October/November, filling up the lake like bathtub, swelling it into a large inland sea and covering all the lowland marshlands, with water from these five rivers. In October and November, the floods subside, the lake loses as much as 90% of its water, and hence vast areas of flat grass-covered marshlands become exposed and are used for grazing by cattle and water buffalo [4, 6]. This forms special scenery of 'A Line at Low Water, An Ocean at Flood' in the lake. The mean annual temperature is 17.6°C with 240–330 days frost-free. The July and January mean temperatures are 29.6° and 5.0°C, respectively. Annual precipitation is about 1528 mm [7], with most of the rain falling between April and September.

The river basin area of Gan river, Fu river, Xin River, Xiu River, Chang River and Le'an River is 80,900 km², 15,800 km², 16,000 km², 14,000 km², 7,036 km² and 8,456 km², respectively. And the lengths of Gan river, Fu river, Xin River, Xiu River, Chang River and Le'an River are 766 km, 312 km, 313 km, 357 km, 85 km and 279 km, respectively.

3. SAMPLING AND ANALYTICAL METHODS

Riverwater, lakewater and groundwater were sampled in August of 2005. In the field, pH, electrical conductivity (EC) and total dissolved solids (TDS) were immediately measured and HCO₃⁻ concentrations were determined using titration assay with 0.01mol/L HCl solution. Samples for isotope analysis were filtered using 0.45µm Millipore filters and collected in acid washed polyethylene bottles without air bubble.

Isotopic compositions of all water samples were analyzed by Finnigan MAT 253 mass spectrometry. Values are reported in per mil (‰) units relative to VSMOW and PDB. The precision of hydrogen, oxygen and carbon isotope results are 1.0, 0.1 and 0.1‰, respectively.

4. RESULTS AND DISCUSSION

The isotopic compositions of ¹⁸O, D, and ¹³C in samples from lakewater, riverwater and from a precipitation event are presented in Figs. 2–4 and Table 1.

4.1. Hydrogen and oxygen isotopes

The hydrogen and oxygen isotopic compositions in Poyang Lake catchment rivers ranges from -7.4 to -5.0 ‰ (averaging -6.4 ‰) and from -55.3 to -27.9 ‰ (averaging -39.4 ‰), respectively. These values are almost the same as those in the lake (averaging -7.0 ‰ and -40.2 ‰, respectively). However, hydrogen and oxygen isotopes significantly differ between riverwater (R) and groundwater (G) sampling at the same sites (Table 1). All the hydrogen isotopes are heavier in groundwater than in riverwater. For the 7 sampling sites, heavier oxygen isotopes occurred in groundwater of 5 sites, only 2 sites showed us heavier oxygen isotopes in riverwater. This can not be explained by nonequilibrium fractionation during evaporation because evaporation is often stronger in riverwater than in groundwater. Therefore, the heavier hydrogen isotopes occurring in groundwater may be the result of mixing with other types of water (e.g. soil water).

The relationship between δD and $\delta^{18}O$ for most meteoric and surface waters around the world that have not experienced significantly evaporation can be approximated by the Global Meteoric Water Line (GMWL) or Craig line [8]. The local meteoric water lines for riverwaters and lakewaters (Fig. 2) in Poyang Lake catchment have the similar slopes, indicating that riverwater is the dominant water source of Poyang Lake. The line for the riverwater data has a y-intercept of 8.56, whereas the line for the lakewater data has a y-intercept of 11.82. As compared to the Craig Line (GMWL), the lines for both riverwater and lakewater data have slightly higher slopes. This divergence reflects the effects of evaporation from the two types of surface water on the isotopic composition. Evaporation is a nonequilibrium process that enriches D less than ^{18}O in the remaining water so that the slope of the D- ^{18}O relation decreases from about 8 (Craig line) to 7.4. Although only a rain water sample was analyzed, the point of this data was obviously below the lines of both

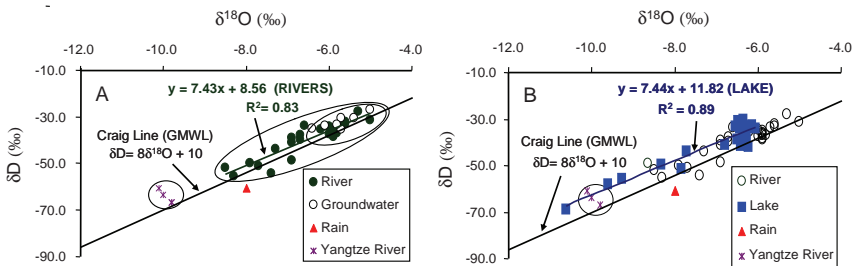


FIG. 2. Isotopic composition in riverwater and lakewater.

TABLE 1. ISOTOPE DIFFERENCES BETWEEN RIVERWATER (R) AND GROUNDWATER (G) SAMPLING AT THE SAME SITES (IN ‰).

Sites	1	2	3	4	5	6	7
Samples	R16 G2	R8 G1	R17 G3	R25 G4	R29 G5	R31 G6	R2 G7
$\delta^{13}\text{C}$ (DIC)	-10.7 -14.3	-15.5 -18.2	-12.6 -17.1	-13.7 -15.1	-12.4 -16.2	-9.1 -21.7	-13.1 -12.4
$\delta^{18}\text{O}$ (H_2O)	-6.1 -5.7	-8.5 -5.7	-6.2 -6.4	-5.3 -5.0	-5.9 -5.4	-5.8 -6.1	-6.9 -5.8
δD (H_2O)	-34.1 -30.7	-51.7 -35.2	-35.5 -35.1	-27.9 -27.1	-36.7 -30.7	-37 -33.6	-48.5 -33.5

riverwater and lakewater data, suggesting the local evaporation is strong in riverwater and lakewater.

4.2. Carbon isotopes of DIC

Dissolved inorganic carbon is the largest carbon pool in most aquatic systems, with bicarbonate being the dominant species [9]. The isotopic composition of the dissolved inorganic carbon ($\delta^{13}\text{C}$) is therefore a DIC useful tracer of processes that dominate the carbon cycle in aquatic systems. These processes occur along the pathway of water transport in catchment basins and can be divided into four groups:

- (1) oxidation of organic matter;
- (2) dissolution of carbonate minerals (when present) in soils, aquifers and surface waters;
- (3) exchanges with atmospheric carbon dioxide and kinetic effects at water/atmosphere interface;
- (4) photosynthetic activity (of algae and macrophytes). All these processes leave isotopic imprints on DIC.

The $\delta^{13}\text{C}_{\text{DIC}}$ values of the Poyang Lake ranged from -18.7 to -8.6‰ , with a mean of -12.3‰ . These values are highly close to those of the catchment rivers (Fig. 3), which have a mean of -12.4‰ (-17.8 to -8.7‰), indicating that they are closely related. The $\delta^{13}\text{C}_{\text{DIC}}$ values of the lake are much lower than those measured for the Great Lakes (-3.6 to $+0.3\text{‰}$; [10]) and Taihu Lake (-10.0 to -1.3‰ ; unpublished data of Xiao). The highly ^{13}C -depleted values in the catchment rivers reflect that bacterial respiration plays an important role in the isotopic composition of DIC and this “bacterial” signature is transmitted from the rivers into Poyang lake. Compared to Poyang Lake, Taihu Lake has higher $\delta^{13}\text{C}_{\text{DIC}}$ values (Fig. 4). This may be because that photosynthesis results in increasing $^{13}\text{C}/^{12}\text{C}$ ratios of the DIC, because algae preferentially remove light carbon (^{12}C) from the DIC pool [11]. Carbon isotope discrimination by algae can be as large as 20‰ [12], but smaller fractionations of only 5‰ have also been reported [13]. This mechanism explains the isotopic discrimination between $\delta^{13}\text{C}_{\text{DIC}}$ and primary production (eutrophication). Although the DIC concentrations are much higher in Yangtze River than in the catchment rivers, the $\delta^{13}\text{C}_{\text{DIC}}$ values are not significantly different.

As listed in table 1, carbon isotope in DIC at most sites show higher values in riverwaters than in groundwater. The largest difference between them reaches 12.6‰ . In the shallow groundwater situation, the gaseous reservoir is soil CO_2 , generally at significantly higher partial pressure. So, the relatively

PRELIMINARY ISOTOPE STUDIES IN POYANG LAKE

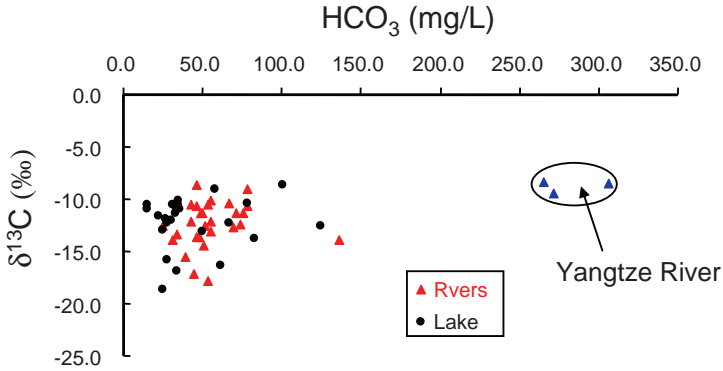


FIG. 3. Carbon isotopic composition in riverwater and lakewater.

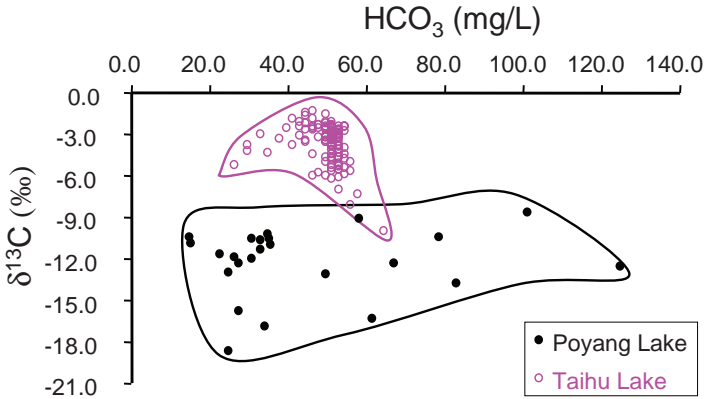


FIG. 4. Comparison of $\delta^{13}\text{C}_{\text{DIC}}$ between Poyang Lake and Taihu Lake.

negative isotopic composition of groundwater shows the influence of the system exchange with more negative $\delta^{13}\text{C}$ soil CO_2 [14].

ACKNOWLEDGEMENTS

This study work was kindly supported by International Science Cooperation project of China through grants 2006DFB91920 (W.B. Zhou) and the National Natural Science Foundation of China through grants 40672159 (W.B. Zhou).

REFERENCES

- [1] MCGUIRE, K.J., DEWALLE, D.R., GBUREK, W.J., Evaluation of mean residence time in subsurface waters using oxygen-18 fluctuations during drought conditions in the mid-Appalachians, *J. Hydrol.* **261** (2002) 132–149.
- [2] TAYLOR, C.B., FOX, V.J., An isotopic study of dissolved inorganic carbon in the catchment of the Waimakariri River and deep ground water of North Canterbury plains, New Zealand, *J. hydrol.* **186** (1996) 161–190.
- [3] YANG, C., TELMER, K., VEIZER, J., Chemical dynamics of the “St. Lawrence” riverine system: δD_{H_2O} , $\delta^{18}O_{H_2O}$, $\delta^{13}C_{DIC}$, $\delta^{34}S_{sulfate}$ and dissolved $^{87}Sr/^{86}Sr$. *Geochim. Cosmochim. Acta.* **60** (1996) 851–866.
- [4] GUO, J.G., ROSS, A.G.P., LIN, D.D., WILLIAMS, G.M., CHEN, H.G., LI, Y.S., DAVIS, G.M., FENG, Z., MCMANUS, D.P., SLEIGH, A.C., A baseline study on the importance of bovines for human *Schistosoma japonicum* infection around Poyang Lake, China, *Am. J. Trop. Med. Hyg.* **65** (2001) 272–278.
- [5] DAVIS, G.M., WU, W.P., CHEN, H.G., LIU, H.Y., GUO, J.G., LIN, D.D., LU, S.B., WILLIAMS, G., SLEIGH, A., FENG, Z., MCMANUS, D.P., A baseline study of importance of bovines for human *Schistosoma japonicum* infections around Poyang Lake, China: villages studied and snail sampling strategy, *Am. J. Trop. Med. Hyg.* **66** (2002) 359–371.
- [6] CHEN, H.G., LIN, D.D., The prevalence and control of schistosomiasis in Poyang Lake region, China. *Parasitol. Int.* **53** (2004) 115–125.
- [7] JIANG, Q.H., PIPERNO, D.R., Environmental and archaeological implications of a late quaternary palynological sequence, Poyang Lake, Southern China, *Quat. Res.* **52** (1999) 250–258.
- [8] CRAIG, H., Isotopic variations in meteoric waters. *Science* **133** (1961) 1702–1703.
- [9] DREVER, J.I., *The Geochemistry of Natural Waters*. Prentice-Hall, New York (1988).
- [10] WEILER, R.R., NRIAGU, J.O., Isotopic composition of dissolved inorganic carbon in the Great Lakes. *J. Fish. Res. Board Canada.* **35** (1978) 422–430.
- [11] FRY, B., SHERR, E.B., $\delta^{13}C$ measurements as indicators of carbon flow in marine and freshwater ecosystems, *Contrib. Mar. Sci.* **27** (1984) 13–47
- [12] HERCZEG, A.L., FAIRBANKS, R.I., Anomalous carbon isotope fractionation between atmospheric CO_2 and dissolved inorganic carbon induced by intense photosynthesis, *Geochim. Cosmochim. Acta* **51** (1987) 895–899.
- [13] FOGEL, M.L., CIFUENTES, L.A., Isotope fractionation during primary production, In: Engel, M.H., Macko, S.A. (Eds), *Organic Geochemistry: Principles and Applications*. Plenum, New York (1993) 73–98.

PRELIMINARY ISOTOPE STUDIES IN POYANG LAKE

- [14] TAYLOR, C.B., On the isotopic composition of dissolved inorganic carbon in rivers and shallow groundwater: A diagrammatic approach to process identification and a more realistic model of the open system, *Radiocarbon*. **39** (1997) 251–268.

LINKING WATER PATHWAYS AND NUTRIENT DYNAMICS IN A SMALL HEAD WATER CATCHMENT: RESULTS OF A CONTROLLED SPRINKLER EXPERIMENT USING A DEUTERIUM TRACER IN WESTERN OREGON

H.R. BARNARD*, W.J. VAN VERSEVELD*, C.B. GRAHAM*,
B.J. BOND*, K. LAJTHA*, J.R. BROOKS**, J.J. MCDONNELL*

*Oregon State University,

**U.S. Environmental Protection Agency,
NHEERL Western Ecology Division

Corvallis, Oregon,
United States of America

Abstract

The linkages between subsurface flow paths, vegetation water use and nutrient dynamics are poorly understood. The few investigations that have explored such relations in forest systems have relied passively on natural rainfall and drainage events. As a result, it has been difficult to identify the first order controls on water-vegetation-biogeochemical processes. This work reports on a sprinkler experiment in Watershed-10 (WS10), H.J. Andrews, Oregon, USA. Discharge from the hillslope remained at steady state for 20 days. A pulse of deuterated water was applied for 24 hours on Day 1 of the experiment to investigate breakthrough of deuterium in hillslope runoff, soil, groundwater and trees. The peak in the hillslope deuterium breakthrough occurred within 24 hours of application. Deuterium enrichment was first observed in xylem samples 3 days following application. Weekly soil samples were taken for extraction of DOC to investigate whether DOC was supply-limited during periods of extended rainfall. Data analysis suggests evidence for depletion of DOC in the upper mineral soil during the experiment.

1. INTRODUCTION

The interdependence of hydrologic processes, vegetation and dissolved organic carbon (DOC) is poorly understood. The few investigations that have

explored such relations in forest systems have relied passively on natural rainfall and drainage events. Water use by vegetation has been closely linked to streamflow patterns on a variety of time scales [1–3]. However, many of the details of these linkages are poorly understood. Furthermore, we often assume an unlimited supply of DOC in our hydro-biogeochemical models, yet few studies have explicitly tested this. As a result, it has been difficult to identify the first order controls on ecohydrological processes. The objectives of this study were: (1) to examine the response of forest transpiration to rapid increases in soil moisture (2) to resolve the dominant flowpaths at the hillslope scale that flush DOC from the soil profile to the stream channel, and (3) to compare the timing of the breakthrough response curve of the deuterium tracer in transpired water versus the hillslope discharge.

2. METHODS

The study hillslope is located in Watershed 10 (WS10), in the HJ Andrews Experimental Forest (HJA) in the western Cascades, Oregon, USA (44.20°N, 122.25°W). Frequent debris flows at WS10 have scoured the stream channel to bedrock removing the riparian area in the lower 200 m of the stream. Soils are gravelly clay loams, classified as Typic Dystrachrepts, with poorly developed structure, high hydraulic conductivities (up to 10 m/hr, decreasing rapidly with depth), and high drainable porosity (15–30%) [4, 5]. Soils on the hillslope range from 10 cm adjacent to the stream, to 2.4 meters at the upper limit of the sprinkled area, have distinct pore size distribution shifts at 0.30, 0.70 and 1.0 m, resulting in transient lateral subsurface flow at 1.0 m [6]. A 10 m wide trench consisting of sheet metal anchored 0.05 m into bedrock and sealed with cement was installed at the intersection of the study hillslope and the bedrock stream channel [4]. Lateral subsurface hillslope discharge was routed to a stilling well with a 30° V-Notch Weir, where a capacitance water level recorder (TruTrack, PLUT-HR) measured stage height at 10 minute intervals.

We conducted the sprinkling experiment for 24 days beginning on July 27, 2005 on an approximately 8 m by 20 m section of the study hillslope directly upslope from the trench. The sprinkled area was chosen so that it would drain downslope into the 10 meter wide collecting trench. Total sprinkled area was 172 m². A rectangular grid of 36 (9 rows of 4) micro-sprinklers delivered water to the study area at an average rate of 3.8 mm/hr to simulate natural precipitation. A pulse of deuterated water was applied to the study via the sprinkling system for approximately 24 hours beginning on Day 1 of the experiment. Approximately, 1 liter of 99.8 at. % of D₂O was well mixed in a 20,000 L reservoir of water having a natural isotopic composition.

LINKING WATER PATHWAYS AND NUTRIENT DYNAMICS

Soil matric potential was measured by 7 fast responding tensiometers (type: UMS T4, 1 bar porous cups), that were installed vertically in an upslope transect, two clusters of tensiometers at 0.3 and 0.7 m depth, and one cluster of tensiometers at 0.3, 0.7 and 1.0 m depth. Soil moisture was measured at 24 locations within the sprinkled area, at 5 depths (0–0.15 m, 0.15–0.30 m, 0.30–0.60 m, 0.60–0.90 m, and 0.90–1.20 m) in each location with a time domain reflectometry (TDR) system. Four groups of tension lysimeters were located on an upslope transect from the slope base. Each group consisted of one lysimeter at the following depths: 0.30, 0.70, and 1.10 m. Water from the lysimeters was collected on a daily basis during the study period. Transpiration was estimated from sapflow measurements of the dominant trees located within or bordering the sprinkled area ($n=9$). Three trees located a minimum of 10 m outside of the sprinkled area were instrumented with sapflow sensors and served as reference trees for baseline rates of transpiration. Sapflow was measured at 15 min intervals using the thermal dissipation technique developed by Granier [7]. Corrections for radial variations in sapflow were estimated from measured radial profiles from the trees of the same species and age at another location [8].

Lateral subsurface flow was sampled with an ISCO sampler every 2 to 4 hours. Fluorescence of lateral subsurface flow was measured continuously at a 5 s. interval using a field fluorometer (10-AU, Turner Designs, Inc., Sunnyvale, CA) equipped with a CDOM Optical Kit (P/N 10-303) to examine DOC flushing. Three plastic zero tension lysimeters of 0.15×0.15 m were located at the hillslope. Two collected water from the organic horizon and 5 mm of upper mineral soil, and one collected water at 0.2 m depth. Twenty five superquartz (Prenart Equipment ApS) tension (0.5 bar) lysimeters installed at a 30° angle [9], were located in an upslope transect at shallow (0.2 m), middle (0.3–0.4 m), and deep (0.7–0.8 m) soil profile positions. For the first 12 days zero tension and tension lysimeters were sampled daily and every other day during the remainder of the experiment. Tension lysimeters were evacuated to -50 kPa and allowed to collect water for 24 hours. Groundwater was sampled daily from two wells that showed consistent transient groundwater and one well located in the seepage area. Samples were analyzed within 24 hours for pH and EC. Samples were filtered through combusted Whatman GF/F glass fiber filters (nominal pore size = $0.7 \mu\text{m}$) and stored frozen until analysis for dissolved organic carbon (DOC). Prenart tension lysimeter samples were not filtered because initial experiments with filtered soil solutions demonstrated that tension lysimeter samples did not need to be filtered [9]. DOC was measured with Pt-catalyzed high-temperature combustion (Shimadzu TOC-V CSH analyzer).

Soil samples were taken from the upper 0.1 m mineral soil 1 week before and three times during the sprinkler experiment at weekly intervals at the

sprinkler plot and an adjacent dry plot (control) for total DOC extraction. The sprinkler and dry plot were divided in 5 blocks of similar size and two composite samples were taken from each two adjacent blocks, resulting in 10 samples from each plot. Sample were sieved through a 1 mm sieve. Approximately 10 g of sieved soil was extracted with 100 mL 0.01 M KCl within 24 hours, shaken for two hours, and filtered with a Whatman no. 40 ashless filter paper.

Samples of subsurface discharge for isotope analysis were collected in 20 mL glass scintillation vials every hour for the first 5 days of the experiment and every 2 to 4 hours in the following days. Soil samples were collected from 0.10, 0.20, 0.30, 0.40, 0.50, 0.75 and 1.0 m depths on days 1, 2, 6, 13, and 27 of the sprinkler experiment. Xylem samples from suberized branches of the sapflow trees were sampled on the same days. Soil and xylem samples water were extracted for isotope analysis using cryogenic vacuum distillation [3]. Water samples were analyzed for hydrogen isotope ratios on an isotope ratio mass spectrometer (Delta plus, ThermoQuest Finnigan, Bremen Germany) interfaced with a high temperature conversion/elemental analyzer (TC/EA, ThermoQuest Finnigan) located at the Integrated Stable Isotope Research Facility at the Western Ecology Division of the EPA, Corvallis, OR. All hydrogen isotope ratios are expressed as δD values relative to Vienna Standard Mean Ocean Water (V-SMOW) in ‰:

$$\delta D = (R_{\text{sample}}/R_{\text{standard}} - 1)1000$$

where R is the ratio of deuterium to hydrogen atoms of the sample and the standard V-SMOW. Measurement precision was 2‰.

3. RESULTS

Hillslope discharge measured at the collecting trench responded quickly to sprinkling, with a detectable rise in discharge within an hour of initiation. Discharge rose from a constant pre-sprinkling daily average rate of 29 L/hr to a steady state daily average value of 209 L/hr in 5 days. Before, during and after the experiment, a clear diurnal pattern in discharge was evident. Steady state discharge was maintained for 13 days, after which a series of sprinkler malfunctions increased discharge over the steady state rate for 3 days. Water enriched in ^2H was observed in the hillslope discharge within 12 hours of application and enrichment peaked after approximately one day.

Transpiration rates of the nine dominant trees within the sprinkled area demonstrated no response to the rapid increase in soil moisture (Fig. 1). In addition, tree within the sprinkled area did not differ in comparison to three

LINKING WATER PATHWAYS AND NUTRIENT DYNAMICS

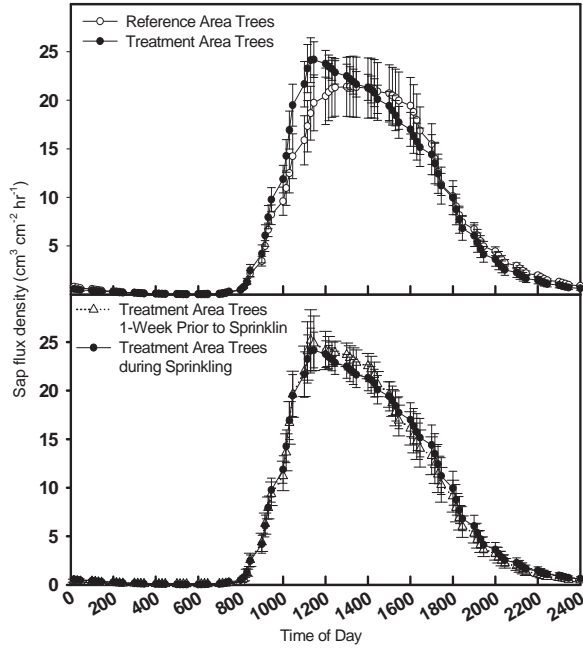


FIG. 1. Mean sap flux density of treatment and reference trees during and prior to sprinkling.

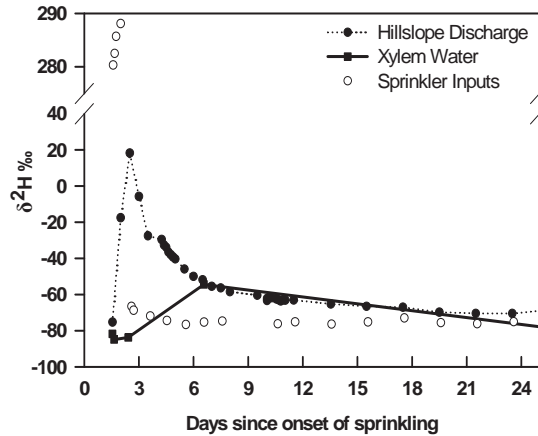


FIG. 2. Deuterium tracer inputs and recovery in hillslope discharge and treatment tree xylem during sprinkling experiment.

measured trees located outside the sprinkled area (Fig. 1). The daily average transpiration rate for the week prior to the onset of sprinkling and for five consecutive days during the steady-state period was 36 L/hr. During steady state, transpiration rate maximized during the day at approximately 13:00 on average. Hillslope discharge was reduced to its minimum rates at approximately 14:00. Minimum soil moisture and maximum soil water tension were observed 3 – 4 hrs after transpiration reached its maximum during the treatment period. Deuterium enriched water appeared in the transpiration stream in upper sunlit branches 3 days after the initial application of the tracer (Fig 2).

Average DOC concentrations and electrical conductivity (EC) in sprinkler water were respectively $4.34 \text{ mg/L} \pm 0.57$ and $48.3 \text{ } \mu\text{S/cm} \pm 2.1$. In contrast, throughfall DOC and EC were respectively on average $1.2 \text{ mg/L} \pm 0.5$, and $3.75 \text{ } \mu\text{S/cm} \pm 0.5$, during natural conditions between Fall 2004 and Spring 2005. DOC from the organic horizon, 0.2 m depth in zero tension lysimeters, tension lysimeters at 0.2 m, and 0.3–0.4 m depth showed a dilution pattern, while DOC from tension lysimeters at 0.7–0.8 m depth remained constant at an average of 2.4 mg/L . Transient groundwater DOC concentrations in two wells were high (on average 6.8 mg/L), indicating preferential flow. Soil extractions for DOC did not show a significant difference between the sprinkler and dry plot. Lateral subsurface flow DOC concentrations increased rapidly at the start of the sprinkler experiment, DOC peaked within 15 hours, and decreased to a ‘constant’ concentration after the third day of sprinkling (day 210) (Fig. 3). Fluorescence showed a diurnal pattern. DOC concentrations showed a weak diurnal pattern, and both EC and pH showed a strong diurnal pattern, indicating this was caused by a concentration effect.

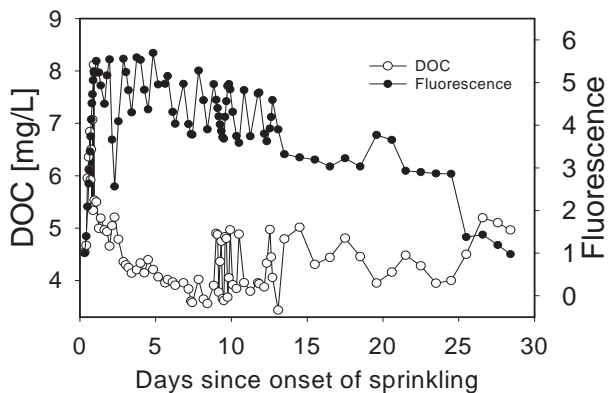


FIG. 3. Hillslope DOC and fluorescence over the course of the sprinkler experiment. Samples were collected from the trench outlet.

LINKING WATER PATHWAYS AND NUTRIENT DYNAMICS

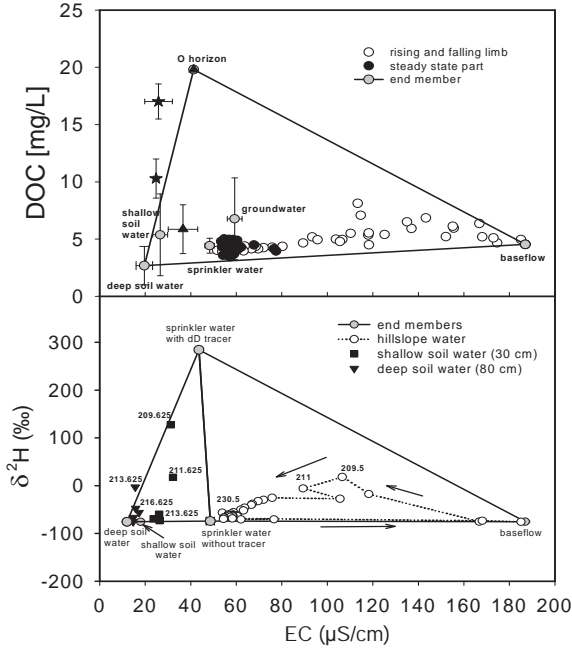


FIG. 4. Multi-end member mixing models of electrical conductivity (EC), DOC, and deuterium. Numbers within the lower panel are the day of year during the experiment. Sprinkling began on Day 208 and ended on day 232.

Lateral subsurface flow can be explained by mixing of the end-members pre-event water (lateral subsurface flow before start sprinkler experiment), organic horizon and deep soil water. The dilution of DOC at the organic horizon (Fig 4: black upwards triangles) and 0.2 m zero tension (Fig 4: black stars) over time is shown, with highest values on day 210, and lower values are an average of the remainder of the sprinkler experiment (Fig 4). In addition, the increase of DOC in lateral subsurface flow at the start of the sprinkler experiment was mainly derived from a water source at a shallow soil depth. Deuterium peaked on day 209 at 0.3 m depth coinciding with nearly saturated to saturated conditions at 0.3 m depth (tensiometer data), and DOC peaked on day 209. After day 212, nearly saturated to saturated conditions occurred at 0.7 m depth, and deeper flowpaths became important, also indicated by the deuterium peak at 0.7–0.8 m at day 213.

4. DISCUSSION

Rapidly increasing soil moisture via sprinkling had no effect on the transpiration rate of the study trees. We anticipated that the trees would rapidly uptake new shallow soil moisture. Although surface soils were relatively dry prior to sprinkling, the soil moisture at depth was great enough to maintain a high transpiration rate in the trees. Stable isotope data indicated that prior to sprinkling the source water for the transpiration stream was located deep in the soil profile (below 0.75 m depth). Enriched water was first observed in the transpiration stream 3 days after the tracer was applied. We are not able at this time to resolve at what depth the transpiration stream originated. After 3 days, the deuterium tracer had moved to depth in the soil and had peaked in the hillslope discharge. Since subsurface water flow is so much faster than uptake by trees, transpiration has little effect on nutrient flushing dynamics.

The dominant flowpath for flushing of DOC from the soil profile to the stream was a shallow water flow path at the beginning of the sprinkler experiment based on tensiometer data and deuterium breakthrough in soil water. DOC throughout the remainder of the experiment was high in aromatic content based on the fluorescence measurements, indicating an organic horizon, shallow soil source. While the bivariate plot of EC and DOC showed that organic horizon, pre-event water and deep soil water encompassed all the variability of the lateral subsurface flow samples, sprinkler water as an end-member instead of deep soil water is in more agreement with other field measurements because of the following reasons. Tensiometer data during natural storms and the sprinkler experiment at the hillslope showed that soil water is dominated by vertical flow. Higher DOC concentrations in the wells with transient groundwater compared to deep soil water from the tension lysimeters indicated that this vertical flow was preferential in the sense that there was not significant soil matrix interaction. In addition DOC concentrations in these wells decreased throughout the experiment to concentrations similar to sprinkler water concentrations. Thus, we argue that flushing was driven by mixing of pre-event water low in DOC concentrations and high transient groundwater DOC concentrations derived from vertical preferential flow from the organic horizon that diluted throughout the sprinkler experiment. Further analysis of deuterium in the groundwater wells throughout the sprinkler experiment will provide more insight into whether sprinkler water or deep soil water was the dominant end-member.

While the DOC dilution pattern of organic horizon and shallow soil water indicated a limited DOC source, DOC soil extractions with 0.01 M KCl from the upper 0.1 m soil profile at a weekly basis at the sprinkler plot and an adjacent dry control plot did not show a significant difference between the two plots

LINKING WATER PATHWAYS AND NUTRIENT DYNAMICS

suggesting an unlimited source of DOC. Thus, at the time scale of this sprinkler experiment water flux through the soil without much soil matrix interaction was the dominant control on DOC flushing, and DOC extracted from the complete soil water domain was disconnected from this mobile soil water.

5. CONCLUSIONS

This work showed that dilution of dissolved organic carbon is an important process and that DOC concentrations of different sources (organic horizon, shallow soil water) can change dramatically. In addition it showed that production in the upper 0.1 m soil profile is disconnected from the mobile soil water that's driving the DOC flushing pattern. These results challenge hydro-biogeochemical models that assume unlimited supply of dissolved organic matter.

ACKNOWLEDGEMENTS

We thank the McKenzie River Ranger District for providing water and infrastructure for the experiment. Aidan Padilla, Matt Bergen, Jessica Mandrick, and John Moreau provided assistance in the field. John Selker and Sherri Johnson provided key field equipment. This project was funded in part by the Ford Foundation, HJ Andrews LTER, and the National Science Foundation IGERT program.

REFERENCES

- [1] BOND, B.J., JONES, J.A., MOORE, G.R., PHILLIPS, N., POST, D., MCDONNELL, J.J., The zone of vegetation influence on baseflow revealed by diel patterns of streamflow and vegetation water use in a headwater basin, *Hydrological Processes* **16** (2002) 1671–1677.
- [2] JONES, J.A., GRANT, G.E., Peak flow response to clear-cutting and roads in small and large basins, western Cascades, Oregon, *Water Resources Research* **32** 4 (1996) 959–974.
- [3] HARR, R.D., LEVNO, A., MERSEREAU, R., Streamflow Changes after Logging 130-Year-Old Douglas Fir in Two Small Watersheds, *Water Resources Research* **18** 3 (1982) 637–644.
- [4] MCGUIRE, K.J., MCDONNELL, J.J., WEILER, M., KENDALL, C., MCGLYNN, B.L., WELKER, J.M., SEIBERT, J., The role of topography on

- catchment-scale water residence time, *Water Resources Research* **41** (2005) W05002 doi:10.1029/2004WR003657.
- [5] RANKEN, D.W., Hydrologic properties of soil and subsoil on a steep, forested slope. M.S. Thesis. Oregon State University, Corvallis, OR (1974).
- [6] HARR, R.D., Water flux in soil and subsoil on a steep forested slope, *Journal of Hydrology* **33** (1977) 37–58.
- [7] GRANIER, A., Sap flow measurements in Douglas-fir tree trunks by means of a new thermal method, *Annales Des Sciences Forestieres* **44** (1987) 1–14
- [8] DOMEQ, J.C., MEINZER, F.C., GARTNER, B.L., WOODRUFF, D., Transpiration-induced axial and radial tension gradients in trunks of Douglas-fir trees, *Tree Physiology* **26** 3 (2006) 275–284.
- [9] LAJTHA, K., CROW, S.E., YANO, Y., KAUSHAL, S.S., SULZMAN, E., SOLLINS, P., SPEARS, J.D.H., Detrital controls on soil solution N and dissolved organic matter in soils: A field experiment, *Biogeochemistry* **76** 2 (2005) 261–281.
- [10] DAWSON, T.E., Water sources of plants as determined from xylem-water isotopic composition: perspectives on plant competition, distribution, and water relations, In *Stable Isotopes and Plant Carbon–Water Relations*, Eds. J.R. Ehleringer, A.E. Hall and G.D. Farquhar, Academic Press, San Diego (1993) 465–496.

GEOCHEMISTRY OF CARBON STABLE ISOTOPES IN SHATT AL-ARAB RIVER AND KHOR AL- ZUBAIR ESTUARY, SOUTH IRAQ

A.H. AFAJ, S.A. THEJEEL
Environmental Research Centre,
Ministry of Science and Technology,
Baghdad, Iraq

Abstract

24 samples of Mollusc shells from Shatt AL-Arab river and Khor AL-Zubair estuary were analyzed in order to determine the concentration of carbon stable isotope and also to clarify the factors that control the geochemical distribution of carbon isotopes in these two different environments. The carbon stable isotope were measured using the closed tube method, in which shell samples are combusted to carbon dioxide for carbon isotope analysis. The carbon dioxide samples are analyzed on a Finnigan Mat 251 isotope ratio mass spectrometer equipped with a triple collector and controlled by an Apple IIe microcomputer. Measurements are made relative to several working standards {Norit (-24‰), NBS-22 (-29‰)}, and several secondary light methane standards at -43.4‰ and -62.6‰. All values are reported versus PDB. These analyses are conducted in the department of Oceanography in Texas A&M University. This study indicates that the differences in carbon stable isotopes were due to three factors: environmental conditions, under which these three molluscs are lived, chemistry of the water in Shatt AL-Arab and Khor AL-Zubair and feeding quality of these of these molluscs. The factors are close related with another important factor that it is the pollution present in these two different environments.

1. INTRODUCTION

Shatt AL-Arab river and Khor AL- Zubair estuaries are the main outlets and waterways to the Arabian Gulf (Fig. 1). Shatt AL-Arab is a tidal river, which located in the south eastern part of Iraq, is a vital source of fresh water for this part of the country, and it forms the outlet of the two main rivers of Iraq, Tigris and Euphrates. The length of Shatt AL-Arab is about 195 km from the confluence at Qurna to Arabian Gulf. The average width approximates 500 m and the depth downstream of Basrah varies between 8–15 m (Fig. 2).

The Karun River, which originates in Iran, is its major tributary. The northern and northwestern parts of the Arabian Gulf are characterized by the existence of various Khors (lagoon and estuarine lagoon) especially at its Arabian coast [1]. These Khors represent marine bars extended in the land. One of these Khors, which is the extension of the Arabian Gulf in Iraq is called Khor AL-Zubair Fig. 3. Khor AL-Zubair is an estuarine lagoon environment [2], situated southwest of Basrah (Fig. 3), which is recently connected with Hor AL-Hammar marsh (permanent marsh) through Shatt AL-Basrah canal. The length of Khor AL-Zubair is about 40 km. Its width varies between 1 to 2 km, and its depth varies between 10 to 20 m. Khor AL-Zubair is covered with fine muddy sediment, where sandy deposits are restricted to the narrow zone of the shallow part near the shore and around the Island slopes [3].

Stable isotopes are increasingly used by geochemists as tracers in environmental studies [4] in order to infer the sources of environmental pollution.

The aims of the present investigation was to determine the geochemical variations of carbon stable isotope in Mollusc shells from Shatt AL-Arab and Khor AL-Zubair in order to improve any environmental pollution in the studied area.

TABLE 1. $\delta^{13}\text{C}$ VALUES OF MOLLUSC SHELLS FROM SHAT AL-ARAB.

Sample	Type of mollusc shell	$\delta^{13}\text{C}$ (‰)
S1	<i>Corb. fluminea</i>	-0.6
S2	<i>Corb. fluminea</i>	-0.6
S3	<i>Corb. fluminea</i>	-8.5
S4	<i>Corb. fluminea</i>	-8.5
S5	<i>Corb. fluminea</i>	-8.6
S6	<i>Viviparus be.</i>	-6.4
S7	<i>Viviparus be.</i>	-7.6
S8	<i>Viviparus be.</i>	-6.4
S9	<i>Viviparus be.</i>	-6.4
S10	<i>Viviparus be.</i>	-6.0
S11	<i>Viviparus be.</i>	-7.1

2. MATERIALS AND METHODS

24 samples of mollusc shells from Shatt AL-Arab and Khor AL-Zubair estuary were analyzed in order to determine the concentration of carbon stable isotopes and also to clarify the factors that control the geochemical distribution of carbon isotopes in these two different environments.

The carbon stable isotope were measured using closed tube method, in which shell samples are combusted to carbon dioxide for carbon isotope analysis. The carbon dioxide samples are analyzed on a Finnigan Mat 251 isotope ratio mass spectrometer equipped with a triple collector and controlled by an Apple IIe microcomputer. Measurements are made relative to several working standards {Norit (-24‰), NBS-22 (-29‰)}, and several secondary light methane standards at -43.4‰ and -62.6‰. All values are reported versus PDB. These analyses are conducted in the department of Oceanography in Texas A&M University.

TABLE 2. $\delta^{13}\text{C}$ VALUES OF MOLLUSC SHELLS FROM KHOR AL-ZUBAIR.

Sample	Type of Mollusc Shell	$\delta^{13}\text{C}$ (‰)
K1	Caryactis cor.	-0.7
K2	Caryactis cor.	-0.5
K3	Caryactis cor.	-0.5
K4	Caryactis cor.	-0.5
K5	Caryactis cor.	-0.7
K6	Placanta placanta	1.0
K7	Placanta placanta	0.7
K8	Placanta placanta	0.3
K9	Placanta placanta	0.7
K10	Thias carinifera	0.6
K11	Thias carinifera	0.9
K12	Thias carinifera	0.1
K13	Thias carinifera	0.7

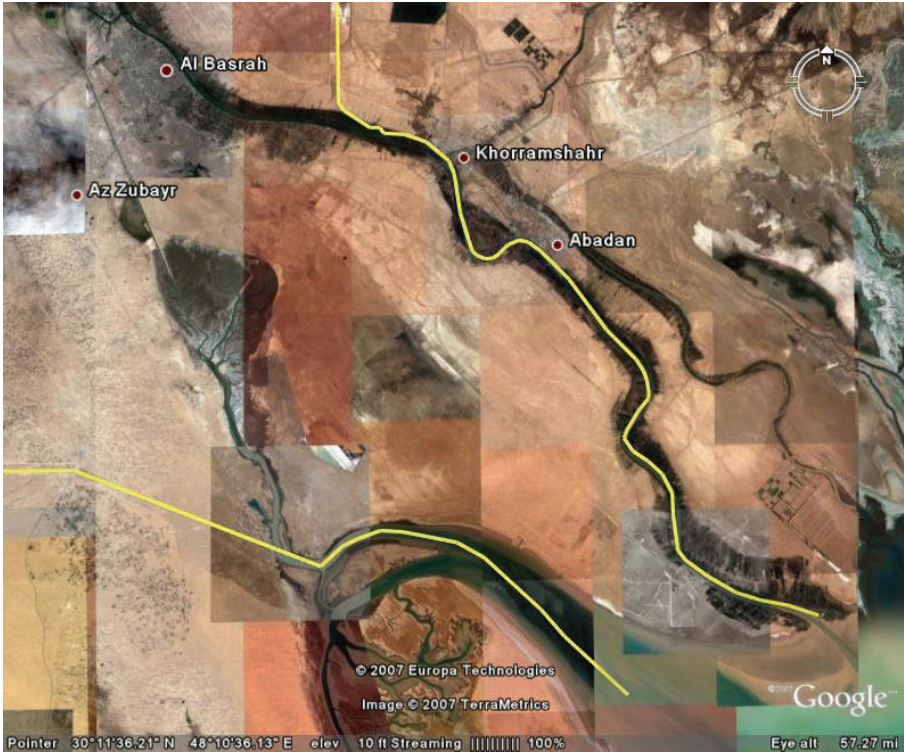


FIG. 1. Southern part of Iraq.

3. RESULTS

The results of the stable carbon isotope analysis of molluscs shell samples collected from Shatt AL-Arab River and Khor AL-Zubair estuary (Fig. 4) appear in Table 1 and Table 2, showed high variability between these two different environments and also between the different species with in the same environment.

4. CONCLUSIONS

This study indicates that the variability of $\delta^{13}\text{C}$ was due to three factors:

- (a) Environmental conditions under which these three molluscs are lived.
- (b) Chemistry of the water in Shatt AL-Arab and Khor AL-Zubair.
- (c) Feeding quality of these of these molluscs.

GEOCHEMISTRY OF CARBON STABLE ISOTOPE IN SHATT AL-ARAB RIVER



FIG. 2. Northern part of Shatt AL-Arab near Basrah City.

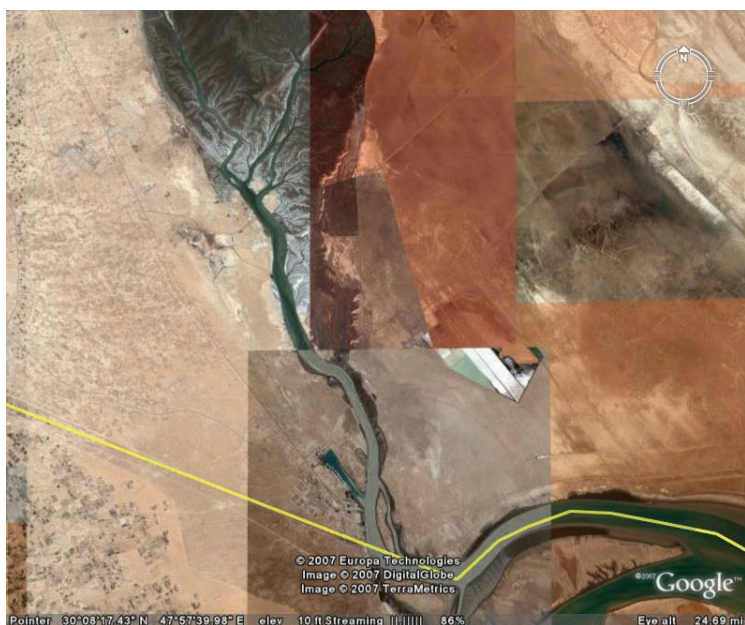


FIG. 3. Khor AL-Zubair.



Caryactis cor.



Thais carinifera



Placanta placanta



Corb. fluminea



Viviparus be.

FIG. 4. Mollusc shells selected for the study.

These factors are close related to another important factor, that it is the pollution present in these two different environments, especially in Shatt AL-Arab River, where sewage of Basrah City is discharged directly to Shatt Al-Arab through different tributaries (Fig. 2). This action may influence the water quality by increasing the nutrient concentration, which may also be associated with high biological activity and growing different food web, especially algae, which represents the food for some molluscs, that is rich in ^{12}C and show a low value of $\delta^{13}\text{C}$ [5, 6].

REFERENCES

- [1] KARIM, H.H., The phenomena of multi lagoonal system in the Northern Arabian Gulf, *Mar. Meropotamica* **3** (1988) 225–238.

GEOCHEMISTRY OF CARBON STABLE ISOTOPE IN SHATT AL-ARAB RIVER

- [2] AL-RAMADHAN, B.M., Introduction to physical oceanography of Khor AL-Zubair. Paper presented in the first symposium on the oceanography of Khor AL-Zubair, Basrah (1986).
- [3] AFAJ, A.H., et al., Some sedimentological aspects of Khor AL-Zubair, Northern Arabian Gulf, *J. Geol. Soc. Iraq* **32** (2004) 55–67.
- [4] PHILLIP, D.L., GREGG, J.W., Source partitioning using stable isotopes: coping with too many sources, *Oecologia*, **136** (2003) 261–269.
- [5] HOEFS, J., *Stable Isotope Geochemistry, Minerals and Rocks*. Springer – Verlag, Berlin. Heidelberg and New York (1980).
- [6] CLOERN, J. E., et al., Stable carbon and nitrogen isotope composition of aquatic and terrestrial plants of the San Francisco bay estuarine system, *Limnol. Oceanogr.* **47** 3 (2002) 713–729.

SURFACE WATER QUALITY

LONG-TERM BEHAVIOR OF CHERNOBYL RADIONUCLIDES IN THE DNEIPER RIVER BASIN

O. ZHUKOVA, Zh. BAKARYKAVA
The Republican Centre of Radiation Control
and Environment Monitoring (RCRCM)

M. GERMENCHUK
Department for Hydrometeorology
of The Ministry for Environment

Minsk, Belarus

Abstract

The analysis of formation of radioactive contamination of rivers of Belarus, entering the Dnieper basin (Dnieper, Sozh, Iput, Besed, Pripyat), after the accident at the ChNPP is given in the paper. The legitimacies and features of behavior of chernobyl radionuclides in surface waters and different types of soils on watersheds are detected. Radionuclide concentration dynamics in surface water of Dnieper river basin for period 1987-2006 are present. Transboundary migration of radionuclides through the river networks of Russia, Belarus and Ukraine is estimated. The transboundary migration of ^{137}Cs has decreased markedly with time. On the other hand, the transboundary migration of ^{90}Sr has fluctuated depending on the extent of annual flooding. Long-term behaviour of chernobyl radionuclides in the difference soil types of Dnieper River watershed are given. Linear velocity of ^{137}Cs , ^{90}Sr for different soil types are found. A forecast of vertical radionuclide migration is made.

1. INTRODUCTION

As a result of the accident at the Chernobyl NPP (ChNPP) a huge amount of radionuclides was ejected into the environment. Those ejections had wide regional character and spread in the whole Eastern and Western Europe. Besides, the greatest amount of radionuclides fell out on the territory of Belarus. In Belarus 23% of the territory was contaminated by ^{137}Cs with the levels from 37 kBq/m² up to 1480 kBq/m² and more, with the total area of 46.45 thousand km² where more than 3600 settlements are located. The main part of radioactive fallouts was concentrated on the watershed territory of the

rivers Dnieper, Pripjat and their tributaries. Just these very territories are and will remain for many years the potential landscape sources of formation of radioactive runoff into the Dnieper-Sozh system, and the surface water — the main transport system of the radionuclides.

During the initial period after the accident at the ChNPP the level dynamics of radioactive contamination was stipulated by radioactive fallouts on water bodies, by physic-chemical properties of aerosols and by hydrology. During the next years (for long-lived radionuclides) their concentration are determined mainly by secondary processes: washout from the contaminated watersheds, access with ground-water, wind carry from the contaminated dry land places on a water surface, interaction with bottom sediments. The processes of radioactive contamination runoff by rain water and melt-water into the river basins are considered to be the most dynamical, long-term and dangerous [1].

2. RESULTS OF RADIATION MONITORING ON THE RIVERS OF DNIEPER BASIN

The data of radiation monitoring of water bodies in Belarus show that the radiation situation on the rivers of the Dnieper-Sozh and Pripjat basins was stabilised, the annual average concentration of ^{137}Cs during the period of observation 1987–2000 in large and medium rivers of Belarus have notably decreased. The exceeding of the National Permissible Level-99 (in drinking water for ^{137}Cs — 10 Bq/l and for ^{90}Sr — 0.37 Bq/l) in water of the rivers was not observed.

The data analysis of ^{137}Cs contents during spring high water of 1999 in the basin of Pripjat river (in Mozyr) showed, that ^{137}Cs concentration in the soluble form have remained at the average values level of concentration for given sampling site for the previous years (1996–2006). However, radionuclide concentrations on the suspensions can considerably increase, this testifies that at present this radionuclide is washed out by floodwater and is transferred in the greater degree with solid material from the river watershed. The similar results on ^{137}Cs transfer into the river network on hard particles at high waters were obtained in Ukraine [2].

At present there is a distinct tendency to decrease ^{137}Cs fluxes by the rivers. The total ^{137}Cs fluxes by the rivers of Belarus for the period 1987–2006 has made for: the river Sozh (in Gomel) — 25.6 TBq, the Dnieper (in Rechitsa) — 18.5 TBq, the Pripjat (in Mozyr) — 14.0 TBq, the Iput (in Dobrush) — 9.6 TBq, the Besed (in Svetilovitchi) — 2.0 TBq.

The dynamics of ^{90}Sr fluxes through the river sampling site shows that this radionuclide migrates mainly in a soluble state. The total ^{90}Sr fluxes by the rivers

LONG-TERM BEHAVIOR OF CHERNOBYL RADIONUCLIDES IN THE DNEIPEP

of Belarus for the period 1990-2006 has made: the Sozh (Gomel) – 4.2 TBq, the Dnieper (Rechitsa) – 3.8 TBq, the Iput (Dobrush) – 1.13 TBq, the Besed (Svetilovitchi) – 0.87 TBq.

Special attention should be paid to the surface waters of a group of small rivers and channels, which catchments are located on the territory of Chernobyl NPP exclusion zone, the largest of which are the Slovechno River, Pogonyanskj Channel, Nizhniya Braginka River and Nesvich River. In these small rivers, a reduction in runoff of ^{137}Cs has been observed for several years however the concentrations of ^{90}Sr still exceed the national maximum permissible level during flood periods. For example, ^{137}Cs concentrations in the Nizhniya Braginka River were (0.03 – 6.4) Bq/L for period 1999–2006 and ^{90}Sr concentrations were (0.3–5.3) Bq/L.

The studies of the bottom sediments of the rivers of the Dnieper and Pripyat basins allow finding radiation dangerous places of radionuclides accumulation in the bottom sediments along the bed of the rivers and reservoirs. Practically on the whole part of the river Nizhniya Braginka near the village Gden and below, ^{137}Cs contamination levels of the bottom sediments in 2006 were 49760, 38135, 30590, 12940, 14340 Bq/kg. Thus, they can be classified as a solid low-level radioactive waste (9630 Bq/kg). The high concentration in the bottom sediments of the forms, which can exchange in the bottom-sediments-water system, is a potential danger of the secondary contamination of the rivers.

3. TRANSBOUNDARY RADIONUCLIDE MIGRATION IN SURFACE WATERS

One of the more serious long-term ecological effects of the Chernobyl fallout was the secondary run-off (“wash-off”) of radionuclides from the initially contaminated areas through the river networks of Russia, Belarus and Ukraine, into the Dnieper reservoir system, thereby expanding the spatial scale of the accident and exposing millions of people who use the downstream resources of the Dnieper River.

Since the Chernobyl accident, water monitoring stations have been established within the Chernobyl exclusion zone and along the major rivers to determine the concentration of radionuclides and their total flow. Although these stations are not ideally suited for monitoring transboundary fluxes estimates have been made for of ^{137}Cs and ^{90}Sr . Estimate results are presented in Figs 1–4.

The transboundary ^{137}Cs migration has decreased markedly with time (Figs 1, 3). On the other hand, the transboundary ^{90}Sr migration has fluctuated

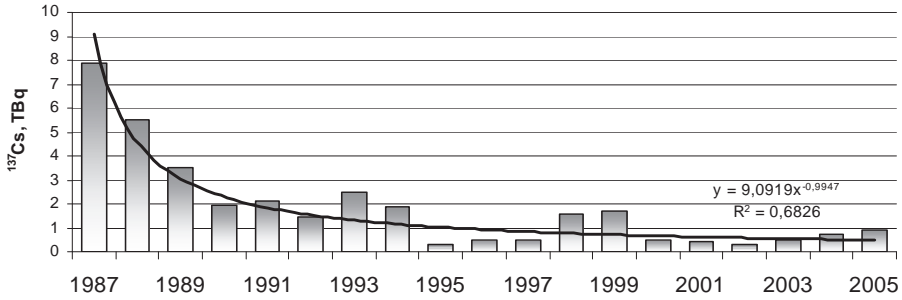


FIG. 1. Dynamics of annual ¹³⁷Cs fluxes by Prypiat surface waters (Belarus-Ukraine border).

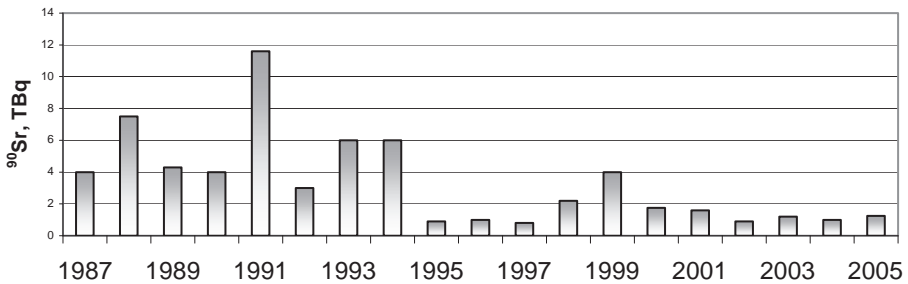


FIG. 2. Dynamics of annual ⁹⁰Sr fluxes in Prypiat surface waters (Belarus-Ukraine border).

from year to year depending on the extent of annual flooding along the banks of the Prypiat River (Fig. 2). Note, however, that the extent of wash out of radionuclides is only a very small percentage of the total inventory in the catchments area.

Transboundary ⁹⁰Sr transfer depends on a degree of annual Pripjat River coast flooding. Total flux of this radionuclide by Prypiat surface waters (border Belarus–Ukraine) for the period 1987–2005 was 62.2 TBq (flux calculation for 1986–1999 was made using data of Ukrainian Hydrometeorological Institute, fluxes calculation for 2000–2005 was made using data of RCRCM). In Fig. 2 dynamics of mid-annual ⁹⁰Sr fluxes by Pripjat surface waters are presented. (Belarus–Ukraine border) [3].

The monitoring data of Belarus indicates that the radionuclide fluxes into the Dnieper river system have stabilized over the past 10–12 years and are now relatively low. During the period 1987–2003 the mean annual concentrations of

LONG-TERM BEHAVIOR OF CHERNOBYL RADIONUCLIDES IN THE DNIEPER

^{137}Cs in the water of large and medium rivers of Belarus was not too large. At present ^{137}Cs runoff from the Russia and Belarus watershed does not represent a substantial contribution to contamination of the Dnieper reservoirs in the territory of the Ukraine. In Fig. 3 dynamics of ^{137}Cs transfer from territory of Russia by surface waters of the Iput and Besed rivers through hydrological post on border Russia–Belarus is presented.

The Iput and Besed rivers are the largest inflows of the Sozh River running through radioactive polluted territories. They belong to Dnieper-Sozh pool and flow on Belarus–Bryansk “cesium spot” with contamination territory levels with ^{137}Cs from 37.0 up to 2220.0 kBq/m².

Since 1991, the clear tendency of reduction of ^{137}Cs fluxes through hydrological post of Belarus Rivers flowing from territory of Russia to Belarus

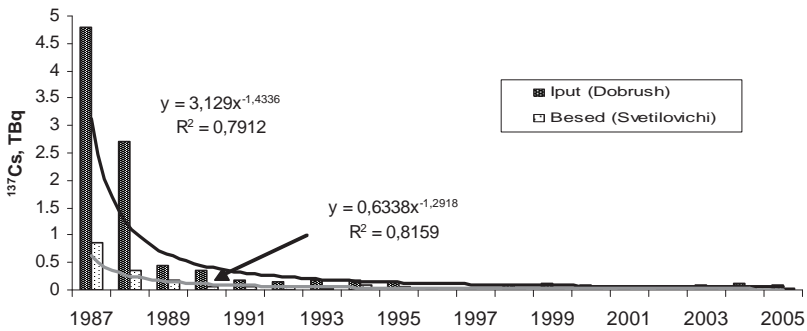


FIG. 3. Dynamics of annual ^{137}Cs fluxes in Iput (Dobrush) and Besed (Svetilovichi) surface waters (Russia-Belarus border) for the period 1987–2005.

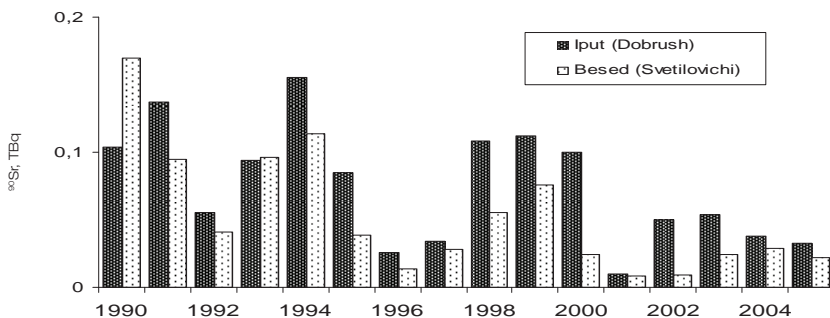


FIG. 4. Annual ^{90}Sr fluxes in Iput river at Dobrus and Besed river at Svetilovichi (Russia-Belarus border) for the period 1990–2005.

shows. A major factor of ^{137}Cs concentration decrease in the dissolved condition is its radioactive decay. In the first some years after Chernobyl accident appreciable transboundary ^{137}Cs fluxes by surface waters of such rivers as Iput and Besed were observed, but now it is insignificant.

The level of water contamination also does not pose any significant risks for water use because, according to the monitoring data of Belarus, the ^{137}Cs concentration in surface waters during the last 5 years remained on the level of 0.01–0.1 Bq/L, which is more than 10 times lower than the national limits for drinking water (10 Bq/L) for ^{137}Cs . Although the wash-off of radionuclides should continue to be monitored, there is no justification for remedial actions in the Upper Dnieper river system.

Fluxes of ^{90}Sr increase markedly during times of high flooding. In Fig. 4 annual fluxes of ^{90}Sr in Iput river at Dobrus and Besed river at Svetilovichi, Russia-Belarus border is shown.

There is still transboundary transfer of radionuclides (mainly ^{90}Sr) by rivers within the Dnieper network. The most important source is the flood plain of the Prypiat River within the Chernobyl exclusion zone.

4. RADIONUCLIDE MIGRATION IN DIFFERENT SOIL TYPES

Natural radionuclide penetration into deep of soil, along with natural decay, is one of the factors of decreasing exposure gamma rates. The most specific form of ^{137}Cs existence is a fixed state on soil particles (85–95%). The portion of forms, capable of increased migration and of penetration into plants through root system, usually is not higher than 10–15%. The relative contribution of mobile forms increases as they penetrate deeper into the soil. ^{90}Sr from Chernobyl migrates more rapidly than ^{137}Cs because of less strong bond with soil absorbing complex [4].

Thirteen years study of radionuclide behaviour on reference sites of RCRCM revealed that by 2006 the main part of ^{137}Cs content is in the top 3–10 cm soil layer. With increase of humidifying degree of soil, the linear velocity of vertical migration increases. So, by 2005 in soddy-podzolic soils with various distribution of sizes, ^{137}Cs penetration depth did not exceed 6–7 cm, in soddy-podzolic soils with attributes of superfluous humidifying — 11–13 cm and more, in soddy-gley soils — 11–14 cm.

Parameters of migration have accounted by convective-diffusion two-box model [5]. By present time the most part ^{137}Cs dropped out on a surface of soil and interacted with a soil absorbing complex is in the fixed form that does not allow ^{137}Cs to penetrate into soil deep together with colloidal particles. This fact explains the decrease of migratory processes intensity in

LONG-TERM BEHAVIOR OF CHERNOBYL RADIONUCLIDES IN THE DNIEPER

all investigated soil in the last years. In Fig. 5 dynamics of average linear ^{137}Cs velocity in different soil types is shown.

^{90}Sr is characterised by higher migration ability in a soil profile. Correspondingly, the contribution of a fast-migrating component is more important, on an average 30–60%. In comparison with ^{137}Cs , the more substantial ^{90}Sr transport from upper to lower soil layers, is specified by relatively high content of mobile forms (water-extractable, exchange, mobile).

In Figs 6, 7 the forecasted soil profiles of ^{137}Cs for most typical Belarusian soils for 30 years (up to 2016 year) and for 40 years (up to 2026 year) are presented.

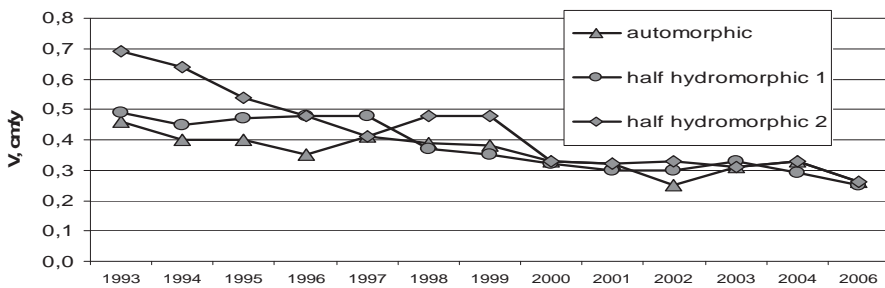


FIG. 5. Dynamics of average linear ^{137}Cs velocity in soddy-podzolic sandy soil (automorphic), soddy-peaty-gley soil (half hydromorphic-1) and peaty-gley soil (half hydromorphic-2).

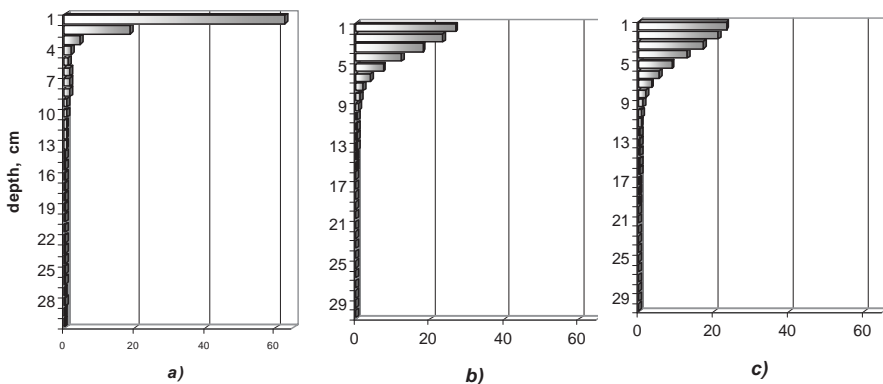


FIG. 6. Actual distribution of ^{137}Cs in soddy-podzolic sandy soil profile in 2006 (a) and prognosis ^{137}Cs migration for 30 years (up to 2016) (b) and for 40 years (up to 2026) (c).

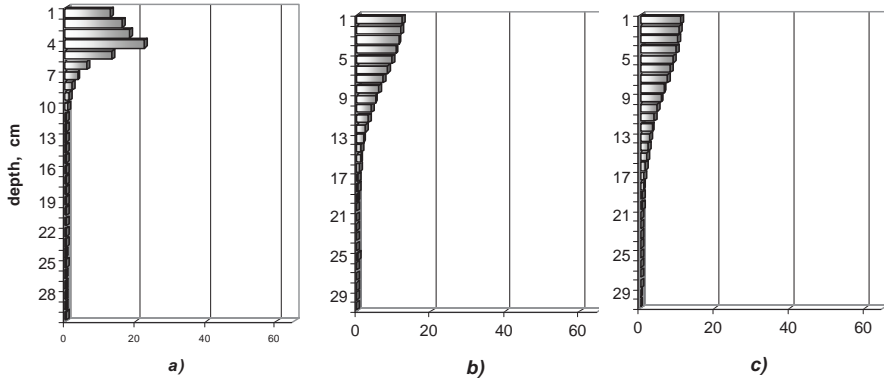


FIG. 7. Actual distribution of ^{137}Cs in peaty-gley soil profile in 2006 (a) and prognosis ^{137}Cs migration for 30 years (up to 2016) (b) and for 40 years (up to 2026) (c).

Figures 6,7 clearly show that by 2026, ^{137}Cs penetration depth in automorphic soil (i.e. the depth where more than 1% from the common ^{137}Cs contents will be contained in 30 cm soil layer) will make 9 cm, and in half-hydromorphic soil — 16 cm. It means that in the near future the main part of radionuclides remains in rooting layer.

5. CONCLUSIONS

- (1) High levels of radioactivity remain within the Chernobyl exclusion zone. Important “hot spots” within this zone are the flood plain along the Prypiat River.
- (2) There is still transboundary transfer of radionuclides (mainly ^{90}Sr) by rivers within the Dnieper network. The most important source is the flood plain of the Prypiat River within the Chernobyl exclusion zone.
- (3) The concentrations of ^{137}Cs and ^{90}Sr in river waters of the Dnieper basin have decreased significantly and are now below maximum permissible levels. Almost all the ^{137}Cs washed out from contaminated areas is immobilized in bottom sediments of the rivers of Dnieper Basin. The impact of these sediments is low and will decline further with decay and further deposition of sediments on top of the contaminated sediments.
- (4) Recent decrease of migratory processes intensity in all investigated soil is observed. In the near future the main part of radionuclides remains in the rooting layer.

REFERENCES

- [1] VAKULOVSKIY, S.M., et al., Contamination of water objects by ^{137}Cs and ^{90}Sr on the territories subjected to the influence of ejections from the ChNPP, *Meteorology and hydrology* **7** (1991) 64–73 (in Russian).
- [2] VOITSEKHOVITCH, O.V., et al., Radiogeoeology of water objects of the zone of influence of the ChNPP accident. Vol.1., *Chernobylinterinform*, Kiev (1997) 82–85 (in Russian).
- [3] ZHUKOVA, O., et al., Transfer of Chernobyl radionuclides in the aquatic systems // *Proceedings of an international conference held in Monaco: Isotopes in Environmental Studies. Aquatic Forum 2004, 25–29 October 2004 / International Atomic Energy Agency, Vienna* (2006) 237–242.
- [4] SHAGALOVA, E. D., PAVLOTSKAYA, F. I., et al., *Soil Sciences*. **10** (1986) 114.
- [5] KONSTANTINOV, I. E., SKOTNIKOVA, O. G., et al., *Soil Sciences*. **5** (1974) 55–58.

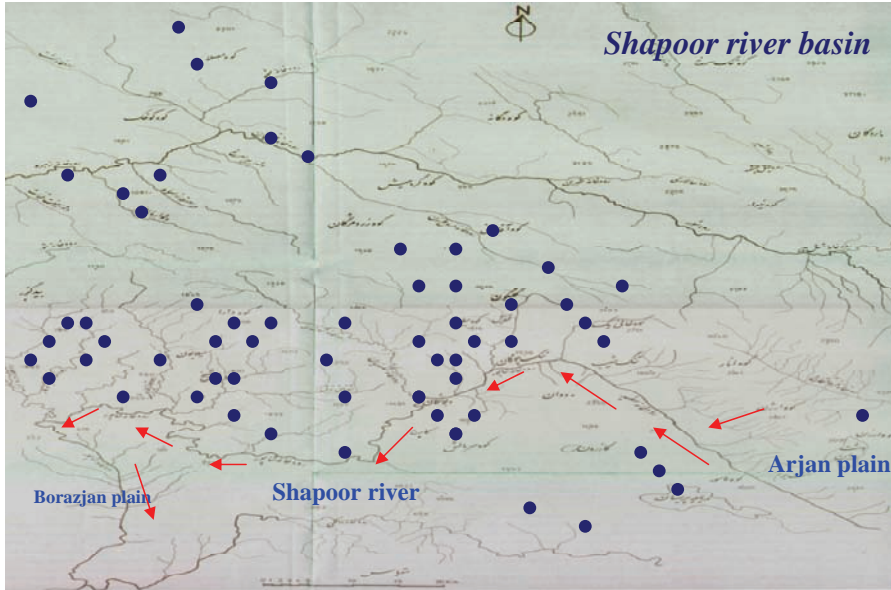
EXAMINATION OF THE SOURCE OF SALINITY IN WATER RESOURCES USING ISOTOPE TECHNIQUES

Case Study: Water Resources of Shapoor River basin

F. HATAMI, Y. KHALAJ AMIRHOSSEINI, M. KUHPUR
Water Research Institute (WRI),
Shahid Abbasspur Blvd., East Vafarda Blvd.,
Tehran, Iran

Abstract

The study area is located in south part of Iran, west part of Fars and the north part of Booshehr province. The area is situated between the longitudes 51°.0' and 52°.0' and latitudes 29° 30' and 30° 20'. The basin is a sedimentary area and hilly with gentle fold which is situated in a part of Zagros chain of mountains, in south-western of Iran. The length and width of the basin are approximately 95 and 70 km² respectively located in both side of Kazeroon fault. From the view of geology the formations of the basin are: series of Hormoz salt which is similar to salt domes, Asmari, Fars and Bakhtiari formations. The limestone formations with high permeability which make the fresh waters reservoirs of the basin are: 1) Asmari formations which is the calcareous main reservoir of ground waters and expands as a folded layer on the surface and depth of the study basin. 2) Sarvak limestone formation which is outcropped in central part of anticlines in east, north and northeast of the basin. The Shapoor river is the main river of the area which originates from the mountains of the east part of Arjan plain, then flows through the Kazeroon fault and after meeting some salt rivers of the middle part of the basin such as Salbiz, Malchesheikh, Chaharbisheh, Daregorg, Tanbakookar and Shekastian, It will enter into the Borazjan plain. Before arriving to the Kazeroon fault, water quality of Shapoor river is good but after contacting with salt rivers and moving through the salt formations of the west part of basin, it severely changes. The main objective of this study is examination of the sources of recharge of salinity resources and examination of all water resources in the study area for controlling water quality of Shapoor river. To access the following objectives more than 50 water samples were taken from different resources such as rivers, wells and springs in both wet and dry seasons. In this regard isotopes (¹⁸O, ²H, T) as well as hydrochemistry analysis and field measurements were carried out.



● Sample location

FIG. 1. Sampling sites in the Shapoor river basin, Fars and Booshehr province, Iran.

1. INTRODUCTION

In hydrology, using of isotope methods is based on isotope composition in the water cycle. Therefore, the basis of isotope study is recognition of isotope composition [1–5]. Isotope composition of water would be changed by some parameters such as passing of time, mixing with other water resources or leaching with salts. Examination of these changes would be helpful to recognize age, origin and relationship between different source and types of water.

2. DESCRIPTION

The aim of this study was to determine the mechanism of salinisation as well as the origin, and the quality of ground water resources in Shapoor river basin (Fig. 1).

The following processes may lead to salinsation of ground waters:

- Leaching of salts by percolating water. The salts may be evaporitic deposits, Aeolian transported salts and products of weathering of surface rocks and soils.

EXAMINATION OF THE SOURCE OF SALINITY IN WATER RESOURCES

- Intrusion of salt water bodies such as sea water, brackish surface water, brines and connate water.
- Concentration of dissolved salts by evaporation.

In arid regions, identifying the mechanism of salinisation is so difficult. Due to the low precipitation and high evaporation in such regions the leaching of salts is local and the transported salts can not move in a long distance, therefore the concentration of salts in ground waters would be so high.

According to the diagram of stable isotopic composition of water resources (Fig. 2) it can be shown that water resources of the basin are divided into two groups:

Group 1: The waters which are affected by evaporation and the ^{18}O and ^2H content are higher than others. These are surface and shallow waters which are evaporated before or after infiltration. This group of samples is near to the evaporation line or mixing with other water resources.

Group 2: the samples which are nearly on the Meteoric Water Line (MWL). This group of waters is only a few. The springs of both east and west part of Kazeroon fault as well as Karstic wells of the east part of this fault and finally Shapoor River which is nearly located on the fault. These waters are directly recharged by precipitation.

In order to explain the scatter of the delta values of the water samples from the mountainous study area, the altitude effect has to be subtracted. As most water samples showed sign of evaporative enrichment of the heavy isotopes, the determined $\delta^{18}\text{O}$ and $\delta^2\text{H}$ values are suitable and they have to be corrected for the fractionation effect. Referring to the global Meteoric Water Line (MWL) with a slope of 8 and a deuterium excess of +22‰ as well as an evaporation line with a slope of 5.02, the following equations are obtained [3]:

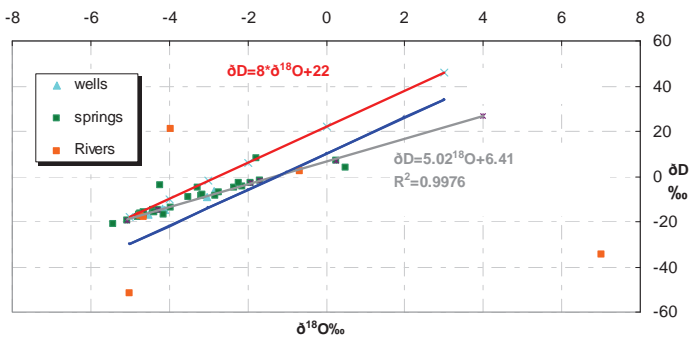


FIG. 2. $\delta^{18}\text{O}/\delta^2\text{H}$ diagram with the MWL and the evaporation.

$$\delta^{18}\text{O}_{\text{corr}} = (\delta^2\text{H} - 5.02 \times \delta^{18}\text{O} - 22)(8 - 5.02)$$

$$\delta^2\text{H}_{\text{corr}} = 8 \times \delta^{18}\text{O}_{\text{corr}} + 22$$

Considering the histograms of ^{18}O (Fig. 3) it can be observed that the ^{18}O values cover a wide range from -5.5‰ to 1.7‰ and have a pronounced peak at -3.2 . The corrected values cover the same range. There are three small peaks which reflect differences in the altitude of the catchments area of the sampling sites. The two peaks with the most negative $\delta^{18}\text{O}$ values are not relevant. Therefore it seems that evaporative isotope enrichment is a natural phenomenon.

3. THE ISOTOPE APPROACH

Stable isotopes provide an independent variable which can assist in identifying the mechanism of salinisation. Salinisation arising from leaching of salts is not accompanied by changes in stable isotopic composition of the leaching water. Thus, the salinity is independent of the stable isotopic composition, but after mixing of a source of saline water with a fresh water, the resultant saline waters will have different salinities and different stable isotopic composition because the stable isotopic composition of the saline source is different from the fresh water prior to salinisation. Therefore, the $\delta^2\text{H}$ and $\delta^{18}\text{O}$ values are both together and individually with the more conservative ionic species such as chloride or sulfate linearly correlated on a mixing line within the limits defined by the fresh water and saline water components.

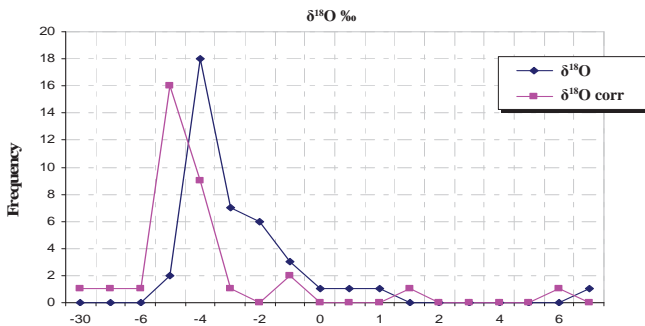


FIG. 3. Histogram $\delta^{18}\text{O}$ values and those corrected for enrichment of the heavy isotopes by evaporation

EXAMINATION OF THE SOURCE OF SALINITY IN WATER RESOURCES

The mechanism of salinisation for surface and ground waters of Shapoor river basin has been illustrated in Figs. 4 and 5. In these diagrams, it can be shown that there are three kinds of waters; the first one are the waters in which leaching of salts lead to salinisation, so there is not any difference between their stable isotope composition. The second is water resources in which salinisation is because of evaporation, thus the $\delta^{18}\text{O}$ values of these waters are completely different.

In this basin in addition to these groups of waters, there are some water resources which are affected by both evaporation and leaching of salts together, so it seems that the intense evaporation and leaching of salt formation in the west part of Kazeroon fault would be the mechanism of salinity in this basin. The surface waters of the central part of the basin are affected by both evaporation and leaching. Some part of these surface waters flows as salt waters and then goes out of the basin via the rivers and other part dissolves the salts

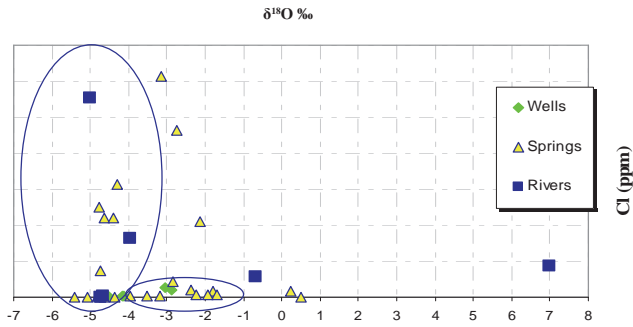


FIG. 4. $\delta^{18}\text{O}$ values versus chloride (ppm).

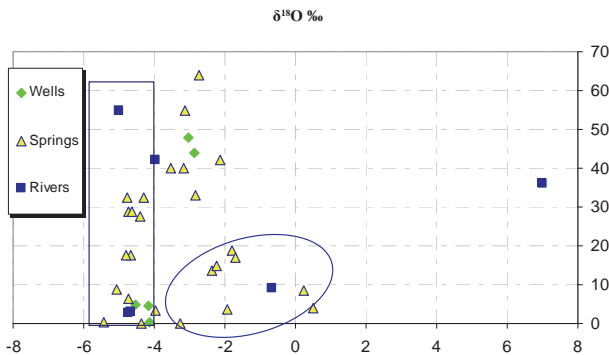


FIG. 5 $\delta^{18}\text{O}$ values versus Sulfate (ppm).

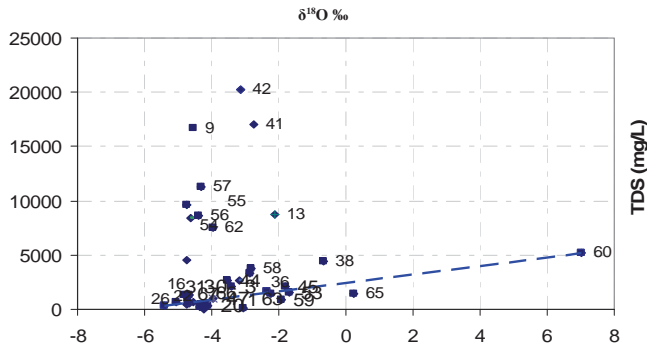


FIG. 6. $\delta^{18}O$ values versus TDS

and meets the ground waters during infiltration. The various salt springs in the central part of the basin are recharged by this way. The quality of these springs is mostly undesirable. The stable isotope values show perfectly the process of evaporation and dissolving of salts together.

The plot $\delta^{18}O$ versus TDS (Fig. 6) shows a clustered triangle, (between 5.5 to 0.2). According to Gat and Gonfiantini [2] the $\delta^{18}O$ values of the water increase by 2.5‰ due to a loss of about 25% water corresponding to a salt enrichment by 30% (dotted line in Fig. 6). As most data are above this line dissolution of salt or admixture of saline water is dominant beside enrichment of heavy isotope by evaporation (especially pronounced for the samples No. 9, 41, and 42)

The origin of the salt may be evaporation of water during summer time. The higher salinity at one site, the higher may be $\delta^{18}O$ in summer time and there will be salt concentration by dissolution.

REFERENCES

- [1] GONFIANTINI, R., DINCER, DEREKOY, T. "Environmental isotope hydrology in the Honda region, Algeria", Isotope Techniques in Groundwater Hydrology 1974 (proc. Symp. Vienna, 1974) vol.1, IAEA, Vienna (1974) 293.
- [2] GAT, J., GONFIANTINI, R. (eds) Stable isotope hydrology. Deuterium and Oxygen 18 in the Water cycle, IAEA, Vienna, Technical reports Series No 210 (1981) 337.
- [3] GEYH, M.A. "Water quality study in the region of 15-Khordad dam, End of mission report of the IAEA TC project IRA/8/014 at Water Research Institute, Tehran, Iran between 16–22 July 1999.

EXAMINATION OF THE SOURCE OF SALINITY IN WATER RESOURCES

- [4] CLARK, I., FRITZ, P., Environmental Isotopes in Hydrology, Part 1.
- [5] Examination of water resources in Shapoor river basin using environmental isotopes (final report).

DEUTERIUM AS INDICATOR OF THE NATURAL AND ANTHROPIC STRESS ON THE WATERS OF THE DANUBE DELTA, ROMANIA¹

V. FEURDEAN, L. FEURDEAN
National Institute for Research and Development
of Isotopic and Molecular Technologies,
Cluj-Napoca, Romania

C. DAVID
Danube Delta National Institute for Research
and Development
Tulcea, Romania

Abstract

The natural flow of water has been examined in the Danube Delta Biosphere Reserve Romania, one of the largest deltas in Europe, using deuterium (²H) as a natural tracer. The understanding of the circulation of the water and pollutants into protected zones is essential to protect the maintenance of all ecological functions of the delta. The isotopic content variations of water due to the climatic changes and anthropogenic activities are fast, the isotopic signature being indicators for the water flow-paths changes before irreversible environmental transformations occur. Contour maps of the mean deuterium concentrations have been used to reveal the changes of the water flow-paths from the running waters (Danube's tributaries, channels/canals with active, controlled or absent circulation of water) and the standing freshwater (lakes with active, reduced or controlled change of water). The isotopic maps show the changes of pathways due to the climatic changes that have the impact on the water balance, the erosion of coastal areas and the man made pressures on the Danube Delta.

1. INTRODUCTION

After flowing 2857 km across Europe, the Danube River (DR) forms at its mouth in the Black Sea one of the largest European deltas considered part of the large European geo-system consisting of the Danube River — Danube

¹ Work performed within the framework of the National R&D Programmes from National Authority for Scientific Research, Romania.

Delta — Black Sea. The Danube Delta (DD) is one of the largest wetland worldwide, especially a waterfowl habitat, contains the greatest reed-bed expanses worldwide, being a real natural museum of biodiversity, which includes 30 types of ecosystems (with 18 sites of 50 600 hectares as strictly protected areas) and a natural genetic bank with incalculable value for the worldwide natural heritage. For these reasons, the Man and Biosphere (MAB) Programme of UNESCO have declared the DD a Biosphere Reserve (which include and geographic divisions, such as sectors of Danube, Razim-Sinoie lagoon complex, coastal marine waters) in 1990, being the only delta in the world as a reserve.

The delta's development, hydrology and health are controlled by natural factors and anthropogenic activities, including and DR drainage basin [1]. After declaring of the Danube Delta as Biosphere Reserve, the main purpose research has been establishing the solutions for protection and ecological reconstruction of the delta [2]. In this context, studies on the detection of the changes occurred at the level of water movement has been achieved. The use of deuterium as a natural tracer offers one global view of key phenomenon and is a sensitive method for evaluation of the environmental changes before irreversible transformations occur.

2. DESCRIPTION OF STUDY AREA

The DD is situated between 44° 47' 25" and 45° 37' 30" North and between 28° 44' 25" and 29° 46' 00" East, with a total area of 4,178 km², of which 3,446 km² (82%) lies in Romania. The delta is situated in an area of high structural mobility, repeatedly affected by strong subsidence and important sediment accumulation [3]. The average altitude of the delta is +0.52 m, 20.5% of the delta area has a level below that of the Black Sea (the water depths in lacustrine depressions do not exceed 3 m), the surfaces between 0 and 1m represent 54.5% and between 1 and 2 m represent 18%, the highest areas are 12.4 m and 8 m on the sand banks of sea origin. The climate is semiarid.

The hydrologic features of the delta are described in detail in Refs. [2–4]. The delta starts from the first bifurcation of the Danube, called Ceatal Chilia, here the river divides into two tributaries: a northern one, the Chilia, and a southern one, the Tulcea. The Tulcea tributary again divides at the second main bifurcation, named Ceatal Sf. Gheorghe, into other two branches: Sulina on the left and Sf. Gheorghe on the right. At its mouth, the Sf. Gheorghe tributary forms a small secondary delta. The maximum depth of the Danube branches is –39 m for Chilia, –34 m for Tulcea, –18 m for Sulina and –26 m for Sf. Gheorghe. The length of the Danube branches is –117 km for Chilia, 17 km for Tulcea, –84 km for Sulina and 110 km for Sf. Gheorghe. The distribution of Danube

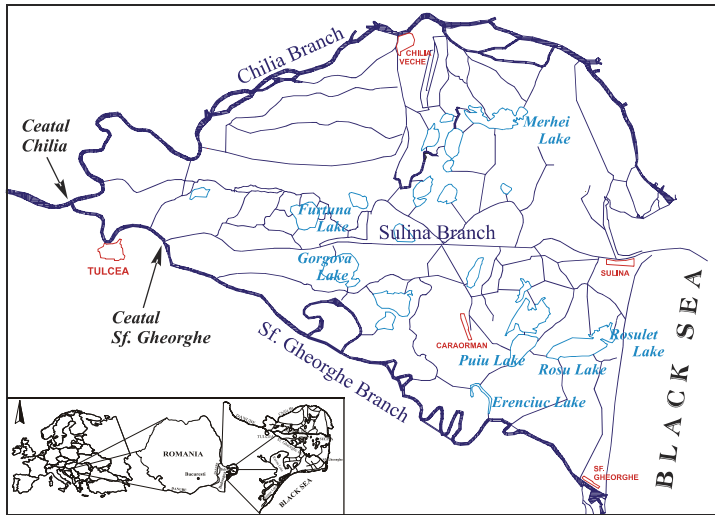


FIG. 1. The Danube Delta: location and study area.

River water discharge among the main delta branches varies in time mainly as a result of natural global changes and anthropic intervention: cut-off projects, damming, channel construction.

Chilia-Sulina intertributary area covers about 160,700 ha and within the fluvial delta plain of this area two depressions are located (the *Sireasa – Sontea – Furtuna Depression* and the *Lopatna – Matita – Merhei Depression*). Sulina – Sf. Gheorghe intertributary area covers a surface of about 101,850ha, and this area is divided into two units: the *Gorgova–Uzlina unit*, within the fluvial delta plain, and *Rosu–Rosulet unit*, located within the marine delta plain. The depth of these lakes fluctuates in terms of time depending on the water level of the main Danube branches: from 3–4 m deep to 1 m in the eastern lakes of the delta (lakes Puiu, Rosu) and from 2–3 m to 1.5–2 m in the western ones (lakes Fortuna, Gorgova, Isac, Matita). Transparency is also influenced by the hydrological phases of the branches (250–359 gr/m³ during the flood period, 15–20 gr/m³ during the autumn-winter phases).

The dense network of natural main and secondary channels as well as artificially dug canals, with active water circulation and sediment inflow into the intertributary depressions, must add to the main hydrographic units described above.

The DD works as a buffering interface between the DR catchments and Western Black Sea. Crossing Europe from West to East, DR, carries downstream its load of pollution originating in all direct or indirect man-made

TABLE 1. THE $\delta^2\text{H}$ AVERAGE VALUES FOR THE MAIN SAMPLING POINTS FROM DANUBE DELTA WATERS.

Sampling Points	$\delta^2\text{H}$ (‰)						
	1993	1994	1995	1996	1998	2005	2006
Ceatal Chilia	-78.3	-71.8	-77.1	-76.8	-75.1	-72.4	-74.2
Ceatal Sf Gheorghe	-77.5	-70.7	-76.3	-77.4	-77.7	-72.5	-77.1
Chilia Branch (Izmail)	-77.0	-72.0	-76.0	-76.8	-78.8	-69.9	-74.0
Sulina Branch (at Sulina)	-76.4	-73.1	-75.8	-76.6	-75.4	-71.6	-73.7
Sf. Gheorghe Branch (at Sf. Gheorghe)	-76.8	-72.6	-75.4	-76.8	-77.3	-74.3	-76.0
Merhei Lake	-56.2	-48.0	-67.9	-67.7	-71.2	-68.6	-71.2
Rosu Lake	-62.8	-57.3	-68.1	-68.7	-68.4	-70.1	-72.3
Erenciuc Lake	-71.8	-61.4	-66.8	-69.3	-69.7	-65.4	-70.1
Lopatna Channal	-70.7	-65.9	-73.2	-73.1	-74.6	-69.1	-73.6
Caraorman Channel	-71.1	-65.9	-70.7	-69.9	-71.8	-66.6	-73.1

pressures and is responsible for the environmental and health state of its delta. During the past 25 years, the lakes from delta have undergone major changes as response to an augmented nutrient influx resulting from increasing agriculture, industrialization in the Danube catchments area and hydro technical works. The water circulation and the equilibrium inside ecosystems from delta change due to the climate changes and to anthropogenic activities. The nutrient loading has promoted progressive eutrophication of lakes and to interpret isotopic values for $\delta^{18}\text{O}$ it is necessary to separate the processes of the oxygen incorporation during photosynthetic blooms of isotope ratio of the waters. This is not an easy process because the variations in chemical and isotopic state of lakes water in the transition states [6]. We used only deuterium as the natural tracer of the water circulation in DD.

3. METHOD AND RESULTS

The monthly collected water samples from March to October from DD (Danube at entrance in delta, branches and lakes) were analyzed for isotopes. Measurements of the hydrogen isotopic ratios ($^2\text{H}/^1\text{H}$) were performed on THN 202 mass spectrometer (system CEA-France) specially constructed for

DEUTERIUM AS INDICATOR OF THE NATURAL AND ANTHROPIC STRESS

natural abundances of deuterium [6]. All samples were analyzed in replicate and reported relative to VSMOW. The analytical reproducibility for $\delta^2\text{H}$ is $\pm 0.5\%$. The $\delta^2\text{H}$ values for deltaic waters are in the normal limits for surface water from Romania and they show a slight increase from the entrance to the delta to the mouths of the Danube. In intertributary space recorded higher values. The $\delta^2\text{H}$ average values for the main sampling points are in Table 1.

The spatio-temporal variation of input of the deuterium natural content in the hydrologic cycle is the key to isotopic interpretation in hydrological investigations. The $\delta^2\text{H}$ values in precipitation over the study area have been estimated with reasonable precision from the database of GNIP, IAEA/WMO [7] and from the values $\delta^2\text{H}$ calculated for mean temperature (T) recorded in delta with the equation established for precipitation fallen over Cluj-Napoca, Romania [8]:

$$\delta^2\text{H}(\text{‰}) = 3.2864 \times T(\text{°C}) - 103.79 \quad R^2 = 0.959$$

Isotopic patterns as a 2-D “isotopic relief” represent the spatial variability of the $\delta^2\text{H}$ values. The most important features of the isotopic contours are the closed isolines and front as a finger pattern. The closed lines (circles or ellipses) delineated the areas with the stagnant water, exposed to higher evaporation process. The parallel and equidistant open isolines correspond to the uniform isotopic gradients and indicate the steady-state flow or uniform horizontal stratification of waters. The high isotopic gradients represent small water flow velocities or long residence time of water. The high variations of the isotopic gradients correspond to the different flow velocities and the front as a finger pattern corresponds to water advance by preferential direction.

4. DISCUSSION

The Danube is a large perennial river that has its headwaters at higher elevation and a large distance away from the arid area of its delta. In spite of the fact that one third of the total Danube drainage basin lays in the lower Danube reach, the tributaries in this section do not make a very significant water contribution to the total. This is the cause for which the deuterium content of the Danube water at the head delta reflects the upstream environment and is distinguishable from the local groundwater of the arid low land of North Dobrogea where is delta located [9]. The deltaic waters from the arid catchments are susceptible to evaporation. The isotopic effects of the evaporation for the water from the Danube branches are not as dramatic as that observed in lakes. The deuterium composition from deltaic lakes can be affected by the

hydrologic inputs (the streamflow and groundwater) and outputs (evaporation, groundwater flow and streamflow out of lake) and by in-lake processes (mixing, biogeochemical processes) [10, 11]. The deuterium content from lakes water must be examined specifically for the lake systems to separate the components that contribute to the isotopic budget. In this paper only the global spatial distribution of deuterium is presented, not the detailed analyses of the isotopic composition of the lakes. Generally, in years with the small Danube discharge at the entrance of delta, the water circulation on channels and the drainage of lakes decreases and the evaporation from lakes increases. The deuterium signals both

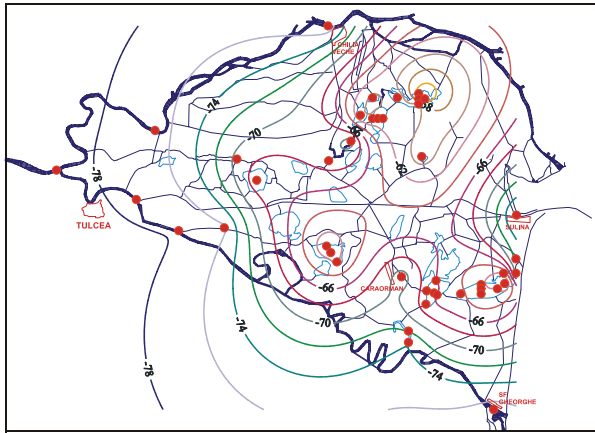


FIG. 2. Isotopic pattern for Danube Delta in 1993.

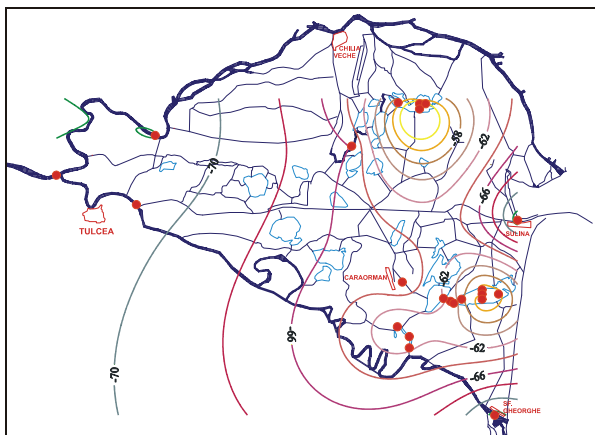


FIG. 3. Isotopic pattern for Danube Delta in 1994.

DEUTERIUM AS INDICATOR OF THE NATURAL AND ANTHROPIC STRESS

for changes of the climate at the local and regional scale and for hydro-technical works are well pointed out on the isotopic maps. Spatial variations of isotopes are important in interpreting of water flow in hydrologic systems in correlations with the climate conditions [11, 12].

The 1993-year was rainy for Central Europe, but dry for the lower Danube and delta. The great precipitation amounts affected the isotopic input in river because the isotopic amount effect that leads to isotopically light precipitation. Local dry climate lead to a decrease of the Danube discharges during summer (~1,650 m³/s during summer months). The $\delta^2\text{H}$ values reveal that the deuterium content of the Danube at the head delta retained a depleted isotopic composition of the headwaters and was relatively unaffected by evaporation during movement through the arid region of low Danube River Basin. The Danube discharges decreased during summer, the water circulation inside of the delta was smaller and the evaporation from deltaic space was bigger (Fig. 2). The lake waters with small drainage were enriched isotopically. The Merhei Lake had reduced water inputs and the result was the increase of large quantities of organic origin deposits, being much affected by eutrophication [1]. The evaporation was 18–20% for Merhei Lake and 8–10% for Rosu Lake [13] calculated by Craig-Gordon relation [14]. The analysis of the deuterium content and salinity values for the Rosu Lake points out both the evaporation and the mixing processes between fresh water of delta and sea water. This fact was confirmed by the chemical analyses [2].

The year was dry both in Central and Eastern Europe. In the delta the precipitation was below 200 mm and the temperatures were higher by 2–3°C than the mean temperature. This fact led to the increase of the $\delta^2\text{H}$ mean values with about 6‰, corresponding to an increase of 2°C for the mean temperature value. The slight isotopic enrichment observed at the delta head is rather due to the influx of tributary water already enriched by evaporation than the direct evaporation from river (Fig. 3).

In 1995–1996–1998 the hydro-meteorological conditions were normalized. The circulation inside of delta recovered. The increased intensity of flushing with river water was the best way to return water systems of the Merhei Lake into a more healthy ecological status. This was possible both the natural hydro-meteorological changes and the anthropogenic activities of conservation and sustainable development of delta. The normalization of the hydrological circulation in the Chilia-Sulina intertributary area was due to the climate conditions and to the restoration works started in 1994 for the Babina polder (2,100 ha) and in 1996 for the Cernovca polder (1580 ha), which in the mid 80's were reclaimed for agriculture and later abandoned. The result of the restoration was the diminishing of the stagnant area in surrounding Merhei Lake. The isotopic maps for 1995–1998 (Figs. 4–6) show the improvements of

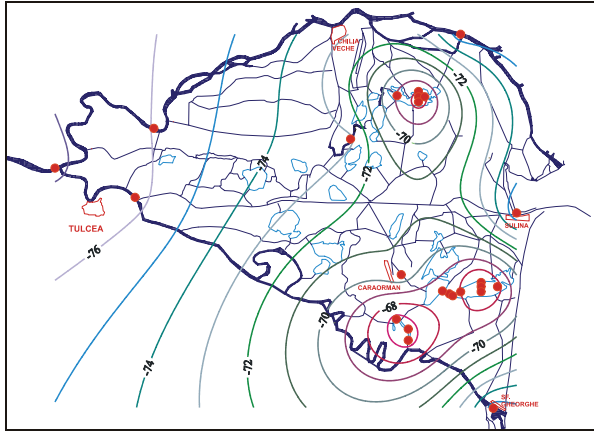


FIG. 4. Isotopic pattern for Danube Delta in 1995.

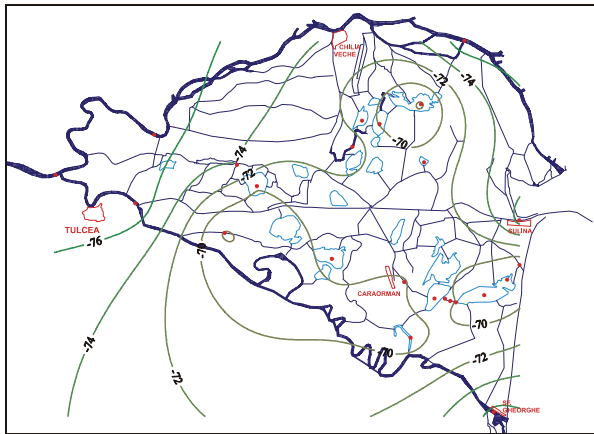


FIG. 5. Isotopic pattern for Danube Delta in 1996.

the water circulation in the fluvial delta plain and a slight shift in deltaic space from the marine delta plain of Sulina-Sf. Gheorghe intertributary space. The finger in the Ceatal Chilia zone is due to the changes in the discharge repartition among the main tributaries in favor of the Sf. Gheorghe branch. The isotopic data are confirmed by the hydrologic measurements [2–4]. These results are due to the completion in 1994 of the works of cutting-off the meander belts of Sf. Gheorghe branch, in order to activate the tributary water and reroute sediment fluxes for equilibrating the sedimentary budget of adjacent sections of the delta

DEUTERIUM AS INDICATOR OF THE NATURAL AND ANTHROPIC STRESS

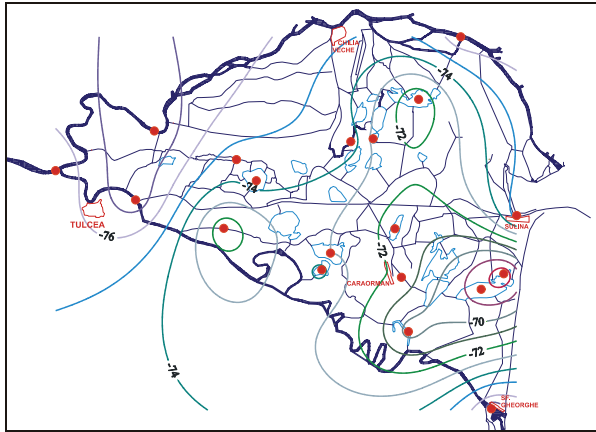


FIG. 6. Isotopic pattern for Danube Delta in 1998.

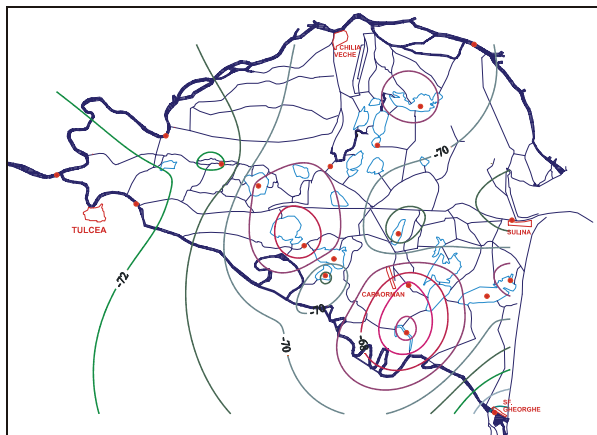


FIG. 7. Isotopic pattern for Danube Delta in 2005.

shore. In the Sulina-Sf. Gheorghe intertributary area the data distinguish a new zone with the stagnant water on Litcov channel, most probably due to the blocking-up of the channel.

In 2005–2006 (Figs. 7 and 8) the Danube discharge was increased and the water circulation was slightly different than that in 1998. For the marine delta plain between Sulina and Sf. Gheorghe branches, it was observed that the stagnant water area moved toward the southwest of the Rosu Lake, and in the eastern part, parallel to shore line, the drainage of deltaic waters was

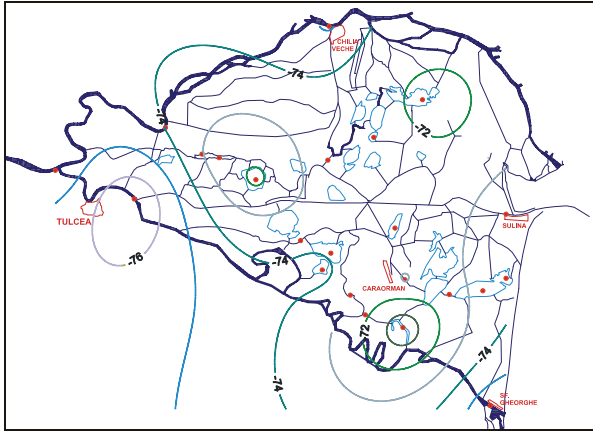


FIG. 8. Isotopic pattern for Danube Delta in 2006.

reestablished due to the opening of the new channel Tataru, parallel to shore line between Sulina and Sf. Gheorghe.

5. CONCLUSIONS

The isotopic content variations of water due to the climatic changes and anthropogenic activities are fast, the isotopic signature being indicators for the water flow-paths changes before irreversible environmental transformations occur. Contours maps of the mean deuterium concentrations can be used to reveal the changes of the water flow-paths from the running waters (Danube's distributaries, channels/canals with active, controlled or absent circulation of water) and the standing freshwater (lakes with active, reduced or controlled change of water). The isotopic maps showed the changes of pathways due to the climatic changes that have the impact on the water balance:

- (a) Between Chilia and Sulina branches there is the improvement of water movement due to the works of ecological restoration of the Babina and Cernovca polders, but the Merhei Lake maintains an area with low drainage.
- (b) Between Sulina and Sf. Gheorghe branches there is a slight drainage of the deltaic water inside the Gorgova unit from the fluvial delta plain and inside the western part of the Rosu–Rosulet unit from maritime delta plain. From the eastern area of the Rosu unit the drainage is much improved.

DEUTERIUM AS INDICATOR OF THE NATURAL AND ANTHROPIC STRESS

- (c) Environmental stresses on delta wetlands have been decreased by the man-made efforts to rehabilitate the environment health status and this was revealed by the isotopic approach.

Danube Delta Biosphere Reserves are excellence sites to explore and demonstrate approaches to conservation and sustainable development on a bioregional scale, with associated research, monitoring, training and education of local people as the driving force for natural conservation of the DD.

REFERENCES

- [1] http://www.geoecomar.ro/c_excel/euroeco-geocentre.htm.
- [2] SCIENTIFIC ANNALS OF THE DANUBE DELTA INSTITUTE, TULCEA, 1993–2002.
- [3] GASTESCU, P., The Danube Delta: Geographical characteristics and ecological recovery. *GeoJournal* **29** 1 (2004) 57–67.
- [4] BONDAR, C., et al., The Danube Delta Hydrologic Data Base and Modelling. Final Report EC: “Fluxes of greenhouse gases in the north-western region of the Black Sea coastal zone: Influence of the Danube River System”, 35, Romania–Italy, (2000).
- [5] McKENZIE, JA., HOLLANDER, D., Oxygen-isotope record in recent carbonate sediments from Lake Greifen, Switzerland, In *Climate Change in Continental Isotopic Records*, Geophysical Monograph **78** (Swart et al., eds), American Geophysical Union (1993) 101–111.
- [6] NIEF, G., BOTTER, R., Mass spectrometric analysis of simple hydrogen compounds, *Advances in Mass Spectrometry*, edited by Walddron J. D (1959) 515.
- [7] <http://isohis.iaea.org/>.
- [8] FEURDEAN, V., FEURDEAN, L., Long term trends (1975–2003) of deuterium content of precipitation from Cluj-Napoca, Romania, poster presented at the International Workshop on the Application of Isotope Techniques in Hydrological and Environmental Studies, UNESCO, Paris, France, 6–8 September (2004).
- [9] INGRAHAM, N.L., et al., Arid Catchments, In: *Isotope Tracers in Catchment Hydrology*, (Kendall C., McDonnell J.J., Eds.), (1998).
- [10] WALKER, J.F., KRABBENHOFT, D.P., Groundwater and Surface-Water Interactions in Riparian and Lake-Dominated Systems In: *Isotope Tracers in Catchment Hydrology*, (Kendall C., McDonnell J.J., Eds.), (1998).
- [11] SHANLEY, J.B. et al., Isotopes as Indicators of Environmental Changes, In: *Isotope Tracers in Catchment Hydrology*, (Kendall C., McDonnell J.J., Eds.), (1998).

- [12] DARLING, W.G., et al., The O & H stable isotopic composition of fresh water in the British Isles. 2. Surface water and groundwater. *Hydrology and Earth System Sciences*, **7** 2 (2003) 183–195.
- [13] FEURDEAN, V., FEURDEAN, L., Deuterium signature in the evaporation processes from few lakes of Danube Delta, Romania, The forth Scientific Session of the Danube Delta Biosphere Reserve, Tulcea, Romania, 16–18 mai, 1995.
- [14] CRAIG, H., GORDON. L.I., Deuterium and oxygen-18 variations in the ocean and marine atmosphere, *Stable Isotopes in Oceanographic Studies and Paleotemperatures*, Lab. di Geologia Nucleare, Pisa, (1965).

TRITIUM CONCENTRATIONS IN THE YUKON RIVER BASIN AND THEIR IMPLICATIONS

R.L. MICHEL
US Geological Survey,
Menlo Park, CA, USA

P. SCHUSTER
US Geological Survey,
Boulder, CO, USA

M. WALVOORD
US Geological Survey Denver,
CO, USA

Abstract

The tritium transient, produced by atmospheric nuclear weapons testing in the 1950s and 1960s, has been used to determine timescales for large-scale hydrologic processes such as the movement of water through river basins. A long-term tritium data base is available from downstream stations on the Yukon River from 1961 to the present. This data has been analyzed using a lumped-sum parameter model to obtain estimates of fraction of base flow and timescales for flow of water through the basin. The data shows that 63% of the water exported by the Yukon River has been retained in the basin less than a year. The average residence time for the older water is approximately 17 years.

1. INTRODUCTION

Recently, there has been concern about the impact of climate and land-use changes on the hydrology and biogeochemistry of watersheds in high northern latitudes. The US Geological Survey has conducted a series of sampling programs to investigate the geochemistry and water cycling of the Yukon River Basin (Fig. 1). One of the crucial requirements for evaluating these changes is an understanding of the timescales for residence times of water within the basin. One method to determine residence times is by the use of tritium data. Tritium was produced in major quantities by nuclear testing in the 1950s and 1960s, overwhelming the natural background concentrations. The

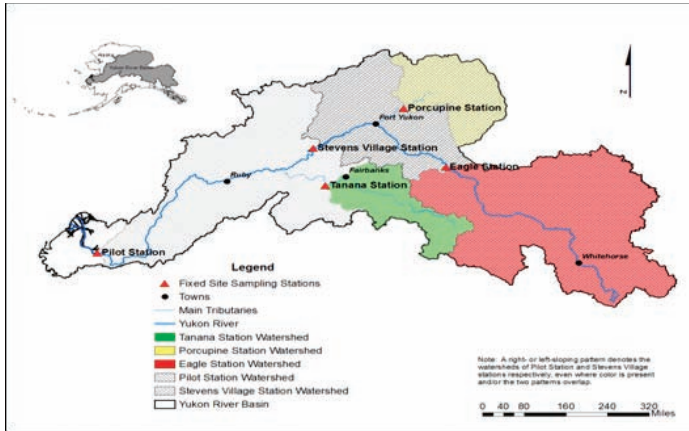


FIG. 1. The US Geological Sampling program in the Yukon River Basin.

tritium inventory on the earth's surface rose from about 3.5 kg to over 600 kg, producing a global tracing experiment for water movement in the environment [1]. The tests produced steep rises in tritium concentrations in precipitation and surface waters with the extent of the increase dependent on geography and atmospheric exchanges.

Most tests were conducted in the Northern Hemisphere and that is where most tritium fallout occurred [2]. Tritium concentrations in precipitation and most surface waters peaked in 1963–1964 and concentrations have dropped since then. Residence times of water in the atmosphere are short so concentrations dropped quickly in precipitation. Tritium concentrations in surface waters never reached the levels of those in precipitation due to mixing with older groundwater which had low tritium concentrations. However, surface waters can retain the memory of the tritium transient much longer due to the groundwater influence and evidence of this elevated input is still present in many watersheds. The concentrations of tritium in surface flow today are a function of the fraction of base flow present and the age of this base flow.

2. APPROACH

One method of obtaining estimates of the age of water within a watershed using tritium data is to apply a lumped-sum parameter model [3]. This approach requires a valid source function for tritium concentrations in precipitation over the time of the tritium transient. No long-term precipitation stations are

TRITIUM CONCENTRATIONS IN THE YUKON RIVER BASIN

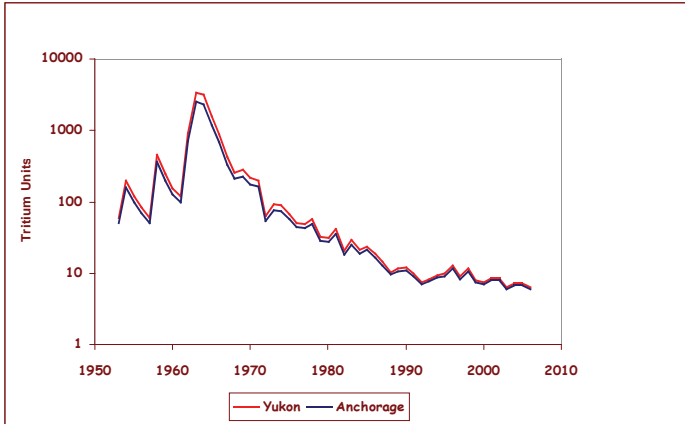


FIG. 2. Tritium concentrations at Anchorage Alaska from measured and correlated data and estimated tritium concentrations in precipitation for the Yukon Basin.

available within the Yukon watershed that record tritium concentrations in wetfall. However, a long-term data base is available at Anchorage, Alaska. It will have a lower tritium concentration because of the oceanic influence. Using Anchorage data ($C_{\text{Anchorage}}$) adjusted with Canadian data, a source function for tritium in precipitation was derived. The concentrations of precipitation in the basin (C_p) are derived as follows

$$1.04 \ln(C_{\text{Anchorage}}) = \ln(C_p).$$

The concentrations obtained are shown in Figure 2.

An understanding of the timescales and sources of water can be derived from long-term tritium data sets [3]. A long-term record of tritium concentrations in Yukon River water was compiled from historical data extending from 1961 to the present, primarily from Pilot Station and Ruby, Alaska records [4]. Tritium concentrations at these stations represent an integration of water composition throughout most of the Yukon River Basin. Water in the river is made up of two primary components, base flow and prompt flow. By definition, prompt flow has been in the water shed less than one year and can be assumed to have a tritium concentration equivalent to precipitation. The tritium concentration of river water is then:

$$C_{\text{river}} = n \times C_p + m \times C_{\text{base}}$$

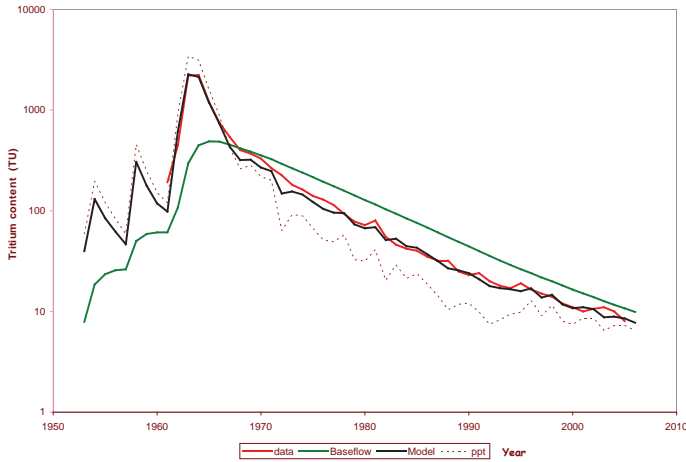


FIG. 3. Tritium concentrations in measured tritium samples from the Yukon River, concentrations in precipitation used for the model, modeled concentrations for the river and concentrations calculated for baseflow assuming a residence time of 17 years.

Where: $n + m = 1$.

Tritium concentrations in baseflow can be derived from the model below:

$$dC_{\text{base}}/dt = k(C_p - C_{\text{base}}) - \lambda C_{\text{base}}$$

Here C_{base} is the tritium concentration of the base flow, C_p is the tritium concentration of precipitation (derived from the above correlation), λ is the decay constant of tritium $=1/\tau = 0.056 \text{ yr}^{-1}$, and $k \text{ (yr}^{-1}\text{)}$ is the rate constant for replacement of water in the baseflow reservoir and the reciprocal of the mean age of the water in the reservoir. The fitting parameters n , m and k can be determined with an inverse modeling approach using the derived tritium input function and measured values of C_{river} over the period 1961–2005.

The values for n , m and k are varied to achieve the best fit of modeled data to the measured data. Figure 3 shows the actual yearly average tritium concentrations, the precipitation source function used, and concentrations derived using the best model concentrations. The goodness of fit between modeled and measured data was determined by running a linear regression with an intercept of zero [5]. The best fit (r^2) was obtained with a value of 0.37 for m (0.63 for n) and a value of 17 years for $1/k$. Walvoord and Striegl [6] reported a value of 0.25 for m using winter streamflow measurements from the Yukon River at Pilot Station. However, they state that their estimate for baseflow

TRITIUM CONCENTRATIONS IN THE YUKON RIVER BASIN

should be considered biased on the low side because shallow groundwater discharge to the Yukon River may increase in the warmer months. A residence time of 17 years is similar decadal scale base flow residence times reported for many other river basins [3, 7, 8].

There are no equivalent long-term tritium data sets for the tributaries of the Yukon River, so no similar approach can be applied. Using the tritium input function and the above model, an estimate of what tritium concentrations would be for different residence times can be calculated. The tritium concentrations measured during this program can be compared to calculated concentrations to estimate residence times. To normalize the data over the four years of the study, the tritium concentrations of the precipitation are divided by the tritium concentrations measured in the river water to produce a ratio (C_P/C_R). This ratio is related to residence times of the waters making up the river water [9]. The ratios obtained from these data vary from greater than 2.5 to less than 0.5. The highest ratio is obtained from runoff from Glakona Glacier which has a large component of pre-bomb water present. The Nares River also has a large component of glacial melt and has tritium concentrations lower than present day precipitation, giving it the second highest ratio.

For sites where no apparent glacial melt is reducing tritium concentrations, the C_{Pre}/C_R can be used to estimate the timescale that waters remain in a given basin. Figure 4 is a graph of the ratios expected for the period of the sampling program using different residence times. The lowest ratios are found for time

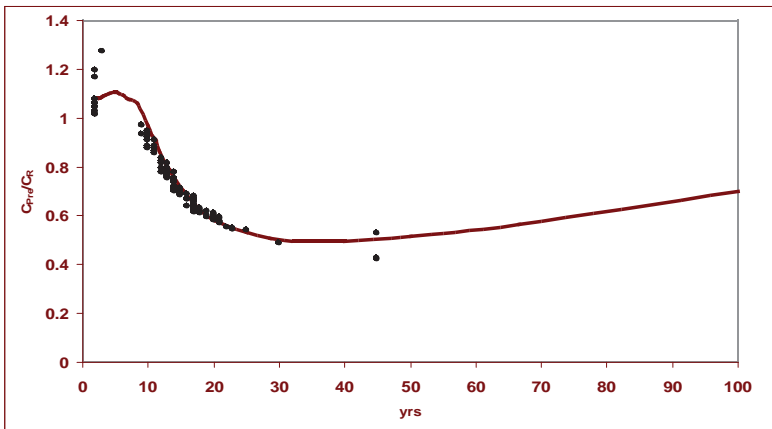


Figure 4. C_{Pre}/C_R ratios for varying timescales for residence times of water in the Yukon River basin. Superimposed on the graph are ratios for samples measured during this program at their location on the residence time curve. Most samples are in the range of 10–20 years.

periods of about 40 years because this is the timescale of the tritium transient. Superimposed on this graph are the ratios for the various stations sampled during this program and the location that they would fall on this curve. There is a wide range of ratios for the present data set but most correspond to residence times of 10-20 years. As these ratios are not corrected for any prompt flow from present day precipitation, they may be expected to be lower than ratios for the baseflow input. Thus the ratio for the base flow can be expected to be shifted to longer residence times in keeping with the results found for the long-term data from the Yukon River.

3. CONCLUSIONS

Tritium concentrations from a long-term data series that effectively integrates water in the Yukon River Basin have been analyzed using a lumped sum parameter model. A best fit between modeled and real data is obtained with a value of 35% for baseflow and a residence time of 17 years for baseflow within the basin. This model is compared to results collected from the tributaries of the Yukon River using the ratio of the concentration in precipitation versus that and of river water. Most results suggest that residence times of baseflow within the watersheds of the tributaries is decadal in scale, in agreement with the results from the integrated model.

REFERENCES

- [1] SUESS, H.E., Tritium geophysics as an international research project, *Science* **163** (1969) 1405–1410.
- [2] INTERNATIONAL ATOMIC ENERGY AGENCY, *Statistical Treatment of Data on Environmental Isotopes in Precipitation* (1992) Vienna, Austria.
- [3] MICHEL, R.L., Residence times in river basins as determined by analysis of long-term tritium records, *J. of Hydrol.* **130** (1992) 367–378.
- [4] LANDA, E.R., BEALS, D.M., HALVERSON, J.E., MICHEL, R.L., CEFUS, G.R., 1999, Tritium and plutonium in waters from the Bering and Chukchi Seas, *Health Physics* **77** (1999) 668–676.
- [5] TAYLOR, J.R., *An Introduction to Error Analysis*, University Science Books, Sausalito, CA USA (1997) 327.
- [6] WALVOORD, M.A., STRIEGL, R. G., Increased groundwater contribution to streamflow in the Yukon River Basin: Potential impacts on carbon and nitrogen export, *Geophysical Res. Lett.*, submitted (2007).

COMBINING HYDROLOGICAL, CHEMICAL AND ISOTOPIC APPROACHES TO IDENTIFY SOURCES AND FATE OF SULFATE AND NITRATE IN THE SOUTH SASKATCHEWAN RIVER SYSTEM, CANADA

B. MAYER*, L.I. WASSENAAR**, L. ROCK*, J.E. MCCALLUM*

*Applied Geochemistry Group,
Department of Geology & Geophysics,
University of Calgary, Calgary

**Science and Technology Branch,
Environment Canada, Saskatoon

Canada

Abstract

River water was seasonally and longitudinally sampled at 25 stations along the South Saskatchewan River and its tributaries from the headwaters in Alberta to the mouth near Prince Albert (Saskatchewan, Canada). River water samples were analyzed for their chemical and isotopic compositions ($\delta^2\text{H}$, $\delta^{18}\text{O}$, $\delta^{13}\text{C}_{\text{DIC}}$, $\delta^{15}\text{N}_{\text{nitrate}}$, $\delta^{18}\text{O}_{\text{nitrate}}$, $\delta^{34}\text{S}_{\text{sulfate}}$, $\delta^{18}\text{O}_{\text{sulfate}}$). Sources and processes responsible for marked changes in riverine sulfate and nitrate fluxes were identified using stable isotope techniques. Geologic (evaporite) sulfate was the predominant sulfate source in the headwaters, while sulfate from anthropogenic sources in urban areas and from pyrite oxidation in the tills of agricultural regions caused markedly elevated sulfate fluxes with increasing distance. Nitrate fluxes in the headwater sections were low, and N and O stable isotope data indicated that the nitrate was mainly derived from nitrification in forest soils. With increasing flow distance, there was clear evidence for nitrate loading from municipal waste water sources and agricultural return flows. This study demonstrates that stable isotope techniques are an effective tool for distinguishing natural and anthropogenic sources and the fate of sulfate and nitrate in large riverine systems, particularly if used in concert with hydrometric and complementary geochemical data.

1. INTRODUCTION

Addition of nitrate, sulphate, and phosphate to surface water or groundwater systems can have major impacts on drinking water quality [1] and can cause acidification [2] and eutrophication [3] of surface waters and even hypoxia [4]. Assessing sources, fate and transport of these anions in riverine systems is, however, often challenging. Stable isotope techniques have the potential to provide unique insights into sources and biogeochemical transformations of nitrate, sulfate and phosphate in riverine systems [5–7], particularly if used in concert with hydrometric and chemical measurements.

The objective of this study was to test the effectiveness of combining hydrological, chemical, and isotopic approaches in differentiating natural and anthropogenic effects on the sulfate and nitrate fluxes in the rivers of the South Saskatchewan River Basin in western Canada with a focus on urban and agricultural impacts.

2. METHODS

River water was seasonally sampled at over 25 sites along the South Saskatchewan River (Figs 1 & 2) and its tributaries between the headwaters in the Rocky Mountains of Alberta and the mouth near Prince Albert (Saskatchewan) during a variety of different flow conditions (snowmelt, base flow, etc.) over a 1 year period. Concentrations and isotopic compositions of sulfate and nitrate were determined. In order to identify the sources and the fate of sulfate and nitrate along the river, riverine sulfate and nitrate fluxes were calculated by combining hydrometric data with concentration measurements. Subsequently, sulfur, nitrogen, and oxygen isotope ratios were analyzed to determine the causes of significant variations in sulfate or nitrate fluxes between subsequent sampling stations.

The procedures for isotopic determination of NO_3^- and SO_4^{2-} were based on methods described by Silva et al. [8], Mayer & Krouse [9], and Kornexl et al. [10]. SO_4^{2-} and NO_3^- were collected on anion exchange columns and were eluted from the columns in the laboratory using 15 ml 3 M HCl. For SO_4^{2-} isotopic analyses, 1 ml of 0.2 M BaCl_2 solution was added to the eluant to precipitate SO_4^{2-} as BaSO_4 . The precipitate was recovered by filtration through a 0.45 μm membrane filter and air-dried. $\text{BaSO}_4\text{-S}$ was converted to SO_2 by high temperature reaction in an elemental analyzer and $^{34}\text{S}/^{32}\text{S}$ ratios were determined using an isotope ratio mass spectrometer in continuous flow mode (CF-IRMS). For O isotopic analyses of SO_4^{2-} , $\text{BaSO}_4\text{-O}$ was converted to CO

COMBINING HYDROLOGICAL, CHEMICAL, AND ISOTOPIC APPROACHES

at 1450°C in a pyrolysis reactor, and $^{18}\text{O}/^{16}\text{O}$ ratios of the gas were measured by CF-IRMS.

To isolate NO_3^- , excess Ba^{2+} was removed from the remaining eluant using a cation exchange column. The eluant then was neutralized with Ag_2O , creating an AgCl precipitate that was removed by filtration. The solution, which contained dissolved Ag^+ and NO_3^- , was freeze-dried to form pure AgNO_3 . The AgNO_3 was converted to N_2 in an elemental analyzer and $^{15}\text{N}/^{14}\text{N}$ ratios were determined using CF-IRMS. For O isotopic analyses of NO_3^- , $\text{AgNO}_3\text{-O}$ was converted to CO at 1350°C in a pyrolysis reactor, and $^{18}\text{O}/^{16}\text{O}$ ratios of the gas were measured by CF-IRMS.

N, S and O isotope ratios are expressed in the internationally accepted delta notation in per mil (‰):

$$\delta(\text{‰}) = [(R_{\text{sample}}/R_{\text{standard}}) - 1] \times 10^3 \quad (1)$$

where R is the $^{34}\text{S}/^{32}\text{S}$ or $^{18}\text{O}/^{16}\text{O}$ ratio of SO_4^{2-} , or $^{15}\text{N}/^{14}\text{N}$ or $^{18}\text{O}/^{16}\text{O}$ ratio of NO_3^- of a sample or standard. The internationally accepted standards are: Vienna Canyon Diablo Troilite (V-CDT) for S isotopes, AIR for N isotopes and Vienna Standard Mean Ocean Water (V-SMOW) for O isotopes. The overall analytical precision including sample pre-treatment, gas preparation, and mass spectrometric analyses was $\pm 0.5\text{‰}$ for $\delta^{34}\text{S}$, $\delta^{15}\text{N}$, and $\delta^{18}\text{O}$ measurements, respectively.

3. RESULTS

Figure 1 displays the average $\delta^{34}\text{S}$ values for riverine sulfate ($n > 4$) at over 20 different sampling stations located in the South Saskatchewan River Basin. Sulfur isotope ratios were highest ($>15\text{‰}$) in the source water regions of the Bow River located in evaporite-containing Paleozoic strata of the Canadian Rocky Mountains. With increasing flow distance, $\delta^{34}\text{S}$ of riverine sulfate decreased to values near 0‰ . The lowest $\delta^{34}\text{S}$ values of riverine sulfate were observed in the agriculturally used portions of the Oldman River basin. Oxygen isotope ratios of sulfate varied between $+8$ and -12‰ .

Figure 2 displays the average $\delta^{15}\text{N}$ values for riverine nitrate at 15 different sampling stations located in the South Saskatchewan River Basin. Nitrogen isotope ratios were lowest ($<4\text{‰}$) throughout the headwater regions. Downstream of major urban centers and intensively used agricultural areas, $\delta^{15}\text{N}$ value of riverine nitrate increased to more than 7‰ . Oxygen isotope ratios of nitrate varied between $+6$ and -8‰ .

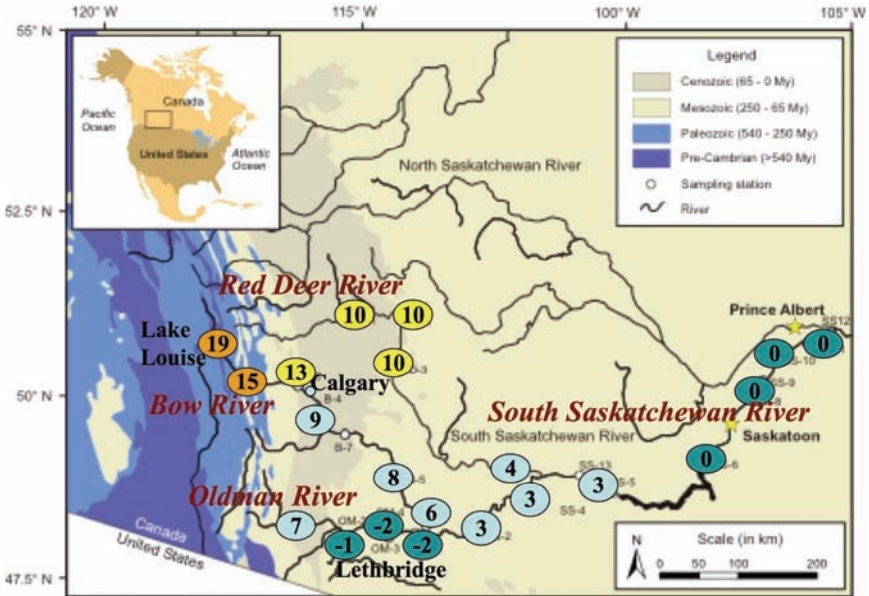


FIG. 1. Mean $\delta^{34}\text{S}$ values of riverine sulfate in ‰ for 21 sampling sites along the South Saskatchewan River and its tributaries. Base map from Ferguson et al. [11].

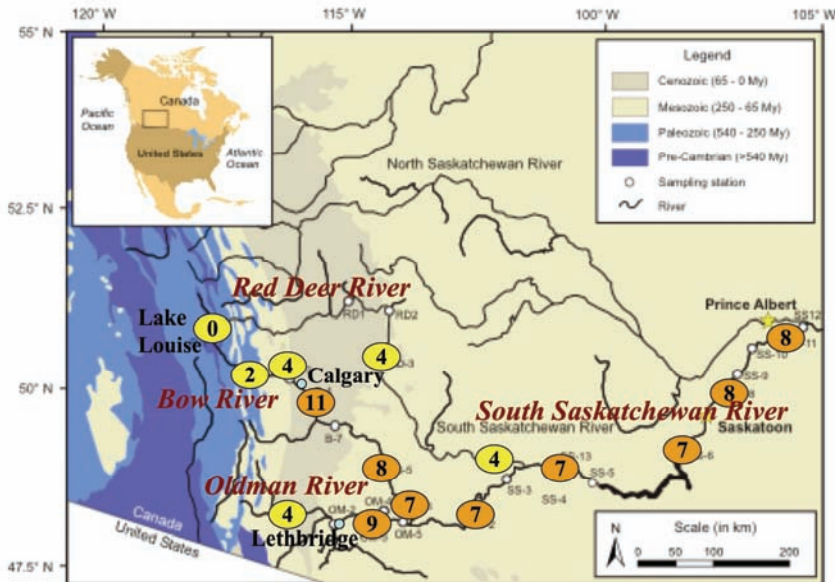


FIG. 2. Mean $\delta^{15}\text{N}$ values of riverine nitrate in ‰ for 15 sampling sites along the South Saskatchewan River and its tributaries. Base map from Ferguson et al. [11].

COMBINING HYDROLOGICAL, CHEMICAL, AND ISOTOPIC APPROACHES

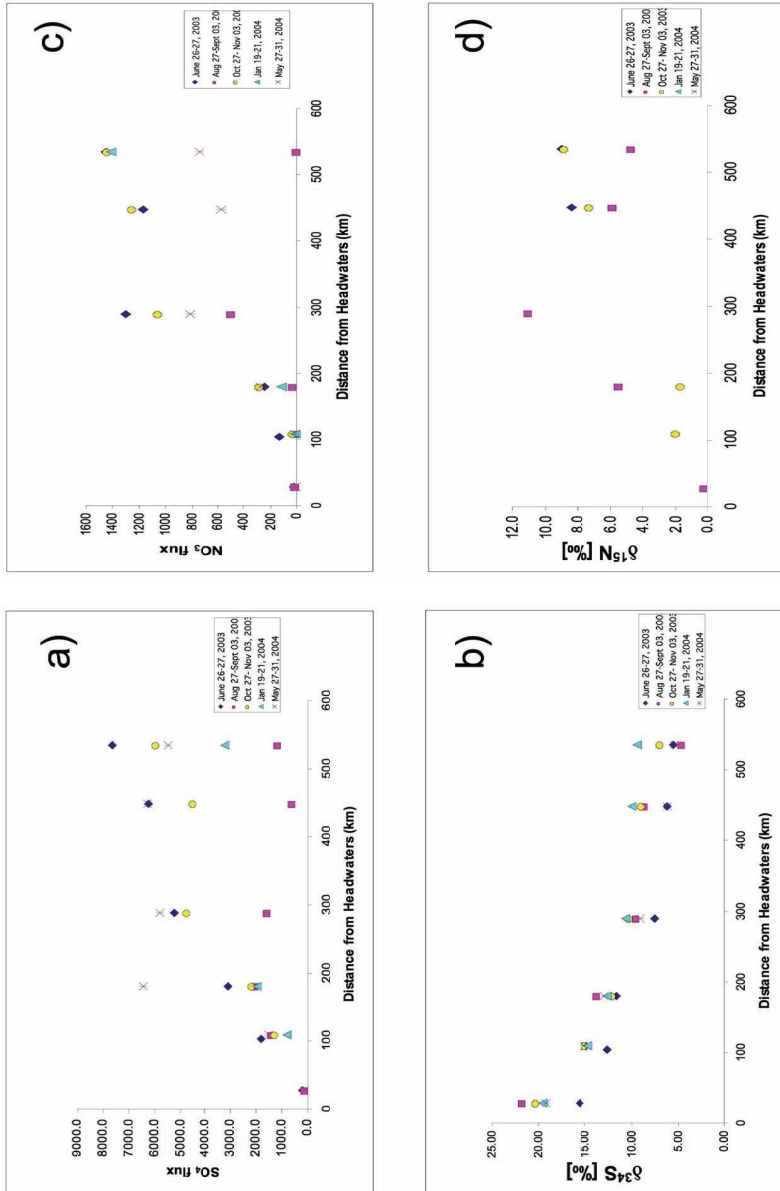


FIG. 3. Fluxes (a) and $\delta^{34}\text{S}$ values (b) of sulfate and fluxes (c) and $\delta^{15}\text{N}$ values (d) of nitrate in the Bow River sampled during a variety of different flow conditions in 2003 and 2004.

4. DISCUSSION

Sulfate fluxes in the headwater regions were low (Fig. 3a) and sulfur isotope ratios indicated that evaporite dissolution was the predominant source of sulfate at some sampling sites (Fig. 3b), besides soil sulfate. With increasing flow distance, sulfate fluxes increased and sulfur isotope ratios decreased significantly. Sulfur isotope data indicated that this was predominantly caused by sulfate derived from anthropogenic sources (Fig. 4a). These include sulfate released via major point source wastewater treatment effluents (e.g. Calgary) with $\delta^{34}\text{S}$ values near 1‰ [12]. In agricultural areas with irrigation districts, sulfate was also derived from oxidation of pyrite in tills, generating sulfate with negative $\delta^{34}\text{S}$ values (Fig. 1) that was delivered via irrigation canals to the river.

Nitrate fluxes in the headwater regions of the Red Deer River, Bow River, and Oldman River were low (Fig. 3c) and the isotopic composition of nitrate (Fig. 3d and 4b) indicated that nitrate was predominantly derived from nitrification in forest soils. At Calgary, nitrate in the waste water treatment plant effluent was found to have a $\delta^{15}\text{N}$ value of 10‰ [12]. Consequently, waste water treatment effluents significantly increased the $\delta^{15}\text{N}$ value of nitrate in the Bow River (Fig. 3d) as well as nitrate fluxes (Fig. 3c). In the Oldman River, manure-derived nitrate in agricultural return flows was identified as the reason for increasing $\delta^{15}\text{N}$ values in riverine nitrate below Lethbridge [13]. While $\delta^{15}\text{N}$ values of nitrate remained elevated in the South Saskatchewan River, it turned out to be challenging to separate the effects of waste water inputs, agricultural return flows, and nitrate assimilating processes in the river. Additional tracer techniques (e.g. boron isotopes [14]) are desirable to better quantify the nitrogen loading and to trace the fate of nitrate from urban and agricultural sources in this river basin.

5. CONCLUSIONS

This study provides evidence that isotope techniques can yield unique information on natural and anthropogenic sources of sulfate and nitrate in riverine systems, particularly if combined with hydrometric and chemical measurements. It was found that distinguishing waste water derived nitrate from manure-derived nitrate can be challenging in riverine systems based on the isotopic composition of nitrate alone. Future work will test complementary tracers such as boron isotopes that may be suitable for distinguishing between waste water derived and agricultural inputs.

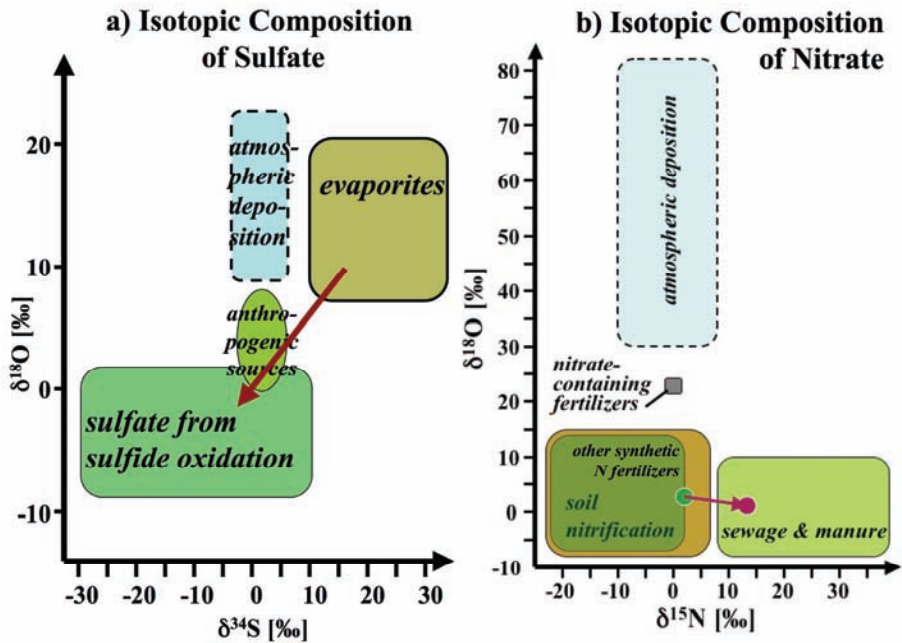


FIG. 4. Isotopic composition of sulfate (a) and nitrate (b) indicating the general trends observed in the South Saskatchewan River with increasing flow distance.

ACKNOWLEDGEMENTS

We gratefully acknowledge the support of Geoff Koehler and Amber Campbell during field sampling and with chemical and isotopic analyses in the laboratory.

REFERENCES

- [1] DAVIES, J.-M., MAZUMDER, A., Health and environmental policy issues in Canada: the role of watershed management in sustaining clean drinking water quality at surface sources, *J. Environ. Management* **68** (2003) 273–286.
- [2] REUSS, J. O., JOHNSON, D. W., Acid deposition and the acidification of soils and waters, *Ecological Studies Vol 59* (1986) Springer, Berlin.
- [3] VITOUSEK, et al. Human alteration of the global nitrogen cycle: sources and consequences, *Ecological Applications* **7** (1997) 737–750.

- [4] GOOLSBY, D. A., Mississippi Basin nitrogen flux believed to cause Gulf hypoxia, *EOS Trans. Am. Geophys. Union* **81** (2000) 321–327.
- [5] MAYER, B., BOYER, E.W., GOODALE, C., JAWORSKI, N.A., VAN BREEMEN, N., HOWARTH, R. W., SEITZINGER, S., BILLEN, G., LAJTHA, K., NADELHOFFER, K., VAN DAM, D., HETLING, L. J., NOSAL, M., PAUSTIAN, K., Sources of nitrate in rivers draining sixteen watersheds in the northeastern U.S.: Isotopic constraints, *Biogeochemistry* **57** (2002) 171–197.
- [6] HITCHON, B., KROUSE, H.R., Hydrogeochemistry of the surface waters of the Mackenzie River drainage basin, Canada — III. Stable isotopes of oxygen, carbon and sulphur, *Geochim. Cosmochim. Acta* **36** (1972) 1337–1357.
- [7] MCLAUGHLIN et al., Phosphate oxygen isotope ratios as a tracer for sources and cycling of phosphate in North San Francisco Bay, California, *J. Geophys. Res. Biogeosci.* **111** (2006) Art. No. G03003.
- [8] SILVA, S.R., KENDALL, C., WILKINSON, D.H., ZIEGLER, A.C., CHANG, C.C.Y., AVANZINO, R.J.A., New method for collection of nitrate from fresh water and the analysis of nitrogen and oxygen isotope ratios, *Journal of Hydrology* **228** (2000) 22–36.
- [9] MAYER, B., KROUSE, H.R., Procedures for sulfur isotope abundance studies. In de Groot, P.A. *Handbook of Stable Isotope Analytical Techniques*, Elsevier, Amsterdam (2004) 538–596.
- [10] KORNEXL, B. E., GEHRE, M., HOFLING, R., WERNER, R. A., On-line $\delta^{18}\text{O}$ measurement of organic and inorganic substances, *Rapid Communications in Mass Spectrometry* **13** (1999) 1685–1693.
- [11] FERGUSON, P.R., WEINRAUCH, N., WASSENAAR, L.I., MAYER, B., VEIZER, J., Isotope constraints on water, carbon, and heat fluxes from the northern Great Plains region of North America, *Global Biogeochemical Cycles*, in press (2007).
- [12] HOGBERG, L. K., JACKSON, L. J., MAYER, B., Submerged macrophyte nutrient limitation in two rivers (Red Deer and Bow) draining the Rocky Mountains of Alberta, Canada, *Freshwater Biology*, in review.
- [13] ROCK, L., MAYER, B., Isotopic assessment of sources of surface water nitrate within the Oldman River basin, Southern Alberta, Canada, *Water, Air, and Soil Pollution: Focus* **4** (2004) 545–562.
- [14] WIDORY, et al., Tracking the sources of nitrate in groundwater using coupled nitrogen and boron isotopes: a synthesis, *Environ. Sci. & Technol.* **39** (2005) 539–548.

ISOTOPE HYDROLOGY AND HYDROCHEMISTRY OF SOME NUTRIENT ENRICHMENT SOURCES TO THE DENSU RIVER BASIN IN GHANA

J.R. FIANKO*, S. OSAE*, D. ADOMAKO**, D.G. ACHEL*

Department of Chemistry,
National Nuclear Research Institute,
Ghana Atomic Energy Commission

Department of Physics
National Nuclear Research Institute,
Ghana Atomic Energy Commission

Legon Accra, Ghana

Abstract

Anthropogenic inputs of nitrogen, phosphorus and oxygen consuming materials to aquatic ecosystems can change nutrient dynamics, deplete oxygen and change abundance and diversity of aquatic plants and animals. The isotopic techniques in groundwater resource management in the Densu River Basin required a research and assessment program to establish the contribution of sewage discharge and agriculture to eutrophication in the Densu River and examine the source of nutrients and other pollutants in the aquatic ecosystem. This will improve the understanding of the interaction between nutrient input, dissolved oxygen and aquatic ecosystem productivity. Combining isotopic and hydrochemical characteristics of samples in the basin will show the influence of natural and anthropogenic source of nutrients in the Densu River Basin.

1. INTRODUCTION

The Densu River is an important source of water for industrial, municipal, irrigation and domestic uses in Ghana and is one of the most exploited rivers in the country. The Densu River basin is one of the largest groundwater reserves in the country. It traverses several towns and serves as the main source of drinking water supply for over seven million people in a number of communities. The water from the Weija Dam supplies the western part of Accra and Kasoa. There are also abstraction points at New Tafo, Apedwa, Koforidua, Akwadum,

and Nsawam for drinking water supply. The catchment area includes parts of six districts in the Eastern Region (Akwapim North and South Districts, East and West Akim Districts, Suhum-Kraboa-Coaltar District, Manya Krobo and the New Juaben Districts), two (2) districts in the Greater Accra Region (Ga District and Accra Metropolitan Area) and one (1) in the Central Region (Awutu-Efutu-Senya District).

The Densu River, however, is extremely susceptible to surface derived contamination. The Densu River Basin was identified by Water Resources Commission of Ghana (WRC, 2003, Amuzu, 1975) as the most problematic and vulnerable catchment on the priority list of issues, especially on water pollution, enhanced use of pesticides and fertilizers, improper land-use, water shortage and lack of adequate data and information for effective management. In the past decade the basin has become the focus of public concern, that has resulted from widespread use of agrochemicals and siting of municipal and domestic refuse dumps on the river banks in many communities. Anthropogenic loading of nitrogen and phosphorus from industrial, municipal, and agricultural sources has increased nutrient concentrations in lakes and rivers worldwide, increased production of aquatic plants, caused changes in the abundance and composition of consumers and contributed to declines in dissolved oxygen. Rivers and lakes receiving elevated input of nutrients in many cases give rise to cultural eutrophication.

The isotopic techniques in groundwater resource management in the Densu River Basin required a research and assessment program to establish the contribution of sewage discharge and agriculture to eutrophication in the Densu River and examine the source of nutrients and other pollutants in the aquatic ecosystem. This will improve the understanding of the interaction between nutrient input, dissolved oxygen and aquatic ecosystem productivity. Combining isotopic and hydrochemical characteristics of samples in the basin will show the influence of natural and anthropogenic source of nutrients in the Densu River Basin.

2. METHODOLOGY

2.1. The study area

The Densu River Basin is located in Southern Ghana and covers the South-Eastern part of the Greater Accra Region and the South-Western portion of the Eastern Region. The Densu River Basin lies between latitude 5°30' N – 6°20' N and longitude 0°10' W – 0°35' W. The river shares its catchment boundary with the Odaw and Volta basins to the east and north respectively, the Birim Basin

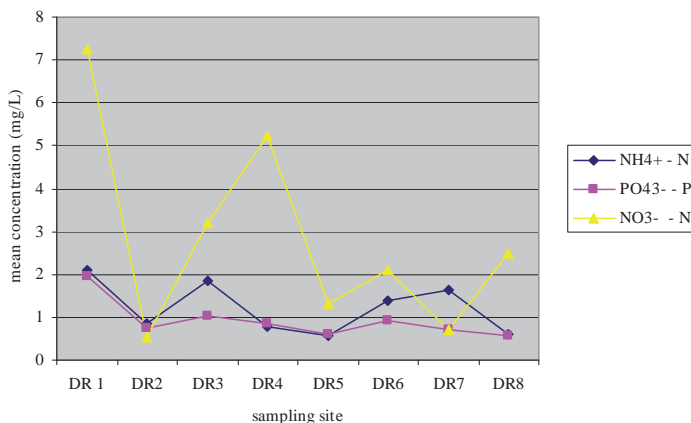


Fig. 2. Mean levels of $\text{NO}_3^- - \text{N}$, $\text{NH}_4^+ - \text{N}$, $\text{PO}_4^{3-} - \text{P}$ in samples.

from mid stream at a depth of 20–30cm over a period of one year which spans both the dry and wet seasons. Electrical conductivity, pH and temperature were measured using digital meters immediately after sampling. Water samples collected in the field were analyzed for chemical constituents such as BOD, COD, SO_4^{2-} , $\text{NO}_3^- - \text{N}$, $\text{NH}_4^+ - \text{N}$, $\text{PO}_4^{3-} - \text{P}$, Cl^- , total hardness and alkalinity in the laboratory using the standard methods for analysis of water and waste water as suggested by the American Public Health Association (APHA, 1998 and EPA, 1983). All reagents used were of analytical grade and instruments pre – calibrated appropriately prior to measurement. Replicate analyses were carried out for each determination to ascertain reproducibility and quality assurance.

4. RESULTS AND DISCUSSION

Understanding the quality of surface water is as important as its quantity because it is the main factor determining its suitability for drinking, domestic, agricultural and industrial processes. Anthropogenic input in a watershed can have significant impacts on the ecology of downstream environments. Surface runoff contributes high concentration of nutrients into the river. The dominant pattern for nutrients phosphate and nitrogen compounds for the Densu River was $\text{NO}_3^- - \text{N} > \text{NH}_4^+ - \text{N} > \text{PO}_4^{3-} - \text{P}$ (Fig.2).

The mean concentration of phosphate was 0.93 mg/L and ranged between 0.42 mg/L to 1.04 mg/L which was higher as a result of washing of phosphate – rich fertilizer from farms in the catchment zone into the river. The concentration of nitrate-N was also high ranging from 0.54 mg/L to 7.25 mg/L

ISOTOPE HYDROLOGY AND HYDROCHEMISTRY OF SOME NUTRIENT

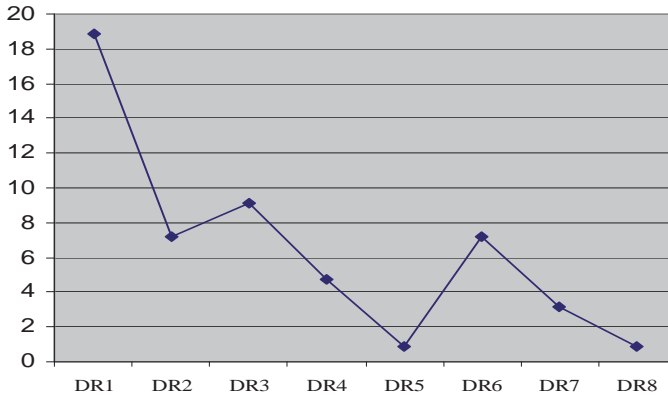


Fig. 3. Mean BOD levels of (mg/L) in samples.

with a mean level of 2.86 mg/L, while $\text{NH}_4^+ -\text{N}$ levels recorded ranged between 0.09 mg/L and 2.10 mg/L with a mean of 1.23 mg/L, suggesting more organic nitrogen input from domestic, agricultural and other anthropogenic origin, since ammonia is a major inorganic product in the decomposition of organic matter. Elevated amount of $\text{NO}_3^- -\text{N}$ in the samples reflects anthropogenic emissions such as combustion of fossil fuels, fertilizer application in these agricultural areas and dumping of domestic and municipal waste into the river. The Densu River had high BOD concentration. The values ranged between 0.87 mg/L and 18.90 mg/L (Fig 3). The high BOD load of the Densu River was a result of dumping domestic and municipal waste into the river course upstream and high organic matter contamination. Anthropogenic enrichment of the Densu River with nutrients and other contaminants lead to production of undesirable effects and cultural eutrophication.

The pH of water samples varied between 6.4 and 8.7 and the average TDS content was 198 mg/L with conductivity of 394 $\mu\text{S}/\text{cm}$. COD, alkalinity and total hardness levels recorded were all within the WHO recommended levels for drinking water (WHO, 1996).

5. CONCLUSIONS

Anthropogenic inputs of nitrogen, phosphorus and oxygen consuming materials to aquatic ecosystems can change nutrient dynamics, deplete oxygen and change abundance and diversity of aquatic plants and animals as well as cultural eutrophication. The nutrient status and hydrochemistry of the Densu

River have been determined in this study. The results of the study have indicated gross pollution of the Densu River with respect to nutrients and organic matter. It also showed the influence of natural and anthropogenic source of nutrients in the river basin.

REFERENCES

- [1] AMUZU, A.T., A survey of the water quality of the River Densu. WRRRI Technical Report, Accra (1975).
- [2] Groundwater Assessment, An Element of Integrated Water Resources Management – the case of Densu River Basin. WRC, Accra (2003).
- [3] EPA, EPA methods of chemical analysis of water and wastewater, EPA/600/4-79/020. USA, 374.3.1-375.4.3 (1983).
- [4] Standard Methods, Standard method for the examination of water and wastewater, 20th Ed. American Public Health Association, Washington DC (1998).
- [5] WHO, Health criteria and other supporting information, 2nd Ed. Guidelines for drinking water, Vol. 2, Geneva (1996).

UNSATURATED ZONE
AND ARTIFICIAL RECHARGE

APPLICATION OF ISOTOPE HYDROLOGY FOR THE ASSESSMENT OF ARTIFICIAL GROUND WATER RECHARGE IN SOME AREAS OF UAE

A.S. EKAABI
Ministry of Environment & Water,
Dubai, UAE

Abstract

Due to recharge — discharge imbalance, severe depletion of groundwater table has occurred in most of the aquifers in United Arab Emirates. Evolved from its prime role to develop the water resources in the country, the Ministry of Environment and Water has constructed a large number of detention and retention dams across the main wadies. To assess groundwater recharge increase due to these dams, isotope methods were used to calculate such increase in three major wadies as Wuraiah, Bih and Tawean. Hydrochemical and isotopic data (^{18}O , ^2H and ^3H) have clearly showed a meaningful contribution to the recharge from the dams. A tentative isotopic balance based on stable isotopes of rains water stored by these dams drove to a quantification of the artificial recharge ranging from 20 to 40%.

1. INTRODUCTION

The United Arab Emirates (UAE) lies in the southern part of the Arabian peninsula between latitudes $22^{\circ}40'$ and $26^{\circ}00'$ North and longitudes $51^{\circ}00'$ and $56^{\circ}00'$ East. It is bounded from the North by the Arabian Gulf, on the East by Sultanate of Oman and the Gulf of Oman and on the South and west by the Kingdom of Saudi Arabia. The total area of the United Arab Emirates is about 83,600 km². Most of the land is desert and characterized by predominance of the Aeolian Landform System. The geomorphologic features include mountains, gravel, sand dunes, coastal zones and draining basins.

The UAE is divided into two distinct zones: the larger low-lying zone and the mountainous zone (Fig. 1). The first covers over 90% of the country's area, extending from the northwest to the eastern part of the country where it is truncated by the mountainous zone [5, 6]. The low-lying zone ranges in altitude from the sea level up to 300 m. Its major part is characterized by the presence of sand dunes which rise gradually from the coastal plain reaching their highest elevation of 250 m above sea level (a.s.l). Along the coast of the Arabian Gulf,



FIG. 1. Map of the United Arab Emirates.

the low-lying land punctuated by ancient raised beaches and isolated hills which may reach up to 40 m (a.s.l) in some locations (Bagdadi in Ref. [5]).

Renewable water recourses in the UAE are very limited. No surface water in the form rivers or lakes is available. Rainwater is very scarce and infrequent. The average rainfall is in the order of 120 mm/yr. However, rainfall is mostly encountered in few events [5].

2. PREVIOUS STUDIES ON THE HYDROLOGY OF SOME DAMS

Evolved from its prime role to develop the water resources in the country, the Ministry of Environment & Water (MOEW) had constructed a large number of detention and retention dams across the main wadis. Detention dams are designed to retard the flow velocities and allow appropriate time for the recharge process to take place. Retention dams are designed for water storage with large quantities and relatively high hydraulic heads. On the other hand, water might be used directly from the storage for irrigation purposes of otherwise. In addition to the numerous dams, several observation wells have been installed to monitor the subsurface water levels.

Within this framework, the current study aims to develop a better understanding of the recharge mechanisms and groundwater flow patterns in the hydrological systems of two selected dam sites, namely Tawiyaen and Wurrayah Wadi sites. This study aiming to the evaluation the effectiveness of dams in recharging groundwater systems, is mainly based on geochemical and isotopic tools which constitute effective and a appropriate methods to investigate the efficiency of artificial recharge of groundwater from surface

APPLICATION OF ISOTOPE HYDROLOGY

TABLE 1. MEAN VALUES OF THE TDS AND MAJOR ELEMENTS CONCENTRATION IN THE WURRAYAH DAM RESERVOIR AND THE OBSERVATION WELLS (IN mg/L).

Mean	TDS	Ca	Mg	Na	K	CO ₃	HCO ₃	Cl	SO ₄	NO ₃
Wur – 3	257.36	6.23	40.09	23.44	2.04	5.96	109.29	48.34	23.19	6.81
Wur – 5	258.50	3.50	32.00	25.50	3.50	4.50	83.50	65.50	65.50	29.00
Wur – 6	278.50	3.70	21.11	49.87	6.15	7.43	92.04	72.27	19.49	3.24
Wur Dam	119.00	16.82	8.68	6.28	1.84	0.00	62.50	21.40	6.56	6.78

impoundment.

2.1. Tawiyaen Wadi basin, Northern Region

The dam in Wadi Tawiyaen was constructed in 1992 on the bedrock consisting of Jurassic to Cretaceous limestone. The capacity of the dam is 18.4 Mio m³. Its catchment area covers 198 km² [4].

2.2. Wurrayah Wadi basin, Eastern Region

The Wurrayah dam was constructed in 1997, approximately 5 km north-west of Khor Fakkan, on the Samail Ophiolite bedrock, which comprises

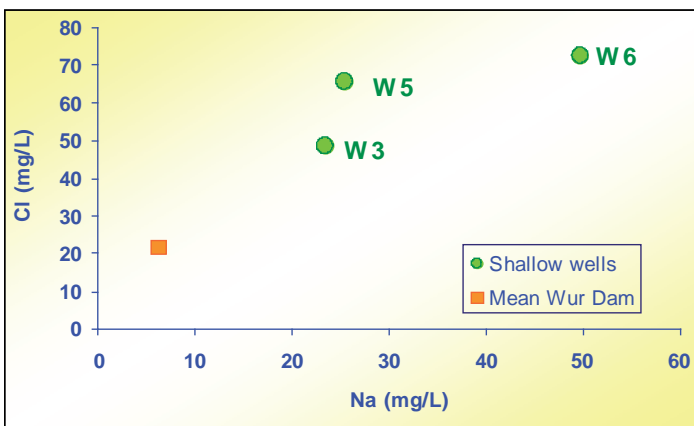


Fig. 2. Cl vs Na contents in the Wurrayah Dam area.

fractured and mineralized assemblages of serpentinite and gabbroic rocks. The catchment area covers 129 km² [3].

Discussion of geochemical data of the Wurrayah Wadi basin

Mean values of the TDS and major elements concentration in the sampled wells are represented in Table 1; the mean TDS value in the dam reservoir water was 119 mg/L. In the shallow wells, the larger the distance from the dam the higher the TDS mean value of groundwater (lowest TDS mean value was registered in Wur 3, which is the nearest well to the dam, while a relatively high value was measured in Wur5, located at larger distance from the dam).

TABLE 2. MAXIMUM AND MINIMUM VALUES OF STABLE ISOTOPES (IN ‰).

	Mean Values		Maximum Values		Minimum Values	
	² H	¹⁸ O	² H	¹⁸ O	² H	¹⁸ O
Wur 3	-5.90	-2.86	-3.60	-2.58	-4.81	-2.71
Wur 5	-2.86	-2.82	-2.54	-2.54	-5.05	-2.53
Wur 6	-2.82	-2.38	-3.32	-2.22	-4.54	-2.32
Wur Dam	-3.83	-3.30	-3.30	-0.78	-1.83	-2.04

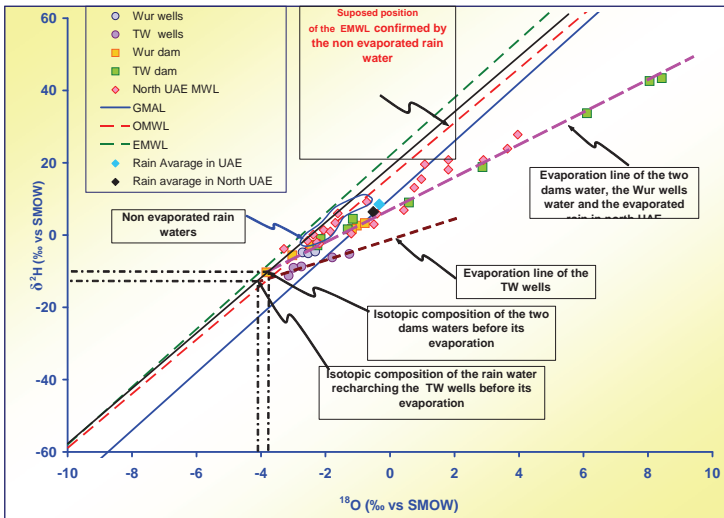


Fig. 3. ¹⁸O / ²H Diagram of Wurrayah , Tawyeen Dams and shallow wells

TABLE 3. DAM RESERVOIR CONTRIBUTION ESTIMATED BY THE ISOTOPIC BALANCE.

	Average ^{18}O (‰)	Dam reservoir contribution (%)
Wur3	-2.71	43.0
Wur5	-2.53	34.1
Wur6	-2.32	22.1

This may indicate that the recharge of these wells is probably derived from the dam reservoir, This hypothesis is confirmed by the diagram shown in Fig. 2.

3. APPLICATION OF ISOTOPE HYDROLOGY FOR THE ASSESSMENT OF ARTIFICIAL GROUND WATER RECHARGE IN SOME AREAS OF UAE

3.1. Discussion of isotopic data

The observation wells and the Wurrayah dam reservoir were sampled for stable isotopes (^{18}O , ^2H) analyses at the end of 2002 (in December) and during the first six months of 2003. The wells Wur3 and Wur6 were sampled 14 times. While the well TW5 and the dam reservoir water was sampled two times and six times respectively. The maximum and the minimum as well as the mean values for each sample are represented in the Table 2.

Mean values of stable isotopes contents in groundwater from observation wells are represented in the $^{18}\text{O}/^2\text{H}$ diagram together with oxygen-18 and deuterium contents of the dam reservoir water and the rainwater samples collected between 1984–1990 in the North and the East of the UAE (Fig. 3). Contrarily to the Tawiyaen basin situation (see below), in the Wurrayah case, the trend constituted by the evaporated samples of precipitation and dam reservoir waters, coincide completely with the evaporation line of the groundwater from the control wells. This evidenced clearly indicate that these waters have the same origin. Thus, the control well groundwater seem to be recharged by the dam reservoir water.

In order to evaluate the dam reservoir water contribution to the shallow aquifer in the Wadi Wurrayah basin, an isotopic balance model has been tentatively established using stable isotopic data and their relationship.

TABLE 4. MEAN VALUES OF THE TDS AND MAJOR ELEMENTS CONCENTRATION IN THE TAWIYEAN DAM RESERVOIR AND THE OBSERVATION WELLS (IN mg/L).

Mean	TDS	Ca	Mg	Na	K	CO ₃	HCO ₃	Cl	SO ₄	NO ₃
TW2	221.83	29.17	16.33	12.00	3.00	2.17	137.00	22.171	14.50	8.50
TW6	504.060	48.60	18.60	83.80	4.80	1.40	213.00	81.40	72.20	22.60
TW8	934.50	22.33	12.83	265.83	5.00	5.83	236.17	248.17	126.50	11.17
TW9	1044.5	39.25	19.23	200.83	4.80	0.08	234.52	168.86	156.20	27.94
TW DAM	253	6.14	3.57	41.00	1.14	2.00	27.14	37.00	35.57	7.57

Computed values of the dam reservoir contribution to the shallow aquifer vary from 22 to 43% (Tab. 3.).

The result of this isotope balance evidenced that groundwater in the observation wells represents mixture between the dam reservoir water and the present rainwater. Indeed, the computed values of dam reservoir water confirm the important contribution of this water in recharging the control wells aquifer, especially in the case of the wells Wur3 and Wur5, which are closer to the dam.

3.2. Discussion of geochemical data of the Tawiyaen Wadi basin

The mean value of salinity and (TDS) concentration of major elements in the sampled wells are reported in Table 4. The TDS mean value in the dam reservoir water was 253 mg/L. In the groundwater from shallow wells this value varied from 222 mg/L measured in the well TW2, to 1044 mg/L measured in the well TW9.

The wells TW2, TW6, TW8 and TW9, located downstream of the dam, showed a TDS values higher than salinity of the dam water. These wells be logically recharged by the dam reservoir water, since the TDS values increase in the same direction the groundwater flow.

3.3. Discussion of isotopic data

The control wells and the Tawiyaen reservoir were sampled during the summer and the spring of 2002 and 2003 for stable isotopes (¹⁸O, ²H) analyses. The maximum and the minimum as well as the mean values for each sample are represented in Table 5.

APPLICATION OF ISOTOPE HYDROLOGY

TABLE 5. MEAN VALUES OF STABLE ISOTOPE CONTENTS IN THE TAWIYEAN BASIN (IN PERMIL VS VSMOW).

	Mean Values		Maximum Values		Minimum Values	
	² H	¹⁸ O	² H	¹⁸ O	² H	¹⁸ O
TW2	-3.14	-11.24	-1.84	-5.55	-3.42	-12.70
TW6	-2.75	-8.69	-2.67	-6.65	-2.84	-9.60
TW8	-2.99	-8.07	-2.92	1.00	-3.11	-11.70
TW9	-1.79	-6.19	-1.42	-4.40	-3.27	-11.80
TW DAM	2.13	16.62	8.43	43.40	-2.25	-2.85

Oxygen- 18 /Deuterium diagram

Mean values of stable isotopes contents in groundwater from control wells were represented in the ¹⁸O/²H diagram together with oxygen-18 and deuterium contents of the dam reservoir water and the rain water samples collected between 1984–1990 in the UAE (Fig. 2) considering the intermediate geographic position of the UAE, and therefore several possible rainwater origins. We represented in this diagram different precipitation water lines, namely the Global meteoric Water line (GMWL) [1, 2], the east Mediterranean water line (EMWL) and the UAE local meteoric water line (equation: ²H = ¹⁸O + 17) [7].

The ¹⁸O/²H diagram shows that the dam reservoir water samples plot on an evaporation line coinciding with that of the rainwater in the UAE. This suggests that the dam water logically derived from the precipitation in the surrounding area. However, the control wells water samples plot on an other evaporation line which trail away from that of the dam water and the UAE meteoric water line.

Tritium data

In the Wadi Tawiyaen basin, tritium analyses were performed during the winter and the summer 2002 and 2003. But, in the Wurrayah basin, these analyses were carried out during the year 2003, excepting one sample which was measured in January 2004.

The tritium concentrations have a limited effectiveness in the determination of the origin of recharge in our case of study, since they present practically the same range of variation, either for the dam water or for an other

recent recharge water deriving from the present-day precipitation. However, it is worth noting that in both cases recharge water in the shallow aquifers.

4. CONCLUSIONS AND RECOMMENDATIONS

Results achieved during this survey allow to highlight the contribution of dams to the recharge of shallow aquifer. Indeed, hydrochemical and isotopic data (^{18}O , ^2H and ^3H), especially those obtained on the Wurrayah basin, clearly show a meaningful contribution to the recharge through the dam. A tentative isotopic balance based on stable isotopes of rains, water stored by this dam and wells drove to a quantification of the artificial recharge ranging from 20 to 40%.

However, chemical and isotopic data obtained on the Tawiyeen basin have not permitted to clearly show recharge from this dam. A recent infiltration seems to exit at the observation wells as shown by the tritium content. On the other hand, considering the scarcity of available data and the inadequate distribution of the sampled wells. It is very difficult to determine how this infiltration takes place, as was the case for the Wurrayah dam.

Hence, and considering the promising and significant results obtained from the Wurrayah basin, it is highly recommended that the Ministry of Environment and Water of the United Arab Emirates continue these investigations and promote the isotopic methods in water management, especially under arid climatic conditions.

REFERENCES

- [1] CRAIG H., Isotopic variation in meteoric waters. *Science* **133** (1961) 1702–1703.
- [2] DANSGAARD W., Stable isotopes in precipitations. *Tellus XVI*, Vol 4 (1964) 436–468.
- [3] ENTEC, Survey on groundwater recharge and flow in wadi ham and Wadi Wurrayah MAF, Vol 2, Wadi Wudrrayah (1964) 17.
- [4] GEYH M.A., Ground water recharge by runoff through dam storage, Isotope Hydrology Techniques in water resources Management (UAE/8/003-01) MAF, Directorate of soil and Water, Section Dams and water (2001) 26.
- [5] MAF and UNITED ARAB EMIRATES UNIVERSITY, Assessment of the effective of Al Bih, Al Tawiyeen and Ham dams in groundwater recharge using numerical models, Interim report, Vol .1 geological, hydro geological and hydrological investigation (2004a).
- [6] MAF and UNITED ARAB EMIRATES UNIVERSITY, Assessment of the effectiveness of dams, Interim report (2004d).

APPLICATION OF ISOTOPE HYDROLOGY

- [7] NIR A., Development of isotope methods applied to groundwater hydrology. Amm Geophs, Union, monographie (1967) 11-09.

QUANTIFICATION OF THE HETEROGENEITY IN WATER TRANSPORT THROUGH THE UNSATURATED ZONE OF SANDY SOILS USING ENVIRONMENTAL ISOTOPES

C. STUMPP, P. MALOSZEWSKI, W. STICHLER
GSF – Institute of Groundwater Ecology,
Neuherberg, Germany

Abstract

A new method, which combines mathematical modelling with environmental and hydrological data, was investigated to estimate the heterogeneity of the unsaturated soils by separation of preferential and matrix flows, quantify both fluxes and determine their transit times. Finally, the transit time distribution functions were used to construct vulnerability diagrams of different soils without plants. The model complexity was simplified using a lumped parameter approach that combines an input and output function of environmental tracer contents with hydraulic measurements. Assuming a two parallel flow-paths model the environmental deuterium (^2H) with its seasonal variation in precipitation and in lysimeters outflow was taken to estimate the mean transit times as well as the amount of preferential and matrix flow and enabled to quantify the heterogeneity of seven sandy lysimeters ($L = 2 \text{ m}$, $A = 0.125 \text{ m}^2$) installed at the area of the GSF, Germany. The calculations were performed using weekly ^2H contents in precipitation and discharge during an eight year period. The fraction of preferential flow directly appearing in the outflow within one week, varied between 17% and 30%. The amount was practically independent from the texture and flow rates. The crucial parameter influencing the fraction of preferential flow was found to be the saturated hydraulic conductivity (K_s). The vulnerability diagrams yielded different patterns for all soil materials depending on the mean water content and the saturated hydraulic conductivity. Coarser material with low mean water content and high K_s showed a short mean transit time for the matrix flow (about 10 weeks) and mean preferential flow equal to or higher than 20%. Finer sand with lower K_s and higher mean water contents resulted in mean transit times of approximately 30 weeks and preferential flow of about 20%.

1. INTRODUCTION

The determination of heterogeneous transport processes in the unsaturated zone is very important for groundwater protection. However, considering heterogeneity of soil structure or preferential flow paths there is no satisfactory quantitative analysis of water fluxes in the unsaturated zone. To develop an adequate model, for heterogeneous medium it is necessary to perform long-term experiments with ideal tracers, such as environmental isotopes (e.g.: ^3H , ^2H , ^{18}O) which were successfully applied for solving different problems in hydrology [1–8]. In the present study such environmental isotopes and hydrological datasets were used to estimate the amount of preferential flow and to quantify the heterogeneity of water transport in the unsaturated zone of seven sandy lysimeters [9].

2. MATERIAL AND METHODS

The lysimeters were homogeneously filled with common soils from Bavaria ranging from quartz and tertiary sands (here referred to as finer material) to quartz and fluvioglacial gravels (here referred to as coarser material). Detailed information about the soil materials and experimental setup is given in Maciejewski et al. [3]. During an eight year observation period

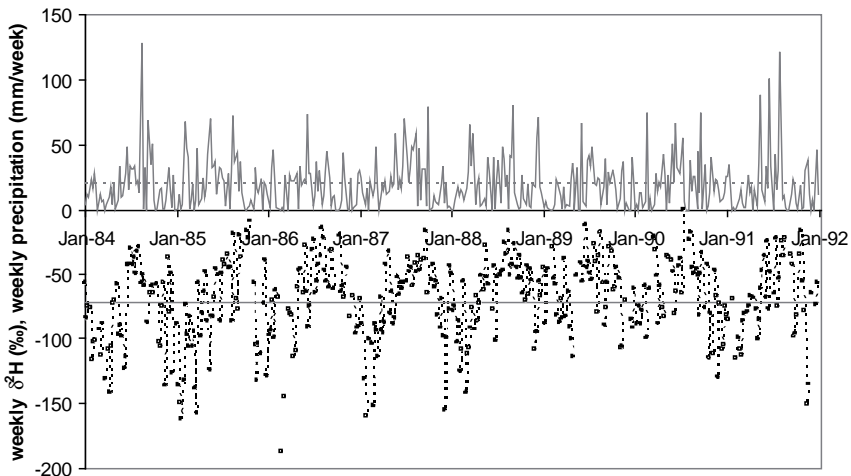


FIG. 1. Weekly precipitation amounts (positive values, solid line) and the corresponding deuterium ratios (negative values, dashed line) of the observation period at the GSF lysimeter research area in Neuherberg, Germany.

QUANTIFICATION OF THE HETEROGENEITY IN WATER TRANSPORT

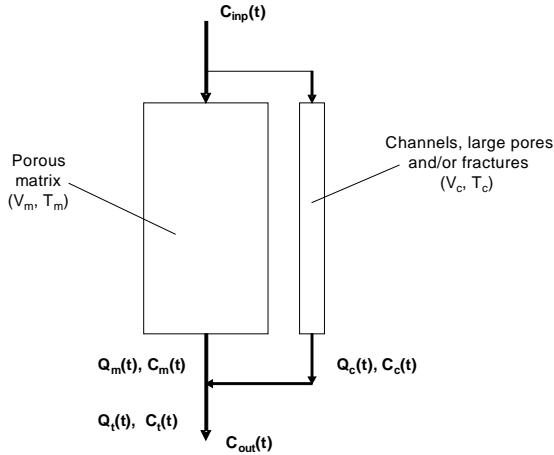


FIG. 2. Conceptual model of water flow through a lysimeter considering preferential and matrix flow, where the input function $C_{inp}(t)$ is transformed into the output function $C_{out}(t)$.

(1984–1991) amounts of precipitation and lysimeters' discharge and deuterium (^2H) contents in precipitation and discharge were measured weekly (Fig. 1). There was no plant coverage to exclude transpiration.

The transport process was described similar to the approach of Maloszewski et al. [10]. Therefore, the water flow through the unsaturated zone is approximated by two parallel systems: matrix and preferential flow paths (Fig. 2). The matrix flow represents the flow through the matrix of the porous material, which includes mobile and stagnant water, while the preferential flow represents the transport through large pores, channels and/or fractures bypassing the matrix flux. To determine transit time distributions a lumped parameter approach was used [11], where the deuterium content in water flowing through the matrix was calculated using the Dispersion Model (DM), which includes both dispersive convective transport in the mobile component and possible diffusive exchange between mobile and stagnant water. The mean transit time of tracer and the apparent dispersion parameter are the two fitting parameters of the Dispersion Model. The transit time distribution of isotopes for preferential flow paths was determined with the Piston Flow Model (PFM). It corresponds to the convective transport for which the transit time is assumed to be within one week. Hence, the weekly deuterium value in precipitation is equivalent to deuterium value of preferential flow in the same week. The fraction of preferential flow compared to the total discharge is then determined by a two component mixing using mass balances of water

and isotope concentrations. Additionally, knowing the transit time distribution functions, their parameters and the mean fraction of preferential water flux calculated for the whole observation time period, so-called vulnerability diagrams were constructed. They can be used to describe the heterogeneity of the soil material and define its vulnerability to pollutants having similar dispersion characteristics as the ideal tracer used in these experiments (worst case calculation).

3. RESULTS AND DISCUSSION

The Dispersion Model applied to the whole observation period yielded mean transit times of deuterium between 9 and 31 weeks for all soils. Whereas lower mean transit times were found in coarser material and higher mean transit times in finer material. Regarding the single calendar years, the transit times varied higher (6–35 weeks) but the relationship to the soil material remained. The apparent dispersion parameter showed the opposite relationship to the soil material. The coarser the material the higher was the apparent dispersion parameter (0.02–0.08). Also here, regarding single calendar years, the dispersion parameter varied higher but stayed in the same range for each soil material. Volumetric mean water contents were calculated from mean flow rates and mean transit times. Over the whole observation period the mean water content varied in all soil materials from 8.4 to 27.3%. Due to short mean transit times

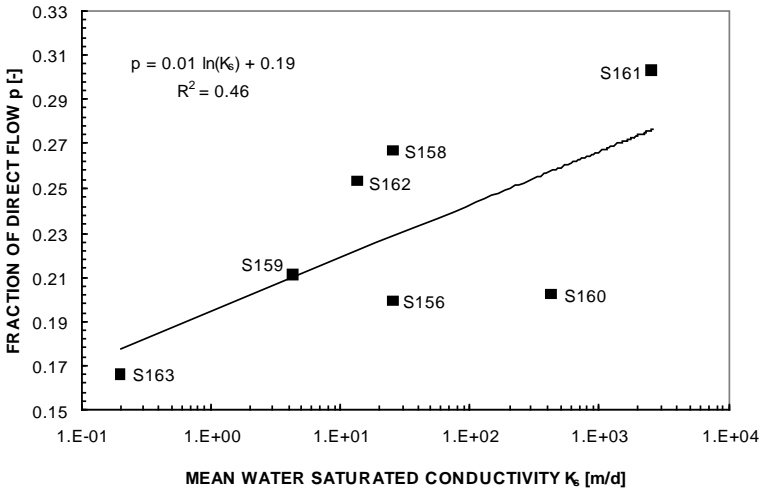


FIG. 3. Relation between fraction of direct flow (p) and the saturated hydraulic conductivity (K_s) found for all lysimeters over the whole observation period.

QUANTIFICATION OF THE HETEROGENEITY IN WATER TRANSPORT

and fast flow velocities, the water content was lowest for coarse material. The calculated mean water content correlates negatively with the fitted apparent dispersion parameter. Higher water contents corresponds to lower apparent dispersion parameters. Similar results were found by Nielsen et al. [12] and Nützmann et al. [13]. In soil column experiments performed under unsaturated conditions they showed that the dispersivity depends on the water content in a power function.

Using the two component mixing approach fractions of preferential flow (p) were calculated for each lysimeter over the whole observation period resulting in mean fractions of preferential flow between 17 and 30%. Here, higher variations of p -values yielded the calibration of the model to each single calendar year. The lowest fraction of the preferential flow (7–9%) was nearly the same for all lysimeters with finer sandy sediments. For coarser material the lowest fraction of preferential flow was nearly two times higher (between 12 and 16%). In general, it was found that the fraction of preferential flow strongly correlates only with the saturated hydraulic conductivity (K_s) of the soil material (Fig. 3). Such relationship was also suggested by Kamra and Lennartz [14]. They stated that preferential flow is more related to soil hydraulic conductivity functions than to soil moisture content or texture. But they also assumed a relationship between infiltration rate and direct flow that was not obvious in the study presented here.

With the knowledge of the mean portion of preferential flow and the transit time distribution functions and their parameters, vulnerability diagrams were constructed for each soil material. Two examples are presented in Fig. 4 representing a coarse material (S161) and a finer sandy soil (S163). Comparing the pattern of these diagrams with soil hydraulic properties it is obvious that the form of the transit time distribution for the matrix flow depends mainly on the mean soil water content. The higher the water content the larger is the mean transit time and the peak of dispersive distribution appears later. The lysimeters containing the coarsest material and having the lowest mean water content showed relatively high fraction of preferential flow ($\geq 20\%$) and the flow through the matrix is comparatively fast with lower variance. Detailed information about the results is given in Stumpp et al. [9].

4. CONCLUSION

The presented study shows that it is possible to estimate and quantify the heterogeneity of the water flux in the unsaturated zone by applying environmental isotope data and a lumped parameter approach. The heterogeneous soil material was approximated in a simple form to contain

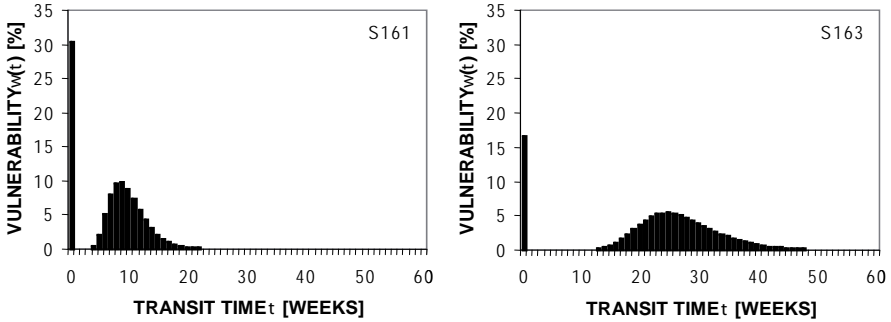


FIG. 4. Vulnerability diagrams calculated for lysimeter filled with Quaternary quartz gravels (left, S161) and Tertiary sand (right, S163).

two flow-paths corresponding to matrix and preferential flow. It was shown that the matrix flow can be satisfactorily described by the Dispersion Model, while the preferential flow lends itself to the Piston Flow Model. The model applied to deuterium contents observed in precipitation and lysimeter's discharge allowed separation and quantification of both flow components and their parameters. For the matrix flow it was found that the apparent dispersion parameter negatively correlates with the calculated mean water content. The fraction of preferential flow in the total outflow varied between 17 and 30%. The fractions were practically independent of flow rates (precipitation amount and discharge). The most crucial parameter influencing the amount of direct outflow is the saturated hydraulic conductivity. Creating vulnerability diagrams revealed different patterns that can be explained by the hydraulic properties of the soils and give information about the heterogeneity. Depending on the mean water content and the saturated hydraulic conductivity such diagrams can give an indication of when so-called conservative pollutants and in which amounts will reach the groundwater. This diagram, calculated for different soil materials, can be used as a powerful tool to estimate exposure of a drinking water resource and improve groundwater protection. In future, the proposed method will be applied to other types of soil, especially for more heterogeneous ones also containing silt and clay, to get a better understanding of the heterogeneity of water transport through the unsaturated zone.

REFERENCES

- [1] ABBOTT, M.D., LINI, A., BIERMAN, P.R., $\delta^{18}\text{O}$, δD and ^3H measurements constrain groundwater recharge patterns in an upland fractured bedrock aquifer, Vermont, USA. *Journal of Hydrology* **228** 1–2 (2000) 101–112.
- [2] GAZIS, C., FENG, X., A stable isotope study of soil water: evidence for mixing and preferential flow paths, *Geoderma*, **119** 1–2 (2004) 97–111.
- [3] MACIEJEWSKI, S., MALOSZEWSKI, P., STUMPP, C., KLOTZ, D., Modelling of water flow through typical Bavarian soils (Germany) based on lysimeter experiments: 1. Estimation of hydraulic characteristics of the unsaturated zone, *Hydrological Sciences Journal* **51** 2 (2006) 285–297.
- [4] MALOSZEWSKI, P. et al., Modelling of water flow through typical Bavarian soils based on lysimeter experiments: 2. Environmental deuterium transport, *Hydrological Sciences Journal* **51** 2 (2006) 298–313.
- [5] MCGUIRE, K.J., DEWALLE, D.R., GBUREK, W.J., Evaluation of mean residence time in subsurface waters using oxygen-18 fluctuations during drought conditions in the mid-Appalachians, *Journal of Hydrology*, **261** 1–4 (2002) 132–149.
- [6] O'DRISCOLL, M.A., DEWALLE, D.R., MCGUIRE, K.J., GBUREK, W.J., Seasonal ^{18}O variations and groundwater recharge for three landscape types in central Pennsylvania, USA, *Journal of Hydrology*, **303** 1–4 (2005) 108–124.
- [7] SWENSEN, B., Unsaturated flow in a layered, glacial-contact delta deposit measured by the use of ^{18}O , Cl^- and Br^- as tracers. *Soil Science*, **162** 4 (1997) 242–253.
- [8] VITVAR, T., BALDERER, W., Estimation of mean water residence times and runoff generation by 180 measurements in a Pre-Alpine catchment (Rietholzbach, Eastern Switzerland), *Applied Geochemistry* **12** 6 (1997) 787–796.
- [9] STUMPP, C., MALOSZEWSKI, P., STICHLER, W., MACIEJEWSKI, S., Quantification of heterogeneity of the unsaturated zone based on environmental deuterium observed in lysimeter experiments, *Hydrological Sciences Journal*, in print (2007).
- [10] MALOSZEWSKI, P., STICHLER, W., ZUBER, A., RANK, D., Identifying the flow systems in a karstic-fissured-porous aquifer, the Schneelpe, Austria, by modelling of environmental ^{18}O and ^3H isotopes. *Journal of Hydrology* **256** 1–2 (2002) 48–59.
- [11] MALOSZEWSKI, P., ZUBER, A., Determining the turnover time of groundwater systems with the aid of environmental tracers, 1. Models and their applicability, *Journal of Hydrology* **52** (1982) 207–231.
- [12] NIELSEN, D.R., VAN GENUCHTEN, M.T., BIGGAR, J.W., Water flow and solute transport processes in the unsaturated zone, *Water Resources Research* **22** (1986) 89–108.

- [13] NÜTZMANN, G., MACIEJEWSKI, S., JOSWIG, K., Estimation of water saturation dependence of dispersion in unsaturated porous media: experiments and modelling analysis, *Advances in Water Resources*, **25** 5 (2002) 565–576.
- [14] KAMRA, S.K., LENNARTZ, B., Quantitative indices to characterize the extent of preferential flow in soils, *Environmental Modelling & Software*, **20** 7 (2005) 903–915.

ISOTOPIC AND GEOCHEMICAL IMPACT OF WATER RELEASES FROM THE SIDI SAÂD DAM ON GROUNDWATER IN KAIROUAN PLAIN (CENTRAL TUNISIA)

S. BELHADJ SALEM, N. CHKIR, K. ZOUARI

Lab. RadioAnalysis and Environment,
National School of Engineering,
Sfax

R. BEJI

Regional Direction of Water Resources Management,
Kairoun

Tunisia

Abstract

Kairouan plain, big endorheic sedimentary basin of 3000 km², contains the most important aquifer of Central Tunisia. The importance of this aquifer is due first to its groundwater reservoir dimension, and then to the high recharge rates by the main wadis (Zeroud and Merguellil) floods and by direct rainfall infiltration. However, since the building of the great dam of Sidi Saâd on oued Zeroud to protect the plain against flooding, natural recharge decreases. Even if regulated dam releases are carried out, a regular depletion of water level is observed due to over exploitation by high anthropic needs. Geochemical and isotopic studies have been conducted in order to quantify the efficiency of artificial recharge. A short time-interval sampling campaign (15 days) has been carried out during the dam release in May 2005 in order to follow up the impact of dam water, whose geochemical and isotopic signatures are well identified on groundwater characteristics.

1. INTRODUCTION

The plain of Kairouan is located in Central Tunisia. The studied zone is limited to the north by the Drâa Affane and Merguellil basin, to south by sebkhet Chrita and Mechertat, to east by sebkhet Kelbia and to west by the mountain chain of Siouf and Cherahil (Fig. 1). The climate of the zone is semi arid with a hot dry summer and a cold wet winter. This aridity increses toward

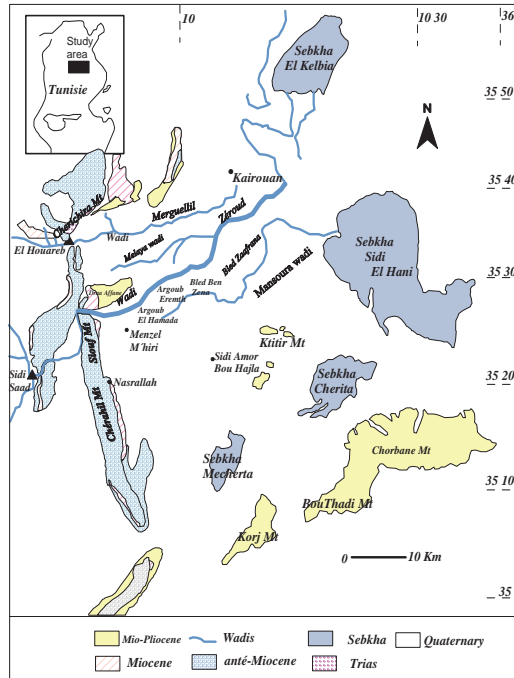


FIG 1. Location map and hydrographic network

the east and the south of the plain. Annual rainfall ranges from 200 to 500 mm but are marked by significant annual and interannual irregularities. Annual evaporation average around 1720 mm while annual mean air temperatures range between 14°C and 20°C.

Even if it is crossed by two important wadis Zeroud and Merguellil, this plain remains known by the scarcity of its perennial water resources. However, the plain constitutes one of the most developed agricultural area of Tunisia thanks to groundwater resources. The aquifer system underlies a 3000 km² area with renewable resources estimated at 44 Mm³ but the exploitation exceeds this potential. The selected site is characterized by an alluvial aquifer known as the largest aquifer system in Central Tunisia. The installation of two dams, Sidi Saad and El Houareb respectively on wadis Zeroud and Merguellil, has greatly disturbed natural surface water flows and has stopped the recharge of the aquifer which was mainly ensured by infiltration from the wadis. This fact has led to a generalized fall of water levels averaging around one meter per year and enhanced by increasing exploitation of groundwater. In order to stop the lowering of the water levels and ensure groundwater resources for farmers'

needs, several campaigns of artificial recharge are carried out through regulated water releases from Sidi Saâd dam.

This study focus on various issues concerning the efficiency of the release campaign of May 2005. We attempt to identify and follow up the response of the aquifer in relation with the released volume in order to assess its influence on groundwater quantity and quality. We base the study on water tracing by stable isotopes (^2H , ^{18}O) while radioactive isotopes (^{14}C , ^3H) have been used to evaluate water residence time and to better characterize hydrodynamic parameters of the aquifer system.

2. GEOLOGY AND HYDROGEOLOGY

The plain of Kairouan corresponds to a vast Quaternary sediments filled basin crossed by the two large wadis Zeroud and Merguellil [1]. The Zeroud basin, in the southern part of the plain of Kairouan, is a part of the Central Atlas, marked by folded lower Cretaceous structures in NE-SW direction [2].

According to the geological map (Fig. 1), no triassic formations outcrop on the Zeroud basin except in the northern part of the plain on Jebel Cherichira. Oldest outcrops correspond to Cretaceous formations observed on Jebels Siouf and Nara. The Paleocene is completely missing, while Eocene-Oligocene series widely outcrop on Jebel Cherahil and Siouf. The Neogene serie is located in Draa Affane and Quaternary deposits are represented by alluvial and crusts limestones. Sedimentary formations in the Zeroud basin can be subdivided in two groups: old formations represented by Cretaceous limestones formations and Eocene or more recent formations (Miocene and Quaternary), marked by a coarser detrital lithology, lying in discordance on the previous ones.

The studied zone is marked by several faults which present major directions of N90, N80 and N120 and which was active until the Quaternary generating SW-NE anticlinal structures [2].

The plain extends over a length of 80 km from north to south and 30 km from west to east with exploitable resources are estimated around 57 Mm^3 . The plain is a collapsed basin filled of Plio-Quaternary continental detrital deposits and marked by lenticular sedimentation of sand alternated with clays.

Hydrogeologic formations in the basin of Zeroud are of Miocene to Quaternary period. Schematic geological cross sections established within this study highlighted three dominant facies (Fig. 2):

- Sands and gravels corresponding to the permeable formations lodging aquiferous levels.

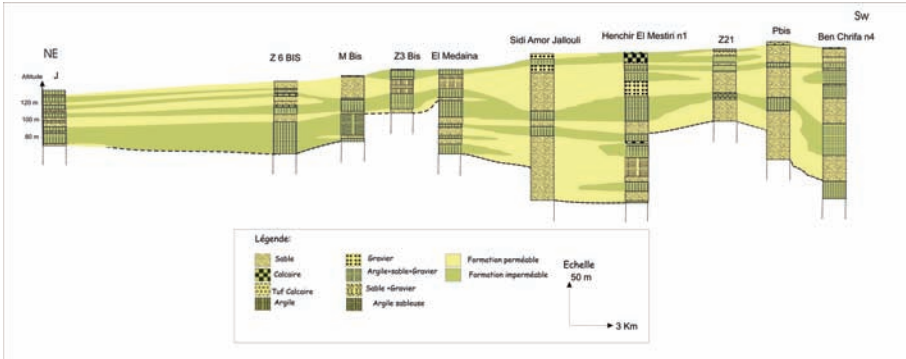


FIG. 2. Simplified geologic cross section through the Zeroud basin from NE to SW.

- Clayey sands and sandy clays corresponding to semi permeable formations.
- Clays and marls corresponding to impermeable formations.

The alternance of sandy horizons of variable thickness with clayey horizons observed in a wide saturated zone allows to estimate the storage capacity of the reservoir to approximatively one billion m³ [3].

The first upper sandy level, hosting the shallow aquifer, is roughly limited to 50 meters of depth and is tapped by several wells. The majority of them are motorised. Several underlying levels, tapping the deep aquifer, are exploited by deeper drillings, up to 500 m of depth. The various superposed aquifer horizons are separated by semi-permeable levels. The number of aquifer levels varies west to east: Under the bed of the wadi, the water level is located at more than 60 m of depth upstream, and less than 10 m downstream. In the central and western parts of the plain, communication and thus mixing between shallow and deeper groundwaters appears to be possible.

3. HYDRODYNAMIC AND HYDROCHEMICAL ASPECTS

Piezometric levels of the aquifer of the Zeroud basin have been mapped for the situation of water table in June 2005 (Fig. 3a) based on 22 piezometers spread over the basin. Groundwaters flow from the surrounding reliefs to the endorheic depression of Sebkhet El Kalbia. In the west, water levels are located at a depth of about 110 m of but decrease eastward to 80 m near Zaafrana Village. In the Argoub Eremth area, isolines highlight the contribution of Zeroud wadi in the recharge of the aquifer.

ISOTOPIC AND GEOCHEMICAL IMPACT OF WATER RELEASES

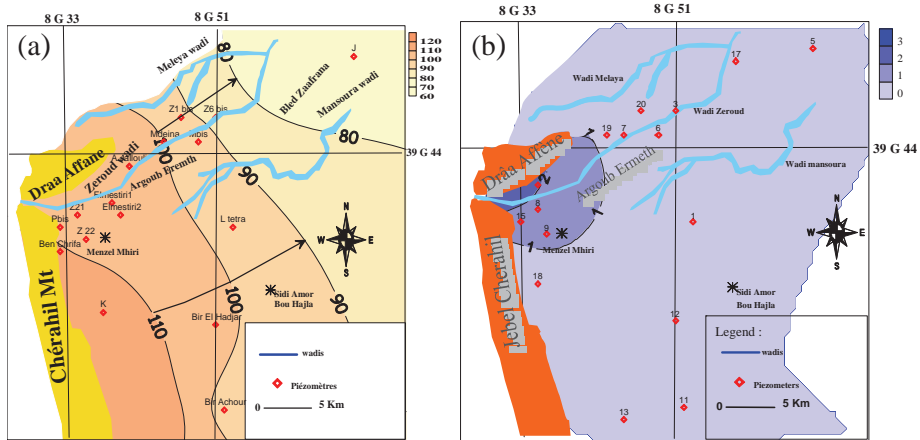


FIG. 3. (a) Potentiometric map of Zeroud basin — June 2005; (b) Water levels increase after May 2005 releases.

Mapping maximum increases of water levels during the release campaign of May 2005 (Fig. 3b) shows that the rise of the piezometric surface has affected all piezometers but with various ranges:

- A first area is characterized by a water level rise exceeding three meters and concerning the piezometers located near the site of release Sidi Salah;
- A second area, in the central part of the basin, shows an increase of the water level ranging between 1 and 3 meters.
- A third part downstream the basin with an increase less than 1 meter and even with no increase related to the long distance which separates the piezometers from the site of release.

Groundwaters of the Kairouan plain are grouped according to two chemical facies (Fig. 4):

- The first group of waters corresponds to the aquifer hosted in Mio-Plio-Quaternary formations with a sulphate-chloride-sodium facies. These groundwaters are characterized by lower capture depth and higher salinity than those located upstream the basin of Zeroud.
- The second group of water corresponds to the majority of groundwaters, characterized by very heterogeneous total mineralization, with values averaging around 2000 mg/L. However, some points, located near the bed of the Zeroud wadi, upstream of the basin, are defined by the lowest salinities and present chloride-sulphate-calcium-magnesium facies which

correspond to the dam water facies. Consequently, these waters seem to be influenced by the Zeroud wadi water and by water released from the dam of Sidi Saad.

The chemical signature of the Zeroud basin groundwaters has been followed up during the release campaign of May 2005 (Fig. 5). In December, at the end of the release campaign, almost all groundwaters present similar facies

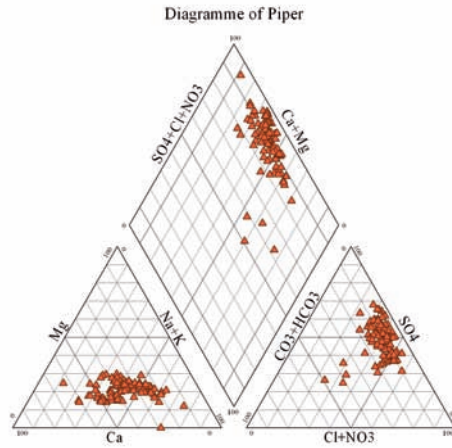


FIG. 4. Chemical facies of groundwaters of the Zeroud basin

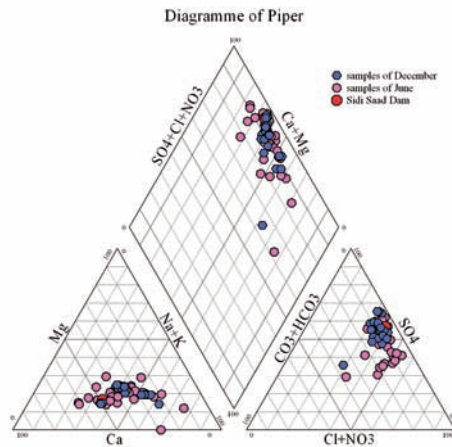


FIG. 5. Variation of chemical facies of the Zeroud basin groundwaters under the influence of water releases from the Dam of Sidi saâd.

ISOTOPIC AND GEOCHEMICAL IMPACT OF WATER RELEASES

less calcium but more sodium and thus close to surface water and particularly to those of Sidi Sâad dam. Consequently, we can suggest that, given a volume of 13 Mm^3 and a flow of $1 \text{ m}^3/\text{s}$, water released from the dam needs at least five months to reach the aquifer.

4. ISOTOPIC STUDY

The first step was to define the stable isotopic signature of dam water in order to identify its influence on groundwaters. Therefore, Sidi Sâad dam waters have been monthly sampled and analysed. Stable isotopes values range between -0.84 to -2.08 ‰ for oxygen 18 and between -9.3 and -14.9 ‰ for deuterium, indicating the effect of evaporation. Even if stable isotopes contents show seasonal variations, they remain the same range and we conduct our study with mean values: -1.25 ‰ for oxygen-18 and -11.41 ‰ for deuterium.

The average composition of groundwater is about -5.35 ± 0.33 ‰ for oxygen 18 and -34.6 ± 2.96 ‰ for deuterium [4]. The stable isotope diagram (Fig. 6) shows that the most enriched shallow groundwaters are in the northeastern part of the basin and along the Zeroud wadi confirming a recent recharge taking place on surrounding reliefs and mainly by wadi infiltration. Almost all points of the deep aquifer show depleted stable isotopes contents suggesting their relatively old origin. For this deep aquifer, enriched groundwaters extend from the upstream part of the basin to the Argoub er Remth and Abida Village

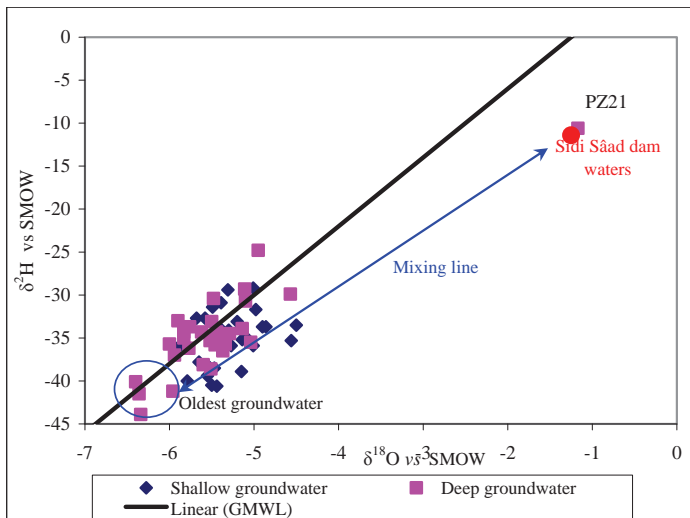


FIG. 6. Stable isotopes diagram for groundwaters of the Zeroud basin

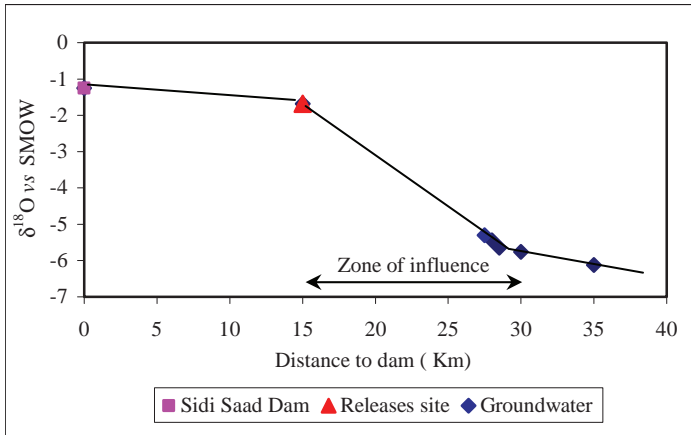


FIG. 7. Isotopic influence of dam water on groundwaters

areas, then a depletion of stable isotopes contents is observed downstream the basin. In the central part of the basin, deuterium excess values are higher what confirms that the recharge has probably took place under wetter conditions than currently.

Surface waters are isotopically the most enriched, as far as moving from the dam waters releases site, groundwaters become more and more depleted in stable isotopes (Fig. 7). This is due to a decrease of the influence of infiltrated dam water and we can estimate that such an influence zone spreads over a length of about fifteen kilometers beyond of which oxygen-18 contents remain constant and thus indicate that groundwater are no more influenced by dam waters.

This recharge process is also confirmed by tritium contents (Fig. 8) and carbon-14 activities (Fig. 9), we can distinguish three water types:

- Water which tritium contents and carbon-14 activities trend to zero, relatively depleted on stable isotopes and corresponding to paleo-water sampled from the deep aquifer, most of these groundwaters are located downstream the basin
- Water not affected by evaporation and recently infiltrated which show variable but significant carbon-14 activities and tritium contents and oxygen-18 values ranging around -5.5‰ vs VSMOW, these waters are sampled from the deep as well as from the shallow aquifers, and are mainly located in the central part of the basin;
- Recent waters marked by an important evaporation so by enriched oxygen-18 values and high carbon-14 activities, these groundwaters are

ISOTOPIC AND GEOCHEMICAL IMPACT OF WATER RELEASES

located upstream the basin, nearby the site where dam are waters released and show high tritium contents.

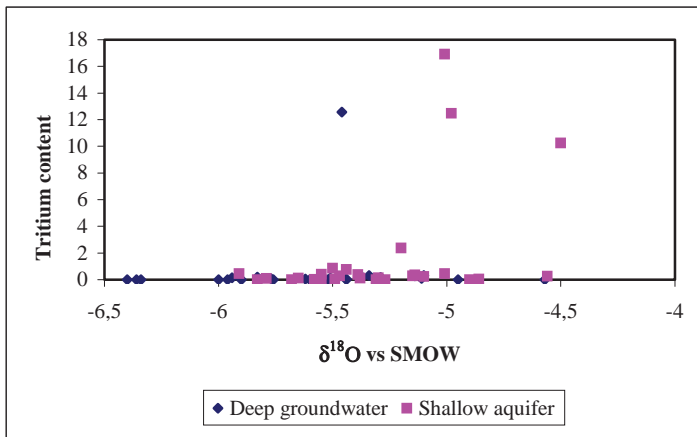


FIG. 8. Relationship between oxygen 18 and tritium for the groundwaters of the Zeroud basin

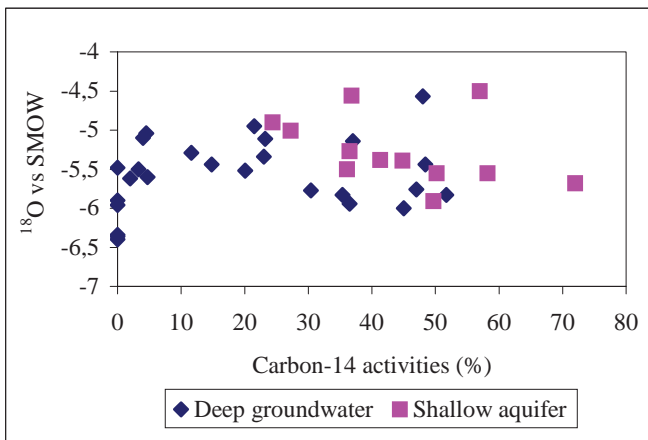


FIG. 9. Relationship between $\delta^{18}\text{O}$ and ^{14}C activities of groundwater of the Zeroud basin.

5. CONCLUSION

Geochemical and isotopic tracing of the Zeroud basin groundwaters response to the water dam releases of the campaign of May 2005 shows that the impact of the artificial recharge is quite low and located close to the site of release. However, we have proven that the affected area is not limited to the area where water level increases, but extends beyond it. Indeed, isotopic fingerprint of evaporated dam waters remains significant up to a distance of 15 km far from the site of release. So, even if the regulated artificial recharge is not enough to compensate the drop of piezometric level over the Zeroud basin, it contributes to slow down this drop and to reduce the effect of summer, dry climatic conditions.

The natural tracing enabled us to conclude that the volume of released waters during this campaign (13 Mm³) is not sufficient to generate a clear response of the aquifer. Further detailed investigations will be carried out during future releases in order to better define various mechanisms taking place in the unsaturated zone and governing the efficiency of artificial recharge.

REFERENCES

- [1] CASTANY, G., Etude géologique de l'Atlas tunisien oriental (1951).
- [2] BEDIR, M., Mécanismes géodynamiques des bassins associés aux couloirs de coulissements de la marge atlasique de la Tunisie, Séismo-stratigraphie, Séismo-tectonique et implications pétrolières, Thèse de Doctorat es-sciences – Fac. Sciences de Tunis (1995).
- [3] HELLER, P., Structure profonde du Sahel Tunisien-Interprétation géodynamique, Thèse de 3ème cycle – Fac. Sciences(1983).
- [4] JERIBI, L., Caractérisation hydrochimique et isotopique des eaux du système aquifère du bassin de Zéroud (Plaine de Kairouan, Tunisie Centrale, Thèse de Doctorat, 3ème Cycle. Fac. Sciences de Tunis (2004).

HYDROCHEMICAL AND ISOTOPIC STUDY OF AL-MOUH SABKHA EVAPORATIC SYSTEM (SYRIA)¹

B. ABOU ZAKHEM, R. HAFEZ
Atomic Energy Commission of Syria (AECS),
Damascus, Syrian Arab Republic

Abstract

Estimation of evaporation rate through unsaturated zone in Al-Mouh sabkha, was done by applying the isotopic model, the mixing ratio between the shallow groundwater and the deep groundwater of Upper Cretaceous aquifer without and with an extensive evaporation process accompanied by precipitation of mineral phases in the sabkha. In this study, the isotopic enrichment peak is determined at a depth of 12 cm for $\delta^{18}\text{O}$ and $\delta^2\text{H}$, that is caused by evaporation through the unsaturated zone. The main evaporation front is located between the surface and a depth of 45 cm. The lower part of the unsaturated zone profile is prone to the capillary effect, where an upward vertical groundwater movement is found. The amount of evaporated water through the unsaturated zone in the sabkha was estimated about 18 Mm³/y using the Barnes and Allison model. The mixing ratio in the sabkha was evaluated using Hydrowin and Netpath programs; it was about 15–20% from surface water and 80–85% from deep groundwater of Upper Cretaceous artesian aquifer. The mixing with extensive evaporation process and precipitation of mineral phases as calcite, dolomite then gypsum and anhydrite, finally, halite, chloride and H₂S gas, that causes a high salinity (100 g/L) of residual water in the sabkha assuming that all the surface water is evaporated completely.

1. INTRODUCTION

Al-Mouh sabkha is located in the central part of the Syrian Arab Republic between 34° latitude, 35° North and 38° latitude, 39° East, in the south and south eastern part of Palmyra city. The sabkha has 24 km length and 10 km width, the total area is about 240 km² and is located at an altitude of about 370 m a.s.l., which is the lowest part in Palmyra region and represents the discharge point for all the surface water and major part of groundwater. It is an evaporative

¹ This study was performed in the co-operation with IAEA on the regional project RAW/8/002 entitled “Isotope hydrology and water management”.

system that causes salt concentration, and where the water type is generally sodium chloride and the salinity reaches 200g/L.

The General Company of Hydraulic Studies (GCHS) has estimated, by classical hydrological method the amount of water loss by evaporation in the sabkha was about $58.2 \times 10^6 \text{ m}^3/\text{y}$ [1]. The Arab Center for the Studies of Arid Zones and Dry Lands (ACSAD) use $62.2 \text{ M m}^3/\text{y}$ for the mathematical modeling of Al Mouh sabkha basin [2] Geyh 1995 [3] working in co-operation with the ACSAD estimated the amount of water loss in sabkha about $0.48 \times 10^6 \text{ m}^3/\text{y}$ that depends on the evaluation of the velocity of groundwater from the Anti-Lebanon recharge area to the sabkha along the Palmyrian chain and Al-Daw basin, and on the transit time for this distance using carbon-14 method.

The aim of this study is to determine the discharged water volume loss by evaporation through the sabkha using Barnes and Allison model (1983) [4], to study the water movement in the unsaturated zone and to estimate the mixing ratio between the surface water and groundwater without and with evaporation and precipitation of mineral phases in the sabkha. Soil profiles were obtained in the unsaturated zone and water samples from deep and shallow groundwater were collected for this purpose. The procedures of extracting water from soil samples under complete vacuum as it is described by [5–9]; the isotopic analyses for $\delta^{18}\text{O}$ and $\delta^2\text{H}$ were performed in the International Atomic Energy Agency (IAEA) laboratory in Vienna. The grain size distribution, moisture content measurements and the mineral analyses using X-Ray diffraction were performed in the (AECS) laboratory. Fig. 1 presents the geological map, groundwater samples and sites where soil profiles were collected.

2. GENERAL BACKGROUND

The area is under a dry climate where the mean annual precipitation is around 120 mm in Palmyra city. The rain occurs during winter (November–April) and the rest of the year is dry. The potential evapotranspiration is about 3162 mm/y in Palmyra city [10].

The Jurassic formations partly outcrop in the central part of the south of the Palmyrian mountain chain, and are composed of dolomitic rocks with some clay layers. The Cretaceous formations are forming most of the southern Palmyrian mountain chain. Upper Cretaceous sediments are formed by marine limestones, while the Maastrichtian is presented by very thick marl and clayey marl layers. The Paleogene formations outcropping at Al-Arak hill consist of marl and phosphate marls and clay limestone, the continental Neogene is exposed towards the East and South of Al-Muoh sabkha depression and consists of conglomerates with continental sand and some evaporites. The depression

HYDROCHEMICAL AND ISOTOPIC STUDY OF AL-MOUH SABKHA

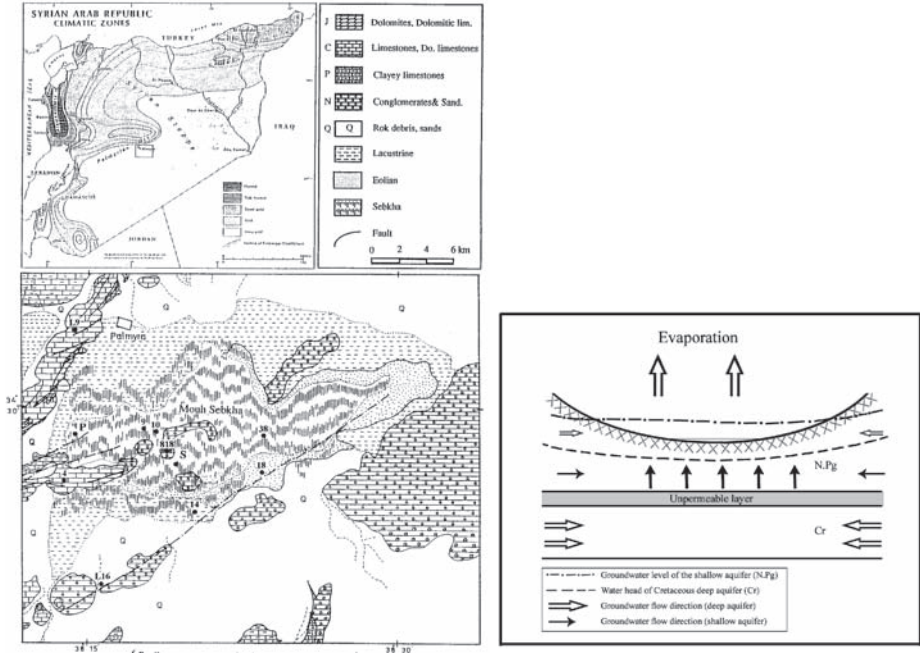


FIG. 1. Geological map and samples location [11] and schematic cross section.

of Al-Mouh sabkha is filled with modern Quaternary deposits which resulted from rock debris from eroded mountains and hills surrounding the sabkha in the North and North West [10–12] (Fig.1).

According to GCHS there are two main aquifers; the Upper Cretaceous confined aquifer and Paleogene, Neogene and Quaternary shallow aquifer.

3. RESULTS AND DISCUSSION

The profile P is located in the western part of the sabkha with 380 cm depth and represents the unsaturated zone in the margin of the sabkha. The clay ratio has 15% in average and could reach 25% near the surface, the fine loam dominates in the profile, has a value between 30–80%, with 55% in average. The coarse loam presents 5%, while the sand and gravel presents the remaining part, 25% in average. The variation of sand and gravel fractions in the upper part and with depth in the profile reflect the importance of evaporites (Fig. 2). The result of mineral analyses shows there is 35% calcite and dolomite in the soil, that reflect the carbonate composition of rocks outcropping in the Palmyrian

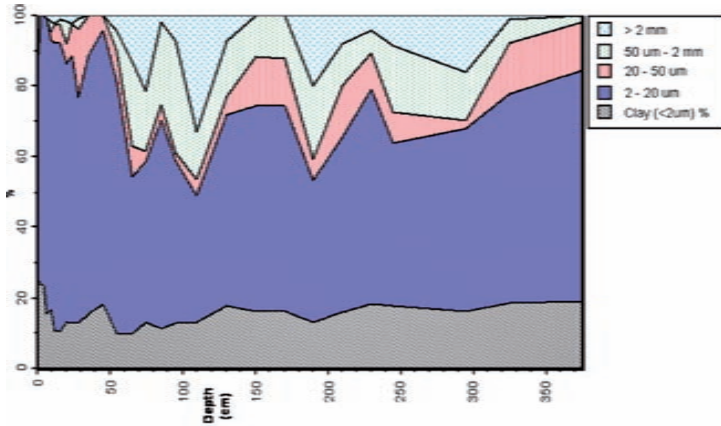


FIG. 2. Particle size (Profile P).

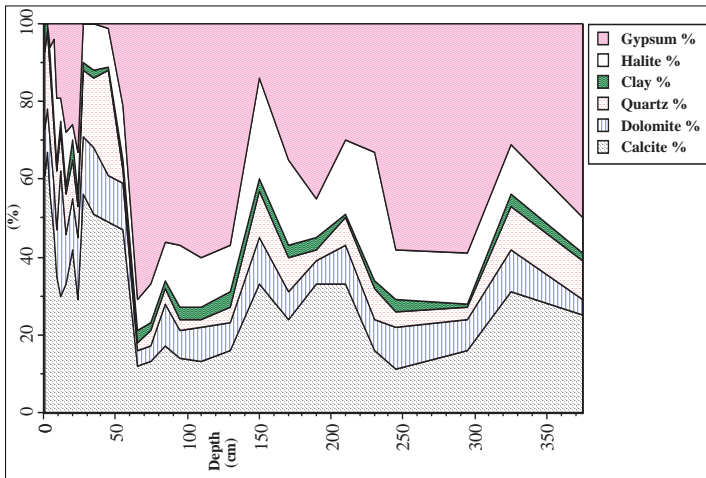


FIG. 3. Mineral analyses by X-Ray diffraction (Profile P).

chain. The 5–15 % of quartz indicate the importance of aeolian erosion. There is 5% of clay in the profile while the gypsum and halite vary between 20 and 80%, in average 50% which reflect the role of sabkha as an evaporatic system and the evaporation rate in respect to the climatic variations (Fig. 3).

The isotopic values vary due to three factors when the soil water moves through the unsaturated zone caused by evaporation [13–16]:

- (1) Vapour diffusion in the upper part of the profile where gas is the dominant phase;
- (2) Downward diffusion of heavy isotopes where liquid is the dominant phase;

HYDROCHEMICAL AND ISOTOPIC STUDY OF AL-MOUH SABKHA

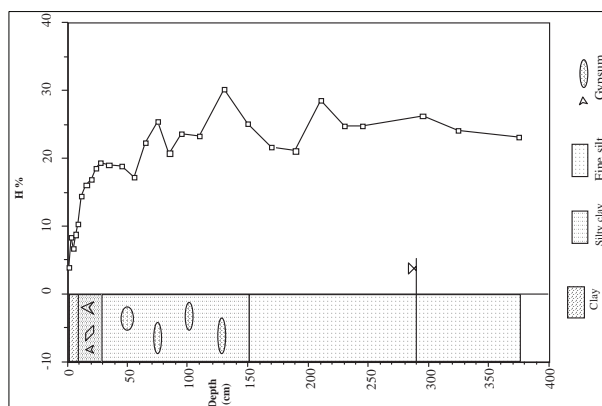


Fig. 4. Lithology and moisture content (Profile P).

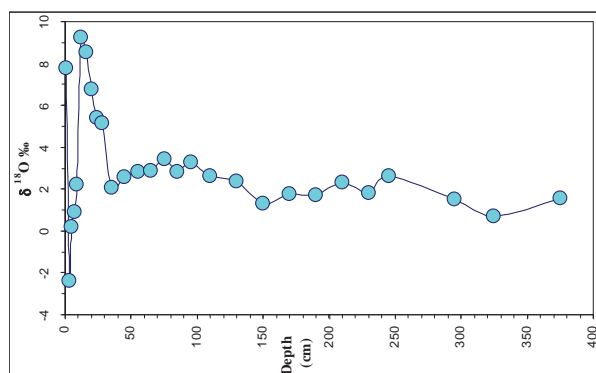


Fig. 5 Variation of $\delta^{18}\text{O}$ with depth (Profile P).

- (3) Isotopic enrichment related to the temperature, relative humidity of the air, isotopic content of water vapor and the isotopic ratio of groundwater.

Profile P has sandy, fine silty and clay soil with some centimetric gypsum crystals and then it becomes very fine loam causing the capillary effect. The moisture content is 4% at 1 cm depth and then it increases up to 20% at a depth of 28 cm, and reaches the saturation level 30% at 130 cm depth. It has the value of 26% in average till the saturated zone at 375 cm (Fig. 4). It is observed that the fine soil in this profile is very wet because of the capillary effect.

Isotopic enrichment peak is located at 12 cm depth where $\delta^{18}\text{O} = 9.26\text{‰}$, $\delta^2\text{H} = 12.5\text{‰}$, this shallow peak related to the soil texture, it can be divided into two parts (Fig. 5, 6):

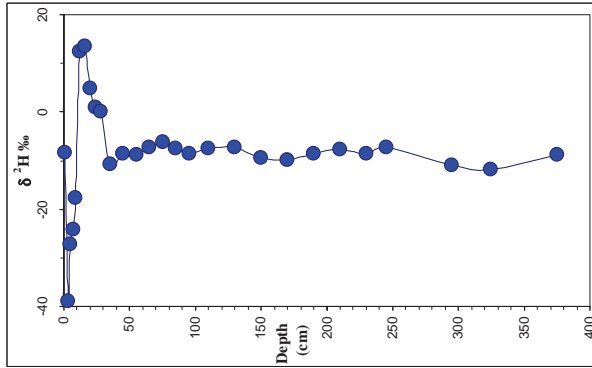


FIG. 6. Variation of $\delta^2\text{H}$ with depth (Profile P).

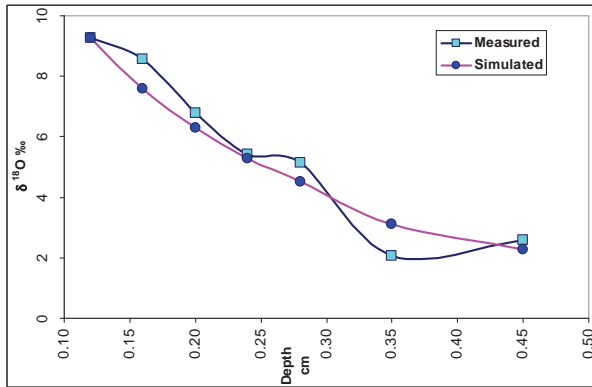


FIG. 7. Evaporation model (Profile P).

- (1) The upper part, from 3–12 cm; the water movement in the vapor phase is dominant, at 3 cm depth the isotopic content is $\delta^2\text{H} = -38.9\text{‰}$, $\delta^{18}\text{O} = -2.37\text{‰}$ while at 12 cm is $\delta^{18}\text{O} = 9.26\text{‰}$, $\delta^2\text{H} = 12.5\text{‰}$.
- (2) The lower part, from 12–375 cm; water movement in liquid phase is dominant. The isotopic contents decrease rapidly till 35 cm depth where $\delta^{18}\text{O} = 2.07\text{‰}$, $\delta^2\text{H} = -10.7\text{‰}$ and at 375 cm has the content $\delta^{18}\text{O} = 2.64\text{‰}$, $\delta^2\text{H} = -12.3\text{‰}$, that present the isotopic contents of saturated zone. The main evaporation front is located between 0–45 cm depth, however, the lower part of profile has minor isotopic variations due to the capillary effect.

HYDROCHEMICAL AND ISOTOPIC STUDY OF AL-MOUH SABKHA

The relation between $\delta^{18}\text{O}$ and δD (Fig. 8) are distributed on two main evaporation lines as follows: samples at less than 45 cm depth, $\delta^2\text{H} = 4.1 \times \delta^{18}\text{O} - 25.3$ and samples at more than 45 cm depth, $\delta^2\text{H} = 1.5 \times \delta^{18}\text{O} - 11.9$. On this plot the following points could be noticed:

- (1) The first point, n°.1, is shifted because of new rain event in the previous week of sampling collection.
- (2) Points from 2–5, till 12 cm depth, present the feeding effect of precipitation and runoff that evaporated completely afterwards.
- (3) Points from 6–12, from 12–45 cm depth, present the maximum evaporation that is linked to precipitation and the upward movement of deep groundwater.
- (4) Points from 45–375 cm depth are located very close to each other on a line with 1.5 slope because of vertical mixing caused by the capillary effect in the sabkha's soil.

Estimation of evaporation rate: Barnes Allison [4] developed a mathematical model describing the isotopic profiles in the unsaturated zone related to the evaporation rate. The following equation describes the lower part of profile where the liquid phase of water is dominant:

$$(\delta_i - \delta_i^{\text{res}}) = (\delta_i^{\text{ef}} - \delta_i^{\text{res}}) \exp [-f(z) \times (z_i)^{-1}]$$

$$f(z) = \theta \int dz (\theta)^{-1} \quad f(z): \text{ is a function of depth } z$$

$$z_i = \theta \tau D_i^1 (E)^{-1} \quad z_i: \text{ is the characteristic length}$$

$[-1(z_i)^{-1}]$: is the slope of the linear equation:

$$\ln (\delta_i - \delta_i^{\text{res}}) \times (\delta_i^{\text{ef}} - \delta_i^{\text{res}})^{-1} \text{ vs } f(z)$$

δ_i	Isotopic content at depth z (i is $\delta^{18}\text{O}$ or $\delta^2\text{H}$)
δ_i^{res}	Isotopic content of groundwater reservoir
δ_i^{ef}	Isotopic content of evaporation front (peak)
τ	Tortuosity
θ	Volumetric water content
D_i^1	Isotopic diffusion coefficient in liquid phase
E	Evaporation rate

In this study the lower part of profile is located between 12 cm and 45 cm depth where the isotopic enrichment has an exponential shape (Fig. 7). After

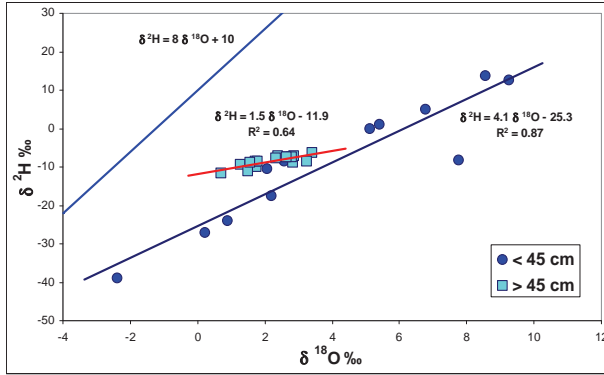


FIG. 8. Correlation between $\delta^{18}O$ and δ^2H (Profile P).

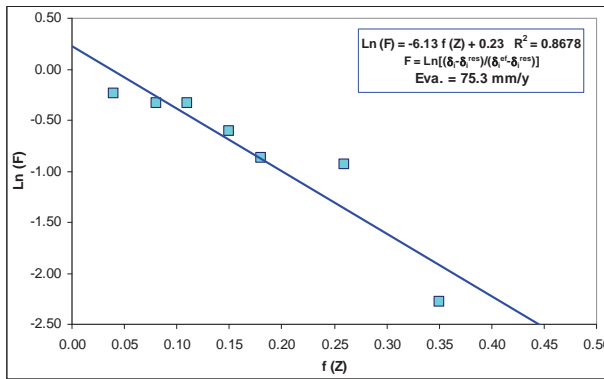


FIG. 9. Correlation between $\ln(F) / f(Z)$ (Profile P).

45 cm depth the isotopic content is affected by the capillary effect which contributed on the evaporation and mixing in the lower part.

Fig. 9 presents a linear relationship between $\ln(F)$ and $f(Z)$, showing the calibration of this model, the mean effective evaporation rate calculated from the model is 75.3 mm/y. As the sabkha has 240 km², the mean evaporated volume through unsaturated zone from the sabkha is:

$$240 \times 10^6 \times 0.0753 = 18 \times 10^6 \text{ m}^3/\text{y}$$

The mean evaporation water volume from the sabkha is 18 M m³/y, excluding the direct evaporation from surface water during the flood period or from saturated wetlands in the sabkha (salt mashes).

HYDROCHEMICAL AND ISOTOPIC STUDY OF AL-MOUH SABKHA

TABLE 1. CHEMICAL COMPOSITION OF GROUNDWATER SAMPLES OF THE AL-MOUH SABKHA BASIN.

n	Date	Cl ⁻	SO ₄ ⁻	HCO ₃ ⁻	K ⁺	Na ⁺	Mg ⁺⁺	Ca ⁺⁺	pH	T°	∑ ions
L16	7/86	308	340.6	585.6	23.85	214.65	75.6	176	7.2	29	1724.3
L9	7/86	588	620.4	231.8	40.2	361.8	17.92	200	7.45	26	2115.4
L14	7/86	63	105	109.4	9.7	87.75	22	28	7.85	28.5	456.18
4	9/86	455	454.2	475.8	27.32	245.88	112.2	180	7.2	-	1950.4
818	9/86	462	604.7	573.4	39.13	352.1	54	220	7.69	-	2336.7
9 *	9/86	123.37	7.932	0.122	7.161	64.456	2.66	1.68	6.84	-	201.24
10 *	9/86	57.4	3.707	0.085	3.4	30.86	1.486	1.68	6.95	-	98.651
14 *	9/86	3.5	1.047	0.891	0.238	2.149	0.183	0.332	7.55	-	8.430
18 *	9/86	26.95	3.521	0.109	1.636	14.73	0.763	1.222	7.59	-	48.932
38 *	9/86	4.305	1.027	0.122	0.255	2.297	0.207	0.336	7.45	-	8.549
Baida	3/74	19.5	32.6	98	5.9	2.3	3	60	8.4	-	221.3
W.Ab.	4/77	50	869	146.4	7.34	60	34	289	7.6	-	1455.8

Concentration in mg/L and * in g/L

As mentioned previously, the sabkha is considered the main drainage area for all surface water and big part of groundwater, especially the Upper Cretaceous artesian aquifer that causes direct upward water movement through the semi-confined layer on the upper part of the aquifer, or from the hidden faults and cracks in the sabkha, so the sabkha forms a place of mixing zone (estuaries, groundwater upward movement and interstitial water) in the sebkha that finally evaporates from the surface or through the unsaturated zone. A set of representative samples of the main water resources has been selected:

- (1) The surface water drainage in Baida and Wadi Abiad is generally calcium bicarbonate or calcium sulfate as Wadi Abiad caused by the veins form of gypsum and anhydrite dissolution in sedimentary layers in the Neogen formation [17].
- (2) The Upper Cretaceous aquifer is confined and has higher salinity than the surface drainage water (1.5 g/L), this water is generally chloride or

sulfate and calcium or magnesium. The dug well (818) indicates the mixing process in Sabkha. L16 (Sukari artesian well), L9 located to the west of Palmyra city, L14 (Arak well) is located to the North West of the sabkha and L4 (Adiya artesian well) is located to the west of the sabkha.

- (3) The interstitial water that is highly evaporated, has a rather high salinity, more than 100 g/L and has very high chloride and sodium values (wells 38, 18, 14, 10, 9). All these analyses were used to study the mixing process of water group in the Sabkha, with and without, evaporation in addition to solid mineral phase precipitation.

Mixing without evaporation: Hydrowin program was used to study this process where some representative samples of the Upper Cretaceous aquifer were selected (L16, L9), and mixed with surface water from Wadi Abiad to obtain groundwater in the dug well (818) as a typical mixing. The optimized mixing ratio given by this program is 15–20% for Wadi Abiad and 80–85% for groundwater of artesian Upper Cretaceous aquifer.

Mixing with evaporation: Netpath program was used to apply the mixing process with a high degree of evaporation and solid mineral precipitation caused by increasing the concentration in the residual water. Surface drainage water presented by one sample from Wadi Abiad was mixed with groundwater from dug well (818) and compared with the well (9) which presents water of high salinity (100 g/L). This mixing followed by high evaporation with supposed mineral phases in the program; calcite or aragonite and dolomite, then sulphate (gypsum and anhydrite), chloride (halite, magnesium and potassium chloride) and the gaseous phase (H_2S gas well observed in the area). One mixing model was selected among several proposed by the program, with precipitation of mineral phases with high concentration in the residual water in the sabkha as in the compared well, assuming all the coming surface water to the sabkha will evaporated completely.

8. CONCLUSION

- (1) The isotopic enrichment peak for stable isotopes ($\delta^{18}O$, δ^2H) was found at a depth of 12 cm in the unsaturated zone profile that has fine sediments near the surface. Generally, the evaporation front is located between the surface to 45 cm depth. The lower part of profile is affected by the capillary effect characterized by the upward vertical movement of water.
- (2) The relationship between $\delta^{18}O$ and δ^2H shows the distribution of unsaturated zone sample points on two evaporation lines:

HYDROCHEMICAL AND ISOTOPIC STUDY OF AL-MOUH SABKHA

- Evaporation line with 4.1 slope. Samples from a depth lower than 45 cm are distributed on this line presenting the main evaporation zone that is related with the precipitation and runoff in one side, and discharged groundwater from the other side.
 - Evaporation line with 1.5 slope. Samples from a depth larger than 45 cm are distributed very close on this line because of feeding the evaporation system from groundwater by vertical mixing.
- (3) The estimated evaporation rate through the unsaturated zone using the Barnes and Allison model is approximately 18×10^6 m³/y in addition to the direct evaporation from surface water that covers part of the sabkha during the flood periods, and from shallow groundwater (Salt marshes).
 - (4) The mixing ratio was estimated using Hydrowin and Netpath programs, 15–20% from surface water and 80–85% from groundwater which is mainly the upper cretaceous artesian water.

The mixing with high evaporation and precipitation of mineral phases as calcite and dolomite, gypsum and anhydrite, then halite and chloride with H₂S gas will lead to increase the concentration of the groundwater the same as in residual water assuming the input surface water will evaporate completely.

ACKNOWLEDGEMENTS

The authors would like to acknowledge the great support of Prof. Dr. I. Othman the general director of Syrian Atomic Energy Commission (SAEC). Thanks are due to the team lab. at the International Atomic Energy Agency (IAEA), and the Jordanian Water Authority for their assistance in performing the isotopic analyses. We are also grateful to the head of the Geology Department and all colleagues in the Department.

REFERENCES

- [1] SELKHOZPROMEXPORT, USSR, Water Resources Use in the Syrian Desert, Syrian Arab Republic, for pasture water supply scheme, I (2), Moscow (1987).
- [2] ACSAD, Mathematical model of Sabkha Al-Mouh, ACSAD/WS/R-92, Water Resources Division, Damascus, Syria (1998).
- [3] GEYH M.A., BENDER H., RAJAB R., WAGNER W., Application of ¹⁴C-groundwater dating to non-steady systems, Proceeding of the Vienna Symposium, August 1994, IAHS Publ. No. 232 (1995).

- [4] BARNES C.J. ALLISON G.B., The distribution of deuterium and oxygen-18 in dry soil (I Theory). *J. Hydrol.* **60** (1995) 141–156.
- [5] GONFIANTINI, R., FONTES, J. Ch., Oxygen isotopic fractionation in the water of crystallization of gypsum. *Nature* **200** 4907 (1963) 644–646.
- [6] GAUVEA DA SILVA, R., Migration des sels et des isotopes lourds à travers des colonnes de sédiments non saturés sous climat semi-aride, Thèse 3^{ème} cycle, Uni. Paris VI (1980).
- [7] ARANYOSSY, J.F., L'apport des techniques isotopiques à l'étude de la recharge des aquifères sous contraintes techniques et climatiques extrêmes, Thèse d'habilitation, Uni. Paris-sud (1991).
- [8] ZOUARI, K., Etude isotopique et géochimique de l'infiltration naturelle en zone non saturée sous climat semi-aride (sud Tunisie), Thèse 3^{ème} cycle, Uni. Paris XI Orsay (1983).
- [9] YOUSFI, M. et al., Etude isotopique des mouvements de l'eau en zone non saturée sous climat aride (Algérie), Tec.Doc. n° 357, IAEA, Vienna (1985) 161–178.
- [10] KHOURI, J., TAYYIB, H., Study of water resources in Al-Daww basin (Syria), Part I, Hydrometeorology & Hydrogeology, ACSAD/dm/t-36 (1983) 205.
- [11] PONIKAROV, V.P. , Explanatory notes on the geological map of Syria, Scale 1/200 000, sheet I-37-XV(Palmyre) "Technoexport" (1966) 104.
- [12] GHALEB, B., Géochimie des familles U & Th et des terres rares dans le bassin de la Sebkhah AL Mouh, Syrie centrale, Thèse de doctorat, Université d'Aix – Marseille II (1988) 218.
- [13] ALLISON, G. B., The relationship between ¹⁸O and ²H in water columns undergoing evaporation, *J. of Hydrology* **55** (1982) 163–169.
- [14] SONNTAG, C. et al., Laboratory and field experiments on infiltration and evaporation of soils by means of deuterium and oxygen-18, Proc. of final mee. "Stable and radioactive isotopes in the study of the unsaturated zone" IAEA-Tec. Doc.-357, Vienna (1985) 145–159.
- [15] BARNES C.J., ALLISON, G.B., Tracing of water movement in the unsaturated zone using stable isotopes of hydrogen and oxygen, *J. of Hydrology* **100** (1988) 143–176.
- [16] ALLISON, G.B., HUGHS, M.W., The use of natural tracers as indicators of soil-water movement in temperate semi-arid region, *J. of Hydrology* **60** (1983) 157–173.
- [17] RASSOUL AGHA, W., DROUBI, A., Study of water resources in Al-Daw basin (Syria), Part II, Hydrometeorology & Hydrogeology, ACSAD/dm/t-36 (1983) 205.

STABLE ISOTOPES AS INDICATORS OF ECOHYDROLOGICAL COUPLING AT THE WATERSHED SCALE

J.R. BROOKS*, H. BARNARD**, J.J. MCDONNELL**,
R. COULOMBE***, C. BURDICK*

*U.S. Environmental Protection Agency,
NHEERL Western Ecology Division,
Corvallis, Oregon, United States of America

**Oregon State University,
Corvallis, Oregon, United States of America

***Dynamac Corporation,
Corvallis, Oregon, United States of America

Abstract

Ecohydrological coupling at the watershed scale is poorly characterized. While soil-water storage is dynamic and strongly influenced by plants, few integrated tools exist for quantifying the spatial and temporal dynamics and interactions among the major components of the terrestrial hydrologic cycle. We analyzed stable isotopes of oxygen ($\delta^{18}\text{O}$) and hydrogen (δD) in soil water to quantify spatial and temporal changes in evaporation, soil water, tree water and stream discharge isotopic signatures in a gauged watershed in the Pacific Northwest, a region with very dry summers and wet winters. At the end of the wet season, soil-water storage was at its maximum, and plant water uptake occurred primarily from the surface soils. As the dry season progressed, plants relied on deeper soil water, and evaporation decreased. Evaporation resulted in a distinct isotopic signature on tightly bound soil water. Our isotope data indicate that most water taken up by plants was affected by evaporation at some point, including soil water deeper than 30 cm. In contrast, stream water did not show any evidence of an evaporation signature even though discharge rates showed distinct diurnal cycles driven by transpiration. We conceptualize these findings as two separate pools of water held within the soil: one a faster moving pool held at relatively weak soil tension, making it more subject to gravitational transport to streams when more water is added to the system. The other pool is water held under higher soil tensions and has a longer residence time within the soil, and a higher propensity to be taken up by plants.

1. INTRODUCTION

The links between forests and streamflow are poorly understood. Despite hundreds of studies over the past 60 years, fundamental questions of forests' effect on the hydrologic cycle remain unanswered: To what extent does transpiration affect streamflow? Why is transpiration so tightly coupled to soil moisture and climate, whereas, streamflow dynamics are dominated by threshold behavior? Until recently, forest hydrologists have relied solely on the paired watershed approach to evaluate forest influences on streamflow. Results from this black-box approach have been highly equivocal where studies have shown that decreases in forest cover result in increased [1, 2], decreased [1, 3] or no net change in stream discharge [1, 4]. In semi-arid zones where paired watershed approaches are infeasible due to limited streamflow, studies of ecohydrological coupling are more advanced and have shown strong relationships between plant physiology and soil infiltration, run-off obstruction, erosion, groundwater depth and discharge [5]. However, in humid, upland regions dominated by forests, detailed process-based studies that explore the interface between plant physiological function and watershed flowpaths, flow sources, and residence times have not been widely attempted. The objective of this study was to understand the coupling between water reservoirs at the watershed scale and to determine the mechanisms that result in temporal and spatial patterns of mobile and poorly mobile water pools. We focused on water held within the soil at various depths, water within trees and stream water as pools of interest at a well-studied research watershed in western Oregon.

2. STUDY SITE

The study site was located in the H. J. Andrews experimental forest in the western Cascade Range of Oregon (44.2° N, 122.2° W). The climate is maritime with wet, mild winters and dry, cool summers. The mean monthly temperature ranges from 1°C in January to 18°C in July. Precipitation increases with elevation from about 230 cm at 410 m elevation to over 355 cm at 1630 m. The study took place in Watershed 10 (WS10), a 10 ha watershed that was 100% clearcut in 1975. Elevation in WS10 ranges between 425 and 700 m. Data has been collected on streamwater discharge, climate, stream chemistry, vegetation since prior to clearcutting. The watershed is dominated by a uniform vegetation cover of young Douglas fir (*Pseudotsuga menziesii*) approximately 30 years of age. During the summer, stream discharge of the watershed is monitored using a V-notch weir and recorded hourly to capture diel fluctuations. The mean residence time of water in stream discharge was found to be 1.2 years [6].

3. METHODS

In the summer of 2004, water samples for isotopic analysis were collected at 32 locations within the watershed associated with permanent vegetation plots which are randomly distributed throughout the watershed covering the range of elevation and aspect. Samples were collected twice during the year: once at the beginning of the dry season, June 28, 2004 and once at the end of the dry season, 9/14/2004. Unfortunately a 30 mm rain event occurred during the last sampling event, but rain samples were not available for isotopic analysis. At each site, xylem samples were collected from suberized xylem of 3 trees, which reflects soil water from where the trees are withdrawing water since trees do not fractionate water during uptake [7]. Soil samples were collected from 5 depths (10 cm, 20 cm, 30 cm, 50 cm and 1 m, if possible) and were divided into two parts, one for isotopic analysis and another for gravimetric soil moisture. In addition, several stream samples were collected at the weir during the day. Samples for soil moisture were transported to the lab in plastic bags, where they were weighed, dried at 50°C until constant weight. Samples for δD and $\delta^{18}O$ analysis in plant and soil water were collected in glass vials with polyseal cone inserts in the cap and sealed to prevent evaporation. Water was extracted from the plant and soil samples using cryogenic vacuum distillation [8]. Water samples were analyzed for δD and $\delta^{18}O$ on an isotope ratio mass spectrometer (Delta plus, Finnigan, Bremen Germany) interfaced with a high-temperature conversion/elemental analyzer (TC/EA, ThermoQuest Finnigan, Bremen, Germany) located at the Integrated Stable Isotope Research Facility at the Western Ecology Division of the EPA, Corvallis Oregon. All δD and $\delta^{18}O$ values are expressed relative to Vienna-standard mean ocean water (V-SMOW) in ‰

$$\delta D \text{ or } \delta^{18}O = \left(\frac{R_{\text{sample}}}{R_{\text{standard}}} - 1 \right) 1000$$

where R is the ratio of deuterium to hydrogen atoms or ^{18}O to ^{16}O atoms of the sample and the standard V_SMOW. Measurement precision was 2‰ for δD and 0.3 ‰ for $\delta^{18}O$.

Soil depth was measured at each water sampling location using a knocking pole cone penetrometer [12]. The maximum rod length was 3 m so that soils deeper than that could not be measured.

4. RESULTS AND DISCUSSION

Stream discharge for the summer period in 2004 showed a distinct diel cycle (Fig. 1), attributable to daily transpiration of the forest cover [9]. In early July, the diurnal variation was about 20–25% of the flow rate, but increased to over 50% by mid August when flows were at their lowest rate during the dry season. This strong linkage between the vegetation and the streamflow indicated that trees used the same water supply water as stream baseflow. We hypothesized that if this was so, the isotopic signal of water in trees should also be similar to the isotopic signal of water entering the stream, and sampling tree water might give a very good estimate of the spatial variation of water supplied to the stream.

Most tree water samples collected on 6/28/04 fell below the Global Meteoric Water Line (GMWL), indicating that trees were using soil water that had experienced some amount of evaporation since the water fell as precipitation (Fig. 2a). Streamwater samples did not show any evaporated signal nor did some soil water samples collected at 1 m. Interestingly stream water, soil water and tree water all showed unique isotopic signals rather than sharing similar isotopic signals as one might expect since the precipitation input was the same for all pools. Stream water had higher δD values than did soil water or tree water indicating that the dominant source was likely warmer precipitation that would plot higher on the GMWL than colder winter rain/snow. This water source appeared not to undergo any evaporation before it reached the stream.

Water sampled from soil cores at 1 m depth had the lowest isotopic values in both $\delta^{18}O$ and δD , indicating cold inputs with little evaporation. Soil water at

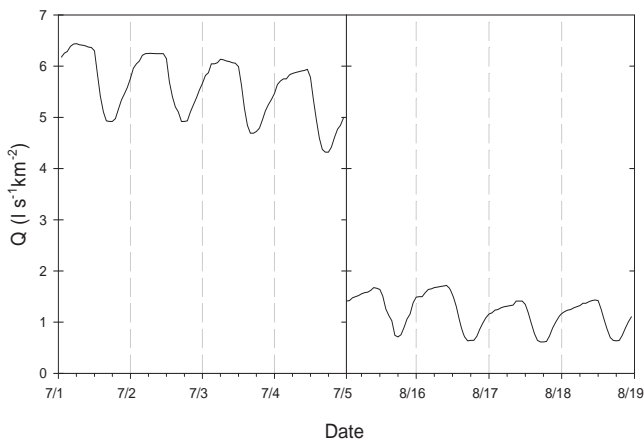


FIG. 1. Flow from HJA Watershed 10 during the early and late summer of 2004.

STABLE ISOTOPES AS INDICATORS OF ECOHYDROLOGICAL COUPLING

10 cm showed the highest evaporation signals. Soil water showed a distinct evaporation signal even as deep as 0.5 m within the soil well below where soil evaporation would be expected to take place. Given the close relationship between transpiration and streamwater discharge (Fig. 1), one might have expected that deep soil water and stream water would be more similar, but deep soil water clearly indicated a colder winter water signal compared to stream water with the soil at 1 m depth averaging -95‰ for δD and -12.5‰ for $\delta^{18}\text{O}$, and streams in June averaging -77‰ for δD and -11.3‰ for $\delta^{18}\text{O}$. These large differences in signals between water bound to soils and stream water indicate that there are stable pools of water within the watershed that may never reach the stream once held by under tension in the soil.

Interestingly, tree water (trees use soil water and do not fractionate water with uptake [7]), did not have the same signal as the soil water, but were distinctly lower in δD than soil water (Fig. 2). The only reasonable explanation for this would be a lag time between recent precipitation inputs and tree water transport to where samples were collected. A major precipitation event occurred two weeks prior to the 6/28/04 sampling, and this warmer summer rain likely did not have time to appear in the xylem water. Our sampled conifers have maximum sap flux velocities of 2–5 m/day [10]. However, this precipitation did mix within the soil water, likely shifting the δD values upward. Thus, the trees represent the pre-event soil water. Another important point is that these differences between pools would not have been found if $\delta^{18}\text{O}$ had been measured alone. This dual isotopic approach has distinct advantages in separating pools when evaporative processes are occurring.

In our second sampling period (9/14/04) following the extended summer drought (and after the first 30 mm rain event of the summer, 1 day beforehand), water pools were generally more enriched in both D and ^{18}O (Fig. 2b, Fig. 3). While the soil samples were much more variable in September compared to June, tree and stream samples were more similar to the soil signal than they had been in June. Soils at 10 cm depth changed the most over the dry summer, increasing in δD and $\delta^{18}\text{O}$ on average by 20 and 3 ‰ respectively, and becoming more evaporated (Fig. 3). In contrast, soils at 1 m depth were very similar between the two sampling events, more so than the stream water or sampled trees. Trees showed less of an evaporated signal overtime reflecting a shift to deeper water sources during the dry summer. However, stream water was more variable with some water samples plotting below the GMWL, thus indicating slightly more evaporation in the signal at the end of the summer.

Significant spatial variation of tree water and soil water isotopic composition were observed on our 6/28/04 sampling date (Fig. 4). The sampled trees were distributed to cover the range of elevation and aspect within the watershed (Fig. 4). In general, soil moisture in the upper 1m was very similar to the mapped soil depth

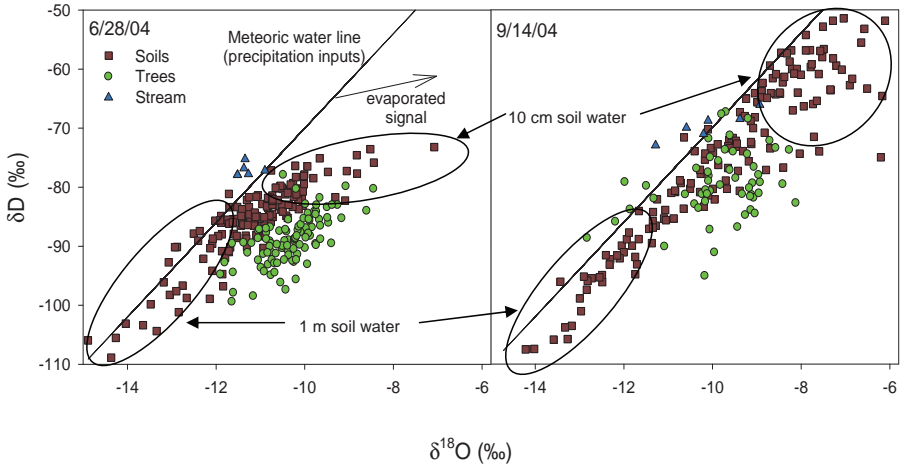


FIG. 2. Water isotope plots for two different dates in HJA Watershed 1. Each point represents a different tree or soil sample from the 32 plots distributed across the watershed, or stream samples from the gauging station. The line is the global meteoric water line, and the arrow is a theoretical evaporation line.

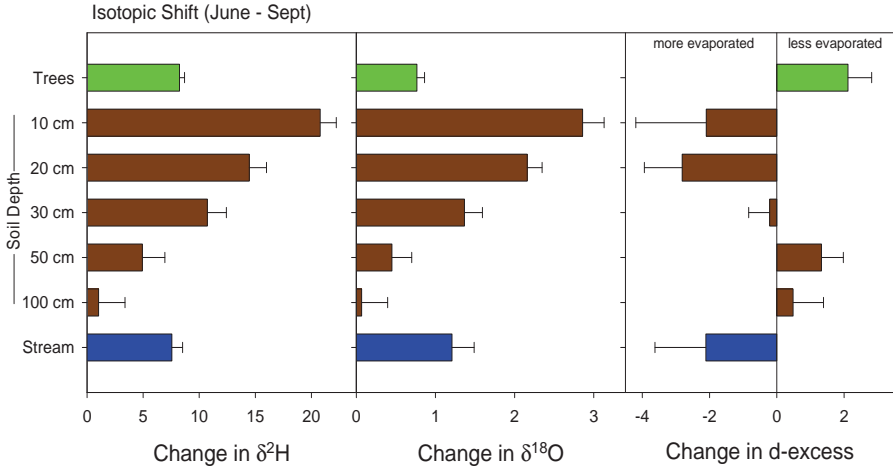


FIG. 3. The isotopic shift from June to September averaged across all 32 sites. The error bars are standard errors

STABLE ISOTOPES AS INDICATORS OF ECOHYDROLOGICAL COUPLING

pattern. The driest upper soils were found in areas with the shallowest soil depth (Fig. 4a,b). Presumably trees in areas with deeper soils accessed deeper water resulted in the upper soils retaining more moisture relative to shallower soils. This hypothesis seems plausible given the pattern of tree water $\delta^{18}\text{O}$ (Fig. 4c). Trees in the deeper soils had water with more negative $\delta^{18}\text{O}$ values than trees in shallow soils, reflected a deeper water source. The $\delta^{18}\text{O}$ of soil water decreased with depth at all locations (data not shown). This pattern with soil depth was likely caused by direct evaporation of soil water from the soil surface which caused enrichment of the surface soil isotopic values. The extent of evaporative enrichment was estimated from the deuterium excess values where samples with a large deviation from the global meteoric water line indicated more evaporation than samples with less deviation (Fig. 2). Highly evaporated soils (those with a large negative deviation from the GMWL) were located primarily on south facing slopes or in the shallow soil region in the lower watershed (Fig. 4d). Isotopic

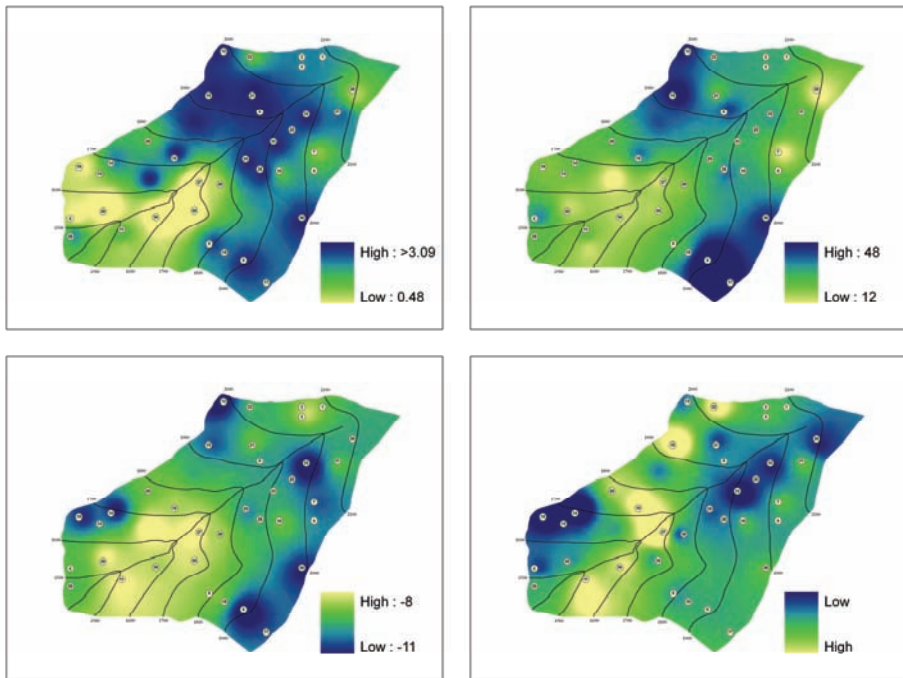


FIG. 4. Maps of WS10 showing the spatial distribution of sample plots, (a) soil depth, (b) gravimetric soil moisture, (c) Tree $\delta^{18}\text{O}$, and (d) soil evaporation as indicated from deuterium excess values for samples collected on June 28, 2004. The dots are the locations of the permanent vegetation plots established in 1973 and monitored every 5 years on average.

shifts for soils at 10 cm depth between June and September were the greatest in the areas with low evaporation and deepest soils, while the evaporated and shallow soils showed less change over time (data not shown), indicating that evaporation over the summer was the greatest in areas of higher surface soil moisture.

Tree water $\delta^{18}\text{O}$ values were most closely correlated with soil moisture in the upper 1 m ($R^2 = 0.34$, $p < 0.001$). Tree water $\delta^{18}\text{O}$ became more negative with increasing moisture soil, which was generally associated with deeper soils as well. However, because we could not measure soil depths greater than 3m, soil depth was not as well correlated with tree water $\delta^{18}\text{O}$ as soil moisture ($R^2 = 0.21$, $p = 0.008$). Since $\delta^{18}\text{O}$ of soil water decreased with depth in the soil, trees with lower $\delta^{18}\text{O}$ water values likely had roots in deeper soils, which would delay the drying of surface soils in those locations [11].

Conclusions: This study examined the coupling between water reservoirs at the watershed scale and quantified the mechanisms that result in temporal and spatial patterns of mobile and poorly mobile water pools. We found that soil water uptake by plants and pools of water within the watershed differed significantly across our small watershed. While a close connection existed between stream flow volume and plant transpiration dynamics (Fig. 1), isotopic data indicated that tree water sources were different from stream water sources (Fig. 2). The disconnect observed between deep soil water and stream water was difficult to explain. Stream water indicated warmer and thus more recent precipitation inputs than did the soil water at 1m, suggesting that flow paths for the recent precipitation did not impact the deep soil water signal. Once soils reach field capacity, soil water pools are stable, and additional water bypasses these pools on its way to deeper reserves used for late-summer stream flow. Tree water does reflect spatial patterns in soil moisture and soil depth. Overall, we conceptualize these findings as two separate pools of water held within the soil: one a mobile pool of water that expressed itself in low tension water and streamflow and the other held under higher soil tension, that is used by plants but does not make its way to the stream. Our future work will search for evaporated water signals in the stream at different times of the hydrologic year. We also plan to examine the $\delta^{18}\text{O}$ of tree rings, which could be a good indicator of historic ecological shifts within watersheds.

ACKNOWLEDGEMENTS

Thanks to Gail Heine, Warren Evans, William Griffis who helped with data collection, water extraction and isotopic analysis, respectively. This document has been reviewed in accordance with U.S. Environmental Protection Agency

policy and approved for publication. Mention of trade names or commercial products does not constitute endorsement or recommendation for use.

REFERENCES

- [1] BOSCH, J.M., HEWLETT, J.D., A review of catchment experiments to determine the effect of vegetation on water yield and evapotranspiration, *Journal of Hydrology* **55** (1982) 3–23.
- [2] CALDER, IR., Water use by forests, limits and controls, *Tree Physiology* **18** (1998) 625–631.
- [3] COSANDEY, C., ANDREASSIAN, V., MARTIN, C., DIDON-LESCOT, J.F., LAVABRE, J., FOLTON, N., MATHYS, N., RICAHRD, D., The hydrologic impact of the Mediterranean forest: a review of French research, *Journal of Hydrology* **301** (2005) 235–249.
- [4] HARR, R.D., MCCORISON, F.M., Initial effects of clearcut logging on size and timing of peak flows in a small watershed in western Oregon, *Water Resources Research* **15** 1 (1979) 90–94.
- [5] HUXMAN, T.E., WILCOX, B.P., BRESHEARS, D.D., SCOTT, R.L., SNYDER, K.A., SMALL, E.E., HULTLINE, K., POCKMAN, W.T., JACKSON, R.B., Ecohydrological implications of woody plant encroachment, *Ecology* **86** 2 (2005) 308–319.
- [6] MCGUIRE, K.J., MCDONNELL, J.J., WEILER, M., KENDALL, C., MCGLYNN, B.L., WELKER, J.M., SEIBERT, J., The role of topography on catchment-scale water residence time, *Water Resources Research* **41** W05002 doi:10.1029/2004WR003657 (2005).
- [7] DAWSON, T.E., Water sources of plants as determined from xylem-water isotopic composition: perspectives on plant competition, distribution, and water relations, In *Stable Isotopes and Plant Carbon-Water Relations* Eds. J.R. Ehleringer, A.E. Hall and G.D. Farquhar, Academic Press, San Diego (1993) 465–496.
- [8] EHLERINGER, J.R., RODEN, J.S., DAWSON, T.E., Assessing ecosystem-level water relations through stable isotope ratio analyses, In *Methods in Ecosystem Science* Ed. R.B.J. O. E. Sala, H. A. Mooney, R. W. Howarth. Springer, New York (2000) 181–198.
- [9] BOND, B.J., JONES, J.A., MOORE, G.R., PHILLIPS, N., POST, D., MCDONNELL, J.J., The zone of vegetation influence on baseflow revealed by diel patterns of streamflow and vegetation water use in a headwater basin, *Hydrological Processes*. **16** (2002) 1671–1677.
- [10] MEINZER, F.C., BROOKS, J.R., DOMEK, J.C., GARTNER, B.L., WARREN, J.M., WOODRUFF, D., BIBLE, K., SHAW, D.C., Dynamics of water transport and

storage in conifers studied with deuterium and heat tracing techniques. *Plant, Cell and Environment* **29** (2006) 105–114.

- [11] BROOKS, J.R., MEINZER, F.C., COULOMBE, R., GREGG, J.W., Hydraulic redistribution of soil water during summer drought in two contrasting Pacific Northwest coniferous forests, *Tree Physiology* **22** (2002) 1107–1117.
- [12] KENDALL, K.A., SHANLEY, J.B., MCDONNELL, J.J., A hydrometric and geochemical approach to testing the transmissivity feedback hypothesis during snowmelt, *Journal of Hydrology* **219** (1999) 188–205.

**USE OF NATURAL TRACERS (MAJOR IONS,
TOTAL ORGANIC CARBON, STABLE ISOTOPES)
TO UNDERSTAND VOLCANIC AQUIFER
FUNCTIONING: AN EXAMPLE FROM THE ARGNAT
BASIN (AUVERGNE, FRANCE)**

G. BERTRAND, H. CELLE-JEANTON, G. CHAZOT
Université Blaise Pascal,
Laboratoire Magmas et Volcans,
Clermont-Ferrand

F. HUNEAU
Université Bordeaux, CDGA,
Talence

France

Abstract

This work focuses on the chemical transfers within volcanic aquifers that are of special interest in Auvergne for they represent 30% of the water supplies (regional project PREVOIR financed by the Région Auvergne). A weekly monitoring of the chemical (major ions, TOC) and isotopic ($\delta^{18}\text{O}$, $\delta^2\text{H}$, $\delta^{13}\text{C}$) composition of rainfalls, unsaturated and saturated zone waters has been scheduled since November 2005. The evolution of the water quality is then followed during its transit towards the saturated zone. A combination of $\delta^{13}\text{C}$, $\delta^{18}\text{O}$ and TOC measurements allow to approach the residence time of water within the unsaturated zone and to comprehend the processes which govern the quality of water during the hydrological cycle. Monthly investigations on the whole basin highlight the specificity of the volcanic environment. Carbon isotopic values range from -8.1‰ $\delta^{13}\text{C}$ to -20.2‰ $\delta^{13}\text{C}$ and then show a participation of deep CO_2 by the way of local faults.

1. INTRODUCTION

This paper presents chemical and isotopic preliminary results obtained from groundwater in a volcanic basin located in the Chaîne des Puys (France).

The purpose is to characterize the modalities of the recharge and of the acquisition of the water chemistry in this kind of environment.

In this way, we adopted two space-time scale approaches during one hydrological year (from April 2006 to April 2007):

- (a) Horizontal transfers are approached with a monthly sampling of nine water catchments within the basin. Major ion concentrations (HCO_3^- , Cl^- , NO_3^- , SO_4^{2-} , Na^+ , K^+ , Mg^{2+} , Ca^{2+}) and Total Organic Carbon (TOC) contents are determined for the whole studied period. The $\delta^{18}\text{O}$, $\delta^2\text{H}$, $\delta^{13}\text{C}$ results are presented for the period April to July 2006.
- (b) Vertical transfers are studied on a weekly time-scale and concern the water catchment of Les Grosliers. Rainfall, unsaturated zone and saturated zone waters are sampled and analyzed for major ions and TOC. $\delta^{13}\text{C}$ measurements are available for the period April to September 2006.

2. GEOLOGICAL AND HYDROGEOLOGICAL SETTINGS

During the last 80 000 years, volcanic activity took place trough tectonic faults on the granitic basement west of the Limagne Basin. Basaltic flows fully covered the area and flowed down on the west fault escarpment to reach the tertiary sediments of the Limagne Basin [1].

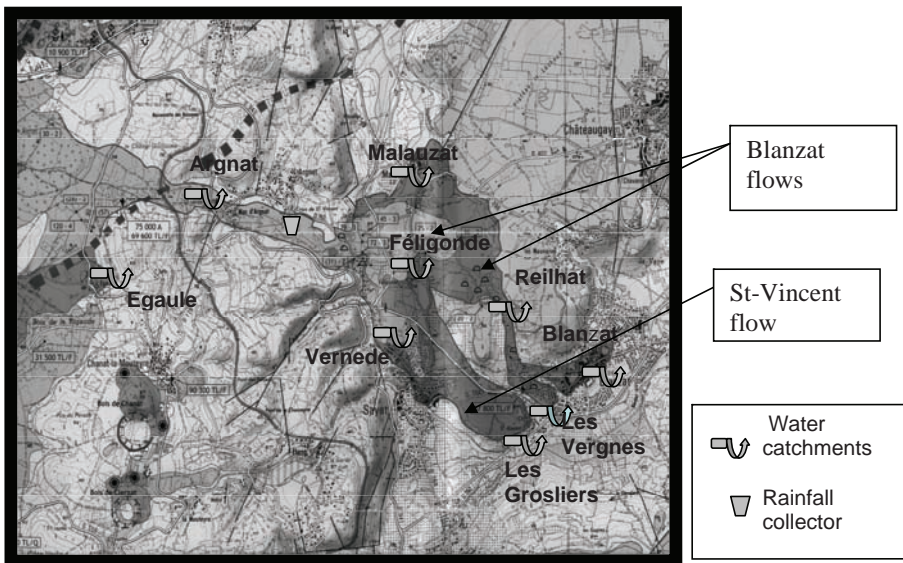


FIG. 1. Geologic setting of the Argnat basin (from [1]).

The Argnat basin is located in the northeastern part of La Chaîne des Puy. It contains several lava flows originated from different volcanoes and superimposed in a deep and narrow thalweg. At the end of the thalweg, the flows separate in two different branches (Fig. 1).

In this kind of environment, precipitation infiltrates on scoria cones, supplying saturated zone through unsaturated zone. Water further circulates in the volcanic flows. The stream coming from the substratum infiltrates near the contact between the basement and the volcanic flows. Thus, water flows in the scoria zone or in the spoiled zone near the volcanic flow/basement contact.

3. HORIZONTAL TRANSFERS

In order to study recharge modalities (season, recharge areas) and horizontal transfers, we established the local meteoric water line (LMWL), using $\delta^{18}\text{O}$ and $\delta^2\text{H}$ signature of rainfall collected in the middle part of the Argnat basin (Fig. 1). The preliminary LMWL (Fig. 2) is based on four months measurements (from April to July 2006) and is similar to the World Meteoric Water Line [2] with a slope of 8.23 and a deuterium excess of 9.03‰.

Calculated means for the four months analyzed from the 8 water catchments plot very close to the LMWL. This first observation shows that the origin of the groundwater is only meteoritic and supplied by current precipitation. [3] showed that this is the general feature for the French mineral waters.

Groundwaters show quite small standard deviation ($-8.3\text{‰} < \delta^{18}\text{O} < -9.2\text{‰}$ and $-60\text{‰} < \delta^2\text{H} < -57\text{‰}$) that could reflect a preferential recharge and/or mixing in the aquifer.

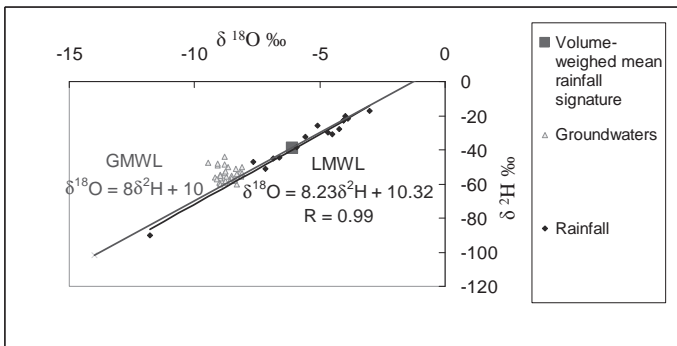


FIG. 2. $\delta^{18}\text{O}$ versus $\delta^2\text{H}$ values for the rainfall, the 8 water catchments of the Argnat basin and the unsaturated zone of Les Grosliers.

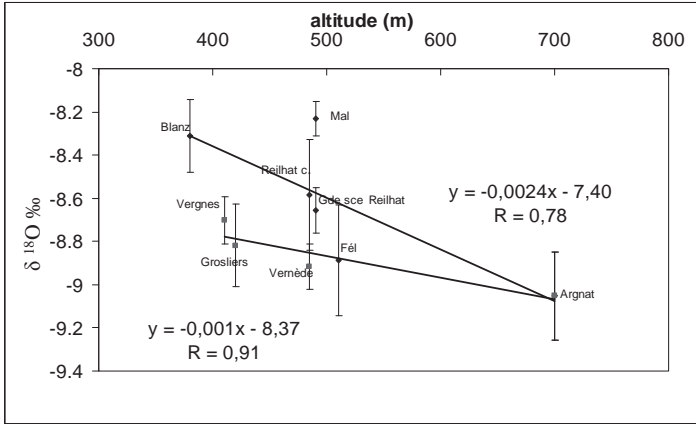


FIG. 3. Four months $\delta^{18}O$ values versus altitude for the 8 water catchments of the Argnat basin.

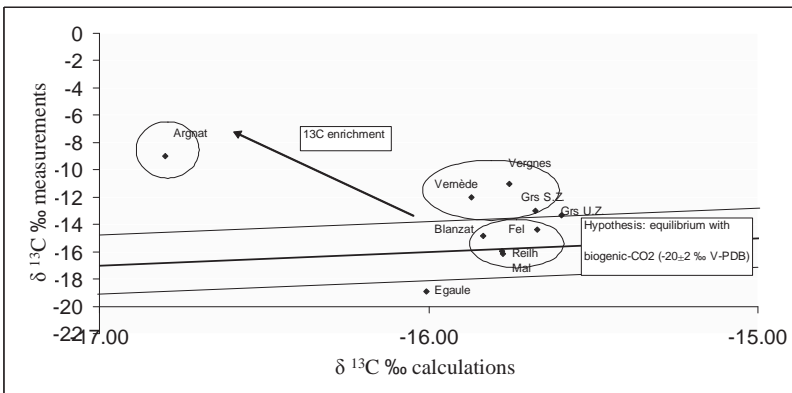


FIG. 4. Measured and calculated of $\delta^{13}C$ for the 8 water catchments and Unsaturated Zone of Les Grosliers.

Fig. 3 presents $\delta^{18}O$ ‰ versus altitude for the four months mean values of the 8 water catchments. Local altitudinal gradients could then be established with values of $-0.24\text{‰}/100\text{ m}$ for the Blanzat volcanic flows and $-0.10\text{‰}/100\text{ m}$ for the Saint-Vincent volcanic flow.

The weak influence of the altitude for the Saint-Vincent volcanic flow could be explained by the existence of 2 different aquifers within the Argnat Basin [4]. A drilling near Feligonde water catchment revealed the presence of these two aquifers: the aquifer of the Blanzat flows is located at upper depth

(-20 m) compared to the Saint-Vincent flow aquifer (-40 m). Moreover, The Saint-Vincent flow is formed by massive, poorly fractured rocks whereas the Blanzat flows are composed of massive parts mixed with scoria where large fissures occur. Precipitation on the Blanzat flows or on the surrounding basement can easily reach the upper aquifer.

Data of $\delta^{13}\text{C}$ show a great spatial variability. Four month mean values range from -18.9‰ for Egaule to -9‰ for Argnat. Comparing these values with theoretical isotopic composition of water in a biogenic CO_2 -open environment (calculations available in [5]), different TDIC origin can be determined for the Argnat basin (Fig. 4).

Fig. 4 shows the existence of four water types. First type is characterized by Argnat groundwater. Using pCO_2 equilibrium calculation [6], we showed that the enriched signature of Argnat water catchment is due to the participation of mantle CO_2 (mean $\text{pCO}_2 \text{ eq} = 1.5 \cdot 10^{-2} \text{ atm.}$). As temperature and conductivity are comparable to the values of other water catchments, we can assume that gaseous CO_2 is coming directly from the upper mantle through regional faults (Fig. 1, [7]). The second cluster includes La Vernède, Les Vergnes, and the saturated zone of Les Grosliers. It shows a quite linear trend to biogenic CO_2 area with smaller $\text{pCO}_2 \text{ eq}$ (about $6 \cdot 10^{-3} \text{ atm.}$) and could indicate a further supply of biogenic CO_2 . The third group (Féligonde, Blanzat, Reilhat and Malauzat) is clearly under the influence of biogenic CO_2 . These two groups correspond to the two different pathways of water identified using stable isotopes. The Blanzat pathway is more open to the biogenic CO_2 than the Saint-Vincent pathway according to its fracturation. Egaule shows a clear biogenic signature. This is not surprising as this locality is located in the upper part of the basin.

Thus, the system is generally open to biogenic CO_2 , and the influence of mantle CO_2 is important around geological faults.

4. VERTICAL TRANSFER

To consider vertical transfer occurring through basaltic flow, both $\delta^{18}\text{O}$ values of saturated (S.Z.) and unsaturated zone (U.Z.) from Les Grosliers water catchments were determined with a weekly time-scale.

- (a) We observe mean values around -8.8‰ (s.d.=0.2, n=20) for the saturated zone and -8.1‰ (s.d.=0.1, n=20) for the unsaturated zone. This difference indicates the existence of different water origins. Recharge of the U.Z. seems to occur at lower altitude than for the S.Z. The standard deviation of 0.1 shows a weekly variability of values for the U.Z that can be due to the existence of a mixing reservoir within the lava flow. This hypothesis

is strengthened by the lack of correlation between precipitation height and the U.Z. weekly volume.

- (b) Chemical contents are also different: U.Z. shows lower Cl^- (from 3.9 to 4.6 mg/L) and NO_3^- (from 3.3 to 4.2 mg/L) contents and higher TOC values (close to rainfall's values) than S.Z. ($18.9 < \text{Cl}^- < 25.0$ mg/L and $11.1 < \text{NO}_3^- < 16.3$ mg/L). This difference points out a different flow path of the water and/or interaction of the system with microbial activity in anaerobic conditions or directly with vegetal activity.
- (c) U.Z. water also shows higher concentration of bicarbonate ($80.5 < \text{HCO}_3^- < 158.6$ mg/L) and silica ($41 < \text{SiO}_2 < 51$ mg/L) compared to SZ ($76.9 < \text{HCO}_3^- < 91.5$ mg/L and $33 < \text{SiO}_2 < 42$ mg/L). This feature could indicate a larger residence time in the basaltic flows and/or larger alteration efficiency for these waters than for the Saturated Zone's waters. Indeed, bicarbonates (and associated cations such as Ca^{2+} , Mg^{2+} , Na^+ , K^+) values evolved during the studied period, consistent with an increase of this alteration efficiency. The ionic content was stable until June, and then increased regularly after the first half of September (F.5) and then decreased.

This trend highlights a seasonal effect that influences dissolved inorganic carbon content of U.Z. During spring and summer, soil activity increases and enhances biogenic CO_2 pressure in the soil. CO_2 equilibrates with water and increases alteration efficiency of the U.Z. water. This seasonal effect allows to approach the transit time of the water in the U.Z.: a maximum of a few weeks. This conclusion is emphasized by the co-variation of rainfall's TOC content and Unsaturated Zone one (Fig. 6).

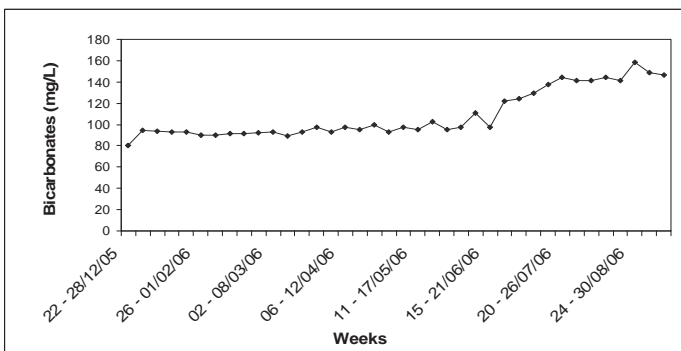


FIG. 5. Evolution of bicarbonate contents of the unsaturated zone of Les Grosliers.

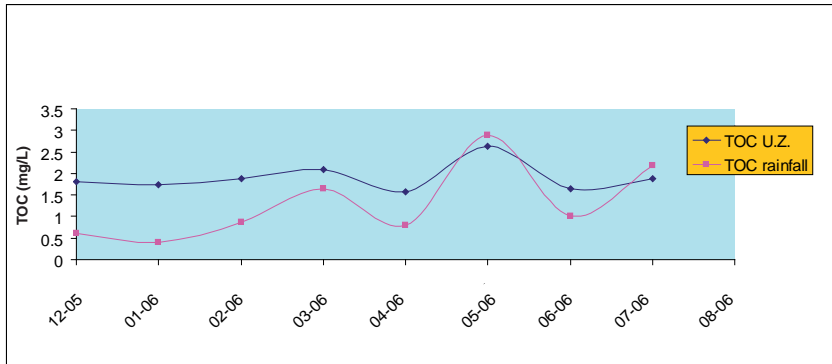


FIG. 6. Evolutions of monthly mean TOC contents of rainfall and U.Z. of Les Grosliers (from December 2005 to July 2006).

This seasonal effect could also occur in the S.Z. However, the high volume water and the mantle CO₂ input near Argnat could overprint this feature.

5. CONCLUSION

This paper presents preliminary isotopic and chemical results obtained studying transfers occurring in volcanic aquifers. Isotopic tools such as ¹⁸O, ²H, ¹³C coupled with chemical analyses allow identifying the processes that govern the functioning of Argnat basin. We determined the LMWL and showed that aquifer's recharge is supplied by current precipitations.

Determination of altitudinal gradient allows us to highlight a different flow path into the two volcanic units and seems to confirm the existence of two different aquifers [4].

Data concerning the carbon isotopes permit us to underline the influence of biogenic CO₂ on the whole basin, which can be disturbed by the arrival of CO₂ from the mantle.

Studying the water catchment of Les Grosliers, we show a great difference between U.Z. and S.Z. The S.Z. seems to be supplied by water coming from the granitic basement as it can be seen with the nitrate concentrations, and also supplied by circulation coming from the high part of the basin and flowing near the bottom of the volcanic flows. The analysis of the U.Z. testifies the existence of a buffer zone into the volcanic flow where water resides as can be seen with carbon isotopes, bicarbonates and associated cations.

These results are preliminary and will be implemented by new data to complete an eighteen months cycle.

REFERENCES

- [1] BOIVIN, P., BESSON, J.C., BRIOT, D., CAMUS, G., DE GOËR DE HERVE, A., GOURGAUD, A., LABAZUY, P., DE LAROUZIERE, F-D., LIVET, M., MERGOIL, J., MIALLIER, D., MOREL, J-M., VERNET, G., VINCENT, P.M. Volcanologie de la Chaîne des Puys, Massif Central Français, 4^{ème} édition, Editions du parc naturel régional des volcans d’Auvergne (2004).
- [2] CRAIG, H., Isotopic variations in meteoric waters, *Science* **133** (1961) 1702–1703.
- [3] BLAVOUX, B., Apports des techniques isotopiques à la connaissances des gisements d’eau minérale, *La Houille Blanche* 2/3 (1995) 1995.
- [4] GAUBI, E.B., Etude hydrogéologique de l’extrémité aval du bassin d’ Argnat (Chaîne des Puys, Massif central Français), Projet de l’Autoroute Périgueux Clermont-Ferrand, Mémoire de DEA national d’hydrogéologie, sciences de l’eau et aménagement, Université de Franche-Comté (1990) 88.
- [5] ROSE, T., DAVISON, M.L., CRISS, R.E., Isotope hydrology of voluminous cold springs in fractured rock from an active volcanic region, northeastern California, *Journal of Hydrology* **179** (1996) 207–236.
- [6] STUMM, W., MORGAN, J.J., Aquatic chemistry: an introduction emphasizing chemical equilibria in natural waters, New-York (1981) 583.
- [7] CAMUS, G., MICHARD, G.P.O., BOIVIN, P., Risque d’éruption gazeuse carbonique en Auvergne, *Bulletin de la Société Géologique de France*, **164** 6 (1993) 767–781.

INFILTRATION PROCESSES AND IMPACT ON SHALLOW GROUNDWATER IN AGRICULTURAL DRY LAND AREAS

E. GAREL*, V. MARC*, S. RUY**, C. DOUSSAN**, R. SIMLER*,
M. DANIEL*, F. TISON**

*Laboratoire d'Hydrogéologie,
Université d'Avignon et des Pays de Vaucluse,
Avignon

**Institut National de la Recherche Agronomique (INRA),
UMR Climat Sol Environnement,
Montfavet

France

Abstract

An investigation of infiltration processes in a Mediterranean agricultural soil was carried out using environmental and artificial tracing. The objective was to assess the impact of the different vertical flow processes on the recharge of the underlying unconfined aquifer. A long term isotopic survey of rainwater, soil water and groundwater enabled us to estimate the seasonal influence of irrigation on the groundwater recharge. According to the rainfall time series over the previous months, the monthly proportions of irrigation ranged from 60% to 98%. These results point out the sensitivity of such shallow groundwater systems in the Mediterranean region, submitted to climate variability and depending on artificial recharge. At plot scale, preferential flow processes were investigated from a simulated rainfall using bromide as tracer (110 mm over 2h 52 min). The impact of this irrigation on the saturated zone was detected about 2 h after the start of the experiment. The hydrological contribution of this local infiltration to the groundwater was low owing to the high transmissivity of the saturated zone and the regional extent of the aquifer. But according to the concentration observed in soil water, solutes fluxes may be significant and local, short-term overtaking of allowable standards for water quality may occur. A rational management of shallow groundwater resources in agricultural regions should consider more explicitly these preferential flow processes in soils.

1. INTRODUCTION

Preferential flows processes in soils have been described since the end of the 80's [1–5]. Different lab and *in situ* experiments have been carried out to investigate the occurrence of such mechanisms. They all have shown that a complex set of parameters was involved comprising soil parameters (texture, structure, water content, heterogeneities, ...) and rainfall features (intensity, frequency, areal variability, ...). These processes are expected to play a significant role in the case of thin unsaturated zones over shallow groundwater systems. This situation is usually found in alluvial environments where water table is constrained by the water level in the stream. In most cases, these groundwaters are also intensively exploited and land use is dominated by agriculture. In this context, the important issues related to rapid vertical flows in soils are both quantitative (aquifer recharge) and qualitative (transfer of pollutants).

The current study was part of the project “Flux d’infiltration, de recharge et hétérogénéité, une approche multi-échelle de la colonne à la parcelle.” funded by the French Ministry of Research in the framework of the National Program for Hydrological Research (PNRH). Beyond the improvement of process knowledge, this project aimed at validating models including preferential flows for water management purposes at the agricultural parcel scale in Mediterranean environment.

The objective of the present study was to use natural and artificial tracing as investigation tool of infiltration processes. An experimental plot dedicated to the study of infiltration processes has been used to elaborate a long term isotopic database of soil waters and groundwaters (from 2004 onwards). This experimental site was also used to carry out a simulated rainfall in summer 2006. Bromide was added to the rainwater as artificial tracer to assess the transit time of infiltration water and the quantitative impact of local infiltration on groundwater.

2. STUDY SITE AND METHODS

The study site is located in the Mediterranean part of the Durance catchment at the confluence with the river Rhone. This is a 2300 km² alluvial area with an intensive market gardening activity (Fig. 1). Due to the Mediterranean context, irrigation is an essential feature of the agricultural practices and is known to have a major impact on the groundwater recharge. Surface irrigation by submersion of the fields is the most usual irrigation technique. Water is collected from the river Durance and conveyed over the whole area using irrigation channels. The climate is pure Mediterranean with a main wet period

INFILTRATION PROCESSES AND IMPACT ON SHALLOW GROUNDWATER

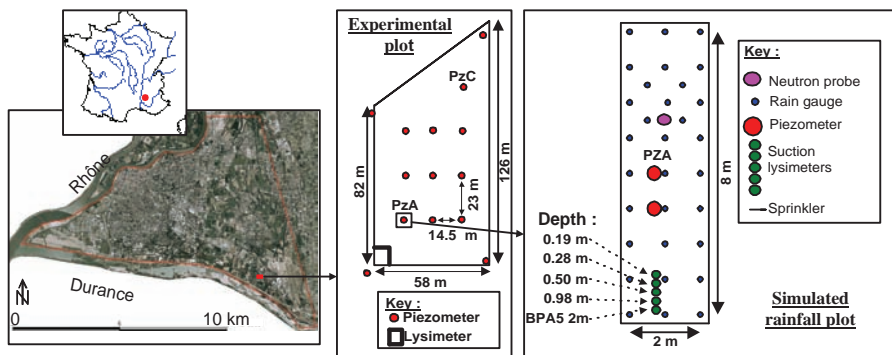


FIG. 1. Localisation of the study site and site instrumentation.

in autumn (high intensity storm events with usually a local extent) and a severe drought in summer. The annual rainfall in 2003–2004 (736 mm, calculated from September to August) was similar to the long term average estimated over the period 1961–2002 (721 mm). By contrast, 2004–2005 and 2005–2006 have been among the driest years for 40 years (415 mm and 472 mm respectively).

The 0.6 ha experimental plot is located at 2 km north of the river Durance (Fig. 1). Soil is composed of clayey silt 2 m thick over 7 m of gravel sand mixture overlying a marl bedrock. The gravel layer comprises a free pressure groundwater system. Transmissivity values range between $4 \cdot 10^{-2} \text{ m}^2/\text{s}$ and $8 \cdot 10^{-2} \text{ m}^2/\text{s}$ [6]. Water table depth varies from 5.5 to 4 m. Due to irrigation, the highest water level is observed in summer. Since the start of the experiment, the plot was planted of different species. Vetsch grass and ray grass were planted in 2005 and 2006 whereas the soil was bare of plants in 2004. Sprinkler irrigation was applied during the Spring and Summer 2005 and 2006.

The experimental plot was instrumented in 2002 of 28 long and short paired piezometers. 14 of them (the long ones) have their filter over the whole thickness of the aquifer whereas the other 14 (the short ones) only reach the upper part of the saturated zone. Suction lysimeters have been set up (5 lysimeters from 19 cm to 200 cm depth) near PZA and PZC (Fig. 1). From early 2004, soil water and groundwater were sampled once a fortnight for chemical and isotopic analyses. In summer 2006, an experiment of artificial rainfall with bromide enriched water was carried out around PZA.

3. LONG TERM ISOTOPIC SURVEY

Monthly data from PZA and from the 2 m depth suction lysimeter BPA5 are presented in Fig. 2 together with the rainfall amounts. The mean ^{18}O isotope content of irrigation water (Durance water) expressed in δ is -10.2‰ . The $\delta^{18}\text{O}$ seasonal variation of the Durance water was not possible to measure. Previous studies [7] have shown that this fluctuation over time (-9.5 in winter to -10.9 in summer) was low compared with the local monthly rainfall $\delta^{18}\text{O}$ (average -5.44‰) [8].

At 2 m depth, the $\delta^{18}\text{O}$ in soil water was due to the damped and time shifted local input (mixing of rainwater and irrigation water). The groundwater isotopic content had a more regional significance (impact of rainfall and irrigation over the whole catchment). In this case, it was observed a greater impact of irrigation water. The proportions of irrigation were computed using the usual mixing model :

$$C = \alpha C_{\text{irr}} + (1 - \alpha)C_{\text{r}}$$

where C_{irr} , C_{r} and C are irrigation concentration, rainfall concentration and resultant mixing water concentration (soil water or groundwater) respectively and α the proportion of irrigation water.

C_{irr} was assumed to be constant. C_{r} was calculated by convoluting the rainwater concentrations C_{in} with an exponential weighting function (exponential model [9]).

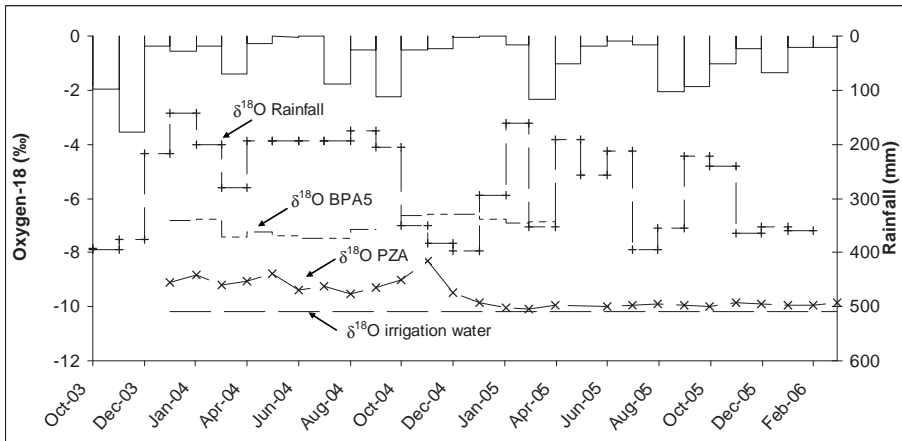


FIG. 2. $\delta^{18}\text{O}$ time series in rainwater, soil water and groundwater.

$$C_r(t) = \int_{-\infty}^t C_{in}(t') g(t-t') dt' \quad \text{or} \quad C_r(t) = \int_0^{\infty} C_{in}(t-t') g(t') dt'$$

where t' is time of entry, $t-t'$ is the transit time, and the $g(t-t')$ function is called the *response function*

In the *exponential model* (EM) approximation, the flow lines are assumed to have the exponential distribution of transit times. There is only one parameter which is T , the mean transit time of tracer.

$$g(t') = T^{-1} \exp(-t'/T)$$

The mixing proportions were calculated for different T estimates to test the sensitivity of the model to this parameter (from 3 months to 24 months, Fig. 3). In soil water, a seasonal fluctuation was observed. The contribution of irrigation increased steadily from the winter (20% in January 2004 and 2005) with a maximum in summer (around 40% in August 2004). According to T , the large differences in the monthly estimates are due to the main contribution of the rainwater component which is very variable over time. This seasonal evolution shows that the mean residence time of soil water (at 2 m depth) is likely less than 6 months. The groundwater isotopic content was also explained by mixing processes but with a greater proportion of the irrigation component. Over the observation period, the contributions of irrigation ranged from a minimum 60% to a maximum 98%. According to T value, a maximum difference of 5% was observed for the monthly proportions (April 2004). The proportion of irrigation time series over the period before January 2005 proved very different of that observed over the subsequent period. In 2004, the average proportion was lower (79%) and standard deviation greater (8%) than in 2005 (respectively 95% and 4%). This is due to the large difference of rainfall amounts between 2003 (annual rainfall close to the long term average) and 2004 (one of the driest year since 1961). In 2004, the impact of the 2003 rainfall (especially the storm events in autumn – 500 mm from September to December, 176 mm in December) showed that the mean transit time of water was between 6 and 12 months. The very low rainfall amount in 2004 resulted in a rise of the irrigation influence over 2005. This impact was also spotted by a steadier time series in 2005 due to a strong stable isotopic signal of the irrigation waters.

The soil capacity to transfer water downwards depends on the rainfall features and the prior soil moisture conditions. For example, in wet conditions, the rainfall events of October 2004 (monthly value of 112.4 mm with a

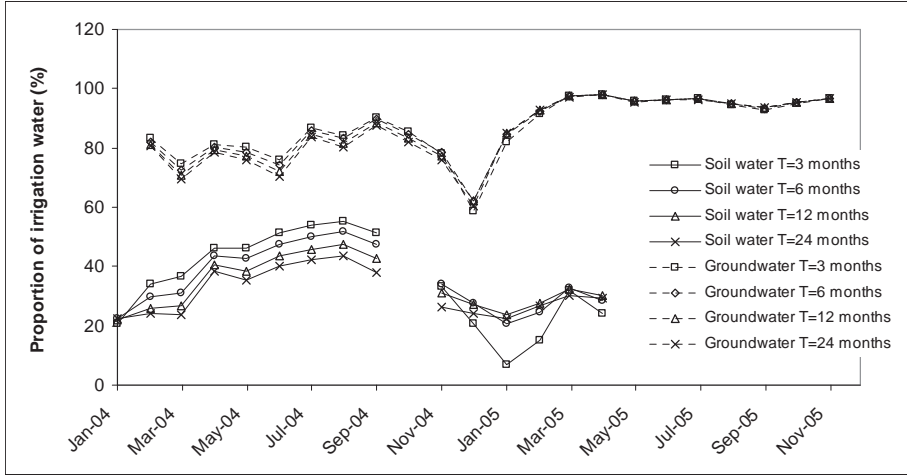


FIG. 3. Contribution of irrigation over time in soil water and groundwater.

maximum daily rainfall of 28 mm) had an impact on soil water in November and on groundwater in December (Fig. 2). Conversely, in a drier context, the rainfall events in April 2005 (117 mm) had no significant influence on the groundwater isotopic content. Large storm events in autumn or spring have often a local extent. This situation may also explain why a significant regional impact on the groundwater is not always detected.

4. SIMULATED RAINFALL EXPERIMENT AND ARTIFICIAL TRACING

An artificial irrigation with bromide-enriched water was carried out in July 2006 on a 16 m² plot around PZA. A 110 mm rainfall was simulated during 2h 52 min. The concentration of bromide was 1600 mg/L during the first 102 minutes of the experiment and 600 mg/L during the remaining 26 minutes. The peak concentration in the groundwater (0.53 mg/L) was observed 2h 10 min after the start of the experiment (Fig. 4). In 2003, an artificial rainfall was simulated on a lysimeter (1.8 × 2.6 × 2.2 m) situated on the same site, using a O¹⁸ depleted water. The lower drains collected the first water and the peak concentration, 20 min and 40 min after the start of the experiment respectively [10]. The results of both experiments are quite similar considering that a shorter transit time is expected in the lysimeter due to the boundary influence. In soil water, the maximum concentration was observed between 327 min and 527 min after the

INFILTRATION PROCESSES AND IMPACT ON SHALLOW GROUNDWATER

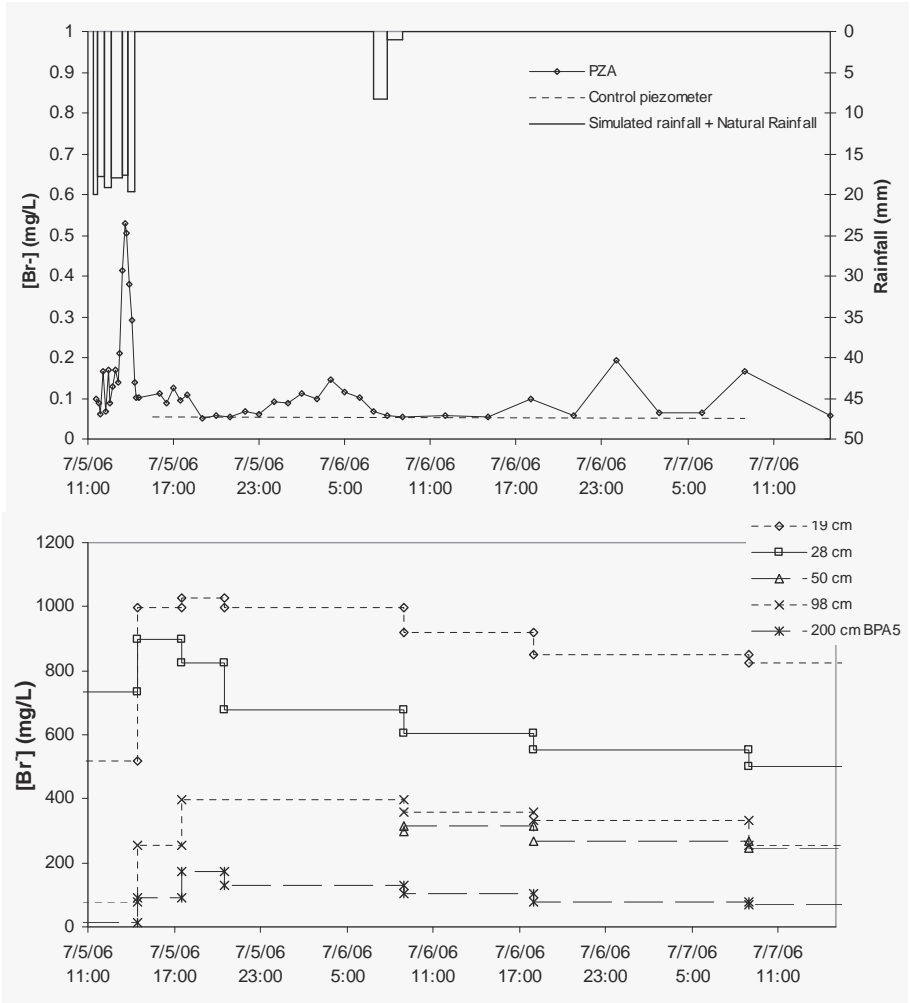


FIG. 4. Concentration variation of bromide in soil water and groundwater during and after the simulated rainfall.

start of the experiment (a 2 h. vacuum was exerted on the suction lysimeters which prevented any precise observation on Br content variation in soil water). The late impact on soil water compared to the rapid impact on groundwater confirmed the role of preferential flows on the groundwater quality variation. The use of suction lysimeters results in a sampling of water which circulates slowly in the soil matrix. Gravitational water involved in rapid preferential flow is not properly sampled with this methodology. Elution curves observed in

soil at different depth provided a good representation of the Darcyan vertical drainage in soil with a damping of concentrations according to depth due to dispersion processes.

5. CONCLUSION

From water tracing investigations, infiltration processes in Mediterranean agricultural soil have been studied at different time and spatial scales. From a long term isotopic survey of rainwaters, soil waters and groundwaters, time variation of the irrigation impact on the shallow unconfined aquifer has been quantified. The contribution of irrigation proved dominant ranging from 60% to 90% according to the rainfall time series over the previous months. These results point out the extreme delicacy of such alluvial groundwater systems in the Mediterranean region. If as forecasted by climate change scenarios the aridity of the climate would increase in the Mediterranean region, irrigation would prove a vital technique not only to maintain agricultural practices but also to recharge alluvial aquifers. At local scale, an *in situ* artificial rainfall experiment using bromide as tracer enabled us to observe processes of rapid water transfer to the saturated zone. The main Br concentration peak was observed in the groundwater only 70 min after the start of the injection. In the conditions of the experiment, these preferential flows had only a minor quantitative impact on the groundwater recharge but evidence of such processes shows that they may occur over the whole recharge area and play a significant quantitative role during particular periods (for example, intense storm events in autumn). In a qualitative point of view, waters involved in rapid vertical flows take solutes (possibly pollutants) down to the groundwater. According to the concentration observed in soil water, solutes fluxes may be significant, and local short-term overtaking of allowable standards for water quality may occur. A rational management of shallow groundwater resources in agricultural regions should consider more explicitly these preferential flow processes in soils.

REFERENCES

- [1] EVERTS, C.J., KANWAR, R.S., ALEXANDER JR., E.C., ALEXANDER, S.C., Comparison of tracer mobilities under laboratory and field conditions, *Journal of Environmental Quality* **18** 4 (1989) 491–498.
- [2] HELLING, C.S., GISH, T.J., Physical and chemical processes affecting preferential flow, pp. 77–86. T.J. Gish and A. Shirmohammadi (ed.) *Preferential flow. Proc. Natl. Symp., Chicago. 16–17 Dec. 1991. ASAE, St. Joseph, MI.*

INFILTRATION PROCESSES AND IMPACT ON SHALLOW GROUNDWATER

- [3] FLURY, M., Experimental evidence of transport of pesticides through field soils – A review. *Journal of Environmental Quality* **25** 1 (1996) 25–45.
- [4] KLADIVKO, E.J., GROCHULSKA, J., TURCO, R.F., VAN SCOYOC, G.E., EIGEL, J.D., Pesticide and nitrate transport into subsurface tile drains of different spacings. *Journal of Environmental Quality* **28** 3 (1999) 997–1004.
- [5] KUNG, K.-J.S., STEENHUIS, T.S., KLADIVKO, E.J., GISH, T.J., BUBENZER, G., HELLING, C.S., Impact of preferential flow on the transport of adsorbing and non-adsorbing tracers. *Soil Science Society of America Journal* **64** 4 (2000) 1290–1296.
- [6] BOGNER, C., Caractérisation hydrogéologique de la nappe des alluvions de la Durance (site expérimental INRA sur les écoulements préférentiels, domaine St Paul, Montfavet), *Memoire DEA SEEC, Montpellier* (2003) 43.
- [7] LACROIX, M., Impact de l'irrigation sur un aquifère alluvial, *Dynamique du système Basse Durance: nitrates et isotopes (cartographie), piézométrie (modélisation mathématique), Thèse de doctorat, Université de Franche-Comté, (1991) 162.*
- [8] CELLE, H., Caractérisation des précipitations sur le pourtour de la Méditerranée occidentale – Approche isotopique et chimique, *Thèse, Université d'Avignon et des pays du Vaucluse* (2000) 222.
- [9] MALOSZEWSKI, P., ZUBER, A., Lumped parameter models for the interpretation of environmental tracer data, *Manual on mathematical models in isotope hydrogeology, IAEA-TECDOC-910, October 1996, 9–58.*
- [10] BOGNER, C., MARC, V., DI PIETRO, L., DOUSSAN, C., RUY, S., GAUDU J.C., PERRIN, P., COGNARD-PLANCQ, A.L., EMBLANCH, C., DANIEL, M., SIMLER, R., Tracer study of infiltration in a field soil – simulated rainfall experiment on a large lysimeter, *International Workshop on the Application of Isotope Techniques in Hydrological and Environmental Studies, Paris* (2004).

USE OF DEUTERATED WATER AS A CONSERVATIVE ARTIFICIAL TRACER IN THE STUDY OF WATER MOVEMENT IN A COARSE GRAVEL UNSATURATED ZONE

N. MALI, J. URBANC
Geological Survey of Slovenia,
Ljubljana, Slovenia

A. LEIS
Institute of Water Resources Management,
Hydrogeology and Geophysics,
Joanneum Research Forschungsgesellschaft mbH
Graz, Austria

Abstract

The processes in a coarse gravel unsaturated zone develop quite differently from those in aquifers with finer unsaturated zone granulation. The aim of a tracing experiment using a lysimeter in the Selniška Dobrava aquifer was to describe the transport processes in a highly permeable coarse gravel unsaturated zone. A combined tracing experiment was performed using both deuterated water and uranine. Deuterated water is known as an effective conservative tracer in hydrogeological studies, but only few studies have focused on the unsaturated zone. Due to its highest degree of conservativeness deuterium was chosen to study water movement, while uranine with its sorption capacity was used as a contaminant transport indicator. Based on the tracing experiment's results, the fastest and dominant flow velocities were estimated. Mean flow velocity and vertical dispersion were assessed by an analytical best-fit method using one-dimensional convection-dispersion-model. Deuterium was confirmed as an ideal conservative tracer and a more suitable tracer than dye (uranine) for the study of water flow in the unsaturated zone of a coarse gravel aquifer.

1. INTRODUCTION

The processes in the coarse gravel unsaturated zone develop quite differently from those in aquifers with finer unsaturated zone granulation. The implementation of measurements in a highly permeable gravel unsaturated zone is quite difficult, sometimes it is almost impossible. A combined tracing

experiment with deuterated water and uranine was performed in a lysimeter in the Selniška Dobrava aquifer to describe the transport processes in highly permeable coarse gravel unsaturated zone. Deuterated water is known as an effective conservative tracer to obtain groundwater transport properties [1] due to its chemical stability, no reactivity, ease of handling and sampling, and reasonable price. Deuterated water has been used as a reference tracer in karsts and porous aquifer studies, but only few studies have focused on the unsaturated zone. Compared to other groundwater tracers, deuterium shows the highest degree of conservativeness [2]. For this reason deuterium was chosen to study water movement, while uranine with its sorption capacity was used as an indicator of possible pollution.

2. AREA DESCRIPTION

Selniška Dobrava is situated in the north-east of Slovenia near Maribor, the capital of the region. The coarse gravel aquifer lies on the north bank of the Drava River (Fig. 1). The aquifer is recharged by the Drava, by infiltration and seepage from the upper terrace aquifer. The thickest coarse gravel deposit is 50 m thick. Groundwater table is found at an average depth of 25 to 37 m, thus the thickness of the saturated layer along the aquifer axis is 7–14 m, possibly even more in the deepest sections. The hydraulic conductivity of the principal aquifer has been reported as 5×10^{-3} m/s [3]. The vegetation covering the larger area of the aquifer is a mixed forest and the soil type is a district cambisol. The

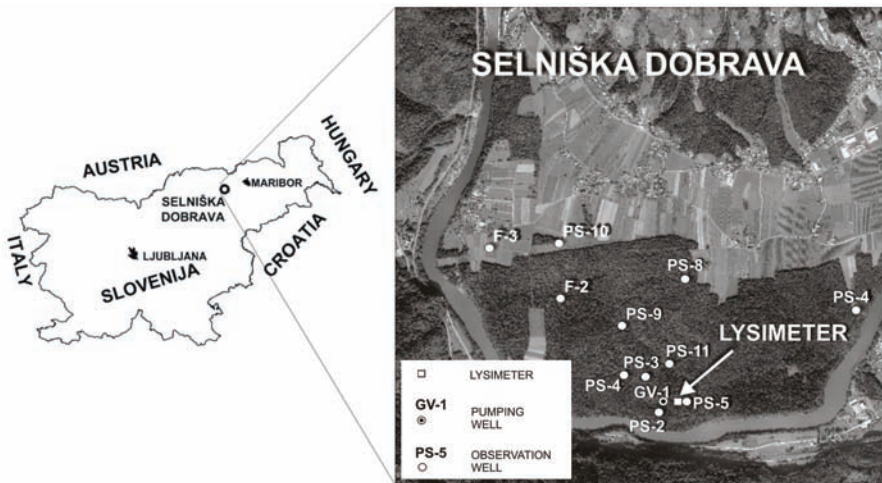


FIG. 1. Study area — location of lysimeter.

USE OF DEUTERATED WATER AS A CONSERVATIVE ARTIFICIAL TRACER

hydraulic conductivity of the soil is $1.5\text{--}4.5 \times 10^{-5}$ m/s. The research area belongs to the moderate continental climate of central Slovenia with a typical continental precipitation regime and an average yearly precipitation between 1200 and 1300 mm. The average yearly air temperature lies between 8 and 12° C.

The lysimeter is in the area of the principal aquifer Selniška Dobrava, downstream from the pumping station GV-1 (Fig. 1). In the conceptual model, the lysimeter area is defined as homogeneous coarse gravel aquifer.

3. METHODS

3.1. Experimental set-up

The lysimeter was constructed as a 2×2 m, 5 m deep concrete box, with 0.2 m thick walls (Fig. 2). It has 10 sampling and measuring points at different depths (JV-1 to JV-10). Sampling point positioning followed a randomized selection over lysimeter width but at approximately equal distances from its depth. For groundwater sampling in the unsaturated zone, 1.7 m drainage samplers with a water collection system at the end were installed (Fig. 2). To sample precipitation, a precipitation station was sited near the lysimeter, while

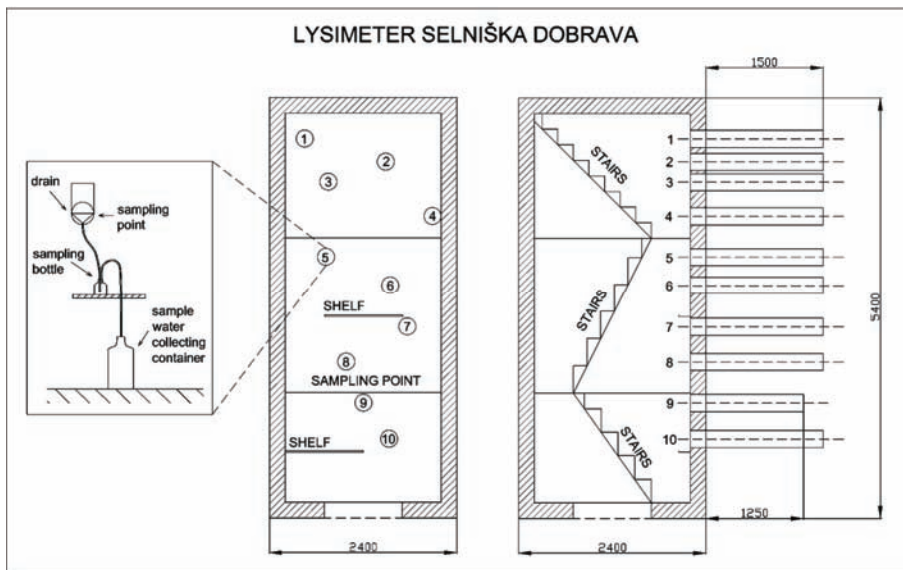


FIG. 2. Lysimeter cross-section.

the nearby Ruše station of the Environmental Agency of the Republic of Slovenia provided precipitation data.

3.2. Combined dye and deuterium tracing experiment

A tracing experiment was performed on April 21, 2004, using deuterated water and uranine as artificial tracers. The period prior to tracer injection was a period of intense snow melting and the saturation of the soil profile was near the field capacity. Before tracer injection, irrigation with groundwater was performed to reach good field capacity. 75 g of uranine and 1100 mL D₂O (55%) were dissolved in 50 L of groundwater and injected by sprinkler irrigation. After injection, the tracer was again splashed by irrigation groundwater. The complete injection was done during 5 hours. The average amount of irrigated water, 107 mm, corresponds to a summer thunderstorm event.

After tracer injection, water in all the outflow sampling points was collected in 120-ml plastic bottles twice on the first day, then once daily for one week; afterwards sampling was performed weekly till October 2005. Both tracers were analysed in the same samples [4].

Based on the injection time, the first tracer appearance time, time of highest concentration and the distance between the top of the lysimeter and observation point, the fastest flow velocity and dominant flow velocity were calculated. The mean flow velocity and vertical dispersion from the results of tracing experiment were estimated using a best-fit method of the computer program TRACI'95 [5]. The analytical solution with one dimensional convection-dispersion-model with standardising values for single porosity was chosen.

The analytical results are presented in ‰ δ²H (difference between the measured ratios of the sample and reference VSMOW (Vienna Standard Mean Ocean Water)). Because the basis of the analytical best-fit model is the concentration of tracer (mg/m³), the ‰ δ²H values of results were converted in the mg/L concentrations of ²H by the slightly modified published equation [1] taking into account the influence of the density of water.

$$Deuterium_{conc} = 34.721 \left[\frac{1000 + \delta D_{VSMOW}}{1000} \right] \quad (1)$$

4. RESULTS AND DISCUSSION

Both tracers were detected in all ten sampling points (Fig. 3). The maximal concentration of tracer at each single measuring point doesn't depend

USE OF DEUTERATED WATER AS A CONSERVATIVE ARTIFICIAL TRACE

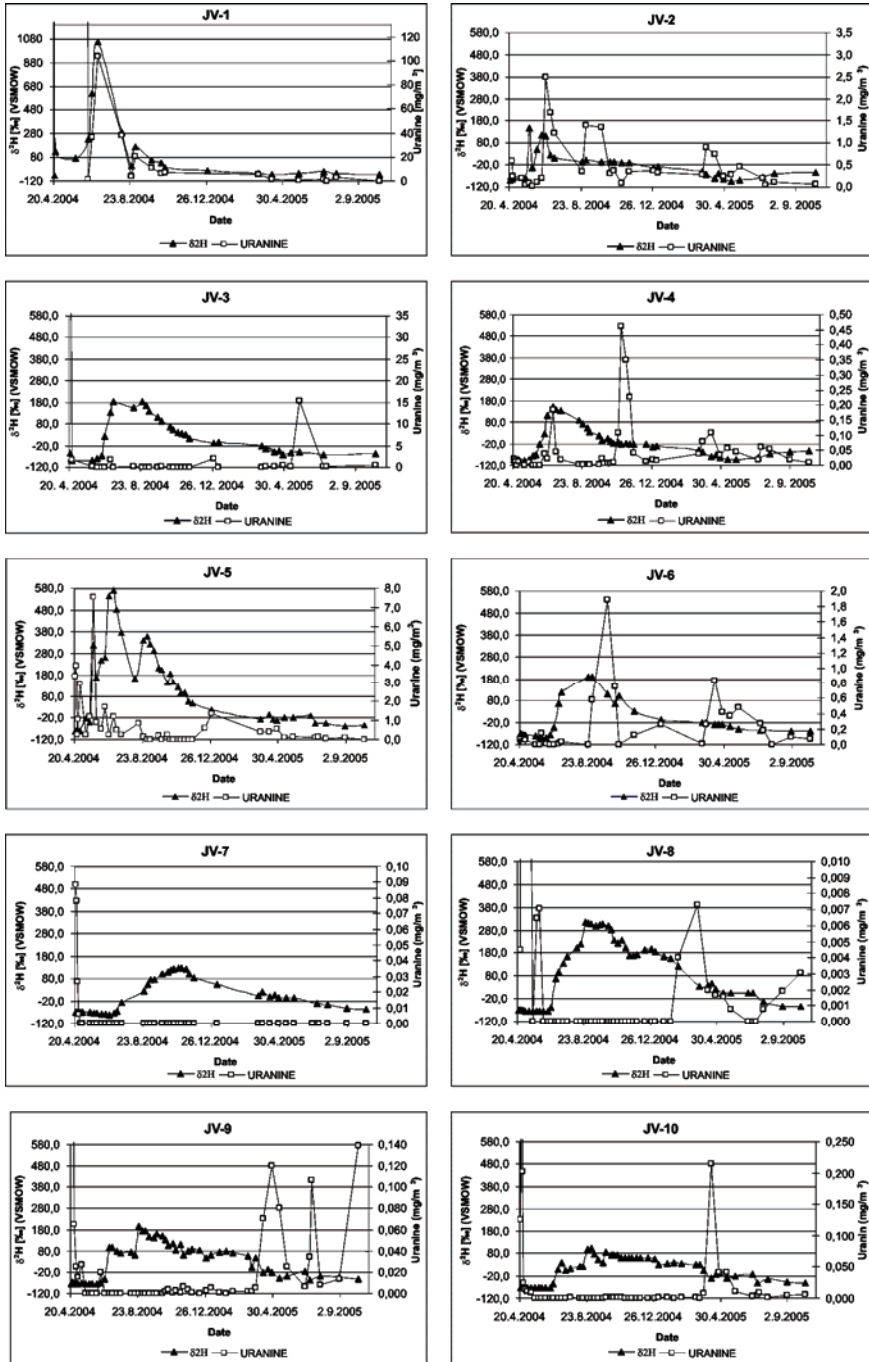


FIG. 3. Deuterium and uranine breakthrough curves.

TABLE 1. CALCULATED FASTEST, DOMINANT AND MEAN FLOW VELOCITY AND RETARDATION FACTOR OF DEUTERIUM AND URANINE TRACERS.

Deuterium	JV-1	JV-2	JV-3	JV-4	JV-5	JV-6	JV-7	JV-8	JV-9	JV-10
Distance	m	0.52	0.82	1.08	1.52	2.41	2.95	3.4	3.93	4.39
Fastest flow	m/d	0.520	0.023	0.023	0.043	0.102	0.042	0.055	0.070	0.071
Dom. flow	m/d	0.520	0.023	0.014	0.021	0.029	0.019	0.015	0.031	0.033
Mean flow	m/d		0.014	0.008	0.014	0.017	0.017	0.011	0.015	0.016
Dispersion	m ² /s	0.488	0	0.001	0.002	0.005	0.004	0.007	0.011	0.015
Uranine	JV-1	JV-2	JV-3	JV-4	JV-5	JV-6	JV-7	JV-8	JV-9	JV-10
Distance	m	0.52	0.82	1.08	1.52	2.41	2.95	3.4	3.93	4.39
Dom. f.	m/d	0.007	0.013	-	0.008	0.015	-	0.010	0.011	0.012
Mean f.	m/d	0.006	0.012	-	0.008	-	0.015	-	0.012	0.012
Rd-meanflow	m/d	1.83	1.17	-	1.75	-	1.13	-	1.25	1.33

on depth or distance from the lysimeter surface. In the first two days after injection of the tracers very high uranine concentrations occurred in several sampling points after that time concentrations declined. It can not be excluded that contamination of some sampling points happened at the time of tracer injection. From precipitation data and tracers' values it is evident that the high intensity and amount of precipitation forced the appearance of the tracer at the different observation points at the same time. Practically higher concentrations of uranine appear impulsively, depending on the quantity and intensity of precipitation. A comparison of the deuterium and uranine breakthrough curves shows that the results of deuterium tracing give more regular distribution of tracer than uranine which shows a strong impulsive appearance of tracer (Fig. 3). If the increase of uranine concentration during the first two days is not considered, a delay in the appearance of the uranine tracer compared to deuterium is recognized.

Table 1 gives the estimation of water fastest, dominant and mean flow velocity obtained from the deuterium and uranine tracing results. Because the uranine tracer appeared in almost immediately after injection on account of contamination, the maximum velocity has not been determined. Based on the knowledge of the aquifer and water flow properties in the lysimeter system, the concentrations of the first few days were omitted from the calculation of dominant velocity. The maximal concentrations of dye tracer after this period were taken in account. For sampling points JV-3 and JV-7 there were no typical breakthrough curves.

Based on the results of tracing experiment, estimations of the mean flow velocity and vertical dispersion (Table 1) were made by analytical best-fit method. One dimensional convection-dispersion-model with standardising values for single porosity was used.

All the results are in Table 1. Based on tracing test results, a strong preferential flow is assumed at sampling point JV-5 and JV-8, at sampling points JV-3 and JV-7 the lowest velocity was recognised.

4.1. Comparison of deuterium and dye tracer

Breakthrough curves of both tracers show retardation in maximum values of dye compared to deuterium. It is presumed that the retardation and impulsive increase of dye tracer concentrations are the result of sorption-desorption processes. These processes slow down the transport, as large parts of the tracer are immobilized on the solid phase for part of the time.

The calculation of the retardation factor for the uranine was made using results of a convection-dispersion model for the estimation of mean flow velocity. Only sampling points JV-2, JV-4, JV-6, JV-8, JV-9 and JV-10 were

included because for these points analytical approaches to calculate mean flow velocity for uranine data could be performed. The retardation factor R was calculated by:

$$R = \frac{v_{aD}}{v_{au}} \quad (2)$$

where R is retardation factor, v_{aD} is mean flow velocity of the deuterium tracer and v_{au} is mean flow velocity of the uranine. The range of retardation factor (Table 3) is from 1.133 (JV-6) to 1.75 (JV-4) which correspond to the published retardation factors for uranine in gravel media determined in the laboratory [6].

4.2. Discussion

A lysimeter tracing experiment showed that deuterated water is more suitable tracer than uranine for the study of water flow properties in unsaturated zone. Both tracers appeared at the sampling points and their arrival to single sampling points was related in both cases to the intensity and amount of precipitation. Uranine came in sight very impulsive (Fig. 3) and its breakthrough curves show several peaks, for which it is difficult to recognize any significant breakthrough curve. On the other hand, the results of deuterium tracer show a typical breakthrough curve (Fig. 3). The retardation factor of the uranine as compared to deuterium was 1.13–1.75 (Table 1), which is in agreement with previously published results [6] for uranine in gravel media determined in laboratory. Deuterated water is thus a useful tracer to detect water movement, while the use of uranine may reflect organic compounds transport. In this study deuterium was confirmed as an ideal conservative tracer for tracer studies in the unsaturated zone.

Based on results of tracing experiment some properties of coarse gravel unsaturated zone at the location of the lysimeter could be described. The

TABLE 2. ESTIMATION OF MEAN RESIDENCE TIME IN THE COARSE GRAVEL UNSATURATED ZONE IN SELNIŠKA DOBRAVA.

Method	m.f. velocity	MRT	MRT	velocity range	MRT-range	MRT-range
	m/d	day	year	m/d	day	year
Convection-dispersion m.	0.015	1833	5.0	0.008–0.017	1618–3438	4.43–9.42

USE OF DEUTERATED WATER AS A CONSERVATIVE ARTIFICIAL TRACE

estimation of the mean flow velocity of the matrix flow is 0.015 m/d (Table 2). If it is assumed that the ground water level is 27.5 m deep, it could be concluded that the mean residence time through unsaturated zone in Selniška Dobrava coarse gravel aquifer is 5.0 years. For groundwater protection and for measures performed because of this protection, the first arrival of the tracer through unsaturated zone is important. If it is accepted that the pollutant behaves like a conservative tracer, and with the estimation of the fastest flow velocity in lysimeter in range 0.1–0.07 m/d (Table 1), a pollutant can reach groundwater in 9–12 months. Based on dominant flow velocity 0.03 m/d the percolation time is 2.5 years.

5. CONCLUSIONS

Tracing with artificial tracers, especially with deuterated water, was found as a very useful tool to assess the properties of water flow in the unsaturated zone also of a coarse gravel aquifer. On the basis of determined range of the water flow properties the estimations of groundwater recharge, pollution influence on aquifer and groundwater protection measures can be provided. Deuterated water was recognised as more suitable tracer than uranine for the study of water flow properties in unsaturated zone. A delay in the appearance of the uranine tracer compared to deuterium is recognized. The calculated retardation factor of uranine as compared to deuterium (1.13–1.75) corresponds to the previously published results. Deuterated water is thus a useful tracer to detect water movement, while the use of uranine may reflect organic compounds transport characteristics. In this study deuterium was confirmed as an ideal conservative tracer for tracer studies in the unsaturated zone. Based on results of tracing experiment some properties of coarse gravel unsaturated zone at the location of the lysimeter were described. Mean flow velocity of the matrix flow is estimated as 0.015 m/d and the mean residence time of the water through the unsaturated zone at the lysimeter location is valued as 5.0 years. At the calculated fastest flow velocity 0.1–0.07 m/d a pollutant can reach groundwater in 9–12 months. Based on dominant flow velocity 0.03 m/d the percolation time is 2.5 years.

ACKNOWLEDGEMENT

The study presented in the paper was carried out within the project Urban Hydrogeology – The impact of Infrastructures on Groundwater, financed by

Ministry of Higher Education, Science and Technology of Republic Slovenia
(Project No. L-1-6670-0215).

REFERENCES

- [1] BECKER, M.W., COPLEN, T.B., Use of deuterated water as a conservative artificial groundwater tracer. *Hydrogeological Journal* **9** (2001) 512–516.
- [2] LEIS, A., BENISCHKE, R., Comparison of different stable hydrogen isotope-ratio measurement techniques for tracer studies with deuterated water in the unsaturated zone in groundwater, Paper presented at the 7th Workshop of European Society for Isotope Research (ESIR), *Berichte des Institutes für Erdwissenschaften Karl-Franzes-Universität Graz, Seggauberg* (2004).
- [3] MALI, N., JANŽA, M., Ocena možnosti zajema podzemne vode z uporabo MIKE SHE programskega orodja za hidrogeološko modeliranje (Evaluation of water resource exploitation options using the MIKE-SHE integrated hydrogeological modelling package – case study Selniška Dobrava), *Geologija* **48** 2 (2005) 281–294.
- [4] MALI, N., URBANC, J., LEIS, A., Tracing of water movement through the unsaturated zone of a coarse gravel aquifer by means of dye and deuterated water, *Environmental Geology* **51** (2007) 1401–1412.
- [5] TRACI'95, Computer program, In: Kass W. (ed) *Tracing techniques in Geohydrology*, A.A. Balkema, Rotterdam (1998).
- [6] KLOTZ, D., Verhalten hydrologischer Tracer in ausgewählten Sanden und Kiesen (Characteristics of hydrological tracers in sand and gravel deposits), *GSF-Bericht* **290** (1982) 17–29.

ASSESSING AGRICULTURE POLLUTION IN THE BEJA AQUIFER USING NITROGEN ISOTOPES (SOUTH PORTUGAL)

E. PARALTA

National Institute of Engineering,
Technology and Innovation (INETI),
Hydrogeology Department,
Amadora

P.M. CARREIRA

Nuclear Technological Institute (ITN),
Chemical Department,
Sacavém

L. RIBEIRO

Lisbon Technical University (IST),
Lisboa

Portugal

Abstract

This paper intent to give scientific support for political decisions, considering the sustainable development of rural regions under semiarid conditions exploiting shallow aquifers, and promote appropriate use of nitrogen fertilizers, based on EC Water Framework Directive and EC Groundwater Framework Directive in the context of vulnerable aquifers. Stable nitrogen isotopes ($^{15}\text{N}/^{14}\text{N}$ ratios) can offer a direct way to identify the pollutant sources in groundwater systems. In the research area two major sources of nitrate were identified, fertilizer and manure, which present different isotopic $\delta^{15}\text{N}$ signatures. The relative contributions of these two sources to groundwater or surface water can be estimated by mass balance. The analysis of nitrate $\delta^{18}\text{O}$ together with $\delta^{15}\text{N}$ improves the ability to trace nitrate sources and cycling. According to field practice in the rural area of Beja, major cause of pollution comes from fertilizers. Isotope results are not conclusive about the possibility that major source of nitrate-N in groundwater comes from agriculture as expected. Further work is required regarding seasonality sampling and laboratory techniques with sufficient precision accuracy.

1. INTRODUCTION

Large-scale diffuse pollution is of great concern in most European countries. Soils and groundwater bodies show increasing nitrates and pesticides concentrations due to intensive agriculture.

This paper will focus on *Assessing the Impacts of Agriculture on Groundwater Quality Using Nitrogen Isotopes* namely in the “Gabbros of Beja Aquifer System” (350 km²) in the vicinities of Beja (south Portugal). This Aquifer System represents the most productive hard aquifer in the region and the best agriculture land use with direct consequences regarding nitrate diffuse pollution.

Nitrate diffuse pollution greatly concerns the scientific Portuguese community and the National Water Authorities (INAG). This situation must be changed according to the EU Nitrate Framework Directive (91/676/EEC) and EC Water Framework Directive (2000/60/EC). In particular, authorities should reevaluate aquifer vulnerability and mobilize funds to promote Nitrogen-use Efficiency and Nitrogen Management, regarding Environmental Farming Proposals (91/2078/EEC) and Drinking Water Regulations (80/778/EEC).

Isotopes of nitrogen were used to distinguish pollutant sources. Nitrate-nitrogen and oxygen isotopes can facilitate the distinction between fertilizer and waste as pollutant sources.

2. STUDY AREA OVERVIEW

The study area is located in South Portugal, between Ferreira do Alentejo and Serpa, covering an area of about 350 km² in Ossa–Morena geotectonic unit. A case study has been established nearby the city of Beja (Fig. 1).

The gabbro-dioritic shallow aquifer is one of the most productive formations of the Alentejo region (south Portugal). Recharge is calculated between 10% and 20% (some places more) of average annual rainfall (500 mm/yr) according to recent recharge models, and occurs mainly between January and March/April [2, 3].

In the study area well productivity's range from 1 to 15 L/s with most frequent average values around 5 L/s and unproductive drills less than 20%. A hydrochemical monitoring was carried out between July 1997 and July 2000 to assess spatial and temporal variability of nitrate contents in the aquifer due to seasonal fertilization and rainfall episodes. A large range of values was recorded but more frequent classes were 50–60 and 70–80 mgNO₃/L. The intra-annual analysis has a large range variation reaching 100 mg/L and median range from 53 mg/L to 86 mgNO₃/L.

ASSESSING AGRICULTURE POLLUTION IN THE BEJA AQUIFER

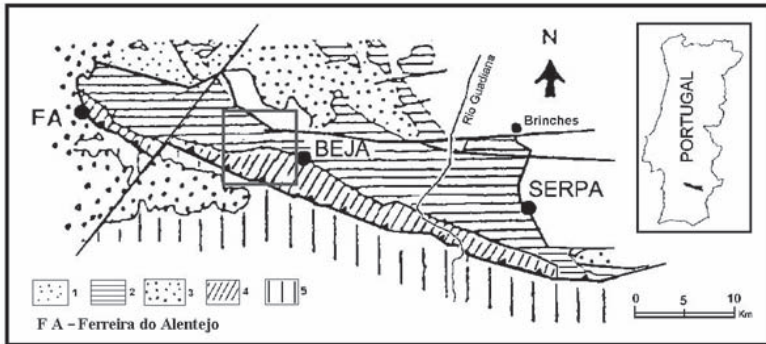


FIG. 1. Geographical location of “Gabbros of Beja” Aquifer (350 km²) and study area (50 km²). General geology adapted from Ref. [1]. 1. Odivelas Volcano-sedimentary Complex. 2. Mafic and intermediate plutonic rocks (Beja’s Gabbro Complex). 3. Plutonic acid and sub-volcanic rocks (Baleizão Porphirs). 4. Beja-Acebuches Ophiolitic Complex (meta-gabbros and basic meta-volcanites). 5. Pulo do Lobo Accretion Terrain (South Portuguese Geotectonic Unit – schists).

Increasing concentrations of nitrate in groundwater supplies for Beja municipality was recognized early in the 1940s due to excessive fertilization directed to increase national grain production. Land use is mainly cereal (wheat) and sunflower or corn as alternative crops. Under intensive cereal crops fertilizer application in the range of 100–150 kg N/ha/yr is common. The nitrate ion content in groundwater is thought to be due mainly to processes of natural nitrification, decomposition of organic material and human pollution, namely agriculture related to the use of nitrogenous fertilizers in farming.

3. ISOTOPIC APPROACH

This paper documents the development of appropriate and innovative techniques to enable isotope measurements in order to discriminate nitrogen source in groundwater of unconfined shallow aquifer near Beja (South Portugal) recently declared as vulnerable area to nitrate diffuse pollution.

The isotopic analyses of the water samples were performed in Instituto Tecnológico e Nuclear (Sacavém-Portugal). All the isotopic determinations ($\delta^2\text{H}$, $\delta^{15}\text{N}$, $\delta^{18}\text{O}_{\text{NO}_3}$ and $\delta^{18}\text{O}$) were carried out using a mass spectrometer for light isotopes.

Pollution associated to agriculture has had a direct and indirect effect on groundwater recharge and on aquifer biogeochemistry rates and composition.

Direct effects include dissolution and transport of excess quantities of fertilizers [4]. Using the mass spectrometry methodology, isotopic differences are found in most terrestrial materials having $\delta^{15}\text{N}$ compositions between -20 and $+30\%$ [5].

The dominant source of nitrogen is the atmosphere ($\delta^{15}\text{N} = 0\%$). Many plants fix nitrogen and organisms cycle this nitrogen into the soil. Other sources of nitrogen to watersheds include fertilizers produced from atmospheric nitrogen with compositions of 0 to 3% and animal manure with nitrate $\delta^{15}\text{N}$ values generally in the range of $+10$ to $+25\%$. Two factors control the $\delta^{15}\text{N}$ values of any N-bearing compound in the subsurface: (1) variations in the $\delta^{15}\text{N}$ values of inputs (sources) and outputs (sinks) of the compound in the subsurface, and (2) chemical, physical and biological transformations of materials within the soil or groundwater that produce or remove the compound.

The analysis of both $\delta^{18}\text{O}$ and $\delta^{15}\text{N}$ of nitrates provides excellent separation of nitrate sources. The nitrates formed in waters with $\delta^{18}\text{O}$ values in the range of -25 to -5% should have $\delta^{18}\text{O}$ values in the range of -9 to $+4\%$. The $\delta^{15}\text{N}$ of atmospheric nitrate has a moderate range of composition around 0% [6].

Under ideal circumstances, stable nitrogen isotopes offer a direct mean of source identification, because the two major sources of nitrate in many agricultural areas, fertilizer and manure, have isotopically distinct $\delta^{15}\text{N}$ values. The relative contributions of these two sources to groundwater or surface water can be estimated by mass balance. However, soil-derived nitrate and fertilizer nitrate commonly have overlapping $\delta^{15}\text{N}$ values, preventing their separation using $\delta^{15}\text{N}$ alone, but the analysis of nitrate $\delta^{18}\text{O}$ together with $\delta^{15}\text{N}$ improves the ability to trace nitrate sources and cycling.

In hydrology studies $\delta^{15}\text{N}$ is used also as a tracer in the identification of aquifer mixtures. According to Ref. [7] the relationships between various aquifers that are linked in succession along a general flow gradient, the nitrate concentrations and the different isotopic $\delta^{15}\text{N}$ content on groundwater allow the identification and quantification of the interconnection between different groundwater systems.

The methodologies and techniques proposed in this study may be obtained through the bibliography. The critical analysis of the methods, with the necessary rigor, would occupy space that isn't available in the format of this paper.

3.1. Results

Field sampling was carried out during December 2004 and May 2006. Waters are medium mineralized, with electrical conductivity (EC) between 300 and $1300 \mu\text{S}/\text{cm}$ and calcium-magnesium facies. Nitrates in groundwater are in the range of 2 to $150 \text{mgNO}_3/\text{L}$ with most common records overlap

ASSESSING AGRICULTURE POLLUTION IN THE BEJA AQUIFER

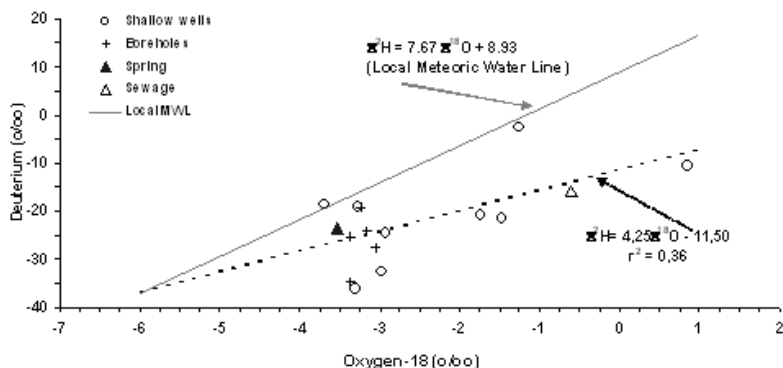


FIG. 2. δ^2H vs $\delta^{18}O$ for groundwater samples from the study area (December 2004).

40 mg NO_3/L . Water sample from wastewater treatment facilities (sample No. 1) shows the highest mineralization ($\text{EC} = 2370 \mu\text{S}/\text{cm}$) and low NO_3 and N-NO_3 content (less than 2 mg/L).

The isotopic composition of the groundwater samples collected in December 2004 was plotted in a δ^2H vs $\delta^{18}O$ diagram (Fig. 2). Also in this figure the Local Meteoric Water Line (LMWL) has been represented, estimated from the isotopic composition of precipitation in Beja meteorological station (ITN database; monthly samples from 1988-2001). The equation of the LMWL is $\delta^2H = 7.67 \times \delta^{18}O + 8.93$.

From the diagram it is possible to observe that the spring is plotted relatively closer to the LMWL, as well as the majority of the borehole water samples. The shallow groundwater samples and sewage present a deviation from this line, most probably related with isotopic fractionation due to evaporation processes. Also from the diagram a good relation between the isotopic composition of the sewage and the isotopic composition of the shallow groundwater samples (wells) can be observed.

Previous work indicates that samples No. 2, 4 and 9 could have domestic/sewage contribution to nitrate content [8]. Fertilizers should influence other samples, since wells are located in the open field (samples Nos. 3, 5, 6, 7, 8, 10, 11, 12, 13, 14, 15 and 16). Isotopic data was used to confirm conceptual model and the magnitude of source contribution. Results of isotopic analyses are shown in Table 1.

Nitrogen isotope ratios of groundwater show a range in $\delta^{15}\text{N}$ from +1‰ to +26‰. For sewage sample, $\delta^{15}\text{N}$ is +16.14‰. These results overlap between the $\delta^{15}\text{N}$ values of both animal and septic tank wastes (Fig. 3).

TABLE 1. ISOTOPE DATA ANALYSES (DECEMBER 2004 AND MAY 2006).

Code	December 2004				May 2006		
	NO ₃ (mg/L)	δ ¹⁵ N (‰)	δ ¹⁸ O (H ₂ O) (‰)	δ ² H (H ₂ O) (‰)	NO ₃ (mg/L)	δ ¹⁵ N (‰)	δ ¹⁸ O (NO ₃) (‰)
1– Sewage	1.28	16.14	-0.60	-15.90	–	–	–
2 – Well	38.97	18.22	-1.46	-21.60	–	–	–
3 – Well	37.78	12.42	-1.26	-2.60	48.37	6.88	4.29
4 – Well	61.73	–	-2.93	-24.60	113.00	8.13	5.35
5 – Well	18.91	26.17	0.86	-10.80	144.20	17.71	-4.71
6 – Well	66.30	3.69	-3.27	-19.20	110.60	1.67	5.35
7 – Well	52.88	3.07	-3.29	-36.30	34.50	16.41	2.63
8 – Well	58.06	13.38	-3.69	-18.70	–	–	–
9 – Well	53.76	13.63	-2.96	-32.60	–	–	–
10 – Well	2.66	11.95	-1.73	-20.90	–	–	–
11 – Borehole	40.96	8.12	-3.37	-25.30	58.40	7.66	-8.16
12 – Borehole	40.34	26.12	-3.37	-34.80	77.70	3.06	4.79
13 – Borehole	45.92	–	-3.17	-24.20	49.60	5.63	9.95
14 – Borehole	56.11	3.50	-3.24	-19.30	–	–	–
15 – Borehole	41.67	–	-3.05	-27.60	–	–	–
16 – Spring	41.50	–	-3.53	-23.60	52.70	–	7.83

Oxygen isotope δ¹⁸O (H₂O) data are in the range of -3.5‰ to +0.9‰ for groundwater and is -0.6‰ for sewage. Oxygen isotope δ¹⁸O (NO₃) data are in the range of -8‰ to +10‰.

Fig. 4 shows the normal range of δ¹⁸O and δ¹⁵N values for dominant sources of nitrate [5]. Nitrate derived from ammonium fertilizer, soil, organic matter and animal manure have overlapping δ¹⁸O values; for these sources δ¹⁵N is a better discriminator. In contrast, nitrate derived from nitrate fertilizer or atmospheric sources are readily separable from microbial nitrate using δ¹⁸O, even though the δ¹⁵N values are overlapping. The dual isotope method has proved quite useful for source identification in some surface-groundwater studies [6].

ASSESSING AGRICULTURE POLLUTION IN THE BEJA AQUIFER

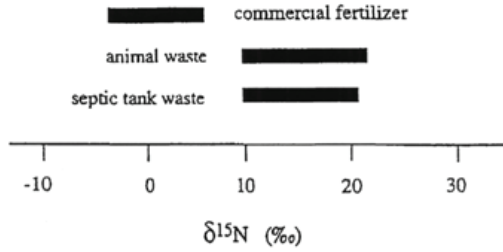


FIG. 3. Range of $\delta^{15}N$ values for the major sources of nitrates into groundwater [8].

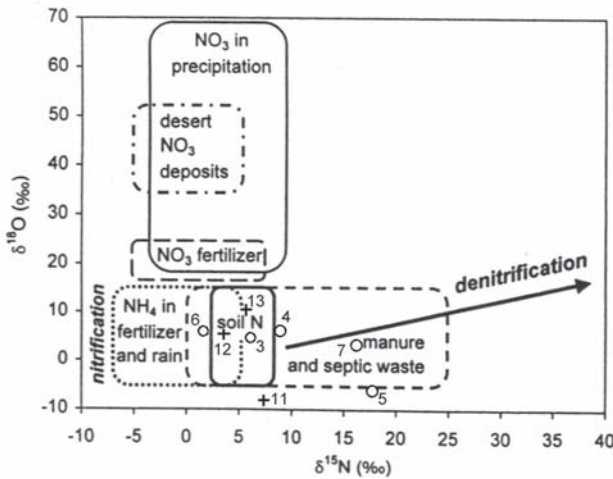


FIG. 4. Schematic of typical ranges of $\delta^{18}O$ and $\delta^{15}N$ values of nitrate from various sources (adapted from Ref.[5]) and sample plot (May 2004).

Nitrification of ammonium and/or organic-N in fertilizer, precipitation, and organic waste can produce a large range of δ values. Soil waters tend to have higher $NO_3-\delta^{18}O$ values and a larger range of $NO_3-\delta^{18}O$ values than groundwaters due to higher $\delta^{18}O$ values of O_2 and/or H_2O in soils. Oxygen isotope from the NO_3 determinations indicates that fertilizers do not provide major source of nitrate to groundwater. The combination of both $\delta^{15}N$ and $\delta^{18}O$ data indicate that signatures observed in groundwater are the result of ammonia nitrification originating from either animal wastes or septic tank wastes, with no significant influence from commercial fertilizers.

4. CONCLUSIONS

Progress has been made in Portuguese research centres to allow determination of $\delta^{18}\text{O}$ and $\delta^{15}\text{N}$ in nitrates. Further work is required to ensure robust techniques with sufficient precision and accuracy.

Using the current techniques it is possible to discriminate different sources of anthropogenic contamination into ground and surface systems.

According field practice and previous monitoring, conceptual model indicates that major cause of pollution comes from fertilizers.

However, preliminary results are not conclusive about the possibility that major source of nitrate-N in groundwater comes from agriculture. There are several factors in the ecosystems that can significantly modify the $\delta^{15}\text{N}$ values. Mixing of point and non-point sources along shallow flowpaths makes determinations of sources, extent and denitrification processes very difficult to identify.

Further work is necessary to verify. The origin of nitrate in “Gabbros of Beja” aquifer system and source contribution.

ACKNOWLEDGEMENTS

The authors wish to express their gratitude to Science and Technology Foundation (FCT) for project financial support and PhD scholarship. Research is based on funding project “Assessing the impacts of agriculture on groundwater quality using nitrogen isotopes” developed in Beja countryside (South Portugal), for the period 2004–2007

REFERENCES

- [1] FONSECA, P., Estudo da Sutura Varisca no SW Ibérico nas regiões de Serpa-Beja-Torrão, Alvito-Viana do Alentejo, PhD Thesis, Universidade de Lisboa, (1995) 325.
- [2] PARALTA, E., RIBEIRO, L., Stochastic Modelling and Probability Risk Maps of Nitrate Pollution in the Vicinities of Beja (Alentejo, South Portugal), In Ribeiro L (ed.) Proc. of 3rd International Conference on Future Groundwater Resources at Risk (FRG'01) (2001) 251–261.
- [3] LTA, E., OLIVEIRA, M., Assessing and modelling hard rock aquifer recharge based on complementary methodologies — A case study in the “Gabbros of Beja” Aquifer System (South Portugal), Proc. 2nd Workshop of the Iberian Regional Working Group on Hard Rock Hydrogeology (2005).

ASSESSING AGRICULTURE POLLUTION IN THE BEJA AQUIFER

- [4] BOHLKE, J-K., Groundwater recharge and agricultural contamination. *Hydrogeology Journal* **10** (2002) 153–179.
- [5] KENDALL, C., McDONNELL, T., Tracing nitrogen sources and cycling in catchments in isotope Tracers in Catchment Hydrology. Chapter 16, Kendall & McDonnell, Elsevier Science (1998).
- [6] KENDALL, C., Use of the $\delta^{18}\text{O}$ and $\delta^{15}\text{N}$ of nitrate to determine sources of nitrate in early spring runoff in forested catchments. In *Isotopes in Water Resources Management*, IAEA, Vol.1 (1996) 167–176.
- [7] JOSEPH, C., et al., Utilisation du traçage isotopique naturel de l'azote¹⁵ pour la mise en évidence de mélanges dans les aquifères complexes, In *Isotope Techniques in Water Resources Development*, IAEA (1987) 351–365.
- [8] PARALTA, E., et al., Assessing the impacts of agriculture on groundwater quality using nitrogen isotopes – preliminary results on the “Gabbros of Beja” Aquifer System (South Portugal), 2nd Workshop of the Iberian Regional Working Group on Hardrock Hydrogeology, Évora, Portugal (2005).
- [9] WASSENAAR, L., Evaluation of the origin and fate of nitrate in the Abbotslord Aquifer using the isotopes of N and O in NO_3^- . *Applied Geochemistry* **10** (1995) 391–405.

DEUTERIUM TRACER EXPERIMENT IN THE UNSATURATED ZONE OF FRACTURED KARST AQUIFERS

B. CENCUR CURK

IRGO – Institute for Mining,
Geotechnology and Environment,
Ljubljana, Slovenia

W. STICHLER

GSF – Institute of Groundwater Ecology,
Neuherberg, Germany

Abstract

In the frame of Association of Tracer Hydrology project a multi-tracer experiment was performed at the research field site (RFS) Sinji Vrh, which consists of surface set-up and a research tunnel, 15 m below the surface. A special construction (1.5 m long segments) for collecting water seeping from the ceiling of the research tunnel was developed. Deuterium (90%), potassium bromide, lithium chloride, zinc sulphate, sulfonic acid, pyranine, naphthionate, uranine, Sulforhodamine B, micro spheres and bacteriophages P22H5 were used as tracers and injected into the borehole. Tracers appeared immediately after the first significant precipitation event, respectively four days after the injection. The most pronounced breakthrough appeared for uranine, deuterium and chlorine ions. This tracer experiment again confirmed the presence of fast flow through a channel above two sampling points (MP4 and MP5), where the response is rapid and the detected concentrations are high. After the injection of tracers, they remain in the microfracture systems of the unsaturated zone and are rinsed by subsequent larger precipitation events even up to several years (in this experiment at least three years) after the injection. The results from Sinji Vrh have shown that the unsaturated zone in the fractured and karstified rocks plays an important role in pollution retardation and storage.

1. INTRODUCTION

Fractured and karstified rocks are very heterogeneous and complex in terms of their geometry and void topology. This results in parameter variability and large uncertainties reflecting complicated hydraulic, mechanical, thermal,

and chemical processes. Therefore, detailed studies of these processes have to be performed on a macro scale at instrumented field research sites [1]. Such a site was established [2] at Sinji Vrh in the western part of Slovenia (Fig. 1). The main goal of the research field site at Sinji Vrh (RFS Sinji Vrh) was the study of flow and solute (particularly pollutant) transport in fractured and karstified rocks, with a focus on the unsaturated zone.

RFS Sinji Vrh is located at the edge of the Trnovski Gozd plateau (Fig. 1; mean altitude of 900 m.a.s.l), which is an overthrust (Trnovo nappe) of carbonate rock over impermeable Eocene ($E_{1,2}$) flysch rocks (turbidites sediments, mainly changing of marble and sandstone). This area is composed of Jurassic (Lias-Dogger) limestone, which passes laterally into crystalline dolomite. The beds dip in general towards south-west and dip angle changes between 30° and 60° . This territory is crossed by the subvertical Avče fault with a Dinaric direction (NW–SE), resulting in crushed and fractured rock. Within

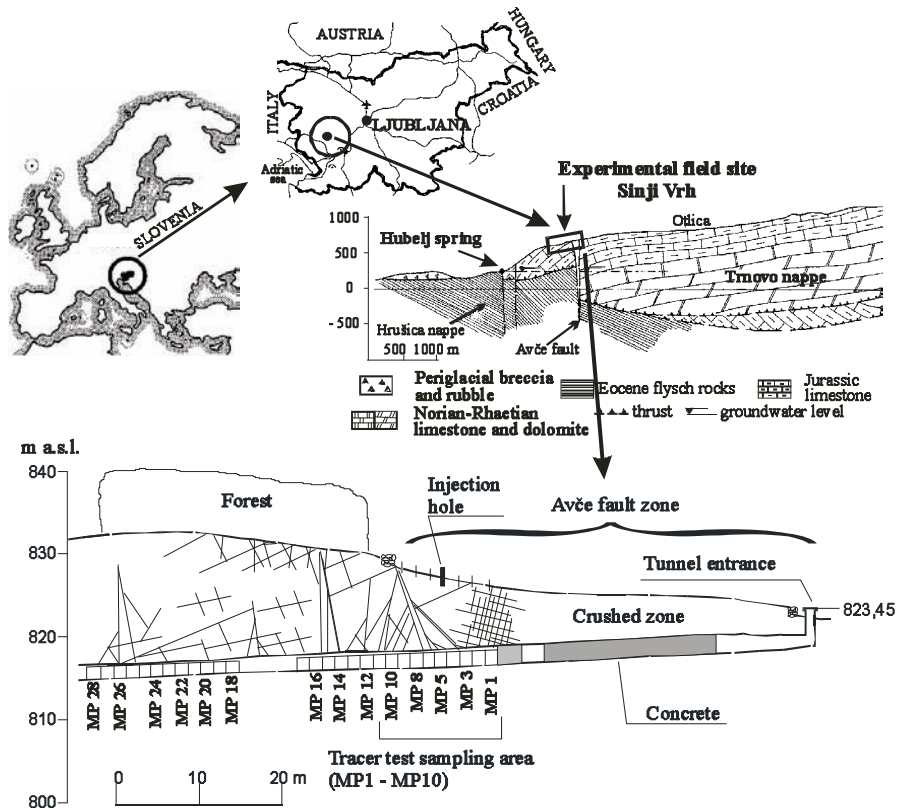


FIG. 1. Location of the research field site Sinji Vrh (RFS Sinji Vrh) with a geological cross-section of Trnovo plateau [6, 7]. Below: Longitudinal section of the RFS Sinji Vrh with tracer tests area and tracer test sampling points in the research tunnel: MP1 – MP10.

DEUTERIUM TRACER EXPERIMENT IN THE UNSATURATED ZONE

the broader fault area numerous accompanying subvertical faults (stretching in NNW–SSE and NNE–SSW directions) are present, branching from the main fault plane and repeatedly joining it [3]. The geological profile of the Trnovski Gozd plateau is presented in Fig. 1 [4]. The groundwater horizon lies extremely deep and appears on the surface at the lowest point of the impermeable flysch border in karstic spring Hubelj (Fig. 1). Average annual precipitation in the catchment is roughly 2450 mm. In this region mainly thin (10–50 cm) carbonate soil types are found. They have low water retention capacities facilitating fast infiltration rates [5].

The research field site in the unsaturated zone of fractured and karstified rock presents a 340 m long artificial tunnel, 5 to 25 meters below the surface (Fig. 1). The tunnel direction is nearly constant running southwest – northeast (N 66° E). The surface is covered with grassland and small beech forests which usually cover outcrops. The unsaturated fractured and karstified limestone has a negligible matrix porosity and very high fracture density with some larger conduits [8]. An agrometeorological station has been installed on the surface, where precipitation, evaporation, air temperature, air moisture, wind speed and direction (both at two levels) are continuously measured. It is located near the tunnel entrance at a height of 825 m.

2. MULTITRACER EXPERIMENT

In the frame of Association of Tracer Hydrology project a multitracer experiment was performed at the RFS Sinji Vrh in autumn 2003. Deuterium (90%; 200 mL), potassium bromide, lithium chloride, zinc sulphate, sulfonic acid, pyranine, naphthionate, uranine, Sulforhodamine B, micro spheres and bacteriophages P22H5 were used as tracers. The aim of this tracer experiment was to quantify channel flow and fractured zone flow and to determine different behaviour of conservative tracers, which was observed in previous tracer experiments. For this tracer experiment a new borehole was drilled through the soil cover on top of the research field (Fig. 1) with a depth of 0.9 m, protected by a PVC pipe, enabling direct injection into the fractured karstified carbonate rock. The tracer solution was slowly poured out into the open borehole. Tracer cocktail was flushed with 25 L water. The injection was performed on a rainy day when the temperature was 11°C, and the next few days were sunny and dry.

A special construction for collecting water penetrating through the rock was developed. The water seeping from the ceiling of the research tunnel is gathered in 1.5 m long segments (MP1–MP10; Fig. 1) with a gathering surface of 2.2 m².

For the multitracer experiment sampling points MP1 to MP10 in the tunnel (Fig. 1) were selected due to the injection position. Two automatic devices for flow rate and conductivity were installed in the sampling points MP4 and MP5. For all other sampling points the amount of water was measured by each sampling campaign. Isotopic analyses of the sampled waters were performed in GSF, Institute of Hydrology, Munich.

3. RESULTS

Tracers appeared immediately after the first significant precipitation event, respectively four days after the injection. The most pronounced breakthrough appeared for uranine, deuterium and chlorine ions. The $\delta^2\text{H}$ composition for all sampling points MP1–MP10 is presented in Fig. 2. This tracer experiment again confirmed the presence of fast flow through a channel above the sampling points MP4 and MP5 (see Fig. 1), where the response is rapid and the detected concentrations are high. The peak $\delta^2\text{H}$ composition in MP5 was 2455‰ and it appeared in the first sample after the injection (four days after the injection and immediately after the first rain event). The highest deuterium value in MP4 appeared after 21 days (18 days after the first rain event) with a composition of 306‰. It should be pointed out, that deuterium was injected at a high enough concentration in order to get significant concentration in fracture system, but this

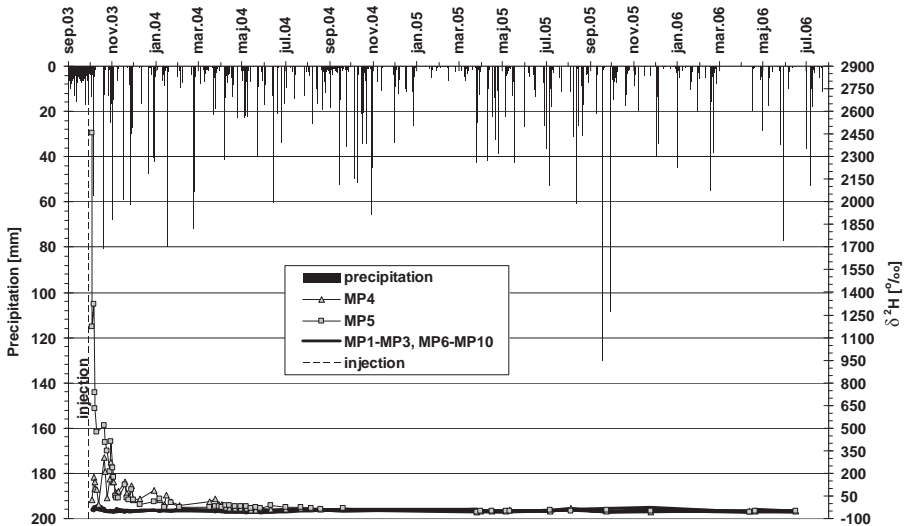


Fig. 2. Deuterium isotope composition of water in sampling points MP1–MP10.

DEUTERIUM TRACER EXPERIMENT IN THE UNSATURATED ZONE

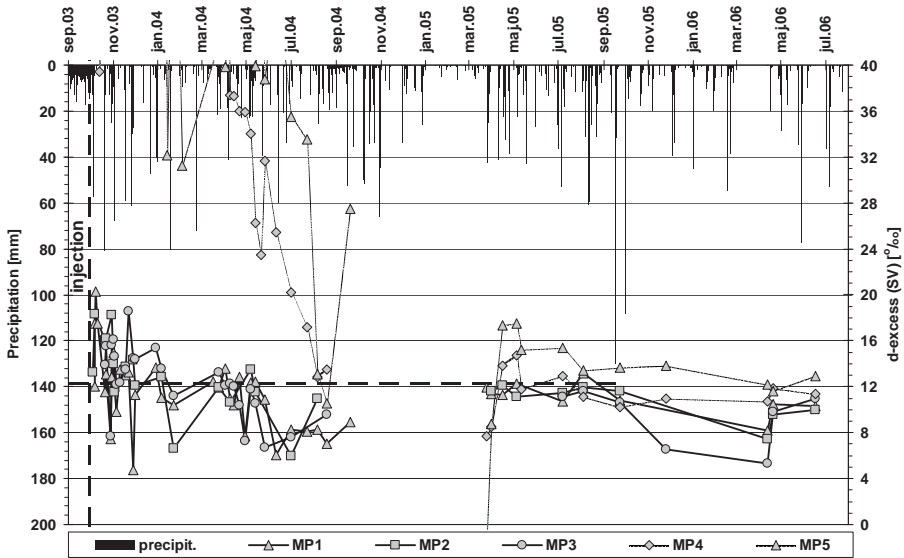


FIG. 3. Deuterium excess in sampling points MP1 – MP5 (vertical dashed line: injection, horizontal dashed line: d-excess for Sinji Vrh unsaturated zone).

caused a high concentration in the fast pathways such as MP4 and MP5. In other sampling points, where the hydraulic permeability is significantly lower, the $\delta^2\text{H}$ composition reached up to -15‰ (MP6). The smallest maximum appeared in MP10 and it was -38‰ . In the fractured system (MP1–MP3, MP6–MP10) the breakthrough was not obvious as it was close to the background variation (-30 to -60‰) in unsaturated zone water (thick line around 0 in Fig. 2).

Besides deuterium $\delta^{18}\text{O}$ was also measured in water samples. The relationship between $\delta^{18}\text{O}$ and $\delta^2\text{H}$ in the unsaturated zone water was determined based on high frequency (monthly) [9] and the last period (quarterly) [10] sampling from 1999–2004 and is: $\delta^2\text{H} = 7.7 \times \delta^{18}\text{O} + 12.3$. In Fig. 3 and Fig. 4 d-excess is depicted for MP1–MP5 and MP6–MP10 in a smaller scale. These figures show significant reaction to precipitation in sampling points MP6, MP8 and MP9. MP6 is connected to the fast channel, whereas MP8 and MP9 represent the broken zone of a fault. MP9 is connected to the fractured zone, which represent a storage zone, where flow is slow with higher dispersion of the tracer, since the maximum concentration appeared 182 days after the injection. In other sampling points (MP1, MP2, MP3, MP7 and MP10) the maximum d-excess values were around 20 but it is not clear whether the isotope composition change depicts tracer breakthrough or only variations in

TABLE 1. THE FIRST APPEARANCE OF DEUTERIUM IN DIFFERENT SAMPLING POINTS AND THE APPEARANCE OF MAXIMUM $\delta^2\text{H}$ COMPOSITION. [11]

	Appearance of tracer (days)	Max. $\delta^2\text{H}$ composition (‰)	Max. value of d-excess (UNZ SV)	Appearance of Max. value (days)
MP1	7.4	-18.5	20.3	8.4
MP2	4.4	-28.4	18.4	6.4
MP3	21.4	-34.6	18.6	52.4
MP4	4.4	305.6	372.0	21.4
MP5	3.4	2454.9	2522.5	3.4
MP6	3.4	-14.9	33.9	6.4
MP7	3.4	-16.6	18.2	22.4
MP8	6.4	-23.1	29.7	7.4
MP9	21.4	-33.65	24.7	182.4
MP10	7.4	-38.3	20.3	7.4

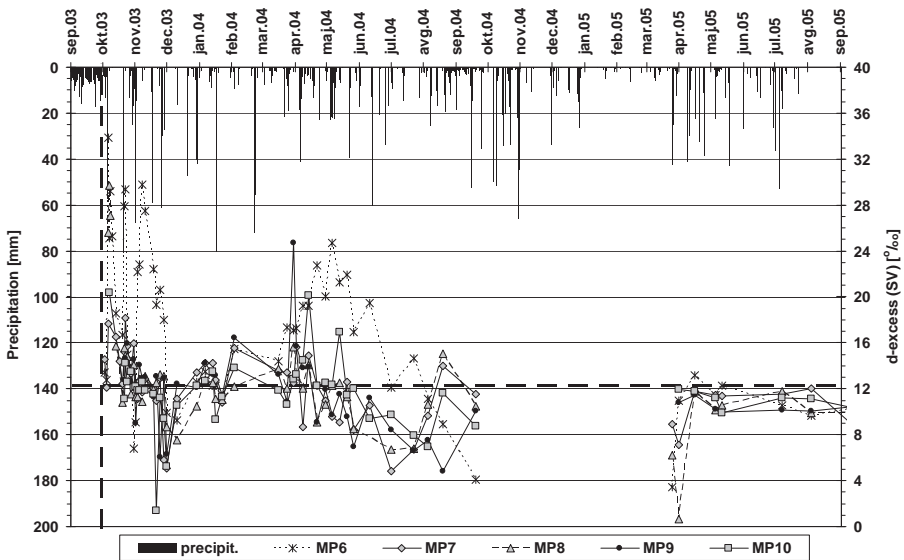


FIG. 4. Deuterium excess in sampling points MP6–MP10 (vertical dashed line: injection, horizontal dashed line: d-excess for Sinji Vrh unsaturated zone).

DEUTERIUM TRACER EXPERIMENT IN THE UNSATURATED ZONE

background. The appearance of deuterium in different sampling points and the appearances of maximum concentrations are summarized in Tab. 1.

4. CONCLUSIONS

Fractured and karstified rocks are highly heterogeneous and complex, therefore knowledge of the rock structure is of paramount significance for predicting flow and transport. The transport of pollutants depends on (i) saturation rate of the soil and unsaturated zone, (ii) on precipitation events and (iii) on the presence of channels and interconnected fracture networks. Pollution remains in the fractures of the upper part of the unsaturated zone and is flushed by subsequent large precipitation events which can occur several months or years afterwards. The degree of flushing is highly dependent on the antecedent moisture conditions within the unsaturated zone.

The new injection borehole for the multi-tracer experiment obviously intercepted the main fracture, therefore the tracer was flushed after the first precipitation event. It is suggested, that tracer dispersed into the smaller surrounding fractures below the borehole (soil — unsaturated rock zone) and was flushed by subsequent larger precipitation events several months or years afterwards. Sampling is still in progress and will close this year and all the calculations will be performed.

The tracer experiment has shown different flow velocities. Karst conduits or large fractures/faults show no storage capacity, the most rapid flow, and very limited dispersion. Broken and fractured zones have some storage capacity, which leads to retardation and the slower flow. The fractured and karstified rock could be seen as discrete conduits within highly fractured rock. The latter could be considered as a permeable matrix, since the rock (limestone) matrix porosity (intracrystalline) is negligible and the system could be best modelled with a hybrid model (comprising discrete conduits and a continuum of dense fractured system) rather than a dual porosity model (where there would be a continuum of conduits and a continuum of dense fractured rock). This is a subject for future research.

ACKNOWLEDGEMENTS

This work was partly supported also by the International Atomic Energy Agency under the research grant No11519. We express our sincere thanks to ATH members for performing the tracer experiment and especially for analysing water samples.

REFERENCES

- [1] ČENČUR CURK, B., Terenski eksperimentalni poligoni kot osnova pri študiju prenosa snovi v nezasičeni kraško-razpoklinski kamnini (Experimental field sites as a basis for the study of solute transport in the vadose zone of karstified rock), *Acta hydrotechnica* **15** 20 (1997) 111, Ljubljana.
- [2] VESELIČ, M., Study of Mass Transport in Fractured and Karstified Rocks. Project Proposal for 1995–1997 Research Grant of the Ministry of Science and Technology of the Republic of Slovenia (1995) 12, Ljubljana.
- [3] ČAR, J., Geological description, in *Karst Hydrogeological Investigations in South-Western Slovenia*, *Acta carsologica* **26** 1 (1997) 68–73, Ljubljana.
- [4] JANEŽ, J., Geological structure and hydrogeological position of the Hubelj spring, in: *Karst Hydrogeological Investigations in South-Western Slovenia*, *Acta carsologica* **26** 1 (1997) 82–86, Ljubljana.
- [5] MATIČIČ, B., Agricultural threats to pollution of water of Trnovsko-Banjška Planota, in: Kranjc, A.(editor), *Karst hydrogeological investigations in south-western Slovenia*, *Acta carsologica* **26** 1 (1997) 102–113, Ljubljana.
- [6] JANEŽ, J., Underground connections in dependency to hydrogeological conditions, in: *Karst Hydrogeological Investigations in South-Western Slovenia*, *Acta carsologica* **26** 1 (1997) 329–332, Ljubljana.
- [7] VESELIČ, M., ČENČUR CURK, B., Test studies of flow and solute transport in the unsaturated fractured and karstified rock on the experimental field site Sinji Vrh, Slovenia, In: K.P. SEILER & S. WOHNLICH (eds.): *New approaches characterizing groundwater flow: proceedings of the XXXI International Association of hydrogeologists Congress, Munich, Germany, 10–14 September 2001* (2001) 211–214, Lisse, Balkema.
- [8] ČENČUR CURK, B., VESELIČ, M., Laboratory and experimental study of contaminant transport in fractured and karstified rock, *RMZ – Materials and Geoenvironment* **46** 3 (1999) 425–442, Ljubljana.
- [9] TRČEK, B., Epikarst zone and the karst aquifer behaviour: a case study of the Hubelj catchment, Slovenia, Ljubljana, *Geološki zavod Slovenije* (2003) 100.
- [10] TRČEK, B., Transport processes in the unsaturated zone of the karst aquifer, Phase report on isotope research, *Geological Survey* **7** (2003) Ljubljana.
- [11] ČENČUR CURK, B., Water dynamics in the unsaturated zone of fractured carbonate rock, in: *Radionuclide transport dynamics in freshwater resources, Final report of a coordinated research project (1999–2005)*, IAEA-TECDOC-xxxx (2007) in press.

CARBON-13 AND CARBON-14 CONTENTS OF GROUNDWATER LOCATED IN SANDY AQUIFER OUTCROPS: DRIVING INFLUENCE OF THE UNSATURATED ZONE

M. GILLON, F. BARBECOT, E. GIBERT, C. MARLIN, M. MASSAULT
Laboratoire IDES (Interactions et
Dynamique des Environnements de Surface),
Université Paris-Sud,
Orsay, France

Abstract

Better assessment of carbon isotopes cycle in the Unsaturated Zone (UZ) is a key point for estimating the ^{14}C residence time of relatively young groundwater. In order to approach the UZ carbon cycle and to quantify C-fluxes, the distribution of the isotopic composition (^{13}C – ^{14}C) of each carbon phase (Dissolved Inorganic Carbon, CO_2 , carbonates) have been investigated on two experimental sites *i.e.* respectively the carbonate-free Fontainebleau sands (Paris Basin, France) and the carbonate Astian sands (South France). Similar matrix properties on both sites allowed identical *in situ* sampling protocols based on water-gas permanent samplers specifically developed for this work. In a carbonate-free UZ, the isotopic composition of water depends essentially on CO_2 diffusion. While, in a carbonated UZ, the carbonates force the isotopic composition of dissolved inorganic carbon and CO_2 . These carbon exchanges lead to a depletion of matrix carbonates by precipitation of secondary calcite.

1. INTRODUCTION

Increasing scarcity of groundwater resources require the improvement of aquifer management. This management consists partly in estimating groundwater residence time in aquifers that can be done through the measurement of radioactive decay of ^{14}C contained in the total dissolved inorganic carbon (TDIC). This approach requires the knowledge of the initial ^{14}C activity of TDIC in recharge water [1], that mainly results of interaction between TDIC, CO_2 produced in soils and carbonates – if existing – within the unsaturated zone (UZ). In aquifers in which dissolution of carbonates impacts the ^{14}C activity of groundwater, several models [2–7] are commonly

used to assess the initial activity. However several questions remain like that concerning the actual ^{14}C activity of recharge groundwater. The study of carbon dynamics in the UZ would lead to a better knowledge of this initial composition of TDIC [8–14]. In the present paper, the turn-over and the fluxes of carbon in the UZ have been characterized by studying spatial and temporal evolution of isotopic contents (^{13}C and ^{14}C) of all the carbon phases (CO_2 , TDIC, carbonates). This monitoring has required the set up of an in-situ specific experimental equipment.

2. METHODOLOGY

In order to characterize transfer mechanisms of TDIC from soils towards the water-table, two sites have been selected and equipped according to two criteria. The sandy nature of the aquifer ensures a more homogeneous transfer of fluids. The presence or not of carbonates in the aquifer allows to identify the carbonate impact on carbon fluxes in recharge area. The equipment required for this study have been set up on outcrop areas of two aquifers, *i.e.* respectively the carbonate-free Fontainebleau sands (Paris Basin, France) and the carbonate Astian sands (South France).

2.1. Field equipment

The experimental equipment set up on field sites has allowed a seasonal sampling of gas, groundwater and soil water at various depths, along vertical profiles within the UZ. During drilling, core samples were collected at different depths for the isotopic study of carbonates. In order to avoid any pollution of the UZ, these drillings have been realized without any fluids (water and air) by using a helicoid drill coupled to a GEOTOOL GTR790. Extracted materials were stored apart from the ground to avoid any biogenic pollution in surface and to allow a backfill of borehole respecting the initial lithology once the scientific material set up.

The hydrogeological setting of the experimental sites has conditioned the drilling. In the case of the Astian sands, only one borehole has been drilled, in an area located above a piezometric dome and characterized by the homogeneity of vegetation cover. For the Fontainebleau sands, three experimental vertical profiles have been equipped along a main flow line of groundwater. Technical characteristics of each profile are given in Table 1.

CARBON 13 AND CARBON-14 CONTENTS OF GROUNDWATER

TABLE 1. TECHNICAL CHARACTERISTICS OF STUDIED BOREHOLES.

Aquifer	Astian sands		Fontainebleau sands	
Borehole No.	1	1	2	3
Borehole depth	25.8 m	16.5 m	22.0 m	9.0 m
Depth to water table	24.3 m	no data	21.6 m	6.5 m
Numbers of screens to sample gas within the UZ	8	7	7	6
Number of ceramic cups to sample interstitial water within the UZ	3	0	3	3
Sampling of groundwater	yes	no	no	yes

2.2. Gas sampling in the unsaturated zone

The equipment set up in the study sites is similar to that of Reardon and co-authors [8]. The sampling device consists on a filtrating stainless steel elements (screen SWADGELock, 140 μm) linked to polyethylene capillary tubes (\varnothing in 2mm) by a pipette tip (polyethylene, 5 ml). Each screen is fixed at a defined depth, outside of the piezometric filled tube (Fig. 1). The capillary tubes connect each screen to the surface. These devices represent a dead volume of 10^{-2} to $3 \cdot 10^{-1}$ L depending on the length of capillary tube. The gas sampling has been made under weak vacuum with a gas syringe, the system being then purged from 4 to 10 times.

2.3. UZ water and groundwater sampling

Interstitial water within the UZ has been sampled using porous ceramic cups. These latter are buried in the UZ from 0.5 to 9 m below ground level. They are connected to the ground via two Teflon capillary tubes (Fig. 1). A vacuum has been applied in the cup using a hand vacuum pump in order to force the entry of soil-water through the porous ceramic. After re-equilibration of pressure (~ 24 hours), water contained in the ceramic cups has been extracted by pushing out the water [3] with an inert gas (Argon; Fig. 1). The sampling method is however restricted to a suction lower than 850 hPa.

3. RESULTS AND DISCUSSION

The CO₂ partial pressures are roughly constant with depth. Carbon transport downward the aquifer likely occurs by water percolation through the UZ but also by diffusion of isotopic species induced by different diffusion coefficients according to the isotope weight.

Concerning the Fontainebleau sands, the isotopic ¹³C and ¹⁴C compositions of CO₂ are quite similar along the three depth profiles. The δ¹³C_{CO₂} and A¹⁴C values range between -27 and -23‰ and 109 and 112 pMC respectively. For the Astian sands area, the ¹³C contents of CO₂ is enriched compared to that of the Fontainebleau sands while ¹⁴C activities are lower, ranging from -24 to -21‰ for carbon-13 and from 80 to 100 pMC for carbon-14.

On both sites, the isotopic composition of dissolved carbon is similar with that of CO₂ gas once corrected from the fractionation factor.

(a) Fontainebleau sands:

- (i) δ¹³C_{groundwater} from -16,5 to -20.5‰,
- (ii) A¹⁴C_{groundwater} from 103 to 112 pMC,
- (iii) δ¹³C_{water of the UZ (0,5-1 m deep)} from -20 to -22‰,
- (iv) A¹⁴C_{water of the UZ (0,5-1 m deep)} of about 108 pMC ;

(b) Astian sands:

- (i) δ¹³C_{groundwater} from -12 to -13 ‰,
- (ii) A¹⁴C_{groundwater} from 70 to 80 pMC,
- (iii) δ¹³C_{water of the UZ at 1 m deep} of about -16 ‰,
- (iv) A¹⁴C_{water of the UZ at 1 m deep} of about 100 pMC.

The two study sites show a wide range of isotopic contents within the first upper metres (0–5 m; Fig. 2). In both aquifers, the upper values are consistent with the modern local vegetation (C3-plants; -27 to -23 ‰). The seasonal isotopic variations observed in the profile tops can be explained by (1) two different ways of CO₂ production, *i.e.* root respiration (vegetative) and CO₂ production via organic matter mineralization by micro-organisms, and/or (2) a situation stress due to water lack or higher temperature of the former production ways [5, 6]. Below 5 m deep, the variability becomes insignificant, with however two different behaviours according the sites: (1) quite constant ¹³C and ¹⁴C contents in the carbonate-free system, and (2) ¹³C contents increasing parallel to decreasing ¹⁴C activities with depth in the carbonated system (Fig. 2).

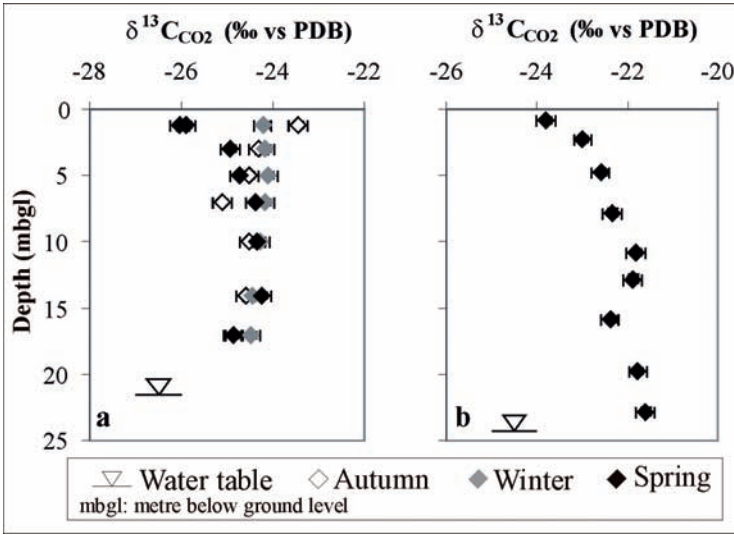


FIG. 2. ^{13}C and ^{14}C contents of CO_2 in the unsaturated zone of (a) Fontainebleau sands (profile 2), and (b) Astian sands.

In the carbonate-free UZ, the isotopic signature of water likely depends on biogenic CO_2 diffusion, the contact time between CO_2 and TDIC being nearly long enough to attain the isotopic equilibrium between the two phases.

In the carbonated UZ, the single diffusion of CO_2 , $^{13}\text{CO}_2$ and $^{14}\text{CO}_2$ cannot explain the observed trend. The carbonates interact with the other C phases and give their signature to both TDIC and CO_2 gas. The isotopic composition of carbonates, more depleted in ^{13}C than the value expected for a marine carbonate ($\delta^{13}\text{C}_{\text{expected}} \sim 0 \text{‰}$, [7]; $\delta^{13}\text{C}_{\text{measured}}$ ranging from -6 to -10‰), also highlights that carbon exchanges occur in between these three C phases. This ^{13}C -depletion of carbonates results from the precipitation of a secondary calcite with an isotopic composition corresponding to that of dissolved carbon once corrected from the fractionation factor.

4. CONCLUSION AND PROSPECTIVE

The monitoring of the isotopic composition of CO_2 , TDIC carbon and carbonates (if present) highlights the interactions existing between the three phases and the variations of isotopic signatures due to the competition between transport and exchanges between the three phases.

CARBON 13 AND CARBON-14 CONTENTS OF GROUNDWATER

Using these results from this work, we are establishing a transport model of carbon and its associated isotopes in the UZ. This model includes:

- fluctuations of temperature and of water content within the UZ, that can be reached with the Hydrous 1D software [8] and by using time-series of meteorological data as input function. Temperature and water contents are at the origin of variations of CO_2 , $^{13}\text{CO}_2$ and $^{14}\text{CO}_2$ diffusion coefficients in the UZ as well as the water advective flux from the ground to the aquifer;
- CO_2 , $^{13}\text{CO}_2$ and $^{14}\text{CO}_2$ diffusion based on the Fick's law;
- water advection;
- carbon exchange between water and gas; these exchange fluxes are calculated assuming that the equilibrium between the two phases is reached at each calculation steps;
- exchanges between carbonates, if present, and the dissolved carbon ;
- ^{14}C radioactive decay;
- the isotopic composition of the atmosphere as the CO_2 input function, and assuming that the water has already reached from the ground, a similar mineralization to that of the aquifer;
- just above the water table, concentration gradients of carbon, temperature and water flux are assumed equal to zero.

Up to now, the field-results allow to adjust the model in order to estimate the respective weight of every above-mentioned parameters (diffusion coefficient, advective flux, exchanges between the different phases) on the fluctuations of the isotopic composition of each phase. This model will ensure the monitoring and evolution of the isotope profile towards the steady state profile over several years and to deduce the "input" isotopic composition of the aquifer.

REFERENCES

- [1] FONTES, J.Ch., Chemical and isotopic constraints on ^{14}C dating of groundwater, Radiocarbon After Four Decades, Taylor R.E., Long A. & Kra R.S (eds.), Springer-Verlag, New-York (1992) 242–261.
- [2] TAMERS, M.A., Radiocarbon ages of groundwater in an arid zone unconfined aquifer, *In* Isotope Techniques in the Hydrologic Cycle, American Geophysical Union Monograph **11** (1967) 143–152.
- [3] INGERSON, E., PEARSON, F.J., Estimation of age and rate of motion of groundwater by the ^{14}C -method. *In* Miyake Y. & Koyama T. (eds), Recent researches in the field of hydrosphere, atmosphere and nuclear geochemistry, Tokyo, Maruzen (1964) 263–283.

- [4] FONTES, J. Ch., GARNIER, J.M., Determination of the initial ^{14}C activity of the total dissolved carbon: a review of the existing models and a new approach, *Water Resources Research* **15** 2 (1979) 399–413
- [5] EVANS, G.V., OTLET, R.L., DOWNING, A., MONKHOUSE, R.A., RAE, G., Some problems in the interpretation of isotope measurements in United Kingdom aquifers, *In Isotope Hydrology II*, Vienna, IAEA (eds) (1979) 679–708.
- [6] EICHINGER, L., A contribution to the interpretation of ^{14}C groundwater ages considering the example of a partially confined sandstone aquifer, *In Stuiiver M. and Kra R.S. (eds), Proceedings of the 10th International ^{14}C conference, Radiocarbon* **25** 2 (1983) 347–356.
- [7] SALEM, O., VISSER, J.H., DRAY, M., and GONFIANTINI, R., Groundwater flow patterns in the western Lybian Arab Jamahiriya, *In Arid-Zones Hydrology: Investigations with isotope techniques*, Vienna, IAEA (Eds) (1980) 165–179.
- [8] REARDON, E.J., ALLISON, G.B., FRITZ, P., Seasonal chemical and isotopic variations of soil CO_2 at Trout Creek, Ontario, *Journal of Hydrology* **43** (1979) 355–371.
- [9] PARIZEK, R.R., LANE, B.E., Soil-water sampling using pan and deep pressure-vacuum lysimeters, *Journal of Hydrology* **11** 1 (1970) 1–21.
- [10] McCREA, J., On the isotope chemistry of carbonates and palaeotemperature scales. *J. of Chem. Phys.* **18** (1950) 849–857.
- [11] ANDREWS, J.F., MATAMALA, R. WESTOVER, K.M., SCHLESINGER, W.H., Temperature effects on the diversity of soil heterotrophs and the $\delta^{13}\text{C}$ of soil-respired CO_2 , *Soil Biology & Biochemistry* **32** (2000) 699–706.
- [12] FARQUHAR, G.D., EHLERINGER J.R., HUBICK, K.T., Carbon isotope discrimination and photosynthesis, *Ann. Rev. Plant Physiol. Plant Mol. Biol.*, **40** (1989) 503–537.
- [13] CLARK I., FRITZ, P. (1997) *Environmental isotopes in hydrogeology*, editions Lewis publisher, Boca Raton, New-York (1997) 290.
- [14] SIMUNEK, J., VAN GENUCHTEN, M. Th., SEJNA, M., Hydrus-1D version 3.00, Code for Simulating the One-Dimensional Movement of Water, Heat, and Multiple Solutes in Variably Saturated Porous Media (2005).

ANALYTICAL DEVELOPMENTS

COMPOUND-SPECIFIC CHLORINE STABLE ISOTOPE OF VINYL CHLORIDE BY CONTINUOUS FLOW-ISOTOPE RATIO MASS SPECTROMETRY (CF-IRMS)

O. SHOUAKAR-STASH*¹, S.K. FRAPE*, A. GARGINI**,
M. PASINI**, R.J. DRIMMIE,* R. ARAVENA*

*Department of Earth Sciences,
University of Waterloo,
Waterloo, Ontario, Canada

**Department of Earth Sciences,
University of Ferrara,
Ferrara, Italy

Abstract

A new method for determining compound-specific chlorine stable isotope was developed for vinyl chloride (VC). The analysis is carried out on a continuous flow-isotope ratio mass spectrometer (CF-IRMS) with special collectors for m/z 64 and 62. The precision of this technique is better than $\pm 0.16\%$ (1σ) for pure phase gas injection and head-space SPME injection. The new methodology was tested in a confined sandy aquifer contaminated with VC located near the city of Ferrara, northern Italy. ^{37}Cl and ^{13}C data on VC showed the contamination is related to the use of VC in the production of PVC manufactured in the Ferrara region during the 70's and 80's. The isotope data also showed VC is attenuated by biodegradation along the groundwater flow system. The development of compound-specific isotope analysis (CSIA) for VC offers a new tool for fingerprinting sources and processes that affect VC in groundwater.

1. INTRODUCTION

Chlorinated solvents have been used as degreasers in a variety of industries such as instrument manufacturing, aerospace, electronic, printing and dry cleaning, and are among the most common groundwater contaminants [1].

¹ Corresponding Author: Department of Earth Sciences, University of Waterloo, 200 University Ave. W., Waterloo, Ontario, Canada N2L 3G1; orfan@uwaterloo.ca; Tel.: 1-519-888-4567 Ext. 35305; Fax: 1-519-746-7484.

VC is classified as a known human carcinogen by the International Agency for Research on Cancer and is considered as one of the most toxic groundwater contaminants. VC occurs in groundwater either as a primary contaminant or as a break-down product from other chlorinated solvent contaminants. The fate of VC is one of the key aspects that need to be addressed in studies dealing with natural attenuation of chlorinated compounds in groundwater. VC can be transformed into ethane which can further be transformed to ethene, methane and/or carbon dioxide. A new approach based on carbon isotope fractionation affecting VC during biodegradation has been proposed as another tool to evaluate processes that affect VC concentration in groundwater [2].

Over the last 10 years attempts have been made to use Cl stable isotopes to investigate groundwater contamination by chlorinated ethenes. Although Cl isotope analysis has a potential to assist in identifying source and processes of contaminants in groundwater, its application is largely limited by the analytical techniques. By using a dual inlet isotope ratio mass spectrometry (DI-IRMS), several analytical methods have been developed to determine chlorine stable isotopic compositions of pure phase or bulk chlorinated ethenes [3–6]. All of these methods involve a conversion of chlorinated ethenes to methyl chloride (CH_3Cl) gas for analysis. The amount of Cl required by these techniques ranged between 10 and 2000 μmol with precisions of $\pm 0.07\%$ and $\pm 0.68\%$. More recently, Thermal Ionization Mass Spectrometry (TIMS) has been introduced to determine Cl isotopic compositions of chlorinated ethenes [7,8]. These two techniques required relatively small sample sizes (0.7 to 2.8 μmol of Cl) and the achieved precision ranged between $\pm 0.10\%$ and $\pm 0.46\%$ depending on the compound and the preparation technique. All of these techniques are used for pure phase or bulk compound analyses and are not capable of CSIA. This fact has limited the use of chlorine stable isotopes in groundwater contamination studies. Requirement of large sample size further limits the application of Cl isotopes.

New possibilities for the chlorine isotope approach have been opened recently by the development of compound-specific Cl isotopes analysis in chlorinated compounds [9]. This paper presents the analytical protocol developed for VC using this new approach. This paper also presents a case study where a combined use of stable carbon and chlorine isotopes identified vinyl chloride as primary contaminant and traced its fate in the groundwater. The study area is of a site where residues from PVC production were disposed and a plume of VC was detected in a sandy aquifer where, other chlorinated ethenes were absent.

2. METHODOLOGY

2.1. Materials

Two different VC products from different years obtained from Fluka were used as standards labeled VC-1 and VC-2.

2.2. Instrumentation

A CF-IRMS (IsoPrime, Micromass, currently GV Instruments) was used in this study. This IRMS is designed to be used in both continuous flow (CF) and dual-inlet (DI) modes, with nine collectors, two of which are in position for mass 62 and 64 to analyze VC. One of the dual inlet bellows is used as the VC reference gas reservoir.

An Agilent 6890 Gas Chromatograph (GC) equipped with a CTC Analytics CombiPAL SPME autosampler is attached to the IRMS. A DB-624 gas chromatographic column (30 m, 0.320 mm, 1.80 μm film thickness from J & W Scientific Inc.) is used for compound separations. A Solid Phase Micro Extraction (SPME) fiber (75 μm Carboxen-PDMS from Merlin MicrosealTM, 23 gauge needle Auto holder from Supelco) was used to extract the VC from aqueous solutions. Four-way Valco valve with two positions installed between the GC and the IRMS is used to direct only VC to the IRMS.

2.3. Standard preparations

Standards were prepared as; pure phase gas and as aqueous solutions. For the pure phase, VC gas was transferred from the tank into special sealed gas bags. Aqueous solutions were prepared in 60 mL VOC vials sealed by open top screw caps with septa (Teflon/Silicone). Stock aqueous solutions with a concentration of 120 mg/L were prepared by adding VC gas into ultra pure deionized water and stirred for 30 minutes. These stock solutions were then used to prepare aqueous standards for the direct head-space and SPME head-space analyses.

2.4. Analysis

The $\delta^{37}\text{Cl}$ composition of VC standards were measured using the 62/64 Faraday cup. The measurements were performed on masses 62 and 64 that were produced in the source by electron bombardment of VC molecules. VC mass fragments and their intensities are illustrated in Fig. 1. The positive masses resulted by the molecules losing an electron get separated according to

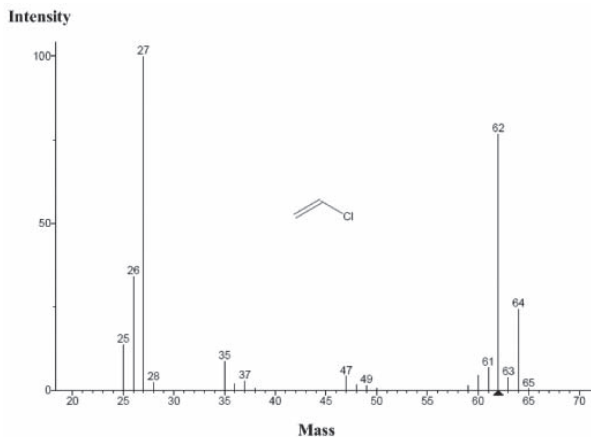


FIG. 1. Mass fragment spectra of VC obtained from the NIST spectral search program for the NIST/EPA/NIH mass spectral library, Demo Version 2.0. Intensities are expressed relative to the highest peak (mass 27).

their mass to charge ratios (m/z) and, finally, are collected in the corresponding Faraday cups.

The Cl isotopic compositions are reported in permil (‰) deviation from isotopic standard reference material using the conventional δ notation, where $\delta = ((R_{\text{sample}}/R_{\text{standard}}) - 1) \times 1000$ and $^{37}\text{Cl}/^{35}\text{Cl}$ is the measured isotopic ratio. The calibration was done by the determination of, the $\delta^{37}\text{Cl}$ values of the two VC standards by the classical technique described in reference [5] on this IRMS in DI mode.

2.5. Results and discussion

The two standards VC-1 and VC-2 were analyzed using the CF-IRMS in three different ways; (1) pure phase direct injection, (2) head-space direct injection, and (3) SPME head-space. For the direct injection 100 μL of VC was injected and a split ratio of 30 was used. Aqueous solutions with concentrations of 300 $\mu\text{g}/\text{L}$ were prepared for the head-space direct injection. 800 μL of head-space was injected and a split ratio of 1 was used. For the SPME head-space, aqueous solutions of 60 $\mu\text{g}/\text{L}$ were prepared. VC was extracted by SPME fiber for 20 minutes and then thermally desorbed from the fiber in the GC inlet port in a splitless mode. The results of these tests are presented in Table 1. The chromatogram in Fig. 2 illustrates a compound specific analysis of VC in a continuous flow mode. The chromatogram shows 4 reference pulses and the

COMPOUND-SPECIFIC CHLORINE STABLE ISOTOPE OF VINYL CHLORIDE

TABLE 1. $\delta^{37}\text{Cl}$ VALUE OF VC-1 AND VC-2 STANDARDS OBTAINED BY ANALYZING THE TWO STANDARDS BY THE CLASSICAL TECHNIQUE [5] AND THE CSIA BY CF-IRMS METHODOLOGY (ALL VALUES ARE CORRECTED TO THE VC-1 AVERAGE VALUE.

Method	VC-1			VC-2		
	n	Mean $\delta^{37}\text{Cl}$ (‰)	STDV (1σ)	n	Mean $\delta^{37}\text{Cl}$ (‰)	STDV (1σ)
Classical Technique [5]	6	0.00	0.07	4	6.25	0.16
CSIA by CF-IRMS						
Pure Phase Gas Injection	6	0.00	0.03	6	6.42	0.16
Head-space Direct Injection	10	0.00	0.09	10	5.96	0.22
Head-space SPME	10	0.00	0.10	10	6.38	0.09

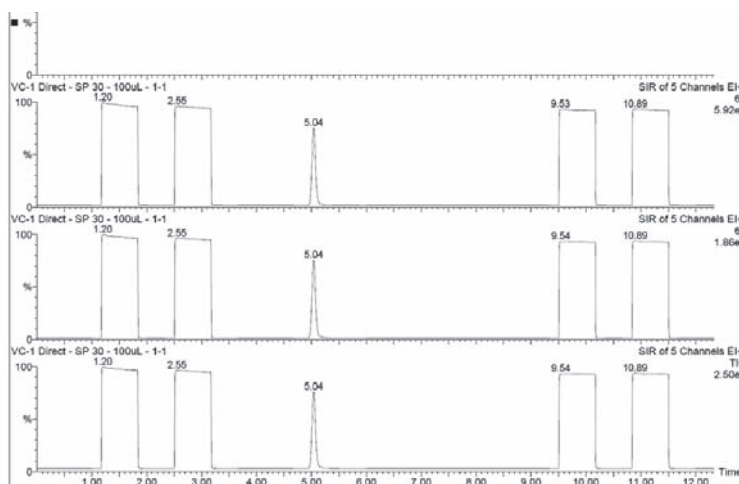


FIG. 2. Chromatogram of VC standard analysis in continuous-flow mode. The chromatogram illustrates four reference pulses and a sample peak. The uppermost trace is the 64/62 ratio, the second trace is the m/z 64 ion current and the lower trace is the m/z 62 ion current.

VC peak. The retention time for the VC peak is around 302 seconds. The total length of the run is 12.5 minutes for the direct injections and 22 minutes for the SPME runs.

The comparison of the isotopic results obtained for the VC standards by the classical technique [5] and the CSIA by CF-IRMS (Table-1) indicate that the new technique provides an excellent accuracy over a range of approximately 6‰ for $\delta^{37}\text{Cl}$. The external precision of the CF-IRMS methodology is better than $\pm 0.16\%$, $\pm 0.22\%$ and $\pm 0.09\%$ for pure phase direct injection, head-space direct injection and SPME head-space, respectively. These results are comparable to that of the classical technique [5] and the limit of quantification (LOQ) of VC is 60 $\mu\text{g/L}$ (ppb) (equivalent to 1 $\mu\text{mol Cl}$) using the SPME head-space. The LOQ is relatively higher (300 $\mu\text{g/L}$) for the head-space direct injection. A linearity test of the technique showed a dependency between the peak area and the delta value of the standard. Therefore, it is recommended to work within a small range of peak area and in order to achieve consistent results, peak area correction is necessary when different peak areas are obtained.

3. CASE STUDY

3.1. Background

The study site is located in the eastern sector of the Padana plain between the historical centre of Ferrara to the south and the Po River to the north. A large petrochemical complex and the public water supply field are located to the southwest and northwest, respectively (Fig. 3). The main geological units in the area include: a shallow silty layer (0–7 m), a clay and silty clay aquitard (7–15 m), a fine to medium grained sand aquifer (15–40 m) and a lower clay unit (40–50 m). VC and other chlorinated ethanes and ethenes were first detected in the shallow and confined units in 1999 in the eastern part of the petrochemical plant with concentrations as high as 2,120 $\mu\text{g/L}$ and VC contamination was later documented in five private and municipal wells in 2001. A detailed evaluation of the VC plume was performed in 2003 and 2004 using about 35 wells and the direct push sampling approach. These data showed a VC plume of about 2100 m in length and about 600 m in width. The main industries that were active in the area during the period of 1937–1998 were related to sugar and PVC production. Vinyl chloride was the main raw material for the production of PVC and the waste products of this industry seems to be the main potential source of the VC contamination found in the groundwater.

For the isotope study, groundwater samples were collected from 5 private wells located within the plume, and two wells, a shallow and a deep, located in

the petrochemical plant. VOCs, dissolved organic carbon and gases, methane (CH_4), ethane (C_2H_6) and ethane (C_2H_4), analyses were performed on the groundwater samples.

3.2. Results and Discussion

The data for the shallow well in the petrochemical plant showed very high concentration for the main chlorinated compounds, PCE (3,270 $\mu\text{g/L}$), TCE (12,804 $\mu\text{g/L}$), cisDCE (7,624 $\mu\text{g/L}$), and VC (4,531 $\mu\text{g/L}$). The carbon isotope data revealed very depleted $\delta^{13}\text{C}$ values for these compounds ranging between -73 and -84‰ , which are significantly more depleted than the values reported for industrial compounds that range between -36 and -23.1‰ [10]. The concentration data in the confined aquifer only showed the presence of VC with concentration ranging between 1,060 and 133 $\mu\text{g/L}$. The $\delta^{13}\text{C}$ and $\delta^{37}\text{Cl}$ values for the VC range between -73 and -52.2‰ and between $+2$ and $+7.5\text{‰}$, respectively. An enrichment trend for both isotopes is observed in these data suggesting biodegradation is affecting VC along the groundwater flow system. Measurements of redox parameters showed that groundwater is under reducing conditions. The absence of ethene and the presence of methane suggest that VC is being biodegraded to methane via oxidative acetogenic and acetrophic methanogenesis. The source of the VC is probably waste residues associated to the older PVC production in the area. This product is produced from polymerization of VC. The extremely depleted values observed for the VC have to be associated with the isotopic composition of the VC source and isotopic fractionation occurring during the production of VC and the polymerization process. A detailed instrumentation is being installed at the site to monitor the behaviour of the VC plume in the aquifer.

4. CONCLUSION

A new CSIA for chlorine stable isotopes analyses was developed for VC. The technique is based on measuring mass fragments by a CF-IRMS with collectors dedicated for m/z 64 and 62. This new methodology offers the following advantages; (1) the capability to analyze VC in complex organic aqueous solutions, (2) a simple and fast methodology due to the elimination of all off-line preparation steps, (3) low limits of quantification (60 $\mu\text{g/L}$ of VC) and, (4) good precision (better than $\pm 0.16\text{‰}$ (1σ) for pure phase gas injection and head-space SPME). The new methodology was tested in a confined sandy aquifer contaminated with VC. ^{37}Cl and ^{13}C data on VC showed that the contamination seems to be related to the use of VC in manufacturing PVC in the Ferrara region during the 70's and 80's. The isotope data also showed VC

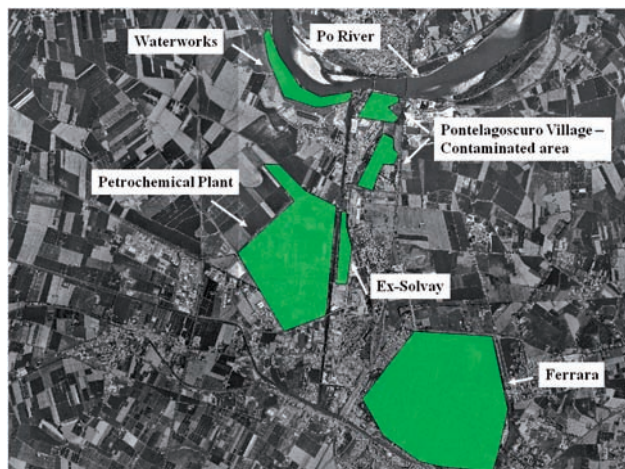


FIG. 3. Map of the location site.

is being attenuated by biodegradation along the groundwater flow system. The development of CSIA for VC offers a new tool for fingerprinting sources and processes that affect VC in groundwater.

REFERENCES

- [1] McCULLOCH, A., MIDGLEY, P.M., The production and global distribution of emissions of trichloroethene, tetrachloroethene and dichloromethane over the period 1988–1992, *Atmospheric Environment* **30** (1996) 601–608.
- [2] HUNKELER, D., ARAVENA, R., COX, E., Carbon isotopes as a tool to evaluate the origin and fate of vinyl chloride: Laboratory experiments and modeling of isotope evolution, *Environmental Science & Technology* **36** (2002) 3378–3384.
- [3] TANAKA, N., RYE, D.M., Chlorine in the stratosphere, *Nature* **353** (1991) 707.
- [4] LONG, A., EASTOE, C.J., KAUFMANN, R.S., MARTIN, J.G., WIRT, L., FINLEY, J.B., High-precision measurement of chlorine stable isotope ratios, *Geochimica et Cosmochimica Acta* **57** (1993) 2907–2912.
- [5] HOLT, B.D., STURCHIO, N.C., ABRAJANO, T., HERATY, L., Conversion of chlorinated volatile organic compounds to carbon dioxide and methyl chloride for isotopic analysis of carbon and chlorine, *Analytical Chemistry* **69** (1997) 2727–2733.
- [6] JENDRZEJEWSKI, N., EGGENKAMP, H.G.H., COLEMAN, M.L., Sequential determination of chlorine and carbon isotopic composition in single microliter samples of chlorinated solvents, *Analytical Chemistry* **69** (1997) 4259–4266.

COMPOUND-SPECIFIC CHLORINE STABLE ISOTOPE OF VINYL CHLORIDE

- [7] NUMATA, M., NAKAMURA, N., KOSHIKAWA, H., TERASHIMA, Y., Chlorine stable isotope measurements of chlorinated aliphatic hydrocarbons by thermal ionization mass spectrometry, *Analytica Chimica Acta* **55** (2002) 1–9.
- [8] HOLMSTRAND, H., ANDERSSON, P., GUSTAFSSON, Ö., Chlorine isotope analysis of submicromole organochlorine samples by sealed tube combustion and thermal ionization mass spectrometry, *Analytical Chemistry* **76** (2004) 2326–2342.
- [9] SHOUAKAR-STASH, O., DRIMMIE, R.J., ZHANG, M., FRAPE, S.K., Compound-specific chlorine isotopes ratio of TCE, PCE and DCE isomers by direct injection using CF-IRM, *Applied Geochemistry* **21** (2006) 766–781.
- [10] SHOUAKAR-STASH, O., FRAPE, S. K., DRIMMIE, R. J., Stable hydrogen, carbon and chlorine isotope measurements of selected chlorinated organic solvents. *Journal of Contaminant Hydrology* **60** (2003) 211–228.

STABLE ISOTOPES IN GACKA RIVER CATCHMENT: INSTALLATION OF A LABORATORY FOR STABLE ISOTOPE ANALYSIS IN CROATIA

Z. ROLLER-LUTZ*, M. MANDIĆ*, D. BOJIĆ*, H.O. LUTZ*+,
S. KAPELJ**

*Laboratory for Environmental Studies,
Medical Faculty,
University of Rijeka, Croatia

+Physics Faculty,
Bielefeld University,
Bielefeld, Germany

**Faculty of Geotechnical Engineering,
Varaždin,
University of Zagreb, Croatia

Abstract

Croatia's first laboratory for stable isotope mass spectroscopy focusing on hydrogeological studies has been set up at Rijeka University. Preliminary $\delta^{18}\text{O}$ results are obtained for the Gacka river catchment and interpreted together with data from the national meteorological and hydrological service.

1. BACKGROUND

Karst is characterized by high permeability, porosity and crevices in which water moves in complex subterranean networks. Thus, water resources in karst areas are very sensitive with respect to the recharge dynamics as well as the potential impact of pollution. This is of particular significance for Croatia since about 50% of the country is karst (Croatian "krš", is the name of the region roughly stretching between the Triest hinterland and the Dinaric ridge along the coast of Croatia). Related studies are a national priority in the program "Preservation of the nature and development of karst regions", and Croatian groups are significant contributors to the numerous international studies on the subject karst. It is, therefore, somewhat surprising that until recently not a single Croatian laboratory existed that could actually participate in the

important issue of stable isotope measurement for water-related studies. This shortcoming has now been eliminated with the installation of a Laboratory for Environmental Studies at the University of Rijeka with a new IRMS system. This laboratory also participates in a larger national joint activity, together with the Laboratory for Measurements of Low-level Radioactivity at the Insitute Rudjer Bošković (measurement and analysis of radioactive isotopes ¹⁴C and tritium) and University of Zagreb, Varaždin branch (application and analysis of hydrochemical tracers).

A program has been initiated to study the dynamics and interactions in karst in order to improve the accuracy and reliability of data for water resource protection and thus to expand the knowledge base for water management. In particular, many kinds of wastes can affect the quality and use of the groundwater. The areas available for the development of settlements, industry, traffic, touristy purposes etc. often belong to the catchments of springs, creating enormous pressure to avoid pollution of available water resources. This requires the re-evaluation of the hydrogeological structure model of the region through data obtained by monitoring tracers and their temporal and spatial variations.

2. THE NEW LABORATORY.

The heart of the new Laboratory for Environmental Studies is a Thermo-Finnigan Delta+XP mass spectrometer, fitted with a gas bench, an autosampler (96 sample positions) and a dual inlet. The central gas supply is connected by capillaries to an overhead distribution console. Electric power is provided via an uninterruptible power supply. In-house water-standards have been produced in fairly large quantities (approx. 35 L each)

TABLE 1. IN-HOUSE WATER STANDARDS AND THE CORRESPONDING $\delta^{18}\text{O}$ (‰ VSMOW) VALUES.

	Origin of water	Rijeka	Jena	Graz	Mean
DZW	De-ionized water from Žut island (Adriatic)	-1.62	-1.58	-1.66	-1.62
RTW	Rijeka tap water	-8.43	-8.54	-8.59	-8.52
MGS	Snow from Moelltal Glacier (Austria)	-19.98	-19.93	-19.89	-19.93
AAS	Antarctic snow	-26.45	-26.24	-26.39	-26.37

INSTALLATION OF A LABORATORY FOR STABLE ISOTOPE ANALYSIS

by collecting various types of waters with different δ -values. After filtering and boiling for sterilization, they are stored in stainless-steel barrels under argon atmosphere. Their $\delta^{18}\text{O}$ values (VSMOW) have been determined in an inter-laboratory comparison of our measurements, those of the Max-Planck-Institute for Biogeochemistry in Jena (Germany), and of Joanneum Research Graz (Austria). The corresponding values and the resulting means are given in Table 1.

For each measurement the autosampler tray is filled to approximately 50% with vials of standards and 50% of unknown samples in predefined positions, each vial containing 0.5 mL. The equilibration time is 24 hours at a temperature (kept by a combination of cooling and heating units) of 20°C. Temperatures higher than room temperature increased the danger of condensation in the capillaries. The δ -values (standard deviations generally below 0.1‰, mostly smaller than 0.05‰) given thus by the NT software are not yet normalized to the VSMOW scale. For this normalization we follow a simplified method as suggested e.g. by Nelson [1]. Three of the internal standards (DZW, MGS, AAS) are used as references, one (RTW) serves as quality control. Assuming a linear relation between the “measured” (as given by the NT software) and the “expected” (VSMOW) δ -values of the DZW, MGS and AAS standards, the regression equation thus derived is used to normalize the δ -values of the unknown samples. The RTW quality control

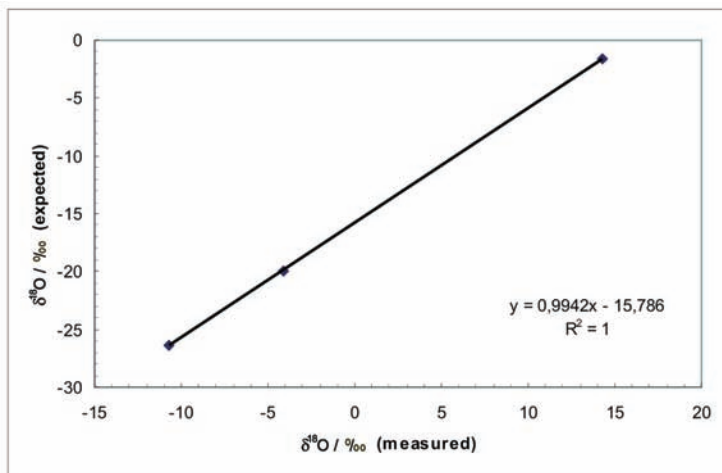


FIG. 1. Example of the DZW, MGS and AAS regression line for a particular run. In this run, the “measured” data for the RTW quality control, inserted into the regression equation, yield a δ -value of -8.43‰ , which differs from the “expected” value (-8.52‰ VSMOW) by 0.09‰ .



FIG. 2. Position of Gacka river and spring area within Croatia.

sample is required to lie within 0.1‰ of its VSMOW value. Fig.1 shows a typical example of this procedure.

3. FIRST RESULTS.

We present examples for three Gacka river springs (Pećina, Tonković(a) vrelo, Majerovo vrelo). The Gacka river is located within the zone of deep karst of the Dinarides at an altitude of about 400 m above sea level (Fig. 2). The climate of the region is continental, but it may occasionally be influenced by maritime air masses from the Mediterranean region.

Firstly, we notice that the three springs have fairly different δ -values (Fig. 3a) although they are located at approximately the same altitude. This indicates that they are fed from different altitudes, the water of Majerovo vrelo coming from the highest altitude on the Kapela mountain, followed by Tonković vrelo and then Pećina. The corresponding differences are roughly 150 m each if a δ -value vs. mean altitude relation of $-0.30\text{‰}/100\text{ m}$ is assumed [2].

INSTALLATION OF A LABORATORY FOR STABLE ISOTOPE ANALYSIS

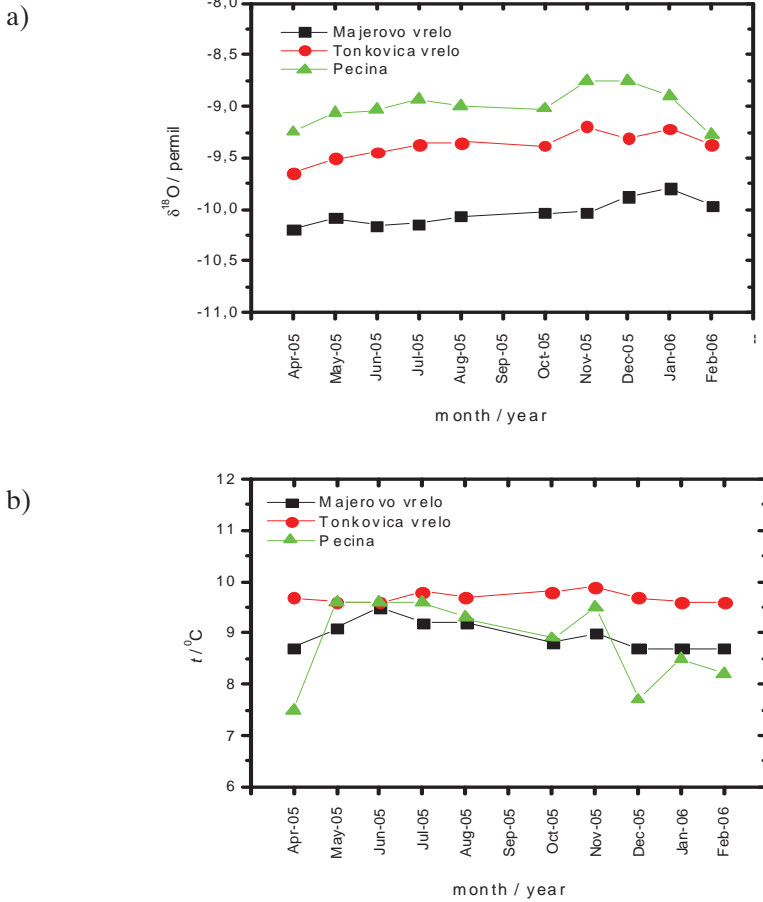


FIG. 3. δ -values in ‰ VSMOW (a) and water temperature (b) of three Gacka river springs.

Secondly, there is no direct correlation of the spring water temperatures (Fig. 3b) with the precipitation amount and temperature, Fig. 4). This is quite evident for Majerovo vrelo and Tonkovića vrelo, the two springs with the highest catchment; Pečina has a restricted outflow due to old artificial barriers constructed for small fish basins which increase the water residence time and expose it to ambient air and evaporation. Similarly, the flow rates (e.g. of Tonkovića and Klanac, Fig. 5) can be compared with the precipitation amounts, and both springs react to precipitation recharge somewhat later, cf. the flow peaks in April (delayed considerably from the winter precipitation probably due to snow melt) and in October (delayed from the August precipitation by about two months).

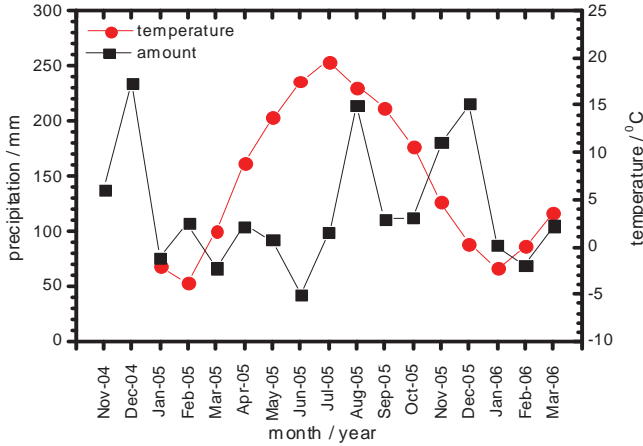


FIG. 4. Monthly precipitation amount and mean (ambient) temperature in the Gacka river area [3].

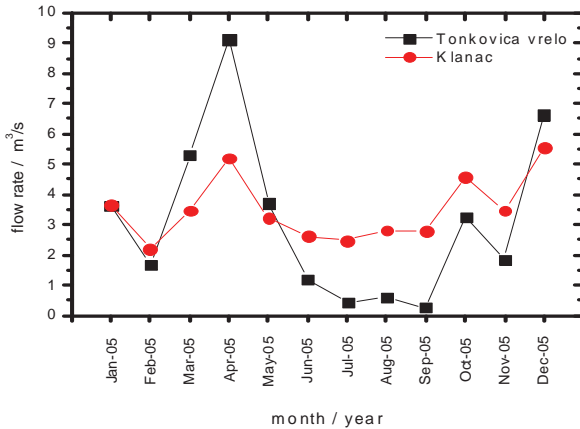


FIG. 5. Mean flow rates of Tonkovića and Klanac springs[3].

Comparison of spring and precipitation δ -values is hampered since our precipitation $\delta^{18}\text{O}$ measurements begin only towards the end of 2005, giving δ -values around -10.5% between November 2005 and February 2006. It may nevertheless be safely assumed that in summer (2005) they are considerably less negative than in the (following) winter months; e.g., also in the summer of 2006 they fluctuate roughly about -8% between March and August (in July they even reached a value of nearly -4%). Even though, the large

INSTALLATION OF A LABORATORY FOR STABLE ISOTOPE ANALYSIS

precipitation amounts in August and November/December 2005 cause an only weak $\delta^{18}\text{O}$ reaction in the following months, again indicating a delayed response and good mixing.

4. CONCLUSIONS.

The new IRMS system has been used for $\delta^{18}\text{O}$ stable isotope analysis of water, and we will add $\delta^{13}\text{C}$ analysis of carbonates as another method. An equilibration device will soon allow for improved precision and high throughput for $\delta^{18}\text{O}$ as well as $\delta^2\text{H}$ measurements. The system has been applied to the study of three springs of the Gacka river. One may conclude that their catchment areas (particularly Majerovo and Tonković) are connected to large and well mixed reservoirs, but of course more detailed studies are required, applying a wider variety of tracers as well as modelling. The end users are the national institutions responsible for water management, foremost the Croatian Water Resources Management (Hrvatske Vode), the IAEA/WMO GNIP network and the local water supply organisations.

ACKNOWLEDGEMENT

We gratefully acknowledge support by the Ministry for Science, Education and Sport (MZOS) of Croatia (projects 062-0982709-0510 and 160-0982709-1709), and the International Atomic Energy Agency (IAEA projects CRO/8/006 and /007). Water samples were collected by the group cooperating in the IAEA projects. We are indebted to Harm Moraal and his colleagues (Northwest University, South Africa) for providing us with the Antarctic snow, to Ines Krajcar Bronić (Institute Rudjer Bošković) for very stimulating discussions, and to Albrecht Leis (Joanneum Research Graz) for sharing his IRMS experience with us.

REFERENCES

- [1] NELSON, S. T., Rapid Commun. Mass Spectrom. **14** 1044 (2000)
- [2] VREČA, P., KRAJCAR BRONIĆ, I., HORVATINČIĆ, N., BAREŠIĆ, J., Hydrol. **330** 457 (2006)
- [3] Croatian Meteorological and Hydrological Services.

**RECENT ADVANCES IN MODERN ION
CHROMATOGRAPHY FOR THE ANALYSIS
OF ENVIRONMENTAL WATER SAMPLES**
*Reagent Free Ion Chromatography Systems using Recycled
Eluent and Their Applications*

S. GHIRLANDA, D. JENSEN
Dionex (Europe) Management AG,
Switzerland

Abstract

Ion Chromatography (IC) is one of the most important analytical techniques for the determination of inorganic ions in water samples. Designed to reduce the working load in modern analytical laboratories, automation in IC plays an important role for actual and future developments. Reagent Free Ion Chromatographs with eluent generation (RFIC-EGTM) enable the user to perform a wide range of ion chromatographic separations using deionised water as the only carrier. RFIC-EG systems provide isocratic and gradient method flexibility for a wide range of IC applications. For laboratories using carbonate- and methanesulfonic-based eluents for isocratic separations Dionex expanded the properties of RFIC with a new technique called RFIC-ERTM (ER: Eluent Regeneration) [1]. We will discuss the principle of this operation mode for IC systems equipped with electrolytic suppressors. It utilizes the fact that the effluent from an electrolytic suppressor operated in the AutoSuppression® mode consists of mainly the eluent used in the IC separation process. The new IC operation mode uses a novel eluent purification cartridge and an efficient analyte trap column to remove electrolysis gases and purify the recycled eluent and is compatible with IC separations using carbonate/bicarbonate and methanesulfonic acid eluents. We will demonstrate the applications of the new IC operation mode in determination of common cations and anions in different sample matrices. RFIC-ER systems are designed specifically for a set of routine IC analyses, such as the determination of anions or cations in drinking water.

1. INTRODUCTION

Since the introduction of ion chromatography (IC) in 1975, Dionex Corp. (Sunnyvale, CA) continuously improved the performance of IC systems while developing new capabilities for the determination of anionic and cationic

components in various water sample matrices. The introduction of RFIC systems fundamentally changed the routine operation of IC by making it an easy-to-use, powerful analytical technique. RFIC systems combine three core technologies:

- Electrolytic Eluent Generation produces acid, base, or salt eluents for IC separations.
- Self-Regenerating Electrolytic Suppression produces the regenerant ions necessary for eluent suppression and allows continuous operation with less maintenance.
- Continuously Regenerated Trap columns (CR-TC) remove trace-level contaminants.

RFIC systems with eluent generation (RFIC-EG™) enable the user to perform a wide range of ion chromatographic separations using deionised water as the only carrier. For many applications, RFIC-EG systems provide high performance with increased sensitivity and the flexibility to perform isocratic and gradient separations using alkali hydroxides (e.g. KOH), methanesulfonic acid eluents, or isocratic separations applying carbonate/bicarbonate buffers. These systems improve the simplicity of operation, ease of use, and improved reproducibility — day to day, operator to operator, and laboratory to laboratory.

To expand RFIC capabilities for frequent-use applications, Dionex is developing RFIC systems with Eluent regeneration: RFIC-ER™ systems. These systems use the electrolytic suppressor to regenerate the starting eluent after suppression. They provide benefits similar to RFIC-EG systems, offering simplicity, ease of use, and high reproducibility. The two technologies differ in the additional advantages they offer for various user needs. While RFIC-EG systems provide isocratic and gradient method flexibility for a wide range of IC applications, RFIC-ER systems are designed specifically for a set of routine IC analysis, such as the determination of anions or cations in drinking water. The major advantages of RFIC-ER are continuous operation, reduced waste disposal, and lower cost of ownership.

2. GENERAL CONSIDERATIONS FOR RFIC-ER SYSTEMS

One key feature of an RFIC-ER system is the operation of the electrolytic suppressor in eluent regeneration mode. Fig. 1 shows the electrochemical processes in an electrolytic suppressor for the determination of anions (Na_2CO_3 based eluent) in an IC system.

RECENT ADVANCES IN MODERN ION CHROMATOGRAPHY

The combined effluent from the suppressor anode and cathode chambers is a mixture of hydrogen gas, oxygen gas, and the aqueous solution containing the eluent components as well as the ions from the injected sample. RFIC-ER systems use novel and patented approaches to remove hydrogen and oxygen gases, sample ions, and other trace contaminants. They purify the suppressor regenerant effluent so that it is converted into the pure electrolyte solution for reuse as the ion chromatographic eluent. Fig. 2 shows the basic components of an RFIC-ER system.

The effluent from the electrolytic suppressor regenerant chamber is passed through the catalytic gas elimination column. The column is packed

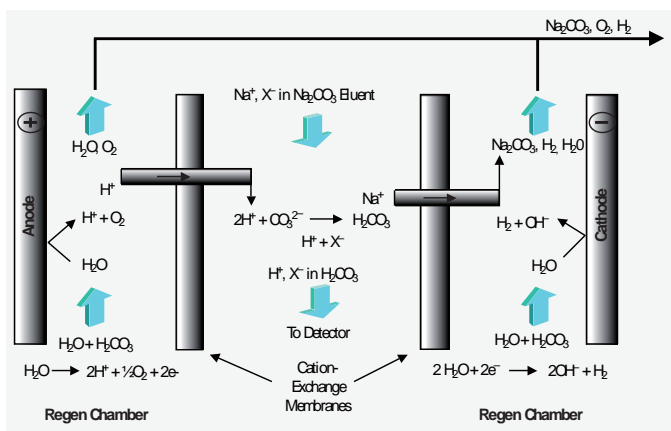


FIG. 1. Electrochemical Processes in an electrolytic suppressor for determination of anions (Na_2CO_3 as the eluent).

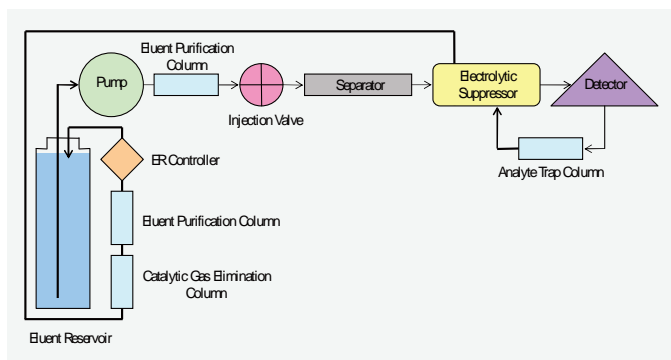


FIG. 2. Block diagram of an RFIC-ER system.

with a noble-metal catalyst that induces the reaction between hydrogen gas and oxygen gas to form water. This serves several important functions. First, it provides a means to conveniently eliminate the build-up of hydrogen and oxygen gases, and thus facilitates the operation of continuous eluent recycle. Second, the water-forming reaction of hydrogen and oxygen is stoichiometric in the column; the amount of water formed is expected to be in principle the same as the amount of water consumed originally to produce hydrogen and oxygen gases in the electrolytic operation of the suppressor. This avoids an increase in the concentration of eluent that would occur due to the consumption of water in the electrolytic operation of the suppressor. In the RFIC-ER system, an analyte trap column is placed after the outlet of a conductivity detector to trap analyte ions. Additionally, eluent purification columns packed with appropriate ion exchange resins are placed in the RFIC-ER system to further purify the regenerated eluent for use in the separation process. This IC operation mode is compatible with IC separations using carbonate/bicarbonate and methanesulfonic acid (MSA) eluents. An RFIC-ER system can operate for up to four weeks without any user intervention apart from loading samples. Under heavy workloads, the analyte trap and eluent purification columns as well as the eluent may require replacement or regeneration more frequently. Chromeleon® chromatography management software (Dionex Corporation, Sunnyvale, CA) provides system wellness features to monitor usage of analyte trap, eluent purification columns, and eluent.

3. APPLICATIONS OF RFIC-ER SYSTEMS

RFIC-ER systems are designed for ion chromatographic determinations of common anions and cations in drinking water samples. The systems can be used to perform isocratic separation of common anions using IonPac® AS22 and AS23 (column ID 4-mm) anion separation columns (Dionex Corporation, Sunnyvale, CA) and carbonate and bicarbonate eluents. The systems are also compatible with isocratic separation of common cations using IonPac CS12A columns (column ID 4-mm) in conjunction with methanesulfonic acid eluents. The systems are suitable for U.S. EPA methods 300.0 Part A and 300.1 Part A, DIN/EN/ISO 10304-1 (Anions), DIN/EN/ISO 14911-E (Cations) or equivalent applications. RFIC-ER systems have been valued for long-term performance in the determination of common anions and cations in water samples. In one of our studies, drinking water samples collected from Fremont, CA, and spiked with 10 pm bromide were analyzed repeatedly. The initial 2 L of eluent, containing 3.5 mmol/L Na_2CO_3 and 1.0 mmol/L NaHCO_3 , were used over a

RECENT ADVANCES IN MODERN ION CHROMATOGRAPHY

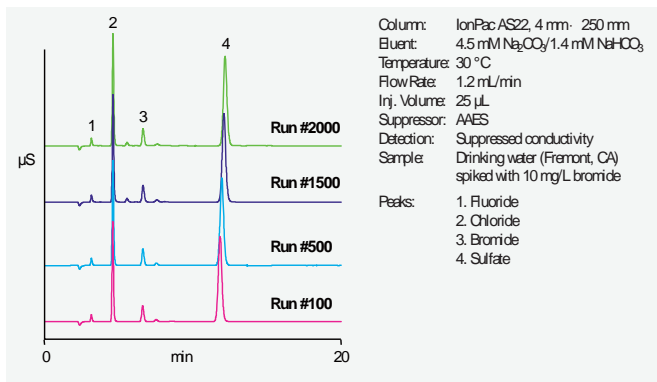


FIG. 3. Separation of common anions in drinkingwater samples on a 4 mm IonPac AS22 column obtained under the RFIC-ER conditions.

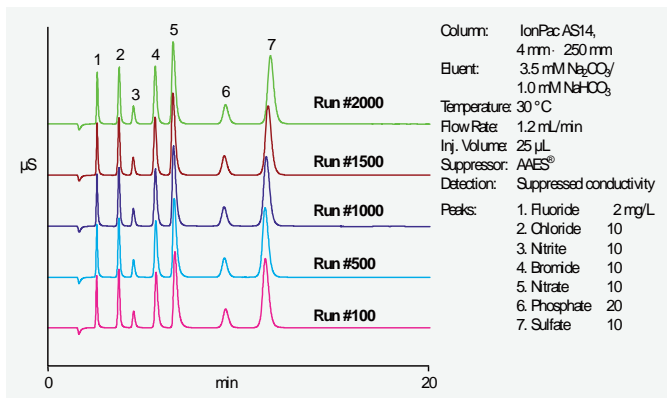


FIG. 4 Separation of seven common anions on a 4 mm IonPac AS14 column obtained under the RFIC-ER conditions.

period of 33 days. Fig. 3 shows representative chromatograms obtained over the course of 2000 injections.

The results demonstrate that the RFIC-ER system provided highly reproducible separation of common anions in drinking water samples over an extended period. The percent retention time change ranged from 0.2% for fluoride to 3.1% for sulfate over the 33-day period. In a second study, an RFIC-ER system was used to separate common cations on a 4 mm CS12A column. The initial 2 L of 20 mmol/L MSA eluent were regenerated over a

period of 52 days. Fig. 4 shows representative chromatograms. The results demonstrate that the RFIC-ER system can provide highly reproducible separations of six target cationic analytes over 2000 injections.

4. CONCLUSION

RFIC-ER systems address the challenges faced by routine IC users such as contract laboratories and municipalities analyzing drinking water samples. The systems offer several advantages when compared to conventional IC systems. Eluent preparation time and waste disposal costs are significantly reduced; a single bottle of eluent can last up to four weeks. Routine IC operation is greatly simplified. The systems can operate continuously for an extended period of time and thus ensure that the system is always equilibrated and ready for sample analysis. They offer enhanced retention time reproducibility, since the same eluent can serve many injections. RFIC-ER systems improve the ease of use and performance of IC methods for routine anion and cation analysis in drinking water.

RFIC-EG systems are recommended for those users with more complex sample matrices and who may require more flexibility in eluent type and gradient capability.

REFERENCE

- [1] LIU, Y., LU, Z., POHL, C., MADDEN, J., SHIRAKWA, N., *American Lab.*, 2, 2007.

COASTAL ZONE HYDROLOGY

SUBMARINE GROUNDWATER DISCHARGE TO THE MEDITERRANEAN SEA: A CASE STUDY OFF MONACO

J.C. SCHOLTEN*, M. SCHUBERT**, A. SCHMIDT**,
M.M. RUTGERS VAN DER LOEFF***, M. SCHLÜTER***,
M.K. PHAM*, K. KNÖLLER**, J.-F. COMANDUCCI*,
J.A. SANCHEZ-CABEZA*

*Marine Environment Laboratories,
International Atomic Energy Agency,
Monaco

**Helmholtz Centre of Environmental Research – UFZ,
Leipzig, Germany

***Alfred-Wegener Institut,
Bremerhaven, Germany

Abstract

Submarine Groundwater Discharge (SGD) is not only a potential fresh water resource, it also represents an important pathway for matter transfer from land to coastal seas. Here we investigate the SGD at Cabbé, a location near Monaco where groundwater from a karst aquifer discharges to the Mediterranean Sea. The discharge was monitored for 24 hours and several parameters (^{222}Rn , ^{223}Ra , ^{224}Ra , ^{228}Ra , ^{226}Ra , salinity, tidal range, nitrate) were measured. The flux of nitrate associated with the SGD to the seawater off Cabbé amounts to $\sim 26.4 \text{ mmol} \cdot \text{day}^{-1} \cdot \text{m}^{-1}$ representing an important nitrate source for the local coastal environment. In contrast to ^{222}Rn , radium isotope concentrations do not vary with the tidal range indicating that the SGD is not a source of radium at Cabbé. We therefore assume that radium isotopes may not be valuable tracers for SGD in cases of focused groundwater discharge from a karst aquifer. Along two ship transects in the Bay of Roquebrune we measured an increase of ^{222}Rn landwards towards Cabbé reflecting the influence of SGD on the composition of local seawater.

1. INTRODUCTION

Submarine Groundwater Discharge (SGD) defined as any flow of water out across the seafloor [1] is now recognized as a potentially important pathway of matter transfer from land to coastal zones. SGD may occur as submarine freshwater springs or as diffusive flows of recirculated seawater. As SGD may be accompanied by enhanced concentrations in dissolved nutrients and potential contaminants it may significantly influence the coastal environment causing e.g. harmful algae blooms, eutrophication and hypoxia [2, 3]. Global estimates of SGD arrived at about 6% of the global river discharge (UNESCO 2004), a number associated with huge uncertainty due to the difficulty of detecting and quantifying SGD and due to its poorly understood spatial and temporal distributions.

Most Mediterranean coastal zones are dominated by a karstic hydrology and thus surface watercourses are limited. As a result a major part of freshwater inflow into the Mediterranean Sea is via SGD from large and dominantly non-renewable regional aquifer systems. SGD is a potentially important freshwater source especially in arid areas and on islands of the Mediterranean Sea. For example along the Cote d'Azur, France, between Nice and Menton over 50 SGD sites have been observed which, based on local hydrogeological water

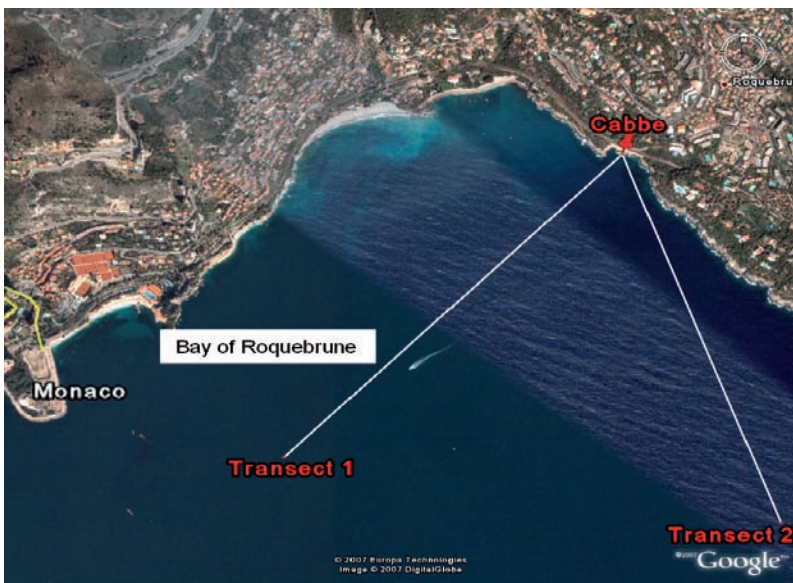


FIG. 1. Locations of the investigated SGD site Cabbe and the two transects in the Bay of Roquebrune.

SUBMARINE GROUNDWATER DISCHARGE TO THE MEDITERRANEAN SEA

mass balances, discharge about 600 L/sec of freshwater to the Mediterranean Sea [4]. Their significance in terms of input of dissolved material has been, however, not explored yet.

Stable and radioactive isotopes have shown to be useful tracers in SGD studies [1]. Measurements of the natural isotopes ^{222}Rn ($T_{1/2} = 3.8$ d), ^{223}Ra ($T_{1/2} = 11.4$ d) and ^{224}Ra ($T_{1/2} = 3.7$ d) can provide estimates of SGD discharge and dispersion rates of groundwater in the coastal environment and have the advantage of integrating a SGD signal over time and space. In groundwaters ^{222}Rn is highly enriched relative to seawater whereas the concentration of radium isotopes is higher in waters having contact with salt water.

At Cabbé we investigated the temporal pattern of SGD over 24 hours and the dispersion of groundwater in the Bay of Roquebrune (Fig.1). Our results suggest that SGD may be an important nitrate source for this region.

2. METHODS

Sampling was conducted on the beach of Cabbé and along two near-shore transects in the Bay of Roquebrune towards Cabbé (Fig. 1). At Cabbé, groundwater enters the sea at the end of a 4 m deep and 3 m wide submarine cave. At this outlet and along the two transects continued measurements of ^{222}Rn were conducted using an RAD7 radon monitor following the procedure described by Dulaiova et al. [5]. These measurements were accompanied by determinations of the tidal range (depth), temperature and salinity using a CTD. Discreet samples for nitrate analyses were obtained at Cabbé (every $\frac{1}{2}$ hour) and along the transects. Nitrate was analysed in duplicates which gives a precision of ± 0.05 μM in the concentration range from zero to 20 μM . About 60–70 L of water was obtained for analyses of radium isotopes (^{223}Ra , ^{224}Ra , ^{228}Ra , ^{226}Ra). The seawater was pumped over manganese fibers, and ^{223}Ra and ^{224}Ra isotopes were measured using the RaDeCC delayed coincidence counting system [6]. The manganese fibers were dried and sealed in tin cans for gamma measurements of ^{228}Ra (via ^{228}Ac) and ^{226}Ra (via ^{214}Pb). Sampling for radium isotopes was also performed along the transects by submerging manganese fibers in seawater for $\frac{1}{2}$ to 1 hour.

3. RESULTS AND DISCUSSION

At Cabbé throughout the first part of the experiment (26.9.06, 18:00 – 27.9.06, 3:00) relatively high salinities are found during both high and low tides, whereas during the second part of the experiment (27.9.06, 6:00–16:00)

TABLE 1. RESULTS OF MEASUREMENTS OF RADIUM ISOTOPES. THE SEAWATER SAMPLES WERE OBTAINED FROM THE MOST SEAWARD POSITION ALONG THE TRANSECTS INVESTIGATED.

	Cabbé (n=4)		Seawater (n=2)	
	dpm/100l	±	dpm/100l	±
^{224}Ra	8.59	1.35	1.72	0.39
^{223}Ra	0.43	0.06	0.06	0.01
$^{224}\text{Ra}/^{223}\text{Ra}^1$	19.9	1.10	26.5	2.30
^{228}Ra	4.99	0.02	2.45	0.40
^{226}Ra	11.4	0.02	6.75	0.43

¹ activity ratio

salinities observed are relatively higher during high tide and lower during low tide (max: 37.35; min: 36.35; Fig. 2). The ^{222}Rn concentrations at Cabbé vary between 413 Bq/m³ and 1,057 Bq/m³ (Fig. 2). During the first part of the experiment (26.9.06, 19:00 – 27.9.06, 3:00) variations in ^{222}Rn concentrations follow those of salinity whereas during the second part of the experiment (27.9.06, 6:00–16:00) the variations in both concentrations are the opposite. Variations of nitrate concentrations (max: 1.48 µM; min: 0.41 µM) basically follow those of ^{222}Rn (Fig. 2). At Cabbé no change of radium concentrations in relation to tidal salinity fluctuations were observed (Fig. 3). The radium isotope concentrations are higher at Cabbé compared to open seawater (Tab. 1). The average $^{224}\text{Ra}/^{223}\text{Ra}$ ratio of 19.9 ± 1.1 measured at Cabbé is near to the natural $^{224}\text{Ra}/^{223}\text{Ra}$ ratio of 21.7 (assuming $^{232}\text{Th}/^{238}\text{U} \sim 1$).

Previous studies have suggested that one of the SGD driving forces is the hydrological gradient between land and sea which is mainly determined by changes in sea level, i.e. the tidal range [7]. During low tide the groundwater discharge should be relatively higher whereas during high tide it should be relatively lower. As groundwater and seawater have different salinity, nitrate and ^{222}Rn concentrations (e.g. at Cabbé groundwater: salinity ~7.2, ^{222}Rn ~28,300 Bq/m³, nitrate ~29.7 µM (note that ^{222}Rn and nitrate end-member concentrations in the groundwater were calculated using the salinity versus ^{222}Rn (nitrate) relationship and a salinity of the groundwater of 7.2); open seawater: salinity ~38.06, ^{222}Rn ~ < 1 Bq/m³; nitrate: below detection) fluctuations of these parameters should follow the tidal cycle, i.e. higher ^{222}Rn and lower salinity during low tide and vice versa during high tide. In our study such a pattern is

SUBMARINE GROUNDWATER DISCHARGE TO THE MEDITERRANEAN SEA

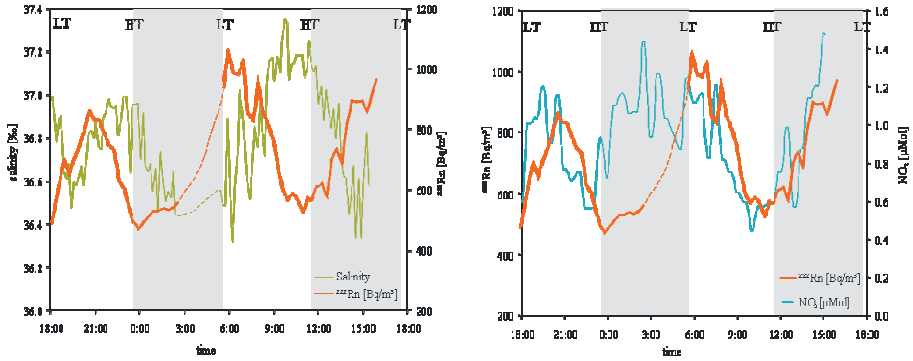


FIG. 2. Variations of salinity, NO_3 and ^{222}Rn concentrations at Cabbé during the experiment (start: 26.9.06, 18:00; end: 27.9.06, 16:15), LT = low tide; HT = high tide; stippled curve: no data; statistical counting error of $^{222}\text{Rn} \sim 12\%$.

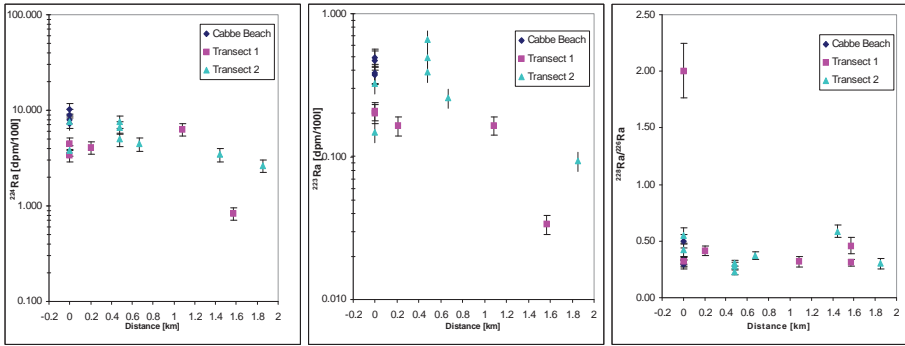


FIG. 3. Distributions of radium isotopes at Cabbé (distance = 0) and along the transects 1 and 2. No clear gradients in the isotope distributions are observed. Note the log scale for ^{224}Ra and ^{223}Ra .

observed during the second part of the investigation (27.9.06, 6:00–16:00) but not at the beginning of the experiment (26.9.06, 19:00–22:00). Here, the parallel fluctuations of ^{222}Rn , nitrate and salinity suggest relatively high groundwater discharge also during high tide. Rough sea conditions prevailing during this part of the experiment as well as heavy rainfall during the days preceding the experiment may have enhanced the groundwater discharge.

The nitrate concentrations in seawater along the transects investigated are below detection limit whereas at Cabbé parallel fluctuations of nitrate and ^{222}Rn concentrations were measured. This suggests that the SGD is a source of

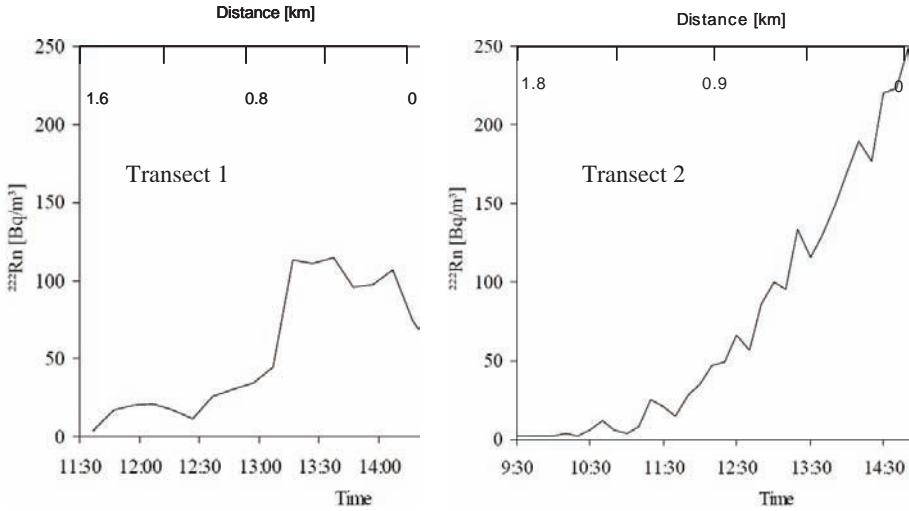


FIG. 4. ^{222}Rn distribution along the transects 1 and 2. The transects started in Bay of Roquebrune (transect 1 starting time: 28.09.06, 11:30; transect 2 starting time: 29.09.06, 9:30) landwards to about 20m off Cabbé (transect 1 end: 28.09.06, 14:30; transect 2 end: 29.09.06, 14:45); the distance from Cabbé is given in the upper scale.

nitrate for the coastal water off Cabbé. Based on the nitrate gradient observed of between 10:00 and 15:00 (27.9.06), a nitrate flux of $26.4 \text{ mmol} \cdot \text{day}^{-1} \cdot \text{m}^{-1}$ can be estimated.

In our study no significant variations of radium concentrations in relation to the tides were observed. This suggests low radium in groundwater probably due to the local geology (low uranium and thorium content in carbonate rocks) and/or short residence times of the groundwater in the karst aquifer. In contrast to other SGD investigations (e. g. [8]), we cannot use the radium distribution at Cabbé as a tracer for submarine groundwater discharge. Therefore, radium may be less useful as a tracer of SGD in cases of focused freshwater discharge from karst aquifers.

We can interpret the distribution of radium measured along the transects as a result of a non-localized release of radium through costal rock/sediment-seawater interaction and mixing of coastal waters. The variable sources of radium combined with variable mixing of coastal waters are probably the reason why no clear gradient for ^{223}Ra , ^{224}Ra and ^{228}Ra was observed.

In contrast to the radium results, a large increase in the ^{222}Rn concentrations was observed along the transects investigated in a landward direction from the Bay of Roquebrune towards Cabbé (Fig. 4). The concentrations observed along

transect 1 were lower than those observed along transect 2. These differences can be explained by diurnal variations in the mixing of ^{222}Rn , supplied by groundwater, with coastal waters. The ^{222}Rn distributions illustrate the far-reaching influence of SGD at Cabbé on the composition of seawater in the Bay of Roquebrune.

ACKNOWLEDGEMENTS

We thank the Service de la Marine, Monaco, for providing a ship for these investigations. We thank Gerhard Kattner and Kai-Uwe Ludwigowski for nitrate analyses. The IAEA is grateful for the support provided to the Marine Environment Laboratories by the Government of the Principality of Monaco.

REFERENCES

- [1] BURNETT, W.C., AGGARWAL, P.K., AURELI, A., BOKUNIEWICZ, H., CABLE, J.E., CHARETTE, M.A., KONTAR, E., KRUPA, S., KULKARNI, K.M., LOVELESS, A., MOORE, W.S., OBERDORFER, J.A., OLIVEIRA, J., OZYURT, N., POVINEC, P., PRIVITERA, A.M.G., RAJAR, R., RAMESSUR, R.T., SCHOLTEN, J., STIEGLITZ, T., TANIGUCHI, M., TURNER, J.V., Quantifying submarine groundwater discharge in the coastal zone via multiple methods, *Science of the Total Environment* **367** (2006) 498–543.
- [2] CORBETT, D.R., CHANTON, J., BURNETT, W., DILLON, K., RUTKOWSKI, C., FOURQUREAN, J.W., Patterns of groundwater discharge into Florida Bay, *Limnol. Oceanogr.* **44** (1999) 1045–1055.
- [3] HUSSAIN, N., TCHURCH, M., KIM, G., Use of ^{222}Rn and ^{226}Ra to trace groundwater discharge into the Chesapeake Bay, *Marine Chemistry* **65** (1999) 127–134.
- [4] GILLI, E., Etudes des sources karstiques sous-marines et littorales des Alpes Maritimes entre Menton et Nice, *Ministre de l'Environnement, Direction Régionale de l'Environnement* (1997) 54.
- [5] DULAIIOVA, H., PETERSON, R.G., BURNETT, W.C., A multi-detector continuous monitor for assessment of ^{222}Rn in the coastal ocean., *Journal Radioanalytical Nuclear Chemistry* **263** (2005) 361–365.
- [6] MOORE, W.S., ARNOLD, R., Measurement of ^{223}Ra and ^{224}Ra in coastal waters using a delayed coincidence counter, *J. Geophys. Res.* **101** (1996) 1321–1329.
- [7] TANIGUCHI, M., ISHITOBI, T., SHIMADA, J., Dynamics of submarine groundwater discharge and freshwater-seawater interface, *Journal Geophysical Research* **111** (2006) C01008; doi:01010.01029/02005JC002924.

- [8] MOORE, W.S., Radium isotopes as tracers of submarine groundwater discharge in Sicily, *Continental Shelf Research* **26** (2006) 852–861.

APPLICATION OF STABLE ISOTOPES TO EVALUATE GROUNDWATER RECHARGE OF A COASTAL AQUIFER IN NORTH-CENTRAL CHILE AND ITS ROLE IN VEGETATION DYNAMICS¹

E. AGUIRRE

Laboratorio de Isótopos Ambientales,
Comisión Chilena de Energía Nuclear,
Santiago, Chile

F.A. SQUEO

Departamento de Biología,
Universidad de La Serena,
Center for Advanced Studies in Arid Zones (CEAZA)
and Institute of Ecology and Biodiversity (IEB),
La Serena, Chile

R. ARAVENA

Department of Earth Sciences,
University of Waterloo,
Waterloo, Canada

Abstract

The understanding of the water sources for plant growth is one of the key elements to evaluate the present and long term primary productivity in arid ecosystems. We use stable isotope tools to evaluate the recharge mechanisms in a coastal aquifer located in the arid zone of north-central Chile. The main water sources in the study area, fog, rain and groundwater, were isotopically characterized over a decade. The isotope data confirmed that fog does not play any role in groundwater recharge. The water table and isotope data showed that during low water conditions (dry periods), the aquifer is maintained primarily by water recharged in the higher part of the Romeral basin. During high water table conditions (wet periods), recharge associated with local precipitation becomes a significant source of groundwater recharge. The aquifer responded very fast to rains with amounts over the average level for precipitation (like El Niño conditions),

¹ This work was supported by FONDECYT 1.030.428 and Compañía Minera del Pacífico

while no recharge was detected with precipitation events lower than the average value for precipitation. The recharge pattern can also influence the behavior of plants characterized by a dimorphic root systems than can perform hydraulic redistribution. Part of the fast recharge of the aquifer could be related to this water redistribution.

1. INTRODUCTION

The dynamics of aquifers are complex and highly dependent of their water sources and recharge mechanisms. The water cycle in north-central Chile is affected by the ENSO (El Niño — Southern Oscillation), which produce a change in the amount of precipitation between years, with rainy years associated with El Niño and dry years during La Niña, and with a El Niño frequency of 3–6 years [1]. Nevertheless, longer climatic cycles (e.g., interdecadal) have also been detected in the Pacific Basin [2]. These correspond to periods where a series of El Niño-La Niña cycles are different in intensity than the following series. The strongest series of El Niño events during the last 20 years of the last century occurred during a positive phase of the Interdecadal Pacific Oscillation (IPO); the present time corresponds to a negative phase of IPO, where less intense El Niño events are to be expected [3]. Furthermore, a clear decline in rainfall since the beginning of the XX century has also been identified in this region [4], so rainfall water contribution for coastal desert ecosystems is decreasing.

Plant productivity in arid ecosystems is highly dependent on seasonal pulses of water contribution from different sources. Therefore rainfall variability can determine pulses in the development of vegetation [5]. Available water for desert plants depends on the balance between the contribution from scarce rainfall (in the form of rain and/or fog) and groundwater, as well as from water losses due to direct evaporation of the soil surface, from transpiration and from the deep percolation [6]. Finally, properties of the local soil determine the amount of water that infiltrates during a period of time and water runoff [6] when rainfall occurs over a short period of time.

Isotopic studies in northern Chile have shown that groundwater plays a significant role as water sources for vegetation in this arid environment [7, 8]. The isotope approach has also been used to evaluate the origin and groundwater residence time and role of fog in groundwater recharge in the Northern Chile region [9]. The purpose of the work presented in this paper is to understand the recharge mechanisms in an unconfined gravel and sand aquifer located in the arid coastal region of north-central Chile. This research, part of a major research program in vegetation ecology in north-central Chile, aims to apply the isotopic fingerprinting approach for evaluating the main water sources for coastal-desert vegetation.

2. METHODS

The study site is part of a coastal-desert ecosystem located at Quebrada El Romeral (29° 43' S, 71° 15' W, 300 m.a.s.l.), 10 kilometers from the coastal border, and 21 km northeast of the city of La Serena (Fig. 1a). The upper part of the El Romeral basin is the Papilones Mount (1,881 m.a.s.l.) (Fig. 1b). The research was carried out during seven years (fall 1996 to December 2003) and a detailed evaluation of seasonal patterns was performed during the last three years of the study.

The Mediterranean arid type climate of La Serena is characterized by a mean annual temperature of 13.5°C, with a mean maximum temperature of 21°C during the warmest month, while the mean minimum temperature reaches 7.0°C during the coldest month. The mean annual rainfall is 114.4 mm, where June the wettest month, and the dry season lasts 9 months. The study site has a mean maximum temperature of 20–21°C during January and a mean minimum temperature of 8–10°C characterizes this last period during July. The July period has no frost occurrences and no vegetative recess. Annual rainfalls reaches 67.4 mm, with a dry period lasting 11–12 months; the annual potential evapotranspiration is 824.3 mm, and the annual hydric deficit reaches 756.9 mm. Annual precipitation at Minas El Romeral (1956–2003) show an average

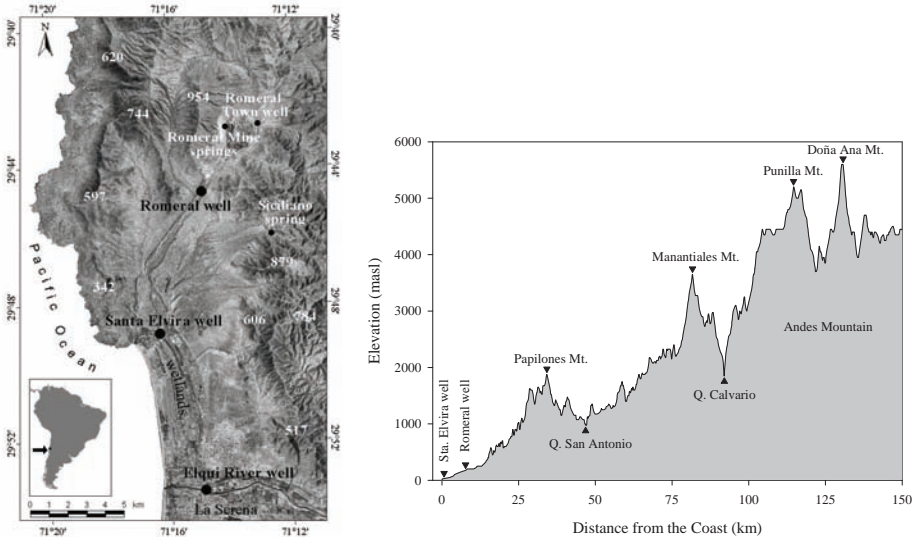


FIG. 1. a) Location of study site and sampling locations, Quebrada El Romeral, north-central Chile. Principal elevation (in m.a.s.l.) are shown. b) Altitude transect from the coast to the West side of the Andes near at 29°45'S (71°20' to 69°55'W).

value of 82.9 mm (76.5 mm in the last 30 years), with rainy years associated to ENSO events.

Groundwater samples were collected from wells located in the middle and lower part of the El Romeral basin (Fig. 1). The Elqui river aquifer in the lower part of the basin was also sampled for isotope analysis. A full sampling program was conducted in 1996, and two selected wells (El Romeral and Santa Elvira) were used to monitor seasonal changes in the isotope composition of the groundwater. Water level was also monitored at the well at Romeral. The depth of this well is 13 m and is tapping the alluvial deposit of the Quebrada El Romeral. The Santa Elvira well has a depth of about 14 m and is tapping the sand deposits of the coastal area of La Serena. Oxygen-18 and deuterium analyses were performed on rain, fog and groundwater samples. Tritium analysis was only performed on groundwater samples collected during 1996 and 1998 sampling events. Hydrogen and oxygen isotope ratios on water samples were measured using a Finnigan MAT 252 isotope ratio mass spectrometer at CCHEN (Chilean Nuclear Energy Commission). The standard used for $\delta^2\text{H}$ and $\delta^{18}\text{O}$ was SMOW and analytical errors were 0.2‰ and 1‰ for $\delta^{18}\text{O}$ and $\delta^2\text{H}$, respectively. Tritium analyses were conducted at the Environmental Isotope Laboratory, University of Waterloo (Canada) by liquid scintillation counting. The tritium data is expressed in tritium units (TU) with an analytical error of 0.8 TU.

3. RESULTS

A wide range in isotope composition that varies between -13 and -1% for $\delta^{18}\text{O}$ and -100 and -1% for $\delta^2\text{H}$ was observed on the different waters that are part of the water cycle in the study area (Fig. 2). Fog waters are the more isotopically enriched waters ranging between -3 and -1% for $\delta^{18}\text{O}$, and -2 and -18% for $\delta^2\text{H}$. Precipitation varies between -9 and -2% for $\delta^2\text{H}$ and -77 and -10% for $\delta^{18}\text{O}$. The weighted mean isotope composition for the precipitation at the Romeral station is -28.1 and -4.8% for $\delta^2\text{H}$ and $\delta^{18}\text{O}$, respectively, which is very similar to the long-term weighted mean isotope composition of the precipitation collected at La Serena.

The overall data for precipitation in the study region is in the same range as isotope precipitation data reported for coastal areas in Chile. The rain isotopic data collected at the Romeral precipitation station define a linear relationship $\delta^2\text{H} = 7.7 \times \delta^{18}\text{O} + 9.6\%$ ($r^2 = 0.91$). This local meteoric water line is close to global meteoric water line $\delta^2\text{H} = 8 \times \delta^{18}\text{O} + 10\%$.

Groundwater collected in the Romeral basin is much more enriched isotopically than the groundwater collected in the lower part of the basin

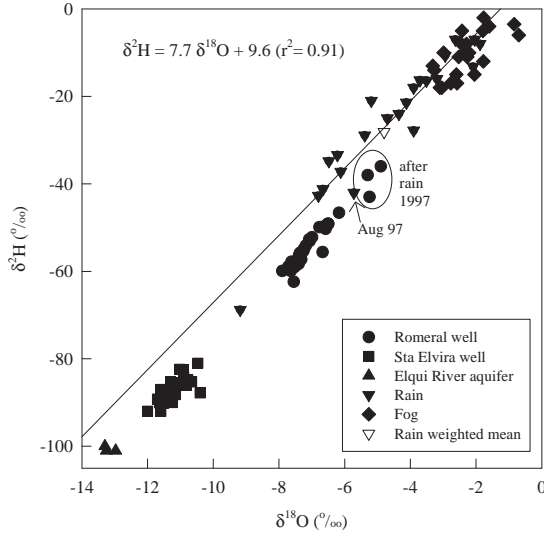


FIG. 2. Relationship between $\delta^{18}\text{O}$ and $\delta^2\text{H}$ for fog, rain and groundwater collected in this study (1996-2003). The local meteoric water line is shown.

(well Santa Elvira) (Fig. 2). In general, the Romeral groundwater is also more depleted isotopically than the isotope composition of the precipitation collected at the Romeral station (Fig. 3), which can be explained by the input of more isotopically depleted precipitation recharging the aquifer in the higher part of the Romeral basin.

However, it is worth noting than the local meteoric water mainly represents the rain in the lower part of the basin. The isotope data showed that coastal fogs do not play any major role in groundwater recharge of the Romeral aquifer. The groundwater collected in the Santa Elvira well with $\delta^{18}\text{O}$ values ranging between -10.5 and -12.0‰ does not seem to receive a significant contribution from the groundwater flow system of the Quebrada El Romeral alluvial aquifer, even though this well is located at the mouth of the Quebrada El Romeral. The aquifer tapped by the Santa Elvira well is clearly part of a discharge zone that has a major contribution of water recharged at higher altitude than the headwater of the Romeral basin. This water is represented by groundwater from the regional aquifer of the Rio Elqui Basin, which is characterized by an isotope composition of around -13 and -100‰ for $\delta^{18}\text{O}$ and $\delta^2\text{H}$, respectively (Fig. 2).

A first approximation for the evaluation of aquifer recharge can be inferred from the seasonal data on precipitation and water level in the aquifer measured at the Romeral well and seasonal data on the isotope composition

of groundwater collected at the Romeral and Santa Elvira wells (Fig. 3). The water table pattern has to be related to a recharge cycle, which is controlled by the precipitation regime in the study area (Fig. 3a). The high water level of 2000 and 2002 could be explained by recharge linked to precipitation that fell during the winter of 2000 and 2002, respectively. The amount of precipitation during this time was higher than the average value for precipitation for the study area. The precipitation that fell during the winter (July–Sept) of 2001 (65.8 mm, Fig. 4a) was lower than the average value, and it seems it did not contribute to recharge which explains the significant drop in the water table observed during the period July 2001 to July 2002 (Fig. 3b). The significant water table drop observed after May 2003 can also be explained by the absence of aquifer recharge due to the dry winter of 2003 (Fig. 3a).

The isotope data suggest that during low water table conditions, the aquifer in El Romeral is mainly maintained by the groundwater recharged in the higher part of the basin (Fig. 3c). The enrichment trend associated with an increase in water table indicated that the aquifer recovery is partially due to more groundwater recharge in the middle and lower part of the basin. During the winter of 2002, the amount of precipitation was significantly higher than the average value. The $\delta^{18}\text{O}$ of precipitation in the lower part of the basin is -4.8‰ . The role of ground water recharge in the middle and lower part of the basin is also supported by isotope data collected on November 1997 that produced the most enriched isotope values for the Romeral groundwater, which was related with an unusual rain event in August 1997 (89.8 mm in two days) characterized by an isotopic composition of -5.7‰ and -42‰ for $\delta^{18}\text{O}$ and $\delta^2\text{H}$, respectively (Fig. 2). It is expected that groundwater recharge during this time was much higher than post 1997 since this year was the wettest year of the last 38 years and was associated with an ENSO event. The enriched isotopic trend started to change toward a depleted pattern after July 2003 that seems to coincide again with a drop in water table similarly to the pattern observed between July 2001 and July 2002.

Similarly, the groundwater collected in the Santa Elvira well seems to show seasonal changes in its isotope composition but are not as well defined as the Romeral groundwater (Fig. 3d). First, a slight trend toward depleted values of $\delta^{18}\text{O}$ is observed between September 2000 and August 2001 then a clear trend toward more enriched isotope values starting from -11.4‰ and reaching values as high as -10.4‰ was observed between October and Dec 2001. This trend is reversed tending to -11.6‰ in July–August 2002. Then, an enriched trend is observed after August 2002 reaching -11‰ in Nov 2002 and reversing toward -11.8‰ after this date. The enrichment pattern observed in the period October–December 2001 could be explained by an increase in the groundwater contribution by the Romeral aquifer, which is characterized by a $\delta^{18}\text{O}$ -7.5‰ and then during low

APPLICATION OF STABLE ISOTOPES TO EVALUATE GROUNDWATER RECHARGE

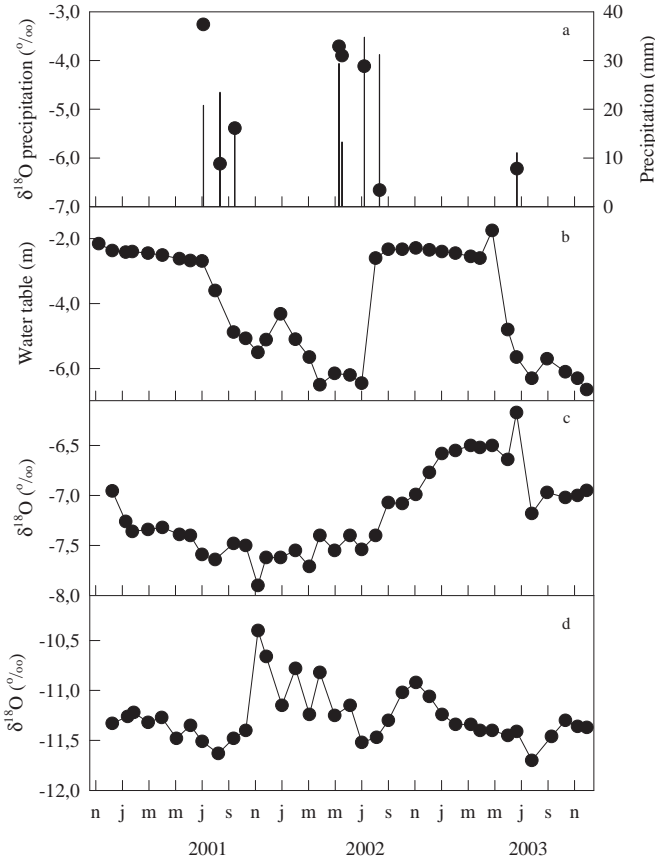


FIG. 3. Precipitation (a), water level Romeral well (b) and $\delta^{18}\text{O}$ for Romeral (c) and Santa Elvira (d) groundwater (2000–2003).

water period observed in the Romeral aquifer, the isotope composition of the Santa Elvira groundwater is mainly controlled by the contribution of the regional aquifer linked to the Elqui basin, which is characterized by $\delta^{18}\text{O}$ of -13.5‰ in the lower part of the basin.

Tritium data collected in 1996 and 1998 in the Romeral basin also provide information about the dynamics of groundwater recharge in the study area. The data collected in December 1996 after four dry years showed the groundwater was devoid of tritium. The precipitation in coastal areas in Chile should have tritium values in the range of 4 to 6 TU. The groundwater tritium data suggested that groundwater in the Romeral aquifer was at least 40 years old. The November 1998 data show 1.5 to 1.8 TU in some wells indicating the recharge of recent

water probably associated with the heavy rains of 1997 linked to an ENSO year. The tritium data agreed with the stable isotope data that showed the Romeral aquifer responded very fast to recharge events associated with rains over the average value for precipitation in the study area. The lack of tritium in the Santa Elvira groundwater and the Elqui River aquifer agreed with the stable isotope data that showed the coastal aquifer tapped by the Santa Elvira well is receiving mainly groundwater linked to the Elqui regional aquifer.

4. CONCLUSIONS

The main conclusion of the present study is that during wet years and especially during ENSO events, the water table recovers very fast and local precipitation plays a significant role in groundwater recharge. This pattern has implications for a functional group of plant species, characterized by a deep root system, that have low capacity to respond directly to precipitation events [11]. However, the fast response of the aquifer to precipitation events that larger than average after a long dry period suggests that this functional group can use groundwater as a main water source for new plant growth and reproduction [11,12]. In the Romeral basin, the plant phenology of 14 native shrub species was evaluated during two contrasting rainfall years. Vegetative growth in deciduous species are strongly related with the winter precipitation while most of the evergreen shrub species are more dependent on groundwater [12]. A field experiment with three shrub species with dimorphic (*Balbisia peduncularis* and *Senna cumingii*) or deep (*Haplopappus parvifolius*) root systems showed that these three species used two water sources (shallow water coming from rainfall and a greater proportion of groundwater) [11]. The species with dimorphic roots are able to reduce their water deficits after the artificial watering in fall, winter and spring, while the deep rooted species only was able to use a proportion of the rain in winter.

The response of the aquifer can also be linked to another functional groups characterized by a dimorphic root systems than have the possibility to perform hydraulic redistribution (i.e., the movement of water through the root system from deep to shallow soils in dry periods, and shallow-wet soil to deep-dry soil in very rainy periods) [13]. Part of the fast recharge of the aquifer could be related to this water redistribution as it has been shown in other desert ecosystems [14]. However, the magnitude of the contribution of the plants in the recharge of this coastal aquifer still needs to be quantified. The other effect of fast water table rebound in the study area could be on seedling recruitment of deep-rooted species. Most of the seeds of shrubs species germinated with precipitation lower than 20 mm [15], but the survival of the new springs of

depth rooted plants required a shallow water table during the next summer to be established.

REFERENCES

- [1] HOLMGREN, M., LÓPEZ, B.C., GUTIÉRREZ, J.R., SQUEO, F.A., Explaining regional differences in ENSO-driven tree establishment in semi-arid South America, *Global Change, Biology* **12** (2006) 2263–2271.
- [2] RUTLLAND, J.A., Aspectos de la circulación atmosférica de gran escala asociada al ciclo ENOS 1997–1999 y sus consecuencias en el régimen de precipitación en Chile central. In: Avaria, S., Carrasco, J., Rutllant, J.A. & Yanez.E. (eds) *El Niño-La Niña 1997–2000, Sus efectos en Chile*, Conaf, Valparaíso (2004) 61–76.
- [3] SALINGER, S.M.J., Interdecadal Pacific Oscillation and South Pacific Climate, *Int. J. Climatology* **21** (2001) 1705–1721.
- [4] SOTO, G., ULLOA, F., Diagnóstico de la Desertificación en Chile, CONAF / FAO / PNUMA, La Serena (1997) 399.
- [5] SQUEO, F.A., EHLERINGER, J.R., OLIVARES, N.C., ARANCIO, G., Variation in leaf level energy balance components of *Encelia canescens* along a precipitation gradient in north-central Chile, *Revista Chilena de Historia Natural* **67** (1994) 143–155.
- [6] NOBLE, I.R., GITAY, H., Deserts in a changing climate: Impacts, In: Watson, R.T., Zinyowera, M.C., Moss, R.H. (Eds.), *Climate Change Impacts, Adaptations and Mitigation of Climate Change: Scientific-Technical Analyses*, Cambridge University Press, New York (1995) 161–169.
- [7] ARAVENA, R., SUZUKI, O., POLLASTRI, A., Coastal fog and its relation to groundwater in the IV Region of northern Chile, *Chemical Geology (Isotope Geoscience Section)* **79** (1989) 83–91.
- [8] SQUEO, F.A., ARAVENA, R., AGUIRRE, E., POLLASTRI, A., JORQUERA, C.B., EHLERINGER, J.R., Groundwater dynamics in a coastal aquifer in North-central Chile: Implications for groundwater recharge in an arid ecosystem, *Journal of Arid Environments* **67** (2006) 240–254.
- [9] ARAVENA, R., Isotope Hydrology and geochemistry of northern Chile groundwaters, *Bull. Inst. Fr. etudes andines* **24** (1995) 495–503.
- [10] TORRES, R., SQUEO, F.A., JORQUERA, C., AGUIRRE, E., EHLERINGER, J.R., Evaluación de la capacidad estacional de utilizar eventos de precipitación en tres especies de arbustos nativos con distintos sistemas radiculares, *Revista Chilena de Historia Natural* **75** (2002) 737–749.

- [11] OLIVARES, S., SQUEO, F.A., Patrones fenológicos en especies arbustivas del desierto costero del norte-centro de Chile. *Revista Chilena de Historia Natural* **72** (1999) 353–370.
- [12] LEÓN, M.Y., SQUEO, F.A., Levantamiento hidráulico: la raíz del asunto, In: Cabrera, H.M. (Ed) *Fisiología Ecológica en Plantas: Mecanismos y Respuestas a Estrés en los Ecosistemas*, Ediciones Pontificia Universidad Católica de Valparaíso, Valparaíso, Chile (2004) 99–109.
- [13] SCHOLZ, F.G., BUCCI, J., GOLDSTEIN, G., MEINZER, F., FRANCO, A., Hydraulic redistribution of soil water by neotropical savanna trees, *Tree Physiology* **22** (2002) 603–61
- [14] MALDONADO, C., PUJADO, E., SQUEO, F.A., El efecto de la disponibilidad de agua durante el crecimiento de *Lycopersicon chilense* sobre la capacidad de sus semillas para germinar a distintas concentraciones de manitol, NaCl y temperatura, *Revista Chilena de Historia Natural* **75** (2002) 651–660.

CHARACTERIZATION OF MARINE INTRUSION AND ORIGIN OF THE MINERALIZATION IN THE ORIENTAL COASTAL AQUIFER OF CAP BON (TUNISIA)

M.F. BEN HAMOUDA

Unité d'Hydrologie et de Géochimie Isotopique,
CNSTN,
Sidi Thabet, Tunisia

K. ZOUARI

Laboratoire de Radioanalyse et Environnement,
ENIS,
Sfax, Tunisia

J. TARHOUNI

Laboratoire des Sciences et Techniques de l'Eau,
INAT,
Tunis, Tunisia

C. LEDUC

Institut de Recherche pour le Développement,
UMR G-EAU, MSE, France

Abstract

The characterization of marine intrusion and the determination of the origin of the salinisation in the plio-quadernary oriental coastal aquifer of Cap Bon (Noth-East of Tunisia), and the understanding of its hydrogeological and geochemical behaviours related to overexploitation of water resources, were studied by the geochemical tools, and by the stable isotopes (^{18}O , ^2H) of water molecules. The study area is bounded by the Gulf of Hammamet in the East, Djebel Sidi Aberahmane in the West, the city of Nabeul in the south and the city Kelibia in the north. The landscape is a coastal plain slightly sloping (3%) towards the sea. The groundwater of the oriental coastal aquifer system occurs mainly at two levels, a shallow aquifer up to depths of about 150 m whose reservoir is consisted by sediments of the plio-quadernary and a deep aquifer between about 150 and 400 m located in the sandstone formations of Miocene and Oligocene of the anticline of Djebel Sidi Abderrahmene. The climate of the region is semi-arid

to sub-humid and of Mediterranean type. The long-term mean annual rainfall varies between 400 and 500mm, and the mean annual potential evaporation is about 1100 mm. The determination of the origin of the mineralization, the piezometric and salinity map were established. The overexploitation of the aquifer is characterized by the decrease of piezometry in the study area, reducing the outflow rate to the sea, and a continuous degradation of the chemical quality of water. Depression cones in various places have dropped to 5 to 10 m below sea level, which demonstrates the inversion of the hydraulic gradient and promotes the invasion of seawater. The increase of the salinity seems mainly linked to the deterioration of the hydrodynamic gradient as suggests the similarity between salinity and piezometric maps. The chloride is strongly correlated to the sodium for the majority of the samples. The predominance of sodium and chloride is explained by the proximity of the sea, via the spray and/or a progress of seawater intrusion. The Br^-/Cl^- ratio is in general lower than the marine ratio. The few points aligned on the dilution line of seawater evoke a possible mixture with the seawater. The plot ^{18}O vs. ^2H for the plio-quadernary aquifer show that the composition of oxygen 18 in the groundwater can be divided in two groups. In the first one, the composition of ^{18}O varies between -4.3 and -5.5 ‰, this group is located between the global meteoric water line (GMWL) and the local water line of Tunis Carthage; (LMWL). The hypothesis of an important contribution of the present rains to the recharge is probable. The second group is composed by the wells located in the region of the piezometric depression, near the sea where the salinity can reach 30 g/L. These waters are more enriched in ^{18}O and ^2H and fall on the mixing line of seawater; confirming the existence of marine origin in these waters. The heterogeneity of the process of salinisation in this coastal region (which has multiple salt origins) requires a combined approach. The results of Hydro-geochemical and isotopic studies have shown the salinity of the groundwater is especially acquired by the dissolution of minerals through the return of irrigation water in the aquifer system, by the contamination of nitrates and by a mixture with seawater. In particular, the area of Korba and Tefelloune strongly is affected, where we observe a negative piezometry and the salinity can reach the 30 g/L.

1. INTRODUCTION

The characterization of marine intrusion and the determination of the origin of the salinisation in the plio-quadernary oriental coastal aquifer of Cap Bon (Noth-East of Tunisia about 60 km south of the Tunis city), and the understanding of its hydrogeological and geochemical behaviours related to overexploitation of water resources, were studied by the geochemical tools (conservative elements: Br^- and Cl^-), and by the stable isotopes (^{18}O , ^2H) of water molecules. The study area is bounded by the Gulf of Hammamet in the East, Djebel Sidi Aberahmane in the West, the city of Nabeul in the south and

CHARACTERIZATION OF MARINE INTRUSION AND ORIGIN

the city Kelibia in the North. The landscape is a coastal plain slightly sloping (3%) towards the sea. The groundwater of the oriental coastal aquifer system occurs mainly at two levels, a shallow aquifer up to depths of about 150 m whose reservoir is consisted by sediments of the Plio-Quaternary and a deep aquifer between about 150 and 400 m located in the sandstone formations of Miocene and Oligocene of the anticline of Djebel Sidi Abderrahmene. The climate of the region is semi-arid to sub-humid and of Mediterranean type. The summer season is dry and hot and rain falls mainly in the cooler winter season. The long-term mean annual rainfall varies between 400 and 450 mm, and the mean annual potential evaporation is about 1100 mm. There are no perennial rivers in this region; but intense storms occasionally cause surface runoff, which is discharged by the oueds. Oued Chiba and Oued Lebna are the major oueds and contain two dams for better management of the groundwater for agriculture in the region.

2. METHOD

To better understand the hydrodynamic processes taking place and flow regime as well as the origin of salinity of the groundwater, samples were analysed for their isotopic compositions (^{18}O , ^2H) and some environmental tracers such as bromide and chloride ions. In fact, they are called conservative ions because their contents are neither influenced by the redox processes, nor controlled by the minerals with low solubility. Thus, the Br^-/Cl^- ratio is always constant, when the two elements have a common and unique origin. For the characterisation of sea water intrusion, piezometric and salinity maps were established. The overexploitation of the aquifer is characterized by the decrease of piezometry in the study area, reducing the outflow rate to the sea, and a continuous degradation of the chemical quality of water. Depression cones in various places have dropped to 5 to 10 m below sea level, which demonstrates the inversion of the hydraulic gradient and promotesthe invasion of seawater.

The increase of the salinity seems mainly linked to the deterioration of the hydrodynamic gradient as suggested by the similarity between salinity and piezometric maps and their conjoined evolution in the time. It is therefore necessary to examine by different geochemical approaches the importance of the marine intrusion in the increase of mineralization.

2.1. Chloride and bromide

The chloride is strongly correlated to the sodium for the majority of the samples (Fig. 1). The predominance of sodium and chloride is explained by the proximity of the sea, via the spray and/or a progress of seawater intrusion.

The waters, whose Na^+/Cl^- is near to the dilution line of the Mediterranean Sea (0.86), are those sampled in wells located in the depression zone and having a mixture with seawater, whereas waters with a lower Na^+/Cl^- ratio (0.5) represent another group, which the origin of the mineralization is especially acquired by the evaporation that is considered in most of semi-arid regions the main reasons of the salinisation. It clearly appears, therefore, that several sources and processes affect with different mineralization participating to the salinisation of the aquifer.

The Br^-/Cl^- provide information inform on the origin of the solutions and/or the identification of possible contribution of sea water [1,3,5]. Actually in seawater, this ratio is relatively constant (1.5×10^{-3}) because of the extremely long residence time in the oceanic masses.

Some samples fall on the dilution line of Mediterranean seawater characterized by molar Br^-/Cl^- ratio of about 1.5×10^{-3} (Fig. 2) and suggests the possibility of mixture with seawater. Other samples, with a lower Br^-/Cl^- ratio, suggest the existence of another type of water with a different mineralization. This suggests a contribution of superficial water and possibly return of water irrigation into the aquifer and an evaporation of water during the infiltration within the aquifer formation.

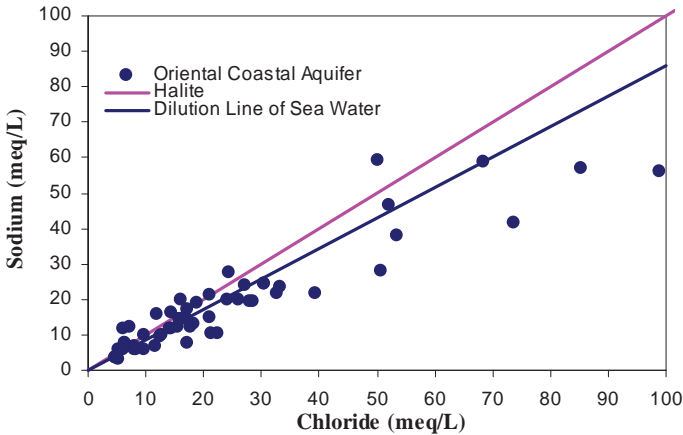


Fig.1. Correlation $[Na^+]/[Cl^-]$ in the groundwater of oriental coastal aquifer of Cap Bon.

CHARACTERIZATION OF MARINE INTRUSION AND ORIGIN

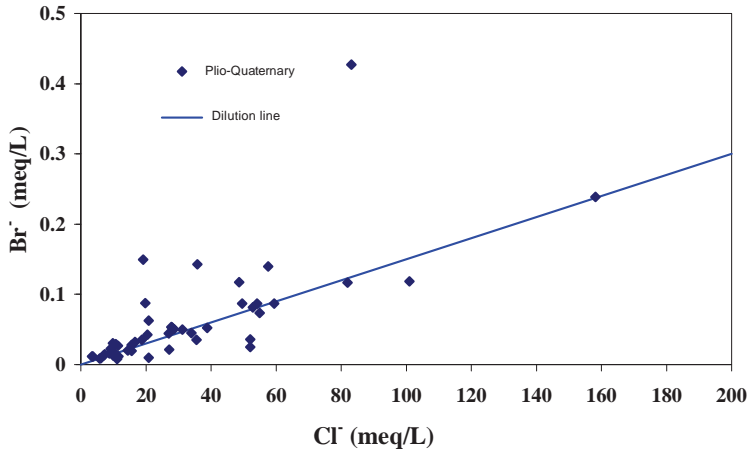


Fig.2. Correlation $[Br^-]/[Cl^-]$ in the the groundwater of oriental coastal aquifer of Cap Bon

The points which the ratio Br^-/Cl^- are located over to the line of dilution of sea water are outside of the seawater intrusion (Fig. 2).

2.2. Stable isotopes

The study of the plot $\delta^{18}O$ vs. δ^2H for the Plio-Quaternary aquifer show that the composition of Oxygen 18 in the groundwater can be divided in two groups (Fig. 3). In the first one, the composition of ^{18}O varies between $-4,3$ and $-5,5$ ‰, this group is located between the global meteoric water line (GMWL) and the local water line of Tunis Carthage; (LMWL). The hypothesis of an important contribution of the present rains to recharge is probable.

The second group is composed by the wells (P19, 11281, 11635, 8684, P3, 5729, 6077, 5994). This entire group is located in the region of the piezometric depression, near the sea where the salinity can reach 30 g/L. These waters are more enriched in ^{18}O and 2H and fall on the mixing line of seawater; So the marine origin of these waters is identified. For the other points situated below this line, they are under the influence of an evaporation.

For the deep Miocene and Oligocene aquifer, the content in oxygen 18 varies between -4.82 and -6.05 ‰. These values are different from the weighted average of the precipitation water of the Tunis Carthage station (-4.41 ‰) and present an isotopic fingerprint characteristic of old water.

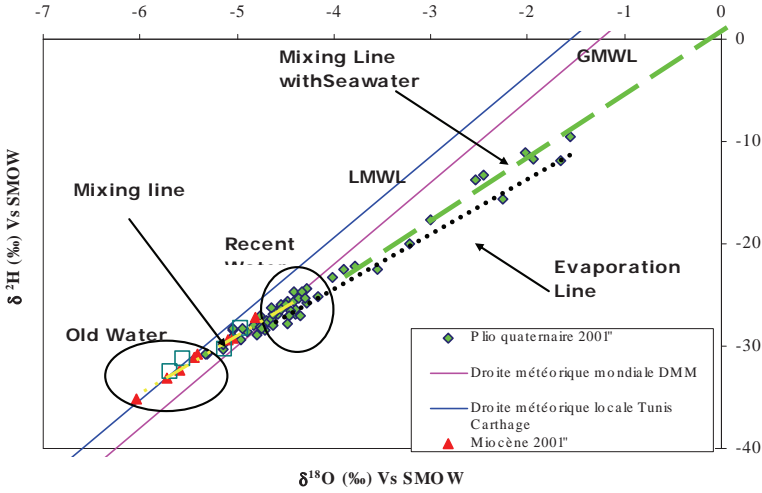


Fig.3. Correlation ¹⁸O-²H in the groundwater of oriental coastal aquifer.

2.3. Sea water contribution

The determination the contribution of seawater in the plio-quaternary aquifer has been based on the calculation of the mass balance of the chloride (conservative element). The fraction F of seawater in every sample affected by the seawater intrusion is calculated by the equation:

$$F = \frac{(mCl_{\text{sample}} - mCl_{\text{fresh}})}{(mCl_{\text{sea}} - mCl_{\text{fresh}})}$$

Where mCl_{sample} , mCl_{fresh} and mCl_{sea} represents the concentration of chloride (mg/L) respectively in the sample, fresh water and seawater.

The concentrations in chloride reach an extreme value of 13824 mg/L (piezometer 13143/2) in the region of Ksar Saad between Korba and Tafelloune. For the other samples, the concentration in chlorides are more or less important and varies from 300 to 11200 mg/L. The average contents of this ion in the most continental part (West) of aquifer and in seawater, are respectively 300 mg/L and 19500 mg/L. Thus, the maximum fraction of the seawater is 70% for piezometer 13143/2, 8% for piezometer 11635/2, and 3.4% for piezometer 11829/2 in Diar Hojjaj. these values show the heterogeneity of the process of salinisation in this region.

3. CONCLUSION

The results of geochemical and isotopic studies have shown that the salinity of the groundwater is generally acquired by dissolution of minerals in the aquifer system. However for the plio-quadernary shallow aquifer a contamination by a mixture with seawater is confirmed, in particular in the area of Korba and Tefelloune, where we observe a negative piezometry and the salinity can reach the 30 g/L, and the sea water intrusion which may reach 70% depending on location.

ACKNOWLEDGEMENTS

The authors wish to thank Mr. C. Gaye from IAEA for providing isotope measurement, Mr. Y. Travi from university of Avignon, France, for bromide measurement and Mr. N. Oueslati from CRDA Nabeul, Tunisia, for assisting with field sampling and measurement. The help of DGRE, Tunisia in aspect of chemical measurement is greatly appreciated. This research was supported by IAEA through TC project TUN/8/015 and TUN/8/017.

REFERENCES

- [1] BARBECOT, F., MARLIN, C., GIBERT, E., DEVER, L., Identification et caractérisation d'un biseau salin dans l'aquifère du Bajocien-Bathonien de la région de Caen (France), *C. R. Acad. Sci. Paris* **326** (1998) 539–544.
- [2] CELLE-JEANTON, H., ZOUARI, K., TRAVI, Y., DAOUD, A., Caractérisation isotopique des pluies en Tunisie, Essai de typologie dans la région de Sfax, *C.R. Acad. Sc.* **333** (2001) 625–631.
- [3] FEDRIGONI, L., KRIMISSA, M., ZOUARI, K., MALIKI, A., ZUPPI, G.M., Origine de la minéralisation et comportement hydrogéochimique d'une nappe phréatique soumise à des contraintes naturelles et anthropiques sévères : exemple de la nappe de Djebeniana, Tunisie, *C. R. Acad. Sci. Paris* **332** (2001) 665–671.
- [4] JONES, B.F., VENGOSH, A., ROSENTHAL, E., YECHIELI, Y., Geochemical investigations, in: J. Bear et al (eds.), *Seawater Intrusion in Coastal Aquifers*, Kluwer Academic Publisher (1999) 51–71.
- [5] KIM, Y., LEE, K., KOH, D., LEE, D., LEE, S., PARK, W., Hydrogeochemical and isotopic evidence of groundwater salinization in a coastal aquifer: a case study in Jeju volcanic island, Korea, *J. Hydrol* **270** (2003) 282–294.

- [6] LOUVAT, D., MICHELOT, J.L., ARANYOSSY, J.F., Origin and residence time of salinity in the Äspö groundwater system, *Applied Geochemistry* **14** (1999) 917–925.
- [7] PANICONI, C., KHLAIFI, I., LECCA, G., GIACOMELLI, A., TARHOUNI, J., A Modelling Study of Seawater Intrusion in the Korba Coastal Plain, Tunisia, *Phys. Chem. Earth* **26** (2001) 345–351.
- [8] PULIDO-LEBOEUF, P., PULIDO-BOSCH, A., CALVACHE, M.L., VALLEJOS, A., ANDREU, J. M., Strontium, $\text{SO}_4^{2-}/\text{Cl}^-$ and $\text{Mg}^{2+}/\text{Ca}^{2+}$ ratios as tracers for the evolution of seawater into coastal aquifers: the example of Castell de Ferro aquifer (SE Spain), *C. R. Geoscience* **335** (2003) 1039–1048.
- [9] BEN HAMOUDA, M.F., ZOUARI, K., TARHOUNI, J., OUSLATI, M.N., GAYE, C.B. (2004), Assessment of marine intrusion in the oriental coastal aquifer of Cap bon, Tunisia, International Workshop on the Application of Isotope Techniques in Hydrological and Environmental Studies UNESCO, Paris, France, September 6–8, 2004
- [10] CUSTUDIO, E., BRUGGEMAN, G.A., Groundwater problems in coastal Aera, Unesco publication, *Studies and reports in hydrology* **45** (1987) 596.
- [11] Ghabayen, S., McKee, M., Kemblowski, M., Ionic and isotopic ratios for identification of salinity sources and missing data in the Gaza aquifer, *Journal of Hydrology* **318** (2006) 360–373.
- [12] SHIVANA, K., KA VADA, S.V., NAIR, A.R., RAO, S.M., Isotope and geochemical evidence of past seawater salinity in Midnapore groundwater, in “Applied isotope techniques in studying past and current environmental changes in the hydrosphere and the atmosphere.”. IAEA, Vienna (1994) 199–212
- [13] VENGOSH, A., BEN-ZVI, A., Formation of a salt plume in the Coastal Plain aquifer of Israel: the Be'er Toviyya region, *J. Hydrol* **160** (1994) 21–52.
- [14] YURTSEVER, Y., (1994), Role of environmental isotopes in studies related to salinization processes and salt water intrusion dynamics. Proc of the 13th saltwater intrusion meeting, Calgary, Italy, 5–10 june (1994) 177–185.

ISOTOPIC CHARACTERISATION OF GROUNDWATER-SEAWATER INTERACTIONS

P.P. POVINEC¹,
International Atomic Energy Agency,
Marine Environment Laboratories,
Monaco

and

Comenius University,
Bratislava, Slovakia

P.K. AGGARWAL, K.M. KULKARNI, M. GROENING, L-F. HAN
International Atomic Energy Agency,
Vienna, Austria

Abstract

Isotopic methods for characterisation of groundwater-seawater interactions have been recently developed, and investigations have been carried out in several coastal regions in the framework of the Coordinated Research Project (CRP) on “Nuclear and Isotopic Techniques for the Characterisation of Submarine Groundwater Discharge in Coastal Zones” coordinated jointly by the IAEA’s Isotope Hydrology Section (Vienna) and Marine Environment Laboratories (Monaco). The CRP was carried out in cooperation with UNESCO’s Intergovernmental Oceanographic Commission (IOC) and the International Hydrological Programme (IHP), and with several laboratories in Brazil, India, Italy, Japan, Russia, Slovenia, Turkey and USA. An isotopic characterisation of groundwater-seawater interactions is illustrated on a case study carried out in the south-eastern Sicily.

1. INTRODUCTION

Studies of groundwater-seawater interactions (GSI) in coastal zones are important for better understanding of coastal processes, input of groundwater

¹ Present address: Comenius University, Faculty of Mathematics, Physics and Informatics, Mlynska dolina F-1, SK-84248 Bratislava, Slovakia. Email address: povinec@fmph.uniba.sk

to the sea via submarine groundwater discharge (SGD), saltwater intrusion in groundwater reservoirs and coastal land, contamination of groundwater and coastal seawater by land based sources, and generally for proper management of fresh water resources in the region. SGD has been recognised as an important pathway for material transport to the marine environment, which can lead to environmental deterioration of coastal zones. [1]. While the major rivers inputs to the ocean are gauged and well analysed, thus allowing relatively precise estimates of fresh water and contaminant inputs to the ocean, assessing groundwater fluxes and their impacts on the near-shore marine environment is much more difficult, as there are no simple means to gauge these fluxes of water and contaminants to the sea. Current estimates of the SGD to the world ocean range from less than ten to nearly fifty percent of total river runoff in temperate and tropical forested regions, as well as in karstic regions [2]. As the Mediterranean Sea is a typical karstic region, the SGD may represent there an important part of the continental water balance requiring more detailed investigations [3]. As almost all coastal zones are subject to flow of groundwater either as submarine springs or disseminated seepage, coastal areas are likely to experience environmental degradation. The direct discharge of groundwater into the near-shore marine environment may have significant environmental consequences because groundwater in many areas has become contaminated with a variety of substances such as heavy metals, radionuclides and organic compounds. Transport of pollutants and nutrients (especially nitrates and nitrites) from the land into coastal waters has caused an eutrophication of coastal ponds, and together with reduced salinity has been implicated in the occurrence of algae blooms, having negative impacts on the economy of coastal zones [1].

Different methods have been developed for measuring the magnitude of the SGD fluxes and studying GSI. Benthic chambers, salinity and temperature measurements, chemical analyses and measurements of a range of isotopic tracers at the aquifer-sea interface helped to estimate local and integrated coastal SGD fluxes [1]. Groundwater seepage is usually patchy, diffuse, temporally variable, and difficult to quantify [4]. Specific methods have been developed for simulating seawater-freshwater interactions and seawater intrusion using temporal salinity/temperature variations, tide pumping, wind and wave modelling [1]. For the estimation of SGD flux to the sea, the most frequently used method is based on seepage rate measurements [5], although because of seawater circulation in the coastal areas it may not give a realistic value for fresh water input into the sea via SGD. As seepage measurements give information on SGD fluxes on local scale only, isotopic tracers have been applied to estimate integrated SGD fluxes over the coast. Isotopic methods using stable (^2H , ^{13}C , ^{15}N , ^{18}O , $^{87/86}\text{Sr}$) as well as radioactive (^3H , ^{14}C , Ra isotopes,

ISOTOPIC CHARACTERISATION OF GROUNDWATER-SEAWATER INTERACTIONS

radon) isotopes have been recently developed, and SGD studies have been carried out in several coastal regions [6–11]. Especially deuterium and ^{18}O are effective conservative tracers of mixing processes at the groundwater-seawater interface, because there is clear isotopic distinction between on-shore meteoric groundwater and seawater. When combined with other isotopic tracers in the mixing zone, $\delta^2\text{H}$ and $\delta^{18}\text{O}$ serve as useful indicators of the mixing dynamics.

There has not been available a standard methodology for assessing groundwater discharge rates into the sea. Estimation of groundwater fluxes into the marine environment has been complicated due to the fact that the direct conventional measurements did not provide comprehensive information on the SGD phenomenon. Therefore to fill existing gaps IAEA launched in 2000 a Coordination Research Project (CRP) on “Nuclear and Isotopic Techniques for the Characterisation of SGD in Coastal Zones”. The aim of the CRP was:

- (i) To improve capabilities for water resources and environmental management of coastal zones.
- (ii) To improve and develop new isotopic techniques suitable for describing the rates and magnitude of groundwater and salt water fluxes in coastal aquifers.
- (iii) To develop a better understanding of influence of SGD on coastal marine processes, on coastal and on-shore groundwater environment and water resources.
- (iv) To carry out several case studies in different geological environments with the aim to study SGD techniques and assist Member States in coastal and water resources management.
- (v) To undertake intercomparison exercises to evaluate various techniques for estimation of SGD fluxes.
- (vi) To transfer know how to Member States by training experts in collecting, interpreting and managing SGD data generated in regional and multidisciplinary isotopic coastal studies.

The CRP was coordinated jointly by the IAEA’s Isotope Hydrology Section (Vienna) and Marine Environment Laboratories (Monaco) and carried out in cooperation with the UNESCO’s Intergovernmental Oceanographic Commission (IOC) and the International Hydrological Programme (IHP). Laboratories from Brazil, India, Italy, Japan, Russia, Slovenia, Turkey and USA participated in the CRP project. Several expeditions were carried out in the framework of the CRP:

- (i) Two expeditions were organised in the south-eastern Sicily (a karstic coastal region) in cooperation with University of Palermo (2001 and 2002).

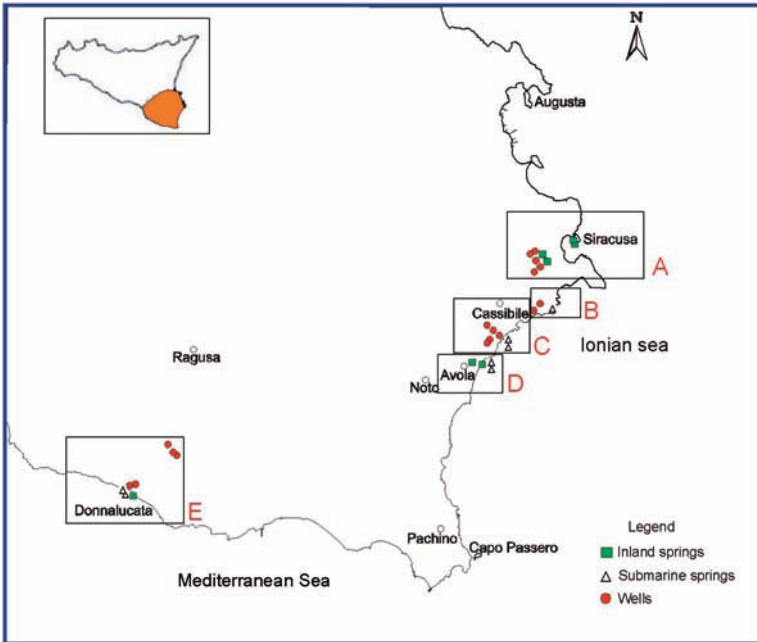


FIG. 1. SGD study areas in the south-eastern Sicily. A – Siracuse/Chiante area; B – Ognina area; C – Cassibile area; D – Avola area; E – Donnalucata area.

- (ii) One expedition was carried out to the south-eastern Brazil (a granite region) in cooperation with Laboratory of Environmental Radiometrics of IPEN and the University of Sao Paulo (2003).
- (iii) One expedition was carried out to Mauritius (an island region) in cooperation with University of Mauritius and the Mauritius Oceanography Institute (2004).

The programme of these expeditions concentrated on field isotopic studies of SGD, and on groundwater, seawater and sediment sampling along the coast. We present here results of SGD investigations carried out in the south-eastern Sicily, as obtained by different isotopic techniques.

2. HYDROGEOLOGY OF THE REGION

The studied area (Fig. 1) belongs to a structure, noted in the literature as the Hyblean Plateau that represents one of the principal structural elements of the eastern Sicily, which has been considered as a part of the African continental

crust. It is a relatively stable plateau, primarily of carbonate in origin. The eastern part has been influenced by a volcanic activity, the western part was formed essentially from carbonate sediments. The most ancient outcrops are represented by limestone marls. Wide carbonate successions known as the Ragusa Formation, that occupies the greatest part of the Hyblean Plateau, were developed in upper layers. The groundwater flows basically along the zones of cracks, fractures and karst hollows. The groundwater also flows through the faults directly to the sea forming submarine springs [12]. The visible submarine springs are located in the port of Donnalucata, at the Avola site, in the inlet of Ognina and in the mouth of the River Cassibile called "Balatone". More to the east, to Syracuse city, the Aretusa spring has been well know from mythology. The vulnerability of the aquifers of the carbonate series is generally high because they are not well protected against possible surface contamination, due to an elevated permeability typical for karst structures.

3. SAMPLING AND METHODOLOGY

Two sampling expeditions dedicated for isotopic studies were carried out in June 2001 and March 2002 to sample groundwater from 15 wells (including 5 borehole wells drilled on the beach) and 7 springs. Further 15 seawater sampling sites along the south-eastern Sicilian coast were visited (see Fig. 1 for visited sites): Siracusa/Ciane (zone A), Ognina (zone B), Cassibile (zone C), Avola (zone D) and Donnalucata (zone E). Water from the visible submarine springs found in the zones B, C, D and E was sampled either by divers, or using a pump and a polyethylene tube located close to a submarine spring.

The water samples for tritium analyses were collected and stored in 1 L polyethylene bottles. Water for $^3\text{H}/^3\text{He}$ measurements was sampled and stored in copper tubes following the procedures described by Ekwurzel et al. [13]. Water for chlorofluorocarbons (CFCs) analyses was sampled and stored in 10 mL glass bottles. Stable isotope measurements were carried out using equilibration technique for ^{18}O [14] and zinc reduction method for ^2H [15] at the IAEA's Isotope Hydrology Laboratory in Vienna and at the Institute of Geological and Nuclear Sciences, Lower Hutt, New Zealand.

Tritium was analysed in samples by ^3He in growth method using a mass spectrometer at the University of Heidelberg, or by liquid scintillation counting following electrolytic enrichment at the IAEA's Isotope Hydrology Laboratory and at the Institute of Geological and Nuclear Sciences, New Zealand

The isotopic results were reported against the international standard VSMOW (Vienna Standard Mean Ocean Water) as defined by Gonfiantini [16] using conventional delta notation. The precision of measurements (1σ)

was $\pm 0.1\text{‰}$ for $\delta^{18}\text{O}$ and $\pm 1\text{‰}$ for $\delta^2\text{H}$. Tritium results are reported in Tritium Units (1 TU = 118 mBq/L of water); the relative precision at 1σ was better than $\pm 10\%$. Standards and IAEA reference materials were used throughout the analyses to ensure data quality of produced results.

4. RESULTS AND DISCUSSION

The samples were analysed for environmental isotopes ^2H , ^{18}O , ^3H , ^3He , and chemistry. In the present contribution we shall discuss only stable isotope results. Fig. 2 shows the plot of $\delta^2\text{H}$ versus $\delta^{18}\text{O}$ in Sicilian groundwater, seawater and mixed samples. The fresh groundwater and some springs discharging groundwater lie between the Mediterranean Meteoric Water Line (MMWL) and the Global Meteoric Water Line (GNWL). The data are depleted in $\delta^{18}\text{O}$ (from -4.5 to -6‰) with respect to the reference VSMOW. The regression line through the groundwater-seawater data set (correlation coefficient $R^2 = 0.98$) shows a lower slope than that for the MMWL, that can be due to seawater-atmospheric water vapour interactions. In contrast, the seawater samples are highly enriched in $\delta^{18}\text{O}$ (from 0 to 1.8‰). The coastal spring and wells, representing submarine groundwater discharge, have $\delta^{18}\text{O}$ values from -2 to -3.3‰ and fall on a mixing line between groundwater and seawater. These samples may consist of about 40–50% fresh groundwater, implying high submarine groundwater discharge in the coastal Sicily. These

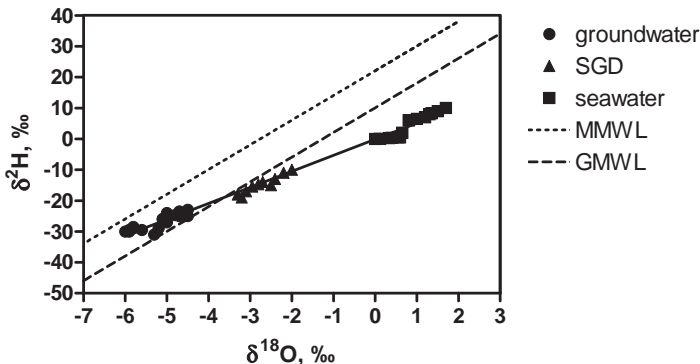


FIG. 2. $\delta^2\text{H}$ versus $\delta^{18}\text{O}$ plot of Sicilian groundwater and seawater samples and their mixtures. The MMWL and GNWL represent the Mediterranean Meteoric Water Line and the Global Meteoric Water Line, respectively.

ISOTOPIC CHARACTERISATION OF GROUNDWATER-SEAWATER INTERACTIONS

data are in reasonable agreement with other results obtained using radium and radon isotopes [11].

The tritium concentrations in groundwater samples varied between 1.5 and 4.1 TU, while in seawater samples they were below 2 TU. The tritiumgenic ^3He content (corrected from terrigenic sources) ranged from 0 to 14 TU. Samples from groundwater wells and springs were used to estimate an apparent age using the $^3\text{H} - ^3\text{He}$ isotope pair. The apparent ages ranged from 14 to 31 years, except a sample collected furthest inland showing a much younger age of about 2 years. The estimated apparent of the Donnalucata beach spring was 8 years.

5. CONCLUSION

The aim of the joint IAEA-UNESCO SGD project was to develop series of complementary isotopic techniques and to undertake intercomparison exercises to evaluate and improve several approaches in the characterisation of SGD in different geological environments. Stable and radioactive isotopes can thus provide a complex approach of SGD investigations, enabling separate estimation of fresh water as well as saline re-circulated groundwater fluxes to the sea. The presented isotopic studies show that discharged waters to the sea consist from about 40 to 50% of fresh groundwater, implying high groundwater discharge in the coastal Sicily.

ACKNOWLEDGEMENTS

The authors would like to thank all CRP participants who contributed to the success of the CRP. Special thanks are to Professor A. Aureli and his group for providing background information on SGD in the south-eastern Sicily, and for technical assistance during 2001 and 2002 expeditions.

REFERENCES

- [1] BURNETT, W.C., et al., Quantifying submarine groundwater discharge in the coastal zone via multiple methods, *Science of the Total Environment* 367 (2006) 498.
- [2] BURNETT, W.C., et al., Assessing methodologies for measuring groundwater discharge to the ocean, *EOS* **83** (2002) 117.
- [3] KONTAR, E.A., BURNETT, W.C., POVINEC, P.P., "Submarine groundwater discharge and its influence on hydrological trends in the Mediterranean Sea",

- Tracing long-term hydrological change in the Mediterranean Sea, CIESM Series, Vol. 16, CIESM, Monaco (2002) 109–113.
- [4] BOKUNIEWICZ, H., Analytical description of subaqueous groundwater seepage. *Estuaries* **15** (1992) 458.
- [5] TANIGUCHI, M., et al., Investigation of submarine groundwater discharge, *Hydrological Processes* **16** (2002) 2115–2129.
- [6] MOORE, W. S., Ages of continental shelf waters determined from ^{223}Ra and ^{224}Ra , *Journal of Geophysical Research* **105** (2000) 22117.
- [7] MOORE, W.S., Radium isotopes as tracers of submarine groundwater discharge in Sicily, *Continental Shelf Research* **26** (2006) 852.
- [8] BURNETT, W.C., DULAIIOVA, H., Estimating the dynamics of groundwater input into the coastal zone via continuous radon-222 measurements, *Journal of Environmental Radioactivity* **69** (2003) 21.
- [9] BURNETT, W.C., DULAIIOVA, H., Radon as a tracer of submarine groundwater discharge into a boat basin in Donnalucata, Sicily, *Continental Shelf Research* **26** (2006) 862.
- [10] AGGARWAL, P.K., et al., “Environmental isotope investigation of submarine groundwater discharge in Sicily, Italy,” *Isotopes in Environmental Studies, C&S Papers Series No. 26/P, IAEA, Vienna* (2006) 212.
- [11] POVINEC, P.P., et al., Characterisation of submarine groundwater discharge offshore south-eastern Sicily, *Journal of Environmental Radioactivity* **89** (2006) 81.
- [12] AURELI, A., The submarine springs in Sicily, Rep. Istituto di Geologia e Geofisica, Universita di Catania, Catania (1992).
- [13] EKWURZEL, B., et al., Dating of shallow groundwater: comparison with transient tracers $^3\text{H}/^3\text{He}$, chlorofluorocarbons, and ^{85}Kr , *Water Resource Research* **30** (1994) 1693.
- [14] SOFER, Z, GAT, J.R., Activities and concentrations of ^{18}O in concentrated aqueous salt solutions: analytical and geophysical implications. *Earth and Planetary Science Letters* **15** (1972) 232.
- [15] COLEMAN, M.L., et al., Reduction of water with zinc for hydrogen isotope analysis, *Analytical Chemistry* **54** (1982) 993.
- [16] GONFIANTINI, R., Standards for stable isotope measurements in natural compounds, *Nature* **271** (1978) 534.

USE OF ENVIRONMENTAL ISOTOPES TO EVALUATE THE SOURCES OF SUBMARINE FRESHWATER IN THE SOUTHERN SHORELINE IN LEBANON

Z. SAAD, V. KAZPARD
Lebanese University,
Faculty of Sciences, Lebanon

and

Lebanese Atomic Energy Commission – CNRS,
Beirut, Lebanon

Abstract

Geochemical and isotopic techniques are applied to evaluate the origin of submarine springs in the southern and northern shoreline in Lebanon. Submarine springs have different geochemistry reflecting a difference in the specific geology of southern and northern shoreline. Environmental isotopes including ^2H , ^{18}O , ^{34}S and ^{18}O in sulfate have proved the different geological features. A more enriched isotopic composition of submarine groundwater is investigated in the south where submarine springs are primarily artesian flows. The deep circulation of groundwater is affected by a high geothermal gradient. Also a high sulfate content is related to a fractionation in ^{34}S isotopic composition. This is due to the dissolution of gypsum minerals and its reduction of marly limestones of the Upper Cretaceous and Lower Eocene in the confined aquifers. In the northern part, a slightly depleted isotopic composition is found for submarine and groundwater. The highly karstified northern region induces a fast infiltration of groundwater till its discharge as submarine springs.

1. INTRODUCTION

Geochemical parameters are important tools to define groundwater quality and its origin with characterization of its path flow in aquifers. During hydro chemical evolution, the concentration of individual ionic species increases, remains constant or decreases. In the case of water-rock interaction in submarine freshwater, changes in calcium, magnesium and sulfate are due to anhydrite

dissolution and dedolomitisation [1]. Sodium increase along the aquifer flow path is attributed to ion exchange with clay minerals [2]. In submarine freshwater, sulphur sources can be divided into mineral or rock contribution, marine and volcanic sources [3]. Ionic molar ratios would distinguish between the different sources of sulfate in water. Environmental stable isotopes (oxygen-18 and deuterium) in combination with the geochemical parameters are used to determine the recharge origin and mixing of groundwater in submarine aquifers. The isotopic compositions of groundwater are governed by recharge from precipitation and infiltration from surface waters.

In karst systems, groundwater mixing is high where connected porosity occurs in small-scale fissures and the porous matrix that provide much of the storage in the system and which contribute to base flow. Stable isotopes of $\delta^{18}\text{O}$ and $\delta^2\text{H}$ can serve to distinguish flow through different systems. In deep and confined aquifers, fractures and faults allow groundwater to discharge as artesian flows into the sea giving submarine freshwater springs. Geothermal gradient within this deep path flow increases the temperature of water. On the other hand, isotopic ratio of sulfur in combination with $\delta^{18}\text{O}$ is applied to observe special chemical processes in surface and groundwater. The stable isotopic ratio of the sulphur isotopes ($\delta^{34}\text{S}$ and $\delta^{18}\text{O}$ in sulfate) allows differentiating between marine, evaporitic and volcanic sources of dissolved sulphate in groundwater [4]. The isotopic composition of sulphur in these sources, with the exception of seawater, varies in a wide range. When sulphur from various natural and anthropogenic sources dissolves in cold groundwater, no appreciable fractionation takes place unless dissolved sulphate is microbially reduced. The exchange of oxygen between SO_4^{2-} and H_2O is extremely slow at the low temperature of groundwater [5]. Therefore, the isotopic composition of oxygen in sulphate reflects either mixing or reduction to sulphides.

These geochemical and isotopic techniques will be applied to delineate the origin of submarine freshwater in different coastal regions in Lebanon. In Lebanon, the heavily uplifted and dissected terrain displays extensive outcrops of an almost complete stratigraphic sequence of Early Jurassic to Quaternary age, mostly in conditions of only minimal tectonic deformation [6, 7]. The Jurassic period includes mainly dolomite and dolomitic limestone. The cretaceous period consists of limestone, marly limestone and dolomite. With respect to groundwater, these are the most important sediments and their widespread and interconnected karstic nature makes them the source of major springs in Lebanon [8]. Some of these springs are extending into the sea such as one 3 km offshore submarine spring beside the Litani river mouth [9]. In coastal Lebanon, the most influencing condition on which water flows from land into the sea is through faults and karstic galleries. Around 54 submarine springs are identified throughout the offshore from the north to the south. It

was found that 52 % of these springs are issuing from karstic rock formation with high flow rate; 22 % are issuing along fault alignments with high flow rate; 18 % are offshore springs with low to high flow rate (interrupting flow) [10,11]. Discharge of springs into submarine freshwater flows is thus influenced by the specific geological features in the different locations. The present study gives an important insight to verify geological differences in submarine springs between the northern and the southern regions in Lebanon, by using hydrochemical and isotopic tools. The origin of recharge in the submarine springs will be determined as a function of variation of water quality throughout water-rock interactions.

2. MATERIALS AND METHODS

The first studied submarine springs are located in the northern region near Chekka bay that flows to the sea via a complex of fault and karstic zones. Submarine springs of the northern coast in Lebanon are estimated to flow from the Turonian-Cenomanian limestones at a mean depth of 120 m below mean sea level and at an average distance from the shoreline that reaches 700 m [10, 12]. The second submarine springs are located in the southern coast where the presence of hydraulic parameters was found to be more developed than the northern part. They exhibit longer lineament extents, dense fracturing systems and conduits extension with the sea [10]. Aquifers in the coastal plateau of South Lebanon are primarily in Cenomano-Turonian strata. In this region, artesian aquifers can extend for considerable distances offshore and occur because of the confining of the aquifer by the cover of marls and marly limestones of the Upper Cretaceous and Lower Eocene. The combined hydrochemical and environmental isotope survey ($\delta^{18}\text{O}$, $\delta^2\text{H}$, $\delta^{34}\text{S}$) was achieved for the following samples: In the north coastal part, sampling sites are 1 coastal groundwater, 2 submarine springs, 1 sea water; In the southern part, sampling sites are 3 coastal surface freshwater, 2 coastal groundwater, 4 submarine springs and 1 sea water. Chemical and isotopic analyses ($\delta^{18}\text{O}$, $\delta^2\text{H}$, $\delta^{34}\text{S}$ and $\delta^{18}\text{O}$ in sulphate) were done after collection.

3. RESULTS AND DISCUSSION

3.1. Hydrochemical characterization of water samples

In order to evaluate the origin of water solutes in coastal and submarine groundwater, variations of sodium and chlorine are plotted as a function of

sulfate concentration (Fig. 1). The plots indicate the distribution of points into three groups. The first group with relatively low concentrations in both Na and Cl is relative to coastal freshwaters. The second group with medium concentrations is relative to submarine water of Chekka (North region). The third group with higher concentrations in sodium and anions is assigned for submarine freshwater in South of Lebanon. This specific distribution of the points indicates that the characteristics of submarine water in Chekka region is close to that of coastal groundwater, whereas a different feature in hydrogeology is recorded for submarine water in South region. This different geochemistry of submarine springs in the north and the south may reflect a difference in the specific geology of the two regions. This specificity must be clarified when using the environmental isotopes analysis.

3.2. Environmental isotopes analysis of submarine and coastal freshwater

Samples of rainwater from coastal and highland regions were taken for environmental isotopes analysis of deuterium and oxygen-18. The local

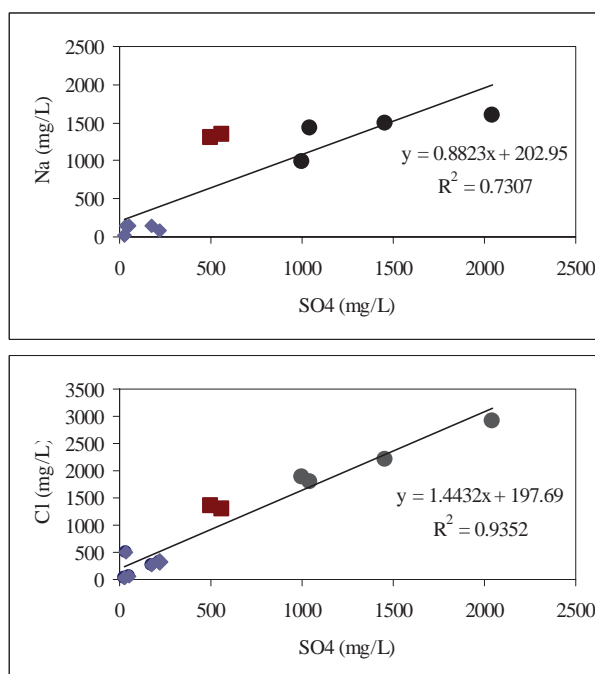


FIG.1. Plot of sulfate concentration vs. the concentrations of Na and Cl in coastal and submarine springs.

USE OF ENVIRONMENTAL ISOTOPES TO EVALUATE THE SOURCES

Lebanese meteoric water line provides a baseline for tracing groundwater recharge [13, 14]. In the Lebanon and Anti-Lebanon mountains where the average temperatures are lower than the coastal areas, precipitation will be isotopically depleted. This altitude effect is useful to distinguish groundwater recharged at high altitudes from that recharged at low altitude. The Lebanese Meteoric water line LMWL is defined by the following equation [14]:

$$\delta^2\text{H} = 7.13 \times \delta^{18}\text{O} + 15.98$$

To establish the origin of water recharge in the different reservoirs (surface water, groundwater, submarine water) the isotopic composition of deuterium and oxygen-18 was determined and compared to the LMWL. Fig. 2 shows the variation of deuterium against oxygen-18 of the submarine, surface and groundwater in the north (Chekka) and the south region (Tyre). All points lie between the Lebanese Meteoric Water Line (LMWL) and the Global Meteoric Water Line (GMWL). Further the distribution of points delineates two groups of waters. The first one includes surface and groundwater with submarine springs in Chekka region that lie near the Lebanese Meteoric water line. The highly karstified region of Chekka, induces a fast infiltration of groundwater in its galleries till they submerge as submarine springs in the sea [10]. These submarine springs of Chekka, estimated to flow at 10 m³/sec, are related to Turonian-Cenomanian limestones aquifer.

The more enriched isotopic composition of submarine groundwater in Tyre region could be explained by either a mixing with sea water or a geothermal effect within the aquifer (Fig. 2). The mixing possibility is a rather bit eliminated because isotopic composition of submarine springs is closer

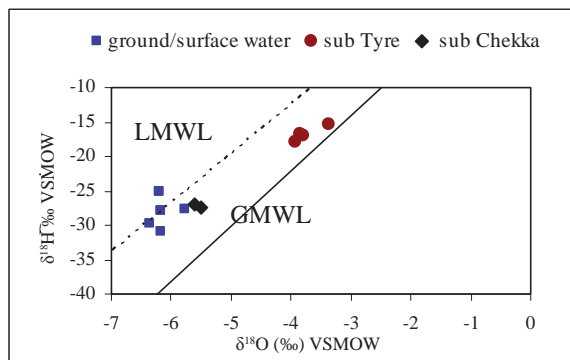


FIG. 2. Isotopic composition of surface, groundwater and submarine springs in different regions.

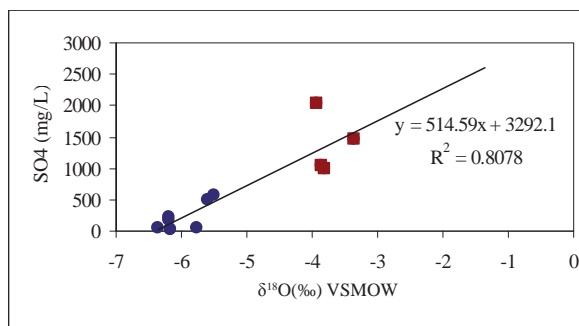


FIG.3. Variation of sulfate against $\delta^{18}\text{O}$ in coastal groundwaters and submarine springs.

to the rainwater data in this region. On the other hand, a specific hydraulic feature exists in this region, according to dense fracturing systems and conduits extension with the sea. Aquifers in the coastal plateau of South Lebanon are primarily in Cenomano-Turonian strata. In this region, the submarine springs are primarily artesian flows that occur in confined aquifers. These aquifers are deep and groundwater reaches great depth before their discharge into the sea. Fractures and faults system assume this deep circulation of groundwater that gain in temperature because of the geothermal gradient. In fact, temperature of submarine springs in the south region is about 42°C that confirms the deep circulation of groundwater before its discharge as submarine spring. Tritium of submarine water ranges between 2.5 and 3.5 TU which is close to the rainwater values in the south region, thus indicating a short subsurface residence time and a high mixing with young meteoric water [15].

When arriving to the confined aquifer, groundwater passes through a layer of marls and marly limestones of the Upper Cretaceous and Lower Eocene. Groundwater will be charged of gypsum minerals ($\text{CaSO}_4 \cdot 2\text{H}_2\text{O}$) when passing through the marl formation. This could be verified in Fig. 3 which shows that submarine samples in the south (square form), enriched with $\delta^{18}\text{O}$, are the most concentrated in sulfate. The deep circulation of groundwater at high temperature promotes the dissolution of gypsum minerals.

At a big depth, usually a certain amount of sulfate is reduced to sulfur via the following equation [2]:



During this complex geochemical transformation of sulfate, fractionation processes affect the stable isotopic compositions of sulfur ($^{34}\text{S}/^{32}\text{S}$) and oxygen

USE OF ENVIRONMENTAL ISOTOPES TO EVALUATE THE SOURCES

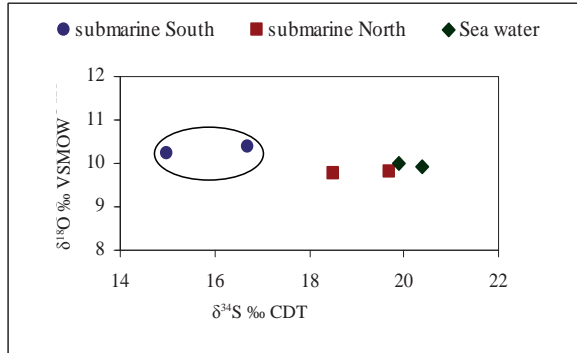


FIG.4. Ranges of variation of $\delta^{34}\text{S}$ and $\delta^{18}\text{O}$ in sulfate of submarine springs (north and south regions) and sea water.

($^{18}\text{O}/^{16}\text{O}$) in sulfate. The temperature of groundwater prevents most of the isotopic fractionation processes to reach isotopic equilibrium and significant isotopic exchange of oxygen between sulfate ions and water [16, 17]. In the present study, isotopic composition of sulfur in dissolved sulfate in sea water is around 20‰ (Fig. 4). This value is concordant with the recent sea water defined by $\delta^{34}\text{S} = 21\text{‰}$.

Fig. 4 does not show important fractionation in $\delta^{18}\text{O}$ of sulfate for all submarine samples. Whereas submarine groundwater in the south region has a lighter isotopic composition of $\delta^{34}\text{S}$ that reaches 15‰. This light fractionation of sulfur isotopic composition verifies the specific hydrogeology in Tyre region associated with the elevated geothermal gradient.

4. CONCLUSIONS

The present study gives an important insight to verify the geological differences between the northern and the southern regions in Lebanon, by using hydrochemical and isotopic tools. This preliminary study shows that submarine springs in the southern and northern shoreline are characterized by different hydrochemical and isotopic parameters. These different characteristics imply a difference in the hydrogeological feature in the two regions. The northern shoreline is affected by a highly karstified region while the southern region exhibits longer lineament extents with dense fracturing system that implies the formation of artesian submarine springs. The elevated temperature of

submarine springs in the south associated with isotopic fractionation of sulfur in dissolved sulfate is related to the geothermal gradient at a big depth.

REFERENCES

- [1] PLUMMER, L.N., PRESTEMON, E.C., PARKHURST, D.L., An interactive code (NETPATH) for modeling Net Geochemical Reactions along a Flow Path. Version 2.0, Water-Resources Investigation Report, 94-4169, U.S. Geol. Survey, Reston (1994) 227.
- [2] CLARK, I.D., FRITZ, P., Environmental Isotopes in Hydrogeology, Lewis Publishers, New York (1997) 328.
- [3] GISLASON, S.R., EUGSTER, H.P., Meteoric water-basalt interactions. II: A field study in N.E. Iceland, *Geochim. Cosmochim. Acta* **51** (1987) 2841–2855.
- [4] KROUSE, H.R., Sulphur isotopes in our environment, In: P. Fritz and J.C. Fontes (Editors), *Handbook of Environmental Isotope Geochemistry Vol. I, The Terrestrial Environment*, Elsevier, Amsterdam (1980) 435–471.
- [5] CHIBA, H., SAKAI, H., Oxygen isotope exchange rate between dissolved sulfate and water at hydrothermal temperatures, *Geochim. Cosmochim. Acta* **49** (1985) 993–1000.
- [6] WALLEY, C. D., A braided strike-slip model for the northern continuation of the Dead Sea Fault and its implications for Levantine tectonics, *Tectonophysics* **145** (1988) 63–72.
- [7] DUBERTRET, L., Introduction à la carte géologique à 1/50000 du Liban, *Notes et Mém. Moyen-Orient* **23** (1975) 345–403.
- [8] MIJATOVIC, B., BAKIC, M., le karst du Liban, étude de son évolution d'après les recherches hydrogéologiques, *BRGM, Chronique d'hydrogéologie, Paris* **10** (1967) 95–107.
- [9] FAO, *Projet de développement hydro-agricole du Liban, Thermometrie aéroportée par infrarouge* (1972).
- [10] SHABAN, A., KHAWLIE, M., ABDALLAH, C., FAOUR, G., Geologic controls of submarine groundwater discharge: application of remote sensing to north Lebanon, *Environ Geol* **47** (2005) 512–522.
- [11] SAAD, Z., KAZPARD, V., SLIM, K., MROUEH, M., A hydrochemical and isotopic study of submarine fresh water along the coast in Lebanon, *Journal of Environmental Hydrology*, vol 13, **8** (2005) 1–16.
- [12] QAREH, R., The submarine springs of Chekka, exploitation of a confined aquifer discharging in the sea, PhD thesis, geology department, American University of Beyrouth (1966).

USE OF ENVIRONMENTAL ISOTOPES TO EVALUATE THE SOURCES

- [13] BARNES, C.J., ALLISON, G.B., Tracing of water movement in the unsaturated zone using stable isotopes of hydrogen and oxygen, *J. Hydrol.* **100** 1-3 (1988) 143–176.
- [14] SAAD, Z., KAZPARD, V., EL SAMRANI, A.G., SLIM, K., Chemical and isotopic composition of rainwater in coastal and highland regions in Lebanon, *Journal of Environmental Hydrology*, vol 13 **29** (2005) 1–11.
- [15] STURCHIO, N.C., AREHART, G., SULTAN, M., SANO, Y., ABOKAMAR, Y., SAYED, M., Composition and origin of thermal waters in the Gulf of Suez area, Egypt, *Applied geochemistry* **11** (1996) 471–479.
- [16] KRAUSE, H.R., Relationships between the sulphur and oxygen isotope composition of dissolved sulphate, In: *Studies on Sulfur Isotope Variations in Nature. Panel Proc. Series, IAEA Vienna* (1987) 31–47.
- [17] FRITZ, P., FRAPE, S.K., DRIMMIE, R.J., APPLEYARD, E.C., HATTORI, K. Sulfate in brines in the crystalline rocks of the Canadian Shield, *Geochim. Cosmochim. Acta* **58** (1994) 57–65.

CHAIRPERSONS OF SESSIONS

OPENING SESSIONS

P.K. AGGARWAL	IAEA
K. FROEHLICH	Germany
R. GONFIANTINI	Italy
N. RAMAMOORTHY	IAEA
H. SAILER	Austria

TECHNICAL SESSIONS

Monday, 21 May 2007	R. GONFIANTINI P. VRECA	Italy Slovenia
Tuesday, 22 May 2007	A. HERCZEG E. SACCHI	Australia Italy
Wednesday, 23 May 200	K. ZOUARI O. ZUKHOVA	Tunisia Belarus
Thursday, 24 May 2007	Y. TRAVI P. CARREIRA	France Portugal
Friday, 25 May 2007	D. MARTINEZ S. CASTANEDA	Argentina Philippines
Roundtable Session 1	D.K. SOLOMON A.L. HERCZEG	USA Australia
Roundtable Session 2	C. TINDIMUGAYA M.A. CHOUDHRY	Uganda IAEA
Closing Session	P.K. AGGARWAL A.L. HERCZEG D.K. SOLOMON C. TINDIMYGAYA	IAEA Australia USA Uganda

PROGRAMME COMMITTEE (IAEA)

P.K. AGGARWAL
L.J. ARAGUAS-ARAGUAS
M.A. CHOUDHRY
W.A. GARNER
M. GROENING
K.M. KULKARNI
T. KURTTAS
B. NEWMAN

SECRETARIAT OF THE SYMPOSIUM

P.K. AGGARWAL	Scientific Secretary
K.M. KULKARNI	Scientific Co-Secretary
H. SCHMID	Conference Services
O. AZUCENA	Administrative Support
C. MANICA	Administrative Support
E. IZEWSKI	Proceedings Support
L. VILLARD	Proceedings Support
G.V. RAMESH	Coordinating Editor

In many parts of the world, surface water and groundwater resources are at risk because of indiscriminate use, rapidly growing populations, increasing agricultural demands, and the threat of pollution. These risks are often compounded by a lack of understanding about local conditions governing the occurrence, distribution and movement of surface and groundwater resources. Historically, the IAEA has played a key role in advancing isotope techniques and in promoting the use of isotopes to address water resource sustainability issues worldwide. The quadrennial IAEA symposia continue to be an important component of the IAEA's mission in water resources management. The 12th symposium in the series was convened from 21 to 25 May 2007 in Vienna with the objectives of: reviewing the state of the art in isotope hydrology; outlining recent developments in the application of isotope techniques to water resources management; and identifying future trends and developments for research and applications. These proceedings — in two volumes — contain the presentations made at the symposium. A CD-ROM containing the complete text of these proceedings is attached to the inside back cover of the second volume.



Water
Resources
Programme

INTERNATIONAL ATOMIC ENERGY AGENCY
VIENNA

ISBN 978-92-0-110207-2

ISSN 0074-1884